

**DEVELOPMENT OF EFFICIENT STRATEGIES FOR THE SYNTHESIS OF  
COMPOUND LIBRARIES OF ANTI-HIV AGENTS THAT BLOCK HIV  
REPLICATION**

by

Maryam Zamiri

B.Sc., The University of British Columbia, 2007

M.Sc., The University of British Columbia, 2013

A THESIS SUBMITTED IN PARTIAL FULFILLMENT OF  
THE REQUIREMENTS FOR THE DEGREE OF

DOCTOR OF PHILOSOPHY

in

THE FACULTY OF GRADUATE AND POSTDOCTORAL STUDIES  
(Pharmaceutical Sciences)

THE UNIVERSITY OF BRITISH COLUMBIA  
(Vancouver)

August 2019

© Maryam Zamiri, 2019

The following individuals certify that they have read, and recommend to the Faculty of Graduate and Postdoctoral Studies for acceptance, the dissertation entitled:

Development of efficient strategies for the synthesis of compound libraries of anti-HIV agents that block HIV replication

---

submitted by Maryam Zamiri in partial fulfillment of the requirements for

the degree of Doctor of Philosophy

in Pharmaceutical Sciences

---

**Examining Committee:**

David Grierson, Pharmaceutical Sciences  
Supervisor

---

Supervisory Committee Member

Urs Häfeli, Pharmaceutical Sciences  
Supervisory Committee Member

Chris Orvig, Chemistry  
University Examiner

Abby Collier, Pharmaceutical Sciences  
University Examiner

**Additional Supervisory Committee Members:**

Adam Frankel, Pharmaceutical Sciences  
Supervisory Committee Member

Glenn Sammis, Chemistry  
Supervisory Committee Member



## Abstract

Worldwide, it is estimated that 37 million people are living with HIV/AIDS. Only 35 years ago, the life expectancy for HIV patients was 1-2 years. Fortunately, with the advent of antiretroviral therapy (ART), where different combinations of drugs targeting the HIV proteins are taken, the morbidity rate has dropped very significantly. However, ART fails to eradicate the latent virus pool from infected cells, and this necessitates strict adherence to lifetime treatment schedules. Prolonged ART therapy also leads to issues of toxicity/side effects and drug resistance. These factors underscore the continued need for new drugs, and especially those acting through novel mechanisms of action. My PhD project focused on developing small molecules that inhibit HIV replication through targeting human serine-arginine (SR) protein splicing factors, rather than viral proteins. Once inside the human, HIV is very dependent on human alternative splicing machinery and this explicit reliance may render it sensitive to even slight disturbances in the progression of the disease. Even low doses can thus impair HIV replication while having no or very limited alteration on human splicing events.

This work was based on the discovery of **IDC16**, which perturbs the alternative splicing of HIV mRNA transcripts, and 5350150, which interferes with HIV mRNA transport. Although, these two molecules have anti-HIV activity, they are toxic to human cells. Using parallel synthesis, a library of amide analogues/mimics of **IDC16** and 5350150 was prepared and screened.

Within the first 2 years of my PhD program, I developed a green and efficient strategy for amide bond formation in which oxo-ester or acid fluoride reacts with N-silylated amines to give di(hetero)arylamides (DHAs) in pure form. This protocol was effective in the production of 92 DHAs in our search for finding new anti-HIV drugs.

The screening of the synthesized molecules for their anti-HIV activity led to the discovery of **4.25kk**(GPS488) and **4.25ww**(GPS491) which are active in both wild type and drug resistant strains, demonstrating that they have a different mechanism of action from the current HIV drugs.drugs.

## Lay Summary

Current anti-HIV drugs target viral proteins to impede its replication. These drugs cannot eradicate all viruses and induce resistance so there is a big demand for drugs and in particular, those acting through new mechanism of actions. This PhD work was based on the discovery of **IDC16** and compound 5350150 which block HIV replication by targeting human alternative splicing machinery which is vital for HIV protein production. Using parallel synthesis, a library of 92 compounds was prepared and screened, which are more drug-like analogues of **IDC16** and compound 5350150. Our newly discovered anti-HIV molecules are active in both wild type and drug resistant HIV strains, suggesting that these molecules have a mechanism of action different from the current HIV drugs.

## Preface

The research described in this dissertation was performed by the author under the guidance and supervision of Dr. David Grierson in the Department of Pharmaceutical Sciences, University of British Columbia, between January 2013 and September 2018. Dr. David Grierson and the author were responsible for designing of the synthetic strategy, data analysis, and interpretation of the results.

Preliminary evaluation of the anti-HIV activity of the synthesized compounds was carried out by Dr. Peter Cheung at BC Centre for Excellence in HIV/AIDS. The drug resistance and EC<sub>50</sub> studies for the most potent molecules were also carried out by Dr. Peter Cheung.

A more detailed study about the effect of our anti-HIV active molecules on cellular gene expression and HIV-1 splicing was done by our collaborators, Dr. Benoit Chabot (Universite de Sherbrooke) and Dr. Alan Cochrane (University of Toronto).

A version of Chapter 2 was published in *American Chemical Society Journal of Medicinal Chemistry*:

Peter K. Cheung, David Horant, Laura E. Bandy, **Maryam Zamiri**, Safwat M. Rabea, Stoyan K. Karagiosov, Mitra Matloobi, Steven McArthur, P. Richard Harrigan, Benoit Chabot, and David S. Grierson. A Parallel Synthesis Approach to the Identification of Novel Diheteroarylamide-Based Compounds Blocking HIV Replication: Potential

Inhibitors of HIV-1 Pre-mRNA Alternative Splicing. *Journal of Medicinal Chemistry*.  
2016, 59 (5), pp 1869–1879

Specifically, my contribution to this paper was focused on the preparation of a series 27 Di(hetero)arylamide possessing a 2-pyridinone or a 4-pyridinone motif as the “left side” scaffold, which are shown in Figure 2.5 and Figure 2.6. Dr. David Horant, Laura E. Bandy, Dr. Safwat M. Rabea, Dr. Stoyan K. Karagiosov, and Dr. Mitra Matloobi synthesized additional **IDC16** mimics for this publication. Dr. Peter K. Cheung and Steven McArthur carried out all the biological testing for the synthesized molecules. Dr. Richard Harrigan, Dr. Benoit Chabot, and Dr. David S. Grierson were the principal investigators for this publication. All authors contributed for the preparation of this manuscript.

A version of Chapter 3 was published in 2 *Synthesis* papers:

**Maryam Zamiri**, and David S. Grierson. A Trimethylsilylamine-Acyl Fluoride Amide Bond Forming Protocol for Weakly Nucleophilic Amines that is Amenable to the Parallel Synthesis of Di(hetero)arylamides. *Synthesis*. 2016, 49 (3), pp 571-578.

Ana Koperniku, **Maryam Zamiri**, David S. Grierson. The Reaction of N-Trimethylsilyl Substituted Heteroarylamines with Thio and Oxoesters: An Efficient Protocol to Access Diheteroarylamides. *Synthesis*. 2019, 51 (08), 1779-1790.

For our 2016 *Synthesis* paper, I synthesized and characterized all the Di(hetero)arylamides. Dr. David Grierson, principle investigator, and I contributed for the preparation of this manuscript.

My contribution to our 2019 *Synthesis* paper focused on the design and synthesis of Di(hetero)arylamides through the reaction of oxo-ester and N-silylated amine, which are shown in Table 3.2. Ana Koperniku designed and synthesized Di(hetero)arylamides through the reaction of thioester and N-silylated amine. All authors contributed for the preparation of this manuscript.

A patent was filed for the findings presented in Chapter 4.

Please note that the numbering of structures in this thesis is done based on the chapter numbers with the exception of **IDC16**, **5350150**, **1C8**, **2D3**, **3C2**, **1E5**, and **ABX464** which are named according to their names in the literature.

## Table of Contents

<b>Abstract.....</b>	<b>iii</b>
<b>Lay Summary .....</b>	<b>v</b>
<b>Preface.....</b>	<b>vi</b>
<b>Table of Contents .....</b>	<b>ix</b>
<b>List of Tables.....</b>	<b>xiii</b>
<b>List of Figures .....</b>	<b>xiv</b>
<b>List of Reaction Schemes .....</b>	<b>xviii</b>
<b>List of Abbreviations.....</b>	<b>xix</b>
<b>Acknowledgements.....</b>	<b>xxii</b>
<b>Dedication .....</b>	<b>xxiii</b>
<b>Chapter 1: Introduction.....</b>	<b>1</b>
1.1    Impact of structural biology in drug discovery .....	2
1.2    Sources of compound libraries.....	3
1.2.1    Natural product libraries.....	3
1.2.2    Industrial (pharmaceutical company) libraries.....	5
1.2.3    Commercial libraries .....	6
1.2.4    Academic libraries.....	6
1.3    Synthesis of compound libraries: combinatorial approach and parallel library synthesis .....	8
1.4    Hit optimization.....	9

1.5	HIV and the application of parallel synthesis to finding a new class of anti-HIV drugs: foundation of my project.....	9
1.5.1	Objective 1: IDC16 and the design of a library of IDC16 mimics .....	12
1.5.2	Objective 2: Construction and evaluation of amide analogues of stilbene 5350150 - discovery of 4.25kk(GPS488) and 4.25ww(GPS491) .....	15
<b>Chapter 2: Discovery of the di(hetero)arylamide type IDC16 mimics 1C8, 2D3, 3C2, 1E5</b>		<b>17</b>
2.1	Discovery of IDC16 and the parallel synthesis/compound library approach to identify active and non-toxic IDC16 “mimics” .....	17
2.2	Compound 1C8 perturbs the function of the SR protein splicing factor SRSF10 .....	26
2.2.1	Alternative splicing and the significance of alternative splicing in HIV replication .....	27
2.2.2	Alternative splicing mechanism .....	28
2.2.3	Alternative splicing in HIV .....	31
2.3	Results for 1C8 on HIV alternative splicing: function of SRSF10 is targeted .....	35
<b>Chapter 3: Development of a new amide bond forming protocol for the parallel synthesis of di(hetero)arylamides .....</b>		<b>38</b>
3.1	Challenges in di(hetero)arylamide (DHA) synthesis and its translation to parallel synthesis .....	40
3.1.1	Peptide coupling methodology .....	40
3.2	Part 1: Coupling of N-silylated (hetero)arylamines with acid fluoride 3.51, a new protocol.....	49
3.2.1	Preparation of N-silylation of (hetero)aryl amines 3.34a to 3.34r .....	49
3.2.2	Preparation of Acid fluoride 3.51.....	50



3.2.3	The coupling step: reaction of acid fluoride 3.51 with N-silylated amines 3.34a-r..	53
3.3	Part 2: coupling of N-silylated amines with oxo-ester .....	58
3.4	DHA synthesis through the reaction of oxo-ester and N-silylated amine .....	61
3.4.1	Preparation of oxo-ester 3.59 .....	61
3.4.2	Reaction of oxo-ester 3.59 with N-silylated amines .....	61
3.5	Conclusions .....	66
3.6	Experimental Section .....	66
3.6.1	Experimental section .....	67
<b>Chapter 4: Targeting HIV rev function: discovery of 4.25kk (GPS488) and 4.25ww (GPS491) .....</b>		<b>90</b>
4.1	Role of SR proteins in mRNA export .....	90
4.2	Conception and design of 5350150-amide analogues .....	94
4.3	Synthesis of amide analogues of 5350150 .....	98
4.4	Preliminary anti-HIV screening for amide 4.6a-xx .....	100
4.5	SAR studies for compounds 4.6kk, qq, ww .....	105
4.6	Calculation of EC50 for 4.25kk (GPS488) and 4.25ww (GPS491) for wild-type and major strains resistant against the four drug classes used in ART .....	110
4.7	Structural similarity of 4.25kk (GPS488) and ABX464 .....	114
4.8	Conclusion and future directions .....	115
4.9	Experimental Section .....	117
<b>Chapter 5: Conclusions .....</b>		<b>168</b>
<b>References .....</b>		<b>170</b>

<b>Appendix: Spectra data for compounds synthesized in Chapter 3 and 4 .....</b>	<b>177</b>
--	------------

## List of Tables

Table 3.1 Synthesis of DHA 3.52a-r from N-silylated amines 3.34a-r.....	55
Table 3.2 Synthesis of DHA 3.57 from oxo-ester and N-TMS amines 3.34. The results from thioesters (synthesized by Ana Koperniku) are also shown for reference purposes.....	64
Table 4.1 The viability of 7 amide analogues of 5350150 with strong anti-HIV activity .....	104

## List of Figures

Figure 1.1 Examples of natural products and their analogues with biological activity .....	4
Figure 1.2 a) Structure of ellipticine, IDC16, and 1C8: ellipticine is a natural product; IDC16 is an analogue of ellipticine; 1C8 is a flexible mimic of IDC16; b) structure of 5350150.....	5
Figure 1.3 a) Solid support synthesis of 1.18 and 1.21 from reacting trienes 1.16 with 2 equivalents of dienophiles b) the structure of calmoduphilin .....	7
Figure 1.4 HIV life cycle highlighting the targets of current anti-HIV drugs .....	11
Figure 1.5 Discovery of IDC16 and its structural relationship to ellipticine .....	14
Figure 1.6 Objective one: preparation of conformationally flexible IDC16 mimics with amide linkers .....	15
Figure 1.7 Objective two: synthesis of amide analogues of 5350150 and their SAR studies.....	16
Figure 2.1 The structure of natural products and derivatives that impact alternative pre-mRNA splicing .....	18
Figure 2.2 a) Structure of olivacine and ellipticine b) IDC16 “mimics” with different linkers; c) structure of 4 DHAs with significant anti-HIV activities .....	20
Figure 2.3 The compilation of all the synthesized IDC16 mimics. Reprinted with permission from "A Parallel Synthesis Approach to the Identification of Novel Diheteroarylamide-Based Compounds Blocking HIV Replication: Potential Inhibitors of HIV-1 Pre-mRNA Alternative Splicing." <u>Journal of Medicinal Chemistry</u> 59(5): 1869-1879. Copyright (2016) American Chemical Society.....	21
Figure 2.4 Evaluation of anti-HIV-1 activity (column) and GXR-CEM cell viability (line) for IDC16 (A) and 1C8 (B) at concentrations between 62.5 nM and 16 $\mu$ M (0 provides the value	

when no compound was added). HIV-1 infection in CEM-GXR cells was assessed by measuring GFP positive cells 3 days after infection. CEM-GXR cell viability was measured after 24 h incubation within the same range of concentrations. Results were expressed from three independent experiments for both the anti-HIV-1 activity and cell viability assays. Reprinted with permission from "A Parallel Synthesis Approach to the Identification of Novel Diheteroarylamide-Based Compounds Blocking HIV Replication: Potential Inhibitors of HIV-1 Pre-mRNA Alternative Splicing." <u>Journal of Medicinal Chemistry</u> 59(5): 1869-1879. Copyright (2016) American Chemical Society .....	23
Figure 2.5 Structure of 18 DHAs bearing 2-pyridinone motif as the “left side” scaffold. Synthesis of these molecules are discussed in Chapter 3.....	25
Figure 2.6 Structure of 9 DHAs bearing 4-pyridinone motif as the “left side” scaffold. Synthesis of these molecules are discussed in Chapter 3. ....	26
Figure 2.7 A schematic presentation defining constitutive splicing and alternative splicing. Adapted with permission from literature <sup>31</sup> .....	28
Figure 2.8 The mechanism of alternative splicing .....	30
Figure 2.9 Position of different regulatory elements on HIV-1 genome. Adapted with permission from literature <sup>32</sup> .....	33
Figure 2.10 HIV-1 genome and different mRNA splicing products. Adapted with permission from literature <sup>32</sup> .....	34
Figure 2.11. Early and late transcripts derived from the viral HIV-1 genome. Adapted with permission from literature <sup>32</sup> .....	35
Figure 3.1 Amide synthesis .....	38
Figure 3.2 Amide bond formation from carboxylic acid and amine .....	41

Figure 3.3 a) Amide bond formation using acid chloride method; b) commonly used carbodiimides; c) amide bond formation using DCC.....	43
Figure 3.4 Acid chloride racemization through a) ketene formation, b) direct enolization, and c) oxazolone formation.....	44
Figure 3.5 A graphical presentation of the electrostatic potential difference on nitrogen in amines 3.30 and 3.32 (Generated using Spartan software) .....	46
Figure 3.6 Generation of amine anions from TMS-amines .....	47
Figure 3.7 Reaction of acid fluoride and chloride with water.....	48
Figure 3.8 Hydration of ketones.....	48
Figure 3.9 Biosynthesis of primary fatty acid amide from Acyl-CoA and glycine .....	58
Figure 3.10 Synthesis of DHAs using thioesters and N-silylated (hetero)aryl amines.....	59
Figure 3.11 Both TBAF and methoxide anion catalyze the formation of amine anion 3.36 .....	60
Figure 4.1 A subset of SR proteins facilitate the export of fully spliced mRNAs from nucleus into cytoplasm. Adapted with permission from literature <sup>89</sup> .....	91
Figure 4.2 Compound 5350150 inhibits HIV replication by altering rev function. Adapted with permission from literature <sup>26</sup> .....	92
Figure 4.3 HIV rev protein mediates movement of US and SS mRNAs from nucleus into cytoplasm. Adapted with permission from literature <sup>90</sup> .....	93
Figure 4.4 Few examples of biologically active molecules bearing stilbene or thiophene moiety. ....	95
Figure 4.5 The anti-HIV activity and viability of 5350150 .....	95
Figure 4.6 Structure of compound 5350150 and our plans for the synthesis and SAR studies of amide analogue of 5350150. ....	97

Figure 4.7 Activity-viability curves for 5350150, 4.6kk (Gps389), 4.6qq (GPS428) and 4.6ww (GPS484).....	102
Figure 4.8 Structure of 17 amide analogues of 5350150 with weak to strong anti-HIV activity	103
Figure 4.9 EC50 curve for 4.29ww (GPS498) and 4.25ww (GPS491) .....	108
Figure 4.10 Activity versus viability for 4.25kk (GPS488) and 5350150 .....	109
Figure 4.11 Activity versus viability for 4.25ww (GPS 491) and 5350150.....	109
Figure 4.12 EC50 curves for 4.25qq (GPS488) and 4.25ww (GPS491) against wild type (WT) and major strains resistant against the four drug classes used in ART: (non)-nucleoside reverse transcriptase inhibitor (N)NRTI, protease inhibitor (PI), integrase inhibitor (INI), and coreceptor inhibitor (CRI).....	113
Figure 4.13 Structure of ABX464 and its 3 points of contacts with 4.25kk (GPS488) .....	114
Figure 4.14 EC50 curve for 4.31 (GPS519), 4.25ww (GPS491), 4.25qq (GPS506), and 4.25kk (GPS488).....	116
Figure 5.1 Future SAR studies for 4.25kk (GPS488) and 4.25ww (GPS491).....	169

## List of Reaction Schemes

Reaction Scheme 3.1 Reagent and conditions: i) 2-bromoethyl methyl ether, CsCO <sub>3</sub> , DMF, 100 °C, 1 h; ii) LiOH, THF/H <sub>2</sub> O (2/1), 4h, r.t.; iii) TFFH, CsF, MeCN, 5 h, r.t.; iv) MeCN, TBAF (cat), 50 °C, 12 h. ....	51
Reaction Scheme 3.2 Reagent and conditions: i) HCl, MeOH; ii) MeI, MeCN, microwave at 120 °C, 1h.....	61
Reaction Scheme 4.1 Reagent and conditions: i) K <sub>2</sub> Cr <sub>2</sub> O <sub>7</sub> , 5N H <sub>2</sub> SO <sub>4</sub> , 100 °C, 2 h; ii) TFFH, CsF, MeCN, r.t., 12 h; iii) TMSCN (neat), 70 °C, reaction time ranges from 7 min to 12 h; iv) MeCN, TBAF (cat), 50 °C, 12 h. ....	99
Reaction Scheme 4.2 Reagent and conditions: i) SOCl <sub>2</sub> , MeOH, 65 °C, 12 h; ii) LiOH, THF/H <sub>2</sub> O (2-1), r.t., 25 min; iii) TFFH, CsF, MeCN, r.t., 22 h; iv) MeCN, TBAF (cat), 50 °C, 48 h; v) LiOH, THF/H <sub>2</sub> O (2-1), r.t., 12 h. ....	106
Reaction Scheme 4.3 Reagent and conditions: i) TFFH, CsF, MeCN, r.t., 12 h; ii) MeCN, 50 °C, 12-48 h.....	107
Reaction Scheme 4.4 Reagents and conditions: i) LiOH, THF/H <sub>2</sub> O (5-3), r.t., 2.5 h; ii) TFFH, CsF, MeCN, r.t., 12 h; iii) MeCN, 50 °C, 12 h. ....	107
Reaction Scheme 4.5 Reagents and conditions: i) LiOH, THF/H <sub>2</sub> O (5-3), r.t., 35 min; ii) TFFH, CsF, MeCN, r.t., 24 h; iii) MeCN, 50 °C, 48 h. ....	108
Reaction Scheme 4.6 Reagents and conditions: i) SnCl <sub>2</sub> , SnCl <sub>4</sub> , HCl, r.t., 4 h; ii) NaNO <sub>2</sub> , HCl, NaN <sub>3</sub> , H <sub>2</sub> O, 0 °C, 2 h, r.t., 1 h .....	116



## List of Abbreviations

ADME properties	Absorption, distribution, metabolism, and excretion properties
AIDS	Acquired immunodeficiency syndrome
ART	Antiretroviral therapy
BPT	Branch point
CB receptors	Cannabinoid receptors
CDCl <sub>3</sub>	Deuterated chloroform
CHO	Aldehyde
CRI	Coreceptor inhibitor
DAST	Diethylaminosulfur trifluoride
DCC	N,N'-Dicyclohexylcarbodiimide
Deoxo-Fluor	Bis(2-methoxyethyl)aminosulfur Trifluoride
DHA	Di(hetero)arylamide
DIC	N,N'-Diisopropylcarbodiimide
DMAP	N,N-Dimethylaminopyridine
DMF	Dimethylformamide
DMSO	Dimethyl sulfoxide
EC <sub>50</sub>	Half maximal effective concentration
EDC	1-Ethyl-3-(3-dimethylaminopropyl) carbodiimide
ESE	Exonic splicing enhancer

ESS	Exonic splicing suppressor
FSC	Forward scattering
HIV	Human immunodeficiency virus
hnRNPs	Heterogeneous nuclear RNPs
HOBT	Hydroxybenzotriazole
HTS	High-throughput screening
INI	Integrase inhibitor
ISE	Intronic splicing enhancer
ISS	Intronic splicing suppressor
mRNA	Messenger RNA
(N)NRTI	(Non)-nucleoside reverse transcriptase inhibitor
N-TMS amine	N-silylated amines
NES	Nuclear export signal
OAc	Acetoxy group
PBMCs	Human peripheral blood mononuclear cells
PI	Protease inhibitor
PPT	Polypyrimidine tract
RRE	Rev-response element
RT	Reverse transcriptase
SAR	Structure activity relationship
SI	Selective index
SN2	Nucleophilic substitution
SNAr reaction	Nucleophilic aromatic substitution reaction

snRNP	Nuclear ribonucleoproteins
SR protein	Serine-arginine protein
SRPK	SR protein kinases
SRSF1	Serine/arginine-rich splicing factor 1
SS	Splicing sites
SS	Singly spliced
Tat	Trans-activator of transcription
TBAF	Tetra- <i>n</i> -butylammonium fluoride
TFFH	Fluoro-N,N,N',N'-tetramethylformamidinium Hexafluorophosphate
THF	Tetrahydrofuran
TMS group	Trimethylsilyl group
TMSCN	Trimethylsilylcyanide
topo I	Topoisomerase I
US	Un-spliced

## Acknowledgements

Foremost, I would like to express my sincere gratitude to my supervisor, Professor David Grierson, for his guidance, patience and encouragement. Thank you for always believing in my strength. It was a great honor to work under supervision of a great mentor who is truly passionate about science.

I would also like to thank my supervisory PhD committee, Dr. Adam Frankel, Dr. Urs Häfeli, Dr. Glenn Sammis, and Dr. Kathleen MacLeod for their guidance and support throughout the years of my research.

Aside from my advisors, I would also like to thank our collaborators, Dr. Peter Cheung, Dr. Benoit Chabot, and Dr. Alan Cochrane for performing all the biological experiments of my synthesized molecules.

I would also like to thank all my lab mates, past and present, for their friendships and insightful discussions. Every single one of you were excellent friends and colleagues in this journey.

Last but not least, my deepest gratitude goes to my family for their unflagging love and support. Thank you for always believing in me.

*To my parents*

## Chapter 1: Introduction

“Medicinal chemistry covers all aspects of the conception, design and synthesis of biologically active compounds with the objective of developing such molecules as therapeutic agents for the treatment of disease, physical injury and other conditions that impair normal human activity. In practice, medicinal chemistry relates the structure of a molecule to its potential to be a drug. This is a highly interdisciplinary activity that combines expertise in synthetic and physical chemistry with biochemistry, pharmacology-toxicology, structural and molecular biology, computational sciences, formulation and delivery technologies, and pharmacognosy. It is not surprising, therefore, that medicinal chemistry plays a major role in essentially all phases of “drug discovery” leading up to the identification of clinical candidate drugs.”<sup>1, 2</sup>

My work in this field has involved the use of small molecule compound libraries, obtained by parallel synthesis, as a research tool to identify active “hit” molecules, which block HIV replication through a novel and, up till recently, unexplored mechanism of action. The molecules identified using this strategy are amongst the first representatives of a new class of anti-HIV agents designed to impact the processing of HIV mRNAs that code for key regulatory proteins essential for HIV replication or their transport. The parallel synthesis approach was chosen for my work, as at the outset of this project, and even today, we do not know the structure or the precise mechanism of action of the serine-arginine (SR) protein splicing factors whose function is being targeted. Indeed, in the absence of any structural data, the “rational drug design” approach to finding active compounds impacting mRNA processing is essentially impossible. Consequently, compound library synthesis-screening represented the only means

available to discover active molecules. As a preamble to the description of my research objectives and results, several of the key concepts and tools important to medicinal chemistry driven drug discovery will be introduced in this chapter.

## **1.1 Impact of structural biology in drug discovery**

In modern drug discovery where high-throughput screening (HTS) and rapid library synthesis techniques are available, structural biology plays an increasingly important role in finding hit/lead compounds. Indeed, when the structural details of the therapeutic targets are known, virtual screening can be used in a rational manner to identify molecules with a high probability of displaying the desired biological activity. In this strategy, computer modeling is used to dock different structures into the target protein binding site and their quality of fit is calculated and ranked.<sup>3-5</sup> Those with the highest ranks will be then synthesized and screened in the relevant assays. This process is cost effective and time efficient, as only selected molecules rather than large diversity-driven libraries are synthesized and screened.

In a less optimum setting, when the 3D structure is not available, but the amino acid sequence of the binding site is known, homology modeling can be used to generate a predicted structure of the protein and its binding/receptor site for virtual screening.<sup>6</sup> This approach is based on the fact that evolutionary related proteins have very similar active site structures.<sup>7</sup>

As alluded to above, my work, involved a more complex scenario. In fact, although their amino acid sequences are known, obtaining structural information on SR proteins is impaired by the

fact that they are inherently disordered and poly-phosphorylated.<sup>8</sup> Conformational mobility and post-translational phosphorylation are requirements for them to carry out the multiple tasks they are implicated in mRNA processing.

## **1.2 Sources of compound libraries**

### **1.2.1 Natural product libraries**

Natural products have been at the heart of drug development for many years, as they have diverse structures and considerable therapeutic potential. For example, digitoxin and digoxin (from foxglove leaves) are used to treat heart conditions; quinine (from cinchona bark) has been used to treat malaria; nicotine (from tobacco leaves) has both stimulant and sedative properties; paclitaxel<sup>9</sup> (from yew tree) is an anticancer drug; and morphine (from opium poppy) acts as an analgesic.<sup>10, 11</sup> The structures of these molecules are shown in Figure 1.1.

The synthesis and screening of natural products and analogues has also been successfully used to identify new biological active molecules. Natural product analogues and analogue libraries are usually made by changing substituents, altering the flexibility/rigidity of the structure, and simplifying their structure. For example, as shown in Figure 1.1, the anticancer drugs docetaxcel **1.6** and paclitaxel **1.5** differ in only two substituents (Phenyl for t-butyl and OAc for OH). Similarly, “peripheral” modification of the structure of morphine **1.7** led to the discovery of opioid agonists hydromorphone **1.8** and oxycodone **1.9**, and the opioid antagonist drugs, naloxone **1.10** and nalorphine **1.11**. This search also resulted in the discovery of a recreational



drug, heroin **1.12**, which is also a therapeutic drug but with high abuse/misuse potential.<sup>12</sup>

Interesting also is the comparison of the structure of anandamide **1.13** (an endogenous cannabinoid) to that of the more rigidified molecule tetrahydrocannabinol **1.14**, the psychoactive ingredient in marijuana/cannabis. Both molecules bind strongly to Cannabinoid (CB) receptors.<sup>13</sup>

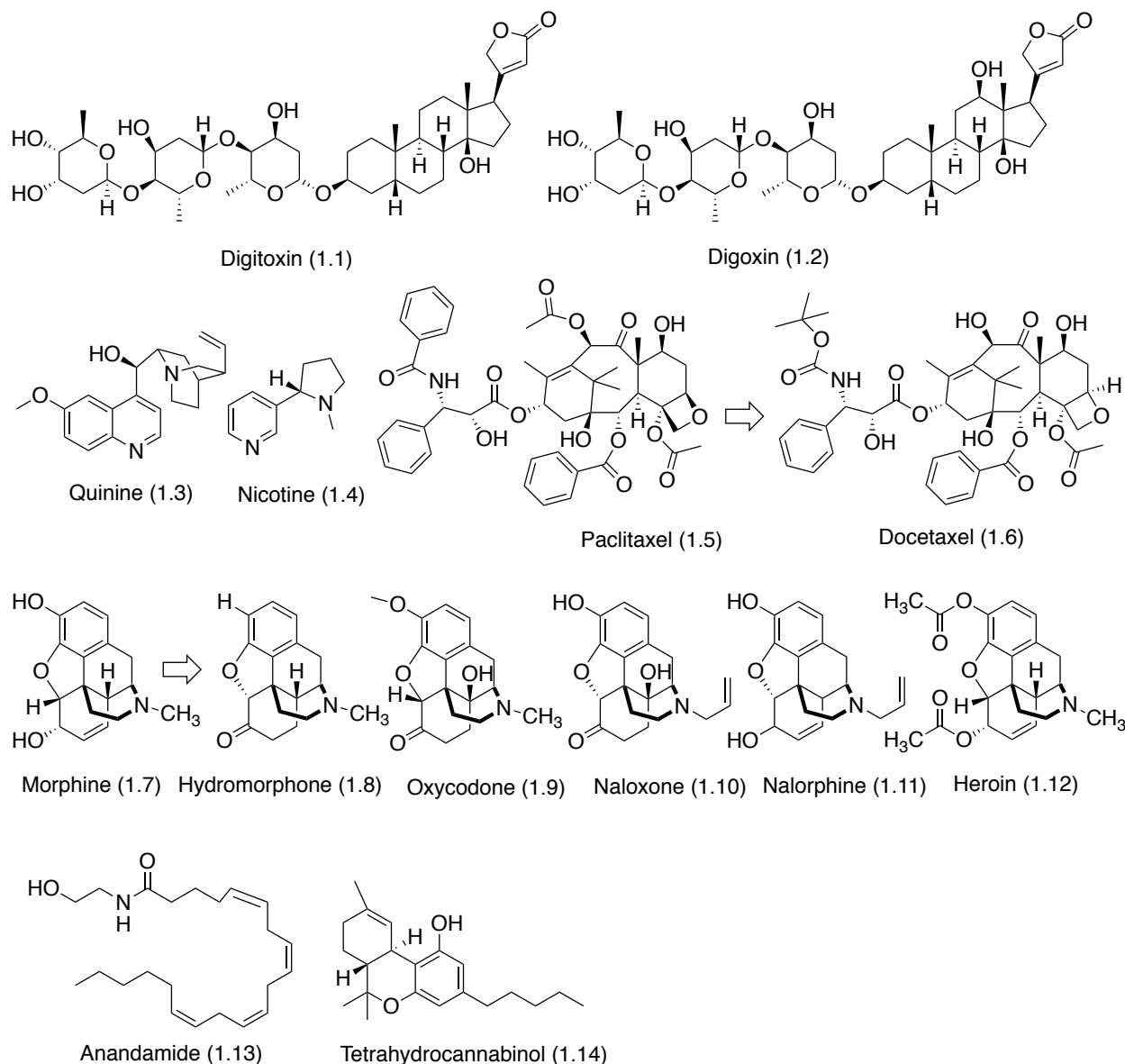


**Figure 1.1** Examples of natural products and their analogues with biological activity

In my work, described in Chapter 2, note that **IDC16** is a natural product analogue of the tetracyclic pyridoctarbazole alkaloid ellipticine **1.15**, and compound **1C8** is a flexible mimic of **IDC16** (Figure 1.2a). Both **IDC16** and **1C8** have anti-HIV activities so this is a clear example of how screening of natural products and their analogues help us to discover new biologically active molecules.

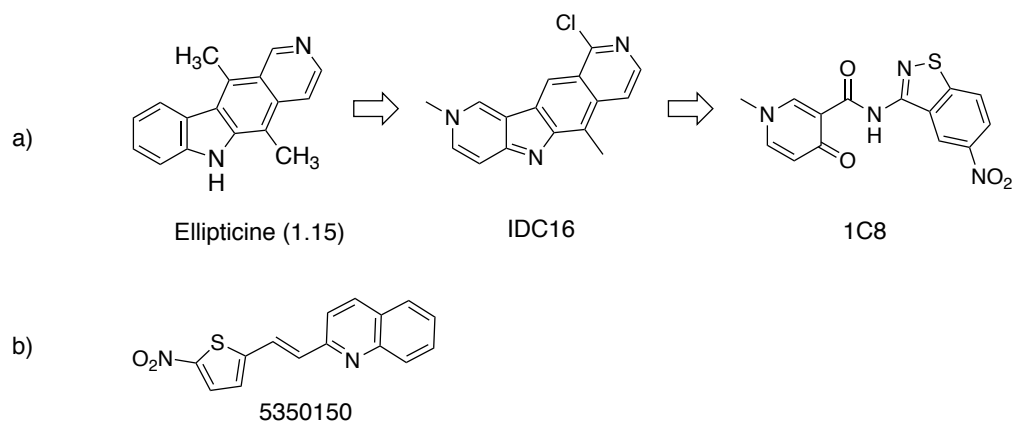


**Figure 1.2 a) Structure of ellipticine, IDC16, and 1C8: ellipticine is a natural product; IDC16 is an analogue of ellipticine; 1C8 is a flexible mimic of IDC16; b) structure of 5350150**

### 1.2.2 Industrial (pharmaceutical company) libraries

Pharmaceutical company libraries are “in house compound libraries” containing compounds collected over many years of research on projects directed to different therapeutic applications. These libraries generally correspond to large number of molecules because for each project the process of going from hit to lead can necessitate the synthesis and screening of up to thousands of molecules. These compound collections are routinely screened for new therapeutic targets in

order to find new hits in new areas. The drawback to pharmaceutical company libraries can be that structural diversity could be limited.

### 1.2.3 Commercial libraries

Commercial libraries contain collections of molecules from different origins. Apart from specialized libraries containing known drugs, the molecules found in commercial libraries were, in many cases, initially prepared for non-medical applications (designing of new dyes for clothing and photography and compounds with optical-electronic properties). Often, such molecules are heterocyclic in structure. For example, compound 5350150 (Figure 1.2b - discussed in Chapter 4) is a thiophenyl-stilbene type compound, available in a commercial library, was found to possess anti-HIV activity.

### 1.2.4 Academic libraries

In academic laboratories, diversity driven parallel synthesis has been exploited to build libraries of both simple and highly complex compounds. Unlike industrial libraries, academic libraries have often been designed to contain molecules with a wide range of different structures. For example, Schreiber et al. used parallel library synthesis to form 29400 polycyclic compounds on solid support.<sup>14</sup> In their study, 41 resin loaded trienes underwent two sequential Diels-Alder reactions with 63 di-, tri-, or tetra-substituted dienophiles to form complex polycyclic compounds. As an example, compound **1.18** and **1.21** (Figure 1.3a) were synthesized from reacting trienes **1.16** with 2 equivalents of dienophiles.

Screening these 29400 molecules in different protein-binding and phenotypic assays revealed that some of these molecules have specific and potent activities. For example, calmoduphilin **1.22** is a calmodulin inhibitor (Figure 1.3b).<sup>15</sup>

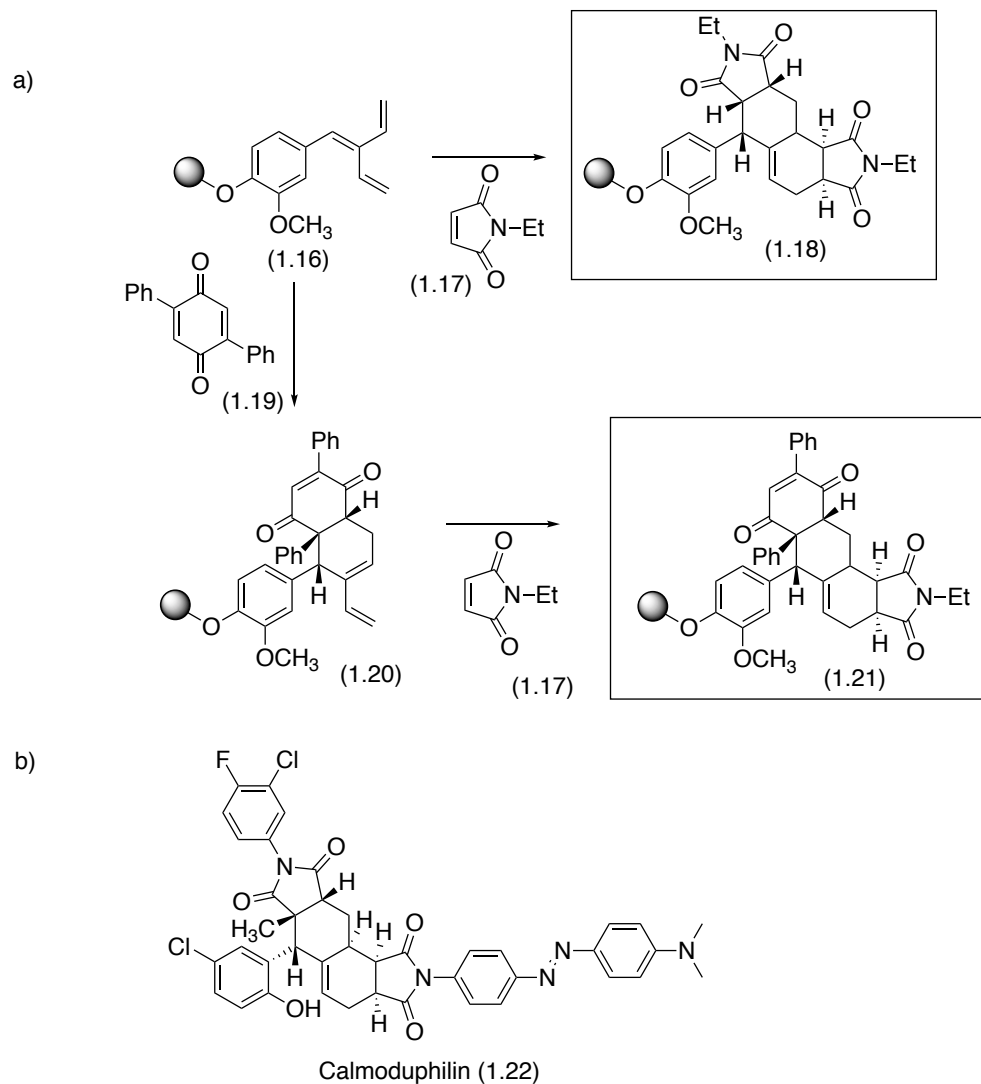


**Figure 1.3 a) Solid support synthesis of 1.18 and 1.21 from reacting trienes 1.16 with 2 equivalents of dienophiles b) the structure of calmoduphilin**

### 1.3 Synthesis of compound libraries: combinatorial approach and parallel library synthesis

The rapid production of compound libraries is possible through the combinatorial chemistry approach in which cocktails of molecules are made simultaneously by applying one or a set of synthetic reactions to different collections of building blocks to connect them in many possible ways.<sup>16</sup> Without isolating each molecule, the resulting mixture of products goes through the screening process. For example, reaction of a set of amines with a set of carboxylic acid in the presence of a peptide coupling reagent gives a mixture of different amides. Once a mixture with biological activities is found, the task of deconvoluting the mixture, i.e., isolating/identifying the active molecule(s), can be difficult. As a consequence, parallel synthesis strategies were developed and optimized. In this technique, robust reactions and conditions are applied to link different building blocks. Here, all combinations are done simultaneously but in separate reaction vessels.<sup>16</sup> Identification of products is made simpler, as each reaction vessel contains, in principle, a predetermined product. The design of robust reactions and conditions applicable to parallel synthesis has its challenges, as several important criteria must be met: the reaction conditions must work for a variety of different substrates, they must involve a minimum number or no purification steps, and they must be cost effective, safe, and easy to execute. Construction of the amide bond is in many situations a robust reaction and many different reagents have been developed for this purpose.<sup>17</sup> However, as described in Chapter 3, it was necessary for our work to design a new set of conditions for this reaction, which could be applied to the coupling of carboxylic acids heterocyclic amines to obtain novel di(hetero)arylamide (DHA)-type compounds.

## **1.4 Hit optimization**

Once hits with acceptable biological activity, chemical stability, and synthetic accessibility are identified, their chemical structures almost invariably need to be modified to further improve their drug-like properties. This entails structure activity relationship (SAR) studies, which both help to understand which parts of the active molecule are important for interaction with biological target and which types of structural modifications (addition of polar/hydrophilic or non-polar/hydrophobic motifs, bioisostere replacement, etc.) will reinforce these interactions (increase potency).<sup>18</sup> The objective of SAR studies is to also obtain compounds with minimum/no toxicity and optimal ADME properties (absorption, distribution, metabolism, and excretion).<sup>16</sup> As it is described in Chapter 4, bioisostere replacement of a double bond by an amide motif was a key feature in the development of a new series of DHA-type anti-HIV agents impacting mRNA processing.

## **1.5 HIV and the application of parallel synthesis to finding a new class of anti-HIV drugs: foundation of my project**

In 2017, the World Health Organization estimated that 37 million people are living with HIV/AIDS, and approximately 2 million new HIV infection occurs and an estimated 1 million dies from AIDS.<sup>19</sup> Indeed, over time, HIV (Human Immunodeficiency Virus) infection can advance to the Acquired Immunodeficiency Syndrome (AIDS), a condition leading to progressive destruction of immune system and consequent vulnerability of the infected person to multiple pathogens and cancer.

HIV can only replicate inside a host cell as it cannot survive long outside the body. Once in the bloodstream, HIV attaches itself into CD4<sup>+</sup> T cells and interacts with CD4 receptors (CCR5 or CXCR4). This results in the fusion of viral and CD4<sup>+</sup> T cell membranes so the viral particles enter the host cell. Once inside, the HIV capsid disintegrates releasing its content: viral RNA, reverse transcriptase, integrase, and protease. In cytoplasm, HIV reverse transcriptase produces viral DNA from its RNA. Then, viral integrase translocates this DNA to CD4<sup>+</sup> T cells nucleus where it can be integrated to the host cell DNA and the cellular machinery does the transcription of the integrated DNA to produce viral genomic RNA (unspliced mRNA). After post-transcriptional modifications, mature mRNA goes to cytoplasm, where translation and production of viral proteins takes place. Complete genomic RNA, gag and Gag-Pol multi-proteins move to cell surface and an immature HIV buds out. Once outside, viral protease becomes active and cuts the gag-pol multi-proteins to form gag, pol, and env proteins to produce mature virus.

Current anti-HIV drugs block different stages of the HIV life cycle (Figure 1.4). These drugs prolong the advancement of HIV infection to AIDS by: i) blocking HIV entry and fusion to CD4 T cells, ii) inhibiting reverse transcription of viral RNA to DNA by the viral polymerase reverse transcriptase (RT), iii) obstructing the function of HIV integrase, and iv) inhibiting the function of the HIV protease.

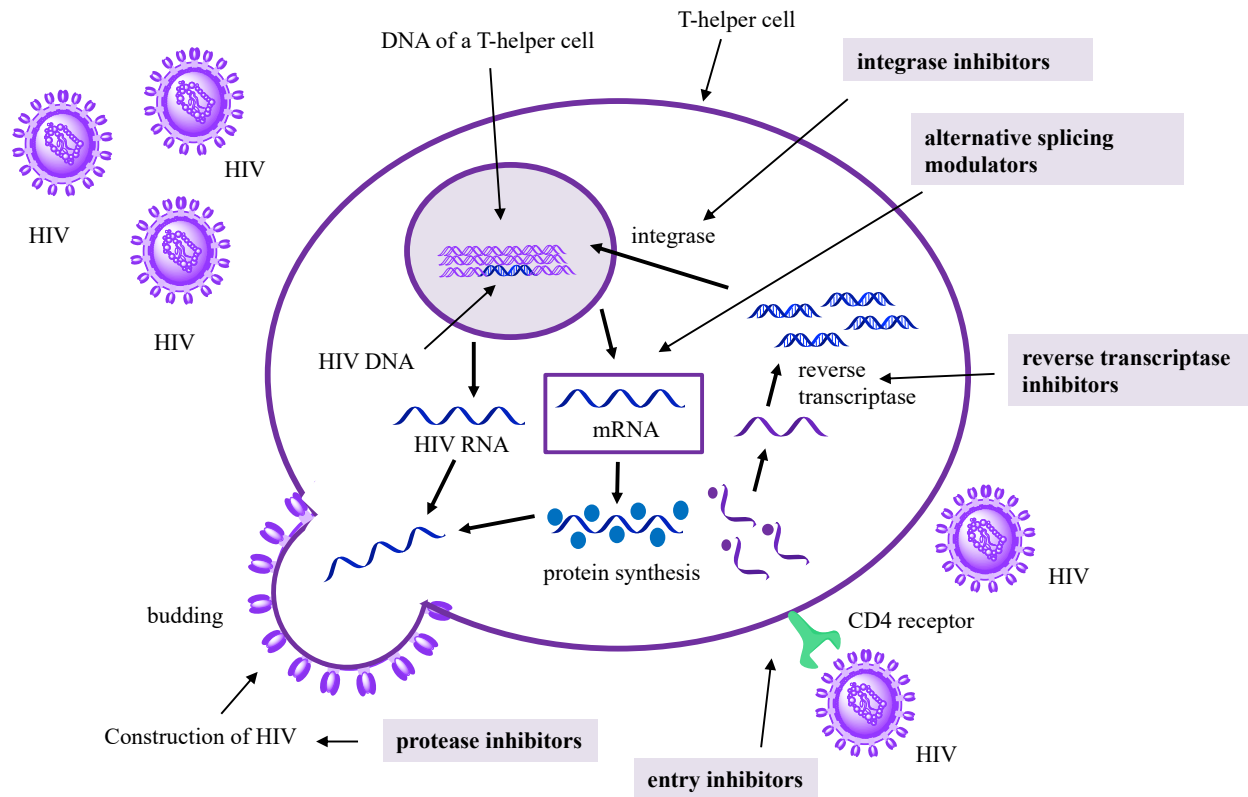


**Figure 1.4 HIV life cycle highlighting the targets of current anti-HIV drugs**

Only 35 years ago, the life expectancy for HIV patients was 1-2 years. Fortunately, with the advent of antiretroviral therapy (ART), where different combinations of drugs targeting these HIV life cycle processes are taken, the morbidity rate has dropped very significantly. In fact, in developed countries, HIV infection is classified as a chronic disease rather than life threatening illness. In light of this success, major steps are now being taken to bring ART to the developing world where the majority of HIV infected people reside. However, ART fails to eradicate the latent virus pool from infected cells, and this necessitates strict adherence to lifetime treatment schedules. Prolonged ART therapy also leads to issues of toxicity/side effects and drug resistance. These problems take on added significance as the scale and diversity of the



populations receiving treatment increases. These factors underscore the continued need for new drugs, and especially those acting through novel mechanisms of action.

In contrast to the current ART drugs, my PhD project aimed at inhibiting HIV replication by targeting human (host) cell proteins involved in the synthesis of the HIV viral proteins, rather than inhibition of the viral proteins themselves. The rationale for this approach is that once inside the host cell, HIV is highly dependent on the cellular mRNA processing machinery (Figure 1.4) to make and/or transport the viral proteins: tat, vpr, rev, nef, vif, env, gag, and pol. Importantly, the exquisite reliance of HIV on this host cell machinery for replication may render it sensitive to even slight disturbances in the progression of the disease. Therefore, at low doses of only weakly (micromolar) active drugs, it may be possible to impair HIV replication, while having no or very limited effects on human splicing events.

### 1.5.1 Objective 1: IDC16 and the design of a library of IDC16 mimics

My project has its origins in a random screening of the Institut Curie-CNRS compound library, which led to the discovery of the tetracyclic indole compound **IDC16** (Figure 1.2a and Figure 1.5) as an anti-HIV agent.<sup>20, 21</sup> Note that **IDC16** is an analogue of the well-known topoisomerase I (topo I) inhibitor ellipticine **1.15** (Figure 1.5), a natural product found in trees within the genera *ochrosia*, *rauwolfia*, *aspidosperma*, and *apocynaceae*.<sup>22</sup>

In fact, the initial objective of this screen was to identify new molecules targeting topo I. This enzyme relieves the tension created by overwinding DNA ahead of a replication fork during

DNA replication and transcription process.<sup>23</sup> This is achieved by cutting the phosphodiester backbone of one DNA strand to unwind the DNA and then resealing the backbone. As this enzyme is overexpressed in cancer cells, it is a target in cancer chemotherapy research.

Inhibition of topo I leads to apoptosis and cell death.

However, pertinent to my project is the fact that, aside from effecting DNA relaxation, topo I also acts as a kinase that phosphorylates different serine residues in the SR protein, SRSF1 (also known as SF2/ASF), a key splicing factor in alternative splicing of mRNA.<sup>20, 24, 25</sup> To identify new topo I inhibitors that alter the kinase activity of topo I, 1500 molecules from Institut Curie–CNRS chemical library were screened. This resulted in the discovery of two ellipticine analogues (Figure 1.5), **1.23** and **1.24**, which target SRSF1 without altering topo I kinase activity. This result suggested that these molecules have a new mechanism of action.

Encouraged by this finding, the further screening of other ellipticine analogues in the Institut Curie–CNRS chemical library led to the discovery of **IDC16** targeting SRSF1. **IDC16** was the first small molecule to show inhibitory effect on HIV replication by blocking alternative splicing that is vital to the production of critical HIV proteins including tat, rev, and nef (collaboration – David Grierson/Claude Monneret: Institut Curie; Jamal Tazi: Universite de Montpellier II).<sup>21</sup> Although interesting, **IDC16** is inherently cytotoxic due to its ability to intercalate DNA. To suppress this unwanted activity, a library of “ring opened” conformationally mobile **IDC16** mimics was designed and evaluated for new compounds displaying the anti-HIV activity of **IDC16** without the associated cytotoxicity.

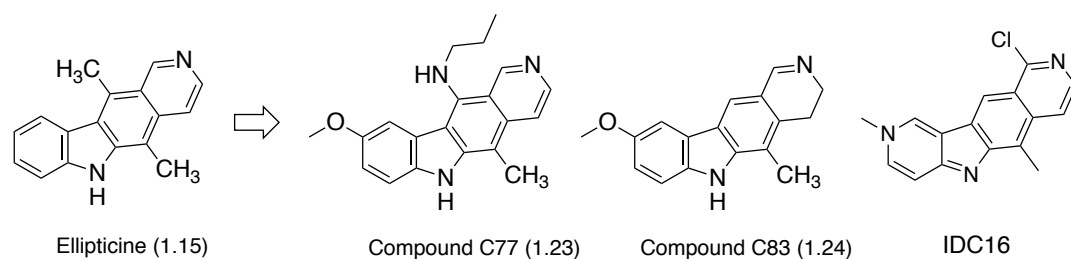


**Figure 1.5** Discovery of IDC16 and its structural relationship to ellipticine

As described in Chapters 2 and 3, the first objective of my research program was to prepare a series of conformationally flexible **IDC16** “mimics”. As shown in Figure 1.6, in these **IDC16** mimics, the **B**- and **C**-rings are replaced by an amide bond. Further for ring **A**, we have a 2-pyridinone or a 4-pyridinone motif and for ring **D**, a series of (hetero)aryl amines were used as the diversity element. These compounds were part of a larger library of 256 **IDC16** mimics that were evaluated for their anti-HIV activity (collaboration with Dr. Peter Cheung: BC Centre for Excellence in HIV/AIDS; Dr. Benoit Chabot: Universite de Sherbrooke; Dr. Alan Cochrane: University of Toronto). The parallel synthesis of our amide based DHAs was achieved by developing an amide synthesis protocol that connects two di(hetero)aryl rings through reaction of an acid fluoride or oxo-ester with N-TMS amines.

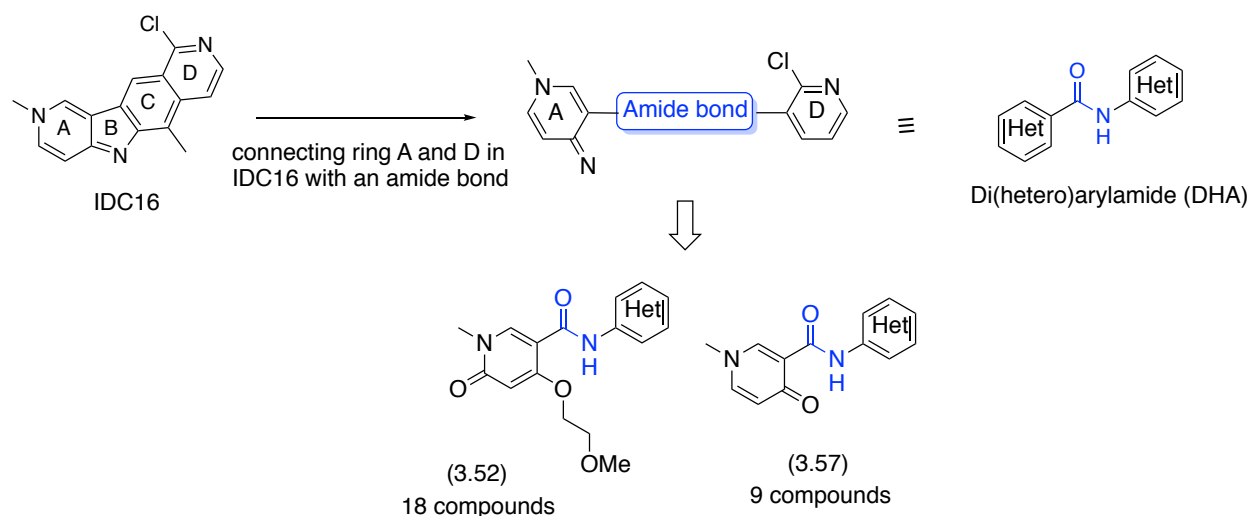


**Figure 1.6 Objective one: preparation of conformationally flexible IDC16 mimics with amide linkers**

### 1.5.2 Objective 2: Construction and evaluation of amide analogues of stilbene 5350150 - discovery of 4.25kk(GPS488) and 4.25ww(GPS491)

Our second compound of interest in this thesis is compound 5350150 (Figure 1.7) which alters HIV replication by impairing rev function.<sup>26</sup> This molecule was discovered by A. Cochrane et al. through random screening of a commercial compound library (ChemBridge Online Chemical Store: [www.hit2lead.com](http://www.hit2lead.com)). This molecule cannot be used for therapeutic purposes, as it is photolabile,<sup>27, 28</sup> toxic, and a ubiquitous hitter in many biological assays.

To conserve the anti-HIV activity but remove the toxicity problem, 50 amide analogues of 5350150 were initially synthesized. The parallel synthesis of this library was done using our acid fluoride-N-TMS amine method which was developed as part of our first objective.

Those molecules with significant anti-HIV activities were subjected to SAR studies. Here, we divided the molecule into 3 segments and each component was studied independently in order to understand which parts of the structure and which functional groups are important for anti-HIV activity. The synthesis of these molecules, their anti-HIV activities, and SAR studies is discussed in Chapter 4.

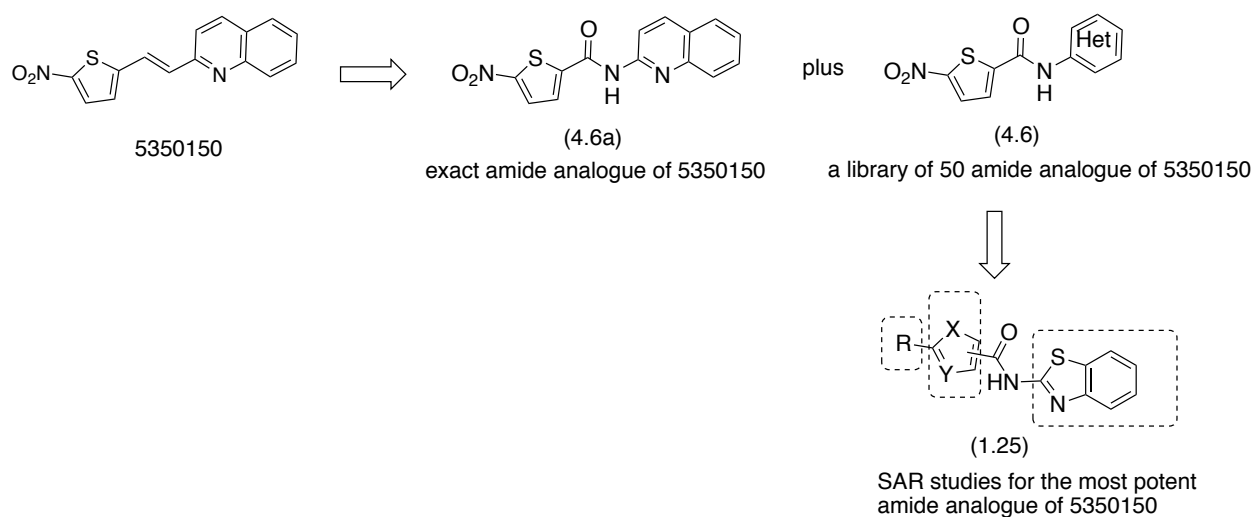


**Figure 1.7 Objective two: synthesis of amide analogues of 5350150 and their SAR studies**

## Chapter 2: Discovery of the di(hetero)arylamide type **IDC16** mimics **1C8**, **2D3**, **3C2**, **1E5**

### 2.1 Discovery of **IDC16** and the parallel synthesis/compound library approach to identify active and non-toxic **IDC16** “mimics”

Although a number of natural products and derivatives have been shown to (or are suspected to) impact alternative pre-mRNA splicing (Figure 2.1),<sup>29</sup> it was the discovery of **IDC16**, the first small molecule to show inhibitory effect on HIV replication by blocking alternative splicing, that catalyzed our effort to design a new generation of anti-HIV agents. Importantly, the evidence obtained at that time suggested that the effect of **IDC16** on SRSF1 (also known as SF2/ASF) function was independent of this enzyme, and that **IDC16** inhibits the exonic splicing enhancer activity of SRSF1.<sup>21</sup> In HIV-1 infected cells, SR proteins specifically regulate alternative splicing events that are vital to the production of critical HIV proteins including tat, rev, and nef.

**IDC16**, an analogue of the natural products ellipticine **1.15** and olivacine **2.20** (Figure 2.2a), is a cytotoxic agent that intercalates DNA. Thus, although it blocks HIV replication at concentrations lower than the threshold of its cytotoxic effect (Figure 2.4), it is not a suitable drug candidate for long term ART. To conserve its impact on HIV alternative splicing and to eliminate its affinity for DNA, a library of 256 ring opened conformationally flexible mimics of **IDC16** were synthesized and evaluated for their anti-HIV activity. A detailed description of this work is featured in our article published in the *Journal of Medicinal Chemistry* (**2016**, 1869-1879).

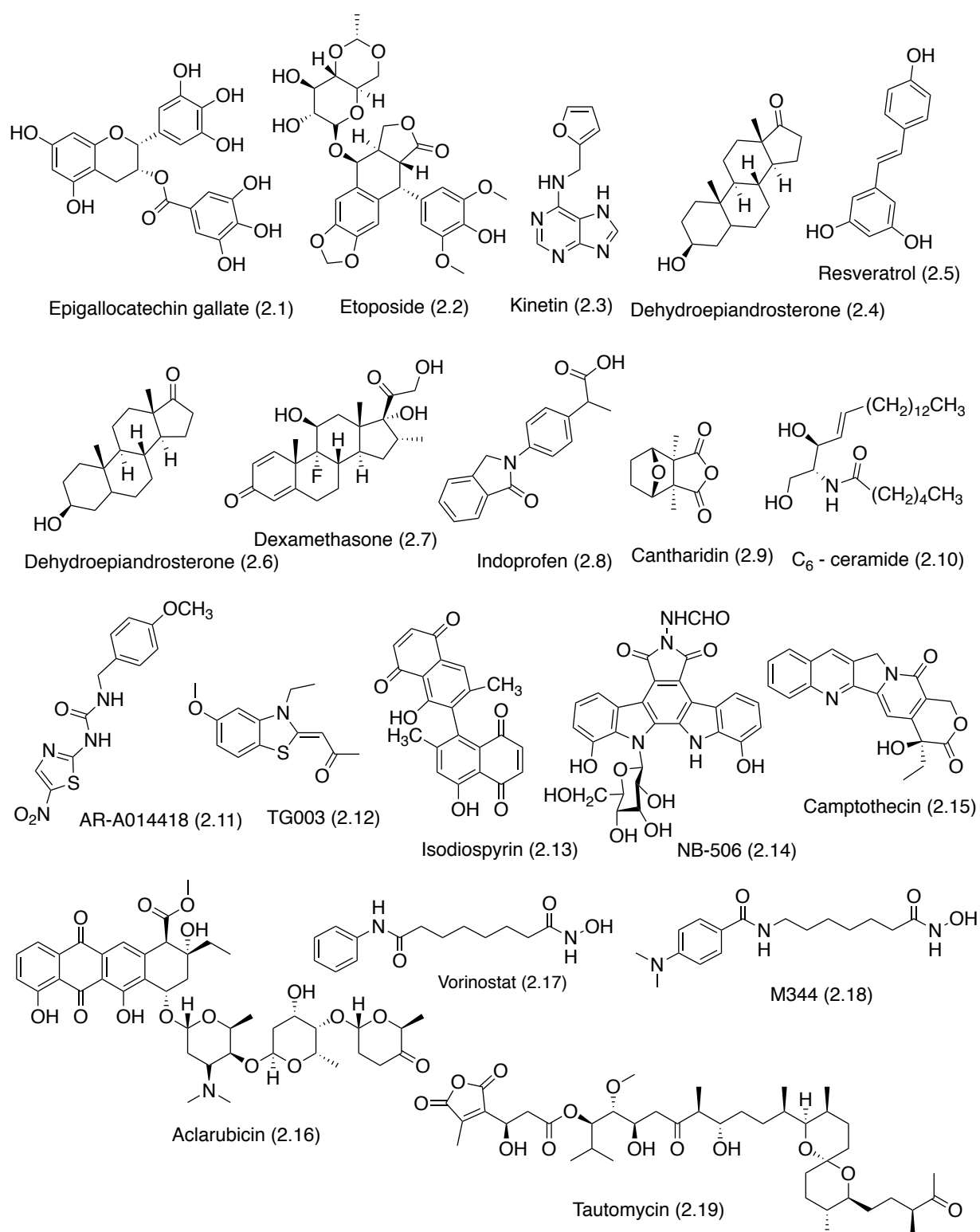


**Figure 2.1** The structure of natural products and derivatives that impact alternative pre-mRNA splicing

As illustrated in Figure 2.2b (Figure 1 in the *Journal of Medicinal Chemistry*, **2016**, 1869- 1879), relative to **IDC16**, the characteristic features of these library molecules (formula **2.21**) was the replacement of **B**- and **C**-rings by different linkers. Linkers included a 1,2,4-oxadiazole motif (i), an extended 1,2,4-oxadiazole-3-carboxamide system (ii), a simple amide function (iii), and bicyclic A/B-type ring systems (imidazopyridine (iv), pyrazolopyridine (v), and pyridoimidazolone (vi)), where the **B**- ring is part of the spacer element and the **C**-ring is eliminated. Ring-**A** and **-D** were replaced by different nitrogen heterocycle motifs. The compilation of all molecules prepared in the library is found in Figure 2.3 (Figure 2 in the *Journal of Medicinal Chemistry*, **2016**, 1869- 1879).



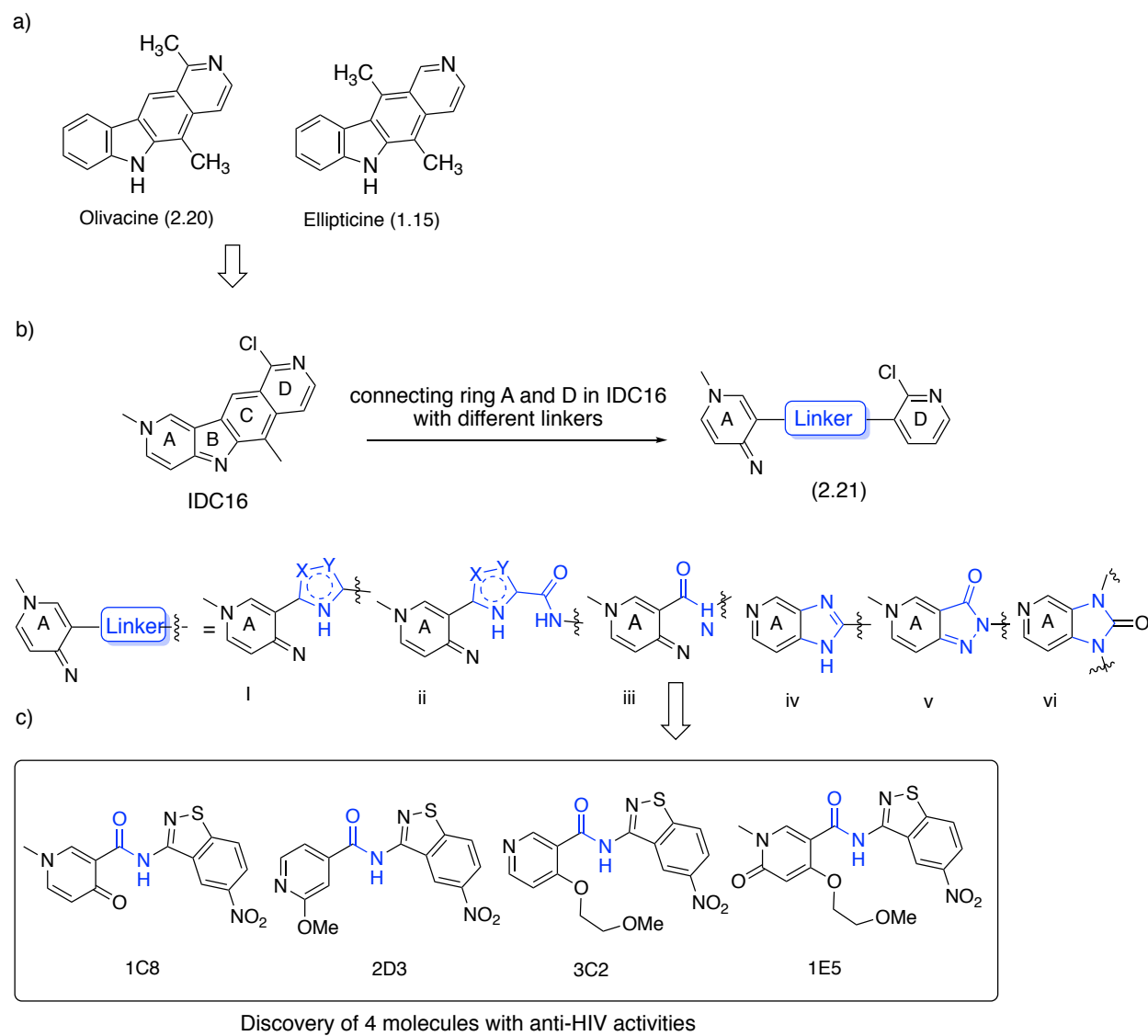


**Figure 2.2 a) Structure of olivacine and ellipticine b) IDC16 “mimics” with different linkers; c) structure of 4 DHAs with significant anti-HIV activities**



The anti-HIV screening (collaboration with Dr. Peter Cheung: BC Centre for Excellence in HIV/AIDS) identified the four active di(hetero)arylamide (DHA) molecules, **1C8**, **1E5**, **2D3**, and **3C2** (Figure 2.2c).<sup>30</sup> In addition to the central amide linker, a common feature in these molecules was the presence of a 1,2-benzisothiazole motif as the “right side” component.

Assessment of dose-response relations of these 4 active molecules indicated that compound **1E5** and **3C2** did not respond to the increasing doses due to their poor solubility in DMSO-H<sub>2</sub>O mixture.<sup>30</sup> Both compound **1C8** and **2D3** displayed good response but as the antiviral potency of **1C8** was approximately 3-fold higher than that of **2D3**, compound **1C8** was selected for further antiviral activity testing.

Compound **1C8** inhibits replication of wild type HIV-1 subtype A and B in T cell-based CEM-GXR reporter cell line.<sup>30</sup> Similarly, it blocks HIV-1 replication in human peripheral blood mononuclear cells (PBMCs) in HeLa rtTA-HIV-ΔMIs (HeLa-HIV) that uses Tet-ON system to activate the HIV-1 expression.

This molecule remains potent in HIV-1 strains that are resistant to each of the current HIV drugs: entry inhibitor based drug (maraviroc), integrase inhibitor drug (raltegravir, eltegravir, and dolutegravir), protease inhibitor drugs (atazabavir and lopinavir) and (non)-nucleoside reverse transcriptase inhibitor drugs (efavirenz, raltegravir, lamivudine, abacavir, zidovudine, and emtricitabine).<sup>30</sup> This suggests that the mechanism of action for **1C8** is different from that for the current HIV drugs.

In comparison to **IDC16**, **1C8** has a similar antiviral activity ( $EC_{50} = 0.959 \pm 0.026$  and  $0.902 \pm 0.113$  for **IDC16** and **1C8** respectively).<sup>30</sup> However, they differ greatly in their cell viability profile. Going from 1  $\mu$ M to 16  $\mu$ M, the cell viability for **IDC16** drops drastically (89.6% at 1  $\mu$ M; 33.2% at 4  $\mu$ M; 19.9% at 8  $\mu$ M; 11.9% at 16  $\mu$ M) while **1C8** has a steady decline (85.5% at 1  $\mu$ M; 81.5% at 4  $\mu$ M; 80.9% at 8  $\mu$ M; 78.7% at 16  $\mu$ M).

In all cases, the Selective Index (SI) for **1C8** is in the range of >66-100.<sup>30</sup> Such a high SI range is an indication of having significant antiviral property with minimum cell toxicity.

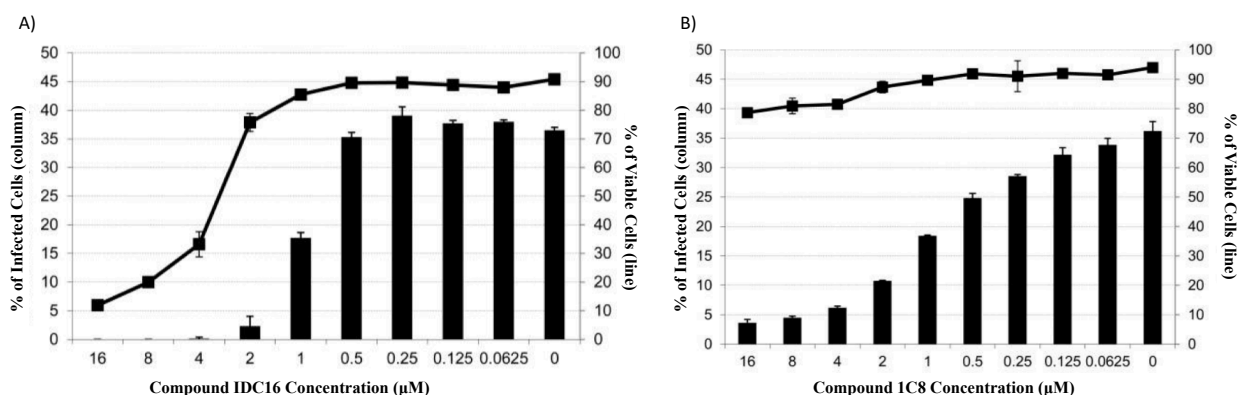


**Figure 2.4** Evaluation of anti-HIV-1 activity (column) and GXR-CEM cell viability (line) for IDC16 (A) and 1C8 (B) at concentrations between 62.5 nM and 16  $\mu$ M (0 provides the value when no compound was added). HIV-1 infection in CEM-GXR cells was assessed by measuring GFP positive cells 3 days after infection. CEM-GXR cell viability was measured after 24 h incubation within the same range of concentrations. Results were expressed from three independent experiments for both the anti-HIV-1 activity and cell viability assays. Reprinted with permission from "A Parallel Synthesis Approach to the Identification of Novel Diheteroarylamide-Based Compounds Blocking HIV Replication: Potential Inhibitors of HIV-1 Pre-mRNA Alternative Splicing." *Journal of Medicinal Chemistry* 59(5): 1869-1879. Copyright (2016) American Chemical Society

Specifically, my contribution to the synthesis of the 256 molecules found in the **IDC16** mimic library was focused on the preparation of a series 27 DHAs possessing a 2-pyridinone or a 4-pyridinone motif as the “left side” scaffold, which are shown in Figure 2.5 and Figure 2.6. The synthesis of these molecules was achieved using the newly developed acyl fluoride-N-trimethylsilylamine coupling protocol discussed in detail in Chapter 3 of this thesis. This series of molecules includes the 2-pyridinone amide **1E5**, one of the four active compounds displaying anti-HIV activity, and different compounds related to the 4-pyridinone **1C8**, prepared in our lab by Dr. David Horhant. It is acknowledged that Laura Bandy, a former Master of Science student, initially synthesized compounds **1E5** (in low yield) using the acid chloride method for formation of the amide bond.

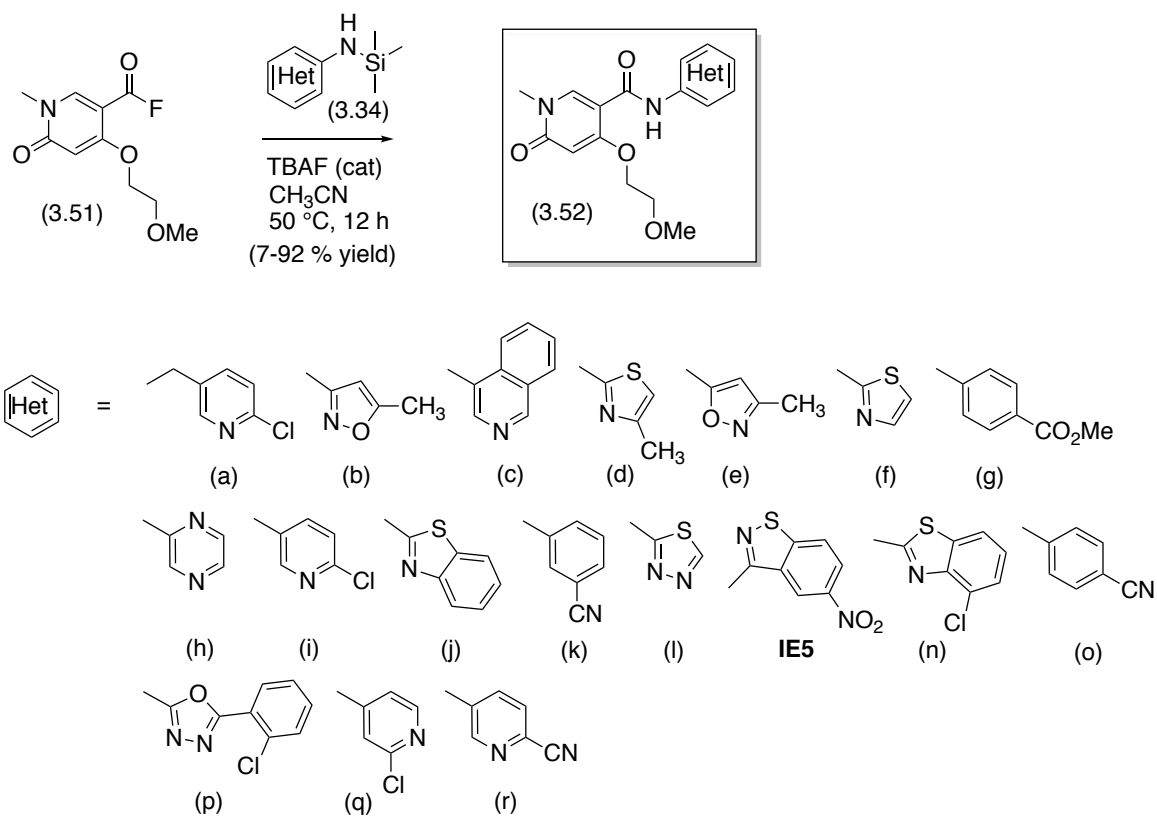


**Figure 2.5** Structure of 18 DHAs bearing 2-pyridinone motif as the “left side” scaffold. Synthesis of these molecules are discussed in Chapter 3.

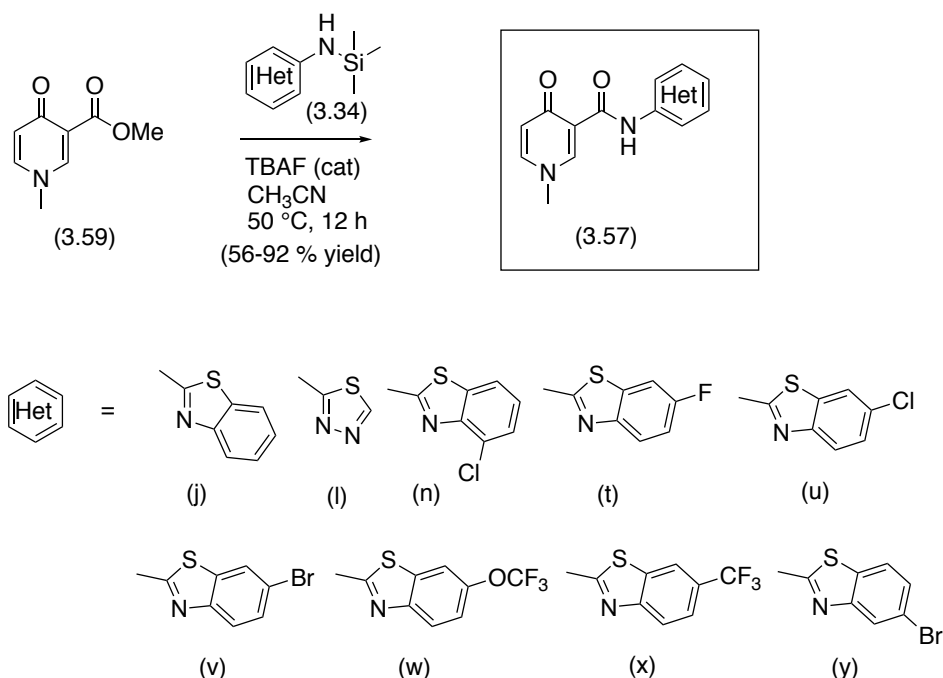


**Figure 2.6** Structure of 9 DHAs bearing 4-pyridinone motif as the “left side” scaffold. Synthesis of these molecules are discussed in Chapter 3.

## 2.2 Compound 1C8 perturbs the function of the SR protein splicing factor SRSF10

The interesting anti-HIV activity observed for **1C8** against drug resistant HIV mutant strains suggested that like **IDC16**, this molecule is targeting HIV alternative splicing and not targeting the classical HIV drug targets. Experiments carried out by Dr. Benoit Chabot (Universite de Sherbrooke) and Dr. Alan Cochrane (University of Toronto) showed that **1C8** perturbs the function of the key SR protein, SRSF10, and not SRSF1 as found for **IDC16**.<sup>26</sup> Following is a brief description of alternative splicing and its significance in HIV-1 replication (section 2.2.1-3). Also, a brief summary of the results obtained by Dr. Chabot and Dr. Cochrane will be presented (section 2.3).

### **2.2.1 Alternative splicing and the significance of alternative splicing in HIV replication**

Cellular RNA polymerase II catalyzes the transcription of the viral DNA that was produced by the viral enzyme reverse transcriptase and incorporated, through the action of the viral enzyme integrase, into the human genome. The product of this transcription process is the HIV pre-mRNA. As for all transcripts, this pre-mRNA contains non-coding introns and coding exons. These non-coding introns must be removed prior to the translation step. Removing introns and reconnecting exons in a linear fashion is called consecutive splicing and it provides a single mRNA, which codes for a unique protein (Figure 2.7). On the other hand, as shown in Figure 2.7, alternative splicing involves reconnecting the mRNA fragments produced on intron excision in different non-linear patterns. Alternative splicing of HIV pre-mRNA produces more than 40 different HIV derived mRNAs (Figure 2.10), which code for the essential viral proteins tat, vpr, rev, nef, vif, env, gag, and pol.



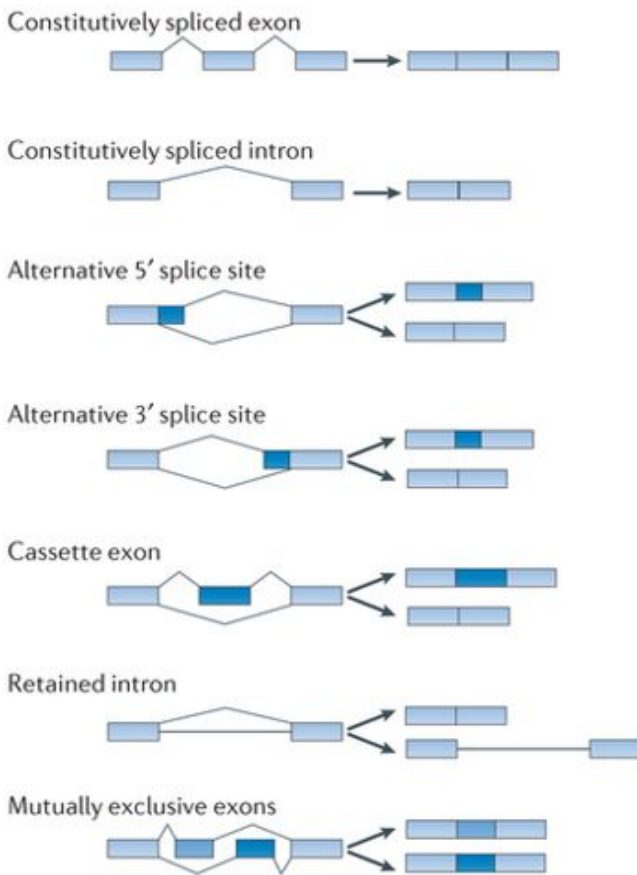


**Figure 2.7** A schematic presentation defining constitutive splicing and alternative splicing. Adapted with permission from literature<sup>31</sup>

### 2.2.2 Alternative splicing mechanism

Consecutive and alternative splicing is carried out by the spliceosome, a macromolecular complex consisting of numerous accessory proteins and 5 small nuclear ribonucleoproteins (snRNP): U1, U2, U4, U5 and U6. These components come together in different combination in different steps of splicing as it is shown in Figure 2.8. The spliceosome recognizes the splicing sites (SS) on a pre-mRNA and carries out two phosphodiesterification steps.<sup>32, 33</sup> Each SS has a

donor and an acceptor site. The donor site (D and also called 5'SS site) is located at the exon/intron junction at the 5' end of the intron and it has a GU dinucleotide in a very loosely conserved sequence. The acceptor site (A and also called 3' SS site) sits in the exon/intron junction at the 3' end of the intron and it has three conserved sequences: a branch point (BPT), a polypyrimidine tract (PPT), and an AG dinucleotide. As shown in Figure 2.8, the first component of spliceosome, U1, binds to the 5'SS while U2 auxiliary factor (U2AF65 and U2AF35) and SF1 (an SR protein) bind concurrently to the 3'SS. More specifically, SF1 binds to BPT and U2AF65 and U2AF35 bind to PPT and AG respectively to construct Complex E. Complex A forms once SF1 is replaced by U2. This is followed by U4, U5, and U6 addition to form Complex B which transforms to Complex C when U6 replaces U1 and U4 leaves. Complex C is the spliceosome's active complex which catalyze the two phosphodiesterification steps. In the first phosphodiesterification step, a 2'-hydroxyl group of an adenosine from BPT does a nucleophilic attack on a 5' end phosphate group of GU sequence at 5'SS giving two fragments: i) a detached 5' exon, ii) a 3' exon attached to a lariat form of the intron. In the second phosphodiesterification step, a 3' hydroxyl group from the detached 5' exon does a nucleophilic attack on a phosphate group at the 3'SS. This results in ligation of 5' and 3' exons and release of the intron still in its lariat configuration.

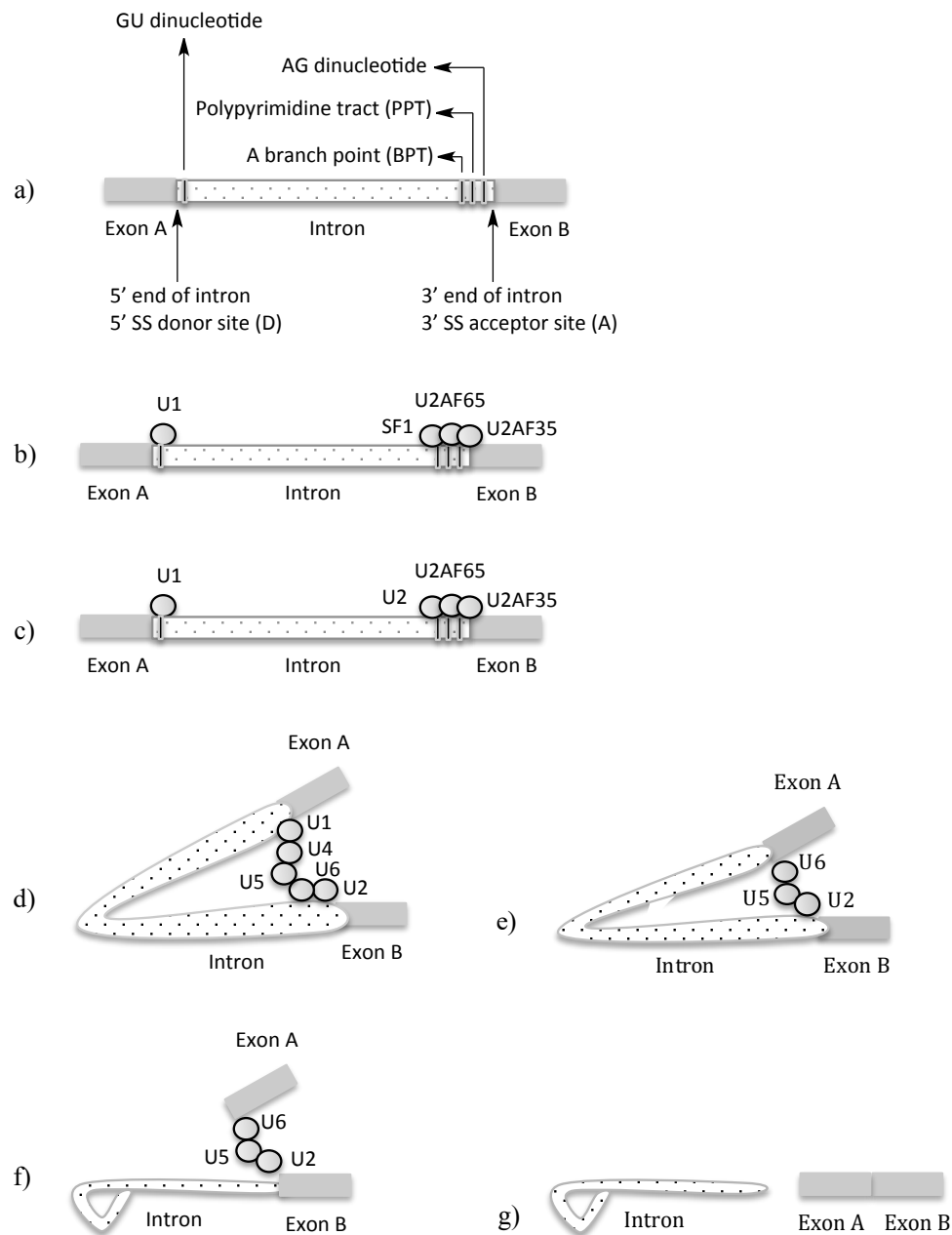


**Figure 2.8 The mechanism of alternative splicing**

Alternative splicing is regulated by cis-regulatory elements that are classified to 4 groups based on their regulatory roles and their location within the pre-mRNA sequence: exonic splicing

enhancer (ESE), intronic splicing enhancer (ISE), exonic splicing suppressor (ESS), and intronic splicing suppressor (ISS).<sup>32</sup> ESEs enhance alternative splicing by facilitating the splice site recognition. They usually bind to SR proteins which are a family of highly conserved proteins that have one or two RNA-recognition motifs in their N-terminal. In the C-terminus of SR proteins, there is a domain that is rich in arginine and serine. The serine residues are usually highly phosphorylated.<sup>33-35</sup> SR proteins use their RNA recognition motif to bind to the pre-mRNA and use their SR domains to recruit U1 to 3'SS and U2AF and U2 to 5'SS.

ESSs and ISSs bind to heterogeneous nuclear RNPs (hnRNPs) and suppress alternative splicing. HnRNPs are made of 20 proteins associated with high-molecular weight nuclear RNA.<sup>33</sup> They inhibit splice site recognition by sterically blocking the access of snRNPs or positive regulators. Splicing is regulated by combination effect of enhancers and suppressors. The position of these elements are important: enhancers are positioned so when splicing factors bind to them, the structure of local mRNA is changed so the splice site is better presented to spliceosome; silencers compete with the component of splicing machinery or change the structure of m-RNA to inhibit splice site recognition.

### **2.2.3 Alternative splicing in HIV**

As shown in Figure 2.9, HIV pre-mRNA has four 5'SS or donor sites (D1, D2, D3, D4) and eight 3'SS or acceptor sites (A1, A2, A3, A4c, A4b, A4a, A5, A7).<sup>32</sup> As shown in Figure 2.10, all the tat mRNAs are spliced at A3, all the nef m-RNAs are spliced at A5 site, and all the rev m-RNAs are spliced at A4a, A4b, or A4c sites.<sup>32</sup> As shown in Figure 2.9, all the ESSs or ISSs at

A2, A3, and A7 sites suppress splicing through interaction with hnRNP proteins.<sup>32</sup> Similarly, all the ESEs at A2, A3, A5, and A7 sites enhance splicing through their association with SR proteins. 3'SSs at A1, A2, and A3 sites are used infrequently which explains the low concentration of tat, vif, and vpr proteins while 3'SS at A4c, A4b, A4a, and A5 are used more frequently which is reflected in high concentration of rev, env, and nef proteins.<sup>36</sup>

In early phase of alternative splicing, only completely spliced mRNAs leave the nucleus and are translated into HIV regulatory proteins: tat, rev, and nef (Figure 2.11).<sup>32</sup> In late phase of alternative splicing, HIV rev protein catalyze the movement of both un-spliced and singly spliced transcripts from nucleus into cytoplasm where they can be translated into HIV structural and accessory proteins respectively. The mechanism for this m-RNA shuttling is discussed in Chapter 4.

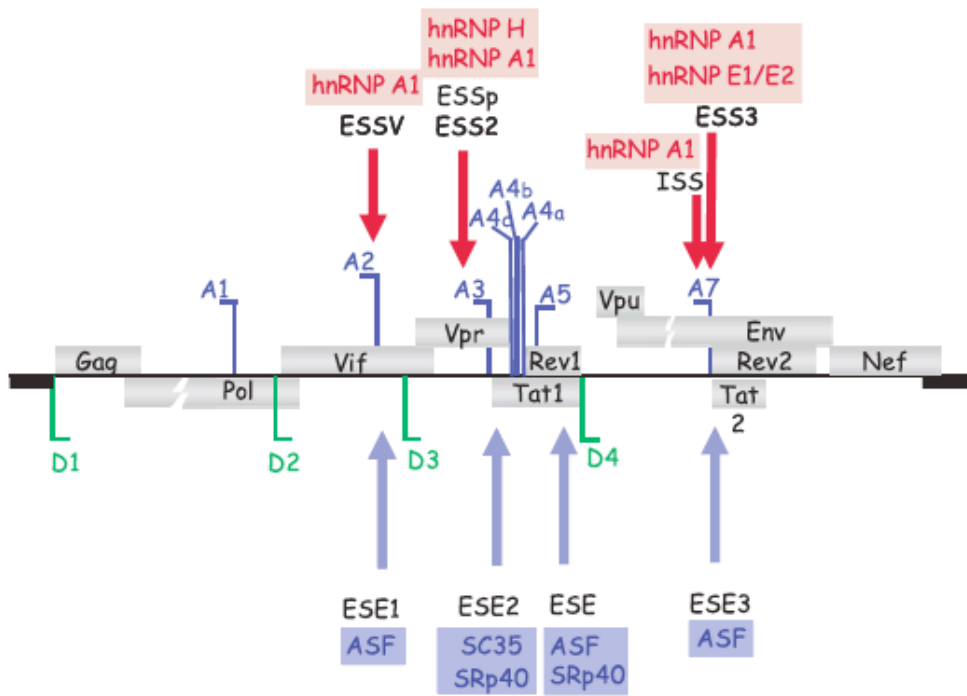


Figure 2.9 Position of different regulatory elements on HIV-1 genome. Adapted with permission from literature<sup>32</sup>

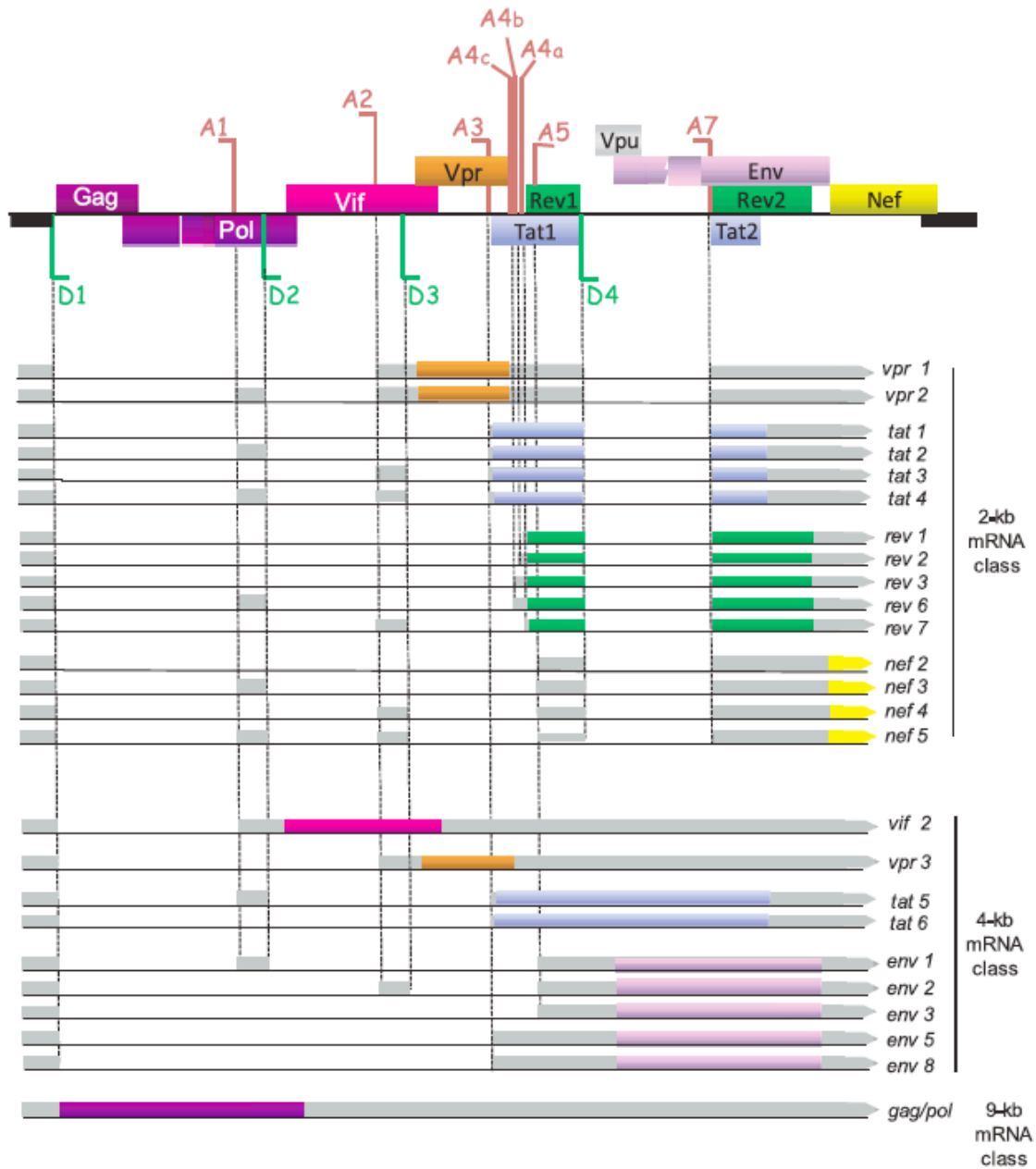


Figure 2.10 HIV-1 genome and different mRNA splicing products. Adapted with permission from literature

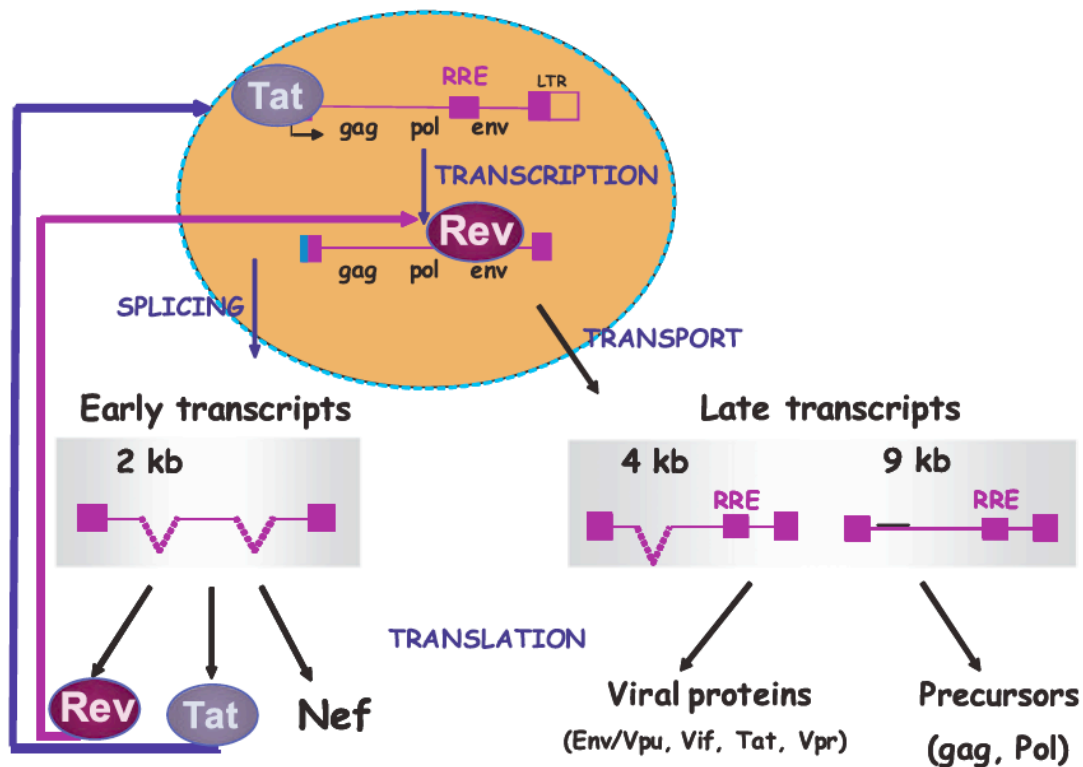


Figure 2.11. Early and late transcripts derived from the viral HIV-1 genome. Adapted with permission from literature<sup>32</sup>

### 2.3 Results for 1C8 on HIV alternative splicing: function of SRSF10 is targeted

A more detailed study about the effect of **1C8** on cellular gene expression and HIV-1 splicing was done by our collaborators, Dr. Benoit Chabot at the Universite de Sherbrooke and Dr. Alan Cochrane at the University of Toronto. Their finding was published in a Nucleic Acids Research paper.<sup>37</sup> The following is a summary of their findings for **1C8**.



For alternative splicing of cellular RNAs, 10-20  $\mu\text{M}$  **1C8** is necessary to have 13-45% alteration in cellular gene expression. Therefore, with an  $\text{EC}_{50} = 0.902 \pm 0.113$  and at low dosage, **1C8** is capable of HIV replication inhibition without any significant interference with host cell pre-mRNA splicing.

Interestingly, **1C8** has selective effect on HIV-1 splicing events as it impedes some but not all HIV-1 m-RNA production. For instance, when looking at the effect of **1C8** on formation of tat1 and nef2 m-RNA, tat1 m-RNA production drops while nef2 m-RNA remain unchanged.

Interestingly, **IDC16** and **1C8** impede HIV-1 splicing through interaction with different SR proteins: **IDC16** alters SRSF1 function while **1C8** targets SRSF10. More specifically, treatment of HeLa-HIV cells with **1C8** gives dephosphorylated form of SRSF10, which represses HIV splicing. In general, phosphorylation of serine residues in RS domain of SR proteins regulates their protein-protein interaction, RNA-protein interaction, and cellular localization. Therefore, as it was expected, dephosphorylated SRSF10 had altered interaction with HIV-1 transcripts and with splicing factors. For example, at 10-25  $\mu\text{M}$  **1C8**, the association of SRSF10 with HIV-1 transcripts drops by 3-4.5 fold. In terms of splicing factors, **1C8** disturbs the interaction of SRSF10 with hnRNP F but enhances its interaction with hTRA2 $\beta$  (a splicing regulator). Splicing factor hnRNP F binds to a specific region of RNA transcript and it can both enhance or inhibit splicing activities.<sup>8</sup> Increased interaction of SRSF10 and hTRA2 $\beta$  leads to assembly of an splicing complex which stimulate a specific splicing site (D3/A3 splicing in Figure 2.9).

There are 3 families of enzymes that catalyze SR protein phosphorylation: SR protein kinases (SRPK), Clk-Sty kinases, and DNA Topoisomerase I (topo 1/kinase).<sup>8, 38</sup> Current studies suggest that it is unlikely for **1C8** to target these kinases because such a broad impact would have a great consequence on cellular pre-mRNA splicing. More assuring, phosphorylation of other SR proteins that share common kinases with SRSF10 are not affected by **1C8**. However, it is possible that **1C8** interact and inhibit SR kinases only when they are in contact with SRSF10.

Our current studies conclude that **1C8** has a cumulative impact on HIV-1 replication. It inhibits some splicing events while enhancing others and this disturbs the steady-state levels of HIV-1 mRNAs. This may not be only through the influence of **1C8** on SRSF10 and other splicing factors could be involved in this. In fact, treatment of HIV-Hela cells with **1C8** resulted in a drop in the concentration of un-spliced HIV-1 mRNA in cytoplasm. This could be because of defective transport of un-spliced HIV-1 mRNA from nucleus to cytoplasm. In Chapter 4, while discussing the mechanism of action of another active molecule, I will explain why export of un-spliced and singly spliced HIV-1 mRNA from nucleus is vital for HIV replication.

## Chapter 3: Development of a new amide bond forming protocol for the parallel synthesis of di(hetero)arylamides

Amide bonds are the fundamental unit connecting the 20 natural amino acids that are the building blocks found in peptides/proteins involved in life. Consequently, a great deal of effort has been devoted to developing peptide coupling reagents to activate the carboxylic acid component **3.1** in amide bond forming reactions (Figure 3.1).<sup>17</sup> They ensure that the process is highly efficient (high yielding), non-racemizing, and ‘clean’, i.e., isolation of the amide product **3.4** does not entail lengthy/difficult product isolation steps and/or production of side-products as contaminants. As an example of the importance of optimizing this process, following the pioneering work by Merrifield and others,<sup>39</sup> it is now, in many cases, routinely possible to rapidly synthesize peptides and small proteins using rapid solid phase synthesis technology.

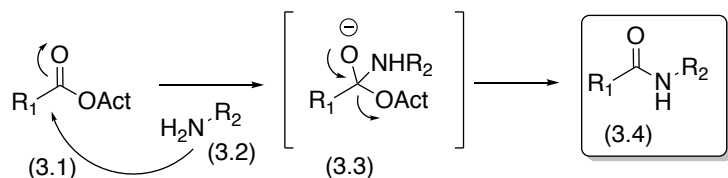


**Figure 3.1 Amide synthesis**

The need for efficient methodology for amide bond synthesis also extends well beyond the coupling of the essential amino acids, as amide motifs are present in approximately 25% of therapeutic drugs<sup>17</sup>, and amide bond formation is very often a crucial step in total synthesis and the preparation of materials for a myriad of applications.

Interestingly, the development of amide coupling reactions between carboxylic acids **3.1** and amines **3.2** has primarily focused on the acid activation step, thereby ensuring that the amine **3.2** will react efficiently at the carbonyl carbon center of acid **3.1**. However, for applications involving electron deficient aromatic and heterocyclic amines, the efficiency of this condensation step is determined by both the reactivity of the carboxylic acid and by the nucleophilicity of the amine partner engaged in the reaction. This is the case for the preparation of the amide-based **IDC16** mimics presented in Chapter 2, which involved reaction of a heterocyclic carboxylic acids (2/4-pyridones and functionalized pyridines) with a diverse series of aromatic and heterocyclic amines of varying nucleophilicity. Indeed, as was ‘painfully” realized during the production of the anti-HIV compounds **1C8**, **2D3**, **3C2**, **1E5**, and the other 115 DHAs in the library using the acid chloride and other classical peptide coupling conditions, the percent conversion to the amide products are low and the desired product is generally produced as a complex mixture with other side products. Due to the polarity of these amide products, their isolation from these mixtures was often difficult to achieve. Taking into account that having to resort to column chromatography as a means to achieve product isolation/purification is a serious limiting operation (time and resource wasting) in any effort to create a library of heterocyclic amide compounds, we found it necessary to develop a new methodology permitting the high yield synthesis and facile isolation of the DHA products under conditions amenable to parallel synthesis.

In “Part 1” of this chapter, we describe the development of a new and efficient protocol for the construction of the amide bond found in DHAs, which is based on the reaction of acyl fluorides with the *N*-TMS derivatives of weakly nucleophilic amines. The synthesis of the 18 DHAs

illustrated in Figure 2.5 was part of the compound library program we undertook to design **IDC16** mimics with anti-HIV activity. From a synthetic point of view, these molecules have two (hetero)aryl systems connected through an amide bond. As a prelude, this sub-chapter includes a brief description of peptide coupling and the reactivity acyl fluorides in this process. Included also are notions concerning the reactivity of aromatic/heteroaromatic substituted amines and the formal conversion to their N-TMS derivatives to their corresponding higher energy/more reactive anion counterparts through reaction with fluoride ion. In Part 2 of this chapter, we further demonstrate that this new methodology to access DHAs can be extended to the reaction of N-TMS (hetero)aryl amines with simple oxo-esters. The synthesis of the 9 DHAs illustrated in Figure 2.6.

### **3.1 Challenges in di(hetero)arylamide (DHA) synthesis and its translation to parallel synthesis**

#### **3.1.1 Peptide coupling methodology**

Condensation of a carboxylic acid with an amine can, in principle, result in formation of an amide bond. However, simple mixing of an amine and a carboxylic acid gives a stable salt which requires very high temperature for the condensation to occur (Figure 3.2, case I).<sup>17</sup> This harsh condition is not compatible with many starting materials, as it causes decomposition and/or side product formation to occur. To overcome this obstacle, the carboxylic acid needs to be activated such that efficient reaction with the amine partner will occur, leading to formation of the amide bond (Figure 3.2, case II).

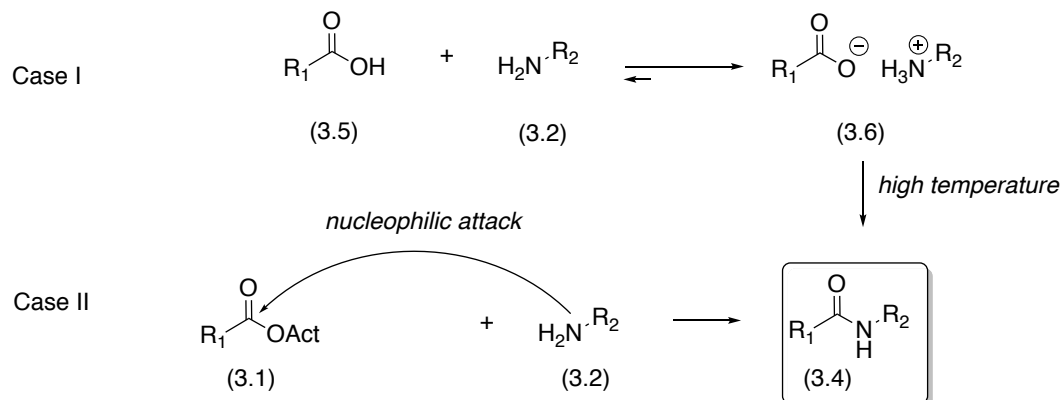


**Figure 3.2 Amide bond formation from carboxylic acid and amine**

There are a large number of reagents that can be used to activate carboxylic acids, the acid chloride approach being traditionally the classical/work-horse method.<sup>17</sup> Thionyl chloride, oxalyl chloride, phosphorus trichloride, phosphorus oxychloride, and phosphorus pentachloride are the reagents commonly used for acid chloride formation.<sup>17</sup> The mechanism of acid chloride formation using thionyl chloride and its coupling with amine is shown in Figure 3.3a. This acid chloride formation liberates HCl and SO<sub>2</sub>, so in order to avoid conversion of amine into an unreactive HCl salt, the coupling step is often carried out in the presence of a hindered tertiary amine base such as triethyl amine or Hunig's base. Formation of the amide product can be accelerated by addition of a catalytic amount of pyridine or N,N-dimethylaminopyridine (DMAP) as shown in Figure 3.3a. Note that under these basic conditions, a reactive N-acylpyridinium salt is generated, which can act as the activated acid component that engages in the amidation reaction.

One limitation to the acid chloride strategy in peptide synthesis is its racemization under basic condition. This occurs through ketene formation, direct enolization, and oxazolone formation (Figure 3.4).<sup>17, 40</sup> As a consequence, this method is not suitable for the coupling of amino acids. This shortcoming led to the development of the carbodiimide-based coupling reagents (DCC, DIC, and EDC) (Figure 3.3b-c). The driving force for amide bond formation using carbodiimides is the formation of a urea by-product. In this one pot reaction, HOBT or DMAP are typically added to minimize N-acylurea generation, which forms through an acetyl transfer. Reaction of HOBT (or DMAP) with O-acylisourea is more rapid than the competing formation of N-acylurea.

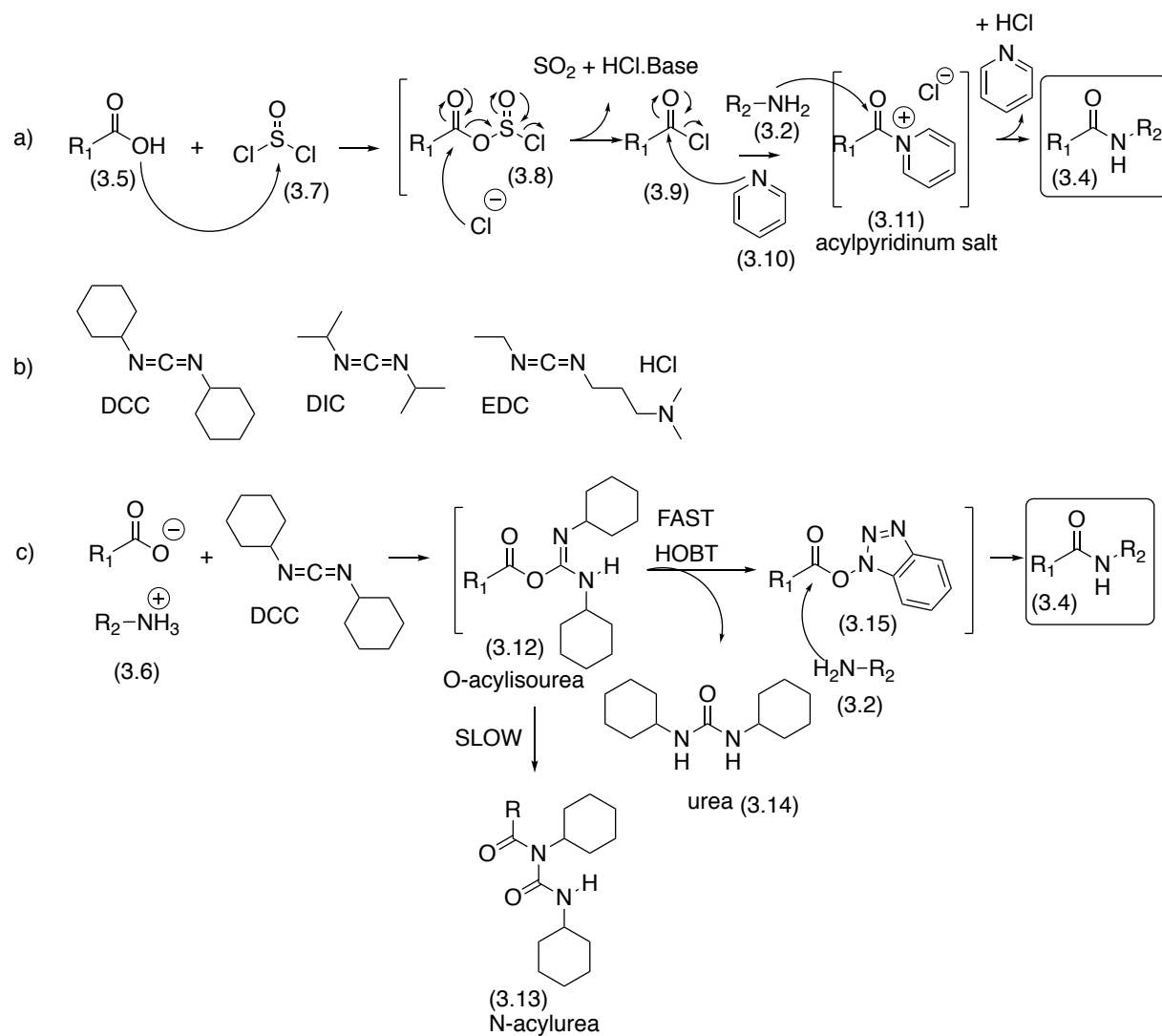
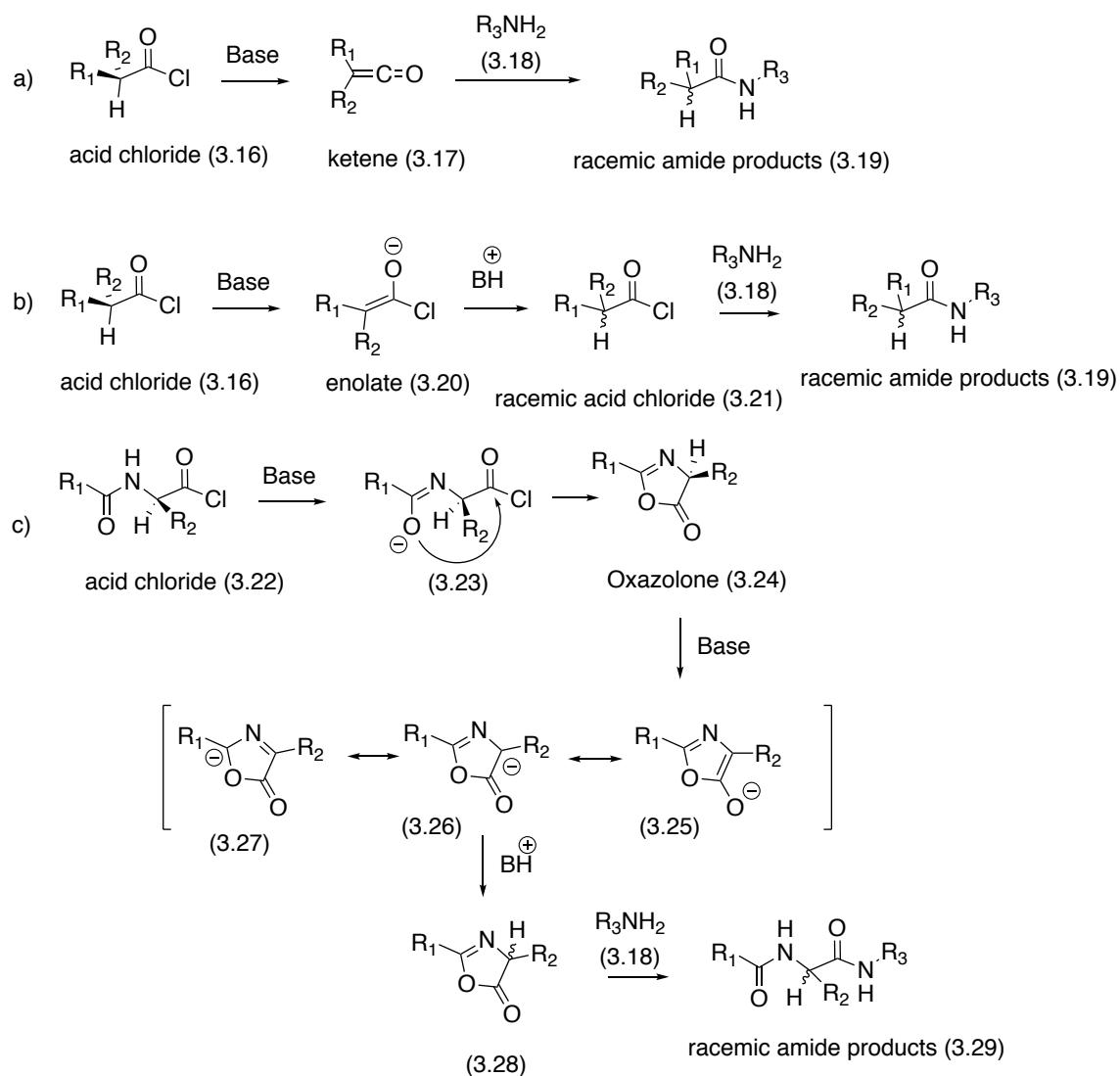


Figure 3.3 a) Amide bond formation using acid chloride method; b) commonly used carbodiimides; c) amide bond formation using DCC





**Figure 3.4 Acid chloride racemization through a) ketene formation, b) direct enolization, and c) oxazolone formation**

Despite the very significant advances in the development of peptide coupling methods, the acid chloride method, or the use of different peptide coupling reagents, was not applicable to our need to make DHA-type compounds, as the amide product yields rarely exceeded 10-30%. This was the consequence of the high reactivity of acid chlorides and to the formation of by products using

other coupling methods/reagents. This led us to look at alternate means to activate the carboxylic acid component, and to find a way to enhance the reactivity of the heterocyclic amines engaged in the coupling reactions.

### **3.1.2 Enhancement of the nucleophilicity of aryl and heteroaryl amines: reaction of TMS-amines with fluoride ion**

In many instances aryl and heteroaryl substituted amines exhibit attenuated/suppressed nucleophilic characteristics due to conjugation/delocalization of the nitrogen lone pair of electrons into the aromatic heteroaromatic ring(s) through resonance. This also magnifies the s-character of the nitrogen as it resonates between sp<sup>3</sup> and sp<sup>2</sup> hybridization (i.e., higher the s character, lower nucleophilicity). As illustrated in Figure 3.5, the exocyclic nitrogen lone pair in 6-chloropyridin-3-amine **3.30** is conjugated with the aromatic ring system giving the resonance structure **3.31**. This nitrogen lone pair delocalization/conjugation is absent in the non-conjugated amines such as (6-chloropyridin-3-yl)methanamine **3.32**. In the latter molecule, the amine nitrogen atom is a better nucleophile. A graphical presentation of the electrostatic potential difference on nitrogen in amines **3.30** and **3.32** (Figure 3.5) illustrates this situation. (Spartan Version 6.1.7; Wavefunction Inc: Irvine (CA, USA), 2014)

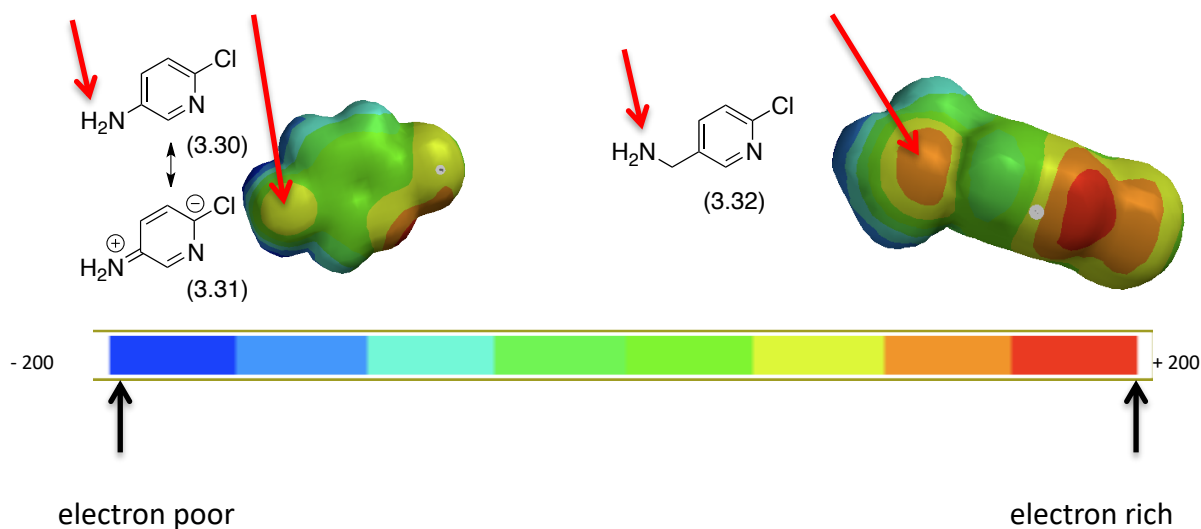


**Figure 3.5** A graphical presentation of the electrostatic potential difference on nitrogen in amines **3.30** and **3.32** (Generated using Spartan software)

For our purposes, the problem of the poor/weak nucleophilicity of (hetero)aryl amines in amide synthesis was resolved by using the amine anion formed *in situ* via the reaction of N-silylated amines with fluoride ion. As shown in Figure 3.6, TMS-amine **3.34** reacts with fluoride ion to form a “hypervalent” silicon species **3.35** which readily decomposes to produce volatile TMSF and an amine anion intermediate **3.36** which is higher in energy and more nucleophilic and reactive than the corresponding free amine **3.33**. Formation of Si-F bond (bond strength = 582 kJ/mol)<sup>41</sup> in TMSF is the driving force for this reaction.

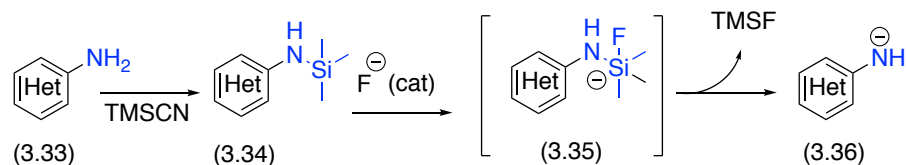


**Figure 3.6 Generation of amine anions from TMS-amines**

### 3.1.3 Acid fluorides in peptide coupling reactions: their enhanced stability relative to acid chlorides

The use of acid fluorides as alternatives to acid chlorides in peptide synthesis has been studied previously.<sup>42-46</sup> Acid fluorides were chosen for our new protocol for several reasons: i) once the reaction is initiated, they are a convenient source of fluoride ion for *in situ* anion generation from TMS amines, ii) they are non-polar and more shelf (hydrolytically) stable than the corresponding acid chlorides. Indeed, in procedures for the preparation of acid fluorides it has been shown that they can be isolated from unwanted side products by washing with water and, and in some cases, can be purified by column chromatography.

Although more stable to water, and less reactive than acid chlorides toward alcohols, acid fluorides react efficiently with amines to give the expected amide products.<sup>42, 47-52</sup> This is intriguing, as one might expect, based on the greater electronegativity of fluoride versus chloride that the carbonyl carbon in acid fluoride would be the more electrophilic, and therefore, more reactive toward nucleophiles. Further, in the ensuing addition reaction where the tetrahedral species **3.38** is formed (Figure 3.7), one might expect rapid loss of fluoride to give the amide product. However, although fluoride would be a better leaving group in this step on the basis of

its electronegativity (analogy to  $\text{S}_{\text{N}}\text{Ar}$  reactions), it is the difference in electronegativity between chloride and fluoride that results in a stabilization of the fluoride containing tetrahedral intermediate **3.38**, lowering the rate of its conversion back to starting material or forward to the amide product. The same pattern of reactivity is observed for ketones bearing alpha-fluoro substituents (e.g.,  $\text{CF}_3$ ) (Figure 3.8). Note, that for non-fluorinated ketones, the keto-form is generally favoured (i.e., the tetrahedral form collapses with loss of  $\text{H}_2\text{O}$ ).

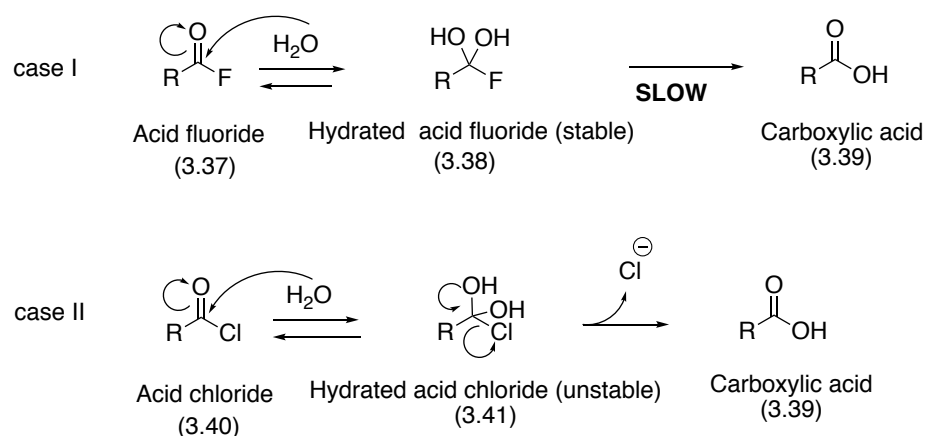


**Figure 3.7 Reaction of acid fluoride and chloride with water**

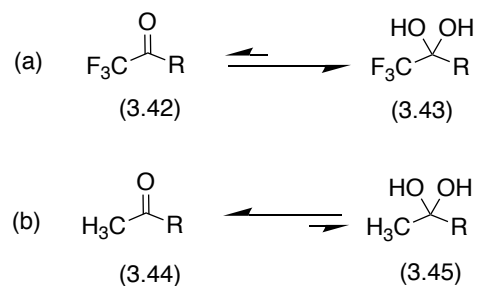


**Figure 3.8 Hydration of ketones**

### **3.2 Part 1: Coupling of N-silylated (hetero)arylamines with acid fluoride 3.51, a new protocol**

In our amide bond forming protocol, it was expected that the fluoride ion liberated through reaction with the acid fluoride would perpetuate the condensation process, rendering it highly efficient. Taking advantage of the reported non-polar nature of acid fluorides and N-TMS amines, it was further anticipated that if an appropriate non-polar solvent was chosen for the reaction, the more polar DHA product may selectively precipitate from the medium, reducing product isolation/purification to a simple vacuum filtration and washing of the precipitated material.

#### **3.2.1 Preparation of N-silylation of (hetero)aryl amines 3.34a to 3.34r**

The most conventional method for N-silylation of (hetero)aryl amines involves their reaction with organolithium base (e.g., *n*-Buli) followed by treatment of the derived anion with an organosilyl chloride (e.g., TBSCl and TMSCl).<sup>53, 54</sup> In most cases, this conversion is sluggish and long reaction hours are necessary. Most importantly, since N-silylated (hetero)aryl amines are moisture sensitive, inert condition is required for work up and purification steps.

To simplify this conversion for the parallel synthesis protocol, we decided to generate the N-TMS amines under essentially neutral (weak acid) conditions and engaged them directly in the condensation step. For our purposes, trimethylsilylcyanide (TMSCN) was used as the N-silylating agent.<sup>55</sup> No purification is required when using this reagent as it reacts effectively with

amines and, the residual TMSCN and liberated HCN, could be readily removed under vacuum (solid NaOH pellets were added in the cold trap of the vacuum line to trap the HCN).

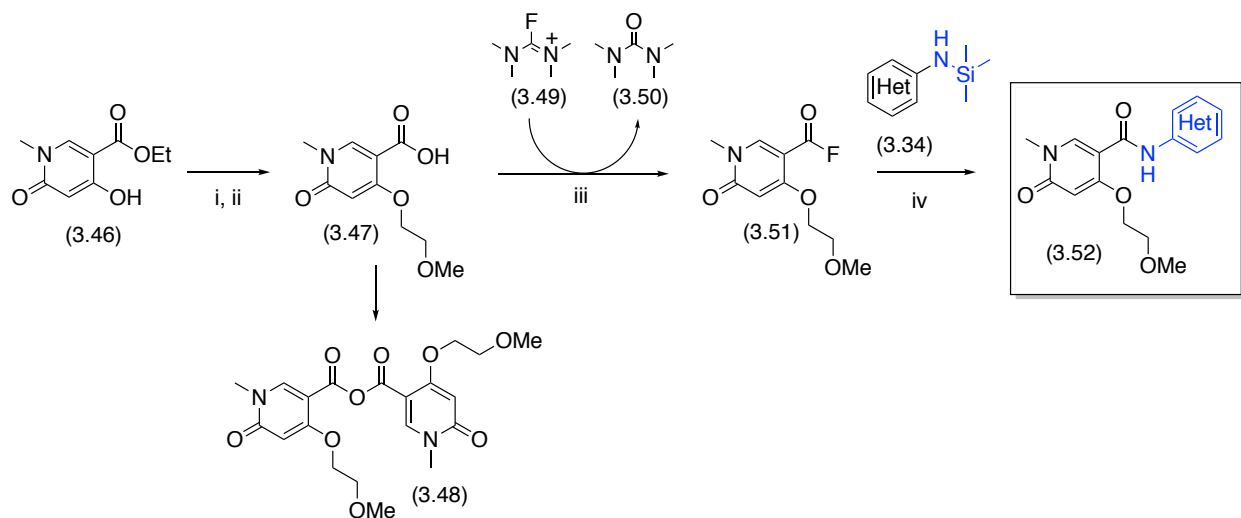
The diversity set of 18 trimethylsilylated (hetero)aryl amines **3.34a-r** used in this study were prepared by reacting 0.5 mmol of the requisite amine in neat TMSCN (0.5 mL) at 70 °C (7 min to 6 h) (Table 3.1). The advancement of each reaction was monitored by <sup>1</sup>H NMR (CDCl<sub>3</sub>). Interestingly, the time required to observe complete dissolution of the amine, i.e., an indicator of complete N-silylation, appeared to be a function of both the reactivity of the amine and its solubility. Indeed, the duration of reaction required did not follow a clear linear relationship to the electrostatic potential on the exocyclic amine nitrogen as calculated using Spartan software (Version 6.1.7; Wavefunction Inc: Irvine (CA, USA), 2014.) (see calculated electrostatic potential in Table 3.1).

### 3.2.2 Preparation of Acid fluoride **3.51**

A 4-methoxyethoxy substituted 2- pyridinone motif with COOH substituent was chosen for the left side component in DHAs **3.52**, since at the start of this study, only five of this type of DHAs were present in our library of **IDC16** mimics with amide linkers. Consequently, it was deemed necessary to synthesize and evaluate a larger number of compounds of this type in order to assess their anti-HIV activity.

Pyridinone carboxylic acid **3.47** was prepared by O<sup>4</sup>-alkylation of 2-pyridinone ester **3.46**<sup>30, 56</sup> with 1-bromo-2-methoxyethane (DMF, Cs<sub>2</sub>CO<sub>3</sub>) and subsequent hydrolysis of the ester group

using LiOH in THF-H<sub>2</sub>O (2:1) (Reaction Scheme 3.1). Conversion of **3.47** to acid fluoride **3.51** was best achieved through reaction with fluoro-N,N,N',N'-tetramethylformamidine hexafluorophosphate (TFFH)<sup>8</sup> **3.49** and cesium fluoride (CsF) in anhydrous MeCN at room temperature for 5 h.



**Reaction Scheme 3.1** Reagent and conditions: i) 2-bromoethyl methyl ether, CsCO<sub>3</sub>, DMF, 100 °C, 1 h; ii) LiOH, THF/H<sub>2</sub>O (2/1), 4h, r.t.; iii) TFFH, CsF, MeCN, 5 h, r.t.; iv) MeCN, TBAF (cat), 50 °C, 12 h.

In addition to TFFH, the most common reagents for conversion of a carboxylic acid to acid fluoride are sulfur tetrafluoride (SF<sub>4</sub>), selenium tetrafluoride (SeF<sub>4</sub>), diethylaminosulfur trifluoride (DAST), bis(2-methoxyethyl)aminosulfur trifluoride (Deoxo-Fluor), aminodifluorosulfinium tetrafluoroborate salts, and cyanuric fluoride ((CNF)<sub>3</sub>). SF<sub>4</sub> is a highly toxic and corrosive gas so its handling requires extensive safety measures and specialized equipment. SeF<sub>4</sub> is liquid but exactly like SF<sub>4</sub>, it has many safety issues. DAST and Deoxo-Fluor are derivatives of SF<sub>4</sub>. Both are liquid and require no addition of base (liberated during the



reaction) for fluorination<sup>17</sup> but they are thermally unstable, and explosive at high temperature or in contact with water. They generate HF gas which is toxic and corrosive to many tissues including bone.<sup>57-59</sup> Crystalline aminodifluorosulfinium tetrafluoroborate salts do not fume and are thermally stable but their reactive species (dialkylaminosulfur trifluoride) has all the disadvantage of DAST and Deoxo-Fluor.<sup>59</sup> Cyanuric fluoride is the most widely used fluorinating agent for acid fluoride formation. However, in large-scale reactions, insoluble cyanuric acid precipitates out during workup. To remove this precipitate, additional extraction with water is required. However, this leads to partial hydrolysis of the acid fluoride.<sup>60</sup> In this project, we used TFFH **3.49** as the fluorinating agent because it is a solid, stable, and non-hygroscopic, which is easy to handle, and cost efficient.<sup>45</sup> It can be used with Hunig's base or inorganic bases (e.g., CsF) and uses urea formation as the driving force. Plus, there is no need for isolation of the intermediate acid fluoride, so one pot coupling can be an option.<sup>17, 61</sup> When using TFFH as the fluorinating agent, the presence of added fluoride ion is mandatory in order to avoid competing formation of the symmetrical anhydride **3.48** (Reaction Scheme 3.1).<sup>62</sup> In my procedure, CsF was used both as the base and as the fluoride ion additive. Unlike amine bases, CsF is not nucleophilic so it does not compete with amide formation.

Compound **3.51** was readily isolated pure as a colorless solid (90%) by washing the crude product mixture with hexane to remove the tetramethylurea **3.50** formed, and then taking the solid material up in DCM, filtering to remove the cesium salts and concentrating to dryness. The structure of **3.51** was confirmed by the presence of a peak at 25.43 ppm in the <sup>19</sup>F NMR spectrum, and by the up-field shift ( $\delta$  0.14 ppm) from  $\delta$  8.34 for the peak for H-6 in the <sup>1</sup>H NMR spectrum. As expected, acid fluoride **3.51** was much more stable than the corresponding (and

corrosive) acid chloride derivative, and could be conveniently stored for periods exceeding one month in an airtight container at 4 °C. In fact, when dissolved in DCM and washed with ice water, it was recovered in greater than 90% yield (purity check by  $^1\text{H}$  NMR).

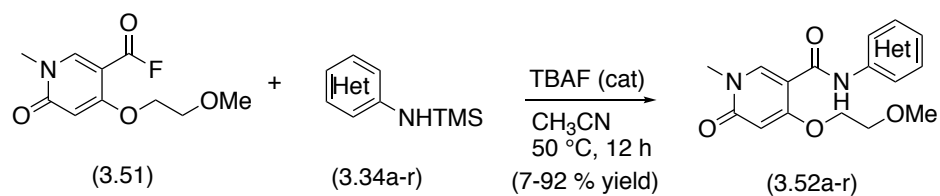
### 3.2.3 The coupling step: reaction of acid fluoride **3.51** with N-silylated amines **3.34a-r**

For the purpose of comparison, we first investigated the reaction of the four non-silylated amines **3.33c**, **3.33g**, **3.33l**, and **3.33n**, with excess of acid fluoride **3.51** in acetonitrile at 50 °C. These reactions were efficient, and the product precipitated from the medium as the reaction progressed and was contaminated with only small quantities (up to 15% based on  $^1\text{H}$  NMR) of residual amine.

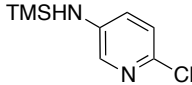
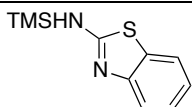
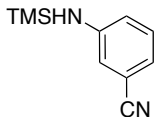
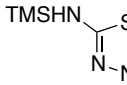
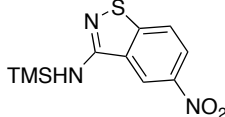
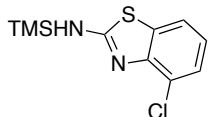
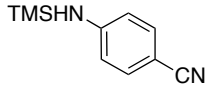
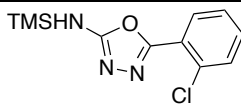
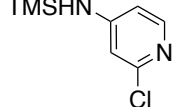
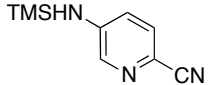
However, when N-silylated amine **3.34n** was reacted with an excess (1.8 equiv.) of acid fluoride **3.51**, no residual amine was present and amide **3.52n** was isolated pure in 47% yield after filtration and drying. Further, a significant improvement in product yield (47% to 92%) was achieved by addition of a catalytic amount of TBAF (2 mol%) at the outset, to initiate reaction of fluoride ion with silicon and formation of the putative amine anion. The protocol that was subsequently employed for the synthesis of the new DHA molecules involved adding acid fluoride **3.51** (0.89 mmol) in acetonitrile (5 mL) to the requisite N-silylated amine **3.34a-r** (0.5 mmol) (prepared immediately before the reaction). TBAF was then added, and the resulting mixture was heated at 50°C overnight. After cooling, the precipitated material was collected by suction filtration and dried. As product purity, and not quantity, was the principle criterion for these reactions, efforts were generally not made to improve the amide product yields beyond

those indicated in Table 3.1. In this context, it was interesting to observe that the yield for the preparation of amide **3.52a** from the electron rich amine **3.34a** was comparable to that for the preparation of **3.52r** from the electron deficient amine **3.34r**. In fact, the initial yield for **3.52a** was 38%, but could be brought up to 78% by washing with a mixture of MeCN-Et<sub>2</sub>O. This reflected the fact that amide **3.52a** is more soluble in MeCN than amide **3.52r**. The relatively lower yields for the isolation of amides **3.52b-d** also reflects their significant solubility in MeCN. For our purposes, <sup>1</sup>H NMR was used to determine product purity. In the large majority of cases, no impurities were detected, and in the few cases where the presence of the amine component persisted, only trace amounts were detectable (purity > 95%).

**Table 3.1 Synthesis of DHA 3.52a-r from N-silylated amines 3.34a-r**



<b>N-TMS Amine 3.34<sup>a</sup></b>	<b>Structure</b>	<b>Electrostatic potential (KJ/mol)</b>	<b>N-Silylation Time</b>	<b>Amide<sup>a,b</sup> 3.52 (Yield)</b>
<b>3. 34a</b>		140.1	7 min (91%) <sup>c</sup>	<b>3.52a</b> (78%)
<b>3. 34b</b> <sup>63</sup>		132.2	30 min	<b>3.52b</b> (7%)
<b>3. 34c</b>		120.0	30 min	<b>3.52c</b> (27%)
<b>3. 34d</b>		119.5	15 min	<b>3.52d</b> (25%)
<b>3. 34e</b>		115.0	30 min	<b>3.52e</b> (53%)
<b>3. 34f</b> <sup>64-67</sup>		112.8	30 min	<b>3.52f</b> (55%)
<b>3. 34g</b> <sup>68</sup>		105.9	3 h	<b>3.52g</b> (89%)
<b>3. 34h</b> <sup>64</sup>		100.5	90 min	<b>3.52h</b> (42%)

<b>3. 34i</b>		98.0	2 h	<b>3.52i</b> (62%)
<b>3. 34j</b>		97.8	30 min	<b>3.52j</b> (71%)
<b>3. 34k</b>		96.0	3 h (96%) <sup>c</sup>	<b>3.52k</b> (85%)
<b>3. 34l</b> <sup>69</sup>		92.9	30 min	<b>3.52l</b> (87%)
<b>3. 34m</b> <sup>30</sup>		88.8	30 min	<b>1E5</b> <sup>Ref: 1a,b</sup> (60%)
<b>3. 34n</b>		88.7	30 min	<b>3.52n</b> (92%)
<b>3. 34o</b> <sup>64</sup>		80.4	3 h	<b>3.52o</b> (81%)
<b>3. 34p</b>		77.3	60 min	<b>3.52p</b> (63%)
<b>3. 34q</b>		74.7	30 min	<b>3.52q</b> (44%)
<b>3. 34r</b>		58.4	6 h (85%) <sup>c</sup>	<b>3.52r</b> (67%)

<sup>a</sup> All known compounds are cited by literature references.

<sup>b</sup> Amide formation: TMS amine (0.5 mmol), acid fluoride (0.89 mmol) in MeCN (5 mL), 50 °C, 12h, (isolated yield).

<sup>c</sup> Percent conversion to N-silylated amine

The results obtained for coupling of acid fluoride **3.51** with 18 different N-TMS amines in acetonitrile demonstrate the simplicity of the protocol and suggests its general applicability to a wide range of amines expressing weak nucleophilic character. Further, as extractive work-up can be avoided, minimum waste is produced. This “green” chemistry method <sup>70-72</sup> can be readily adapted to rapid parallel synthesis of libraries of DHA-based compounds.

### 3.3 Part 2: coupling of N-silylated amines with oxo-ester

Having successfully demonstrated that weakly nucleophilic heterocyclic N-TMS amines readily react with the acid fluorides of 2-pyridinone **3.51**, our objective became to determine whether this methodology could be extended to other activated acid derivatives, and in particular to the reaction with thioesters and oxo esters.

The reaction with thioesters was undertaken by a PhD thesis student in our laboratory, Ana Koperniku. Thioester was chosen as the active ester since they are more stable than acid fluorides and more reactive than oxo-esters. Indeed, precedent for their ability to react with amines was inspired by the reaction of acyl-CoA **3.53** with glycine **3.54** in biosynthesis of primary fatty acid amides **3.55** (Figure 3.9).<sup>73</sup>

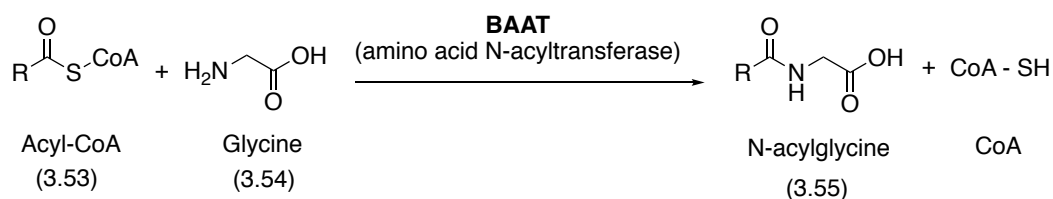


**Figure 3.9 Biosynthesis of primary fatty acid amide from Acyl-CoA and glycine**

Through the synthesis of a representative library of 19 DHAs, Ana Koperniku demonstrated that thioesters **3.56a** and **3.56b** react readily with a diverse set of N-silylated (hetero)aryl amines in presence of quantitative amount of TBAF (Figure 3.10).<sup>74</sup> All the products were isolated with simple filtration and the yield ranges from 11% to 96%.

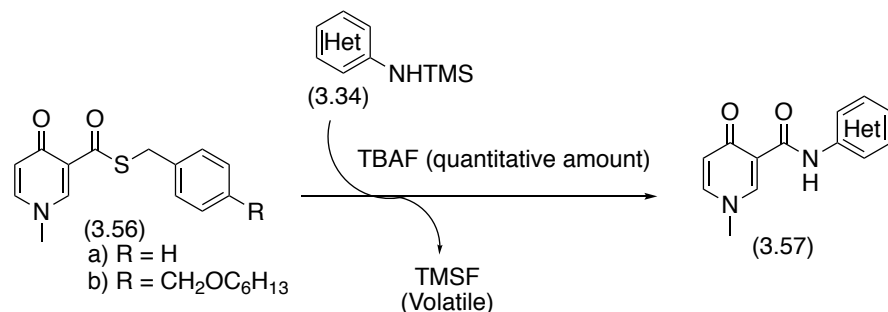


**Figure 3.10** Synthesis of DHAs using thioesters and N-silylated (hetero)aryl amines

Motivated by this result, it was decided to push the limits of the methodology even further by exploring the reactivity of N-silylated amines with oxo-esters. A major consideration in this choice was that neutral esters, rather than polar acid functions are often proffered as intermediates in synthesis. Furthermore, this will economize the number of steps in synthesis of **3.52** in our future work, as conversion of 2-pyridinone ester, **3.46** to acid **3.47** to acid fluoride **3.51** can be avoided.

However, oxo-esters are not the conventional activated acid form for amide bond formation.<sup>17</sup> In fact, the ester group finds use as an acid protecting group in peptide coupling reactions. As it is well documented that in the absence of metal promoters/catalysts, the reaction of esters with amines, and in particular aromatic and heteroaromatic amines is generally inefficient, even at elevated temperatures. However, it has been shown that amine anions, generated by the reaction of amines with strong bases such as NaH<sup>75-77</sup>, BuLi<sup>78-80</sup>, and KOt-Bu<sup>81, 82</sup>, react with esters to form amide products. This suggests that oxo-ester can also react with the amine anion generated through reaction of a N-silylated amine with a catalytic quantity of fluoride anion to produce the desired amide product.



As is shown in Figure 3.11, oxo-ester **3.59** react with amine anion **3.36** to liberates methoxide anion **3.58**, as a byproduct, along with the coupling product **3.57**. As shown in **path b** in this figure, **3.58** also helps in conversion of N-silylated amine **3.34** to its amine anion form **3.36**. Consequently, both bond formation of Si-F in TMSF and Si-O in TMSOMe (bond strength = 425.6 kJ/mol)<sup>83</sup> are the driving force for this amide formation.

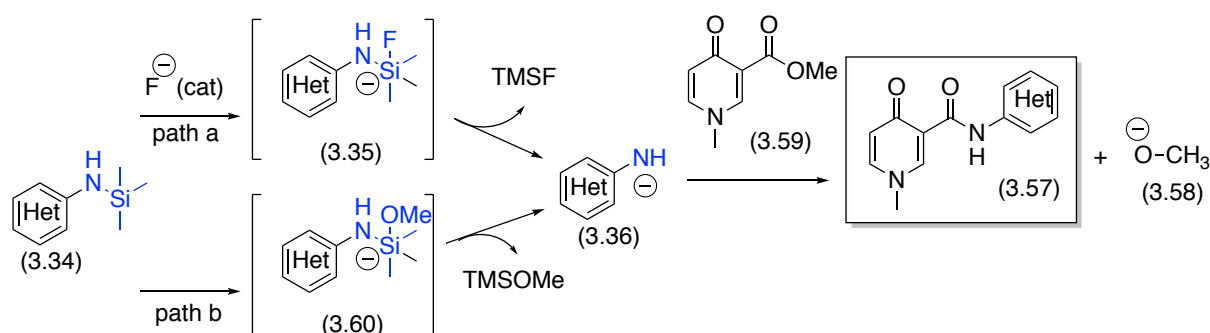


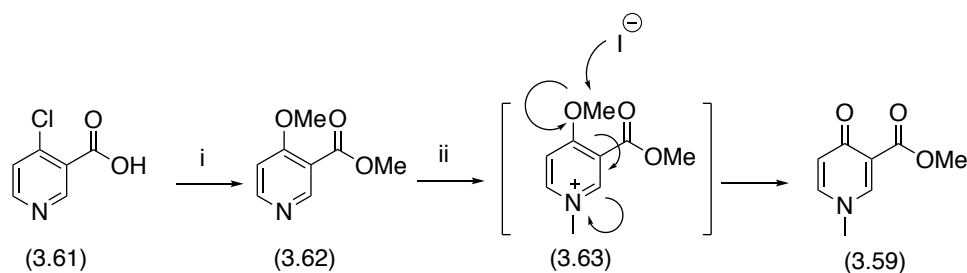
**Figure 3.11 Both TBAF and methoxide anion catalyze the formation of amine anion 3.36**

In an identical manner to the reactivity of amides **3.52**, synthesized from acid fluoride **3.51** and N-silylated (hetero)aryl amine **3.34**, due to high polarity difference between synthons and products in MeCN, polar DHA products **3.57** were isolated through a simple filtration and no farther purification was necessary.

### 3.4 DHA synthesis through the reaction of oxo-ester and N-silylated amine

#### 3.4.1 Preparation of oxo-ester 3.59

Oxo-ester **3.59**, and intermediate used in our laboratory to prepare **1C8** was obtained in two steps from 4-chloronicotinic acid **3.61**, involving its reaction with methanol-HCl<sup>84, 85</sup>, followed by treatment of the derived 4-methoxypyridine methyl ester intermediate **3.62** with a sub-stoichiometric quantity of MeI under microwave heating conditions (Reaction Scheme 3.2). This latter transformation most likely proceeded by *N*-methylation of the pyridine nitrogen atom in **3.62** and iodide ion induced SN2 reaction at the 4-methoxy methyl group center in the quaternary salt **3.63**.<sup>86, 87</sup> In this step the N-alkyl-4-pyridinone system is created and MeI is regenerated.



Reaction Scheme 3.2 Reagent and conditions: i) HCl, MeOH; ii) MeI, MeCN, microwave at 120 °C, 1h

#### 3.4.2 Reaction of oxo-ester 3.59 with N-silylated amines

The efficiency of oxo-ester **3.59** for DHA synthesis was evaluated through its reaction with a total of 11 N-silylated amines. Table 3.2 summarizes the result of these experiments. As a point

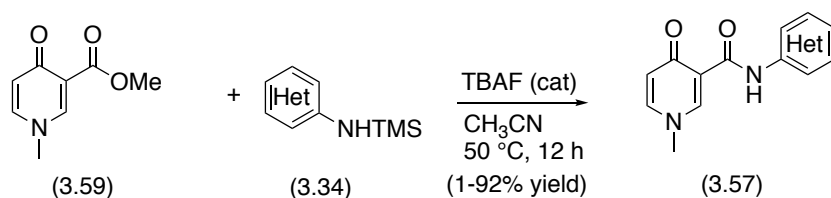
of reference, in this table, we also included the results obtained by Ana Koperniku for the synthesis of these DHA starting from thioesters **3.56a,b**.

To evaluate the influence of varying amount of TBAF used in the protocol, methyl ester **3.59** was initially reacted with the thiadiazole-based amine **3.34l**. In the presence of 1.1 equivalents of TBAF, the desired amide product **3.57l** was isolated in 78% yield. More exciting, compound **3.57l** was isolated in 88% yield when only 0.25 equivalents of TBAF was employed. This latter result demonstrated that methoxide anion **3.58** contributes to product formation. It further showed that the efficiency of the reaction is comparable to that observed (92/96%) for thioesters **3.57a/b**.

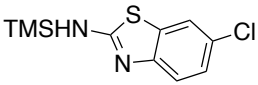
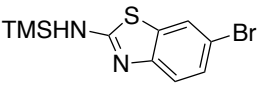
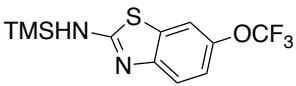
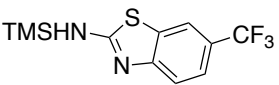
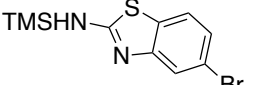
Encouraged by this result, methyl ester **3.59** was reacted in acetonitrile under the standard conditions (50 °C, overnight) with the other ten other N-silylated amines **3.34e**, **3.34j**, **3.34n**, **3.34s**, **3.34t**, **3.34u-y** (Table 3.2). Precipitate formation was observed in all cases. Although compound **3.57x** was isolated in moderate yield (56%), the seven amide products (**3.57j**, **3.57n**, **3.57t**, **3.57u-w**, and **3.57y**) were isolated high to excellent yields (75-92%) by simple vacuum filtration and washing with cold acetonitrile (> 95% purity by <sup>1</sup>H NMR). On the other hand, the precipitate recovered for the reaction with N-silylated amine **3.34e** corresponded to an 8-2 mixture of amide **3.57e** contaminated with the starting ester **3.59** (calculated yield for **3.57e** = 12%), reflecting the fact that the amide product and the ester have similar solubility in acetonitrile. Note here, that as the objective of this work was to have a simple protocol for parallel synthesis, no effort was made to isolate pure **3.57e** by recrystallization of the precipitate or by column chromatography of the concentrated mother liquor.

Lastly, in the reaction of oxo- ester **3.59** with TMS-amine **3.34s**, amide **3.57s** was obtained in only 1% yield. Interestingly, the yields for the preparation of this amide **3.57s** from thioesters **3.56a/b** was markedly higher (88%). In the reaction with oxo-ester **3.59**, the major component in the isolated precipitate was the starting amine. Suggesting that N-silylated amine **3.34s** is unstable under the reaction conditions. One possibility is that there is rapid loss of the trimethylsilyl (TMS) group due to the presence of adventitious water (hydroxide ions) in the added TBAF solution. In the reaction with the thioesters **3.56a/b**, a high yield conversion to product may also be the consequence of using a four-fold excess of a more reactive activated acid component.

**Table 3.2 Synthesis of DHA 3.57 from oxo-ester and N-TMS amines 3.34. The results from thioesters (synthesized by Ana Koperniku) are also shown for reference purposes.**



N-TMS Amine 3.34	Structure	Electrostatic Potential (KJ/mol)	N- Silylation Time	Amide from thioesters 3.56a/3.56b (Yield) <sup>a</sup>	Amide from oxo- ester 3.57 (Yield) <sup>b</sup>
3.34e		115.0	30 min	3.57e (24%/17%)	3.57e (12%)
3.34j		97.8	30 min	3.57j (70%/70%)	3.57j (75%)
3.34l		92.9	30 min	3.57l (92%/96%)	3.57l (88%)
3.34n		97.8	30 min	3.57n (68%/68%)	3.57n (90%)
3.34s		95.7	30 min	3.57s (88%/88%)	3.57s (1%)
3.34t		93.7	14 h	3.57t (68%/68%)	3.57t (92%)

<b>3.34u</b>		81.7	14 h	<b>3.57u</b> (85%/84%)	<b>3.57u</b> (91%)
<b>3.34v</b>		81.5	14 h	<b>3.57v</b> (82%/86%)	<b>3.57v</b> (78%)
<b>3.34w</b>		75.9	14 h	<b>3.57w</b> (67%/69%)	<b>3.57w</b> (75%)
<b>3.34x</b>		72.0	14 h	<b>3.57x</b> (69%/63%)	<b>3.57x</b> (56%)
<b>3.34y</b>		26.1	14 h	<b>3.57y</b> (80%/81%)	<b>3.57y</b> (70%)

<sup>a</sup> *Synthesis* (2019, 1779-1790)

<sup>b</sup> Amide formation: TMS amine (0.6 mmol) + acid fluoride (1.2 mmol) in MeCN (2 mL), 50 °C, 16h, (isolated yield).

### 3.5 Conclusions

This study established that both an acid fluoride and an oxo-ester are valuable starting compounds for the preparation of DHAs through reaction with the *in situ* generated anion derived from N-silylated (hetero)aryl amines. Further, the results for **3.34s** suggested that, even if extra steps are required to access thioester, in certain cases thioester may be preferred. In Chapter 4, acid fluoride and N-TMS amine method was used to synthesize a library of DHAs. This was done prior to the development of ester method. We believe that the ester and N-TMS amine method has the potential to be a general method for future DHA library synthesis.

### 3.6 Experimental Section

All chemicals were purchased from Sigma Aldrich or Oakwood Chemicals and they were used without purification unless mentioned. All solvents were dried and kept under N<sub>2</sub>. <sup>1</sup>H and <sup>13</sup>C NMR spectra were recorded at 400 and 100 MHz, respectively, on a Bruker AC 400 Ultrashield 10 spectrophotometer. Chemical shifts are expressed in ppm, ( $\delta$  scale). When peak multiplicities are reported, the following abbreviations are used: s (singlet), d (doublet), m (multiplet), dd (doublet of doublet). Coupling constants are reported in Hertz (Hz). High resolution mass spectra was recorded on a Thermo Scientific Q Exactive Orbitrap High Resolution Mass Spectrometer. Flash column chromatography was performed using silica gel (Silicycle, Siliaflash F60, 40-63 $\mu$ m, 230-400 mesh), or on a Biotage Isolera purification system, (PartnerTech Atvidaberg AB) using pre-packed silica gel columns (Biotage, part no. FSKO-1107-0010, FSKO-1107-0025, or FSKO-1107-0050). Infrared spectra were recorded on a Agilent Technologies (Cary 600 series)

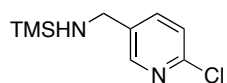
FT-IR spectrometer, using a PIKE MIRacle ATR accessory for sampling ( $\nu$  in  $\text{cm}^{-1}$ ). Melting points were obtained using a Mel-Temp II apparatus.

### 3.6.1 Experimental section

#### General procedure for the synthesis of 3.34a-y

The starting amines were dried under high vacuum for 12 h. Then, a solution/mixture of the requisite amine (0.5 mmol) in  $\text{Me}_3\text{SiCN}$  (0.5 mL) was heated at 70 °C for the required time (Table 3.1 and Table 3.2). Without removing the hot oil bath, the resulting solution was flushed with  $\text{N}_2$  for 15 min and then concentrated under high vacuum. The percent conversion of each amine to its N-silylated derivative was determined by  $^1\text{H}$  NMR in  $\text{CDCl}_3$  (passed through a basic alumina column prior to use). The synthesis of **3.34s-y**, were done according to the reported procedure.<sup>74, 88</sup>

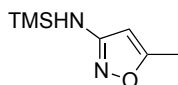
#### *N*-((6-Chloropyridin-3-yl)methyl)-1,1,1-trimethylsilanamine (**3.34a**)



Heated for 7 min (yellow oil; 91% conversion).

$^1\text{H}$  NMR (400 MHz,  $\text{CDCl}_3$ ):  $\delta$  = 8.22 (s, 1 H), 7.54 (d,  $J$  = 8.1 Hz, 1 H), 7.18 (d,  $J$  = 8.1 Hz, 1 H), 3.85 (d,  $J$  = Hz, 2 H), 0.00 (s, 9 H).

#### 5-Methyl-N-(trimethylsilyl)isoxazol-3-amine (**3.34b**)

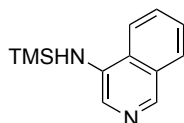




Heated for 30 min (yellow solid; 100% conversion).

$^1\text{H}$  NMR (400 MHz,  $\text{CDCl}_3$ ):  $\delta$  = 5.46 (s, 1 H), 3.75 (s, 1 H), 2.24 (s, 3 H), 0.23 (s, 9 H).

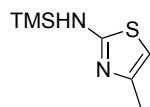
**N-(Trimethylsilyl)isoquinolin-4-amine (3.34c)**



Heated for 30 min (yellow solid; 100% conversion).

$^1\text{H}$  NMR (400 MHz,  $\text{CDCl}_3$ ):  $\delta$  = 8.62 (s, 1 H), 8.03 (s, 1 H), 7.79 (d,  $J$  = 7.8 Hz, 1 H), 7.73 (d,  $J$  = 8.4 Hz, 1 H), 7.55 (t,  $J$  = 7.7 Hz, 1 H), 7.46 (d,  $J$  = 7.7 Hz, 1 H), 3.88 (s, 1 H), 0.30 (s, 9 H).

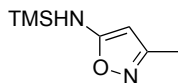
**4-Methyl-N-(trimethylsilyl)thiazol-2-amine (3.34d)**



Heated for 15 min (yellow oil; 100% conversion).

$^1\text{H}$  NMR (400 MHz,  $\text{CDCl}_3$ ):  $\delta$  = 5.95 (s, 1 H), 4.84 (s, 1 H), 2.14 (s, 3 H), 0.23 (s, 9 H).

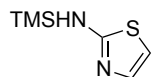
**3-Methyl-N-(trimethylsilyl)isoxazol-5-amine (3.34e)**



Heated for 30 min (orange solid; 100% conversion).

$^1\text{H}$  NMR (400 MHz,  $\text{CDCl}_3$ ):  $\delta$  = 4.78 (s, 1 H), 4.30 (s, 1 H), 2.08 (s, 3 H), 0.21 (s, 9 H).

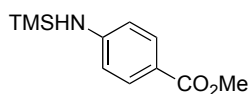
**N-(Trimethylsilyl)thiazol-2-amine (3.34f)**



Heated for 30 min (orange oil; 100% conversion).

$^1\text{H}$  NMR (400 MHz,  $\text{CDCl}_3$ ):  $\delta$  = 7.02 (s, 1 H), 6.40 (s, 1 H), 5.20 (s, 1 H), 0.25 (s, 9 H).

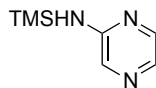
**Methyl 4-((trimethylsilyl)amino)benzoate (3.34g)**



Heated for 180 min (yellow oil; 100% conversion).

$^1\text{H}$  NMR (400 MHz,  $\text{CDCl}_3$ ):  $\delta$  = 7.68 (d,  $J$  = 7.8 Hz, 2 H), 6.48 (d,  $J$  = 7.9 Hz, 2 H), 3.69 (s, 4 H), 0.14 (s, 9 H).

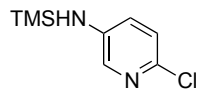
**N-(Trimethylsilyl)pyrazin-2-amine (3.34h)**



Heated for 90 min (yellow oil; 100% conversion).

$^1\text{H}$  NMR (400 MHz,  $\text{CDCl}_3$ ):  $\delta$  = 7.83 (t,  $J$  = 1.2 Hz, 3 H), 4.23 (s, 1 H), 0.24 (s, 9 H).

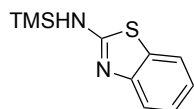
**6-Chloro-N-(trimethylsilyl)pyridin-3-amine (3.34i)**



Heated for 120 min (purple solid, 100% conversion).

$^1\text{H}$  NMR (400 MHz,  $\text{CDCl}_3$ ):  $\delta$  = 7.73 (s, 1 H), 6.97 (d,  $J$  = 8.7 Hz, 1 H), 6.85 (d,  $J$  = 8.7 Hz, 1 H), 3.44 (s, 1 H), 0.20 (s, 9 H).

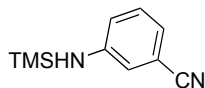
**N-(Trimethylsilyl)benzo[d]thiazol-2-amine (3.34j)**



Heated for 30 min (yellow oil; 100% conversion).

$^1\text{H}$  NMR (400 MHz,  $\text{CDCl}_3$ ):  $\delta$  = 7.41 (s, 2 H), 7.13 (s, 1 H), 6.93 (s, 1 H), 4.91 (s, 1 H), 0.21 (s, 9 H).

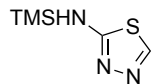
**3-((Trimethylsilyl)amino)benzonitrile (3.34k)**



Heated for 180 min (yellow oil; 96% conversion).

$^1\text{H}$  NMR (400 MHz,  $\text{CDCl}_3$ ):  $\delta$  = 7.03 (t,  $J$  = 7.8 Hz, 1 H), 6.81 (d,  $J$  = 7.5 Hz, 1 H), 6.69 (m, 2H), 3.51 (s, 1 H), 0.13 (s, 9 H).

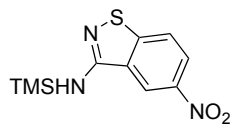
**N-(Trimethylsilyl)-1,3,4-thiadiazol-2-amine (3.34l)**



Heated for 30 min (yellow solid; 100% conversion).

$^1\text{H}$  NMR (400 MHz,  $\text{CDCl}_3$ ):  $\delta$  = 8.35 (s, 1 H), 6.01 (s, 1 H), 0.32 (s, 9 H).

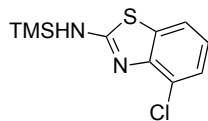
**5-Nitro-N-(trimethylsilyl)benzo[d]isothiazol-3-amine (3.34m)**



Heated for 30 min (red/orange solid; 100% conversion).

$^1\text{H}$  NMR (400 MHz,  $\text{CDCl}_3$ ):  $\delta$  = 8.70 (s, 1 H), 7.99 (s, 1 H), 7.40 (s, 1 H), 5.96 (s, 1 H), 0.43 (s, 9 H).

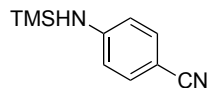
**4-Chloro-N-(trimethylsilyl)benzo[d]thiazol-2-amine (3.34n)**



Heated for 30 min (yellow oil; 100% conversion).

$^1\text{H}$  NMR (400 MHz,  $\text{CDCl}_3$ ):  $\delta$  = 7.37 (d,  $J$  = 7.7 Hz, 1 H), 7.23 (d,  $J$  = 7.8 Hz, 1 H), 6.92 (t,  $J$  = 7.7 Hz, 1 H), 5.22 (s, 1 H), 0.30 (s, 9 H).

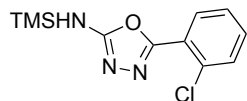
**4-((Trimethylsilyl)amino)benzonitrile (3.34o)**



Heated for 180 min (yellow oil; 100% conversion).

$^1\text{H}$  NMR (400 MHz,  $\text{CDCl}_3$ ):  $\delta$  = 7.23 (d,  $J$  = 8.0 Hz, 2 H), 6.49 (d,  $J$  = 8.0 Hz, 2 H), 3.79 (s, 1 H), 0.14 (s, 9 H).

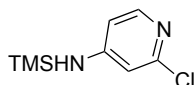
**5-(2-Chlorophenyl)-N-(trimethylsilyl)-1,3,4-oxadiazol-2-amine (3.34p)**



Heated for 60 min (white solid; 100% conversion).

$^1\text{H}$  NMR (400 MHz,  $\text{CDCl}_3$ ):  $\delta$  = 7.85 (d,  $J$  = 7.3 Hz, 1 H), 7.43 (d,  $J$  = 7.5 Hz, 1 H), 7.30 (m, 2 H), 5.45 (s, 1 H), 0.32 (s, 9 H).

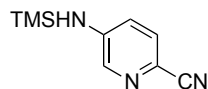
**2-Chloro-N-(trimethylsilyl)pyridin-4-amine (3.34q)**



Heated for 30 min (orange oil; 100% conversion).

$^1\text{H}$  NMR (400 MHz,  $\text{CDCl}_3$ ):  $\delta$  = 7.87 (d,  $J$  = 5.7 Hz, 1 H), 6.47 (s, 1 H), 6.38 (d,  $J$  = 5.6 Hz, 1 H), 4.09 (s, 1 H), 0.24 (s, 9 H).

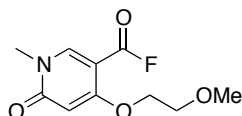
**5-((Trimethylsilyl)amino)picolinonitrile (3.34r)**



Heated for 6 h (orange solid; 85% conversion).

$^1\text{H}$  NMR (400 MHz,  $\text{CDCl}_3$ ):  $\delta$  = 8.01 (s, 1 H), 7.37 (d,  $J$  = 8.6 Hz, 1 H), 6.88 (d,  $J$  = 8.6 Hz, 1 H), 3.99 (s, 1 H), 0.26 (s, 9 H).

**4-(2-Methoxyethoxy)-1-methyl-6-oxo-1,6-dihydropyridine-3-carbonyl fluoride (3.51)**



A mixture of **3.47** (1.0 g, 4.40 mmol), TFFH (1.18 g, 4.40 mmol), and CsF (1.57 g, 10.3 mmol) in CH<sub>3</sub>CN (22 mL) was stirred for 12 h at room temperature. The mixture was then concentrated under reduced pressure and washed with hexanes to remove the tetramethylurea formed. The product mixture was then dissolved in DCM and filtered to remove the excess CsF. The filtrate was concentrated and dried under high vacuum for 2 days to afford **3.51** as a beige solid (0.91 g, 90%).

IR: 1814, 1778, 1678, 1617, 1530 cm<sup>-1</sup>.

<sup>1</sup>H NMR (400 MHz, CDCl<sub>3</sub>):  $\delta$  = 8.20 (s, 1 H), 5.91 (s, 1 H), 4.13 (t,  $J$  = 4.3 Hz, 2 H), 3.81 (t,  $J$  = 4.3 Hz, 2 H), 3.57 (s, 3 H), 3.46 (s, 3 H).

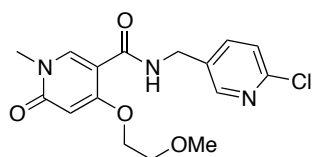
<sup>19</sup>F NMR (400 MHz, CDCl<sub>3</sub>):  $\delta$  = 25.43.

<sup>13</sup>C NMR (100 MHz, CDCl<sub>3</sub>):  $\delta$  = 165.6, 163.5, 154.1, 150.8, 148.1, 97.3, 70.1, 69.0, 59.6, 37.8.

### General procedure for the synthesis of **3.52a-r**

Acid fluoride **3.51** (200mg, 0.89 mmol) in CH<sub>3</sub>CN (5 mL) was added in one portion to the silylated amine **3.34a-r** (0.50 mmol) at room temperature. This was quickly followed by addition of 1M TBAF in THF (10  $\mu$ L, 0.01 mmol). The reaction mixture/solution was stirred at 50 °C for 12 h. The precipitated product was collected with suction filtration and washed with CH<sub>3</sub>CN or the specified solvent.

### *N*-((6-Chloropyridin-3-yl)methyl)-4-(2-methoxyethoxy)-1-methyl-6-oxo-1,6-dihydropyridine-3-carboxamide (**3.52a**)



From **3.34a**. The precipitated product was washed with CH<sub>3</sub>CN/Et<sub>2</sub>O (1:1) to afford **3.52a** as a white solid; yield: 274 mg (78%); mp 187-188 °C.

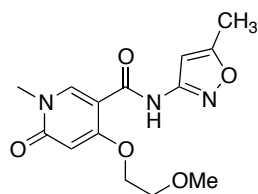
IR: 3393, 1675, 1632, 1528 cm<sup>-1</sup>.

<sup>1</sup>H NMR (400 MHz, DMSO-*d*<sub>6</sub>): δ = 8.37 (d, *J* = 2.4 Hz, 1 H), 8.28 (m, 2 H), 7.78 (dd, *J* = 2.5, 8.2 Hz, 1 H), 7.50 (d, *J* = 8.2 Hz, 1 H), 5.92 (s, 1 H), 4.49 (d, *J* = 5.9 Hz, 2 H), 4.19 (m, 2 H), 3.67 (m, 2 H), 3.42 (s, 3 H), 3.19 (s, 3 H).

<sup>13</sup>C NMR (100 MHz, DMSO-*d*<sub>6</sub>): δ = 163.7, 162.7, 162.5, 148.9, 148.8, 144.5, 138.9, 134.5, 124.0, 105.7, 96.3, 69.3, 68.0, 58.1, 36.3.

HRMS (HESI): *m/z* [M - H]<sup>-</sup> calcd for C<sub>16</sub>H<sub>17</sub>ClN<sub>3</sub>O<sub>4</sub>: 350.0913; found 350.0916.

**4-(2-Methoxyethoxy)-1-methyl-*N*-(5-methylisoxazol-3-yl)-6-oxo-1,6-dihydropyridine-3-carboxamide (3.52b)**



From **3.34b**. The precipitated product was washed with CH<sub>3</sub>CN to afford **3.52b** as a pale yellow solid; yield: 21 mg (7%); mp 179-181 °C.

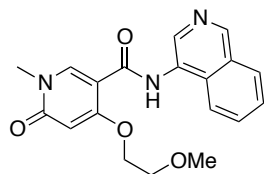
IR: 3337, 1685, 1660, 1612, 1548 cm<sup>-1</sup>.

<sup>1</sup>H NMR (400 MHz, CDCl<sub>3</sub>): δ = 9.98 (s, 1 H), 8.36 (s, 1 H), 6.71 (s, 1 H), 5.94 (s, 1 H), 4.24 (t, *J* = 3.8 Hz, 2 H), 3.85 (t, *J* = 3.7 Hz, 2 H), 3.58 (s, 3 H), 3.54 (s, 3 H), 2.41 (s, 3 H).

<sup>13</sup>C NMR (100 MHz, CDCl<sub>3</sub>): δ = 169.8, 163.9, 163.8, 160.8, 158.2, 145.9, 105.6, 97.3, 97.1, 69.6, 68.7, 59.6, 37.7, 12.8.

HRMS (HESI): *m/z* [M - H]<sup>+</sup> calcd for C<sub>14</sub>H<sub>16</sub>N<sub>3</sub>O<sub>5</sub>: 306.1095; found: 306.1102.

***N*-(Isoquinolin-4-yl)-4-(2-methoxyethoxy)-1-methyl-6-oxo-1,6-dihydropyridine-3-carboxamide (3.52c)**



From **3.34c**. The precipitated product was washed with Et<sub>2</sub>O to afford **3.52c** as a white solid; yield: 95 mg (27%); mp 213-214 °C.

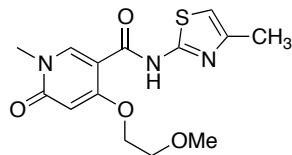
IR: 3286, 1664, 1627, 1543 cm<sup>-1</sup>.

<sup>1</sup>H NMR (400 MHz, DMSO-*d*<sub>6</sub>): δ = 9.88 (s, 1 H), 9.20 (s, 1 H), 8.85 (s, 1 H), 8.48 (s, 1 H), 8.20 (d, *J* = 8.5 Hz, 1 H), 8.06 (d, *J* = 8.5 Hz, 1 H), 7.87 (d, *J* = 15.2 Hz, 1 H), 7.75 (d, *J* = 15.2 Hz, 1 H), 6.07 (s, 1 H), 4.36 (m, 2 H), 3.80 (m, 2 H), 3.50 (s, 3 H), 3.19 (s, 3 H).

<sup>13</sup>C NMR (100 MHz, DMSO-*d*<sub>6</sub>): δ = 163.6, 162.8, 161.8, 149.5, 145.3, 138.4, 130.7, 130.0, 128.4, 128.3, 127.9, 127.7, 121.3, 105.8, 96.5, 69.4, 68.5, 58.2, 36.4.

HRMS (HESI): *m/z* [M + H]<sup>+</sup> calcd for C<sub>19</sub>H<sub>20</sub>N<sub>3</sub>O<sub>4</sub>: 354.1448; found: 354.1449.

**4-(2-Methoxyethoxy)-1-methyl-*N*-(4-methylthiazol-2-yl)-6-oxo-1,6-dihydropyridine-3-carboxamide (3.52d)**



From **3.34d**. The precipitated product was washed with Et<sub>2</sub>O to afford **3.52d** as a yellow solid; yield: 110 mg (34%); mp 189-190 °C.

IR: 3308, 1680, 1635, 1530 cm<sup>-1</sup>.

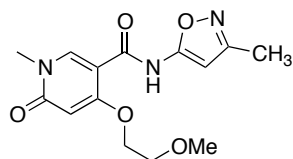


$^1\text{H}$  NMR (400 MHz, DMSO- $d_6$ ):  $\delta$  = 11.07 (s, 1 H), 8.48 (s, 1 H), 6.81 (s, 1 H), 6.00 (s, 1 H), 4.27 (m, 2 H), 3.75 (m, 2 H), 3.47 (s, 3 H), 3.40 (s, 3 H), 2.27 (s, 3 H).

$^{13}\text{C}$  NMR (100 MHz, DMSO- $d_6$ ):  $\delta$  = 163.3, 162.7, 160.3, 156.5, 147.0, 145.8, 108.4, 104.0, 96.4, 69.4, 68.5, 58.5, 36.5, 16.9.

HRMS (HESI):  $m/z$   $[\text{M} + \text{H}]^+$  calcd for  $\text{C}_{14}\text{H}_{18}\text{N}_3\text{O}_4\text{S}$ : 324.1013; found: 324.1015.

**4-(2-Methoxyethoxy)-1-methyl-*N*-(3-methylisoxazol-5-yl)-6-oxo-1,6-dihydropyridine-3-carboxamide (3.52e)**



From **3.34e**. The precipitated product was washed with  $\text{Et}_2\text{O}$  to afford **3.52e** as a white solid; yield: 163 mg (53%); mp 211-213  $^\circ\text{C}$ .

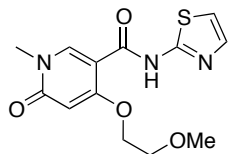
IR: 3306, 1694, 1656, 1610, 1528  $\text{cm}^{-1}$ .

$^1\text{H}$  NMR (400 MHz, DMSO- $d_6$ ):  $\delta$  = 10.72 (s, 1 H), 8.42 (s, 1 H), 6.24 (s, 1 H), 5.99 (s, 1 H), 4.25 (m, 2 H), 3.74 (m, 2 H), 3.46 (s, 3 H), 3.36 (s, 3 H), 2.21 (s, 3 H).

$^{13}\text{C}$  NMR (100 MHz, DMSO- $d_6$ ):  $\delta$  = 162.7, 160.8, 160.4, 159.1, 145.7, 104.6, 96.4, 89.3, 69.4, 68.3, 58.3, 36.5, 11.4.

HRMS (HESI):  $m/z$   $[\text{M} - \text{H}]^-$  calcd for  $\text{C}_{14}\text{H}_{16}\text{N}_3\text{O}_5$ : 306.1095; found: 306.1102.

**4-(2-Methoxyethoxy)-1-methyl-6-oxo-*N*-(thiazol-2-yl)-1,6-dihydropyridine-3-carboxamide (3.52f)**



From **3.34f**. The precipitated product was washed with Et<sub>2</sub>O to afford **3.52f** as a pale yellow solid; yield: 170 mg (55%); mp 185-186 °C.

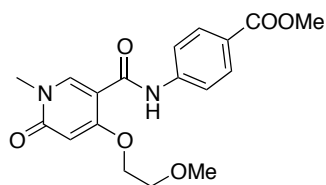
IR: 3311, 1678, 1632, 1612, 1530 cm<sup>-1</sup>.

<sup>1</sup>H NMR (400 MHz, DMSO-*d*<sub>6</sub>): δ = 11.14 (s, 1 H), 8.50 (s, 1 H), 7.50 (d, *J* = 3.5 Hz, 1 H), 7.27 (d, *J* = 3.5 Hz, 1 H), 6.01 (s, 1 H), 4.28 (m, 2 H), 3.76 (m, 2 H), 3.47 (s, 3 H), 3.38 (s, 3 H).

<sup>13</sup>C NMR (100 MHz, DMSO-*d*<sub>6</sub>): δ = 163.3, 162.7, 160.4, 157.3, 145.8, 138.0, 114.2, 104.0, 96.4, 69.4, 68.5, 58.5, 36.5.

HRMS (HESI): *m/z* [M - H]<sup>-</sup> calcd for C<sub>13</sub>H<sub>14</sub>N<sub>3</sub>O<sub>4</sub>S: 308.0711; found: 308.0696.

**Methyl 4-(4-(2-methoxyethoxy)-1-methyl-6-oxo-1,6-dihydropyridine-3-carboxamido)benzoate (3.52g)**



From **3.34g**. The precipitated product was washed with CH<sub>3</sub>CN to afford **3.52g** as a white solid; yield: 321 mg (89%); mp 213-215 °C.

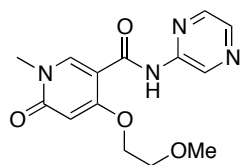
IR: 3348, 1688, 1656, 1592, 1527 cm<sup>-1</sup>.

<sup>1</sup>H NMR (400 MHz, CDCl<sub>3</sub>): δ = 9.76 (s, 1 H), 8.41 (s, 1 H), 8.03 (d, *J* = 8.6 Hz, 2 H), 7.73 (d, *J* = 8.6 Hz, 2 H), 6.04 (s, 1 H), 4.28 (t, *J* = 3.9 Hz, 2 H), 3.90 (m, 5 H), 3.61 (s, 3 H), 3.53 (s, 3 H).

<sup>13</sup>C NMR (100 MHz, CDCl<sub>3</sub>): δ = 166.8, 163.9, 163.7, 161.1, 145.7, 142.7, 130.9, 125.6, 119.5, 106.3, 97.3, 69.8, 68.0, 59.1, 52.2, 37.7.

HRMS (HESI):  $m/z$   $[M - H]^-$  calcd for  $C_{18}H_{19}N_2O_6$ : 359.1249; found: 359.1251.

**4-(2-Methoxyethoxy)-1-methyl-6-oxo-*N*-(pyrazin-2-yl)-1,6-dihydropyridine-3-carboxamide (3.52h)**



From **3.34h**. The precipitated product was washed with  $Et_2O$  to afford **3.52h** as a white solid; yield: 128 mg (42%); mp 191-193 °C.

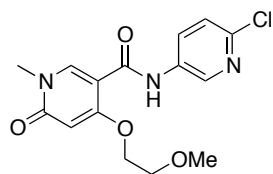
IR: 3331, 1693, 1645, 1528  $cm^{-1}$ .

$^1H$  NMR (400 MHz,  $DMSO-d_6$ ):  $\delta$  = 10.20 (s, 1 H), 9.44 (d,  $J$  = 1.5 Hz, 1 H), 8.53 (s, 1 H), 8.43 (m, 2 H), 6.01 (s, 1 H), 4.29 (m, 2 H), 3.76 (m, 2 H), 3.49 (s, 3 H), 3.36 (s, 3 H).

$^{13}C$  NMR (100 MHz,  $DMSO-d_6$ ):  $\delta$  = 163.3, 162.7, 161.1, 148.3, 146.2, 142.9, 140.2, 136.3, 104.5, 96.4, 69.5, 68.8, 58.4, 36.6.

HRMS (HESI):  $m/z$   $[M + Na]^+$  calcd for  $C_{14}H_{16}N_4O_4Na$ : 327.1064; found: 327.1062.

***N*-(6-Chloropyridin-3-yl)-4-(2-methoxyethoxy)-1-methyl-6-oxo-1,6-dihydropyridine-3-carboxamide (3.52i)**



From **3.34i**. The precipitated product was washed with  $CH_3CN$  to afford **3.52i** as a white solid; yield: 209 mg (62%); mp 195-196 °C.

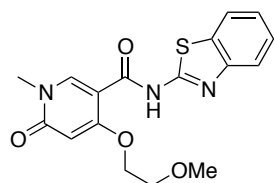
IR: 3329, 1694, 1649, 1596, 1529  $cm^{-1}$ .

$^1\text{H}$  NMR (400 MHz, DMSO- $d_6$ ):  $\delta$  = 9.96 (s, 1 H), 8.63 (d,  $J$  = 2.5 Hz, 1 H), 8.41 (s, 1 H), 8.16 (dd,  $J$  = 2.8, 8.7 Hz, 1 H), 7.54 (d,  $J$  = 8.8 Hz, 1 H), 6.00 (s, 1 H), 4.27 (m, 2 H), 3.79 (m, 2 H), 3.47 (s, 3 H), 3.33 (s, 3 H).

$^{13}\text{C}$  NMR (100 MHz, DMSO- $d_6$ ):  $\delta$  = 163.3, 162.7, 161.4, 145.2, 143.9, 140.8, 134.9, 130.2, 124.3, 105.6, 96.3, 69.4, 67.9, 58.1, 36.5.

HRMS (HESI):  $m/z$   $[\text{M} - \text{H}]^-$  calcd for  $\text{C}_{15}\text{H}_{15}\text{ClN}_3\text{O}_4$ : 336.0757; found: 336.0765.

***N*-(Benzo[d]thiazol-2-yl)-4-(2-methoxyethoxy)-1-methyl-6-oxo-1,6-dihydropyridine-3-carboxamide (3.52j)**



From **3.34j**. The precipitated product was washed with  $\text{CH}_3\text{CN}$  to afford to give **3.52j** as a white solid; yield: 255 mg (71%); mp 209-211  $^\circ\text{C}$ .

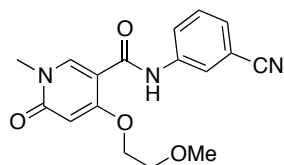
IR: 3302, 1684, 1640, 1600, 1530  $\text{cm}^{-1}$ .

$^1\text{H}$  NMR (400 MHz,  $\text{CDCl}_3$ ):  $\delta$  = 11.01 (s, 1 H), 8.45 (s, 1 H), 7.81 (dd,  $J$  = 7.9, 19.0 Hz, 2 H), 7.44 (t,  $J$  = 7.5 Hz, 1 H), 7.30 (t,  $J$  = 7.5 Hz, 1 H), 5.99 (s, 1 H), 4.34 (s, 2 H), 3.94 (s, 2 H), 3.64 (s, 3 H), 3.60 (s, 3 H).

$^{13}\text{C}$  NMR (100 MHz,  $\text{CDCl}_3$ ):  $\delta$  = 163.7, 161.1, 157.8, 148.4, 146.3, 132.4, 126.3, 124.1, 121.5, 121.1, 104.4, 97.5, 69.8, 68.9, 59.7, 37.8.

HRMS (HESI):  $m/z$   $[\text{M} - \text{H}]^-$  calcd for  $\text{C}_{17}\text{H}_{16}\text{N}_3\text{O}_4\text{S}$ : 358.0867; found: 358.0849.

***N*-(3-Cyanophenyl)-4-(2-methoxyethoxy)-1-methyl-6-oxo-1,6-dihydropyridine-3-carboxamide (3.52k)**



From **3.34k**. The precipitated product was washed with CH<sub>3</sub>CN and MeOH to afford **3.52k** as a white solid; yield: 278 mg (85%); mp 236-238 °C.

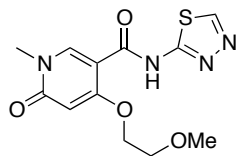
IR: 3356, 2227, 1690, 1649, 1591, 1555 cm<sup>-1</sup>.

<sup>1</sup>H NMR (400 MHz, DMSO-*d*<sub>6</sub>): δ = 9.98 (s, 1 H), 8.40 (s, 1 H), 8.09 (s, 1 H), 7.90 (td, *J* = 1.9, 7.6 Hz, 1 H), 7.58 (m, 2 H), 5.99 (s, 1 H), 4.27 (m, 2 H), 3.80 (m, 2 H), 3.47 (s, 3 H), 3.35 (s, 3 H).

<sup>13</sup>C NMR (100 MHz, DMSO-*d*<sub>6</sub>): δ = 163.3, 162.7, 161.3, 145.2, 139.4, 130.4, 127.2, 124.1, 122.3, 118.6, 111.7, 105.7, 96.3, 69.4, 68.0, 58.0, 36.5.

HRMS (HESI): *m/z* [M - H]<sup>-</sup> calcd for C<sub>17</sub>H<sub>16</sub>N<sub>3</sub>O<sub>4</sub>: 326.1146; found: 326.1152.

**4-(2-Methoxyethoxy)-1-methyl-6-oxo-*N*-(1,3,4-thiadiazol-2-yl)-1,6-dihydropyridine-3-carboxamide (3.52l)**



From **3.34l**. The precipitated product was washed with CH<sub>3</sub>CN to afford **3.52l** as a white solid; yield: 270 mg (87%); mp 234-236 °C.

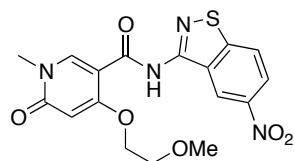
IR: 3308, 1686, 1636, 1611, 1528 cm<sup>-1</sup>.

$^1\text{H}$  NMR (400 MHz, DMSO- $d_6$ ):  $\delta$  = 11.51 (s, 1 H), 9.20 (s, 1 H), 8.51 (s, 1 H), 6.01 (s, 1 H), 4.28 (m, 2 H), 3.76 (m, 2 H), 3.47 (s, 3 H), 3.39 (s, 3 H).

$^{13}\text{C}$  NMR (100 MHz, DMSO- $d_6$ ):  $\delta$  = 163.4, 162.7, 160.9, 158.2, 149.2, 146.0, 103.8, 96.4, 69.4, 68.5, 58.5, 36.5.

HRMS (HESI):  $m/z$   $[\text{M} - \text{H}]^-$  calcd for  $\text{C}_{12}\text{H}_{13}\text{N}_4\text{O}_4\text{S}$ : 309.0663; found: 309.0647.

**4-(2-Methoxyethoxy)-1-methyl-*N*-(5-nitrobenzo[d]isothiazol-3-yl)-6-oxo-1,6-dihydropyridine-3-carboxamide (1E5)**



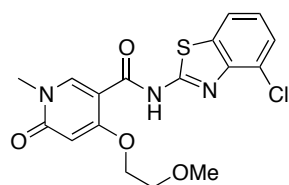
From **3.34m**. The precipitated product was washed with  $\text{CH}_3\text{CN}$  and acetone to afford **1E5** as a yellow solid; yield: 242 mg (60%); mp 296-298 °C.

IR: 3297, 1692, 1638, 1610, 1511  $\text{cm}^{-1}$ .

$^1\text{H}/^{13}\text{C}$  NMR: see reference 30.

HRMS (HESI):  $m/z$   $[\text{M} - \text{H}]^-$  calcd for  $\text{C}_{17}\text{H}_{15}\text{N}_4\text{O}_6\text{S}$ : 403.0718; found: 403.0695.

***N*-(4-Chlorobenzo[d]thiazol-2-yl)-4-(2-methoxyethoxy)-1-methyl-6-oxo-1,6-dihydropyridine-3-carboxamide (3.52n)**



From **3.34n**. The precipitated product was washed with  $\text{CH}_3\text{CN}$  to afford **3.52n** as a white solid; yield: 362 mg (92%); mp 266-267 °C.

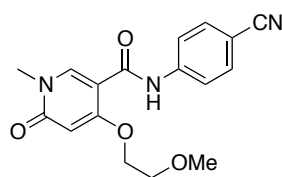
IR: 3288, 1684, 1638, 1589, 1527  $\text{cm}^{-1}$ .

$^1\text{H}$  NMR (400 MHz,  $\text{DMSO}-d_6$ ):  $\delta$  = 11.61 (s, 1 H), 8.55 (s, 1 H), 7.99 (d,  $J$  = 7.5 Hz, 1 H), 7.54 (dd,  $J$  = 7.8 Hz, 1 H), 7.32 (t,  $J$  = 7.9 Hz, 1 H), 6.02 (s, 1 H), 4.29 (m, 2 H), 3.79 (m, 2 H), 3.48 (s, 6 H).

$^{13}\text{C}$  NMR (100 MHz,  $\text{DMSO}-d_6$ ):  $\delta$  = 163.4, 162.7, 161.7, 158.4, 146.2, 145.4, 133.4, 126.3, 124.6, 124.5, 120.9, 103.8, 96.4, 69.5, 68.6, 58.8, 36.5.

HRMS (HESI):  $m/z$   $[\text{M} - \text{H}]^-$  calcd for  $\text{C}_{17}\text{H}_{15}\text{ClN}_3\text{O}_4\text{S}$ : 392.0477; found: 392.0461.

***N*-(4-Cyanophenyl)-4-(2-methoxyethoxy)-1-methyl-6-oxo-1,6-dihydropyridine-3-carboxamide (3.52o)**



From **3.34o**. The precipitated product was washed with MeOH to afford **3.52o** as a white solid; yield: 265 mg (81%); mp 249-251  $^{\circ}\text{C}$ .

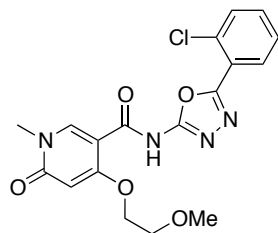
IR: 3364, 2219, 1687, 1645, 1589, 1527  $\text{cm}^{-1}$ .

$^1\text{H}$  NMR (400 MHz,  $\text{DMSO}-d_6$ ):  $\delta$  = 10.06 (s, 1 H), 8.40 (s, 1 H), 7.83 (s, 4 H), 5.99 (s, 1 H), 4.27 (m, 2 H), 3.78 (m, 2 H), 3.47 (s, 3 H), 3.33 (s, 3 H).

$^{13}\text{C}$  NMR (100 MHz,  $\text{DMSO}-d_6$ ):  $\delta$  = 163.3, 162.7, 161.4, 145.2, 142.8, 133.4, 119.6, 119.0, 105.9, 105.4, 96.3, 69.4, 68.0, 58.1, 36.4.

HRMS (HESI):  $m/z$   $[\text{M} - \text{H}]^-$  calcd for  $\text{C}_{17}\text{H}_{16}\text{N}_3\text{O}_4$ : 326.1146; found: 326.1153.

***N*-(5-(2-Chlorophenyl)-1,3,4-oxadiazol-2-yl)-4-(2-methoxyethoxy)-1-methyl-6-oxo-1,6-dihydropyridine-3-carboxamide (3.52p)**



From **3.34p**. The precipitated product was washed with CH<sub>3</sub>CN to afford **3.52p** as a pale yellow solid; yield: 255 mg (63%); mp 190-192 °C.

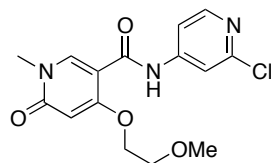
IR: 3289, 1698, 1667, 1594, 1528 cm<sup>-1</sup>.

<sup>1</sup>H NMR (400 MHz, DMSO-*d*<sub>6</sub>): δ = 11.09 (s, 1 H), 8.41 (s, 1 H), 7.93 (dd, *J* = 1.7 , 7.7 Hz, 1 H), 7.64 (dddd, *J* = 1.2, 7.8, 15.0, 27 Hz, 3 H), 5.98 (s, 1 H), 4.22 (m, 2 H), 3.71 (m, 2 H), 3.46 (s, 3 H), 3.31 (s, 3 H).

<sup>13</sup>C NMR (100 MHz, DMSO-*d*<sub>6</sub>): δ = 163.3, 162.7, 160.4, 158.9, 157.6, 145.6, 133.1, 131.6, 131.1, 131.0, 127.9, 122.5, 105.1, 96.3, 69.4, 68.4, 58.3, 36.5.

HRMS (HESI): *m/z* [M - H]<sup>-</sup> calcd for C<sub>18</sub>H<sub>16</sub>ClN<sub>4</sub>O<sub>5</sub>: 403.0815; found: 403.0823.

***N*-(2-Chloropyridin-4-yl)-4-(2-methoxyethoxy)-1-methyl-6-oxo-1,6-dihydropyridine-3-carboxamide (3.52q)**



From **3.34q**. The precipitated product was washed with CH<sub>3</sub>CN to afford **3.52q** as a white solid; yield: 148 mg (44%); mp 228-229 °C.

IR: 3332, 1700, 1655, 1580, 1509 cm<sup>-1</sup>.

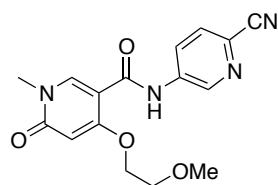


$^1\text{H}$  NMR (400 MHz, DMSO- $d_6$ ):  $\delta$  = 10.16 (s, 1 H), 8.41 (s, 1 H), 8.32 (d,  $J$  = 5.6 Hz, 1 H), 7.75 (d,  $J$  = 1.5 Hz, 1 H), 7.58 (dd,  $J$  = 1.7, 5.6 Hz, 1 H), 6.00 (s, 1 H), 4.26 (m, 2 H), 3.78 (m, 2 H), 3.47 (s, 3 H), 3.34 (s, 3 H).

$^{13}\text{C}$  NMR (100 MHz, DMSO- $d_6$ ):  $\delta$  = 163.7, 163.1, 162.5, 151.5, 151.0, 148.2, 146.0, 113.5, 113.3, 106.0, 96.7, 69.9, 68.5, 58.5, 37.0.

HRMS (HESI):  $m/z$   $[\text{M} - \text{H}]^-$  calcd for  $\text{C}_{15}\text{H}_{15}\text{ClN}_3\text{O}_4$ : 336.0757; found: 336.0764.

***N*-(6-Cyanopyridin-3-yl)-4-(2-methoxyethoxy)-1-methyl-6-oxo-1,6-dihydropyridine-3-carboxamide (3.52r)**



From **3.34r**. The precipitated product was washed with  $\text{CH}_3\text{CN}/\text{Et}_2\text{O}$  (1:1) to afford **3.52r** as a pale yellow solid; yield: 220 mg (67%); mp 255-256 °C.

IR: 3312, 2225, 1684, 1648, 1580, 1540  $\text{cm}^{-1}$ .

$^1\text{H}$  NMR (400 MHz, DMSO- $d_6$ ):  $\delta$  = 10.22 (s, 1 H), 8.87 (d,  $J$  = 2.1 Hz, 1 H), 8.43 (s, 1 H), 8.36 (dd,  $J$  = 2.3, 8.6 Hz, 1 H), 8.05 (d,  $J$  = 8.7 Hz, 1 H), 6.01 (s, 1 H), 4.27 (m, 2 H), 3.79 (m, 2 H), 3.47 (s, 3 H).

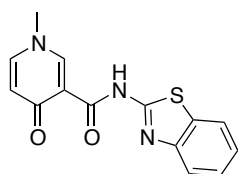
$^{13}\text{C}$  NMR (100 MHz, DMSO- $d_6$ ):  $\delta$  = 163.2, 162.7, 161.9, 145.4, 142.3, 138.5, 129.8, 126.3, 126.2, 117.7, 105.5, 96.3, 69.4, 68.0, 58.0, 36.5.

HRMS (HESI):  $m/z$   $[\text{M} - \text{H}]^-$  calcd for  $\text{C}_{16}\text{H}_{15}\text{N}_4\text{O}_4$ : 327.1099; found: 327.1106.

**General procedure for synthesis of 3.57j, 3.57l, 3.57n, 3.57t, 3.57u, 3.57v, 3.57w, 3.57x, 3.57y**

A solution of methyl ester **3.59** (1.2 mmol, 2 equivs) in MeCN (2 mL) was transferred to a narrow vial (diameter: 1-1.5 cm; height: 8-15 cm) containing the requisite N-silylated amine **3.34** (0.6 mmol), and the mixture was stirred for 10 min under nitrogen. Then, TBAF 1 M in THF (0.15 mmol) was added and the solution was stirred at 50 °C overnight (16 h). After heating, the precipitated product was collected by suction filtration and washed with cold MeCN.

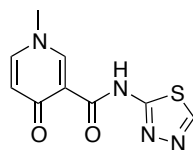
**N-(Benzo[d]thiazol-2-yl)-1-methyl-4-oxo-1,4-dihydropyridine-3-carboxamide (3.57j)**



From TMS-amine **3.34j**. The precipitated product was washed with cold CH<sub>3</sub>CN to afford **3.57j** as a white solid; yield: 129 mg (75%).

<sup>1</sup>H NMR (400 MHz, DMSO-*d*<sub>6</sub>): δ = 14.44 (s, 1 H), 8.77 (d, *J* = 2.4 Hz, 1 H), 8.01 (d, *J* = 7.8 Hz, 1 H), 7.96 (d, *J* = 7.5, 2.4 Hz, 1 H), 7.78 (d, *J* = 8.1 Hz, 1 H), 7.45 (t, *J* = 7.6 Hz, 1 H), 7.33 (t, *J* = 7.9 Hz, 1 H), 6.66 (d, *J* = 7.4 Hz, 1 H), 3.88 (s, 3 H).

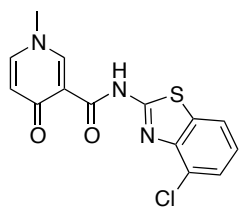
**1-Methyl-4-oxo-N-(1,3,4-thiadiazol-2-yl)-1,4-dihydropyridine-3-carboxamide (3.57l)**



From TMS-amine **3.34l**. The precipitated product was washed with cold CH<sub>3</sub>CN to afford **3.57l** as a white solid; yield: 124 mg (88%).

$^1\text{H}$  NMR (400 MHz, DMSO- $d_6$ ):  $\delta$  = 14.61 (s, 1 H), 9.21 (s, 1 H), 8.75 (d,  $J$  = 2.4 Hz, 1 H), 7.96 (dd,  $J$  = 7.5, 2.3 Hz, 1 H), 6.66 (d,  $J$  = 7.5 Hz, 1 H), 3.87 (s, 3 H).

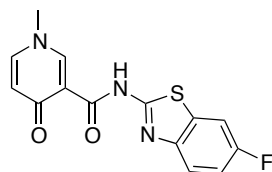
**N-(4-Chlorobenzo[d]thiazol-2-yl)-1-methyl-4-oxo-1,4-dihydropyridine-3-carboxamide**  
**(3.57n)**



From TMS-amine **3.34n**. The precipitated product was washed with cold  $\text{CH}_3\text{CN}$  to afford **3.57n** as a white solid; yield: 173 mg (90%).

$^1\text{H}$  NMR (400 MHz, DMSO- $d_6$ ):  $\delta$  = 14.58 (s, 1 H), 8.79 (s, 1 H), 7.99 (m, 2 H), 7.55 (d,  $J$  = 7.6 Hz, 1 H), 7.32 (t,  $J$  = 8.0 Hz, 1 H), 6.69 (d,  $J$  = 7.5 Hz, 1 H), 3.88 (s, 3 H).

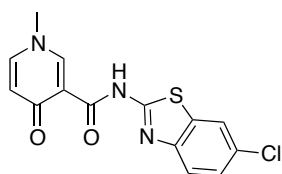
**N-(6-Fluorobenzo[d]thiazol-2-yl)-1-methyl-4-oxo-1,4-dihydropyridine-3-carboxamide**  
**(3.57t)**



From TMS-amine **3.34t**. The precipitated product was washed with cold  $\text{CH}_3\text{CN}$  to afford **3.57t** as a white solid; yield: 168 mg (92%).

$^1\text{H}$  NMR (400 MHz,  $\text{DMSO-}d_6$ ):  $\delta$  = 14.47 (s, 1 H), 8.78 (d,  $J$  = 2.2 Hz, 1 H), 7.94 (ddd,  $J$  = 2.3, 7.8, 10.6 Hz, 2 H), 7.79 (dd,  $J$  = 5.0, 8.7 Hz, 1 H), 7.31 (td,  $J$  = 2.9, 9.1 Hz, 1 H), 6.66 (d,  $J$  = 7.4 Hz, 1 H), 3.88 (s, 3 H).

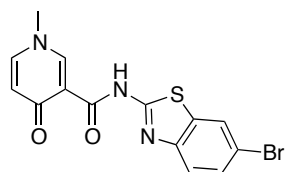
**N-(6-Chlorobenzo[d]thiazol-2-yl)-1-methyl-4-oxo-1,4-dihydropyridine-3-carboxamide**  
**(3.57u)**



From TMS-amine **3.34u**. The precipitated product was washed with cold  $\text{CH}_3\text{CN}$  to afford **3.57u** as a white solid; yield: 175 mg (91%).

$^1\text{H}$  NMR (400 MHz,  $\text{DMSO-}d_6$ ):  $\delta$  = 14.53 (s, 1 H), 8.77 (d,  $J$  = 2.3 Hz, 1 H), 8.16 (d,  $J$  = 2.1 Hz, 1 H), 7.96 (dd,  $J$  = 2.1, 7.1 Hz, 1 H), 7.77 (d,  $J$  = 8.6 Hz, 1 H), 7.47 (dd,  $J$  = 2.1, 8.8 Hz, 1 H), 6.66 (d,  $J$  = 7.5 Hz, 1 H), 3.88 (s, 3 H).

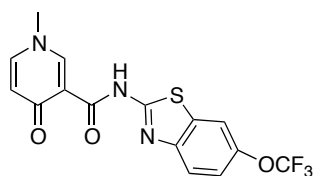
**N-(6-Bromobenzo[d]thiazol-2-yl)-1-methyl-4-oxo-1,4-dihydropyridine-3-carboxamide**  
**(3.57v)**



From TMS-amine **3.34v**. The precipitated product was washed with cold  $\text{CH}_3\text{CN}$  to afford **3.57v** as a white solid; yield: 170 mg (78%).

$^1\text{H}$  NMR (400 MHz,  $\text{DMSO}-d_6$ ):  $\delta$  = 14.53 (s, 1 H), 8.77 (d,  $J$  = 2.3 Hz, 1 H), 8.29 (d,  $J$  = 2.2 Hz, 1 H), 7.96 (dd,  $J$  = 2.4, 7.6 Hz, 1 H), 7.72 (d,  $J$  = 8.7 Hz, 1 H), 7.59 (dd,  $J$  = 2.1, 8.6 Hz, 1 H), 6.66 (d,  $J$  = 7.5 Hz, 1 H), 3.88 (s, 3 H).

**1-Methyl-4-oxo-N-(6-(trifluoromethoxy)benzo[d]thiazol-2-yl)-1,4-dihydropyridine-3-carboxamide (3.57w)**

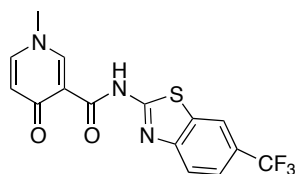


From TMS-amine **3.34w**. The precipitated product was washed with cold  $\text{CH}_3\text{CN}$  to afford **3.57w** as a white solid; yield: 167 mg (75%).

$^1\text{H}$  NMR (400 MHz,  $\text{DMSO}-d_6$ ):  $\delta$  = 14.56 (s, 1 H), 8.78 (d,  $J$  = 2.3 Hz, 1 H), 8.16 (d,  $J$  = 2.6 Hz, 1 H), 7.96 (dd,  $J$  = 2.3, 7.4 Hz, 1 H), 7.86 (d,  $J$  = 8.8 Hz, 1 H), 7.44 (dd,  $J$  = 2.5, 8.6 Hz, 1 H), 6.67 (d,  $J$  = 7.4 Hz, 1 H), 3.88 (s, 3 H).

$^{19}\text{F}$  NMR (400 MHz,  $\text{DMSO}-d_6$ ):  $\delta$  = - 56.99.

**1-Methyl-4-oxo-N-(6-(trifluoromethyl)benzo[d]thiazol-2-yl)-1,4-dihydropyridine-3-carboxamide (3.57x)**

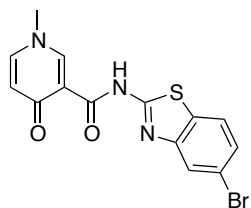


From TMS-amine **3.34x**. The precipitated product was washed with cold  $\text{CH}_3\text{CN}$  to afford **3.57x** as a white solid; yield: 119 mg (56%).

$^1\text{H}$  NMR (400 MHz,  $\text{DMSO-}d_6$ ):  $\delta$  = 14.67 (s, 1 H), 8.79 (d,  $J$  = 2.3 Hz, 1 H), 8.53 (s, 1 H), 7.96 (ddd,  $J$  = 1.7, 7.5, 8.9 Hz, 2 H), 7.76 (dd,  $J$  = 1.8, 8.7 Hz, 1 H), 6.68 (d,  $J$  = 7.4 Hz, 1 H), 3.89 (s, 3H).

$^{19}\text{F}$  NMR (400 MHz,  $\text{DMSO-}d_6$ ):  $\delta$  = -59.43.

**N-(5-Bromobenzo[d]thiazol-2-yl)-1-methyl-4-oxo-1,4-dihydropyridine-3-carboxamide (3.57y)**



From TMS-amine **3.34y**. The precipitated product was washed with cold  $\text{CH}_3\text{CN}$  to afford **3.57y** as a white solid; yield: 152 mg (70%).

$^1\text{H}$  NMR (400 MHz,  $\text{DMSO-}d_6$ ):  $\delta$  = 14.56 (s, 1 H), 8.78 (d,  $J$  = 2.3 Hz, 1 H), 7.99 (m, 3 H), 7.49 (dd,  $J$  = 2.0, 8.5 Hz, 1 H), 6.67 (d,  $J$  = 7.4 Hz, 1 H), 3.89 (s, 3 H).

## **Chapter 4: Targeting HIV rev function: discovery of 4.25kk (GPS488) and 4.25ww (GPS491)**

Compound 5350150, identified by random screening of a commercial compound library, inhibits HIV replication by altering rev function. Evidence at the time suggested that this results from a shifting of rev's subcellular distribution, which causes in a reduction in gag and env expression and decrease in the concentration of HIV-1 un-spliced (US) mRNAs in the cytoplasm.<sup>26</sup> In contrast to **1C8**, this molecule works without affecting splice site usage, the total abundance of HIV-1 mRNAs, or host cell alternative mRNA splicing. It is very likely that compound 5350150 targets rev function by altering the abundance of regulatory factors needed for rev translocation between cytoplasm and nucleus. This is done without modulating rev expression. SR proteins play a role in this process. The objective in this chapter is to use 5350150 as a starting point for the development of another new type of anti-HIV agent targeting HIV mRNA processing. This research led to the identification of two lead compounds, **4.25kk** (GPS488) and **4.25ww** (GPS491).

### **4.1 Role of SR proteins in mRNA export**

SR proteins are positive regulators of HIV-1 alternative splicing. These proteins mediate spliceosome complex formation in their phosphorylated form but once they are dephosphorylated, splicing catalysis starts.<sup>89</sup> As shown in Figure 4.1, once fully spliced transcripts are made, a subset of SR proteins, acting as adaptor molecules, facilitate their export from the nucleus. In the cytoplasm, these SR proteins are phosphorylated, and mature mRNAs

are released. Phosphorylated SR proteins can go back to the nucleus for another round of splicing event while the newly exported fully spliced mRNAs are translated into HIV proteins: rev, nef, vpr, and tat. In early phase of HIV-1 expression, only these 4 viral proteins are expressed (Figure 4.2) because in eukaryotic cells, only fully spliced mRNAs can leave the nucleus.<sup>32, 90</sup> However, HIV escapes this barrier by expressing the protein rev, which shuttles un-spliced (US) and singly spliced (SS) HIV-1 mRNAs from nucleus to the cytoplasm. Therefore, in the late phase of HIV-1 expression, env, vpu, vif, tat, and vpr proteins and gag and pol precursor proteins are formed.

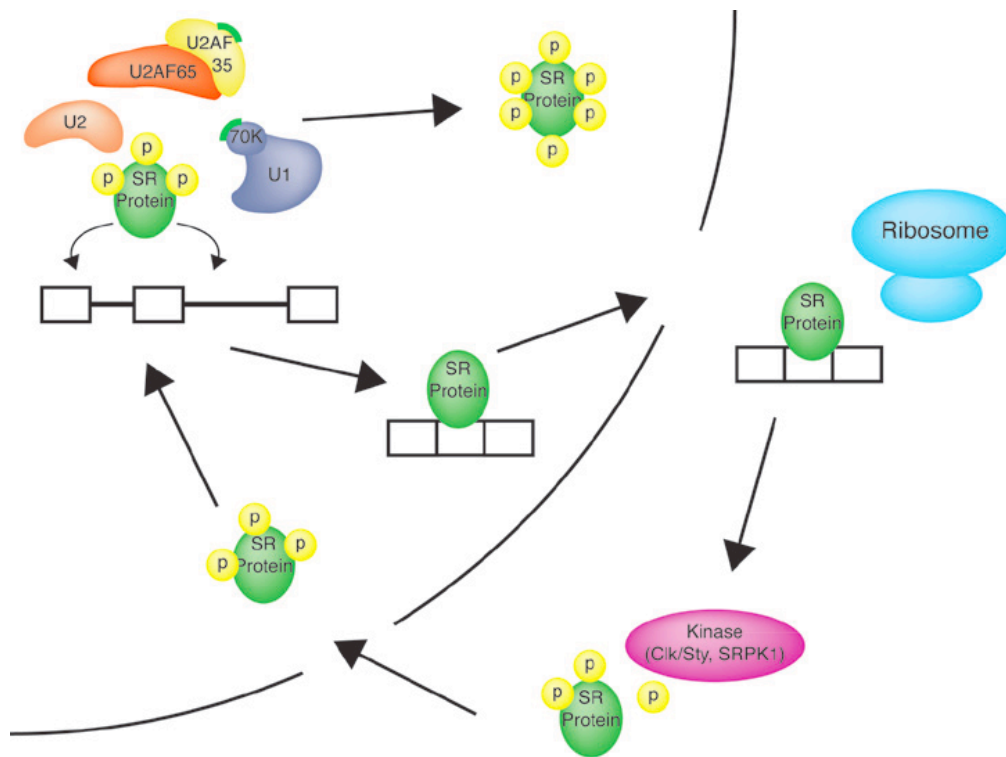


**Figure 4.1 A subset of SR proteins facilitate the export of fully spliced mRNAs from nucleus into cytoplasm.**

Adapted with permission from literature<sup>89</sup>



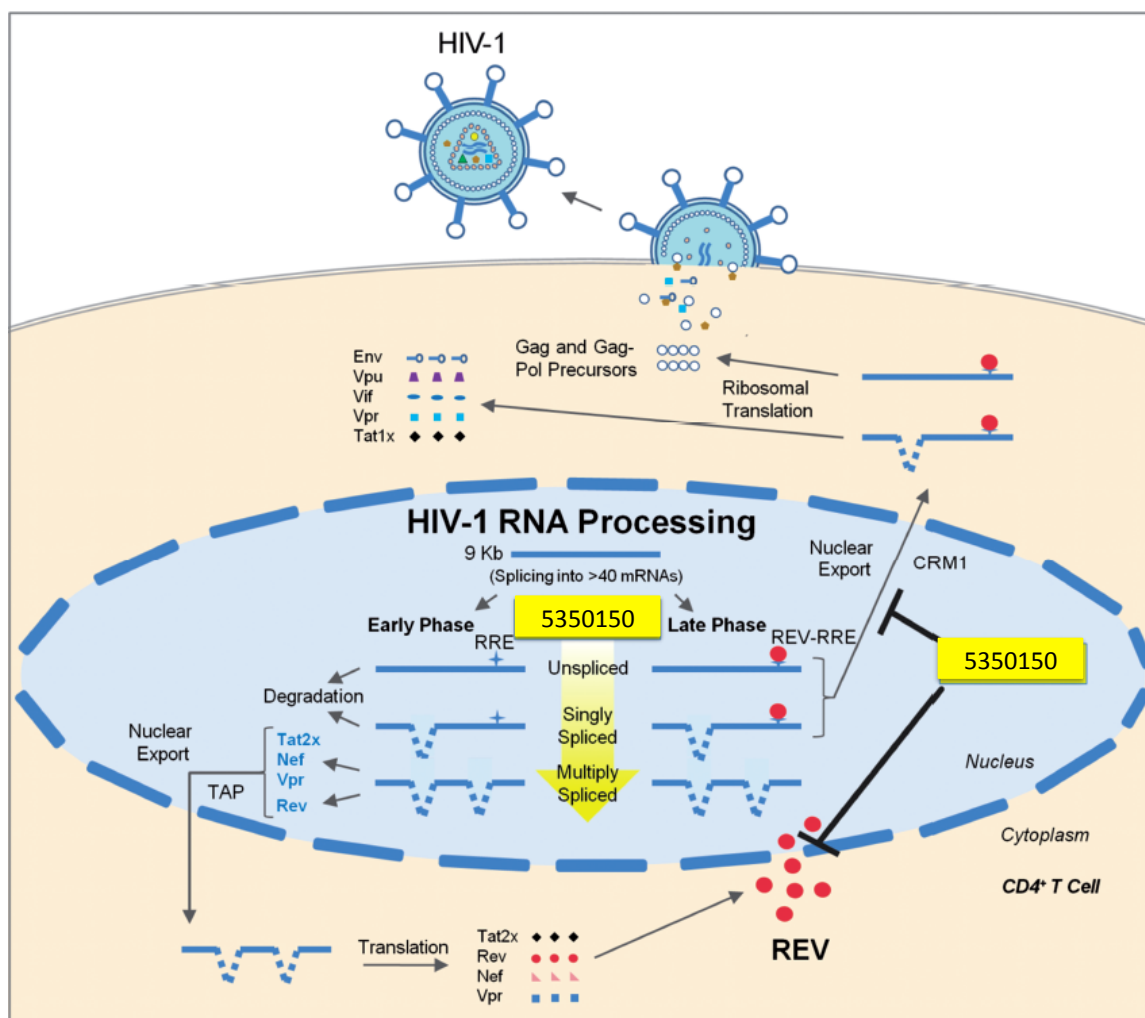


**Figure 4.2 Compound 5350150 inhibits HIV replication by altering rev function. Adapted with permission from literature<sup>26</sup>**

Both US and SS mRNAs express rev-response element (RRE), which binds to rev, and moves into cytoplasm after forming a complex with CRM1 and Ran-GTP as it is illustrated in Figure 4.3.<sup>90</sup> CRM1 is a transport factor<sup>91</sup> that binds to nuclear export signal (NES) in rev. Ran is a GTPase enzyme which hydrolyzes GTP to GDP. The shuttling of incompletely spliced mRNAs from the nucleus into the cytoplasm also requires association of two nucleoporins, Nup214 and

Nup98, which are part of the nuclear pore complex. Once moved into the cytoplasm, Ran-GTP is hydrolyzed into Ran-GDP, causing the complex to dissociate releasing US and SS mRNAs. Discharged CRM1 goes back to nucleus while rev forms a complex with importin $\beta$  (a transport factor) and Ran-GDP and moves back to nucleus. In the nucleus, Ran-GTP is hydrolyzed to Ran-GDP releasing rev, which is now available for another round of export.

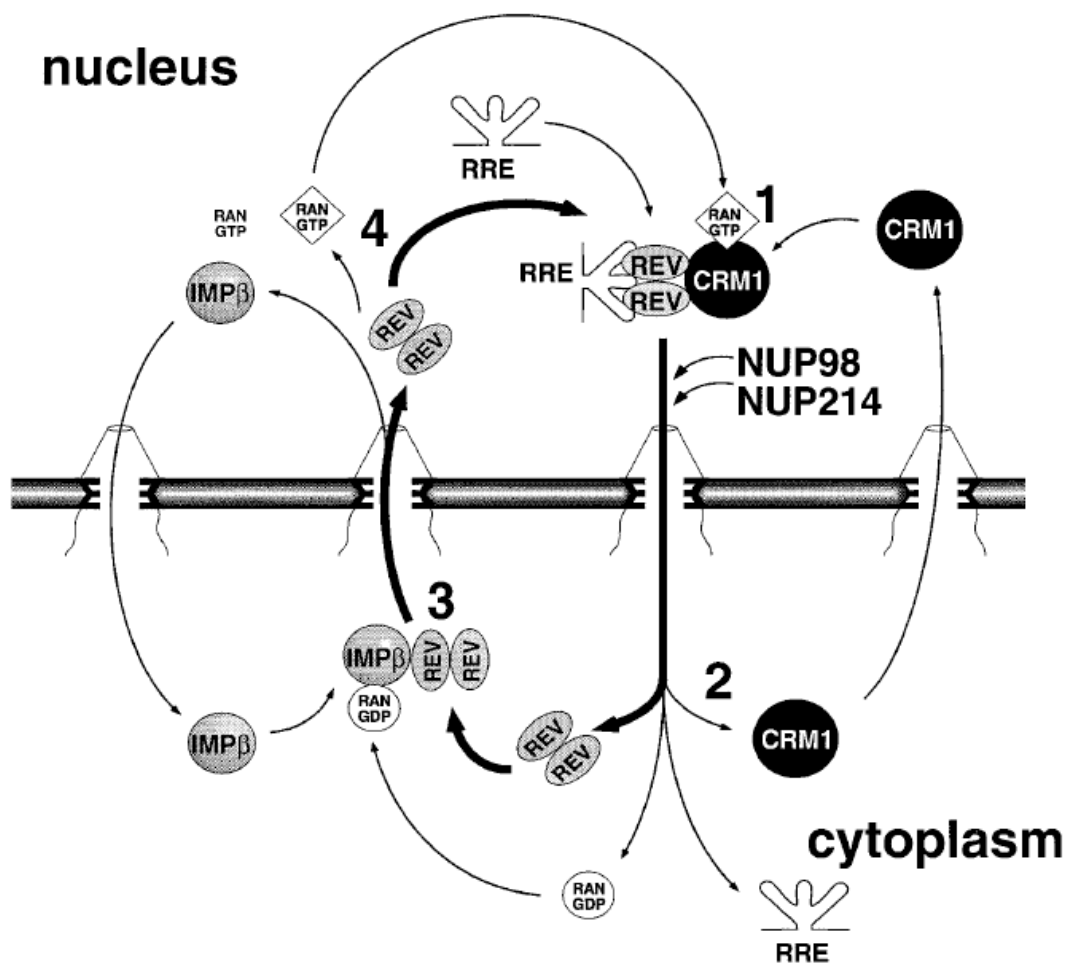
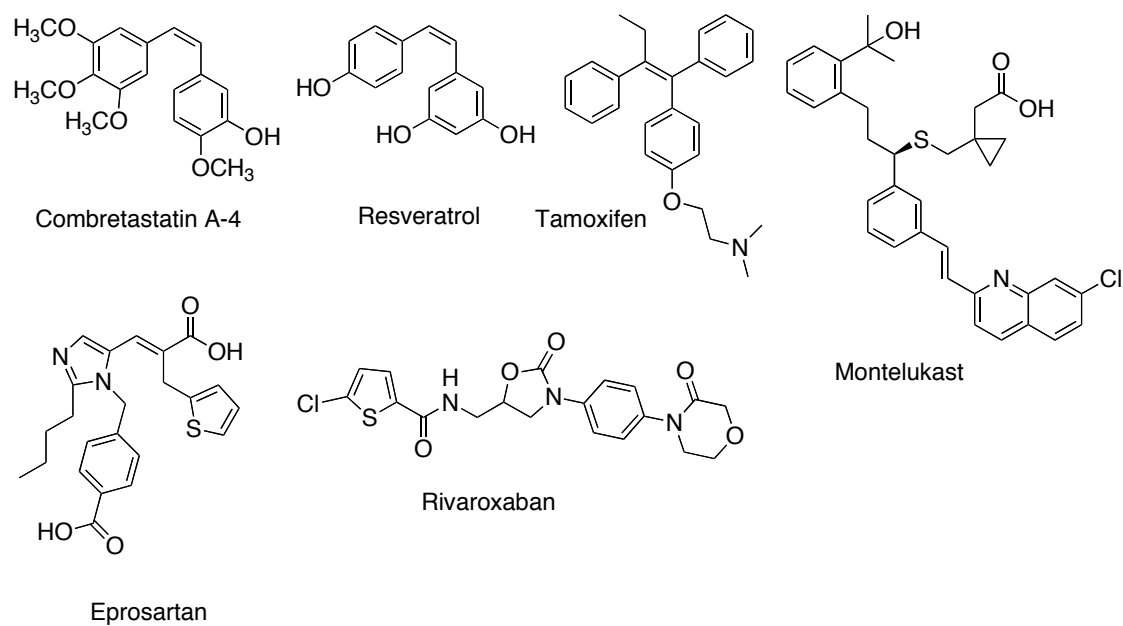


Figure 4.3 HIV rev protein mediates movement of US and SS mRNAs from nucleus into cytoplasm. Adapted with permission from literature <sup>90</sup>

Expression of skeletal and accessory viral proteins and formation of viral RNA genome for HIV-1 replication are very dependent on rev function. Having such a vital role on HIV-1 life cycle, rev function seems to be a sensible target in the search for a new class of anti-HIV-1 drugs.

## **4.2 Conception and design of 5350150-amide analogues**

Although an interesting hit, compound 5350150 is a photolabile molecule,<sup>27, 28</sup> and inherently cytotoxic in vivo. This negates any possibility of using it in prolonged ART. Although stilbene-type compounds have been extensively investigated for their biological properties<sup>92</sup> (e.g., combretastatin A-4 and resveratrol in Figure 4.4), and therapeutic properties (e.g., tamoxifen and montelukast in Figure 4.4), it was considered probable that the toxic properties observed by us for 5350150 (Figure 4.5) would most probably be associated with the C=C double bond that enables conjugation through the thiophene ring to the nitro substituent. The sulfur atom in the molecule could also be a source of toxicity (bioactivation), but a thiophene motif has been successfully used in drug development as a bioisostere of a phenyl ring.<sup>93</sup> For example, both eprosartan and rivaroxaban (Figure 4.4) have thiophene moieties in their structures but they don't form any reactive metabolites from their thiophene ring. These two drugs are used for hypertension and anticoagulant treatments, respectively.



**Figure 4.4** Few examples of biologically active molecules bearing stilbene or thiophene moiety.

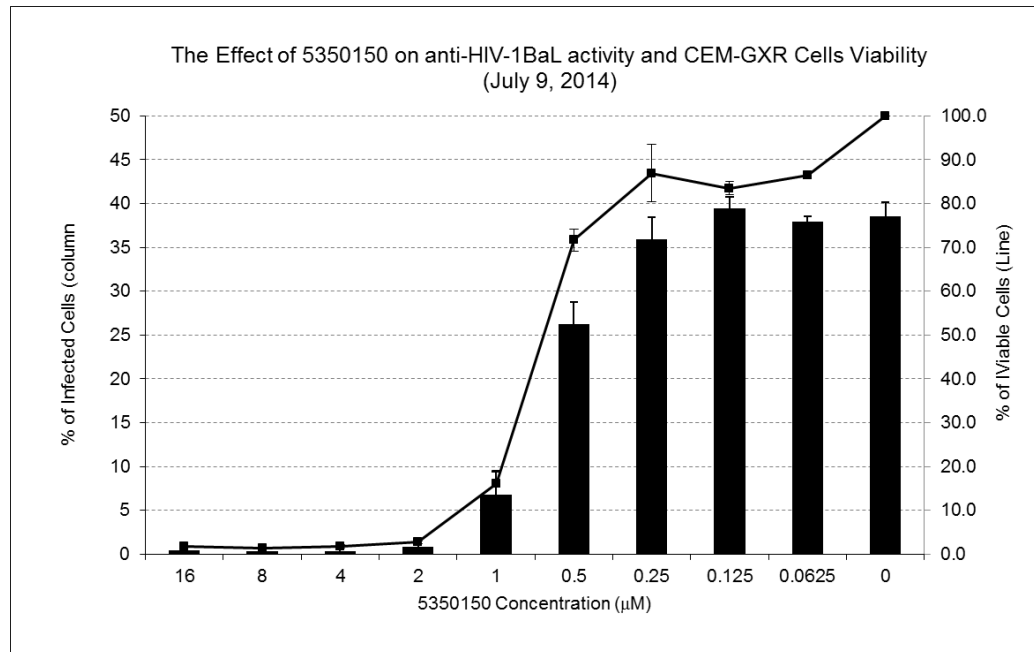


**Figure 4.5** The anti-HIV activity and viability of 5350150

Although 5350150 manifested its activity at concentrations inferior to its toxicity threshold, any effort to exploit the anti-HIV properties of this system would have to begin with replacement of the central stilbene double bond. Taking into consideration that a C=C is an amide bioisostere, one obvious strategy to identify less toxic compounds will be to prepare and evaluate the corresponding more drug-like amide analogues.<sup>94</sup> In terms of geometry, both –CONH– and C=C are planar. Furthermore, the amide modification may improve drug-like character (e.g., stability) of the derived molecules.

However, it was necessary to keep in mind that the most obvious **IDC16** mimic, where the **A**- and **D**-rings were conserved and the **B/C**-rings were replaced by a –CONH– motif was inactive. Indeed, it proved necessary to synthesize a library of **IDC16** mimics in order to identify active molecules. Consequently, it was not certain that the simple C=C double bond isostere replacement in 5350150 itself would result in a 5350150-amide analogue displaying activity. For this reason, we embarked on a new library synthesis project to prepare 5350150 analogues in which the right side quinoline component was replaced by diverse aromatic and mono and bicyclic heteroaromatic systems.

Our acid fluoride-N-silylated amine coupling protocol from Chapter 3 has been effective for the rapid parallel library synthesis of amide analogues of 5350150. Further, depending upon the results obtained, additional exploration would involve replacing the nitro substituent and thiophene ring by other motifs and varying the position of attachment of the amide motif to the left side component. These planned objectives for our library synthesis and SAR exploration are illustrated in Figure 4.6.

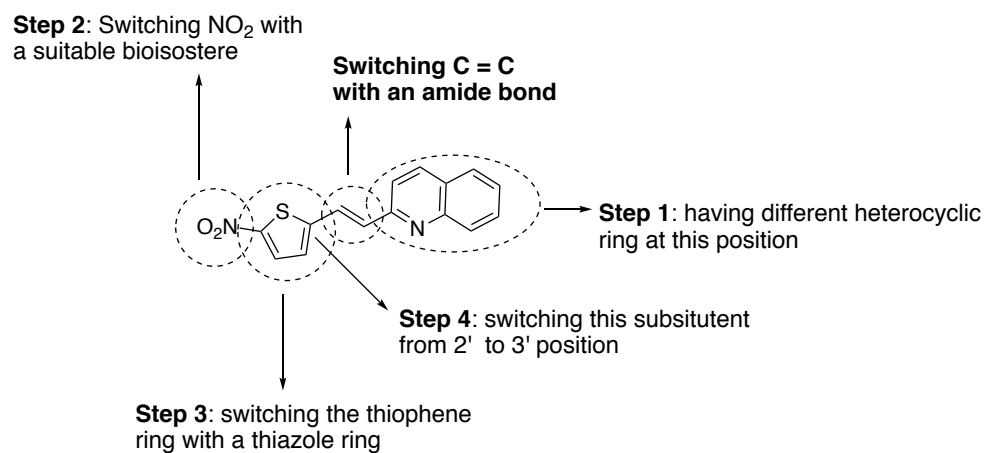


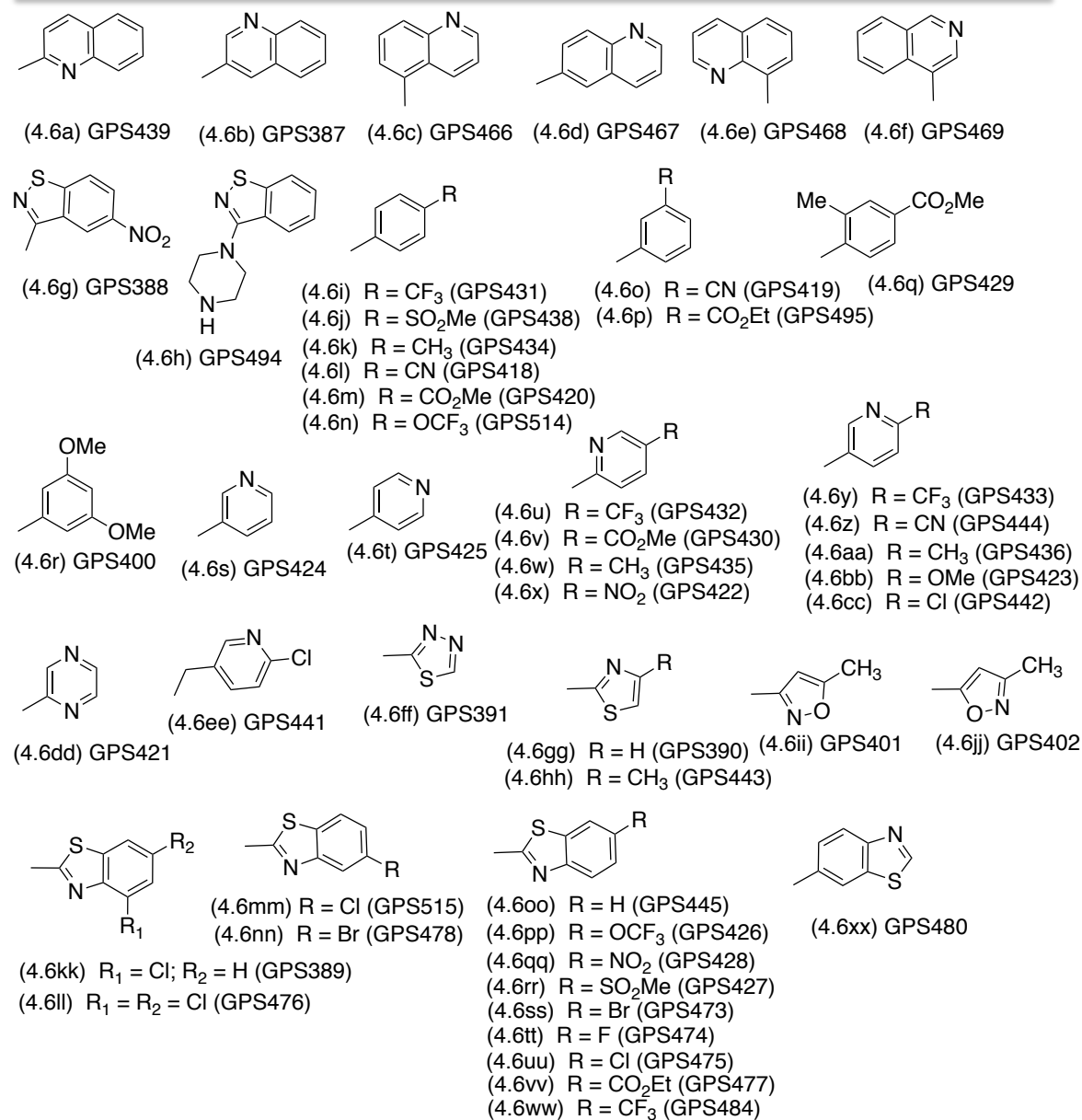
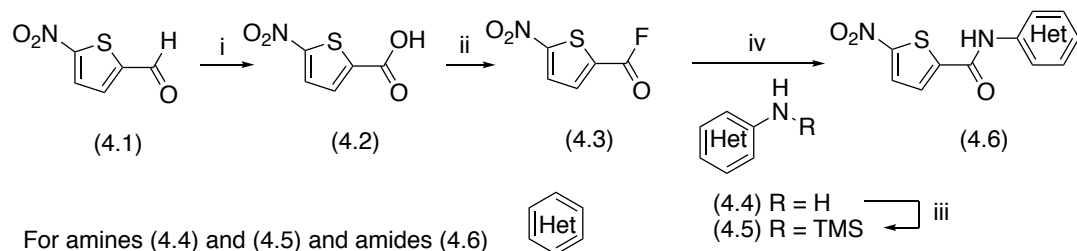
**Figure 4.6** Structure of compound 5350150 and our plans for the synthesis and SAR studies of amide analogue of 5350150.

### 4.3 Synthesis of amide analogues of 5350150

Taking into consideration that the identification of the active DHA analogues of **IDC16** required evaluation of a broad range of compounds, it was anticipated that a similar course of action would have to be followed to identify active amide analogues of 5350150.

Consequently, as it is illustrated in Reaction Scheme 4.1, the 2-nitrothiophene-4 carboxylic acid fluoride intermediate **4.3** was reacted with a set of 50 mono and bicyclic *N*-TMS substituted hetero(aryl)amines **4.5a-xx** to give the amide products **4.6a** to **4.6xx**.

The synthesis of compounds **4.6a-xx** involved conversion of 5-nitrothiophene-2-carboxylic acid **4.2** (itself available by dichromate oxidation of aldehyde **4.1** in 82%) to acid fluoride **4.3** through reaction with TFFH and CsF, and reaction of this intermediate with the requisite *N*-TMS amines **4.5a-xx** in the presence of TBAF.<sup>88</sup> Because both acid fluoride and urea by-product were soluble in hexanes, acid fluoride **4.3** was isolated as a 1:1 mixture with the fluorination reaction side-product *N,N,N,N*-tetramethylurea. However, as the use of acetonitrile as solvent for the coupling step favoured precipitation of the desired amide products **4.6a-xx**, the non-polar urea contaminant and other impurities were readily separated from the target amides by simple vacuum filtration. With the exception of compound **4.6g**, **4.6n**, **4.6pp**, whose isolation required a further column chromatography operation, vacuum filtration was sufficient to obtain amides **4.6** in >95% purity.



**Reaction Scheme 4.1** Reagent and conditions: i) K<sub>2</sub>Cr<sub>2</sub>O<sub>7</sub>, 5N H<sub>2</sub>SO<sub>4</sub>, 100 °C, 2 h; ii) TFFH, CsF, MeCN, r.t., 12 h; iii) TMSCN (neat), 70 °C, reaction time ranges from 7 min to 12 h; iv) MeCN, TBAF (cat), 50 °C, 12 h.



#### 4.4 Preliminary anti-HIV screening for amide 4.6a-xx

Preliminary evaluation of the anti-HIV activity of these compounds was carried out by Dr. Peter Cheung (BC Centre for Excellence in HIV/AIDS), using a cell-based screen<sup>30</sup> in which reporter CEM-GXR cells were infected by co-culture with one percent HIV-1<sub>NL4-3</sub> infected (GFP positive) cells at the start of the assay (day 0). CEM-GXR cells are an immortalized CD4<sup>+</sup> T-lymphocyte line that expresses GFP due to the activation of the tat-dependent promoter upon HIV-1 infection.<sup>95</sup> A different library molecule in DMSO was added to the culture in each microplate well immediately after the inoculation by infected cells. The final library compound concentration was fixed at 5 different concentrations: 0, 1.25, 2.5, 5, and 10  $\mu$ M, and the final DMSO concentration was less than 0.1%. The percent of infected cells in the culture was determined by flow cytometry on day 3.

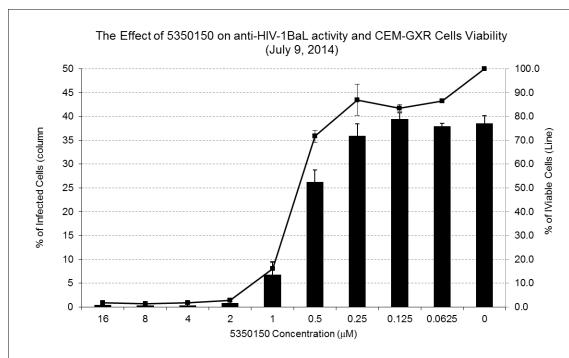
Preliminary screening of the 50 amide analogues of 5350150 (Reaction Scheme 4.1) resulted in finding 17 compounds with weak to strong anti-HIV activities (Figure 4.8). Interestingly, the exact amide analogue of 5350150, **4.6a**, in which C=C replaced by amide, but nitro thiophene and quinoline motifs conserved, displayed no anti-HIV activity. This suggests that the amide motif alters binding and does not perfectly emulate C=C. Exploring 5 additional quinolone and isoquinoline rings, **4.6b-f**, only resulted in one anti-HIV active molecule, **4.6d**, with moderate activity. Similarly, **4.6g**, an analogue of **1C8** was inactive indicating that 5-nitrothiophene does not represent an alternative to the 4-pyridinone ring that characterizes **1C8**. This also suggests that **1C8** and amide analogues of 5350150 have different targets.

Switching to a different ring system, it was observed that 5 and 6-membered aryl or heterocyclic (oxadiazole, pyridine, etc) rings do not improve the anti-HIV activity. It is worth mentioning that amides **4.6i**, **m**, **r**, and **u** have low to moderate activities but after exploring 28 amides with different mono cyclic rings and finding no molecule with strong potency, it was evident that this system has a general poor anti-HIV profile. This outcome took a sharp turn once we started exploring benzothiazole-based analogues. Interestingly, the majority of the synthesized amides bearing benzothiazole ring in Reaction Scheme 4.1 have low to strong anti-HIV activities. For those with strong anti-HIV activity, we measured their viability (Table 4.1). Here, the potential adverse effect of these molecules on CEM-GXR cells viability was determined by the Guava ViaCount assay. This assay differentially stains viable and nonviable cells based on their permeability to the DNA-binding dyes and uses the forward scatter (FSC) properties to distinguish free nuclei and cellular debris from intact cells to quantify cell count. CEM-GXR cells were incubated with compound at concentrations ranging between 0.5 and 100  $\mu$ M for 24 h.

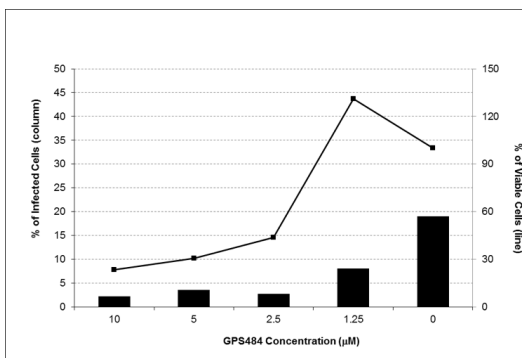
Amides **4.6kk**, **4.6ll**, **4.6nn**, **4.6uu** have strong anti-HIV activities but those with a substituent at C5 or C6 position of the benzothiazole ring, **4.6ll**, **4.6nn**, **4.6uu**, have poor viabilities. Contrary to this, **4.6pp** and **4.6qq** have substituents at C6 but both have strong anti-HIV activity and good viability. Importantly, it was found that the NO<sub>2</sub> substituent in **4.6qq** could be changed to CF<sub>3</sub>, suggesting that this functionality could act as a bioisostere of a nitro group,<sup>96</sup> as compound **4.6ww** is equally potent but has better viability profile.

It was also observed that having no substituent on benzothiazole ring (**4.6oo**) or having SO<sub>2</sub>Me, Br, or F at C6 (**4.6rr**, **ss**, **tt**) diminishes anti-HIV activity.

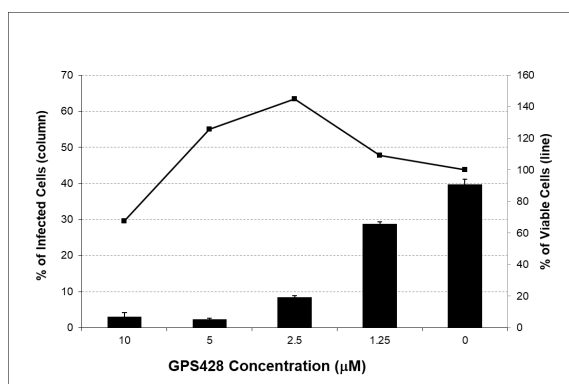
Considering anti-HIV activity and viability together (Figure 4.7 and Table 4.1), compounds **4.6kk**, **qq**, **ww** were selected for more in-depth SAR studies.



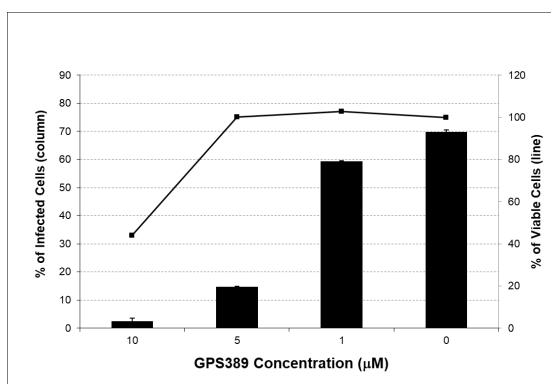
**5350150**



**4.6ww (GPS484)**



**4.6qq (GPS428)**



**4.6kk (GPS389)**

**Figure 4.7 Activity-viability curves for 5350150, 4.6kk (Gps389), 4.6qq (GPS428) and 4.6ww (GPS484)**

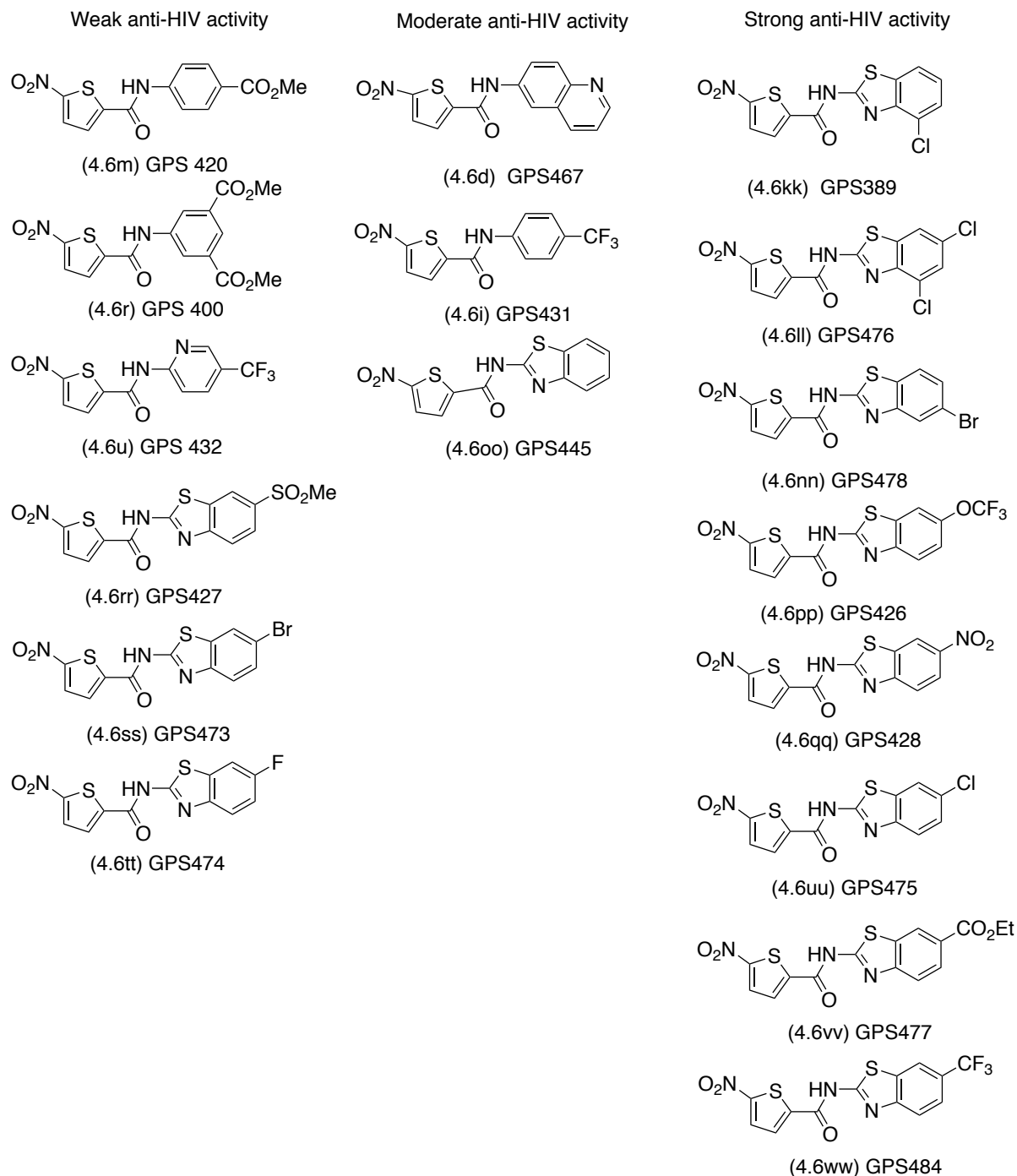


**Figure 4.8 Structure of 17 amide analogues of 5350150 with weak to strong anti-HIV activity**

**Table 4.1 The viability of 7 amide analogues of 5350150 with strong anti-HIV activity**

Compounds with strong anti-HIV activity	Viability
4.6kk	100%
4.6ll	60%
4.6nn	74%
4.6pp	82%
4.6qq	114%
4.6uu	51%
4.6ww	133%

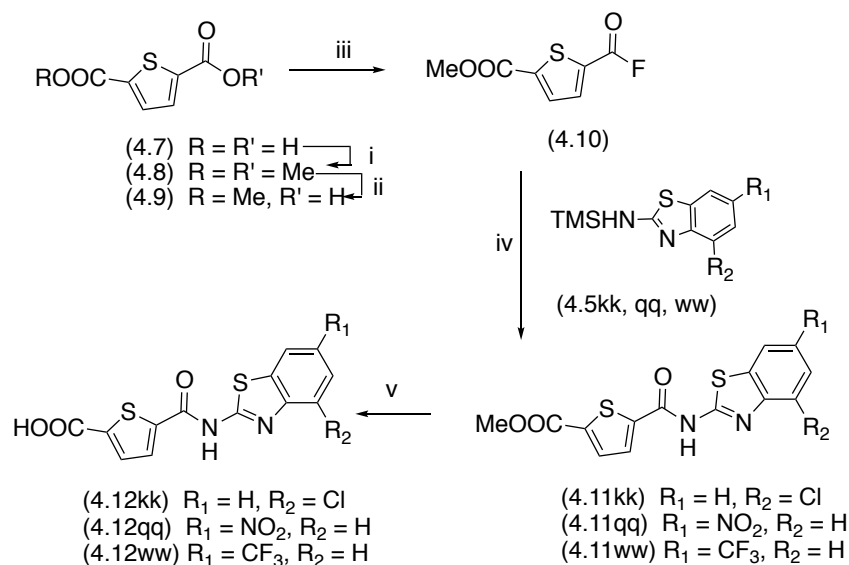
#### 4.5 SAR studies for compounds **4.6kk**, **qq**, **ww**

To study its influence on anti-HIV activity, the C-5 nitro group in compounds **4.6kk**, **qq**, and **ww** was exchanged for a methyl ester and a carboxylic acid function. In terms of its electronic properties, a CO<sub>2</sub>H function was considered to be isoelectronic with the 5-nitro functionality in **4.6kk**, **qq**, and **ww**. To access the ester analogues **4.11kk**, **qq**, and **ww** (Reaction Scheme 4.2) thiophene 2,5-dicarboxylic acid **4.7** was reacted with HCl-MeOH, and the resulting diester **4.8** was partially hydrolyzed to give ester-acid **4.9**.

Mono acid **4.9** was subsequently converted to acid fluoride **4.10** through reaction with TFFH and CsF, and this intermediate (isolated as a 1:1 mixture with the N,N,N,N-tetramethylurea side product) was reacted with the requisite N-TMS amines **4.5kk**, **qq**, and **ww** in the presence of TBAF.<sup>88</sup> Once again, the use of acetonitrile as solvent for the coupling step favoured precipitation of the desired amide products **4.11kk**, **qq**, **ww**, permitting isolation of the three target amides in pure form by simple vacuum filtration.

Treatment of amides **4.11** with LiOH in THF-H<sub>2</sub>O effected ester hydrolysis, giving access to the corresponding acid analogues **4.12kk**, **qq**, and **ww**.

Contrary to expectation, neither the ester substituted amides **4.11kk**, **qq**, **ww** or the CO<sub>2</sub>H substituted amides **4.12kk**, **qq**, **ww** displayed no anti-HIV activity, indicating that both CO<sub>2</sub>Me and CO<sub>2</sub>H are not suitable replacements for NO<sub>2</sub> group in **4.6kk**, **qq**, **ww**.

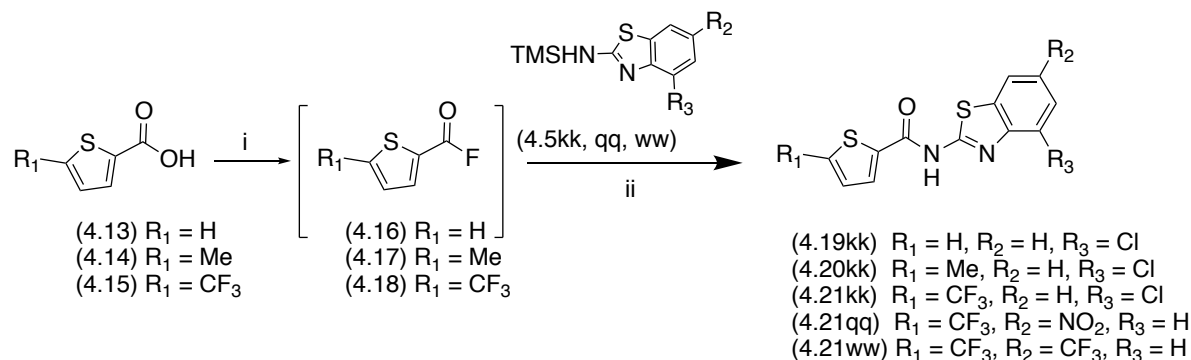


**Reaction Scheme 4.2** Reagent and conditions: i)  $SOCl_2$ , MeOH, 65 °C, 12 h; ii) LiOH, THF/H<sub>2</sub>O (2-1), r.t., 25 min; iii) TFFH, CsF, MeCN, r.t., 22 h; iv) MeCN, TBAF (cat), 50 °C, 48 h; v) LiOH, THF/H<sub>2</sub>O (2-1), r.t., 12 h.

To further study the influence of the C-5 substituent on anti-HIV activity and cell viability, the 5350150 amides **4.19kk** ( $R_1 = H$ ), **4.20kk** ( $R_1 = Me$ ), and amides **4.21kk**, **qq**, and **ww** ( $R_1 = CF_3$ ), were prepared from the commercially available thiophenes **14.13**, **4.14**, and **4.15** (Reaction Scheme 4.3). To access these target amides, the coupling protocol to prepare compounds **4.6a-xx** was modified such that the N-TMS amines **4.5kk**, **qq**, **ww** were reacted with the acid fluoride **4.16-4.18** generated *in situ*. Further, in this “one pot” operation, the presence of CsF in the reaction medium eliminated the need to add TBAF to initiate the coupling reaction.

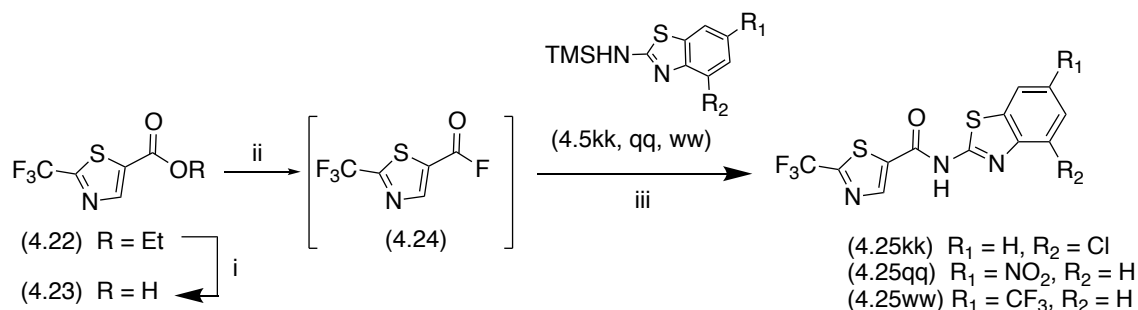
In the screen, no anti-HIV activity was observed for **4.19kk** and **4.20kk** indicating that  $NO_2$  group at C-5 position of the thiophene cannot be eliminated or replaced by a methyl group.

However, anti-HIV activity was observed for the 3 amides **4.21kk**, **qq**, and **ww**, showing that CF<sub>3</sub> is indeed a suitable bioisostere for the C-5 NO<sub>2</sub> group.



**Reaction Scheme 4.3 Reagent and conditions:** i) TFFH, CsF, MeCN, r.t., 12 h; ii) MeCN, 50 °C, 12-48 h.

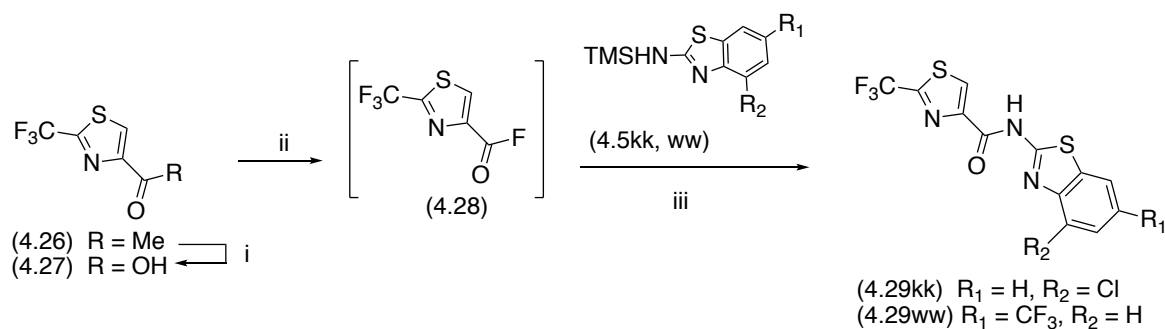
To expand on this finding, we decided to make **4.21** more drug-like by replacing its thiophene ring with a thiazole ring. The preparation of amides **4.25kk**, **qq**, and **ww** was again achieved through reaction of N-TMS amines **4.5kk**, **qq**, **ww** with the *in situ* generated acid fluoride **4.24** (Reaction Scheme 4.4). It was exciting to observe that the thiazole amides **4.25kk**, **qq**, **ww** were anti-HIV active with EC<sub>50</sub> 3.6 μM, 2.4 μM, and 0.6 μM respectively.



**Reaction Scheme 4.4 Reagents and conditions:** i) LiOH, THF/H<sub>2</sub>O (5-3), r.t., 2.5 h; ii) TFFH, CsF, MeCN, r.t., 12 h; iii) MeCN, 50 °C, 12 h.

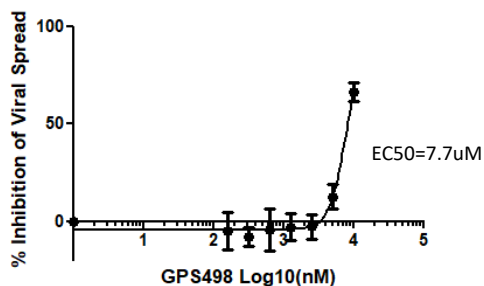


In the final modification to the 5350150-amide series studied, the isomeric C-2 substituted thiazole-based compounds **4.29kk** and **ww** were prepared from the commercially available thiazole **4.26** through coupling of the requisite N-TMS amines with the *in situ* generated of acid fluoride **4.28**. In these compounds, the appending carboxamide function was attached to C-5 (adjacent to the ring nitrogen atom) (Reaction Scheme 4.5). Isomeric C-2 substituted thiazole-based compounds **4.29kk** and **ww** were similarly active, but amides but **4.25 kk**, **qq**, and **ww** have better anti-HIV activity.



Reaction Scheme 4.5 Reagents and conditions: i) LiOH, THF/H<sub>2</sub>O (5-3), r.t., 35 min; ii) TFFH, CsF, MeCN, r.t., 24 h; iii) MeCN, 50 °C, 48 h.

The Antiviral Effect GPS498 on HIV-1NL4-3 Strain



The Antiviral Effect GPS491 on HIV-1NL4-3 Strain

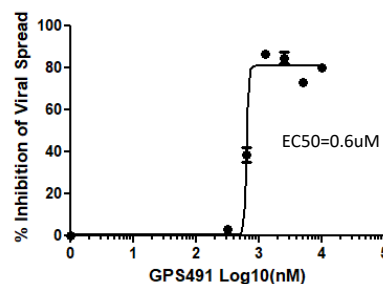
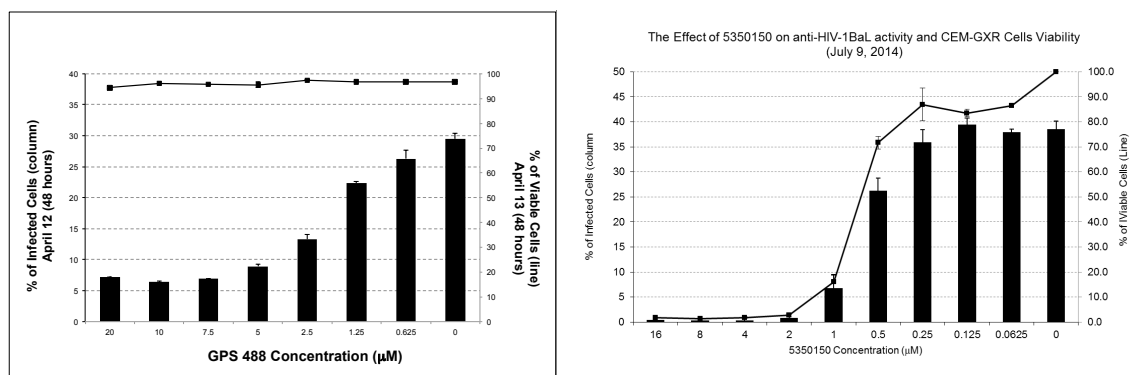
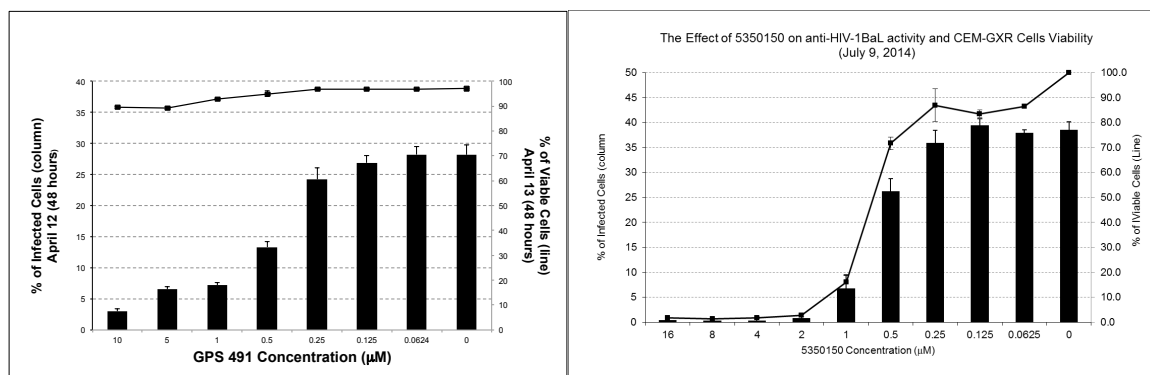


Figure 4.9 EC<sub>50</sub> curve for 4.29ww (GPS498) and 4.25ww (GPS491)

Again, considering both activity and viability (Figure 4.10 and Figure 4.11), amides **4.25kk** (GPS488) and **4.25ww** (GPS491) were chosen for extended biological studies. Both of these molecules have improved viability with respect to 5350150.



**Figure 4.10 Activity versus viability for 4.25kk (GPS488) and 5350150**



**Figure 4.11 Activity versus viability for 4.25ww (GPS 491) and 5350150**

#### **4.6 Calculation of EC50 for 4.25kk (GPS488) and 4.25ww (GPS491) for wild-type and major strains resistant against the four drug classes used in ART**

The resistance and EC50 studies were done by Dr. Peter Cheung (BC Centre for Excellence in HIV/AIDS). The following is a summary of the findings for **4.25kk** (GPS488) and **4.25ww** (GPS491).

Given that the antiviral activity of anti-HIV drugs can vary significantly due to the genetic variation of HIV-1 subtypes and its coreceptor usage, compounds **4.25kk** (GPS488) and **4.25ww** (GPS491) were evaluated for their anti-HIV activity in different HIV-1 subtypes and tropisms. In the experiment, the culture contained serial dilutions of molecule **4.25kk** (GPS488) and **4.25ww** (GPS491) in final concentrations between 100 nM and 10  $\mu$ M, and the half maximal effective concentration (EC50) values were calculated by nonlinear regression with GraphPad Prism software. The compounds exhibited activity against wild-type HIV-1IIIB (subtype B, X4-tropic), and HIV-1 97USSN54 (subtype A, R5-tropic) with EC50 values of 1.29 and 0.955  $\mu$ M for **4.25kk** (GPS488) and 0.248 and 0.176  $\mu$ M for **4.25 ww** (GPS491) (Figure 4.12). Note that compound **4.25 ww** (GPS491) was 5.5 times more potent than **4.25kk** (GPS488) in these assays.

To assess its potential against drug-resistant strains, the antiretroviral activity of the **4.25kk** (GPS488) and **4.25ww** (GPS491) were tested against key HIV-1 strains resistant to at least one of the current four major drug target categories: (non)-nucleoside reverse transcriptase inhibitor (N)NRTI, protease inhibitor (PI), integrase inhibitor (INI), and coreceptor inhibitor (CRI).

Compounds **4.25kk** (GPS488) and **4.25ww** (GPS491) were evaluated against the isolate (E00443), which greatly reduces susceptibility to both NNRTI's and NRTI's. Indeed, this isolate harbor a variety of mutations, including the widely recognized NNRTI-resistance mutation K103N that confer high level resistance to efavirenz and nevirapine. This virus also carries the NRTI-resistance mutations D67N, K70R, Y115F, Q151M, M184V, and K219Q, which confer high-level resistance to lamivudine, abacavir, zidovudine, and emtricitabine. In the assay, compounds **4.25kk** (GPS488) and **4.25ww** (GPS491) remained active, with an EC<sub>50</sub> of 1.157 and 0.235  $\mu$ M respectively.

Compounds **4.25kk** (GPS488) and **4.25ww** (GPS491) similarly retained their potency (EC<sub>50</sub> of 1.168 and 0.230  $\mu$ M respectively) against the PI-resistant isolate (2948), which contains substitutions G48V and L90M. This combination reduces the susceptibility to atazanavir and lopinavir, currently the two of the three most frequently prescribed HIV protease inhibitors.

To determine whether **4.25kk** (GPS488) and **4.25ww** (GPS491) targets HIV-1 integrase, it was tested against a clinical isolate (11845), which harbors G140S and Q148H substitutions that reduce susceptibility to raltegravir and elvitegravir more than 100- fold and reduce sensitivity toward dolutegravir up to 10-fold. Compound **4.25kk** (GPS488) and **4.25ww** (GPS491) showed activity against this isolate with an EC<sub>50</sub> of 0.951 and 0.203  $\mu$ M respectively.

Lastly, **4.25kk** (GPS488) and **4.25ww** (GPS491) retained activity EC<sub>50</sub> of 0.969 and 0.216  $\mu$ M respectively against an HIV-1 strain that is resistant to the entry inhibitor-based drug maraviroc. This maraviroc-resistant variant derived from a R5 strain of HIV-1<sub>BaL</sub> contains five mutations

within the envelope V3 loop: A19T, L20F, T22A, E25D, and I26V.

Having activity against the drug resistant strains indicates that both compounds **4.25kk** (GPS488) and **4.25ww** (GPS491) likely display no affinity for the classical HIV target proteins and have different mechanism of action than the current HIV drugs.

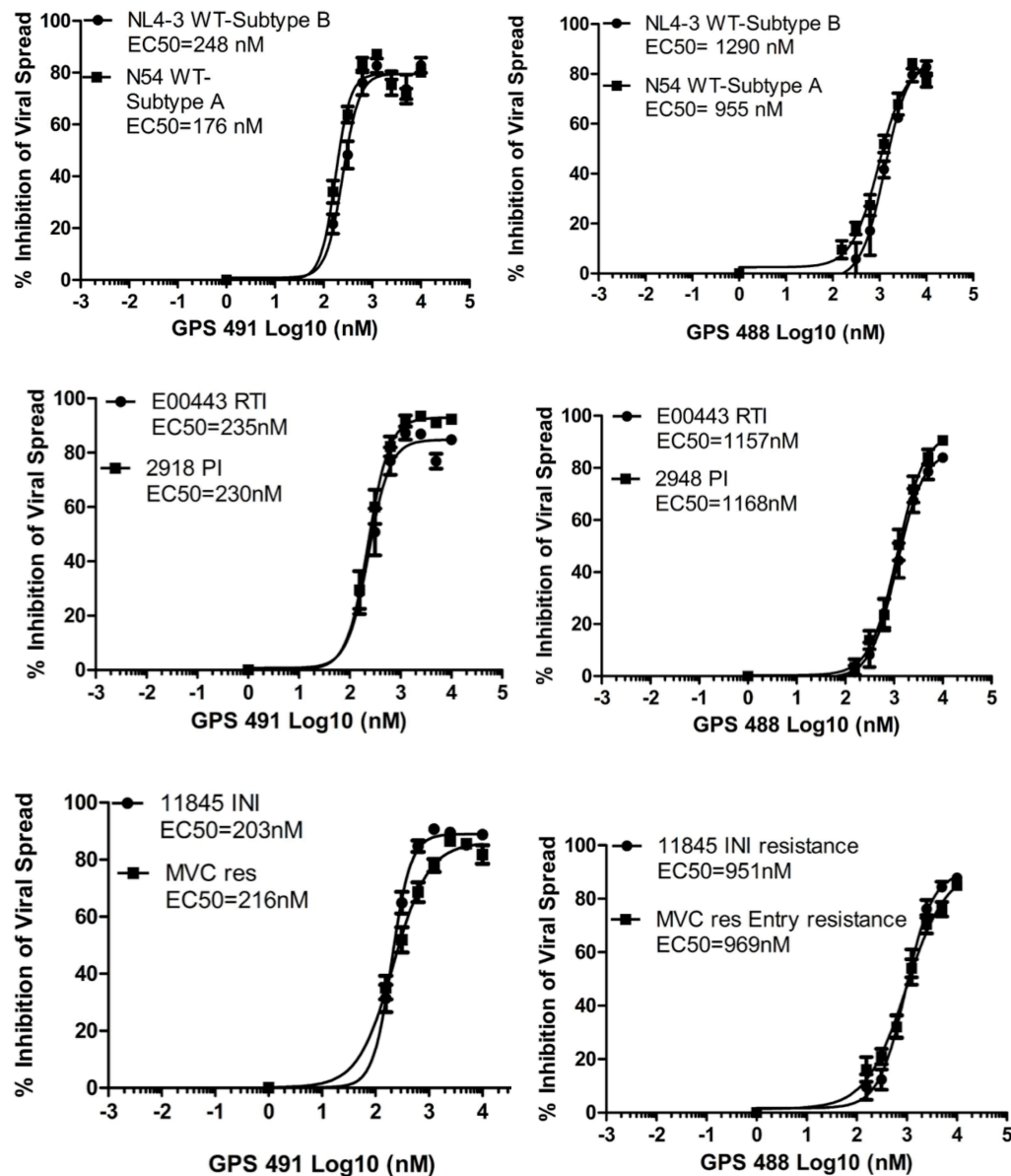


Figure 4.12 EC50 curves for 4.25qq (GPS488) and 4.25ww (GPS491) against wild type (WT) and major strains resistant against the four drug classes used in ART: (non)-nucleoside reverse transcriptase inhibitor (N)NRTI, protease inhibitor (PI), integrase inhibitor (INI), and coreceptor inhibitor (CRI)

#### 4.7 Structural similarity of 4.25kk (GPS488) and ABX464

Interestingly, **4.25kk**(GPS488) and **ABX464** have several structural similarities that “invite” the temptation to generation pharmacophore model based on 3 points of contacts (Figure 4.13).

**ABX464** was also designed as an **IDC16** mimic, and its development has been pursued by the groups at institut curie and the Universite De Montpellier II. This compound also functions as an anti-HIV agent by impairing rev function. Indeed, the current evidence indicates that it amplifies the concentration of spliced mRNA but reduces the abundance of SS and US mRNAs with no significant effect on cellular splicing. Currently, **ABX464** is in Phase II clinical trials. In vitro studies have shown that this molecule has activity on different HIV subtype and mutant viruses and because it has cellular rather than viral targets, **ABX464** resistance seems to be unlikely.<sup>97</sup> In humanized mouse models, 52 days post-treatment, there was a substantial reduction in viral rebound.<sup>98</sup> In human studies, **ABX464** was well tolerated in healthy and HIV positive volunteers and at high dosage (150 mg) reduction of viral load was observed.<sup>99, 100</sup> Studies are in progress in our laboratories to compare the anti-HIV profiles and mechanism of action of **4.25kk** (GPS488) and **4.25ww** (GPS491) and the current lead compound in the field **ABX-464**.

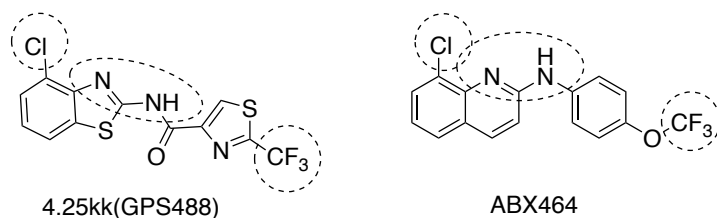


Figure 4.13 Structure of ABX464 and its 3 points of contacts with 4.25kk (GPS488)

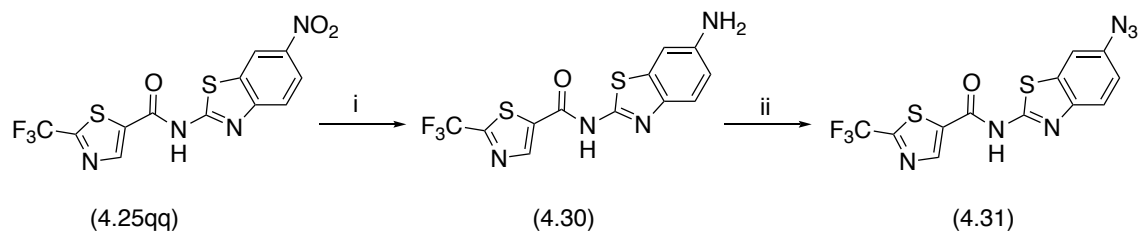
## 4.8 Conclusion and future directions

Synthesis and screening of 50 amide analogues of 5350150 led to the discovery of 3 anti-HIV active molecules, **4.6kk**, **qq**, **ww**. Our SAR studies on these 3 molecules gave more drug-like compounds, **4.25kk** (GPS488) and **4.25ww** (GPS491), which have anti-HIV activities in both wild-type HIV strains and major HIV strains resistant against the four drug classes used in ART. This implies that **4.25kk** (GPS488) and **4.25ww** (GPS491) have different mechanism of action than the current HIV drugs.

For target validation, the plan is to use the anti-HIV active analogue of **4.25ww** (GPS491), **4.31** (Reaction Scheme 4.6) bearing a photolabile azide motif which form a covalent bond with its target molecule. Using a chromatographic co-elution (TICC) approach,<sup>101</sup> cells will be incubated with compound **4.31** at one of two concentrations: the maximum dose that has no effect on HIV-1 gene expression and the minimum dose required to fully inhibit viral protein synthesis. After irradiation to induce covalent linkage to host factors, cell lysates will be prepared and fractionated by HPLC using various column matrices (most likely ion exchange supports). Fractions will be monitored for the presence of **4.31** (differential UV absorbance), and will be analyzed by mass spectrometry to identify the protein(s) that share the same elution profile and, thus, are likely targets. Comparison of the proteins co-eluting with the attached **4.31** at the two doses will define those interactions that correlate with the inhibition of viral gene expression.

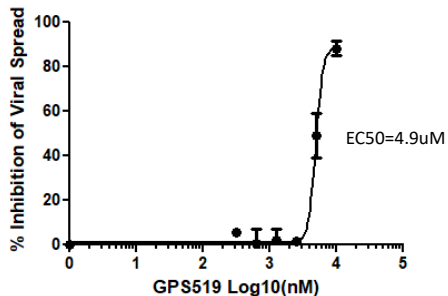


Compound **4.31** was synthesized by first reduction<sup>102</sup> of the NO<sub>2</sub> group in **4.25qq** to NH<sub>2</sub> and then applying a diazotization-azidation procedure to get the azide product.<sup>103-105</sup> This molecule is anti-HIV active with an EC<sub>50</sub> of 4.9 μM.

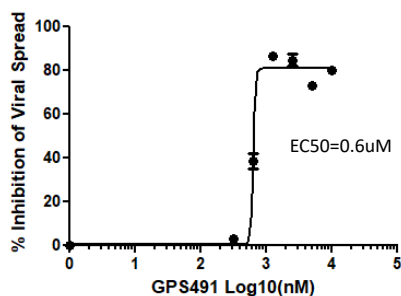


Reaction Scheme 4.6 Reagents and conditions: i) SnCl<sub>2</sub>, SnCl<sub>4</sub>, HCl, r.t., 4 h; ii) NaNO<sub>2</sub>, HCl, NaN<sub>3</sub>, H<sub>2</sub>O, 0 °C, 2 h, r.t., 1 h

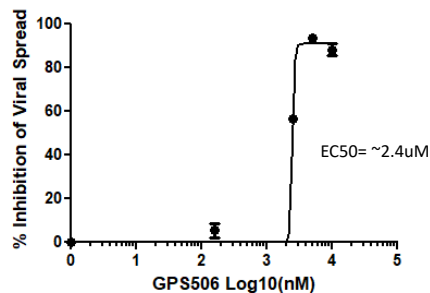
The Antiviral Effect GPS519 on HIV-1NL4-3 Strain



The Antiviral Effect GPS491 on HIV-1NL4-3 Strain



The Antiviral Effect GPS506 on HIV-1NL4-3 Strain



The Antiviral Effect GPS488 on HIV-1NL Strain

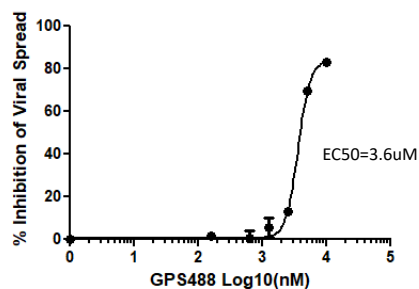


Figure 4.14 EC<sub>50</sub> curve for 4.31 (GPS519), 4.25ww (GPS491), 4.25qq (GPS506), and 4.25kk (GPS488).

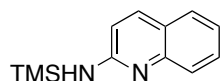
## 4.9 Experimental Section

All chemicals were purchased from Sigma-Aldrich or Oakwood Chemicals, and they were used without purification unless mentioned. All solvents were dried and kept under N<sub>2</sub>. <sup>1</sup>H, <sup>13</sup>C, and <sup>19</sup>F NMR spectra were recorded at 400, 100, and 400 MHz, respectively, on a Bruker AC 400 Ultrashield 10 spectrophotometer. Chemical shifts are expressed in ppm, (δ scale). When peak multiplicities are reported, the following abbreviations are used: s (singlet), d (doublet), dd (doublet of doublet), ddd (doublet of doublet of doublet), t (triplet) td (triplet of doublet), q (quartet), m (multiplet). Coupling constants are reported in Hz. All high-resolution mass spectra were recorded on a Thermo Scientific Q Exactive Orbitrap High Resolution Mass Spectrometer. Flash column chromatography was performed using silica gel (Silicycle, Siliaflash F60, 40–63 μm, 230–400 mesh) or on a Biotage Isolera purification system, (PartnerTechAtvidaberg AB) using prepacked silica gel columns (Biotage, part no. FSKO-1107-0010, FSKO-1107-0025, or FSKO-1107-0050).

## General Procedure for N-silylation: Preparation of compounds 4.5a-4.5xx

N-trimethylsilylated amines **4.5a-4.5xx** were prepared by reaction of their corresponding heteroaromatic amine precursors (0.5 mmol) (dried under high vacuum for 12 h before use) in neat TMSCN (0.5 mL), with stirring under nitrogen at 70 °C for the indicated time. The excess TMSCN was removed under high vacuum and the derived N-silylated amine was used without purification in the amide bond forming reaction. The percent conversion of each amine to its N-silylated derivative was determined by  $^1\text{H}$  NMR analysis in  $\text{CDCl}_3$  (passed through a basic alumina column prior to use). The synthesis of **4.5b**, **4.5d**, **4.5f**, **4.5g**, **4.5l**, **4.5m**, **4.5o**, **4.5z**, **4.5cc**, **4.5dd**, **4.5ee**, **4.5ff**, **4.5gg**, **4.5hh**, **4.5ii**, **4.5jj**, **4.5kk**, **4.5nn**, **4.5oo**, **4.5pp**, **4.5ss**, **4.5tt**, **4.5uu**, and **4.5ww** were done according to the reported procedure.<sup>74, 88</sup>

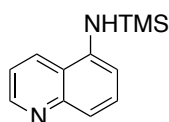
### N-(Trimethylsilyl)quinolin-2-amine (**4.5a**)



Heated for 4 h; dark orange oil; 100% conversion.

$^1\text{H}$  NMR (400 MHz,  $\text{CDCl}_3$ ):  $\delta$  = 7.73 (d,  $J$  = 8.9 Hz, 1 H), 7.59 (d,  $J$  = 8.0 Hz, 1 H), 7.51 (d,  $J$  = 8.0 Hz, 1 H), 7.44 (m, 1 H), 7.13 (m, 1 H), 6.59 (d,  $J$  = 8.7 Hz, 1 H), 4.34 (s, 1 H), 0.28 (s, 9 H, TMS).

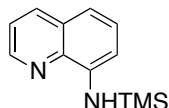
### N-(Trimethylsilyl)quinolin-5-amine (**4.5c**)



Heated for 12 h; brown oil; 79% conversion.

$^1\text{H}$  NMR (400 MHz,  $\text{CDCl}_3$ ):  $\delta$  = 8.69 (dd,  $J$  = 1.6, 4.3 Hz, 1 H), 8.01 (dd,  $J$  = 1.6, 8.6 Hz, 1 H), 7.37 (m, 2 H), 7.16 (q,  $J$  = 4.3 Hz, 1 H), 6.69 (t,  $J$  = 4.4 Hz, 1 H), 3.95 (s, 1 H), 0.21 (s, 9 H).

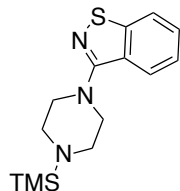
### **N-(Trimethylsilyl)quinolin-8-amine (4.5e)**



Heated for 20 h; green oil; 100% conversion.

$^1\text{H}$  NMR (400 MHz,  $\text{CDCl}_3$ ):  $\delta$  = 8.66 (dd,  $J$  = 1.6, 4.4 Hz, 1 H), 7.97 (dd,  $J$  = 1.6, 8.2 Hz, 1 H), 7.27 (m, 2 H), 7.02 (d,  $J$  = 8.2 Hz, 1 H), 6.84 (d,  $J$  = 7.8 Hz, 1 H), 6.07 (bs, 1 H), 0.31 (s, 9 H).

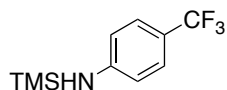
### **3-(4-(Trimethylsilyl)piperazin-1-yl)benzo[d]isothiazole (4.5h)**



Heated for 12 h; yellow solid; 66% conversion.

$^1\text{H}$  NMR (400 MHz,  $\text{CDCl}_3$ ):  $\delta$  = 7.81 (d,  $J$  = 8.2 Hz, 1 H), 7.69 (d,  $J$  = 8.0 Hz, 1 H), 7.35 (m, 1 H), 7.24 (m, 1 H), 3.27 (m, 4 H), 2.99 (m, 4 H), 0.00 (s, 9 H).

### **1,1,1-Trimethyl-N-(4-(trifluoromethyl)phenyl)silanamine (4.5i)**

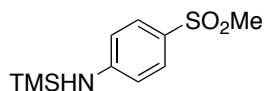


Heated for 12 h; orange oil; 88% conversion.

$^1\text{H}$  NMR (400 MHz,  $\text{CDCl}_3$ ):  $\delta$  = 7.22 (d,  $J$  = 8.0 Hz, 2 H), 6.51 (d,  $J$  = 8.3 Hz, 2 H), 3.55 (s, 1 H), 0.13 (s, 9 H).

$^{19}\text{F}$  NMR (400 MHz,  $\text{CDCl}_3$ ):  $\delta$  = - 61.01.

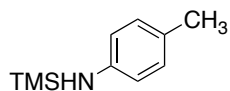
**1,1,1-Trimethyl-N-(4-(methylsulfonyl)phenyl)silanamine (4.5j)**



Heated for 20 h; orange oil and solid; 82% conversion.

$^1\text{H}$  NMR (400 MHz,  $\text{CDCl}_3$ ):  $\delta$  = 7.59 (d,  $J$  = 8.7 Hz, 2 H), 6.65 (d,  $J$  = 8.2 Hz, 2 H), 4.03 (s, 1 H), 2.93 (s, 3 H), 0.24 (s, 9 H).

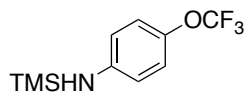
**1,1,1-Trimethyl-N-(p-tolyl)silanamine (4.5k)**



Heated for 2 h; orange oil; 92% conversion.

$^1\text{H}$  NMR (400 MHz,  $\text{CDCl}_3$ ):  $\delta$  = 6.79 (d,  $J$  = 7.8 Hz, 2 H), 6.41 (d,  $J$  = 7.8 Hz, 2 H), 3.16 (s, 1 H), 2.08 (s, 3 H), 0.10 (s, 9 H).

**1,1,1-Trimethyl-N-(4-(trifluoromethoxy)phenyl)silanamine (4.5n)**

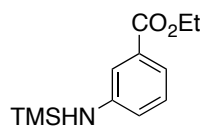


Heated for 20h; orange oil; 90% conversion.

$^1\text{H}$  NMR (400 MHz,  $\text{CDCl}_3$ ):  $\delta$  = 6.83 (d,  $J$  = 8.6 Hz, 2 H), 6.44 (d,  $J$  = 9.0 Hz, 2 H), 3.31 (s, 1 H), 0.11 (s, 9 H).

$^{19}\text{F}$  NMR (400 MHz,  $\text{CDCl}_3$ ):  $\delta = -58.46$ .

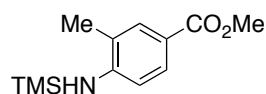
**Ethyl 3-((trimethylsilyl)amino)benzoate (4.5p)**



Heated for 12 h; orange oil; 92% conversion.

$^1\text{H}$  NMR (400 MHz,  $\text{CDCl}_3$ ):  $\delta = 7.23$  (dt,  $J = 1.2, 7.7$  Hz, 1 H),  $7.19$  (t,  $J = 2.0$  Hz, 1 H),  $7.03$  (t,  $J = 7.9$  Hz, 1 H),  $6.67$  (ddd,  $J = 1.0, 2.6, 8.0$  Hz, 1 H),  $4.19$  (q,  $J = 7.1$  Hz, 2 H),  $3.44$  (bs, 1 H),  $1.22$  (t,  $J = 7.2$  Hz, 3 H),  $0.13$  (s, 9 H).

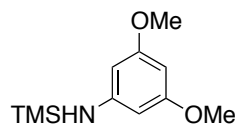
**Methyl 3-methyl-4-((trimethylsilyl)amino)benzoate (4.5q)**



Heated for 12 h; yellow solid; 73% conversion.

$^1\text{H}$  NMR (400 MHz,  $\text{CDCl}_3$ ):  $\delta = 7.60$  (s, 2 H),  $6.56$  (d,  $J = 8.7$  Hz, 1 H),  $3.69$  (s, 3 H),  $3.50$  (s, 1 H),  $2.01$  (s, 3 H),  $0.16$  (s, 9 H).

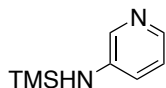
**N-(3,5-Dimethoxyphenyl)-1,1,1-trimethylsilanamine (4.5r)**



Heated for 30 min; yellow oil; 100% conversion.

$^1\text{H}$  NMR (400 MHz,  $\text{CDCl}_3$ ):  $\delta = 5.82$  (s, 1 H),  $5.78$  (s, 2 H),  $3.66$  (s, 6 H),  $3.40$  (s, 1 H),  $0.20$  (s, 9 H).

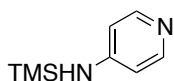
**N-(Trimethylsilyl)pyridin-3-amine (4.5s)**



Heated for 4 h; orange oil; 100% conversion.

$^1\text{H}$  NMR (400 MHz,  $\text{CDCl}_3$ ):  $\delta$  = 8.00 (s, 1 H), 7.89 (s, 1 H), 6.96 (m, 1 H), 6.87 (m, 1 H), 3.51 (s, 1 H), 0.21 (s, 9 H).

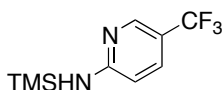
**N-(Trimethylsilyl)pyridin-4-amine (4.5t)**



Heated for 2 h; black oil; 100% conversion.

$^1\text{H}$  NMR (400 MHz,  $\text{CDCl}_3$ ):  $\delta$  = 7.96 (s, 2 H), 6.39 (s, 2 H), 4.28 (s, 1 H), 0.13 (s, 9 H).

**5-(Trifluoromethyl)-N-(trimethylsilyl)pyridin-2-amine (4.5u)**

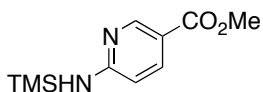


Heated for 4 h; orange oil; 100% conversion.

$^1\text{H}$  NMR (400 MHz,  $\text{CDCl}_3$ ):  $\delta$  = 8.18 (s, 1 H), 7.39 (d,  $J$  = 8.6 Hz, 1 H), 6.29 (d,  $J$  = 8.9 Hz, 1 H), 4.27 (s, 1 H), 0.15 (s, 9 H).

$^{19}\text{F}$  NMR (400 MHz,  $\text{CDCl}_3$ ):  $\delta$  = - 61.20.

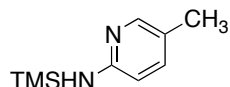
**Methyl 6-((trimethylsilyl)amino)nicotinate (4.5v)**



Heated for 2 h; pale yellow solid; 100% conversion.

$^1\text{H}$  NMR (400 MHz,  $\text{CDCl}_3$ ):  $\delta$  = 8.59 (s, 1 H), 7.80 (d,  $J$  = 8.7 Hz, 1 H), 6.26 (d,  $J$  = 8.5 Hz, 1 H), 4.41 (s, 1 H), 3.71 (s, 3 H), 0.15 (s, 9 H).

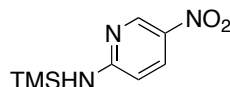
#### 5-Methyl-N-(trimethylsilyl)pyridin-2-amine (4.5w)



Heated for 30 min; orange oil; 100% conversion.

$^1\text{H}$  NMR (400 MHz,  $\text{CDCl}_3$ ):  $\delta$  = 7.82 (s, 1 H), 7.12 (d,  $J$  = 8.3 Hz, 1 H), 6.28 (d,  $J$  = 8.6 Hz, 1 H), 3.99 (bs, 1 H), 2.09 (s, 3 H), 0.20 (s, 9 H).

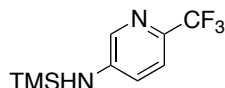
#### 5-Nitro-N-(trimethylsilyl)pyridin-2-amine (4.5x)



Heated for 12 h; brown solid; 100% conversion.

$^1\text{H}$  NMR (400 MHz,  $\text{CDCl}_3$ ):  $\delta$  = 9.00 (bs, 1 H), 8.14 (bs, 1 H), 6.43 (bs, 1 H), 4.83 (bs, 1 H), 0.30 (bs, 9 H).

#### 6-(Trifluoromethyl)-N-(trimethylsilyl)pyridin-3-amine (4.5y)



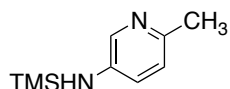
Heated for 12 h; orange oil; 96% conversion.

$^1\text{H}$  NMR (400 MHz,  $\text{CDCl}_3$ ):  $\delta$  = 7.95 (s, 1 H), 7.26 (d,  $J$  = 8.4 Hz, 1 H), 6.84 (d,  $J$  = 8.4 Hz, 1 H), 3.68 (s, 1 H), 0.16 (s, 9 H).



$^{19}\text{F}$  NMR (400 MHz,  $\text{CDCl}_3$ ):  $\delta = -66.53$ .

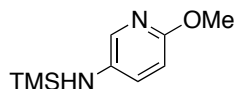
**6-Methyl-N-(trimethylsilyl)pyridin-3-amine (4.5aa)**



Heated for 2 h; brown solid; 100% conversion.

$^1\text{H}$  NMR (400 MHz,  $\text{CDCl}_3$ ):  $\delta = 7.97$  (s, 1 H), 6.88 (m, 2 H), 3.36 (s, 1 H), 2.41 (bs, 3 H), 0.26 (s, 9 H).

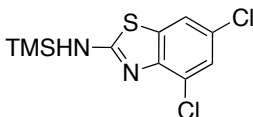
**6-Methoxy-N-(trimethylsilyl)pyridin-3-amine (4.5bb)**



Heated for 12 h; red oil; 86% conversion.

$^1\text{H}$  NMR (400 MHz,  $\text{CDCl}_3$ ):  $\delta = 7.38$  (s, 1 H), 6.73 (d,  $J = 8.9$  Hz, 1 H), 6.33 (d,  $J = 8.4$  Hz, 1 H), 3.61 (s, 3 H), 2.91 (s, 1 H), 0.00 (s, 9 H).

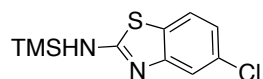
**4,6-Dichloro-N,N-bis(trimethylsilyl)benzo[d]thiazol-2-amine (4.5ll)**



Heated for 12 h; orange oil; 100% conversion.

$^1\text{H}$  NMR (400 MHz,  $\text{CDCl}_3$ ):  $\delta = 7.36$  (d,  $J = 2.1$  Hz, 1 H), 7.24 (d,  $J = 2.0$  Hz, 1 H), 5.16 (s, 1 H), 0.31 (s, 18 H).

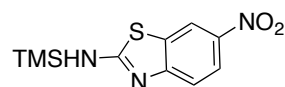
**5-Chloro-N-(trimethylsilyl)benzo[d]thiazol-2-amine (4.5mm)**



Heated for 20 h; yellow solid; 100% conversion.

$^1\text{H}$  NMR (400 MHz,  $\text{CDCl}_3$ ):  $\delta$  = 7.45 (d,  $J$  = 2.2 Hz, 1 H), 7.36 (d,  $J$  = 8.4 Hz, 1 H), 6.97 (dd,  $J$  = 8.4, 2.1 Hz, 1 H), 5.10 (s, 1 H), 0.28 (s, 9 H).

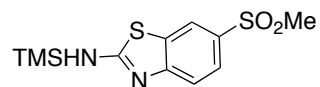
**6-Nitro-N-(trimethylsilyl)benzo[d]thiazol-2-amine (4.5qq)**



Heated for 12 h; yellow oil; 100% conversion

$^1\text{H}$  NMR (400 MHz,  $\text{CDCl}_3$ ):  $\delta$  = 8.41 (s, 1H), 8.11 (d,  $J$  = 9.0 Hz, 1H), 7.46 (d,  $J$  = 8.9 Hz, 1H), 5.28 (s, 1H), 0.34 (s, 9H).

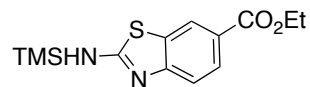
**6-(Methylsulfonyl)-N-(trimethylsilyl)benzo[d]thiazol-2-amine (4.5rr)**



Heated for 20 h; brown solid; 100% conversion.

$^1\text{H}$  NMR (400 MHz,  $\text{CDCl}_3$ ):  $\delta$  = 8.10 (s, 1 H), 7.75 (d,  $J$  = 8.0 Hz, 1 H), 7.55 (d,  $J$  = 8.0 Hz, 1 H), 5.42 (s, 1 H), 3.01 (s, 3 H), 0.32 (s, 9 H).

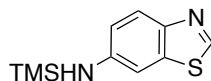
**Ethyl 2-((trimethylsilyl)amino)benzo[d]thiazole-6-carboxylate (4.5vv)**



Heated for 12 h; brown solid; 100% conversion.

$^1\text{H}$  NMR (400 MHz,  $\text{CDCl}_3$ ):  $\delta$  = 8.22 (s, 1 H), 7.92 (d,  $J$  = 7.2 Hz, 1 H), 7.46 (d,  $J$  = 7.4 Hz, 1 H), 5.29 (bs, 1 H), 4.30 (bs, 2 H), 1.33 (bs, 3 H), 0.31 (s, 9 H).

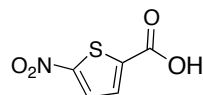
#### **N-(Trimethylsilyl)benzo[d]thiazol-6-amine (4.5xx)**



Heated for 12 h; black oil; 100% conversion.

$^1\text{H}$  NMR (400 MHz,  $\text{CDCl}_3$ ):  $\delta$  = 8.51 (s, 1 H), 7.71 (d,  $J$  = 8.8 Hz, 1 H), 6.96 (d,  $J$  = 2.4 Hz, 1 H), 6.68 (dd,  $J$  = 2.4, 8.8 Hz, 1 H), 3.50 (s, 1 H), 0.16 (s, 9 H).

#### **5-Nitrothiophene-2-carboxylic (4.2)**



To a stirred solution of potassium dichromate (2.8 g, 11.5 mmol) in 5 N  $\text{H}_2\text{SO}_4$  (40 mL) was added 5-nitro-2-thiophenecarboxaldehyde **4.1** (4 g, 25.5 mmol) and the reaction was heated at 100 °C for 2 h. The mixture was then cooled in an ice bath and diluted with water (40 mL). The resulting precipitate was collected by suction filtration, washed with ice water (5 x 20 mL), and dried under high vacuum to afford **4.2** as a green solid (3.6 g, 20.8 mmol, 82% yield).

$^1\text{H}$  NMR (400 MHz,  $\text{DMSO}-d_6$ ):  $\delta$  = 13.9 (s, 1 H), 8.12 (d,  $J$  = 4.1 Hz, 1 H), 7.74 (d,  $J$  = 4.1 Hz, 1 H).

HRMS (HESI)  $m/z$   $[\text{M}-\text{H}]^-$  calcd for  $\text{C}_5\text{H}_2\text{NO}_4\text{S}$ : 171.9710; found: 171.96967.

### General procedure for the preparation of di(hetero)arylamides **4.6a-zz** via coupling of N-TMS amines **4.5a-zz** with 5-nitrothiophene-2-carbonyl fluoride **4.3**

A mixture of thiophene-2-carboxylic acid **4.2** (800 mg, 4.64 mmol), TFFH (1.22 g, 4.64 mmol), and CsF (1.36 g, 8.96 mmol) in MeCN (24 mL) was stirred for 12 h at room temperature. The product mixture was then concentrated under reduced pressure, taken up in hexane and filtered to remove the cesium salts. The filtrate was concentrated to give a yellowish oil, which was dried under high vacuum for 5 h. Based on its  $^1\text{H}$  NMR spectrum, the isolated material corresponded to a 1:1 mixture of acid fluoride **4.3** and the 1,1,3,3-tetramethylurea side product. Peaks for trace amounts of unidentified material were also observed. The product mixture was estimated to contain 714 mg (4.08 mmol, 88% conversion) of acid fluoride **4.3**.

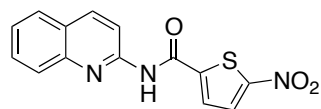
$^1\text{H}$  NMR (400 MHz,  $\text{CD}_3\text{CN}$ ):  $\delta$  = 8.01 (m, 1 H), 7.94 (m, 1 H), 2.73 (s, 12 H, NMe).

$^{19}\text{F}$  NMR (400 MHz,  $\text{CD}_3\text{CN}$ ):  $\delta$  = 23.74.

$^{19}\text{F}$  NMR (400 MHz,  $\text{CDCl}_3$ ):  $\delta$  = 25.55.

For the coupling experiments, the mixture containing the freshly prepared acid fluoride **4.3** was dissolved in MeCN (24 ml). Aliquots of this stock solution was divided to 4 portions (each portion containing 179 mg, 1.02 mmol, 1.28 equivalents of **4.3** in 6 ml MeCN) and each portion was added to one of four reaction vessels, each containing a different TMS-amine **4.5** (0.8 mmol). This was quickly followed by the addition of 1 M TBAF in THF (10  $\mu\text{L}$ , 0.01 mmol) to each reaction vessel. The resultant mixtures were stirred at 50  $^\circ\text{C}$  for 12 h. The desired amide products **4.6a-xx** precipitated from the reaction, and, with the exception of **4.6g**, **4.6n**, and **4.6pp**, were isolated pure by simple vacuum filtration.

### 5-Nitro-N-(quinolin-2-yl)thiophene-2-carboxamide (4.6a)



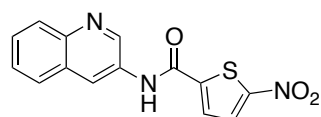
From **4.5a**. The precipitated product was washed with MeCN and then hexanes to afford **4.6a** as a yellow solid; yield 22% (53 mg, 0.18 mmol)

$^1\text{H}$  NMR (400 MHz, DMSO- $d_6$ ):  $\delta$  = 11.76 (s, 1 H), 8.44 (d,  $J$  = 9.1 Hz, 1 H), 8.30 (m, 2 H), 8.20 (d,  $J$  = 4.4 Hz, 1 H), 7.97 (d,  $J$  = 8.2 Hz, 1 H), 7.91 (d,  $J$  = 8.4 Hz, 1 H), 7.76 (t,  $J$  = 7.6 Hz, 1 H), 7.56 (t,  $J$  = 7.5 Hz, 1 H).

$^{13}\text{C}$  NMR (100 MHz, DMSO- $d_6$ ):  $\delta$  = 159.5, 154.0, 151.0, 146.3, 145.7, 138.6, 130.3, 130.2, 129.5, 127.9, 127.1, 126.0, 125.7, 115.3.

$^{13}\text{C}$  DEPT 90 NMR (100 MHz, DMSO- $d_6$ ):  $\delta$  = 138.6, 130.3, 130.2, 129.5, 127.9, 127.1, 125.6, 115.3.

### 5-Nitro-N-(quinolin-3-yl)thiophene-2-carboxamide (4.6b)

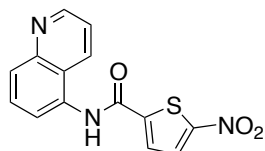


From **4.5b**. The precipitated product was washed with MeCN and then hexanes to afford **4.6b** as a yellow solid; yield 49% (117 mg, 0.39 mmol).

$^1\text{H}$  NMR (400 MHz, DMSO- $d_6$ ):  $\delta$  = 11.09 (s, 1 H), 9.11 (d,  $J$  = 2.6 Hz, 1 H), 8.79 (d,  $J$  = 2.5 Hz, 1 H), 8.25 (d,  $J$  = 4.4 Hz, 1 H), 8.12 (d,  $J$  = 4.4 Hz, 1 H), 7.99 (ddd,  $J$  = 8.2, 2.2, 1.1 Hz, 2H), 7.70 (ddd,  $J$  = 8.4, 6.9, 1.5 Hz, 1 H), 7.61 (ddd,  $J$  = 8.1, 6.9, 1.2 Hz, 1 H).

$^{13}\text{C}$  NMR (100 MHz, DMSO- $d_6$ ):  $\delta$  = 158.9, 153.7, 145.5, 145.1, 144.7, 131.8, 130.2, 128.9, 128.6 (for two carbons), 128.0, 127.6, 127.3, 124.3.

**5-Nitro-N-(quinolin-5-yl)thiophene-2-carboxamide (4.6c)**

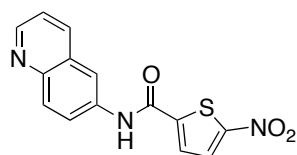


From **4.5c**. The precipitated product was washed with MeCN and then hexanes to afford **4.6c** as a yellow solid; 73% (174 mg, 0.58 mmol).

$^1\text{H}$  NMR (400 MHz, DMSO- $d_6$ ):  $\delta$  = 11.02 (s, 1 H), 8.96 (dd,  $J$  = 1.7, 4.2 Hz, 1 H), 8.43 (d,  $J$  = 8.6 Hz, 1 H), 8.27 (d,  $J$  = 4.4 Hz, 1 H), 8.17 (d,  $J$  = 4.4 Hz, 1 H), 8.01 (d,  $J$  = 8.5 Hz, 1 H), 7.83 (t,  $J$  = 8.0 Hz, 1 H), 7.72 (d,  $J$  = 7.4 Hz, 1 H), 7.59 (dd,  $J$  = 4.2, 8.6 Hz, 1 H).

$^{13}\text{C}$  NMR (100 MHz, DMSO- $d_6$ ):  $\delta$  = 159.4, 153.5, 150.8, 148.1, 145.7, 132.7, 132.0, 130.2, 129.1, 128.8, 128.0, 124.2, 124.1, 121.4.

**5-Nitro-N-(quinolin-6-yl)thiophene-2-carboxamide (4.6d)**

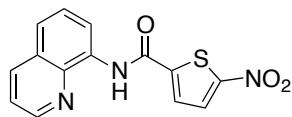


From **4.5d**. The precipitated product was washed with MeCN and then hexanes to afford **4.6d** as a yellow solid; 31% (75 mg, 0.25 mmol) TY= 239.23 mg.

$^1\text{H}$  NMR (400 MHz, DMSO- $d_6$ ):  $\delta$  = 10.95 (s, 1 H), 8.84 (dd,  $J$  = 1.7, 4.2 Hz, 1H), 8.47 (d,  $J$  = 2.1 Hz, 1 H), 8.35 (dd,  $J$  = 1.6, 8.3 Hz, 1 H), 8.23 (d,  $J$  = 4.3 Hz, 1 H), 8.13 (d,  $J$  = 4.4 Hz, 1 H), 7.99-8.06 (m, 2 H), 7.52 (dd,  $J$  = 4.2, 8.3 Hz, 1 H).

$^{13}\text{C}$  NMR (100 MHz, DMSO- $d_6$ ):  $\delta$  = 158.6, 153.5, 149.8, 146.0, 145.2, 135.9, 135.8, 130.2, 129.7, 128.6, 128.1, 124.0, 122.0, 117.1.

### 5-Nitro-N-(quinolin-8-yl)thiophene-2-carboxamide (4.6e)

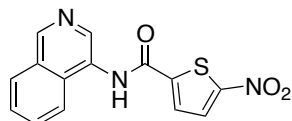


From **4.5e**. The precipitated product was washed with MeCN and then hexanes to afford **4.6e** as a brown solid; 65% (156 mg, 0.52 mmol).

$^1\text{H}$  NMR (400 MHz, DMSO- $d_6$ ):  $\delta$  = 10.85 (s, 1 H), 8.99 (dd,  $J$  = 1.7, 4.3 Hz, 1 H), 8.45-8.49 (m, 2 H), 8.22 (d,  $J$  = 4.4 Hz, 1 H), 8.12 (d,  $J$  = 4.4 Hz, 1 H), 7.83 (dd,  $J$  = 1.5, 8.3 Hz, 1 H), 7.65-7.70 (m, 2 H).

$^{13}\text{C}$  NMR (100 MHz, DMSO- $d_6$ ):  $\delta$  = 158.1, 153.6, 149.6, 145.6, 139.1, 136.7, 133.1, 130.3, 128.4, 128.0, 126.8, 124.0, 122.4, 119.4.

### N-(Isoquinolin-4-yl)-5-nitrothiophene-2-carboxamide (4.6f)



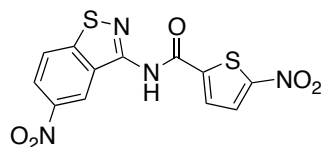
From **4.5f**. The precipitated product was washed with MeCN and then hexanes to afford **4.6f** as a yellow solid; yield 52% (125 mg, 0.42 mmol).

$^1\text{H}$  NMR (400 MHz, DMSO- $d_6$ ):  $\delta$  = 11.02 (s, 1 H), 9.30 (s, 1 H), 8.62 (s, 1 H), 8.28 (d,  $J$  = 4.4 Hz, 1 H), 8.22 (d,  $J$  = 8.3 Hz, 1 H), 8.16 (d,  $J$  = 4.4 Hz, 1 H), 8.02 (dd,  $J$  = 0.8, 8.4 Hz, 1 H), 7.86 (ddd,  $J$  = 1.3, 6.9, 8.2 Hz, 1 H), 7.76 (ddd,  $J$  = 1.0, 6.9, 8.2 Hz, 1 H).

$^{13}\text{C}$  NMR (100 MHz, DMSO- $d_6$ ):  $\delta$  = 159.6, 153.6, 151.2, 145.4, 140.6, 131.5, 130.9, 130.3, 128.9, 128.5, 127.9 (2 carbons), 127.6, 122.4.

HRMS (HESI):  $m/z$   $[\text{M}-\text{H}]^-$  calcd for  $\text{C}_{14}\text{H}_8\text{N}_3\text{O}_3\text{S}$ : 298.02919; found: 298.02896.

**5-Nitro-N-(5-nitrobenzo[d]isothiazol-3-yl)thiophene-2-carboxamide (4.6g)**



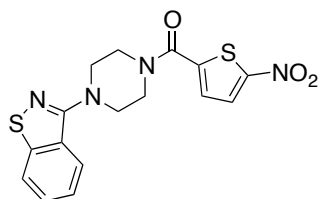
From **4.5g**. The precipitated product was purified by flash column chromatography (EtOAc/MeOH 95:5) to afford **4.6g** as an orange solid; yield 18% (50 mg, 0.14 mmol).

$^1\text{H}$  NMR (400 MHz, DMSO- $d_6$ ):  $\delta$  = 9.36 (s, 1 H), 8.19 (m, 3 H), 7.68 (d,  $J$  = 9.4 Hz, 1 H).

$^{13}\text{C}$  NMR (100 MHz, DMSO- $d_6$ ):  $\delta$  = 154.3, 141.3, 130.9, 130.1, 123.6, 120.3, 120.2, (5 carbons are missing).

DEPT 135 NMR (100 MHz, DMSO- $d_6$ ):  $\delta$  = 130.9, 130.1, 123.6, 120.3.

**(4-(Benzo[d]isothiazol-3-yl)piperazin-1-yl)(5-nitrothiophen-2-yl)methanone (4.6h)**



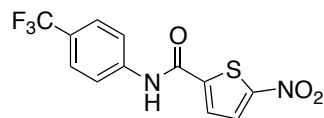
From **4.5h**. The product was crystalized in MeCN and then washed with Et<sub>2</sub>O and then hexanes to afford **4.6h** as a purple crystals; 63% (188 mg, 0.50 mmol).

$^1\text{H}$  NMR (400 MHz, DMSO- $d_6$ ):  $\delta$  = 8.10 (m, 3 H), 7.58 (ddd,  $J$  = 1.0, 7.1, 8.1 Hz, 1H), 7.54 (d,  $J$  = 4.3 Hz, 1H), 7.46 (ddd,  $J$  = 1.2, 6.9, 8.2 Hz, 1 H), 3.87 (m, 4 H), 3.56 (m, 4 H).

$^{13}\text{C}$  NMR (100 MHz, DMSO- $d_6$ ):  $\delta$  = 162.9, 160.4, 152.2, 152.1, 143.9, 129.3, 128.6, 128.0, 127.2, 124.5, 124.1, 121.2, 49.3, 48.6.



#### 5-Nitro-N-(4-(trifluoromethyl)phenyl)thiophene-2-carboxamide (4.6i)



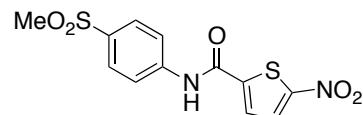
From **4.5i**. The precipitated product was washed with MeCN and then hexanes to afford **4.6i** as a light brown solid; 7% (17 mg, 0.05 mmol).

$^1\text{H}$  NMR (400 MHz, DMSO- $d_6$ ):  $\delta$  = 10.93 (s, 1 H), 8.23 (d,  $J$  = 4.4 Hz, 1 H), 8.10 (d,  $J$  = 4.4 Hz, 1 H), 7.96 (d,  $J$  = 8.6 Hz, 2 H), 7.77 (d,  $J$  = 8.7 Hz, 2 H).

$^{13}\text{C}$  NMR (100 MHz, DMSO- $d_6$ ):  $\delta$  = 158.8, 153.7, 145.6, 141.6, 130.1, 129.0, 126.2 (q,  $J$  = 3.7 Hz), 124.5 (q,  $J$  = 32.6 Hz), 124.3 (q,  $J$  = 271.2 Hz), 120.5.

$^{19}\text{F}$  NMR (400 MHz, DMSO- $d_6$ ):  $\delta$  = - 60.50.

#### N-(4-(Methylsulfonyl)phenyl)-5-nitrothiophene-2-carboxamide (4.6j)

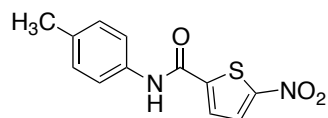


From **4.5j**. The precipitated product was washed with MeCN and then hexanes to afford **4.6j** as a pale yellow solid; 53% (138 mg, 0.42 mmol).

$^1\text{H}$  NMR (400 MHz, DMSO- $d_6$ ):  $\delta$  = 11.00 (s, 1 H), 8.23 (d,  $J$  = 4.4 Hz, 1 H), 8.11 (d,  $J$  = 4.4 Hz, 1 H), 7.97 (ddd,  $J$  = 4.2, 8.7, 20.9 Hz, 4 H), 3.20 (s, 3 H).

$^{13}\text{C}$  NMR (100 MHz, DMSO- $d_6$ ):  $\delta$  = 158.8, 153.8, 145.4, 142.5, 136.0, 130.1, 129.1, 128.2, 120.4, 43.7.

#### 5-Nitro-N-(p-tolyl)thiophene-2-carboxamide (4.6k)

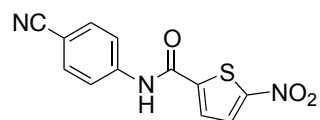


From **4.5k**. The precipitated product was washed with ice MeCN and then hexanes to afford **4.6k** as a yellow solid; 28% (59 mg, 0.23 mmol) TY = 209.63 mg.

$^1\text{H}$  NMR (400 MHz, DMSO- $d_6$ ):  $\delta$  = 10.58 (s, 1 H), 8.21 (d,  $J$  = 4.45 Hz, 1 H), 8.04 (d,  $J$  = 4.43 Hz, 1 H), 7.60 (dd,  $J$  = 8.61 Hz, 2 H), 7.20 (d,  $J$  = 8.86 Hz, 2 H), 2.29 (s, 3 H).

$^{13}\text{C}$  NMR (100 MHz, DMSO- $d_6$ ):  $\delta$  = 158.0, 153.3, 146.6, 135.4, 133.8, 130.2, 129.3, 128.2, 120.6, 20.5.

#### N-(4-Cyanophenyl)-5-nitrothiophene-2-carboxamide (**4.6l**)

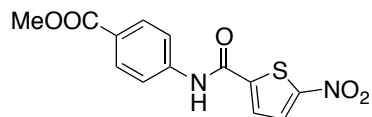


From **4.5l**. The precipitated product was washed with MeCN and then hexanes to afford **4.6l** as a white solid; yield 5% (12 mg, 0.04mmol).

$^1\text{H}$  NMR (400 MHz, DMSO- $d_6$ ):  $\delta$  = 10.97 (s, 1H), 8.23(d,  $J$  = 4.1Hz, 1 H), 8.09 (d,  $J$  = 4.0 Hz, 1 H), 7.93 (d,  $J$  = 8.4 Hz, 2 H), 7.86 (d,  $J$  = 8.3 Hz, 2 H).

$^{13}\text{C}$  NMR (100 MHz, DMSO- $d_6$ ):  $\delta$  = 158.9, 153.8, 145.3, 142.3, 133.3, 130.1, 129.2, 120.5, 118.9, 106.3.

#### Methyl 4-(5-nitrothiophene-2-carboxamido)benzoate (**4.6m**)

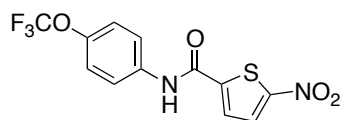


From **4.5m**. The precipitated product was washed with Et<sub>2</sub>O and then hexanes to afford **4.6m** as a yellow solid; yield 39% (95 mg, 0.31 mmol).

<sup>1</sup>H NMR (400 MHz, DMSO-*d*<sub>6</sub>): δ = 10.90 (s, 1 H), 8.22 (d, *J* = 4.4 Hz, 1 H), 8.10 (d, *J* = 4.4 Hz, 1 H), 7.99 (d, *J* = 8.6 Hz, 2 H), 7.89 (d, *J* = 8.7 Hz, 2 H), 3.84 (s, 3 H).

<sup>13</sup>C NMR (100 MHz, DMSO-*d*<sub>6</sub>): δ = 165.7, 158.6, 153.7, 145.7, 142.4, 130.2, 130.1, 128.9, 125.2, 119.9, 52.0.

#### 5-Nitro-N-(4-(trifluoromethoxy)phenyl)thiophene-2-carboxamide (**4.6n**)



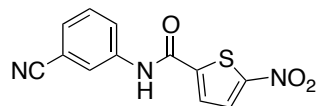
From **4.5n**. The precipitated product was purified by flash column chromatography (Hexanes/EtOAc 7:3) to afford **4.6n** as a orange solid; 27% yield (71 mg, 0.21 mmol)

<sup>1</sup>H NMR (400 MHz, DMSO-*d*<sub>6</sub>): δ = 10.78 (s, 1 H), 8.21 (d, *J* = 4.4 Hz, 1 H), 8.06 (d, *J* = 4.4 Hz, 1 H), 7.84 (d, *J* = 9.1 Hz, 2 H), 7.40 (d, *J* = 8.8 Hz, 2 H).

<sup>13</sup>C NMR (100 MHz, DMSO-*d*<sub>6</sub>): δ = 158.4, 153.5, 145.8, 144.5, 137.1, 130.0, 128.6, 122.0, 121.6, 120.1 (q, *J* = 255.1 Hz).

<sup>19</sup>F NMR (400 MHz, DMSO-*d*<sub>6</sub>): δ = - 57.00.

#### N-(3-Cyanophenyl)-5-nitrothiophene-2-carboxamide (**4.6o**)

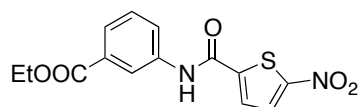


From **4.5o**. The precipitated product was washed with MeCN and then hexanes to afford **4.6o** as a white solid; 6% yield (14 mg, 0.05 mmol).

$^1\text{H}$  NMR (400 MHz, DMSO- $d_6$ ):  $\delta$  = 10.92 (s, 1 H), 8.23 (d,  $J$  = 4.5 Hz, 1 H), 8.18 (bs, 1 H), 8.06 (d,  $J$  = 4.4 Hz, 1 H), 7.99 (dt,  $J$  = 7.2 Hz, 1 H), 7.62 (m, 2 H).

$^{13}\text{C}$  NMR (100 MHz, DMSO- $d_6$ ):  $\delta$  = 158.7, 153.7, 145.4, 138.8, 130.4, 130.2, 128.9, 128.1, 125.2, 123.4, 118.5, 111.7.

### Ethyl 3-(5-nitrothiophene-2-carboxamido)benzoate (**4.6p**)

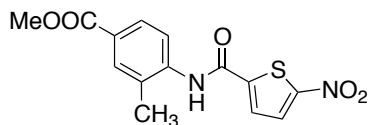


From **4.5p**. The product was crystalized in MeCN and then washed with iced cold MeCN and then hexanes to afford **4.6p** as a yellow solid; yield 41% (105 mg, 0.33 mmol).

$^1\text{H}$  NMR (400 MHz, DMSO- $d_6$ ):  $\delta$  = 10.84 (s, 1 H), 8.34 (t,  $J$  = 1.9 Hz, 1 H), 8.22 (d,  $J$  = 4.4 Hz, 1 H), 8.09 (d,  $J$  = 4.5 Hz, 1 H), 8.06 (dq,  $J$  = 1.1, 8.1 Hz, 1 H), 7.75 (dt,  $J$  = 1.3, 7.9 Hz, 1 H), 7.54 (t,  $J$  = 8.4 Hz, 1 H), 4.34 (q,  $J$  = 7.1 Hz, 2 H), 1.33 (s, 3 H).

$^{13}\text{C}$  NMR (100 MHz, DMSO- $d_6$ ):  $\delta$  = 165.4, 158.5, 153.6, 145.9, 138.4, 130.5, 130.2, 129.4, 128.6, 125.1, 124.9, 120.9, 61.0, 14.2.

### Methyl 3-methyl-4-(5-nitrothiophene-2-carboxamido)benzoate (**4.6q**)

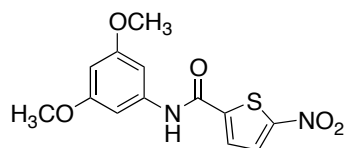


From **4.5q**. The precipitated product was washed with MeCN and then hexanes to afford **4.6q** as a yellow solid; yield 14% (35 mg, 0.11 mmol) TY = 256.04 mg.

$^1\text{H}$  NMR (400 MHz, DMSO- $d_6$ ):  $\delta$  = 10.51 (s, 1 H), 8.22 (d,  $J$  = 4.4 Hz, 1 H), 8.04 (d,  $J$  = 4.4 Hz, 1 H), 7.91 (d,  $J$  = 2.0 Hz, 1 H), 7.84 (dd,  $J$  = 2.1, 8.3 Hz, 1 H), 7.55 (d,  $J$  = 8.3 Hz, 1 H), 3.85 (s, 3 H), 2.32 (s, 3 H).

$^{13}\text{C}$  NMR (100 MHz, DMSO- $d_6$ ):  $\delta$  = 165.9, 158.4, 153.5, 145.5, 139.6, 133.8, 131.5, 130.2, 128.7, 127.4, 127.3, 126.4, 52.2, 17.8.

#### N-(3,5-Dimethoxyphenyl)-5-nitrothiophene-2-carboxamide (4.6r)

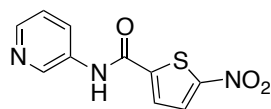


From **4.5r**. The product was crystalized in MeCN and then washed with MeCN and then hexanes to afford **4.6r** as a yellow solid; yield 29% (72 mg, 0.23 mmol).

$^1\text{H}$  NMR (400 MHz, DMSO- $d_6$ ):  $\delta$  = 10.52 (s, 1 H), 8.20 (d,  $J$  = 4.5 Hz, 1 H), 8.04 (d,  $J$  = 4.4 Hz, 1 H), 6.99 (s, 2 H), 6.32 (s, 1 H), 3.74 (s, 6 H).

$^{13}\text{C}$  NMR (100 MHz, DMSO- $d_6$ ):  $\delta$  = 160.5, 158.2, 153.4, 146.3, 139.6, 130.1, 128.3, 98.7, 96.6, 55.2.

#### 5-Nitro-N-(pyridin-3-yl)thiophene-2-carboxamide (4.6s)

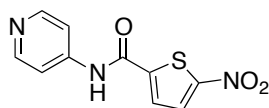


From **4.5s**. The precipitated product was washed with MeCN and then hexanes to afford **4.6s** as a brownish yellow; 60% (120 mg, 0.48 mmol).

$^1\text{H}$  NMR (400 MHz,  $\text{DMSO}-d_6$ ):  $\delta$  = 10.85 (s, 1 H), 8.89 (d,  $J$  = 2.56 Hz, 1 H), 8.37 (dd,  $J$  = 1.53, 4.67 Hz, 1 H), 8.23 (d,  $J$  = 4.42 Hz, 1 H), 8.13 (ddd,  $J$  = 1.58, 2.61, 8.38 Hz, 1 H), 8.06 (d,  $J$  = 4.42 Hz, 1 H), 7.44 (dd,  $J$  = 4.69, 8.13 Hz, 1 H).

$^{13}\text{C}$  NMR (100 MHz,  $\text{DMSO}-d_6$ ):  $\delta$  = 158.7, 153.6, 145.5 (for two carbons), 142.1, 134.7, 130.2, 128.8, 127.8, 123.8.

#### 5-Nitro-N-(pyridin-4-yl)thiophene-2-carboxamide (4.6t)

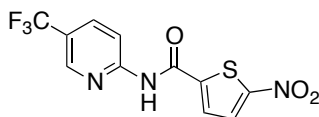


From **4.5t**. The precipitated product was washed with MeCN and then hexanes to afford **4.6t** as a beige solid; 58% (116 mg, 0.47 mmol) TY = 199.22 mg.

$^1\text{H}$  NMR (400 MHz,  $\text{DMSO}-d_6$ ):  $\delta$  = 10.95 (s, 1 H), 8.53 (dd,  $J$  = 1.68, 4.78 Hz, 2 H), 8.23 (d,  $J$  = 4.43 Hz, 1 H), 8.09 (d,  $J$  = 4.41 Hz, 1 H), 7.74 (dd,  $J$  = 1.66, 4.77 Hz, 2 H).

$^{13}\text{C}$  NMR (100 MHz,  $\text{DMSO}-d_6$ ):  $\delta$  = 159.2, 153.9, 150.4, 145.1, 145.0, 130.1, 129.3, 114.2.

#### 5-Nitro-N-(5-(trifluoromethyl)pyridin-2-yl)thiophene-2-carboxamide (4.6u)



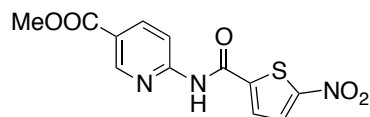
From **4.5u**. The precipitated product was washed with MeCN and then hexanes to afford **4.6u** as a pale green solid; 21% (54 mg, 0.17 mmol) TY = 253.61 mg.

$^1\text{H}$  NMR (400 MHz,  $\text{DMSO}-d_6$ ):  $\delta$  = 11.86 (s, 1 H), 8.84 (s, 1 H), 8.27-8.35 (m, 3 H), 8.20 (d,  $J$  = 4.4 Hz, 1 H).

$^{13}\text{C}$  NMR (100 MHz, DMSO- $d_6$ ):  $\delta$  = 159.5, 154.5, 154.2, 145.4 (q,  $J$  = 3.8 Hz), 144.9, 136.2, 130.1, 129.9, 123.8 (q,  $J$  = 269.0 Hz), 121.3 (q,  $J$  = 32.4 Hz), 114.5.

$^{19}\text{F}$  NMR (400 MHz,  $\text{CDCl}_3$ ):  $\delta$  = - 60.32.

#### Methyl 6-(5-nitrothiophene-2-carboxamido)nicotinate (4.6v)

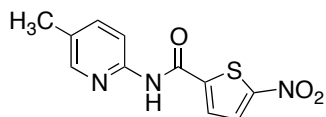


From **4.5v**. The precipitated product was washed with MeCN and then hexanes to afford **4.6v** as a pale green solid; 79% (195 mg, 0.64 mmol).

$^1\text{H}$  NMR (400 MHz, DMSO- $d_6$ ):  $\delta$  = 11.81 (s, 1 H), 8.93 (d,  $J$  = 2.4 Hz, 1 H), 8.35 (dd,  $J$  8.8, 2.4 Hz, 1 H), 8.17-8.29 (m, 3 H), 3.87 (s, 3 H).

$^{13}\text{C}$  NMR (100 MHz, DMSO- $d_6$ ):  $\delta$  = 164.7, 159.4, 154.6, 154.2, 149.4, 145.1, 139.5, 130.1, 129.8, 121.9, 114.0, 52.3.

#### N-(5-Methylpyridin-2-yl)-5-nitrothiophene-2-carboxamide (4.6w)

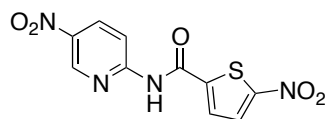


From **4.5w**. The precipitated product was washed with MeCN and then hexanes to afford **4.6w** as a greenish yellow solid; yield 29% (60 mg, 0.23 mmol).

$^1\text{H}$  NMR (400 MHz, DMSO- $d_6$ ):  $\delta$  = 11.37 (s, 1 H), 8.24-8.27 (m, 2 H), 8.18 (d,  $J$  = 4.4 Hz, 1 H), 8.02 (d,  $J$  = 8.48 Hz, 1 H), 7.70 (dd,  $J$  = 2.56, 8.44 Hz, 1 H), 2.29 (s, 3 H).

$^{13}\text{C}$  NMR (100 MHz, DMSO- $d_6$ ):  $\delta$  = 158.7, 153.7, 149.1, 147.9, 146.0, 138.8, 130.2, 129.7, 129.0, 114.6, 17.4.

**5-Nitro-N-(5-nitropyridin-2-yl)thiophene-2-carboxamide (4.6x)**

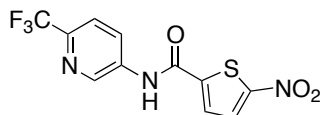


From **4.5x**. The precipitated product was washed with MeCN and then hexanes to afford **4.6x** as a beige solid; 25% (58 mg, 0.20 mmol).

$^1\text{H}$  NMR (400 MHz, DMSO- $d_6$ ):  $\delta$  = 12.10 (s, 1 H), 9.27 (s, 1 H), 8.69 (d,  $J$  = 8.9 Hz, 1 H), 8.21-8.38 (m, 3 H).

$^{13}\text{C}$  NMR (100 MHz, DMSO- $d_6$ ):  $\delta$  = 159.7, 155.6, 154.4, 144.6 (for 2 carbons), 140.6, 134.5, 130.2, 130.1, 114.1.

**5-Nitro-N-(6-(trifluoromethyl)pyridin-3-yl)thiophene-2-carboxamide (4.6y)**



From **4.5y**. The precipitated product was washed with MeCN and then hexanes to afford **4.6y** as a off white solid; 19% (48 mg, 0.15 mmol).

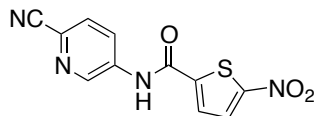
$^1\text{H}$  NMR (400 MHz, DMSO- $d_6$ ):  $\delta$  = 11.17 (s, 1 H), 9.05 (d,  $J$  = 2.5 Hz, 1 H), 8.43 (dd,  $J$  = 2.6, 8.6 Hz, 1 H), 8.24 (d,  $J$  = 4.4 Hz, 1 H), 8.09 (d,  $J$  = 4.4 Hz, 1 H), 7.95 (d,  $J$  = 8.7, 1 H).

$^{13}\text{C}$  NMR (100 MHz, DMSO- $d_6$ ):  $\delta$  = 159.2, 154.0, 144.7, 141.9, 141.5 (q,  $J$  = 34.5 Hz), 137.8, 130.1, 129.4, 128.2, 121.7 (q,  $J$  = 274.1 Hz), 121.3.

$^{19}\text{F}$  NMR (400 MHz, DMSO- $d_6$ ):  $\delta$  = - 65.80.

**N-(6-Cyanopyridin-3-yl)-5-nitrothiophene-2-carboxamide (4.6z)**



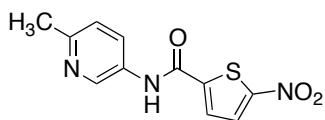


From **4.5z**. The precipitated product was washed with MeCN and then hexanes to afford **4.6z** as a beige solid; 39% (86 mg, 0.31 mmol).

$^1\text{H}$  NMR (400 MHz, DMSO- $d_6$ ):  $\delta$  = 11.19 (s, 1 H), 9.03 (d,  $J$  = 2.5 Hz, 1 H), 8.38 (dd,  $J$  = 2.5, 8.6 Hz, 1 H), 8.24 (d,  $J$  = 4.4 Hz, 1 H), 8.07 (m, 2 H).

$^{13}\text{C}$  NMR (100 MHz, DMSO- $d_6$ ):  $\delta$  = 159.2, 154.1, 144.5, 142.9, 138.2, 130.1, 129.6 (for 2 carbons), 127.4, 127.1, 117.6.

#### N-(6-Methylpyridin-3-yl)-5-nitrothiophene-2-carboxamide (**4.6aa**)

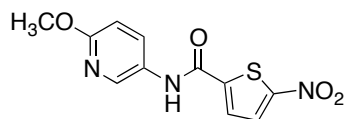


From **4.5aa**. The precipitated product was washed with MeCN and then hexanes to afford **4.6aa** as a yellow solid; 57% (120 mg, 0.46 mmol).

$^1\text{H}$  NMR (400 MHz, DMSO- $d_6$ ):  $\delta$  = 10.77 (s, 1 H), 8.74 (d,  $J$  = 2.52 Hz, 1 H), 8.22 (d,  $J$  = 4.44 Hz, 1 H), 8.04 (d,  $J$  = 4.43 Hz, 1 H), 8.01 (dd,  $J$  = 2.78, 8.39 Hz, 1 H), 7.29 (d,  $J$  = 8.46 Hz, 1 H), 2.45 (s, 3 H).

$^{13}\text{C}$  NMR (100 MHz, DMSO- $d_6$ ):  $\delta$  = 158.5, 153.8, 153.5, 145.7, 141.3, 132.2, 130.2, 128.6, 128.4, 123.0, 23.5.

#### N-(6-Methoxypyridin-3-yl)-5-nitrothiophene-2-carboxamide (**4.6bb**)

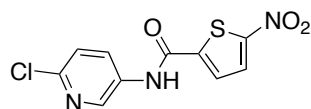


From **4.5bb**. The precipitated product was washed with MeCN and then hexanes to afford **4.6bb** as a yellow solid; 30 % (68 mg, 0.24 mmol).

$^1\text{H}$  NMR (400 MHz, DMSO- $d_6$ ):  $\delta$  = 10.71 (s, 1 H), 8.47 (d,  $J$  = 2.6 Hz, 1 H), 8.21 (d,  $J$  = 4.4 Hz, 1 H), 7.98-8.02 (m, 2 H), 6.87 (d,  $J$  = 8.9 Hz, 1 H), 3.85 (s, 3 H).

$^{13}\text{C}$  NMR (100 MHz, DMSO- $d_6$ ):  $\delta$  = 160.5, 158.3, 153.4, 145.9, 139.3, 132.8, 130.2, 128.8, 128.4, 110.3, 53.3.

#### N-(6-Chloropyridin-3-yl)-5-nitrothiophene-2-carboxamide (**4.6cc**)



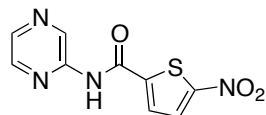
From **4.5cc**. The precipitated product was washed with MeCN and then hexanes to afford **4.6cc** as a yellow solid; yield 64% (146 mg, 0.52 mmol).

$^1\text{H}$  NMR (400 MHz, DMSO- $d_6$ ):  $\delta$  = 10.97 (s, 1 H), 8.74 (d,  $J$  = 2.8 Hz, 1 H), 8.23 (d,  $J$  = 4.4 Hz, 1 H), 8.19 (dd,  $J$  = 2.8, 8.7 Hz, 1 H), 8.04 (d,  $J$  = 4.4 Hz, 1 H), 7.56 (d,  $J$  = 8.7, 1 H).

$^{13}\text{C}$  NMR (100 MHz, DMSO- $d_6$ ):  $\delta$  = 158.8, 153.8, 145.1, 144.9, 141.7, 134.4, 131.3, 130.2, 129.0, 124.4.

HRMS (HESI):  $m/z$   $[\text{M}]^+$  calcd for  $\text{C}_{10}\text{H}_6\text{ClN}_3\text{O}_3\text{S}$ ; ; found: .

#### 5-Nitro-N-(pyrazin-2-yl)thiophene-2-carboxamide (**4.6dd**)

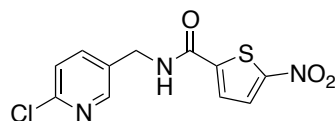


From **4.5dd**. The product was crystallized in MeCN and washed with Et<sub>2</sub>O and then hexanes to afford **4.6dd** as a brown solid; yield 44% (87 mg, 0.35 mmol).

$^1\text{H}$  NMR (400 MHz, DMSO- $d_6$ ):  $\delta$  = 11.72 (s, 1 H), 9.36 (d,  $J$  = 1.5 Hz, 1 H), 8.52 (m, 1 H), 8.47 (d,  $J$  = 2.5 Hz, 1 H), 8.26 (d,  $J$  = 4.4 Hz, 1 H), 8.20 (d,  $J$  = 4.4 Hz, 1 H).

$^{13}\text{C}$  NMR (100 MHz, DMSO- $d_6$ ):  $\delta$  = 159.1, 154.1, 148.2, 144.7, 142.7, 140.7, 137.5, 130.1, 129.8.

#### N-((6-Chloropyridin-3-yl)methyl)-5-nitrothiophene-2-carboxamide (**4.6ee**)



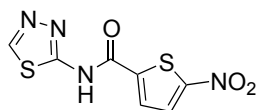
From **4.5ee**. The precipitated product was washed with MeCN/ether (1:1) to afford **4.6ee** as a pale yellow solid; 13 % (31 mg, 0.10 mmol)

$^1\text{H}$  NMR (400 MHz, DMSO- $d_6$ ):  $\delta$  = 9.58 (s, 1 H), 8.40 (d,  $J$  = 2.6 Hz, 1 H), 8.15 (d,  $J$  = 4.4 Hz, 1 H), 7.81 (m, 2 H), 7.51 (d,  $J$  = 8.2 Hz, 1 H), 4.50 (s, 2 H).

$^{13}\text{C}$  NMR (100 MHz, DMSO- $d_6$ ):  $\delta$  = 159.8, 153.1, 149.1, 149.0, 145.7, 139.2, 133.8, 130.2, 127.7, 124.2, 39.9.

DEPT 135 NMR (100 MHz, DMSO- $d_6$ ):  $\delta$  = 149.1, 139.2, 130.2, 127.7, 124.2, 39.9.

#### 5-Nitro-N-(1,3,4-thiadiazol-2-yl)thiophene-2-carboxamide (**4.6ff**)

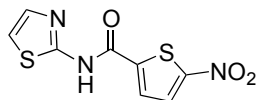


From **4.5ff**. The precipitated product was washed with MeCN and then hexanes to afford **4.6ff** as a yellow solid; yield 78% (160 mg, 0.63mmol)

$^1\text{H}$  NMR (400 MHz, DMSO- $d_6$ ):  $\delta$  = 13.65 (s, 1 H), 9.22 (s, 1 H), 8.21 (d,  $J$  = 4.0 Hz, 2 H).

HRMS (HESI):  $m/z$   $[\text{M-H}]^-$  calcd for  $\text{C}_7\text{H}_3\text{N}_4\text{O}_3\text{S}_2$ : 254.9652; found: 254.96541.

#### 5-Nitro-N-(thiazol-2-yl)thiophene-2-carboxamide (4.6gg)



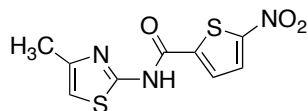
From **4.5gg**. The precipitated product was washed with MeCN and then hexanes to afford **4.6gg** as a yellow solid; yield 22% (45 mg, 0.18 mmol).

$^1\text{H}$  NMR (400 MHz, DMSO- $d_6$ ):  $\delta$  = 13.33 (s, 1 H), 8.17 (d,  $J$  = 4.2 Hz, 1 H), 8.04 (s, 1 H), 7.59 (d,  $J$  = 3.8 Hz, 1 H), 7.30 (d,  $J$  = 3.7 Hz, 1 H).

$^{13}\text{C}$  DEPT90 NMR (100 MHz, DMSO- $d_6$ ):  $\delta$  = 130.0, 129.2.

HRMS (HESI):  $m/z$   $[\text{M}-\text{H}]^-$  calcd for  $\text{C}_8\text{H}_4\text{N}_3\text{O}_3\text{S}_2$ : 253.96996; found: 253.97020.

#### N-(4-Methylthiazol-2-yl)-5-nitrothiophene-2-carboxamide (4.6hh)

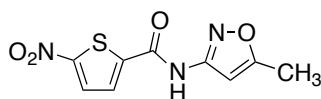


From **4.5hh**. The precipitated product was washed with MeCN and then hexanes to afford **4.6hh** as an orange solid; 36% (78 mg, 0.29 mmol).

$^1\text{H}$  NMR (400 MHz, DMSO- $d_6$ ):  $\delta$  = 13.27 (s, 1 H), 8.15 (d,  $J$  = 4.2 Hz, 1 H), 7.93 (bs, 1 H), 6.82 (s, 1 H), 2.28 (s, 3 H).

$^{13}\text{C}$  DEPT 90/135 NMR (100 MHz, DMSO- $d_6$ ):  $\delta$  = 130.2, 129.2.

#### N-(5-Methylisoxazol-3-yl)-5-nitrothiophene-2-carboxamide (4.6ii)

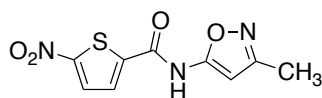


From **4.5ii**. The precipitated product was washed with MeCN and then hexanes to afford **4.6ii** as a white solid; 21% (42 mg, 0.17 mmol).

$^1\text{H}$  NMR (400 MHz, DMSO- $d_6$ ):  $\delta$  = 11.90 (s, 1 H), 8.16 (dd,  $J$  = 4.6, 15.5 Hz, 2 H), 6.72 (s, 1 H), 2.42 (s, 3 H).

$^{13}\text{C}$  NMR (100 MHz, DMSO- $d_6$ ):  $\delta$  = 170.0, 158.4, 157.9, 154.0, 144.4, 130.1, 129.5, 96.8, 12.1.

**N-(3-Methylisoxazol-5-yl)-5-nitrothiophene-2-carboxamide (4.6jj)**

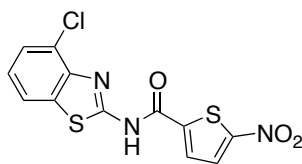


From **4.5jj**. The product crystallized in MeCN and was washed with Et<sub>2</sub>O and then hexanes to afford **4.6jj** as a dark green crystal; yield 26% (53 mg, 0.21 mmol)

$^1\text{H}$  NMR (400 MHz, DMSO- $d_6$ ):  $\delta$  = 12.48 (s, 1 H), 8.20 (d,  $J$  = 4.5 Hz, 1 H), 8.11 (d,  $J$  = 4.3 Hz, 1 H), 6.31 (s, 1 H), 2.23 (s, 3 H).

$^{13}\text{C}$  NMR (100 MHz, DMSO- $d_6$ ):  $\delta$  = 160.9, 160.4, 156.8, 154.3, 143.5, 130.1, 129.7, 90.5, 11.4.

**N-(4-Chlorobenzo[d]thiazol-2-yl)-5-nitrothiophene-2-carboxamide (4.6kk)**



From N-TMS amine **4.5kk**. The precipitated product was washed with MeCN and then hexanes to afford **4.6kk** as a yellow solid; 40% (108 mg, 0.32 mmol).

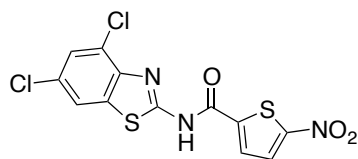
$^1\text{H}$  NMR (400 MHz, DMSO- $d_6$ ):  $\delta$  = 13.73 (s, 1 H), 8.32 (d,  $J$  = 4.2 Hz, 1 H), 8.20 (d,  $J$  = 4.2 Hz, 1 H), 8.02 (d,  $J$  = 8.0 Hz, 1 H), 7.57 (d,  $J$  = 7.8 Hz, 1 H), 7.34 (t,  $J$  = 7.9 Hz, 1H).

$^{13}\text{C}$  NMR (100 MHz,  $\text{DMSO-}d_6$ ):  $\delta = 154.7, 133.3, 130.6, 130.2, 126.5, 124.9, 121.0$  (5 carbons are missing).

DEPT-135 NMR (100 MHz,  $\text{DMSO-}d_6$ ):  $\delta = 130.6, 130.2, 126.5, 124.9, 121.0$

HRMS (HESI):  $m/z$   $[\text{M-H}]^-$  calcd for  $\text{C}_{12}\text{H}_5\text{ClN}_3\text{O}_3\text{S}_2$ : 337.94663; found: 337.94647.

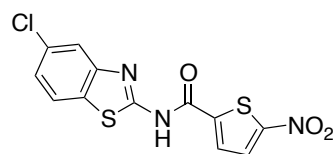
**N-(4,6-Dichlorobenzo[d]thiazol-2-yl)-5-nitrothiophene-2-carboxamide (4.6II)**



From **4.5II**. The precipitated product was washed with MeCN and then hexanes to afford **4.6II** as a greenish yellow solid; 70% (210 mg, 0.56 mmol).

$^1\text{H}$  NMR (400 MHz,  $\text{DMSO-}d_6$ ):  $\delta = 13.82$  (s, 1 H), 8.15-8.38 (m, 3 H), 7.72 (s, 1 H).

**N-(5-Chlorobenzo[d]thiazol-2-yl)-5-nitrothiophene-2-carboxamide (4.4mm)**



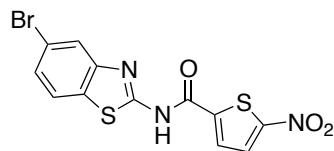
From **4.5mm**.

$^1\text{H}$  NMR (400 MHz,  $\text{DMSO-}d_6$ ):  $\delta = 8.21$  (d,  $J = 4.3$  Hz, 1 H), 8.17 (s, 1H), 8.06 (d,  $J = 8.5$  Hz, 1 H), 7.81 (s, 1 H), 7.41 (dd,  $J = 2.0, 8.5$  Hz, 1 H).

$^{13}\text{C}$  NMR (100 MHz,  $\text{DMSO-}d_6$ ):  $\delta = 154.4, 131.2, 130.4, 130.2, 124.1, 123.8$ , (6 carbons are missing).

DEPT 90 NMR (100 MHz,  $\text{DMSO-}d_6$ ):  $\delta = 130.4, 130.2, 124.1, 123.8$ .

**N-(5-Bromobenzo[d]thiazol-2-yl)-5-nitrothiophene-2-carboxamide (4.4nn)**

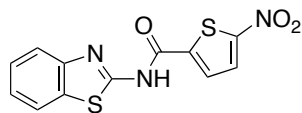


From **4.5nn**. The precipitated product was washed with MeCN and then hexanes to afford **4.6nn** as a yellow solid; 54% (164 mg, 0.43 mmol).

$^1\text{H}$  NMR (400 MHz, DMSO- $d_6$ ):  $\delta$  = 13.66 (s, 1 H), 8.17-8.21 (m, 2 H), 8.01 (d,  $J$  = 8.4 Hz, 1 H), 7.93 (s, 1 H), 7.52 (dd,  $J$  = 2.1, 8.5 Hz, 1 H).

$^{13}\text{C}$  DEPT90 NMR (100 MHz, DMSO- $d_6$ ):  $\delta$  = 130.2, 126.6, 124.0.

**N-(Benzo[d]thiazol-2-yl)-5-nitrothiophene-2-carboxamide (4.6oo)**



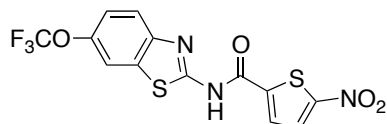
From **4.5oo**. The precipitated product was washed with MeCN and then hexanes to afford **4.6oo** as a yellow solid; 55% (133 mg, 0.44 mmol).

$^1\text{H}$  NMR (400 MHz, DMSO- $d_6$ ):  $\delta$  = 13.61 (s, 1 H), 7.98-8.18 (m, 3 H), 7.69 (s, 1 H), 7.49 (t,  $J$  = 7.6 Hz, 1 H), 7.36 (t,  $J$  = 7.6 Hz, 1 H).

$^{13}\text{C}$  NMR (100 MHz, DMSO- $d_6$ ):  $\delta$  = 154.0, 130.2, 130.1, 126.9, 124.1, 122.4, (6 carbons are missing).

DEPT-135 NMR (100 MHz, DMSO- $d_6$ ):  $\delta$  = 130.2, 130.1, 126.8, 124.1, 122.4.

**5-Nitro-N-(6-(trifluoromethoxy)benzo[d]thiazol-2-yl)thiophene-2-carboxamide (4.6pp)**



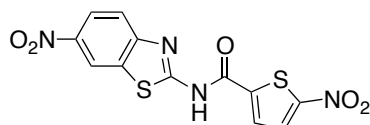
From N-TMS amine **4.5pp**. The precipitated product was further purified by flash column chromatography (EtOAc/MeOH 9:1) to remove minor impurities. Compound **4.6pp** was obtained as a yellow solid; 22 % (70 mg, 0.18 mmol).

$^1\text{H}$  NMR (400 MHz, Acetone- $d_6$ ):  $\delta$  = 8.19 (d,  $J$  = 4.2 Hz, 1 H), 8.11 (d,  $J$  = 4.3 Hz, 1 H), 8.04 (s, 1H), 7.83 (d,  $J$  = 8.8 Hz, 1 H), 7.45 (d,  $J$  = 8.8 Hz, 1 H).

$^{13}\text{C}$  NMR (100 MHz, Acetone- $d_6$ ):  $\delta$  = 162.4, 162.3, 156.1, 146.2, 145.7, 144.7, 133.3, 130.7, 130.2, 121.6 (q,  $J$  = 255.0 Hz), 121.3, 116.0.

$^{19}\text{F}$  NMR (400 MHz, Acetone- $d_6$ ):  $\delta$  = - 58.86.

#### 5-Nitro-N-(6-nitrobenzo[d]thiazol-2-yl)thiophene-2-carboxamide (4.4qq)



From N-TMS amine **4.5qq**. The precipitated product was washed with MeCN and then hexanes to afford **4.6qq** as a yellow solid; 45% (126 mg, 0.36 mmol).

$^1\text{H}$  NMR (400 MHz, DMSO- $d_6$ ):  $\delta$  = 13.91 (s, 1 H), 9.07 (s, 1 H), 8.30 (dd,  $J$  = 2.4, 9.0 Hz, 1 H), 8.22 (m, 2 H), 7.90 (dd,  $J$  = 8.8 Hz, 1 H).

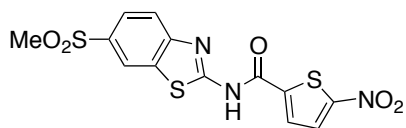
$^{13}\text{C}$  NMR (100 MHz, DMSO- $d_6$ ):  $\delta$  = 154.6, 143.3, 130.8, 130.2, 122.2, 119.4, (6 carbons are missing).

DEPT 90 NMR (100 MHz, DMSO- $d_6$ ):  $\delta$  = 130.8, 130.2, 122.2, 119.4.

HRMS (HESI):  $m/z$   $[\text{M-H}]^-$  calcd for  $\text{C}_{12}\text{H}_5\text{N}_4\text{O}_5\text{S}_2$ : 348.97068; found: 348.97015.



**N-(6-(Methylsulfonyl)benzo[d]thiazol-2-yl)-5-nitrothiophene-2-carboxamide (4.6rr)**



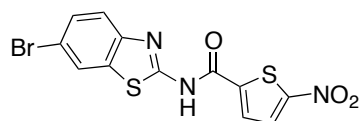
From **4.5rr**. The precipitated product was washed with MeCN and then hexanes to afford **4.6rr** as a yellow solid; 74% (226 mg, 0.59 mmol).

$^1\text{H}$  NMR (400 MHz, DMSO- $d_6$ ):  $\delta$  = 13.84 (s, 1 H), 8.69 (s, 1 H), 8.22 (m, 2 H), 8.00 (dd,  $J$  = 1.8, 8.5 Hz, 1 H), 7.95 (d,  $J$  = 8.2 Hz, 1 H), 3.26 (s, 3 H).

$^{13}\text{C}$  NMR (100 MHz, DMSO- $d_6$ ):  $\delta$  = 154.5, 135.9, 130.6, 130.2, 125.4, 122.5, 44.0, (6 carbons are missing).

DEPT 135 NMR (100 MHz, DMSO- $d_6$ ):  $\delta$  = 130.6, 130.2, 125.4, 122.5.

**N-(6-Bromobenzo[d]thiazol-2-yl)-5-nitrothiophene-2-carboxamide (4.6ss)**



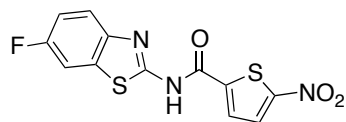
From **4.5v**. The precipitated product was washed with MeCN and then hexanes to afford **4.6ss** as a yellow solid; 45% (138 mg, 0.36 mmol).

$^1\text{H}$  NMR (400 MHz, DMSO- $d_6$ ):  $\delta$  = 13.60 (s, 1 H), 8.18-8.28 (m, 3 H), 7.60-7.6 (m, 2 H).

$^{13}\text{C}$  NMR (100 MHz, DMSO- $d_6$ ):  $\delta$  = 154.3, 130.4, 130.2, 129.7, 124.7, 116.1, (6 carbons are missing).

DEPT 135 NMR (100 MHz, DMSO- $d_6$ ):  $\delta$  = 130.3, 130.2, 129.6, 124.7.

**N-(6-Fluorobenzo[d]thiazol-2-yl)-5-nitrothiophene-2-carboxamide (4.6tt)**



From **4.5tt**. The precipitated product was washed with MeCN and then hexanes to afford **4.6tt** as a yellow solid; 79% (205 mg, 0.63 mmol).

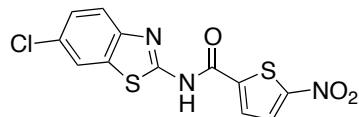
$^1\text{H}$  NMR (400 MHz, DMSO- $d_6$ ):  $\delta$  = 13.55 (s, 1 H), 8.10-8.18 (m, 2 H), 7.92 (dd,  $J$  = 2.7, 8.7 Hz, 1 H), 7.74 (bs, 1 H), 7.33 (td,  $J$  = 2.8, 9.1 Hz, 1 H).

$^{13}\text{C}$  NMR (100 MHz, DMSO- $d_6$ ):  $\delta$  = 168.3, 160.1, 157.7, 154.3, 147.4, 130.3, 130.2, 114.9, 114.7, 108.5, (2 carbons missing).

DEPT 90 NMR (100 MHz, DMSO- $d_6$ ):  $\delta$  = 130.3, 130.2, 114.9, 114.7.

$^{19}\text{F}$  NMR (400 MHz,  $\text{CDCl}_3$ ):  $\delta$  = - 117.57.

**N-(6-Chlorobenzo[d]thiazol-2-yl)-5-nitrothiophene-2-carboxamide (4.6uu)**



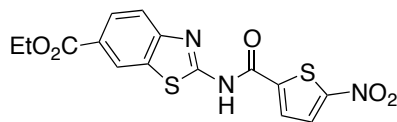
From N-TMS amine **4.5uu**. The precipitated product was washed with MeCN and then hexanes to afford **4.6uu** as a yellow solid; 80% (218 mg, 0.64 mmol).

$^1\text{H}$  NMR (400 MHz, DMSO- $d_6$ ):  $\delta$  = 13.60 (s, 1 H), 8.13-8.18 (m, 3 H), 7.70-7.72 (m, 1 H), 7.50 (dd,  $J$  = 2.21, 8.59 Hz, 1 H).

$^{13}\text{C}$  NMR (100 MHz, DMSO- $d_6$ ):  $\delta$  = 154.3, 130.3, 130.2, 128.2, 128.0, 127.0, 121.9, (5 carbons are missing).

DEPT-90 NMR (100 MHz, DMSO- $d_6$ ):  $\delta$  = 130.3, 130.2, 127.0, 121.9.

**Ethyl 2-(5-nitrothiophene-2-carboxamido)benzo[d]thiazole-6-carboxylate (4.6vv)**



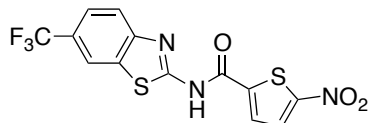
From **4.5vv**. The precipitated product was washed with MeCN and then hexanes to afford **4.6vv** as a greenish yellow solid; 88% (264 mg, 0.70 mmol).

$^1\text{H}$  NMR (400 MHz, DMSO- $d_6$ ):  $\delta$  = 13.72 (s, 1 H), 8.60 (s, 1 H), 8.00-8.16 (m, 3 H), 7.75 (m, 1 H), 4.32 (q,  $J$  = 7.1 Hz, 2 H), 1.34 (t,  $J$  = 7.1 Hz, 3 H).

$^{13}\text{C}$  NMR (100 MHz, DMSO- $d_6$ ):  $\delta$  = 165.3, 154.2, 130.4, 130.2, 127.6, 125.3, 124.1, 60.9, 14.2, (6 carbons are missing).

DEPT-135 NMR (100 MHz, DMSO- $d_6$ ):  $\delta$  = 130.4, 130.1, 127.6, 124.1, 60.9, 14.2.

**5-Nitro-N-(6-(trifluoromethyl)benzo[d]thiazol-2-yl)thiophene-2-carboxamide (4.6ww)**



From **4.5ww**. The precipitated product was washed with MeCN and then hexanes to afford **4.6ww** as a yellow solid; 60% (180 mg, 0.48 mmol).

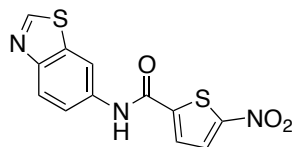
$^1\text{H}$  NMR (400 MHz, DMSO- $d_6$ ):  $\delta$  = 13.77 (s, 1H), 8.51 (s, 1H), 8.18 (d,  $J$  = 4.2 Hz, 1H), 8.16 (bs, 1H), 7.88 (m, 1H), 7.78 (dd,  $J$  = 8.6, 1.7 Hz, 1H).

$^{13}\text{C}$  NMR (100 MHz, DMSO- $d_6$ ):  $\delta$  = 154.4, 130.5, 130.2, 128.5, 125.8, 124.5 (q,  $J$  = 270.4 Hz), 124.2 (q,  $J$  = 32.1 Hz), 123.4, 120.3, (4 carbons missing).

DEPT-90 NMR (100 MHz, DMSO- $d_6$ ):  $\delta$  = 130.5, 130.2, 123.4, 120.3.

$^{19}\text{F}$  NMR (400 MHz, DMSO- $d_6$ ):  $\delta$  = - 59.62.

#### N-(Benzo[d]thiazol-6-yl)-5-nitrothiophene-2-carboxamide (4.6xx)



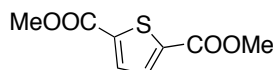
From **4.5xx**. The precipitated product was washed with MeCN and then hexanes to afford **4.6xx** as a brown solid; yield 15% (37 mg, 0.12 mmol).

$^1\text{H}$  NMR (400 MHz, DMSO- $d_6$ ):  $\delta$  = 10.90 (s, 1 H), 9.34 (s, 1 H), 8.63 (d,  $J$  = 2.1 Hz, 1 H), 8.23 (d,  $J$  = 4.4 Hz, 1 H), 8.10 (m, 2 H), 7.79 (dd,  $J$  = 2.2, 9.1 Hz, 1 H).

$^{13}\text{C}$  NMR (100 MHz, DMSO- $d_6$ ):  $\delta$  = 158.4, 155.8, 153.5, 150.0, 146.1, 135.5, 134.2, 130.2, 128.6, 123.1, 120.0, 113.6.

HRMS (HESI):  $m/z$   $[\text{M}]^+$  calcd for  $\text{C}_{12}\text{H}_7\text{N}_3\text{O}_3\text{S}_2$ ; found: .

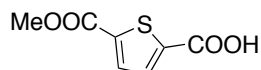
#### Dimethyl thiophene-2,5-dicarboxylate (4.8)



Thionyl chloride (1.16 mL, 16.0 mmol) was added dropwise to an ice-bath cooled solution of 2,5-thiophenedicarboxylic acid **4.7** (1 g, 5.8 mmol) in MeOH (20 mL). After the addition, the solution was stirred at 65 °C for 12 h. After cooling to room temperature, the reaction mixture was poured into ice water (25 mL). The precipitate that formed was collected by suction filtration and washed with ice MeOH to give **4.8** in 86% yield (1 g, 5 mmol).

$^1\text{H}$  NMR (400 MHz, DMSO- $d_6$ ):  $\delta$  = 7.82 (s, 2H), 3.86 (s, 6H).

#### 5-(Methoxycarbonyl)thiophene-2-carboxylic acid (4.9)



A mixture of **4.8** (3 g, 15 mmol) and LiOH (600 mg, 24 mmol) in THF/ H<sub>2</sub>O (2-1) (225 mL) was stirred for 25 min at room temperature. The solution was then acidified to pH 1 using concentrated HCl. The product was extracted with EtOAc, and the aqueous layer was washed with EtOAc (4 X 20 mL). The combined organic layers were dried over Na<sub>2</sub>SO<sub>4</sub>, filtrated, and concentrated. The solid obtained was purified by flash column chromatography (0-50% EtOAc in Hexanes) to afford **4.9** as a white solid in 46% yield (1.3 g, 6.98 mmol).

<sup>1</sup>H NMR (400 MHz, DMSO-*d*<sub>6</sub>): δ = 7.79 (d, *J* = 4.0 Hz, 1H), 7.73 (d, *J* = 4.0 Hz, 1H), 3.85 (s, 3H).

<sup>13</sup>C NMR (100 MHz, DMSO-*d*<sub>6</sub>): δ = 162.3, 161.4, 140.4, 137.6, 133.8, 133.3, 52.8

#### **General Procedure for the synthesis of 4.11kk, qq, ww**

A mixture of **4.9** (180 mg, 1 mmol), TFFH (260 mg, 1 mmol), and CsF (300 mg, 2 mmol) in MeCN (5 mL) was stirred for 22 h at room temperature. The product mixture was then concentrated under reduced pressure, taken up in hexane and filtered to remove the cesium salts. The filtrate was concentrated to give a yellowish oil, which was dried under high vacuum for 5 h. Based on its <sup>1</sup>H NMR spectrum, the isolated material corresponded to a 3:1 mixture of acid fluoride **4.3** and the 1,1,3,3-tetramethylurea side product. The product mixture was estimated to contain 188 mg (1 mmol, 100% conversion) of acid fluoride **4.3**.

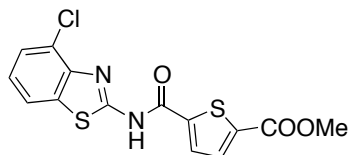
<sup>1</sup>H NMR (400 MHz, CD<sub>3</sub>CN-*d*<sub>3</sub>): 7.94 (m, 1H), 7.80 (m, 1H), 3.87 (s, 3H), 2.70 (s, 4 H, NMe).

<sup>19</sup>F NMR (400 MHz, CD<sub>3</sub>CN-*d*<sub>3</sub>): δ = 23.62.

For the coupling experiments, the mixture containing the freshly prepared acid fluoride (in mix with 1,1,3,3-tetramethylurea) was dissolved in MeCN (5 mL) and was added in one portion to the corresponding N-silylated amine (0.7 mmol) at room temperature. This was quickly followed

by addition of 1 M TBAF in THF (10  $\mu$ L, 0.01 mmol). The reaction mixture was stirred at 50  $^{\circ}$ C for 48 h. The precipitated product was collected with suction filtration and washed with MeCN and hexanes.

**Methyl 5-((4-chlorobenzo[d]thiazol-2-yl)carbamoyl)thiophene-2-carboxylate (4.11kk)**



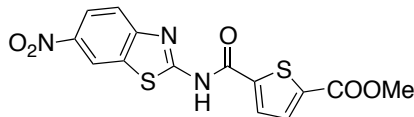
From **4.5kk** to afford **4.11kk** as a white solid in 53% yield (130 mg, 0.37 mmol).

$^1\text{H}$  NMR (400 MHz, DMSO- $d_6$ ):  $\delta$  = 13.55 (s, 1 H), 8.35 (d,  $J$  = 4.1 Hz, 1 H), 8.00 (d,  $J$  = 7.9 Hz, 1 H), 7.87 (d,  $J$  = 4.1 Hz, 1 H), 7.55 (d,  $J$  = 7.8 Hz, 1 H), 7.33 (t,  $J$  = 7.9 Hz, 1 H), 3.86 (s, 3 H).

$^{13}\text{C}$  NMR (100 MHz, DMSO- $d_6$ ):  $\delta$  = 161.3, 145.5, 138.2, 134.2, 133.3, 131.6, 126.3, 124.7, 124.5, 120.9, 52.8, (3 carbons are missing).

$^{13}\text{C}$  DEPT 135 NMR (100 MHz, DMSO- $d_6$ ):  $\delta$  = 134.2, 131.6, 126.3, 124.6, 120.9, 52.8.

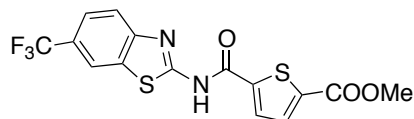
**Methyl 5-((6-nitrobenzo[d]thiazol-2-yl)carbamoyl)thiophene-2-carboxylate (4.11qq)**



From **4.5qq** to afford **4.11qq** as a very pale green solid in 77% yield (195 mg, 0.54 mmol).

$^1\text{H}$  NMR (400 MHz, DMSO- $d_6$ ):  $\delta$  = 13.68 (s, 1 H), 9.09 (s, 1 H), 8.30 (m, 2 H), 7.91-7.93 (m, 2 H), 3.88 (s, 3 H).

**Methyl 5-((6-(trifluoromethyl)benzo[d]thiazol-2-yl)carbamoyl)thiophene-2-carboxylate**  
**(4.11ww)**



From **4.5ww** to afford **4.11ww** as a pale yellow solid in 58% yield (156 mg, 0.40 mmol).

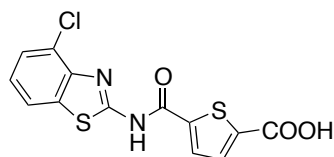
$^1\text{H}$  NMR (400 MHz, DMSO- $d_6$ ):  $\delta$  = 13.51 (s, 1 H), 8.52 (s, 1 H), 8.26 (s, 1 H), 7.91 (d,  $J$  = 8.4 Hz, 1 H), 7.87 (d,  $J$  = 4.2 Hz, 1 H), 7.77 (dd,  $J$  = 1.9, 8.6 Hz, 1 H), 3.87 (s, 3 H).

$^{13}\text{C}$  NMR (100 MHz, DMSO- $d_6$ ):  $\delta$  = 161.3, 142.8, 138.1, 134.1, 131.6, 124.5 (q,  $J$  = 272.3 Hz), 124.0 (q,  $J$  = 31.9 Hz), 123.2 (q,  $J$  = 3.6 Hz), 120.0 (q,  $J$  = 4.1 Hz), 52.7, (5 carbons missing).

DEPT 135 NMR (100 MHz, DMSO- $d_6$ ):  $\delta$  = 134.1, 131.6, 123.2 (q,  $J$  = 3.6 Hz), 120.0 (q,  $J$  = 4.1 Hz).

$^{19}\text{F}$  NMR (400 MHz,  $\text{CDCl}_3$ ):  $\delta$  = - 59.53.

**5-((4-Chlorobenzo[d]thiazol-2-yl)carbamoyl)thiophene-2-carboxylic acid (4.12kk)**

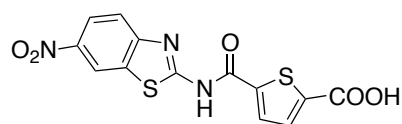


A mixture of **4.11kk** (230 mg, 0.65 mmol) and LiOH (153 mg, 6.12 mmol) in THF/ $\text{H}_2\text{O}$  (2-1) (24 mL) was stirred for 12 h at room temperature. The mixture was then acidified to pH 1 using concentrated HCl. The precipitate that formed was collected by suction filtration and washed with ice water. The product was then dried in oven (80  $^\circ\text{C}$ ) for few hours to afford **4.12kk** as a white solid in 80% (175 mg, 0.52 mmol).

$^1\text{H}$  NMR (400 MHz,  $\text{DMSO}-d_6$ ):  $\delta$  = 13.71 (s, 1 H), 13.52 (s, 1 H), 8.35 (d,  $J$  = 4.0 Hz, 1 H), 8.03 (d,  $J$  = 7.9 Hz, 1 H), 7.80 (d,  $J$  = 4.1 Hz, 1 H), 7.57 (d,  $J$  = 7.8 Hz, 1 H), 7.35 (t,  $J$  = 8.0 Hz, 1 H).

$^{13}\text{C}$  NMR (100 MHz,  $\text{DMSO}-d_6$ ):  $\delta$  = 162.4, 160.1, 159.3, 145.4, 141.6, 140.7, 133.6, 133.3, 131.8, 126.4, 124.8, 124.6, 120.9.

**5-((6-Nitrobenzo[d]thiazol-2-yl)carbamoyl)thiophene-2-carboxylic acid (4.12qq)**

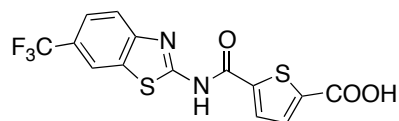


A mixture of **4.11qq** (217 mg, 0.60 mmol) and LiOH (118 mg, 4.72 mmol) in THF/ $\text{H}_2\text{O}$  (2-1) (21 mL) was stirred for 12 h at room temperature. The mixture was then acidified to pH 1 using concentrated HCl. The precipitate that formed was collected by suction filtration and washed with ice water. The product was then dried in oven (80 °C) for few hours to afford **4.12qq** as a very pale yellow solid in 83% (174 mg, 0.50 mmol).

$^1\text{H}$  NMR (400 MHz,  $\text{DMSO}-d_6$ ):  $\delta$  = 13.68 (s, 2 H), 9.10 (s, 1 H), 8.30-8.33 (m, 1 H), 8.28 (bs, 1 H), 7.93 (d,  $J$  = 8.9 Hz, 1 H), 7.81 (d,  $J$  = 4.1 Hz, 1 H).

$^{13}\text{C}$  NMR (100 MHz,  $\text{DMSO}-d_6$ ):  $\delta$  = 164.2, 162.3, 160.8, 152.6, 143.1, 141.7, 140.8, 133.6, 132.1, 131.9, 121.9, 120.2, 119.2.

**5-((6-(Trifluoromethyl)benzo[d]thiazol-2-yl)carbamoyl)thiophene-2-carboxylic acid (4.12ww)**





A mixture of **4.11ww** (90 mg, 0.23 mmol) and LiOH (45 mg, 1.84 mmol) in THF/H<sub>2</sub>O (2-1) (7.5 mL) was stirred for 12 h at room temperature. The mixture was then acidified to pH 1 using concentrated HCl. The precipitate that formed was collected by suction filtration and washed with ice water. The product was then dried in oven (80 °C) for few hours to afford **4.12ww** as a white solid in 22% (19 mg, 0.05 mmol).

<sup>1</sup>H NMR (400 MHz, DMSO-*d*<sub>6</sub>): δ = 13.50 (s, 1 H), 8.55 (s, 1 H), 8.26 (bs, 1 H), 7.93-7.95 (m, 1 H), 7.78-7.81 (m, 2 H).

<sup>13</sup>C NMR (100 MHz, DMSO-*d*<sub>6</sub>): δ = 162.3, 140.5, 133.5, 131.8, 124.5 (q, J = 271.6 Hz), 124.0 (q, J = 31.8 Hz), 123.2, 120.1, (6 carbons are missing).

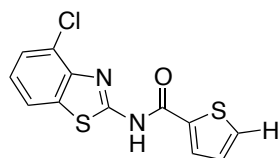
<sup>13</sup>C DEPT 90 NMR (100 MHz, DMSO-*d*<sub>6</sub>): δ = 133.6, 131.8, 123.2, 120.1

<sup>19</sup>F NMR (400 MHz, DMSO-*d*<sub>6</sub>): δ = - 59.51.

#### Preparation of amides **4.19kk**, **4.20kk**, and **4.21kk**, **qq**, **ww** :

To access the target amides **4.19kk**, **4.20kk**, and **4.21kk**, **qq**, **ww**, the method to prepare compounds **4.6a-xx** was modified such that the *N*-TMS amines **4.5kk**, **qq**, and **ww** were reacted with the *in situ* generated acid fluoride **4.16-4.18**. Further, in this “one pot” operation, the presence of CsF in the reaction medium eliminated the need to add TBAF to initiate the coupling reaction.

#### N-(4-Chlorobenzo[d]thiazol-2-yl)thiophene-2-carboxamide (**4.19kk**)

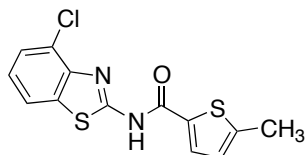


A mixture of **4.13** (130 mg, 1 mmol), TFFH (265mg, 1mmol) and CsF (400 mg, 2.67 mmol) in MeCN (5 mL) was stirred for 12 h at room temperature. To the mixture containing the *in situ* generated acid fluoride **4.16** was added a solution of TMS-amine **4.5kk** (0.7 mmol) in MeCN (5 mL). The reaction mixture was stirred at 50 °C for 48 h. The mixture was then concentrated under reduced and the solid obtained was silica-gel flash column chromatographed (Hex/EtOAc 9:1 to Hex/EtOAc 7:3) to afford **4.19kk** as a pale yellow solid in 12% (25 mg, 0.09 mmol).

<sup>1</sup>H NMR (400 MHz, DMSO-*d*<sub>6</sub>): δ = 13.28 (s, 1 H), 8.40 (d, *J* = 3.7 Hz, 1 H), 8.04 (dd, *J* = 0.9, 4.9 Hz, 1 H), 8.00 (dd, *J* = 0.9, 7.9 Hz, 1 H), 7.55 (dd, *J* = 0.9, 7.9 Hz, 1 H), 7.32 (t, *J* = 7.9 Hz, 1 H), 7.29 (t, *J* = 4.6 Hz, 1 H).

<sup>13</sup>C NMR (100 MHz, DMSO-*d*<sub>6</sub>): δ = 160.5, 159.6, 145.5, 136.7, 134.6, 133.3, 131.9, 128.8, 126.3, 124.5, 124.4, 120.8.

#### N-(4-Chlorobenzo[d]thiazol-2-yl)-5-methylthiophene-2-carboxamide (**4.20kk**)

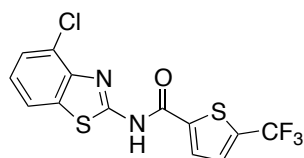


A mixture of **4.14** (142 mg, 1 mmol), TFFH (265mg, 1mmol) and CsF (240 mg, 1.60 mmol) in MeCN (5 mL) was stirred for 12 h at room temperature. To the mixture containing the *in situ* generated acid fluoride **4.17** was added a solution of TMS-amine **4.5kk** (0.7 mmol) in MeCN (5 mL). The reaction mixture was stirred at 50 °C for 48 h. The mixture was then concentrated under reduced and the solid obtained was silica-gel flash column chromatographed (Hex/EtOAc 9:1) to afford **4.20kk** as a yellow solid in 25% (53 mg, 0.17 mmol).

$^1\text{H}$  NMR (400 MHz,  $\text{DMSO}-d_6$ ):  $\delta$  = 13.16 (s, 1 H), 8.21 (d,  $J$  = 3.8 Hz, 1 H), 7.99 (dd,  $J$  = 1.0, 7.9 Hz, 1 H), 7.54 (dd,  $J$  = 1.1, 7.8 Hz, 1 H), 7.31 (t,  $J$  = 7.9 Hz, 1 H), 6.99 (dd,  $J$  = 1.2, 3.9 Hz, 1 H), 2.53 (s, 3 H).

$^{13}\text{C}$  NMR (100 MHz,  $\text{DMSO}-d_6$ ):  $\delta$  = 160.3, 159.6, 149.0, 145.5, 134.0, 133.3, 132.3, 127.5, 126.3, 124.5, 124.4, 120.8, 15.5.

**N-(4-Chlorobenzo[d]thiazol-2-yl)-5-(trifluoromethyl)thiophene-2-carboxamide (4.21kk)**



A mixture of 5-trifluoromethylthiophene-2-carboxylic acid **4.15** (115 mg, 0.6 mmol), TFFH (160 mg, 0.6 mmol), and CsF (160 mg, 1.05 mmol) in MeCN (3 mL) was stirred for 12 h at room temperature. To the mixture containing the *in situ* generated acid fluoride **4.18** was added a solution of TMS-amine **4.5kk** (0.4 mmol) in MeCN (3 mL). The resultant mixture was stirred at 50 °C for 48 h. It was then concentrated under reduced pressure and the solid obtained was silica-gel flash column chromatographed (0-100% EtOAc in Hex) to afford **4.21kk** as a pale pink solid in 66% (95 mg, 0.26 mmol).

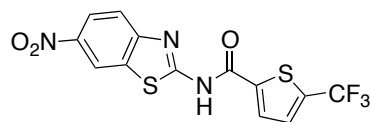
$^1\text{H}$  NMR (400 MHz,  $\text{DMSO}-d_6$ ):  $\delta$  = 13.62 (s, 1 H), 8.40 (s, 1 H), 8.02 (d,  $J$  = 7.9 Hz, 1 H), 7.90 (d,  $J$  = 4.1 Hz, 1 H), 7.57 (d,  $J$  = 7.8 Hz, 1 H), 7.34 (t,  $J$  = 7.9 Hz, 1 H).

$^{13}\text{C}$  NMR (100 MHz,  $\text{DMSO}-d_6$ ):  $\delta$  = 159.7, 159.2, 145.4, 141.2, 134.7 (q,  $J$  = 37.8 Hz), 133.3, 131.3, 126.4, 124.8, 124.6, 121.9 (q,  $J$  = 271.2 Hz), 121.0, (one carbon is missing).

DEPT 135  $^{13}\text{C}$  NMR (100 MHz,  $\text{DMSO}-d_6$ ):  $\delta$  = 131.3, 126.4, 124.8, 121.0.

$^{19}\text{F}$  NMR (400 MHz,  $\text{DMSO}-d_6$ ):  $\delta$  = -54.73.

**N-(6-Nitrobenzo[d]thiazol-2-yl)-5-(trifluoromethyl)thiophene-2-carboxamide (4.21qq)**

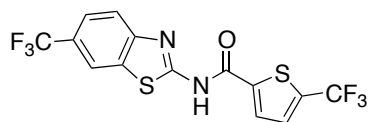


A mixture of carboxylic acid **4.15** (115 mg, 0.6 mmol), TFFH (160 mg, 0.6 mmol), and CsF (300 mg, 2.00 mmol) in MeCN (3 mL) was stirred for 12 h at room temperature. To the mixture containing the *in situ* generated acid fluoride **4.18** was added a solution of TMS-amine **4.5qq** (0.4 mmol) in MeCN (3 mL). The resultant mixture was stirred at 50 °C for 48 h. It was then concentrated under reduced pressure and the solid obtained was silica-gel flash column chromatographed (Hex/EtOAc 7:3) to afford **4.21qq** as a pale yellow solid in 16% (23.5 mg, 0.06 mmol).

<sup>1</sup>H NMR (400 MHz, DMSO-*d*<sub>6</sub>): δ = 13.78 (s, 1 H), 9.10 (s, 1 H), 8.30-8.34 (m, 2 H), 7.91-7.94 (m, 2 H).

<sup>19</sup>F NMR (400 MHz, DMSO-*d*<sub>6</sub>): δ = - 54.73.

**5-(Trifluoromethyl)-N-(6-(trifluoromethyl)benzo[d]thiazol-2-yl)thiophene-2-carboxamide (4.21ww)**



A mixture of carboxylic acid **4.15** (115 mg, 0.6 mmol), TFFH (160 mg, 0.6 mmol), and CsF (500 mg, 3.30 mmol) in MeCN (3 mL) was stirred for 12 h at room temperature. To the mixture containing the *in situ* generated acid fluoride **4.18** was added a solution of TMS-amine **4.5ww** (0.4 mmol) in MeCN (3 mL). The resultant mixture was stirred at 50 °C for 48 h. It was then concentrated under reduced pressure and the solid obtained was silica-gel flash column

chromatographed (Hex/EtOAc 7:3) to afford **4.21ww** as a pale yellow solid in 48% (76 mg, 0.19 mmol).

$^1\text{H}$  NMR (400 MHz, DMSO- $d_6$ ):  $\delta$  = 13.62 (s, 1 H), 8.53 (s, 1 H), 8.28 (s, 1 H), 7.88-7.92 (m, 2 H), 7.77-7.79 (dd,  $J$  = 1.9, 8.5 Hz, 1 H).

$^{13}\text{C}$  NMR (100 MHz, DMSO- $d_6$ ):  $\delta$  = 141.8, 134.5 (q,  $J$  = 37.8 Hz), 131.3, 128.6, 126.0, 124.5 (q,  $J$  = 270.7 Hz), 124.1 (q,  $J$  = 32.0 Hz), 123.3, 120.6, 120.2, (4 carbons missing).

DEPT 135  $^{13}\text{C}$  NMR (100 MHz, DMSO- $d_6$ ):  $\delta$  = 131.3, 123.3, 120.2.

$^{19}\text{F}$  NMR (400 MHz, DMSO- $d_6$ ):  $\delta$  = - 54.75, - 59.54.

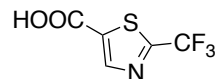
$^1\text{H}$  NMR (400 MHz, acetone- $d_6$ ):  $\delta$  = 8.43 (bs, 1 H), 8.30 (dt,  $J$  = 1.4, 4.0 Hz, 1 H), 7.93 (d,  $J$  = 8.6 Hz, 1 H), 7.79 (m, 2 H).

$^{13}\text{C}$  NMR (100 MHz, acetone- $d_6$ ):  $\delta$  = 162.7, 161.6, 150.9, 142.7, 136.8 (q,  $J$  = 38.2 Hz), 133.1, 131.5, 131.3 (q,  $J$  = 3.6 Hz), 126.1 (q,  $J$  = 32.7 Hz), 125.6 (q,  $J$  = 271.2 Hz), 124.1 (q,  $J$  = 3.1 Hz), 123.0 (q,  $J$  = 271.2 Hz), 121.4, 120.5 (q,  $J$  = 3.9 Hz).

DEPT 135  $^{13}\text{C}$  NMR (100 MHz, acetone- $d_6$ ):  $\delta$  = 131.5, 131.3 (q,  $J$  = 3.6 Hz), 124.1 (q,  $J$  = 3.1 Hz), 121.4, 120.5 (q,  $J$  = 3.9 Hz).

$^{19}\text{F}$  NMR (400 MHz, acetone- $d_6$ ):  $\delta$  = - 56.74, - 61.64.

### 2-(Trifluoromethyl)thiazole-5-carboxylic acid (**4.23**)



A mixture of ester **4.22** (0.97 g, 4.31 mmol) and LiOH (220 mg, 9.17 mmol) in THF/H<sub>2</sub>O (5-3) (80 mL) was stirred for 2.5 h at room temperature. The mixture was then acidified to pH 1 using concentrated HCl. The mixture was extracted with CH<sub>2</sub>Cl<sub>2</sub>, and the aqueous layer was washed with CH<sub>2</sub>Cl<sub>2</sub> (4 X, 20 mL). The combined organic layers were dried over Na<sub>2</sub>SO<sub>4</sub>, filtrated, and concentrated to afford **4.23** as a yellow solid 93% (790 mg, 4.01 mmol).

<sup>1</sup>H NMR (400 MHz, DMSO-*d*<sub>6</sub>): δ = 8.61 (s, 1 H).

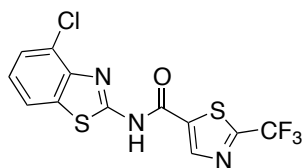
<sup>13</sup>C NMR (400 MHz, DMSO-*d*<sub>6</sub>): δ = 161.1, 157.5 (q, *J* = 40.0 Hz), 148.3, 135.6, 119.2 (q, *J* = 272.6 Hz).

<sup>19</sup>F NMR (400 MHz, DMSO-*d*<sub>6</sub>): δ = - 60.66.

### Preparation of amides **4.25kk**, **qq**, **ww** from 2-trifluoromethylthiazole-5-carboxylic acid,

**4.23**: The protocol used to prepare amides **4.19kk**, **4.20kk**, and **4.21kk**, **qq**, **ww** was further used to access the 2-trifluoromethylthiazole-based amides **4.25kk**, **qq**, **ww**.

### N-(4-Chlorobenzo[d]thiazol-2-yl)-2-(trifluoromethyl)thiazole-5-carboxamide (**4.25kk**)



A mixture of carboxylic acid **4.23** (300 mg, 1.5 mmol), TFFH (400 mg, 1.5 mmol), and CsF (340 mg, 2.25 mmol) in MeCN (8 mL) was stirred for 12 h at room temperature. To the mixture containing the *in situ* generated acid fluoride **4.24** was added a solution of TMS-amine **4.5kk** (1

mmol) in MeCN (8 mL). The resultant mixture was stirred at 50 °C for 12 h. It was then concentrated under reduced pressure and the solid obtained was silica-gel flash column chromatographed (Hex/EtOAc 7:3) to afford **4.25kk** as a white solid in 58% (210 mg, 0.58 mmol).

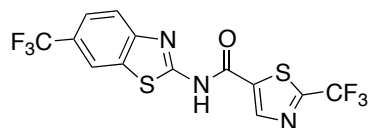
<sup>1</sup>H NMR (400 MHz, DMSO-*d*<sub>6</sub>): δ = 13.84 (s, 1 H), 9.10 (s, 1 H), 8.03 (d, *J* = 7.9 Hz, 1 H), 7.58 (d, *J* = 7.7 Hz, 1 H), 7.36 (t, *J* = 7.9 Hz, 1 H).

<sup>13</sup>C NMR (400 MHz, DMSO-*d*<sub>6</sub>): δ = 159.0, 158.6, 158.0 (q, *J* = 40.0 Hz), 146.5, 145.3, 137.9, 133.2, 126.5, 125.0, 124.6, 121.0, 119.2 (q, *J* = 273.3 Hz).

DEPT 135 <sup>13</sup>C NMR (400 MHz, DMSO-*d*<sub>6</sub>): δ = 146.5, 126.5, 125.0, 121.1.

<sup>19</sup>F NMR (400 MHz, DMSO-*d*<sub>6</sub>): δ = - 60.57.

**2-(Trifluoromethyl)-N-(6-(trifluoromethyl)benzo[d]thiazol-2-yl)thiazole-5-carboxamide (4.25ww)**



A mixture of carboxylic acid **4.23** (250 mg, 1.27 mmol), TFFH (340 mg, 1.28 mmol), and CsF (600 mg, 3.95 mmol) in MeCN (6 mL) was stirred for 12 h at room temperature. To the mixture containing the *in situ* generated acid fluoride, **4.24** was added a solution of TMS-amine **4.5ww** (0.85 mmol) in MeCN (6 mL). The resultant mixture was stirred at 50 °C for 12 h. It was then concentrated under reduced pressure and the solid obtained was silica-gel flash column chromatographed (100% EtOAc) and then recrystallized in EtOAc to afford **4.25ww** as a white solid in 55% (184 mg, 0.46 mmol).

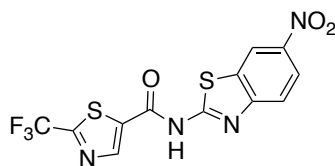
$^1\text{H}$  NMR (400 MHz,  $\text{DMSO}-d_6$ ):  $\delta$  = 13.87 (s, 1 H), 8.95 (s, 1 H), 8.52 (s, 1 H), 7.89 (d,  $J$  = 8.2 Hz, 1 H), 7.78 (d,  $J$  = 8.7 Hz, 1 H).

$^{13}\text{C}$  NMR (400 MHz,  $\text{DMSO}-d_6$ ):  $\delta$  = 157.7 (q,  $J$  = 40.1 Hz), 146.5, 138.7, 131.1, 124.5 (q,  $J$  = 272.7 Hz), 124.2 (q,  $J$  = 32.1 Hz), 123.5 (2XCH), 120.3, 119.2 (q,  $J$  = 271.9 Hz), (3 carbons are missing).

DEPT 135  $^{13}\text{C}$  NMR (400 MHz,  $\text{DMSO}-d_6$ ):  $\delta$  = 146.5, 123.5, 120.3.

$^{19}\text{F}$  NMR (400 MHz,  $\text{DMSO}-d_6$ ):  $\delta$  = - 60.59, - 59.63.

#### ***N*-(6-Nitrobenzo[d]thiazol-2-yl)-2-(trifluoromethyl)thiazole-5-carboxamide (4.25qq)**



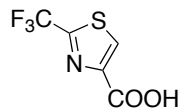
A mixture of carboxylic acid **4.23** (267 mg, 1.35 mmol), TFFH (362 mg, 1.37 mmol), and CsF (500 mg, 3.31 mmol) in MeCN (6 mL) was stirred for 27 h at room temperature. To the mixture containing the *in situ* generated acid fluoride **4.24** was added a solution of TMS-amine **4.5qq** (0.85 mmol) in MeCN (6 mL). The resultant mixture was stirred at 50 °C for 48 h. It was then concentrated under reduced pressure to afford **4.25qq** in pure form as a yellow solid in 119% (380 mg, 1.01 mmol).

$^1\text{H}$  NMR (400 MHz,  $\text{DMSO}-d_6$ ):  $\delta$  = 11.84 (s, 1H), 8.67 (d,  $J$  = 2.5 Hz, 1H), 8.41 (s, 1H), 8.11 (dd,  $J$  = 2.5, 8.9 Hz, 1H), 7.55 (d,  $J$  = 8.9 Hz, 1H).

$^{19}\text{F}$  NMR (400 MHz,  $\text{DMSO}-d_6$ ):  $\delta$  = - 60.24

#### **2-(Trifluoromethyl)thiazole-4-carboxylic acid (4.27)**





A mixture of **4.26** (560 mg, 2.49 mmol) and LiOH (125 mg, 5.21 mmol) in THF/H<sub>2</sub>O (5-3) (40 mL) was stirred for 35 min at room temperature. The solution was then acidified to pH 1 using concentrated HCl. The product was extracted with EtOAc, and the aqueous layer was washed with EtOAc (4 X 25 mL). The combined organic layers were dried over Na<sub>2</sub>SO<sub>4</sub>, filtrated, and concentrated to afford **4.27** as a pale pink solid in quantitative yield.

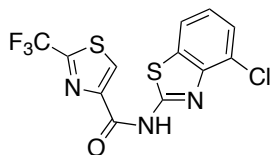
<sup>1</sup>H NMR (400 MHz, DMSO-*d*<sub>6</sub>): δ = 8.84 (s, 1 H).

<sup>13</sup>C NMR (400 MHz, DMSO-*d*<sub>6</sub>): δ = 161.0, 154.4 (q, *J* = 40.5 Hz), 148.2, 132.8, 119.4 (q, *J* = 119.4 Hz).

<sup>19</sup>F NMR (400 MHz, DMSO-*d*<sub>6</sub>): δ = - 60.29.

**Preparation of amides 4.29kk and 4.29 ww from 2-(trifluoromethyl)thiazole-4-carboxylic acid, 4.27:** The protocol used to prepare amides **4.19kk**, **4.20kk**, and **4.21kk**, **qq**, **ww** was further used to access **4.29kk** and **4.29ww**.

#### **N-(4-Chlorobenzo[d]thiazol-2-yl)-2-(trifluoromethyl)thiazole-4-carboxamide (4.29kk)**



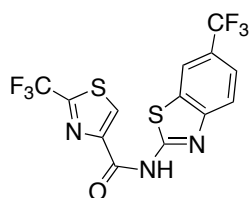
A mixture of **4.27** (150 mg, 0.76 mmol), TFFH (200 mg, 0.76 mmol), and CsF (220 mg, 1.47 mmol) in MeCN (4 mL) was stirred for 24 h at room temperatures. Then, **4.5kk** (0.5 mmol) in MeCN (4 mL) was added in one portion at room temperature. The reaction mixture was stirred at 50 °C for 45 h. The mixture was then concentrated under reduced and the solid obtained was

silica-gel flash column chromatographed (100 % EtOAc) to afford **4.29kk** as a white solid in 93% yield (169 mg, 0.47 mmol).

$^1\text{H}$  NMR (400 MHz, DMSO- $d_6$ ):  $\delta$  = 13.34 (s, 1 H), 9.20 (s, 1 H), 8.04 (d,  $J$  = 7.9 Hz, 1 H), 7.58 (d,  $J$  = 7.8 Hz, 1 H), 7.35 (t,  $J$  = 7.9 Hz, 1 H).

$^{19}\text{F}$  NMR (400 MHz,  $\text{CDCl}_3$ ):  $\delta$  = -60.10.

**2-(Trifluoromethyl)-N-(6-(trifluoromethyl)benzo[d]thiazol-2-yl)thiazole-4-carboxamide (4.29ww)**



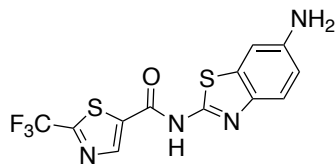
A mixture of **4.27** (150 mg, 0.76 mmol), TFFH (200 mg, 0.76 mmol), and CsF (350 mg) in MeCN (4 mL) was stirred for 24 h at room temperature. Then, **4.5ww** (0.5 mmol) in MeCN (4 mL) was added in one portion at room temperature. The reaction mixture was stirred at 50 °C for 48 h. The mixture was then concentrated under reduced and the solid obtained was silica-gel flash column chromatographed (100% EtOAc) to afford **4.29ww** as a white solid in 59% yield (118 mg, 0.30 mmol).

$^1\text{H}$  NMR (400 MHz, DMSO- $d_6$ ):  $\delta$  = 9.13 (s, 1H), 8.54 (s, 1H), 7.96 (d,  $J$  = 9.0 Hz, 1 H), 7.78 (dd,  $J$  = 8.7, 2.2 Hz, 1 H)

DEPT-90 NMR (100 MHz, Acetone- $d_6$ ):  $\delta$  = 131.9, 123.8 (q,  $J$  = 3.5 Hz), 122.3, 120.23 (q,  $J$  = 4.4 Hz)

$^{19}\text{F}$  NMR (400 MHz, DMSO- $d_6$ ):  $\delta$  = -59.46, -60.06

***N*-(6-Aminobenzo[*d*]thiazol-2-yl)-2-(trifluoromethyl)thiazole-5-carboxamide (4.30)**

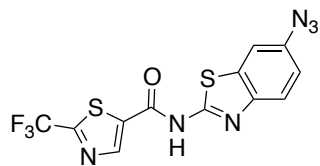


Nitro compound **4.25qq** (377 mg, 1 mmol) was added to a cooled solution of 1M SnCl<sub>4</sub> in DCM (1.75 mL, 1.75 mmol) and concentrated HCl (0.9 mL). The resulting mixture was stirred at 0 °C for 10 minutes before dropwise addition (over 30 minutes) of SnCl<sub>2</sub> (682 mg, 3.6 mmol in 0.5 mL concentrated HCl) at 0 °C. The resulting mixture was stirred for 30 minutes at 0C and then 45 minutes at room temperature. The reaction mixture was then diluted with Et<sub>2</sub>O and filtered. The isolated product was passed through a short silica gel column and 100% MeOH was used as eluent. After concentrating the isolated product, it was dissolved in EtOAc and then washed with H<sub>2</sub>O to afford **4.30** in 28% yield (95mg, 0.28 mmol)

<sup>1</sup>H NMR (400 MHz, DMSO-*d*<sub>6</sub>): δ = 8.97 (bs, 1 H), 8.03 (s, 1 H), 7.83 (bs, 1 H), 7.46 (dd, *J* = 2.1, 8.6 Hz, 1 H)

<sup>19</sup>F NMR (400 MHz, DMSO-*d*<sub>6</sub>): δ = - 60.44

***N*-(6-Azidobenzo[*d*]thiazol-2-yl)-2-(trifluoromethyl)thiazole-5-carboxamide (4.31)**



Amine **4.30** (75 mg, 0.20 mmol) dissolved in 2.36N hydrochloric acid (0.7 mL) and cooled to 0C in an ice bath. To this stirred mixture, NaNO<sub>2</sub> (16 mg, 40 mmol) in 1.1 mL of water was added and stirred for 30 minutes at room temperature. After that, the reaction mixture was gradually neutralized to pH 6.0-7.0 with sodium acetate. Then, the aqueous solution of sodium azide (0.26

mmol in 1.1 mL of water) was gradually added and the mixture was stirred at -5 °C for 30 minutes. The reaction mixture was then diluted with EtOAc (4.5 mL) and extracted with 3 x 5 mL of EtOAc. The combined organic layers were dried over sodium sulfate and concentrated under reduced pressure. The isolated crude product was purified by column chromatography (100% EtOAc) to afford **4.31** in 3% yield (3 mg, 0.008mmol).

<sup>1</sup>H NMR (400 MHz, DMSO-*d*<sub>6</sub>): δ = 13.68 (s, 1 H), 8.94 (bs, 1 H), 7.89 (s, 1 H), 7.75 (bs, 1 H), 7.23 (dd, *J* = 2.5, 8.6 Hz, 1 H)

<sup>19</sup>F NMR (400 MHz, DMSO-*d*<sub>6</sub>): δ = - 60.51

## Chapter 5: Conclusions

Both **IDC16** and compound 5350150 blocks anti-HIV replication by blocking alternative splicing that is vital to the production of critical HIV proteins. In search for more drug-like analogues of these two molecules, in my PhD work, I synthesized 27 **IDC16** “mimics” and 67 amide analogues of 5350150. For parallel synthesis of these DHA-type molecules, first we developed an efficient protocol for amide bond formation suitable for weakly nucleophilic amines. Reaction of acid fluoride with N-TMS amines in MeCN turned out to be effective in the synthesis of DHAs and depending on the solubility of DHAs in MeCN and stability of acid fluoride, in most cases, the target DHAs were isolated in pure form with a simple filtration without the need for work up or column chromatography. Toward the end of my PhD work, we learned that the coupling of oxo-ester with N-TMS amines can also be used for DHA synthesis. Since ester is much more stable and easier accessible than acid fluoride, ester and N-TMS method has the potential to be the general method for our future DHA library synthesis.

For **IDC16** “mimics”, 18 DHAs were synthesized using acid fluoride and N-TMS amines method and 9 DHAs were synthesized through reaction of oxo-ester and N-TMS amines. These DHAs are part of our “in house compound library” of 256 molecules screened for their anti-HIV activity. Within this library, 4 molecules, **1C8**, **1E5**, **2D3**, and **3C2**, have significant anti-HIV activity and **1C8** is the most potent molecule with good dose-response relation. Our current studies show that **1C8** perturbs the function of the key SR protein, SRSF10.

For amide analogues of 5350150, 67 DHAs were synthesized using acid fluoride and N-TMS amines method. Within this library, **4.25kk** (GPS488) and **4.25ww** (GPS491) are the most anti-HIV active molecules. Their activities are conserved for wild-type HIV strains and major HIV strains resistant against the four drug classes used in ART. This indicates that these two molecules have different mechanism of action than the current HIV drugs.

Future studies are aimed at target validation as discussed in section 4.7. Aside from this, we are also planning to do additional SAR studies on **4.25kk** (GPS488) and **4.25ww** (GPS491) hoping to find additional potent molecules with good viability. This future plan includes switching the benzothiazole ring with a benzoxazole ring, thiazole ring with a oxazole ring, and changing the CF<sub>3</sub> group on the thiazole ring with a CN, and reversing the amide bond.

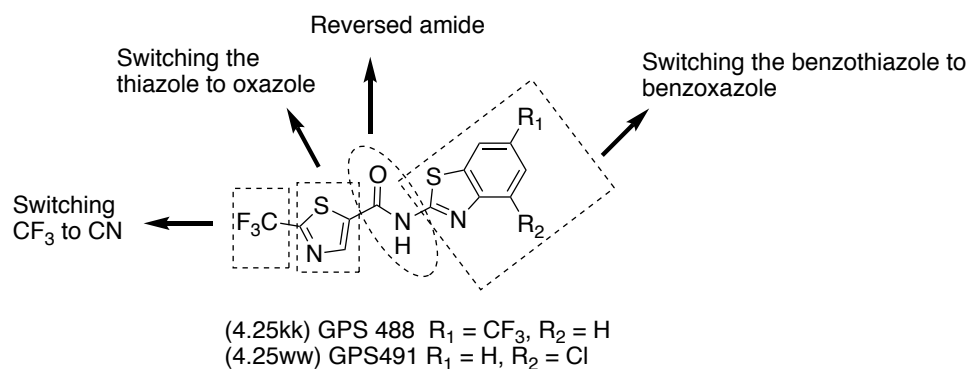


**Figure 5.1 Future SAR studies for 4.25kk (GPS488) and 4.25ww (GPS491)**

## References

1. Lombardino, J. G.; Lowe Iii, J. A., A guide to drug discovery: the role of the medicinal chemist in drug discovery—then and now. *Nature reviews Drug discovery* **2004**, *3*, 853-862.
2. Grierson, D. S., Medicinal Chemistry part 1 - Therapeutic Targets and Drug Design. *Pharmacy Foundation Review Guide*.
3. Shoichet, B. K., Virtual screening of chemical libraries. *Nature* **2004**, *432*, 862-865.
4. Kitchen, D. B.; Decornez, H.; Furr, J. R.; Bajorath, J., Docking and scoring in virtual screening for drug discovery: methods and applications. *Nature reviews Drug discovery* **2004**, *3*, 935-949.
5. Lyne, P. D., Structure-based virtual screening: an overview. *Drug discovery today* **2002**, *7*, 1047-1055.
6. Muhammed, M. T.; Aki-Yalcin, E., Homology modeling in drug discovery: Overview, current applications, and future perspectives. *Chemical biology & drug design* **2019**, *93*, 12-20.
7. Evans, B. E.; Rittle, K. E.; Bock, M. G.; DiPardo, R. M.; Freidinger, R. M.; Whitter, W. L.; Lundell, G. F.; Veber, D. F.; Anderson, P. S.; Chang, R. S. L., Methods for drug discovery: development of potent, selective, orally effective cholecystokinin antagonists. *Journal of medicinal chemistry* **1988**, *31*, 2235-2246.
8. Soret, J.; Tazi, J., Phosphorylation-dependent control of the pre-mRNA splicing machinery. In *Regulation of Alternative Splicing*, Springer: 2003; pp 89-126.
9. Rowinsky, E. K.; Donehower, R. C., Paclitaxel (Taxol). *New England Journal of Medicine* **1995**, *332*, 1004-1014.
10. Dias, D. A.; Urban, S.; Roessner, U., A historical overview of natural products in drug discovery. *Metabolites* **2012**, *2*, 303-36.
11. Cutler, H. G.; Cutler, S. J., *Biologically active natural products: pharmaceuticals*. CRC Press: 1999.
12. Sneader, W., The discovery of heroin. *The Lancet* **1998**, *352*, 1697-1699.
13. Watanabe, K.; Kayano, Y.; Matsunaga, T.; Yamamoto, I.; Yoshimura, H., Inhibition of anandamide amidase activity in mouse brain microsomes by cannabinoids. *Biological and Pharmaceutical Bulletin* **1996**, *19*, 1109-1111.
14. Kwon, O.; Park, S. B.; Schreiber, S. L., Skeletal diversity via a branched pathway: efficient synthesis of 29 400 discrete, polycyclic compounds and their arraying into stock solutions. *Journal of the American Chemical Society* **2002**, *124*, 13402-13404.
15. Schreiber, S. L., The small-molecule approach to biology. *Chem. Eng. News* **2003**, *81*, 51-61.
16. Bleicher, K. H.; Böhm, H.-J.; Müller, K.; Alanine, A. I., A guide to drug discovery: hit and lead generation: beyond high-throughput screening. *Nature reviews Drug discovery* **2003**, *2*, 369-378.
17. Montalbetti, C. A. G. N.; Falque, V., Amide bond formation and peptide coupling. *Tetrahedron* **2005**, *61*, 10827-10852.
18. Guha, R., On exploring structure-activity relationships. *Methods Mol Biol* **2013**, *993*, 81-94.
19. WHO HIV/AIDS. <https://http://www.who.int/news-room/fact-sheets/detail/hiv-aids> (June 22),

20. Soret, J.; Bakkour, N.; Maire, S.; Durand, S.; Zekri, L.; Gabut, M.; Fic, W.; Divita, G.; Rivalle, C.; Dauzonne, D., Selective modification of alternative splicing by indole derivatives that target serine-arginine-rich protein splicing factors. *PNAS* **2005**, *102*, 8764-8769.
21. Bakkour, N.; Lin, Y.-L.; Maire, S.; Ayadi, L.; Mahuteau-Betzer, F.; Nguyen, C. H.; Mettling, C.; Portales, P.; Grierson, D.; Chabot, B., Small-molecule inhibition of HIV pre-mRNA splicing as a novel antiretroviral therapy to overcome drug resistance. *PLoS pathogens* **2007**, *3*, 1530-1539.
22. Isah, T., Anticancer alkaloids from trees: Development into drugs. *Pharmacognosy reviews* **2016**, *10*, 90-99.
23. Wang, J. C., Cellular roles of DNA topoisomerases: a molecular perspective. *Nature Reviews Molecular Cell Biology* **2002**, *3*, 430-440.
24. Pilch, B.; Allemand, E.; Facompré, M.; Bailly, C.; Riou, J.-F.; Soret, J.; Tazi, J., Specific inhibition of serine-and arginine-rich splicing factors phosphorylation, spliceosome assembly, and splicing by the antitumor drug NB-506. *Cancer research* **2001**, *61*, 6876-6884.
25. Labourier, E.; Riou, J.-F.; Prudhomme, M.; Carrasco, C.; Bailly, C.; Tazi, J., Poisoning of topoisomerase I by an antitumor indolocarbazole drug: stabilization of topoisomerase I-DNA covalent complexes and specific inhibition of the protein kinase activity. *Cancer research* **1999**, *59*, 52-55.
26. Wong, R. W.; Balachandran, A.; Haaland, M.; Stoilov, P.; Cochrane, A., Characterization of novel inhibitors of HIV-1 replication that function via alteration of viral RNA processing and rev function. *Nucleic acids research* **2013**, *41*, 9471-9483.
27. Ho, T.-I.; Ho, J.-H.; Wu, J.-Y., Novel acid-catalyzed hydrolysis of an intermediate from a photorearrangement of stilbenes. *Journal of the American Chemical Society* **2000**, *122*, 8575-8576.
28. Wu, J.-Y.; Ho, J.-H.; Shih, S.-M.; Hsieh, T.-L.; Ho, T.-I., Solvent-dependent photochemical rearrangements of ethers of styrylheterocycles. *Organic letters* **1999**, *1*, 1039-1041.
29. Sumanasekera, C.; Watt, D. S.; Stamm, S., Substances that can change alternative splice-site selection. *Biochemical Society transactions* **2008**, *36*, 483-90.
30. Cheung, P. K.; Horhant, D.; Bandy, L. E.; Zamiri, M.; Rabea, S. M.; Karagiosov, S. K.; Matloobi, M.; McArthur, S.; Harrigan, P. R.; Chabot, B.; Grierson, D. S., A Parallel Synthesis Approach to the Identification of Novel Diheteroarylamide-Based Compounds Blocking HIV Replication: Potential Inhibitors of HIV-1 Pre-mRNA Alternative Splicing. *J Med Chem* **2016**, *59*, 1869-79.
31. Dvinge, H.; Kim, E.; Abdel-Wahab, O.; Bradley, R. K., RNA splicing factors as oncoproteins and tumour suppressors. *Nature Reviews Cancer* **2016**, *16*, 413.
32. Tazi, J.; Bakkour, N.; Marchand, V.; Ayadi, L.; Aboufirassi, A.; Branlant, C., Alternative splicing: regulation of HIV-1 multiplication as a target for therapeutic action. *FEBS J.* **2010**, *277*, 867-876.
33. Black, D. L., Mechanisms of alternative pre-messenger RNA splicing. *Annual review of biochemistry* **2003**, *72*, 291-336.
34. Matlin, A. J.; Clark, F.; Smith, C. W., Understanding alternative splicing: towards a cellular code. *Nature Reviews Molecular Cell Biology* **2005**, *6*, 386-398.
35. Rajan, P.; Elliott, D. J.; Robson, C. N.; Leung, H. Y., Alternative splicing and biological heterogeneity in prostate cancer. *Nature Reviews Urology* **2009**, *6*, 454-460.
36. Stoltzfus, C. M.; Madsen, J. M., Role of viral splicing elements and cellular RNA binding proteins in regulation of HIV-1 alternative RNA splicing. *Curr. HIV Res.* **2006**, *4*, 43-55.



37. Shkreta, L.; Blanchette, M.; Toutant, J.; Wilhelm, E.; Bell, B.; Story, B. A.; Balachandran, A.; Cochrane, A.; Cheung, P. K.; Harrigan, P. R.; Grierson, D. S.; Chabot, B., Modulation of the splicing regulatory function of SRSF10 by a novel compound that impairs HIV-1 replication. *Nucleic Acids Res* **2017**, *45*, 4051-4067.
38. Long, J. C.; Caceres, J. F., The SR protein family of splicing factors: master regulators of gene expression. *The Biochemical journal* **2009**, *417*, 15-27.
39. Merrifield, R. B., Solid phase peptide synthesis. I. The synthesis of a tetrapeptide. *Journal of the American Chemical Society* **1963**, *85*, 2149-2154
40. El-Faham, A.; Albericio, F., Peptide coupling reagents, more than a letter soup. *Chemical reviews* **2011**, *111*, 6557-6602.
41. Ou, X.; Janzen, A. F., Silicon– Fluorine and Silicon– Carbon Bond Cleavage in Organofluorosilicates: A Molecular Orbital Study. *Inorganic Chemistry* **1997**, *36*, 392-395.
42. Rajeswari, S.; Jones, R. J.; Cava, M. P., A new synthesis of amides from acyl fluorides and N-silylamines. *Tetrahedron letters* **1987**, *28*, 5099-5102.
43. Rajeswari, S.; Adesomoju, A. A.; Cava, M. P., Synthesis of new gramine-type analogs of CC-1065. *J. Heterocycl. Chem.* **1989**, *26*, 557-64.
44. Carpino, L. A.; Ionescu, D.; El-Faham, A.; Beyermann, M.; Henklein, P.; Hanay, C.; Wenschuh, H.; Bienert, M., Complex Polyfluoride Additives in Fmoc-Amino Acid Fluoride Coupling Processes. Enhanced Reactivity and Avoidance of Stereomutation. *Org. Lett.* **2003**, *5*, 975-977.
45. Carpino, L. A.; El-Faham, A., Tetramethylfluoroformamidinium Hexafluorophosphate: A Rapid-Acting Peptide Coupling Reagent for Solution and Solid Phase Peptide Synthesis. *J. Am. Chem. Soc.* **1995**, *117*, 5401-2.
46. Carpino, L. A.; Mansour, E. S. M. E., Protected  $\beta$ - and  $\gamma$ -aspartic and -glutamic acid fluorides. *J. Org. Chem.* **1992**, *57*, 6371-3.
47. Lippert Iii, J. W., Amide bond formation by using amino acid fluorides. *Arkivoc* **2005**, *14*, 87-95.
48. Carpino, L. A.; Beyermann, M.; Wenschuh, H.; Bienert, M., Peptide synthesis via amino acid halides. *Accounts of chemical research* **1996**, *29*, 268-274.
49. Carpino, L. A.; Sadat-Aalae, D.; Chao, H. G.; DeSelms, R. H., [(9-Fluorenylmethyl)oxy]carbonyl (Fmoc) amino acid fluorides. Convenient new peptide coupling reagents applicable to the Fmoc/*tert*-butyl strategy for solution and solid-phase syntheses. *J. Am. Chem. Soc.* **1990**, *112*, 9651-2.
50. Wenschuh, H.; Beyermann, M.; Winter, R.; Bienert, M.; Ionescu, D.; Carpino, L. A., Fmoc amino acid fluorides in peptide synthesis—Extension of the method to extremely hindered amino acids. *Tetrahedron letters* **1996**, *37*, 5483-5486
51. Kim, H.-O.; Gardner, B.; Kahn, M., Acylation of sterically hindered secondary amines and acyl hydrazides. *Tetrahedron letters* **1995**, *36*, 6013-6016.
52. Sakamoto, K.; Nakahara, Y.; Ito, Y., Combination of silyl carbamate and amino acid fluoride for solid-phase peptide synthesis. *Tetrahedron letters* **2002**, *43*, 1515-1518.
53. Kraushaar, K.; Herbig, M.; Schmidt, D.; Wagler, J.; Böhme, U.; Kroke, E., Insertion of phenyl isocyanate into mono- and diaminosilanes. *Zeitschrift für Naturforschung B* **2017**, *72*, 909-921.
54. Schulz, A.; Villinger, A.; Westenkirchner, A., Synthesis of 1, 3-Dichloro-cyclo-1, 3-diphosphadiazanes from Silylated Amino (dichloro) phosphanes. *Inorganic Chemistry* **2013**, *52*, 11457-11468

55. Mai, K.; Patil, G., Alkylsilyl cyanides as silylating agents. *The Journal of Organic Chemistry* **1986**, *51*, 3545-3548.
56. Wallace, E. M.; Lyssikatos, J.; Blake, J. F.; Seo, J.; Yang, H. W.; Yeh, T. C.; Perrier, M.; Jarski, H.; Marsh, V.; Poch, G., Potent and selective mitogen-activated protein kinase kinase (MEK) 1, 2 inhibitors. 1. 4-(4-Bromo-2-fluorophenylamino)-1-methylpyridin-2 (1 H)-ones. *Journal of medicinal chemistry* **2006**, *49*, 441-444.
57. L'Heureux, A.; Beaulieu, F.; Bennett, C.; Bill, D. R.; Clayton, S.; La Flamme, F.; Mirmehrabi, M.; Tadayan, S.; Tovell, D.; Couturier, M., Aminodifluorosulfonium Salts: Selective Fluorination Reagents with Enhanced Thermal Stability and Ease of Handling. *J. Org. Chem.* **2010**, *75*, 3401-3411.
58. Kim, J.-G.; Jang, D. O., A convenient, one-pot procedure for the preparation of acyl and sulfonyl fluorides using Cl<sub>3</sub>CCN, Ph<sub>3</sub>P, and TBAF(t-BuOH)<sub>4</sub>. *Synlett* **2010**, 3049-3052.
59. Umemoto, T.; Singh, R. P.; Xu, Y.; Saito, N., Discovery of 4-tert-Butyl-2,6-dimethylphenylsulfur Trifluoride as a Deoxofluorinating Agent with High Thermal Stability as Well as Unusual Resistance to Aqueous Hydrolysis, and Its Diverse Fluorination Capabilities Including Deoxofluoro-Arylsulfonylation with High Stereoselectivity. *J. Am. Chem. Soc.* **2010**, *132*, 18199-18205.
60. Kaduk, C.; Wenschuh, H.; Beyermann, M.; Forner, K.; Carpino, L. A.; Bienert, M., Synthesis of Fmoc-amino acid fluorides via DAST, an alternative fluorinating agent. *Lett. Pept. Sci.* **1996**, *2*, 285-8.
61. Fiammengo, R.; Licini, G.; Nicotra, A.; Modena, G.; Pasquato, L.; Scrimin, P.; Broxterman, Q. B.; Kaptein, B., Duality of Mechanism in the Tetramethylfluoroformamidinium Hexafluorophosphate-Mediated Synthesis of N-Benzylloxycarbonylamino Acid Fluorides. *J. Org. Chem.* **2001**, *66*, 5905-5910.
62. Joullié, M. M.; Lassen, K. M., Evolution of amide bond formation. *Arkivoc* **2010**, *8*, 189-250.
63. Sircar, J. C.; Capiris, T.; Bobovski, T. P.; Schwender, C. F., Synthesis of 4-hydroxy-N-[5-(hydroxymethyl)-3-isoxazolyl]-2-methyl-2H-1, 2-benzothiazine-3-carboxamide 1, 1-dioxide and [(5-methyl-3-isoxazolyl) amino] oxoacetic acid. Major metabolites of isoxicam. *The Journal of Organic Chemistry* **1985**, *50*, 5723-5727
64. Bryce, M. R.; Heaton, J. N.; Taylor, P. C.; Anderson, M., Diels–Alder and ene reactions of new transient thionitrosoarenes (Ar-NS) and thionitrosoheteroarenes (Het-NS) generated from N-(arylamino)sulfanyl and N-(heteroarylamino)sulfanyl-phthalimides: synthesis of cyclic and acyclic sulfenamides. *Journal of the Chemical Society, Perkin Transactions 1* **1994**, 1935-1944.
65. El-Tamany, E.-S. H.; Sowellim, S. Z.; Hamed, A. A.; Radwan, A. S., Synthesis and antimicrobial activity of some isoindole derivatives. *Research on Chemical Intermediates* **2015**, *41*, 2675-2685
66. El-Tammany, E.-S. H.; Hamed, A. A.; Sowellim, S. Z. A.; Radwan, A. S., Azoniaallene salts as versatile building blocks in the synthesis of antibacterial and antifungal heterocyclic compounds. *Natural Science* **2012**, *4*, 1013-1021.
67. Schmidt, U.; Schwochau, M.,  $\beta$ -Polycarbonylverbindungen, 3. Mitt.: Über Synthesen mit den Trimethylsilylestern der Acetessigsäure und Malonsäure. Ein neuer Weg zu Diacyl-methanen und Diacyl-essigsäureestern. *Monatshefte für Chemie und verwandte Teile anderer Wissenschaften* **1967**, *98*, 1492-1511.

68. Fuchter, M. J.; Smith, C. J.; Tsang, M. W. S.; Boyer, A.; Saubern, S.; Ryan, J. H.; Holmes, A. B., Clean and efficient synthesis of O-silylcarbamates and ureas in supercritical carbon dioxide. *Chemical Communications* **2008**, 2152-2154.
69. Kricheldorf, H. R., N-Silylierte Isothioharnstoff-Derivate. *Justus Liebigs Annalen der Chemie* **1971**, 745, 81-86.
70. Pattabiraman, V. R.; Bode, J. W., Rethinking amide bond synthesis. *Nature* **2011**, 480, 471-9.
71. Gernigon, N.; Al-Zoubi, R. M.; Hall, D. G., Direct amidation of carboxylic acids catalyzed by ortho-iodo arylboronic acids: catalyst optimization, scope, and preliminary mechanistic study supporting a peculiar halogen acceleration effect. *J Org Chem* **2012**, 77, 8386-400.
72. García-Álvarez, R.; Crochet, P.; Cadierno, V., Metal-catalyzed amide bond forming reactions in an environmentally friendly aqueous medium: nitrile hydrations and beyond. *Green Chem.* **2013**, 15, 46-66.
73. Jeffries, K. A.; Dempsey, D. R.; Behari, A. L.; Anderson, R. L.; Merkler, D. J., Drosophila melanogaster as a model system to study long-chain fatty acid amide metabolism. *FEBS letters* **2014**, 588, 1596-1602.
74. Koperniku, A.; Zamiri, M.; Grierson, D. S., The Reaction of N-Trimethylsilyl-Substituted Heteroarylamines with Esters and Thioesters: An Efficient Protocol To Access Diheteroarylamides. *Synthesis* **2019**, 51, 1779-1790.
75. Wu, Y.-Y.; Chen, Y.; Gou, G.-Z.; Mu, W.-H.; Lv, X.-J.; Du, M.-L.; Fu, W.-F., Large Stokes shift induced by intramolecular charge transfer in N, O-Chelated Naphthyridine-BF<sub>2</sub> complexes. *Organic letters* **2012**, 14, 5226-5229.
76. Chen, X.; Wen, Z.; Xian, M.; Wang, K.; Ramachandran, N.; Tang, X.; Schlegel, H. B.; Mutus, B.; Wang, P. G., Fluorophore-labeled S-nitrosothiols. *The Journal of Organic Chemistry* **2001**, 66, 6064-6073.
77. Singh, B., Synthesis of amides by aminolysis of esters using sodium hydride in dimethyl sulfoxide. *Tetrahedron letters* **1971**, 12, 321-322.
78. Yang, K.-W.; Cannon, J. G.; Rose, J. G., N-butyllithium in aminolysis and ammonolysis of esters. *Tetrahedron letters* **1970**, 11, 1791-1794.
79. Ruggeri, R. B.; Heathcock, C. H., Synthesis of polycyclic lactam and lactone ethers by intramolecular Reformatskii reactions. A model for construction of the daphnilactone A ring system. *The Journal of Organic Chemistry* **1987**, 52, 5745-5746.
80. Ooi, T.; Tayama, E.; Yamada, M.; Maruoka, K., Efficient synthesis of aromatic sec-amides from esters: synthetic utility of bislithium amides. *Synlett* **1999**, 6, 729-730.
81. Tanwar, B.; Kumar, A.; Yogeewari, P.; Sriram, D.; Chakraborti, A. K., Design, development of new synthetic methodology, and biological evaluation of substituted quinolines as new anti-tubercular leads. *Bioorganic & medicinal chemistry letters* **2016**, 26, 5960-5966.
82. Kim, B. R.; Lee, H.-G.; Kang, S.-B.; Sung, G. H.; Kim, J.-J.; Park, J. K.; Lee, S.-G.; Yoon, Y.-J., tert-Butoxide-assisted amidation of esters under green conditions. *Synthesis* **2012**, 44, 42-50.
83. Stauch, T.; Dreuw, A., A quantitative quantum-chemical analysis tool for the distribution of mechanical force in molecules. *J Chem Phys* **2014**, 140, 134107.
84. Lang, R.; Wahl, A.; Skurk, T.; Yagar, E. F.; Schmiech, L.; Eggers, R.; Hauner, H.; Hofmann, T., Development of a hydrophilic liquid interaction chromatography– high-performance liquid chromatography– tandem mass spectrometry based stable isotope dilution analysis and pharmacokinetic studies on bioactive pyridines in human plasma and urine after coffee consumption. *Analytical chemistry* **2010**, 82, 1486-1497.

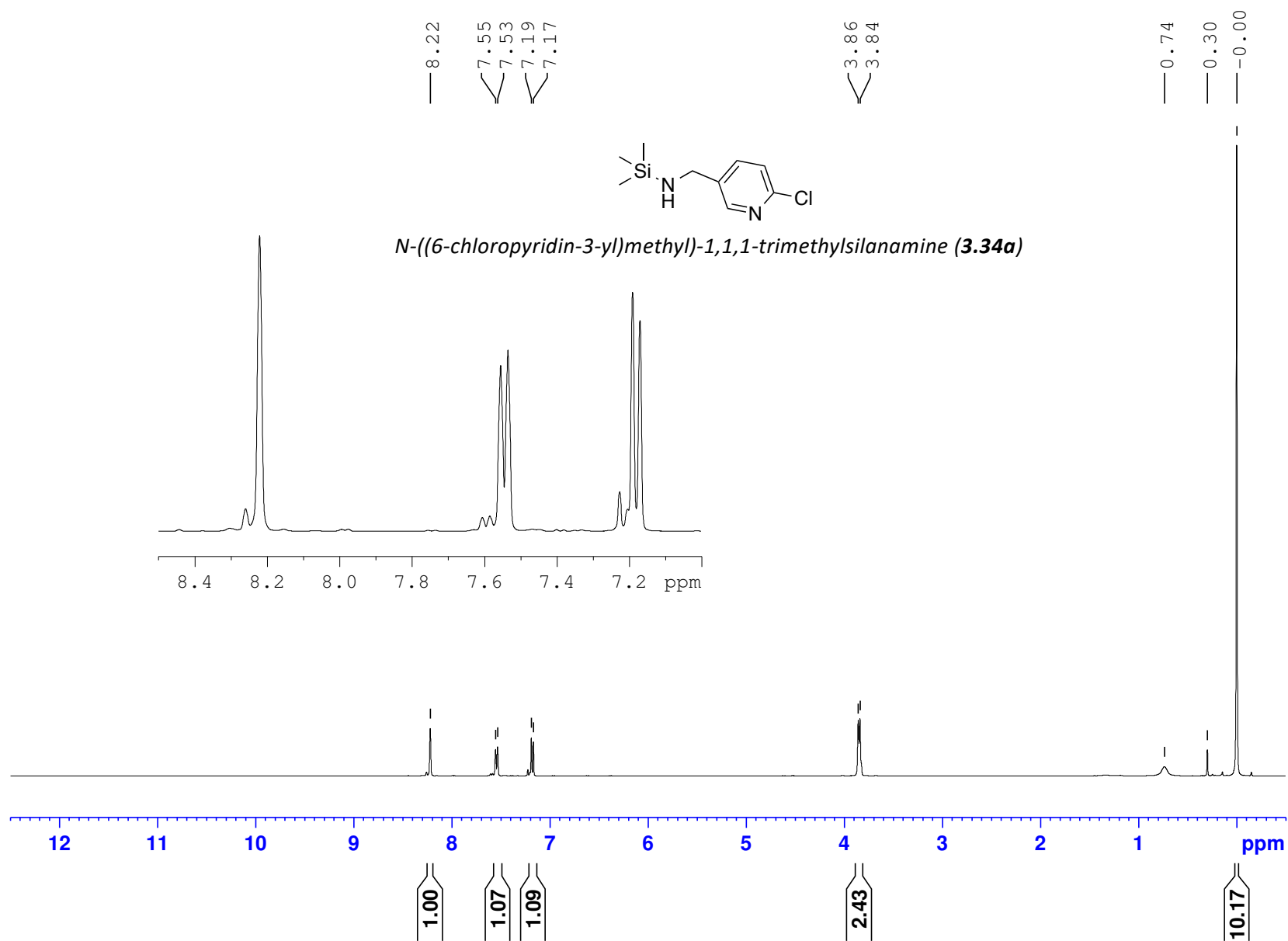
85. Ross, W. C. J., The preparation of some 4-substituted nicotinic acids and nicotinamides. *Journal of the Chemical Society C: Organic* **1966**, 1816-1821.
86. Yi, X.; Chen, J.; Xu, X.; Ma, Y., Solvent and substituent effects on the conversion of 4-methoxypyridines to N-methyl-4-pyridones. *Synthetic Communications* **2017**, *47*, 872-877.
87. Ma, Y. M.; Hider, R. C., Design and synthesis of fluorine-substituted 3-hydroxypyridin-4-ones. *Tetrahedron letters* **2010**, *51*, 5230-5233
88. Zamiri, M.; Grierson, D. S., A Trimethylsilylamine-Acyl Fluoride Amide Bond Forming Protocol for Weakly Nucleophilic Amines that is Amenable to the Parallel Synthesis of Di (hetero) arylamides. *Synthesis* **2017**, *49*, 571-578
89. Mueller, W. F.; Hertel, K. J., The role of SR and SR-related proteins in pre-mRNA splicing. *In RNA Binding Proteins* **2011**, 27-46.
90. Hope, T. J., The ins and outs of HIV Rev. *Archives of biochemistry and biophysics* **1999**, *365*, 186-191.
91. Hutten, S.; Kehlenbach, R. H., CRM1-mediated nuclear export: to the pore and beyond. *Trends in cell biology* **2007**, *17*, 193-201
92. Giacomini, E.; Rupiani, S.; Guidotti, L.; Recanatini, M.; Roberti, M., The use of stilbene scaffold in medicinal chemistry and multi-target drug design. *Current Medicinal Chemistry* **2016**, *23*, 2439-2489.
93. Gramec, D.; Peterlin Mašič, L.; Sollner Dolenc, M., Bioactivation potential of thiophene-containing drugs. *Chemical research in toxicology* **2014**, *27*, 1344-1358.
94. Gaikwad, P. L.; Gandhi, P. S.; Jagdale, D. M.; Kadam, V. J., The use of bioisosterism in drug design and molecular modification. *American Journal of PharmTech Research* **2012**, *2*, 1-23.
95. Brockman, M. A.; Tanzi, G. O.; Walker, B. D.; Allen, T. M., Use of a novel GFP reporter cell line to examine replication capacity of CXCR4- and CCR5-tropic HIV-1 by flow cytometry. *Journal of virological methods* **2006**, *131*, 134-42.
96. Chiarelli, L. R.; Mori, M.; Beretta, G.; Gelain, A.; Pini, E.; Sammartino, J. C.; Stelitano, G.; Barlocco, D.; Costantino, L.; Lapillo, M.; Poli, G.; Caligiuri, I.; Rizzolio, F.; Bellinzoni, M.; Tuccinardi, T.; Villa, S.; Meneghetti, F., New insight into structure-activity of furan-based salicylate synthase (MbtI) inhibitors as potential antitubercular agents. *J Enzyme Inhib Med Chem* **2019**, *34*, 823-828.
97. Campos, N.; Myburgh, R.; Garcel, A.; Vautrin, A.; Lapasset, L.; Nadal, E. S.; Mahuteau-Betzer, F.; Najman, R.; Fornarelli, P.; Tantale, K.; Basyuk, E.; Seveno, M.; Venables, J. P.; Pau, B.; Bertrand, E.; Wainberg, M. A.; Speck, R. F.; Scherrer, D.; Tazi, J., Long lasting control of viral rebound with a new drug ABX464 targeting Rev - mediated viral RNA biogenesis. *Retrovirology* **2015**, *12*, 30.
98. Scherrer, D.; Rouzier, R.; Noel Barrett, P.; Steens, J. M.; Gineste, P.; Murphy, R. L.; Tazi, J.; Ehrlich, H. J., Pharmacokinetics and tolerability of ABX464, a novel first-in-class compound to treat HIV infection, in healthy HIV-uninfected subjects. *The Journal of antimicrobial chemotherapy* **2017**, *72*, 820-828.
99. <Safety, Pharmacokinetics, and Antiviral Activity of a Novel HIV Antiviral, ABX464, in Treatment-Naïve HIV-Infected Subjects in a Phase 2 Randomized, Controlled Study.pdf>.
100. Steens, J.-M.; Scherrer, D.; Gineste, P.; Barrett, P. N.; Khuanchai, S.; Winai, R.; Ruxrungtham, K.; Tazi, J.; Murphy, R.; Ehrlich, H., Safety, pharmacokinetics, and antiviral activity of a novel HIV antiviral, ABX464, in treatment-naïve HIV-infected subjects in a phase 2 randomized, controlled study. *Antimicrobial agents and chemotherapy* **2017**, *61*, e00545-17

101. Chan, J. N.; Vuckovic, D.; Sleno, L.; Olsen, J. B.; Pogoutse, O.; Havugimana, P.; Hewel, J. A.; Bajaj, N.; Wang, Y.; Musteata, M. F.; Nislow, C.; Emili, A., Target identification by chromatographic co-elution: monitoring of drug-protein interactions without immobilization or chemical derivatization. *Molecular & cellular proteomics : MCP* **2012**, *11*, M111 016642.
102. Wrubel, J., 3-Substituierte 5-Amino-1,2-benzisoxazole. *Zeitschrift für Chemie* **1980**, *20*, 18.
103. Kofman, T. P.; Namestnikov, V. I., Synthesis of 3-Azido-5-amino-1,2,4-triazole. *Russian journal of organic chemistry* **2003**, *39*, 579-584.
104. Srinivas, D.; Ghule, V. D.; Muralidharan, K., Synthesis of nitrogen-rich imidazole, 1,2,4-triazole and tetrazole-based compounds. *RSC Advances* **2014**, *4*, 7041-7051.
105. Sanphanya, K.; Wattanapitayakul, S. K.; Phowichit, S.; Fokin, V. V.; Vajragupta, O., Novel VEGFR-2 kinase inhibitors identified by the back-to-front approach. *Bioorganic & medicinal chemistry letters* **2013**, *23*, 2962-7.

## **Appendix: Spectra data for compounds synthesized in Chapter 3 and 4**

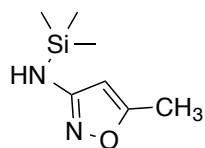
MZP147\_Si-A18\_CDCl3

(400 MHz, 297.2K, CDCl<sub>3</sub>)

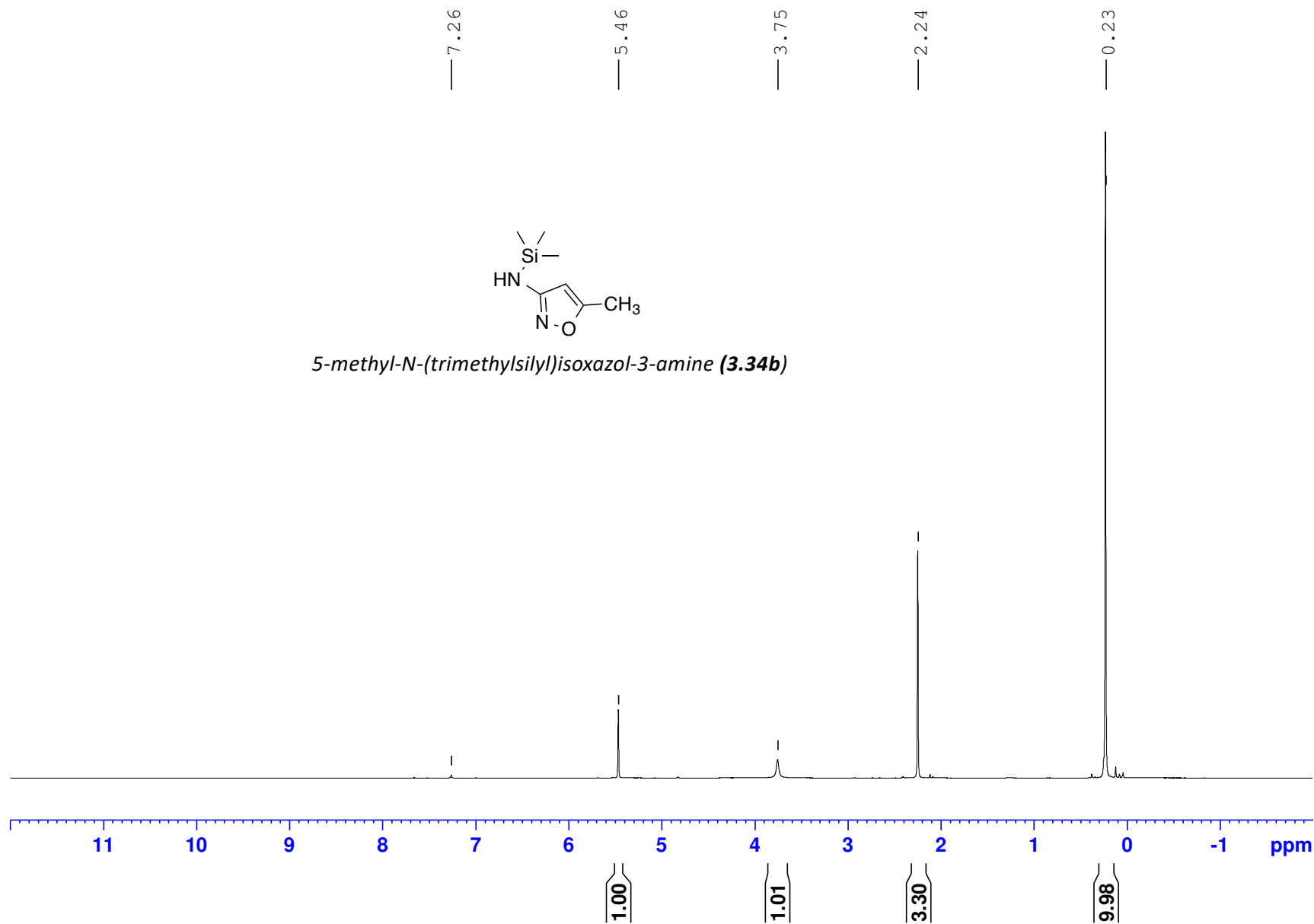


MZP118\_Si-A16\_CDC13

(400 MHz, 297.2K, CDCl<sub>3</sub>)



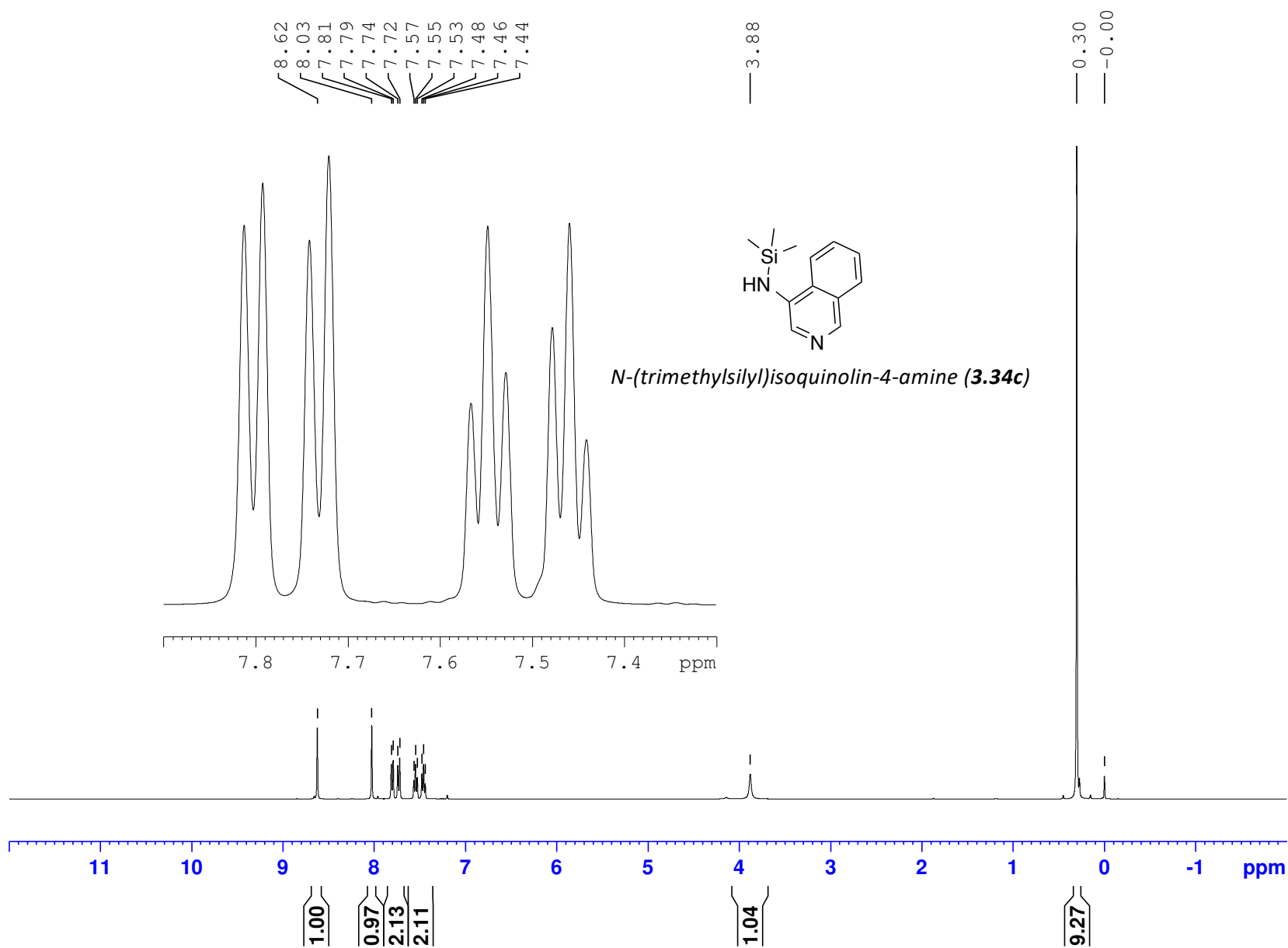
5-methyl-N-(trimethylsilyl)isoxazol-3-amine (**3.34b**)





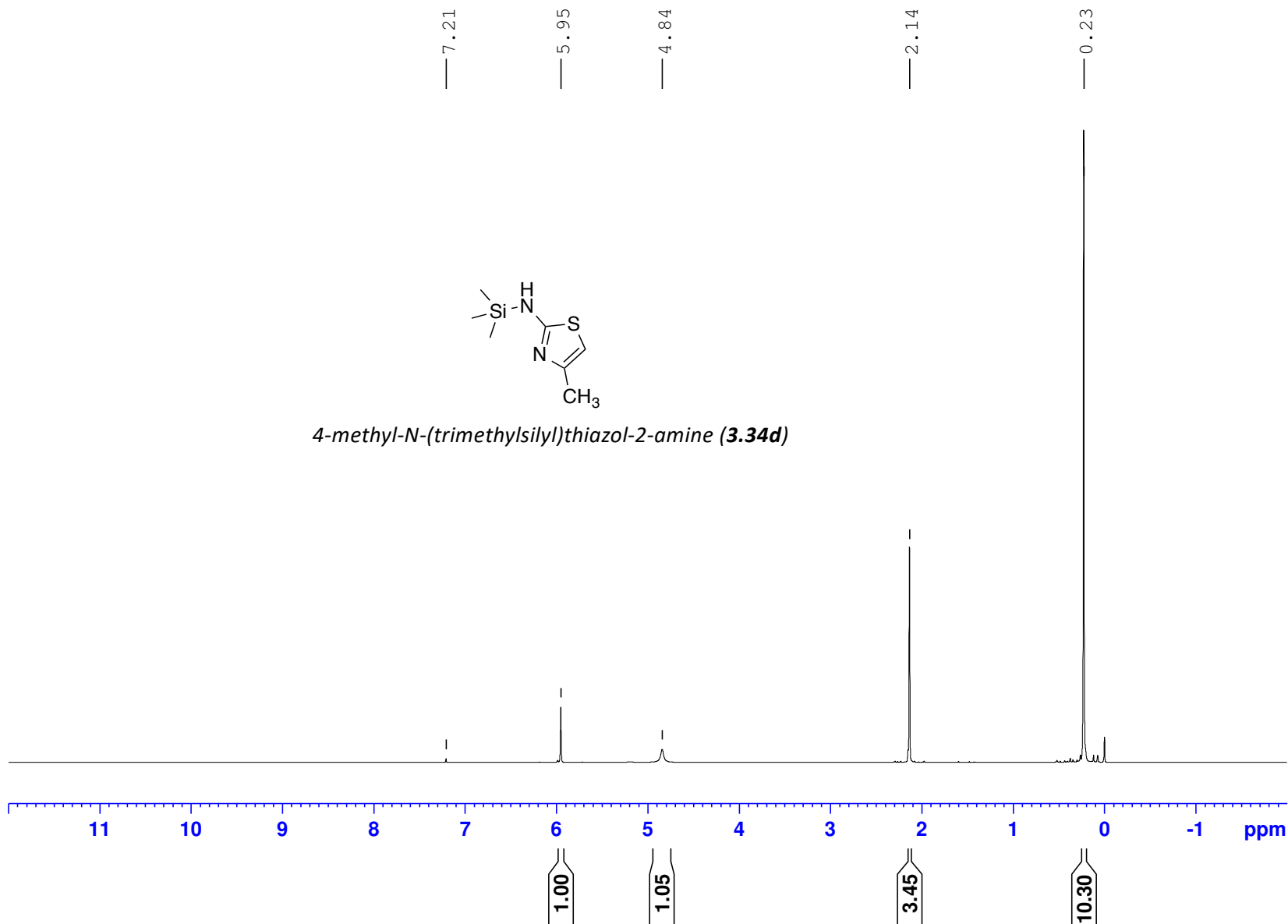
MZP132\_Si-4225\_CDC13

(400 MHz, 297.2K, CDCl<sub>3</sub>)



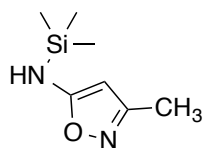
MZP117\_Si-A17\_CDC13

(400 MHz, 297.2K, CDCl<sub>3</sub>)

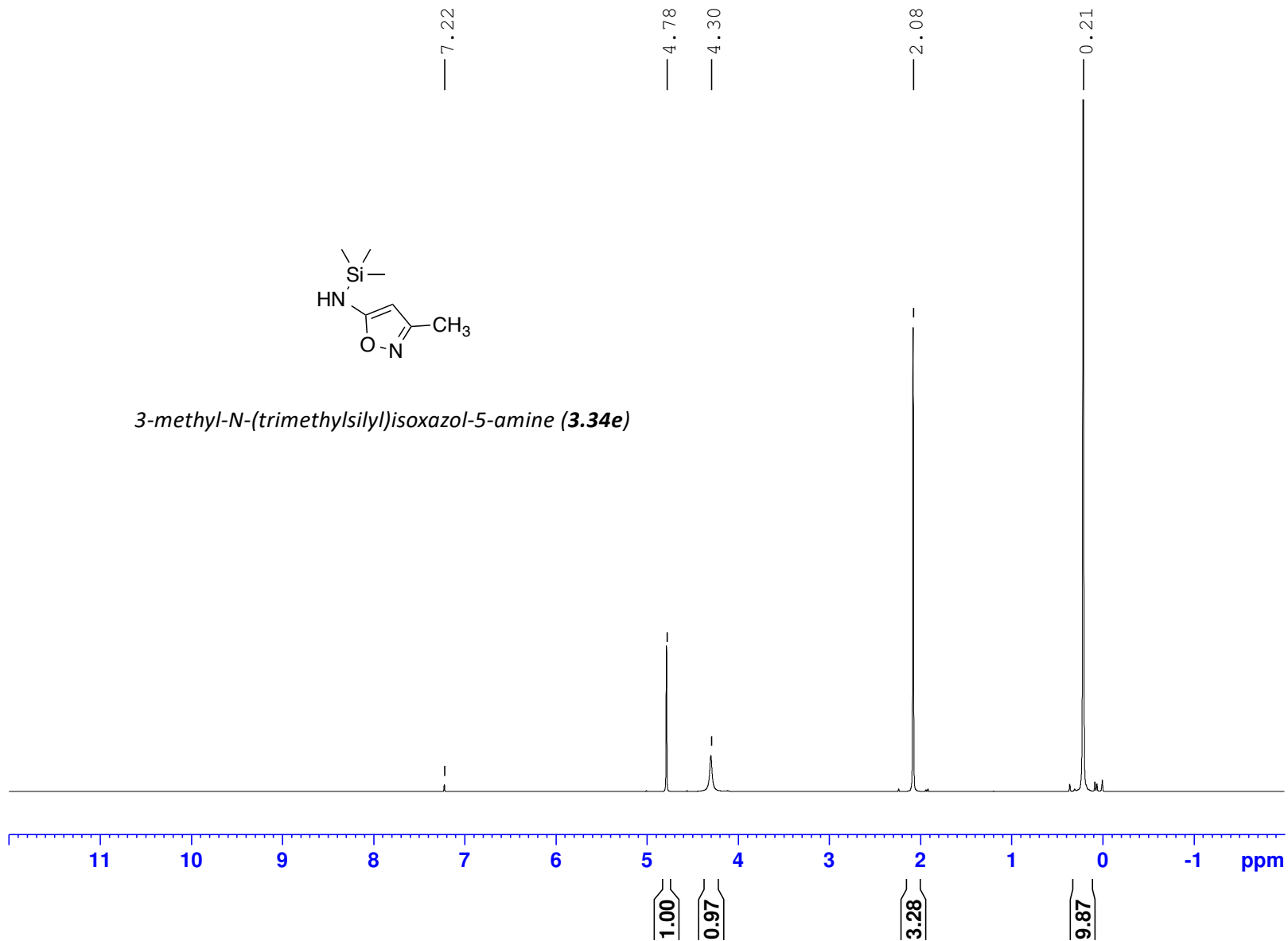


MZP131\_Si-A31\_CDC13

(400 MHz, 297.2K, CDCl<sub>3</sub>)

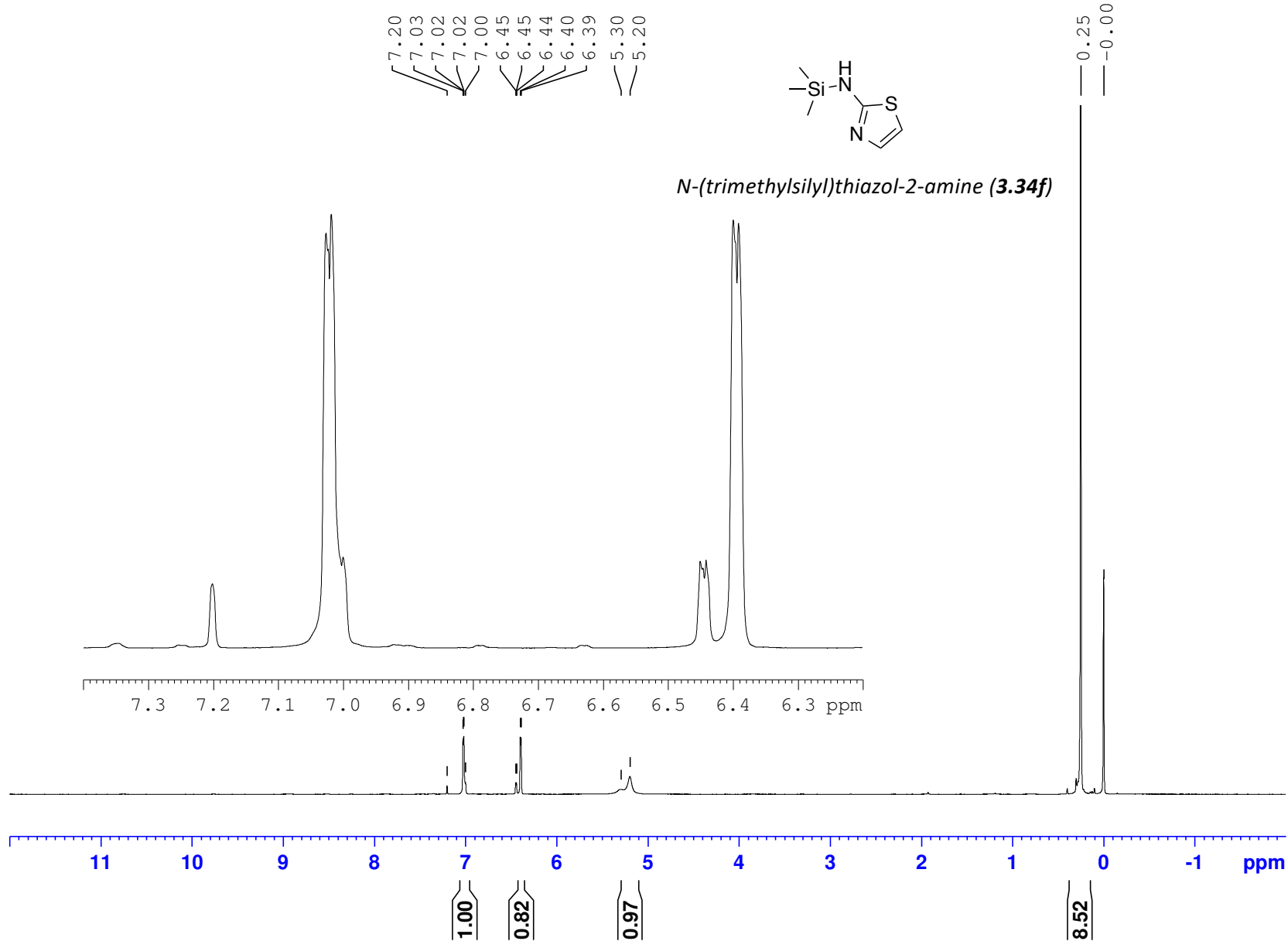


*3-methyl-N-(trimethylsilyl)isoxazol-5-amine (3.34e)*



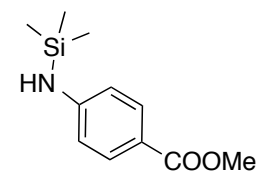
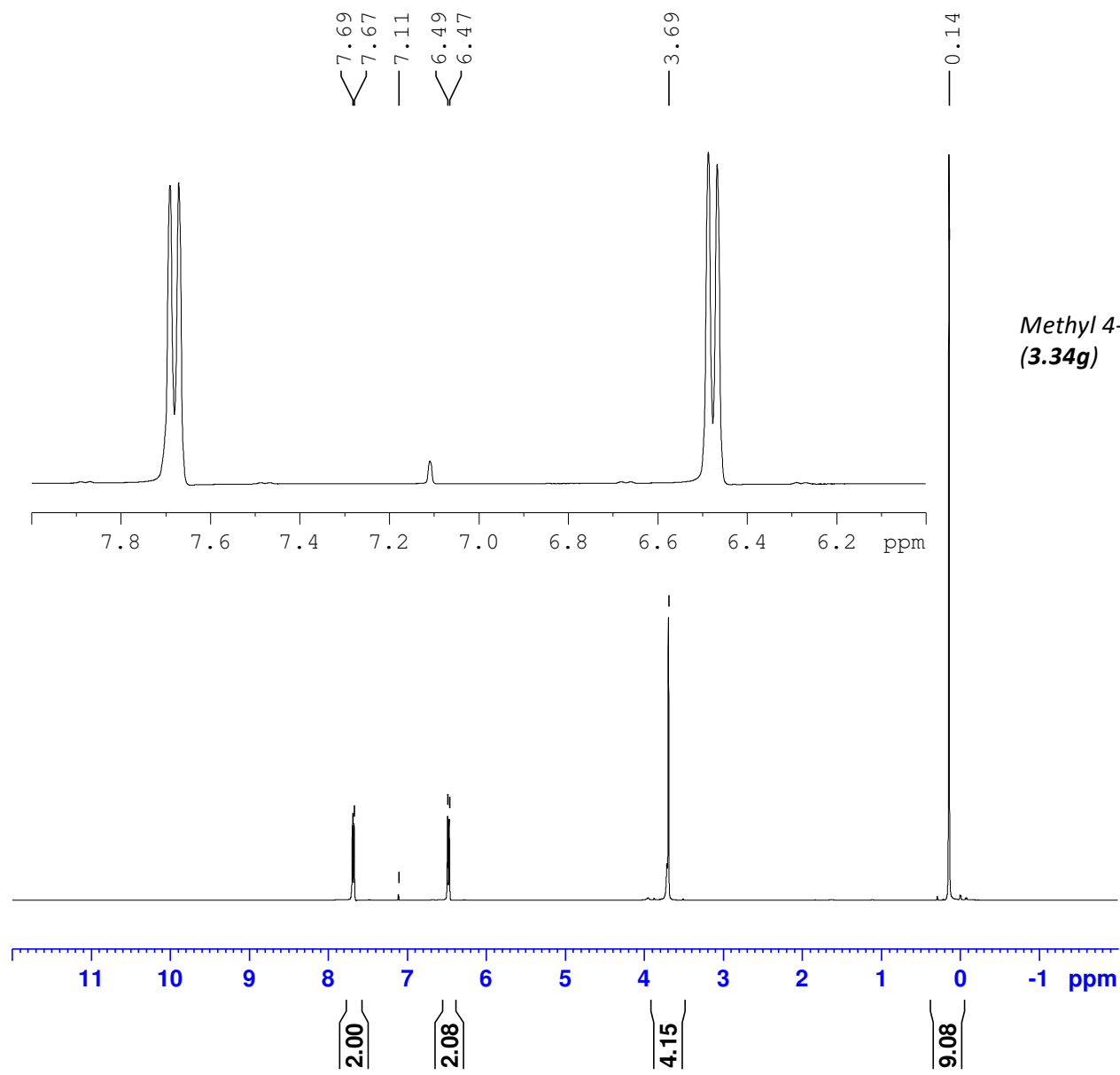
MZP130\_Si-3129\_CDCl3

(400 MHz, 297.2K, CDCl<sub>3</sub>)



MZP148\_Si-A109B\_CDCl3

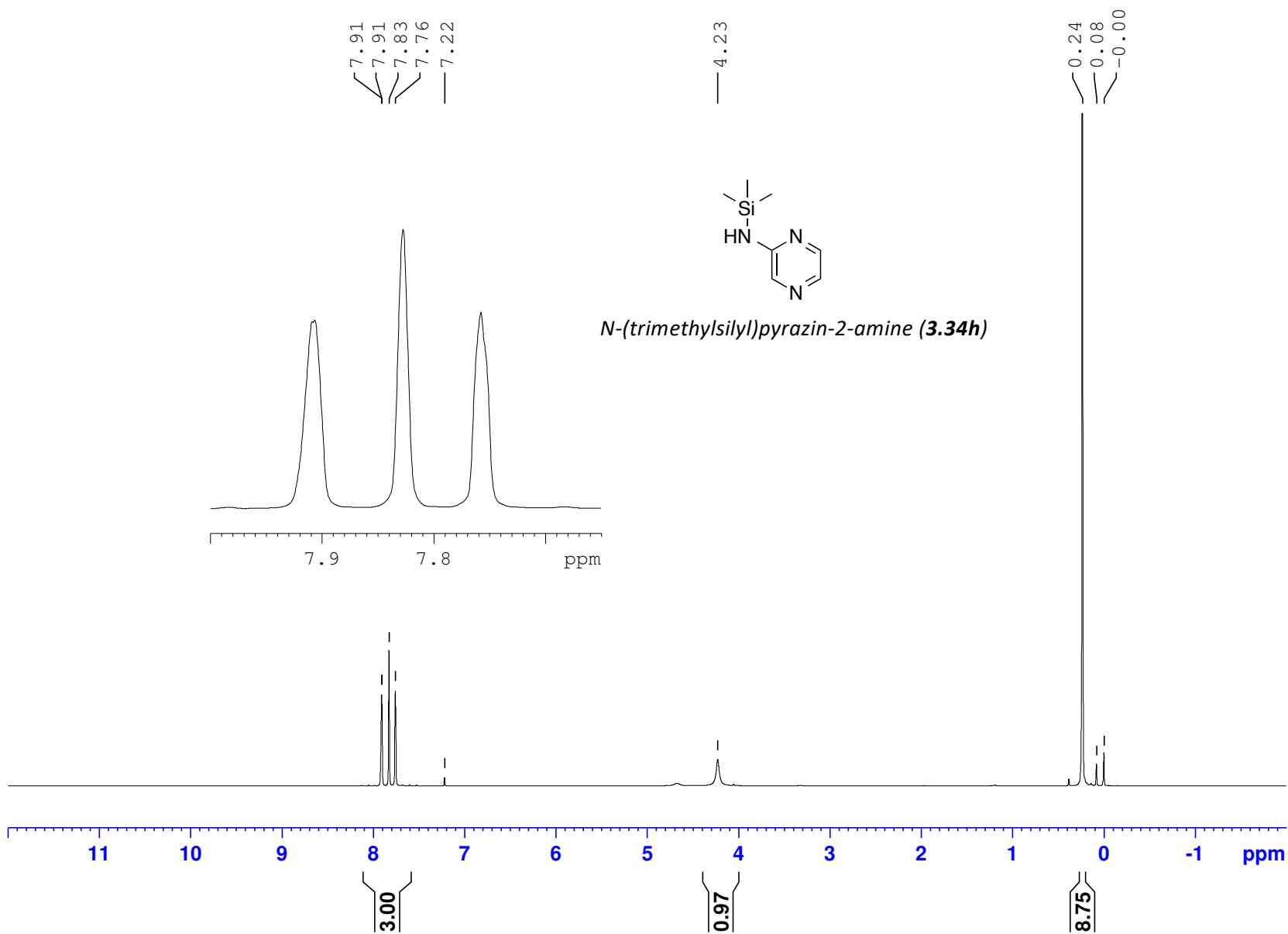
(400 MHz, 297.2K, CDCl<sub>3</sub>)



Methyl 4-((trimethylsilyl)amino)benzoate  
(3.34g)

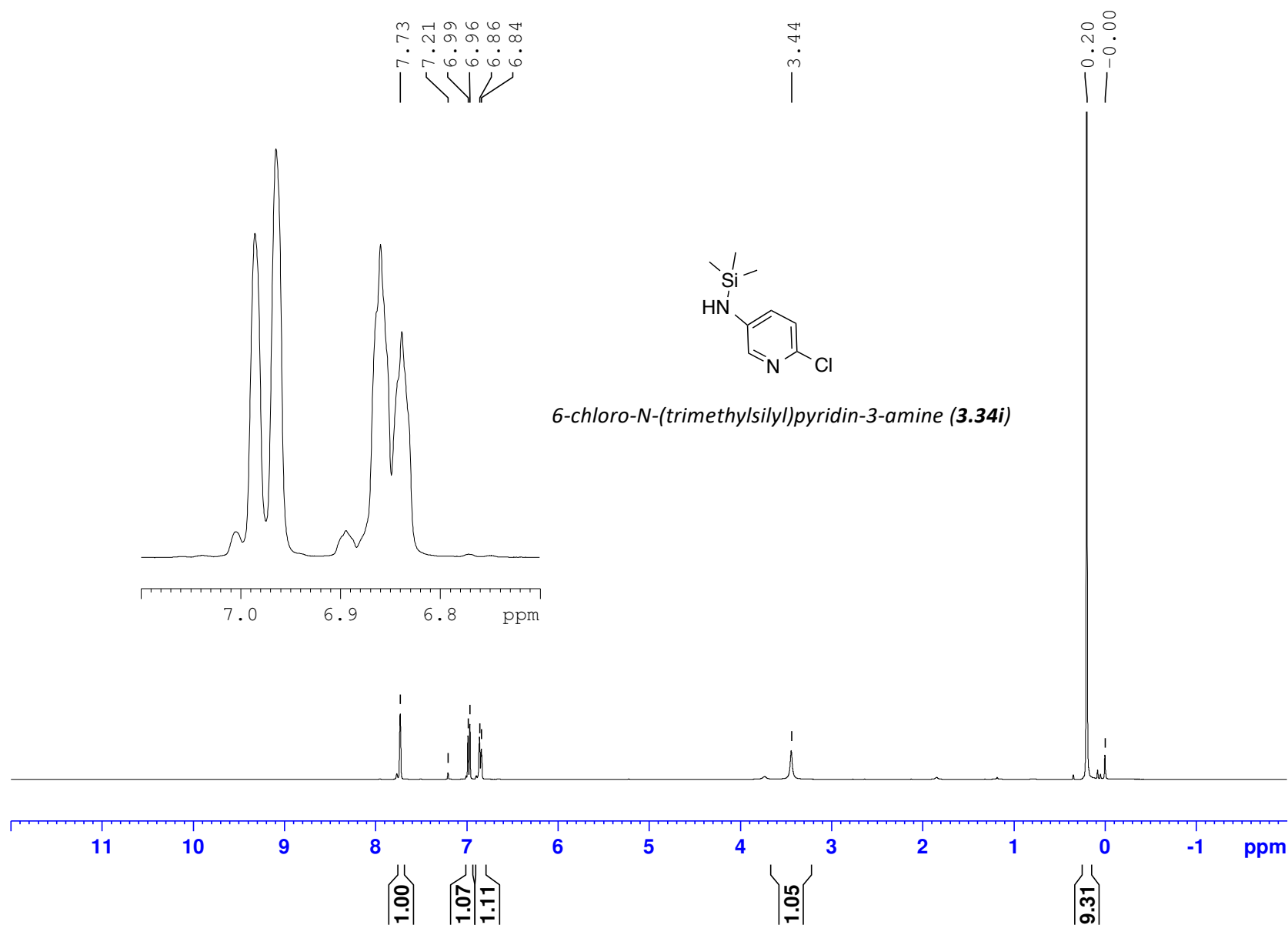
MZP142\_Si-6958\_CDC13

(400 MHz, 297.2K, CDCl<sub>3</sub>)



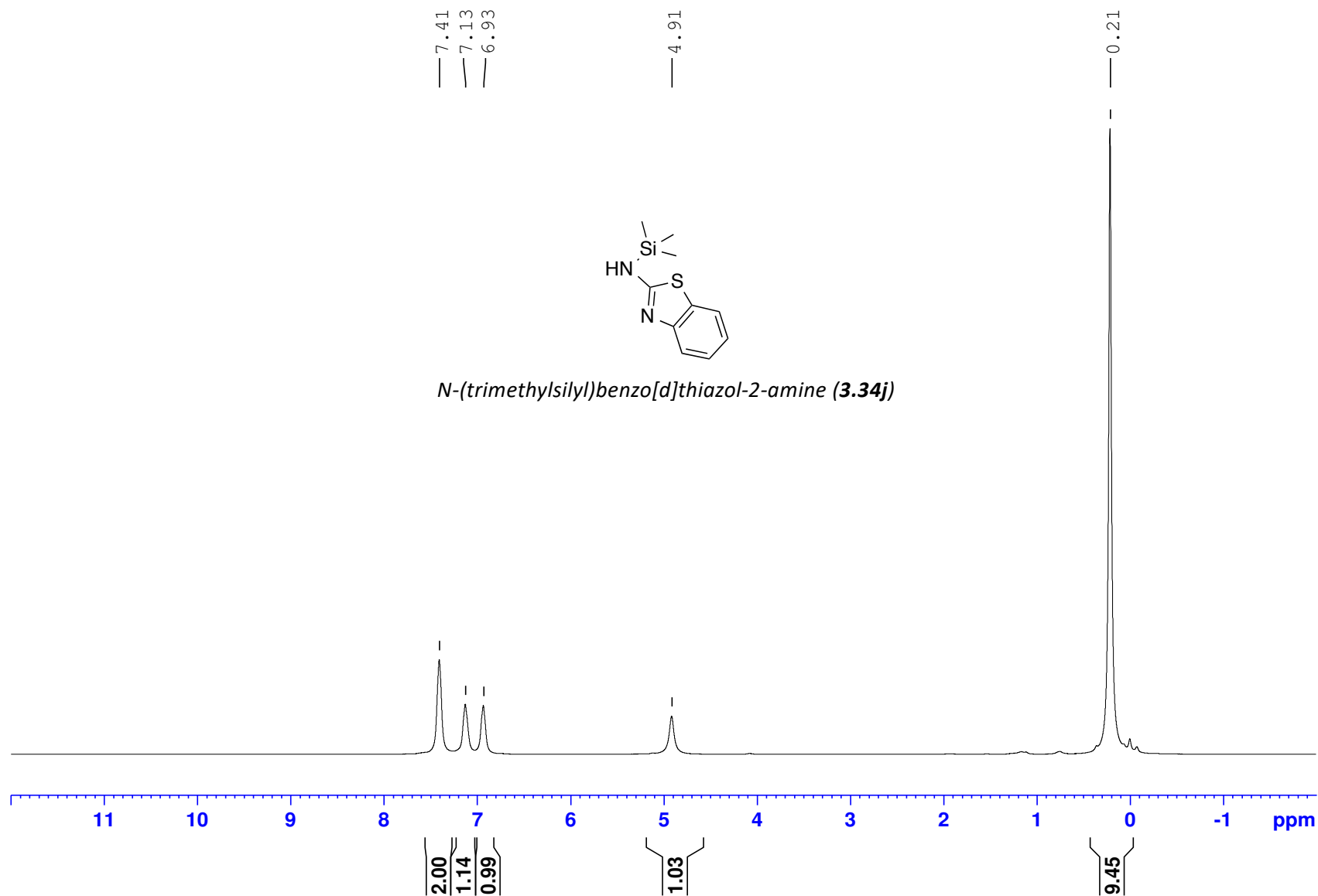
MZP\_Si-109B\_2.5h\_CDCl3

(400 MHz, 297.2K, CDCl<sub>3</sub>)



MZP107\_Si-8812\_CDCl3

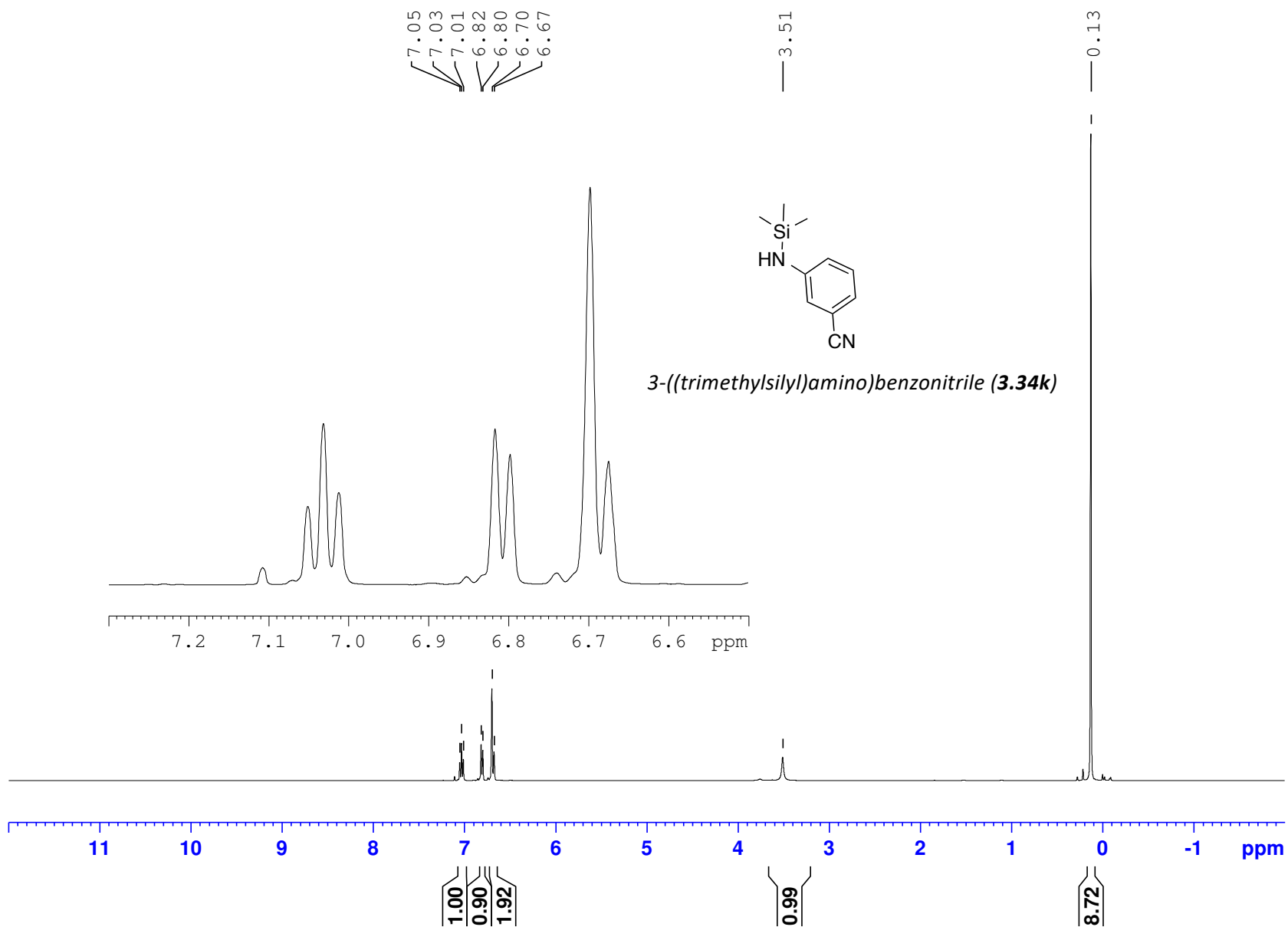
(400 MHz, 297.2K, CDCl<sub>3</sub>)





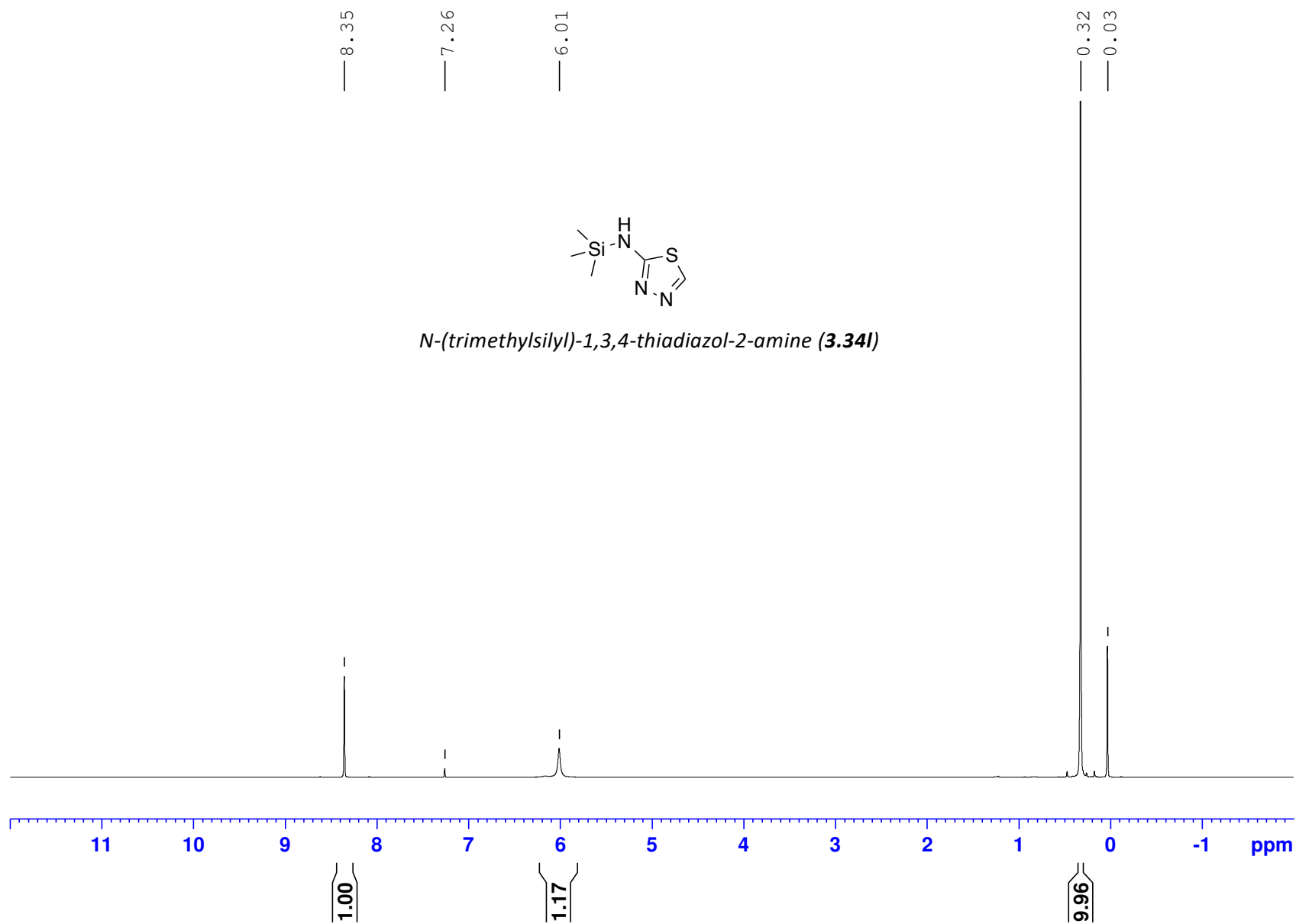
MZP150\_Si-A14\_CDCl3

(400 MHz, 297.2K, CDCl<sub>3</sub>)



MZP109\_Si-8881\_CDCl3

(400 MHz, 297.2K, CDCl<sub>3</sub>)



MZP105\_Si-C20\_CDC13

(400 MHz, 297.2K, CDCl<sub>3</sub>)

— 8.70

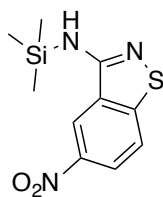
— 7.99

— 7.40

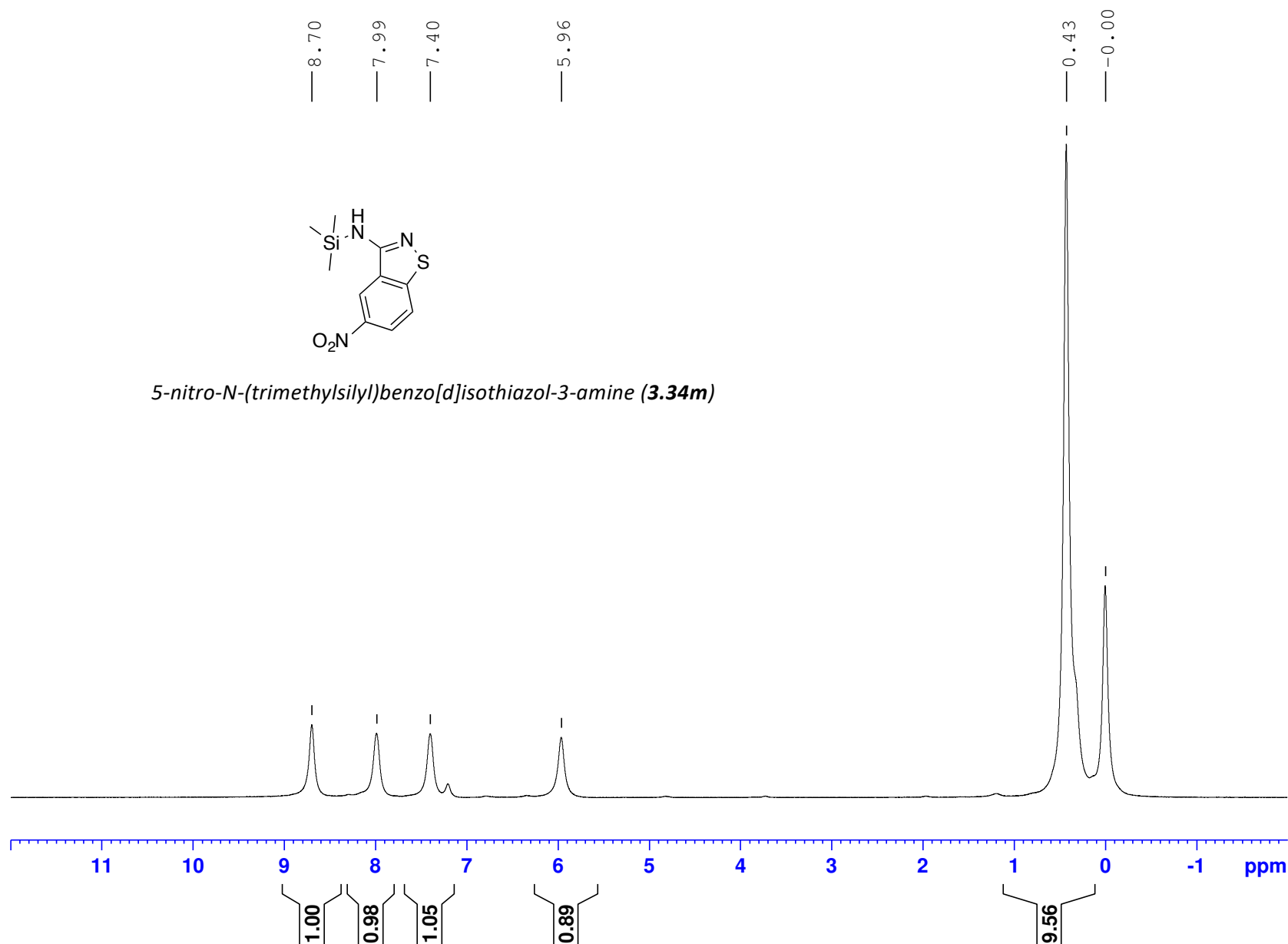
— 5.96

— 0.43

— -0.00

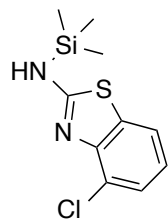


5-nitro-N-(trimethylsilyl)benzo[d]isothiazol-3-amine (**3.34m**)

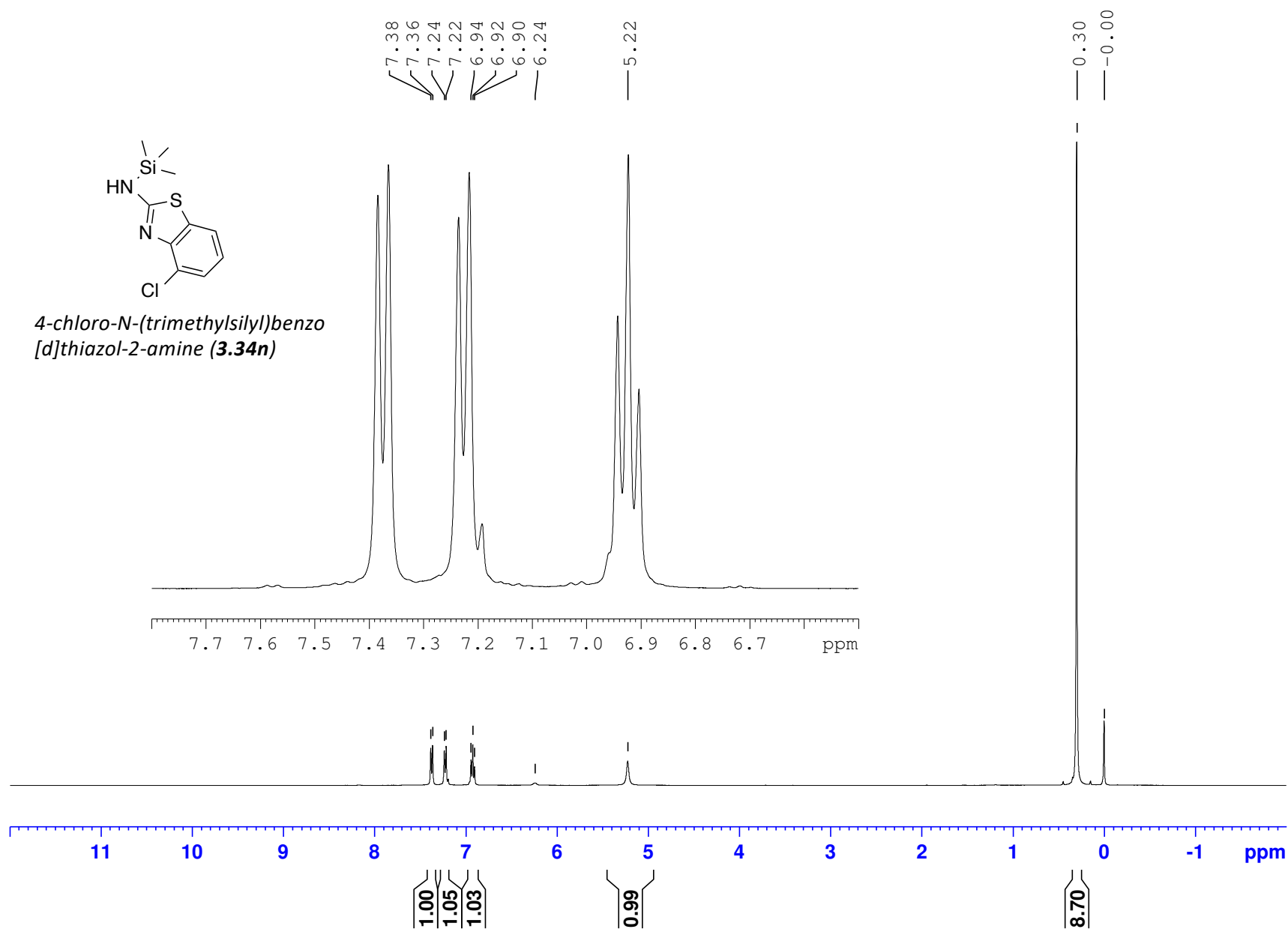


MZP106\_Si-A42\_CDC13

(400 MHz, 297.2K, CDCl<sub>3</sub>)

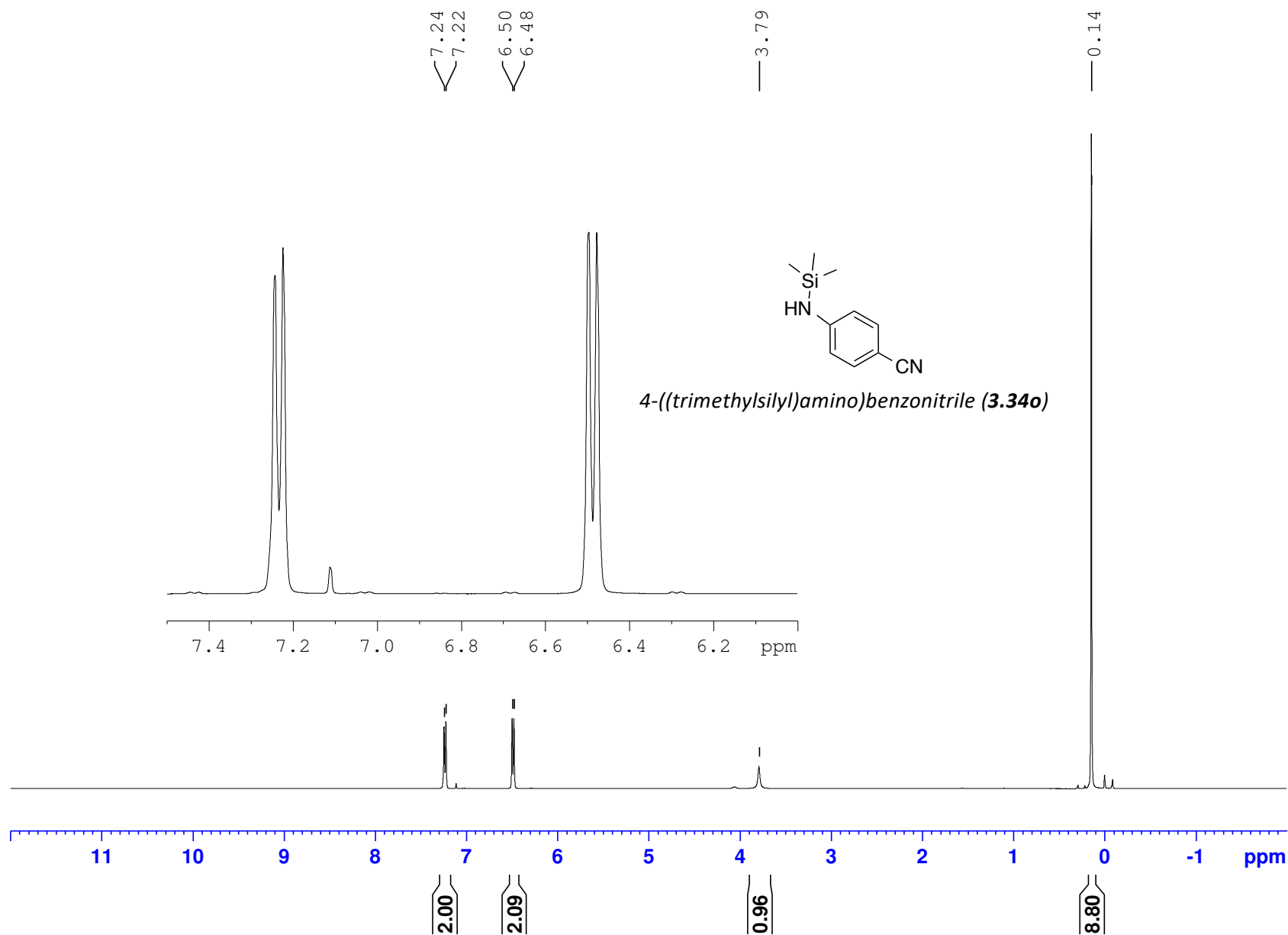


4-chloro-N-(trimethylsilyl)benzo[d]thiazol-2-amine (**3.34n**)



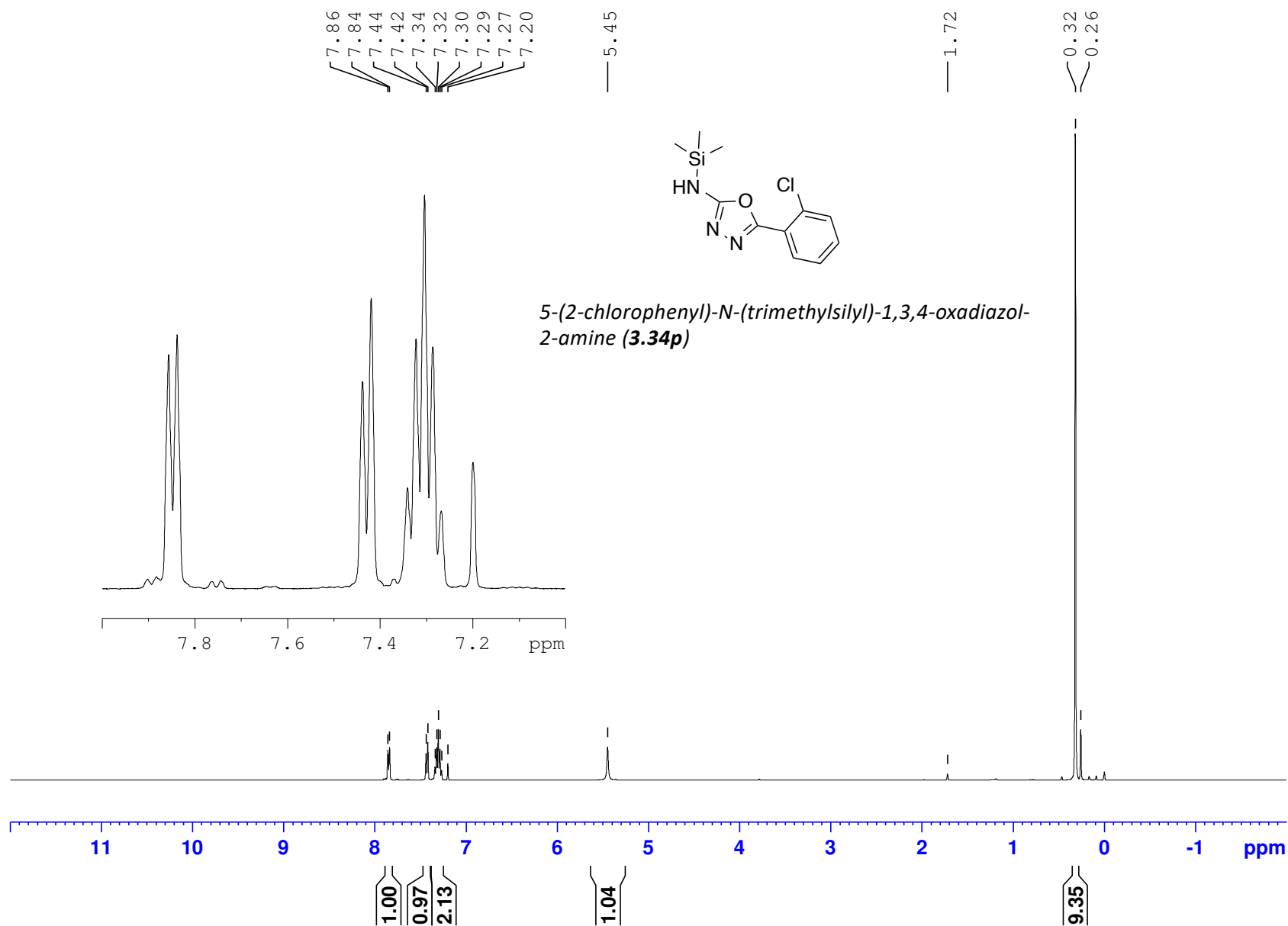
MZP149\_Si-A112C\_CDC13

(400 MHz, 297.2K, CDCl<sub>3</sub>)



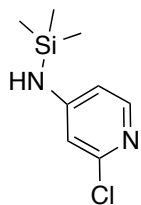
MZP137\_Si-A30\_CDC13

(400 MHz, 297.2K, CDCl<sub>3</sub>)

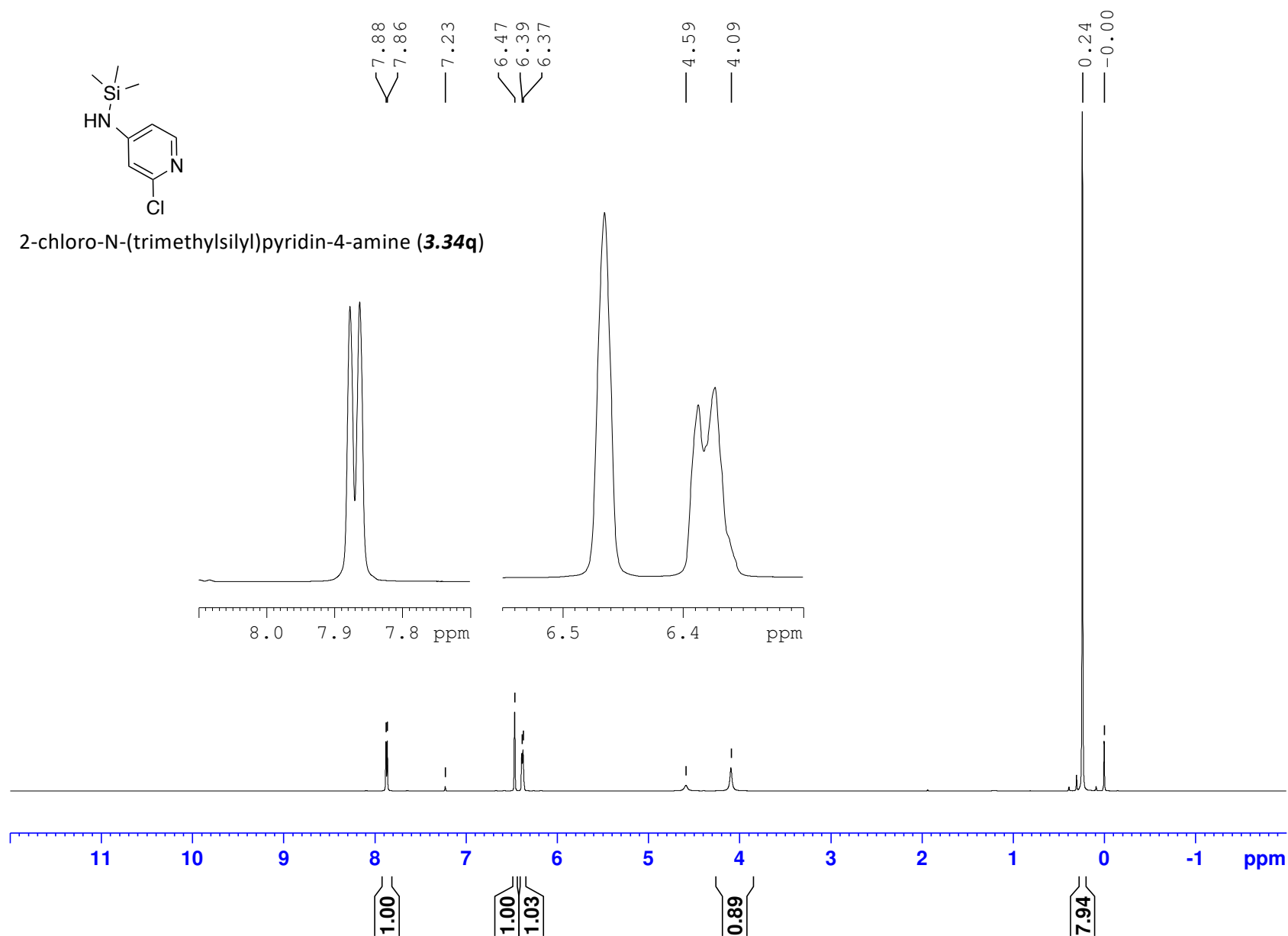


MZP135\_Si-A13\_CDC13

(400 MHz, 297.2K, CDCl<sub>3</sub>)

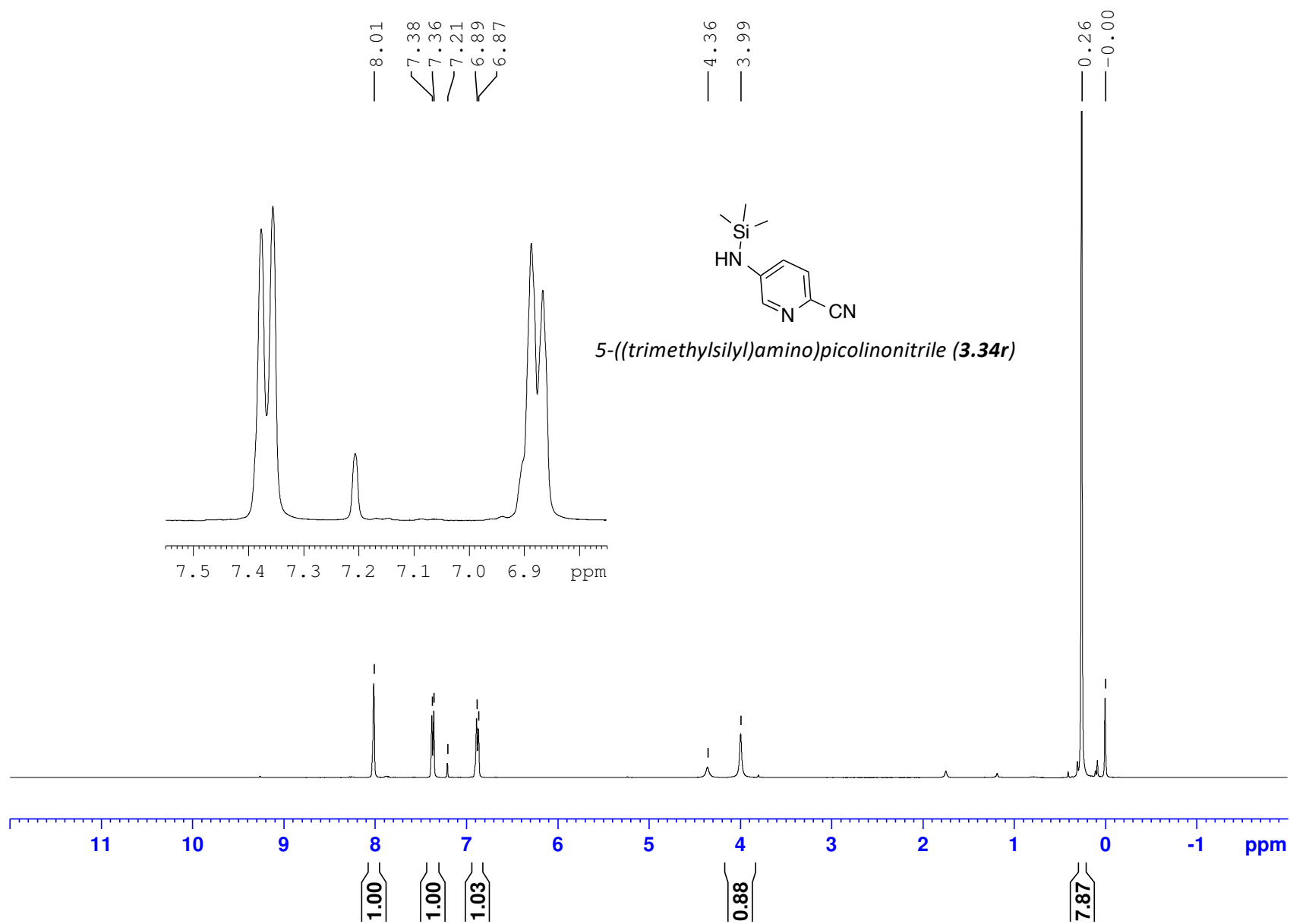


2-chloro-N-(trimethylsilyl)pyridin-4-amine (**3.34q**)



MZP\_Si-101C\_6h\_CDC13

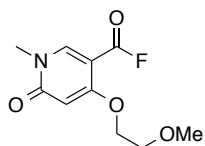
(400 MHz, 297.2K, CDCl<sub>3</sub>)



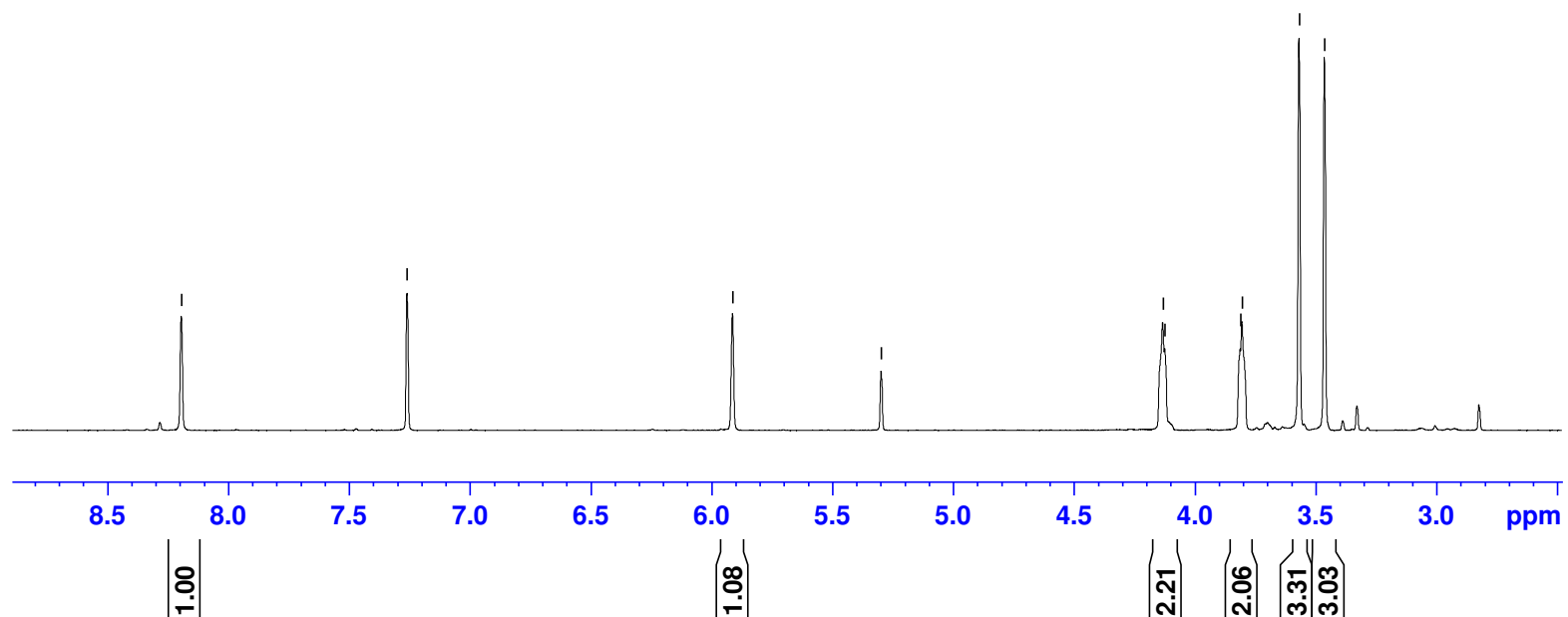


MZP-COF-1H-NMR-Feb2015

(400 MHz, 297.2K, CDCl<sub>3</sub>)



4-(2-methoxyethoxy)-1-methyl-6-oxo-1,6-dihydropyridine-3-carbonyl fluoride (**3.51**)



MZP54-10-COF-13C-NMR-CDC13

(100 MHz, 297.2K, CDCl<sub>3</sub>)

165.58  
163.54

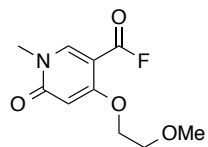
154.14  
150.82  
148.06

97.30

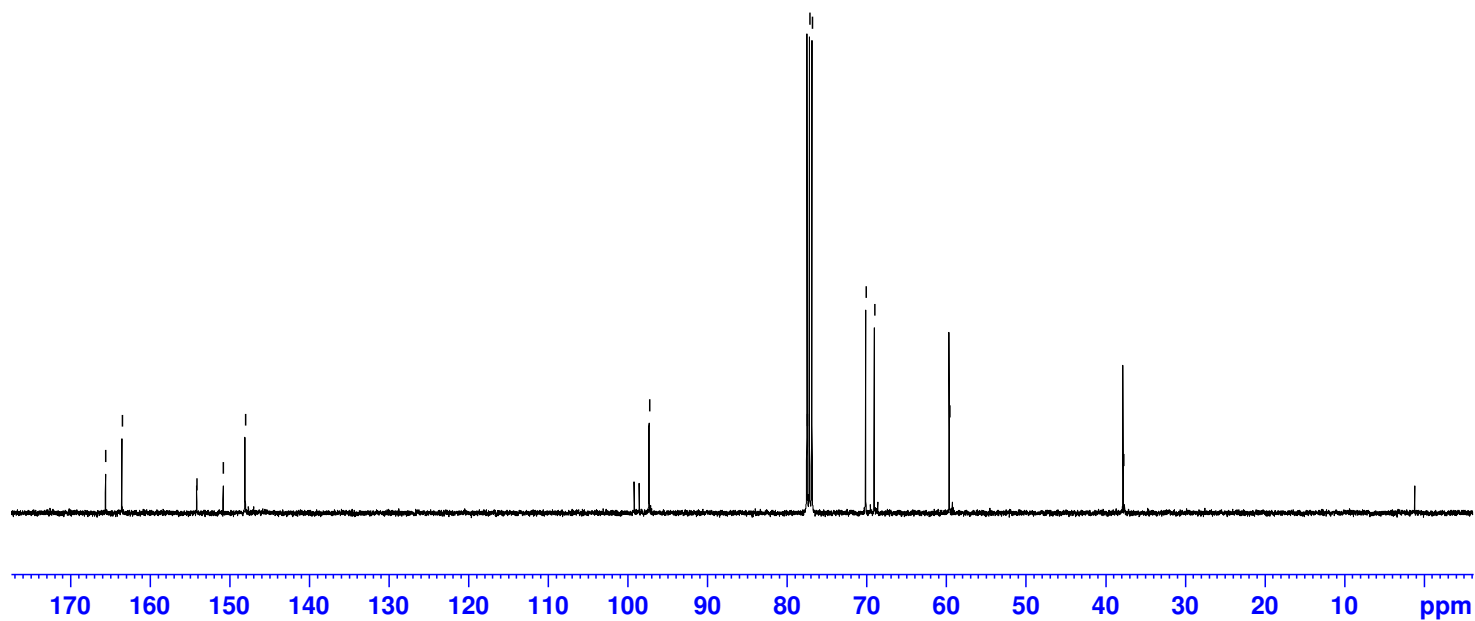
77.48  
77.16  
76.84  
70.09  
69.03

59.61

37.77

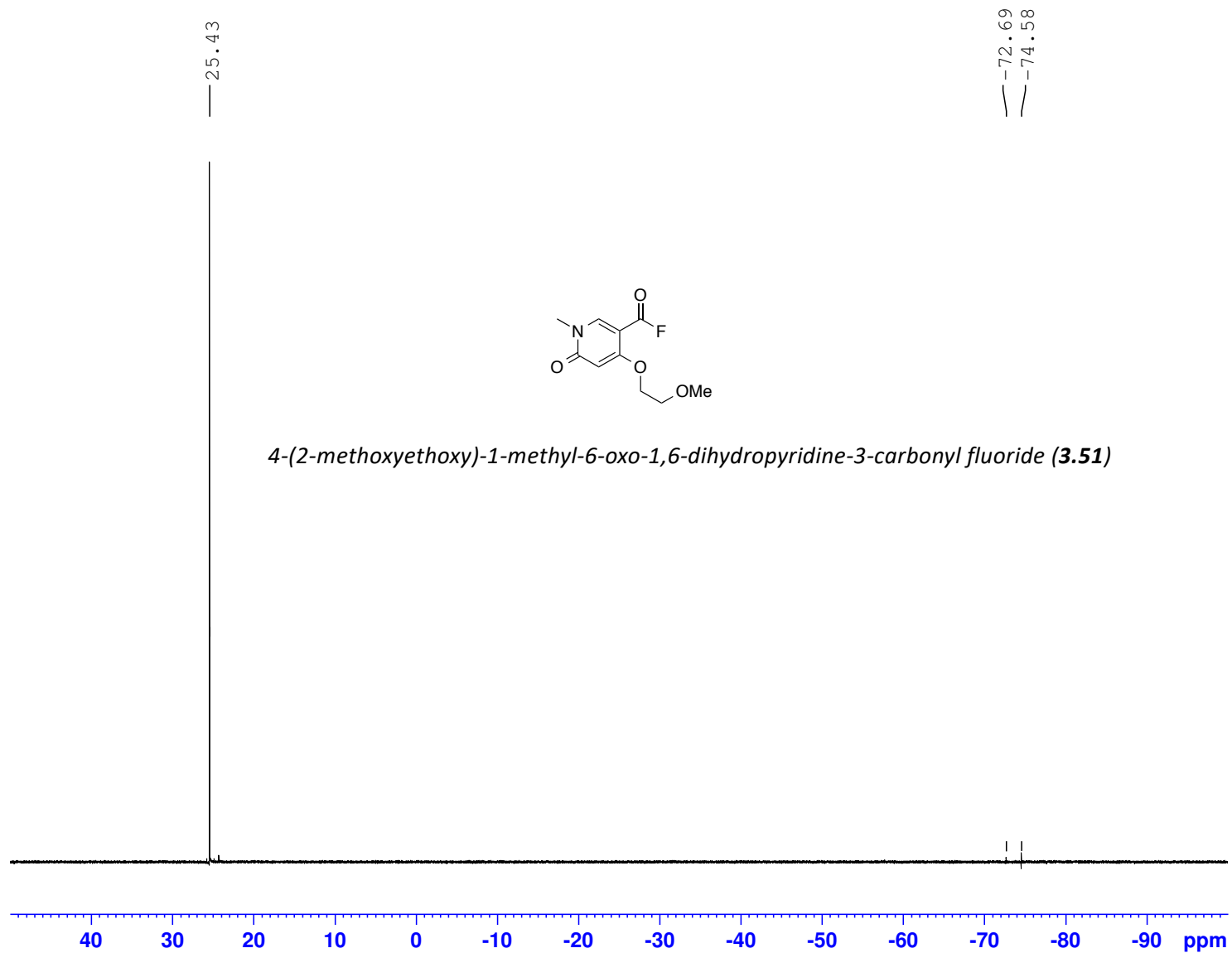


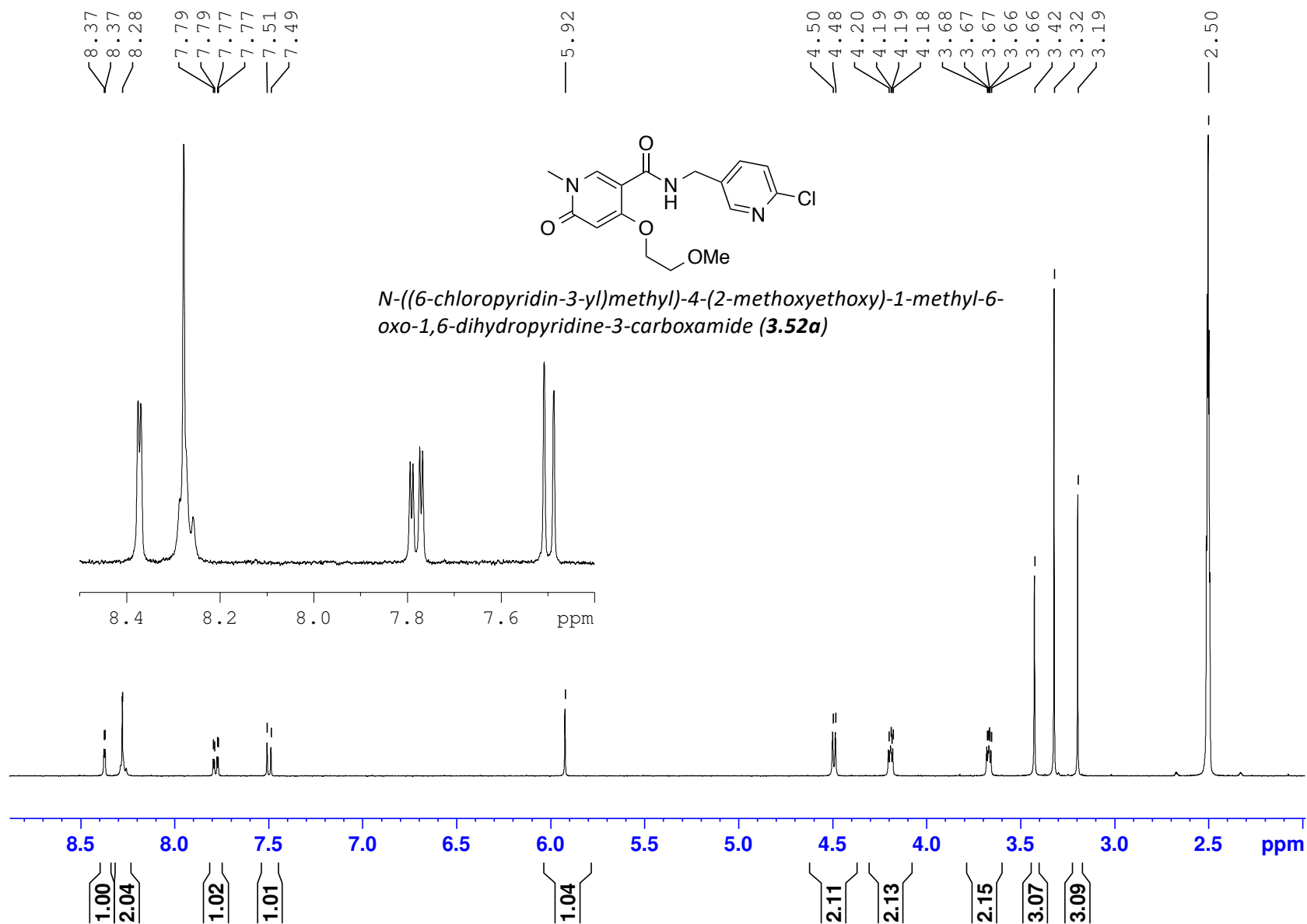
4-(2-methoxyethoxy)-1-methyl-6-oxo-1,6-dihydropyridine-3-carbonyl fluoride (**3.51**)



MZP\_COF\_Dec2014\_19F-NMR\_CDC13

(400 MHz, 297.2K, CDCl<sub>3</sub>)





(100 MHz, 297.2 K, DMSO-d6)

MZP-Amide-A18-13CBB-DMSO

163.68  
162.71  
162.49

148.93  
148.78  
144.54

138.88  
134.51

124.01

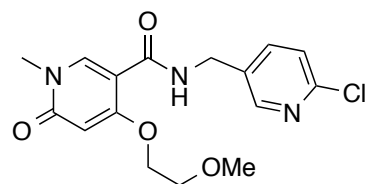
105.69

96.25

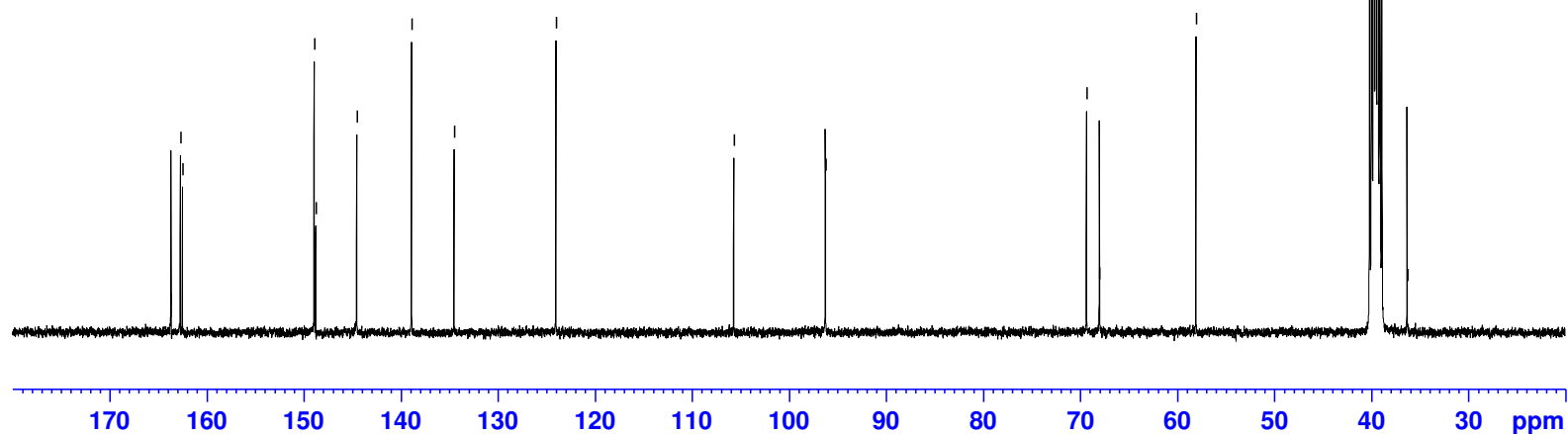
69.34  
68.01

58.06

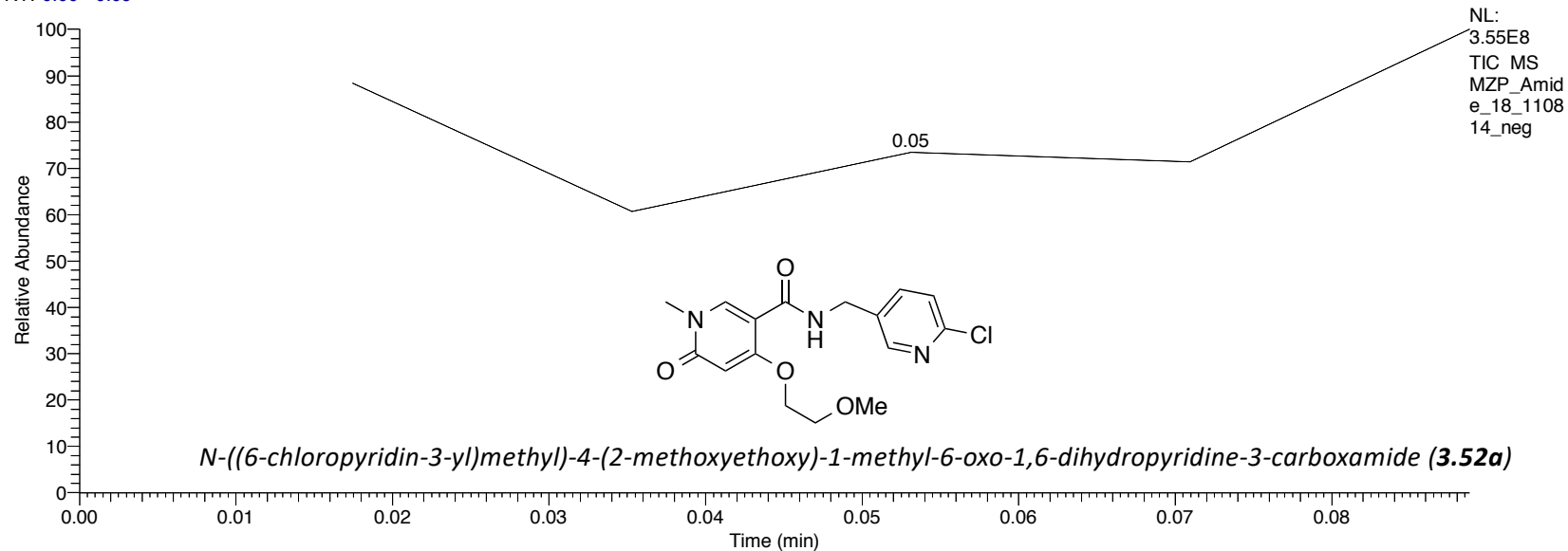
39.52  
36.31



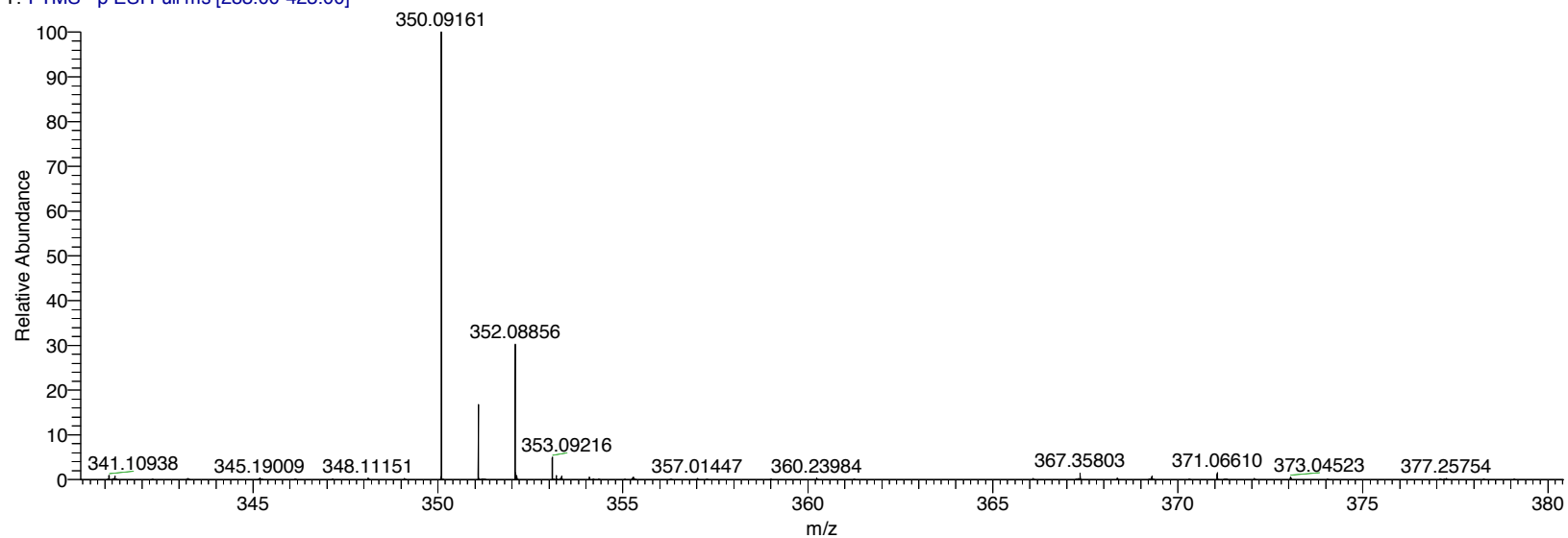
*N*-((6-chloropyridin-3-yl)methyl)-4-(2-methoxyethoxy)-1-methyl-6-oxo-1,6-dihydropyridine-3-carboxamide (**3.52a**)

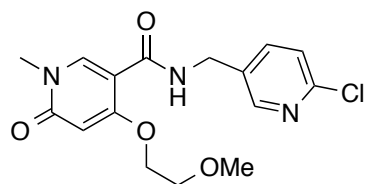


RT: 0.00 - 0.09

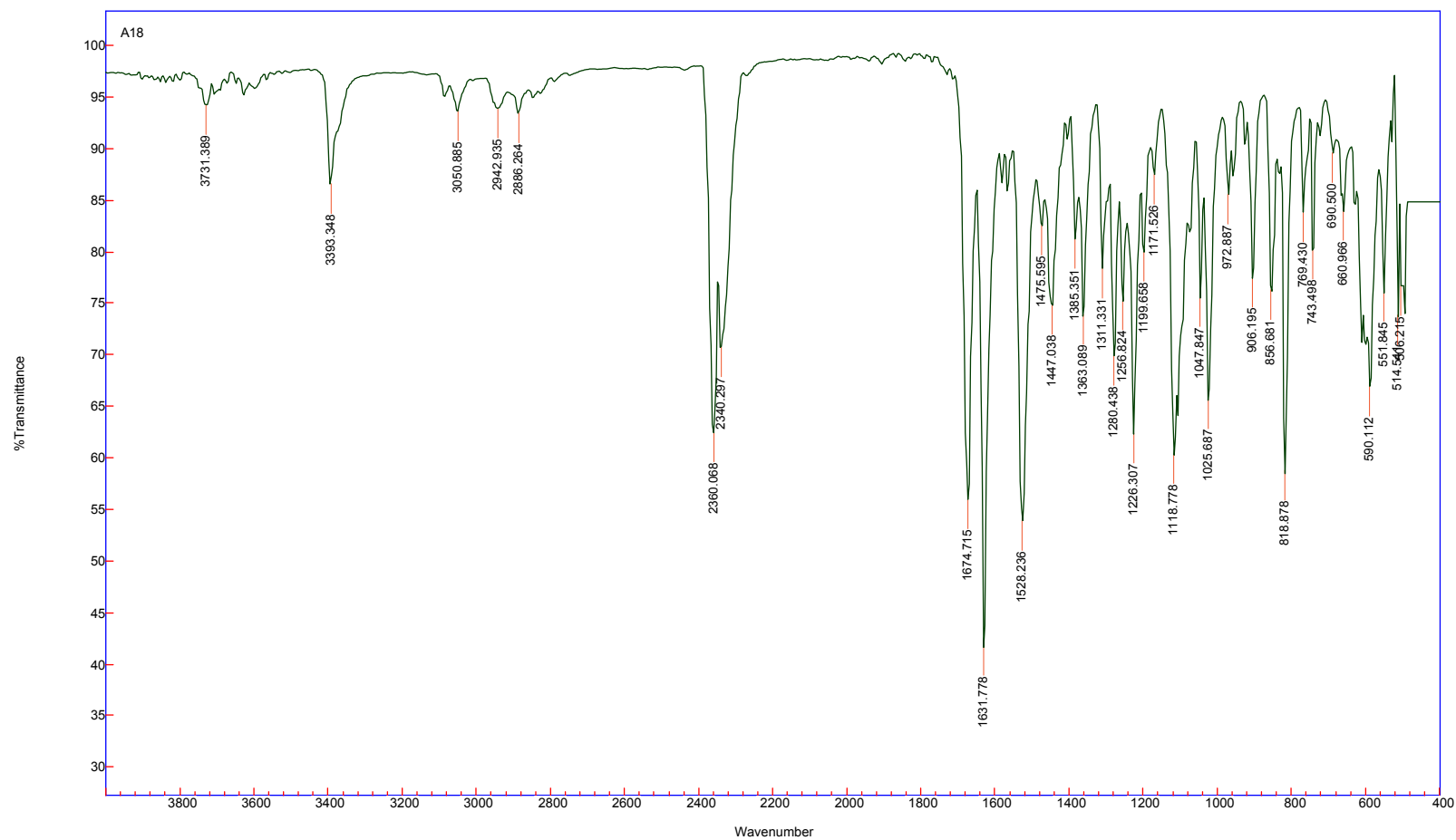


MZIP\_Amide\_18\_110814\_neg #1 RT: 0.02 AV: 1 NL: 1.00E8  
T: FTMS - p ESI Full ms [283.00-423.00]



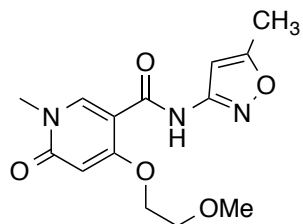


*N*-((6-chloropyridin-3-yl)methyl)-4-(2-methoxyethoxy)-1-methyl-6-oxo-1,6-dihydropyridine-3-carboxamide (**3.52a**)

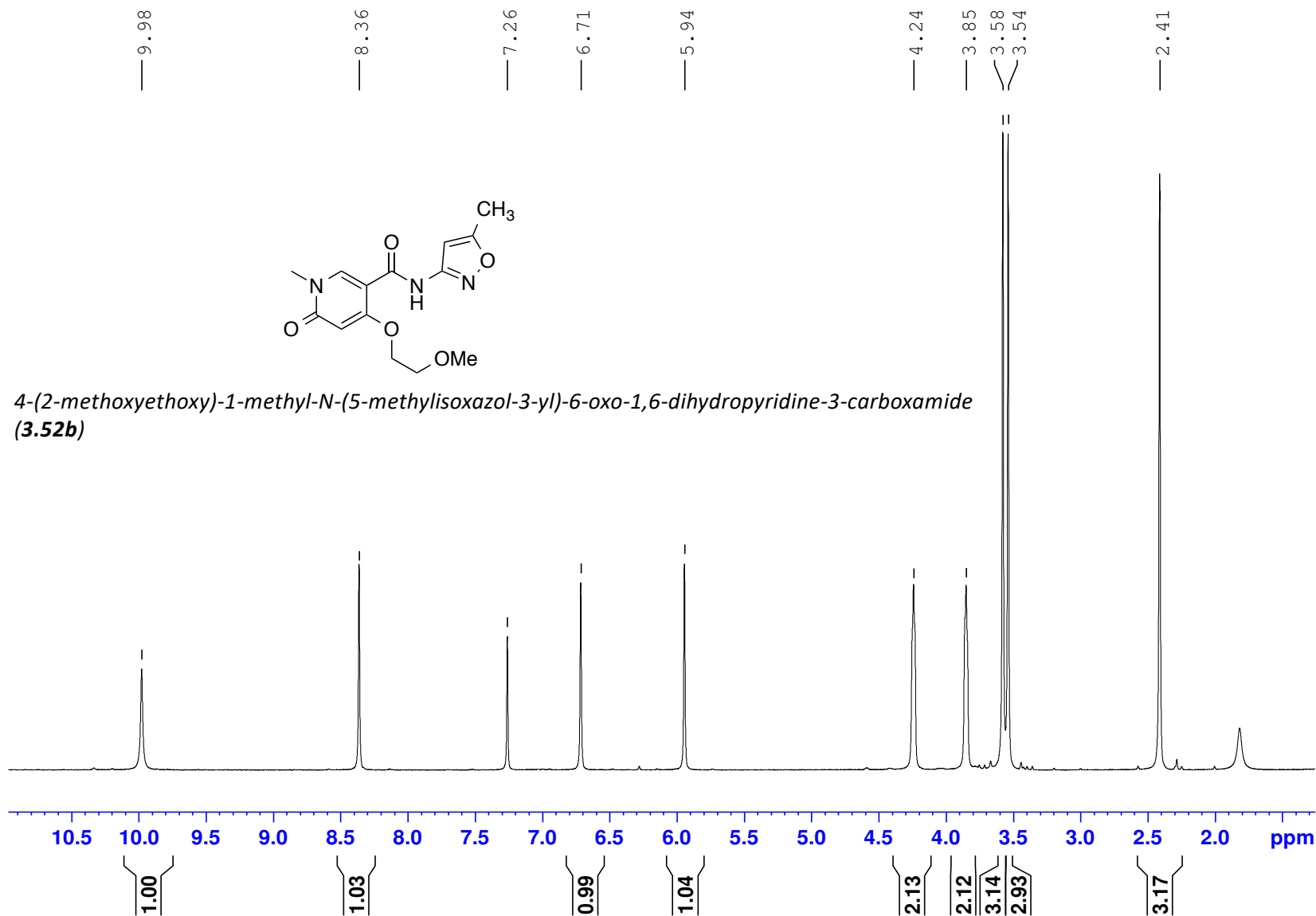


MZP-amide-A16-10mg-1H CDCl<sub>3</sub>

(400 MHz, 297.2 K, CDCl<sub>3</sub>)



4-(2-methoxyethoxy)-1-methyl-N-(5-methylisoxazol-3-yl)-6-oxo-1,6-dihydropyridine-3-carboxamide  
(**3.52b**)





(100 MHz, 297.2 K, CDCl<sub>3</sub>)

MZP-Amide-16-10mg\_13CBB CDCl<sub>3</sub>

— 169.84  
— 163.88  
— 163.84  
— 160.81  
— 158.20

— 145.87

— 105.56

— 97.34  
— 97.08

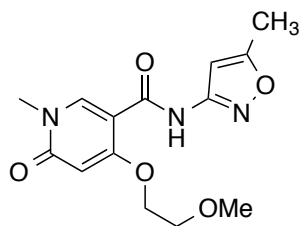
— 77.16

— 69.64  
— 68.67

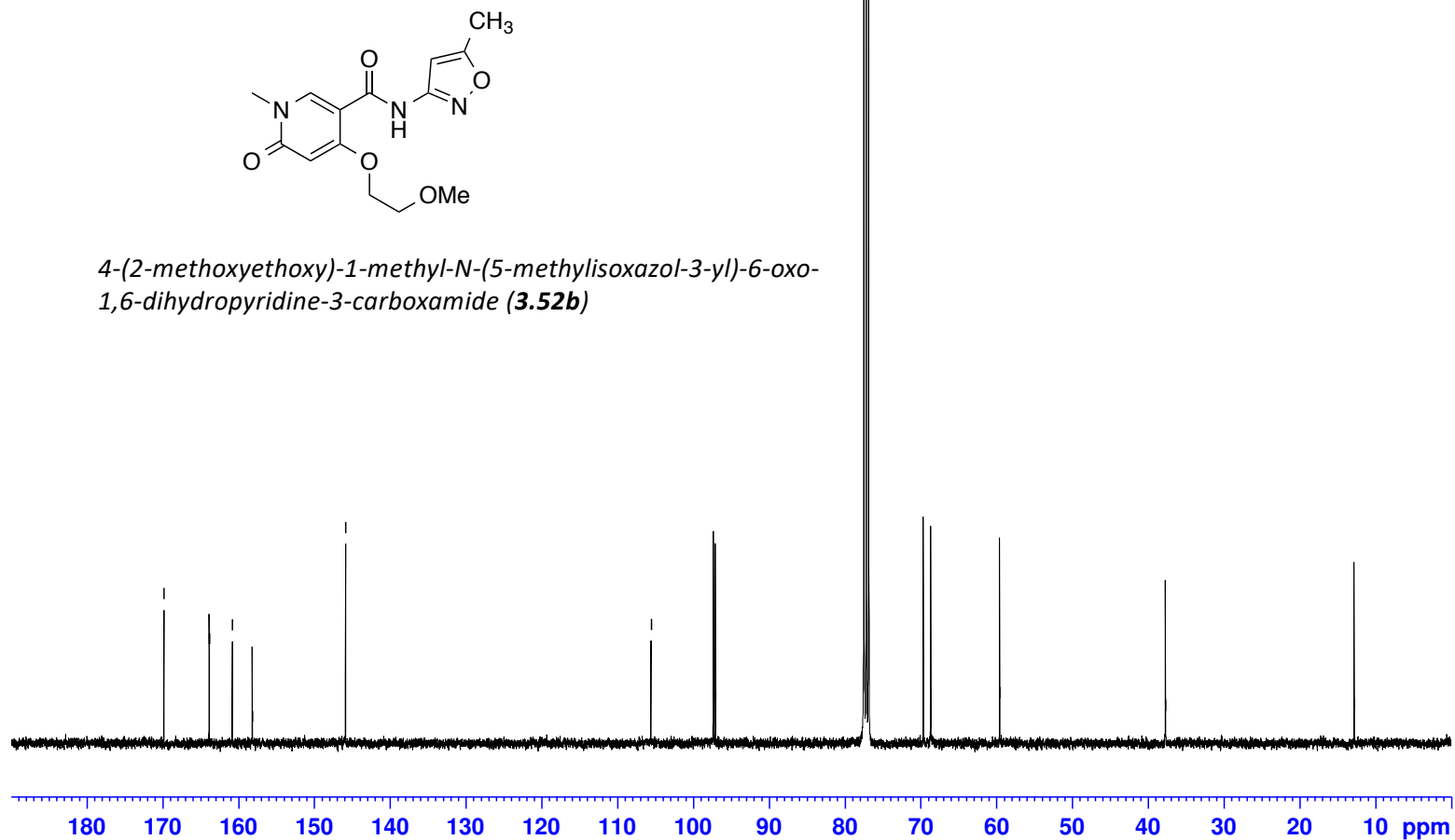
— 59.58

— 37.71

— 12.80

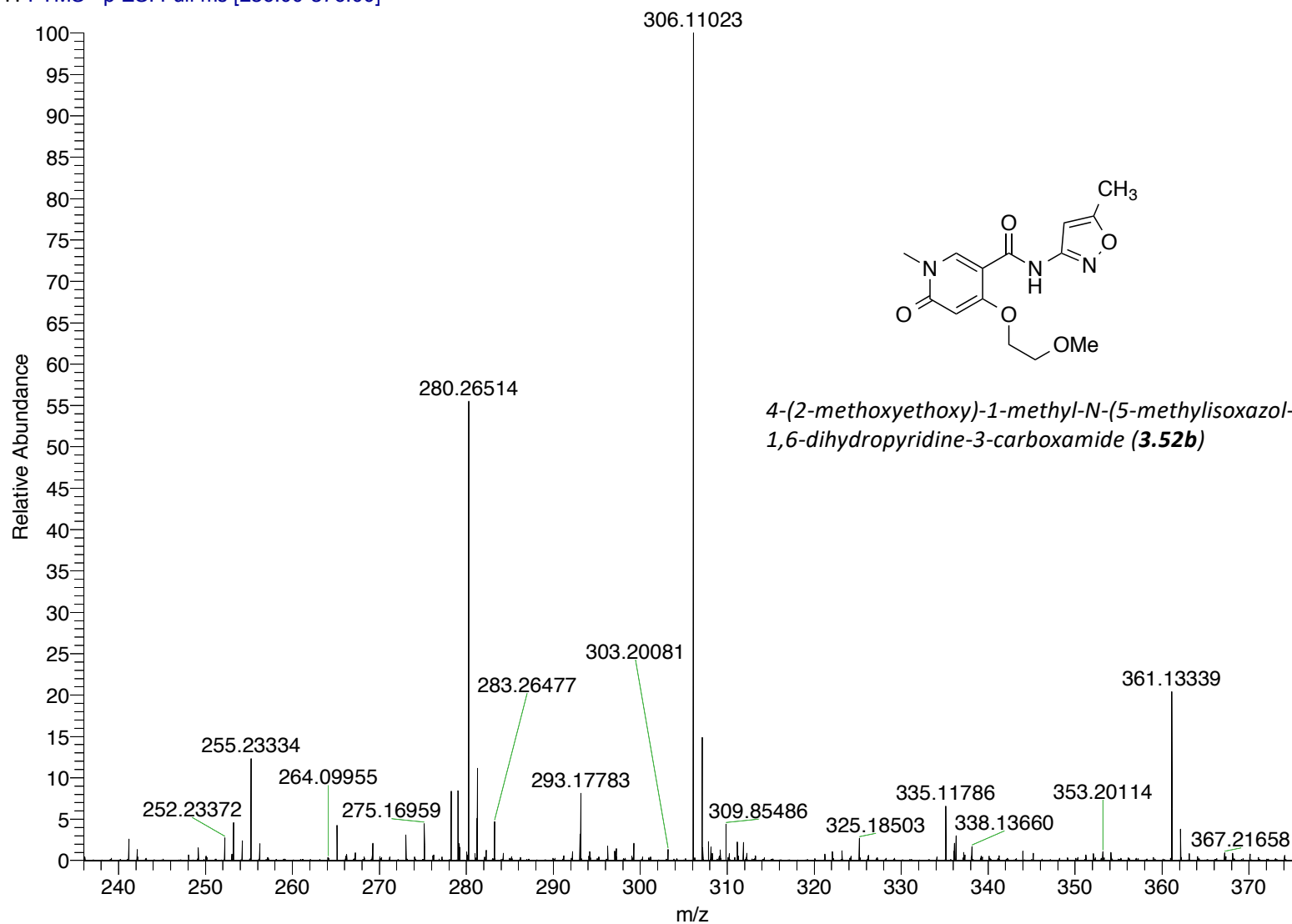


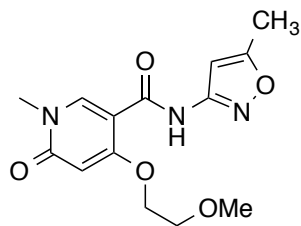
4-(2-methoxyethoxy)-1-methyl-N-(5-methylisoxazol-3-yl)-6-oxo-1,6-dihydropyridine-3-carboxamide (**3.52b**)



MZIP-Amide-A16-Feb15-2015-neg #25 RT: 0.45 AV: 1 NL: 3.16E7

T: FTMS - p ESI Full ms [236.00-376.00]



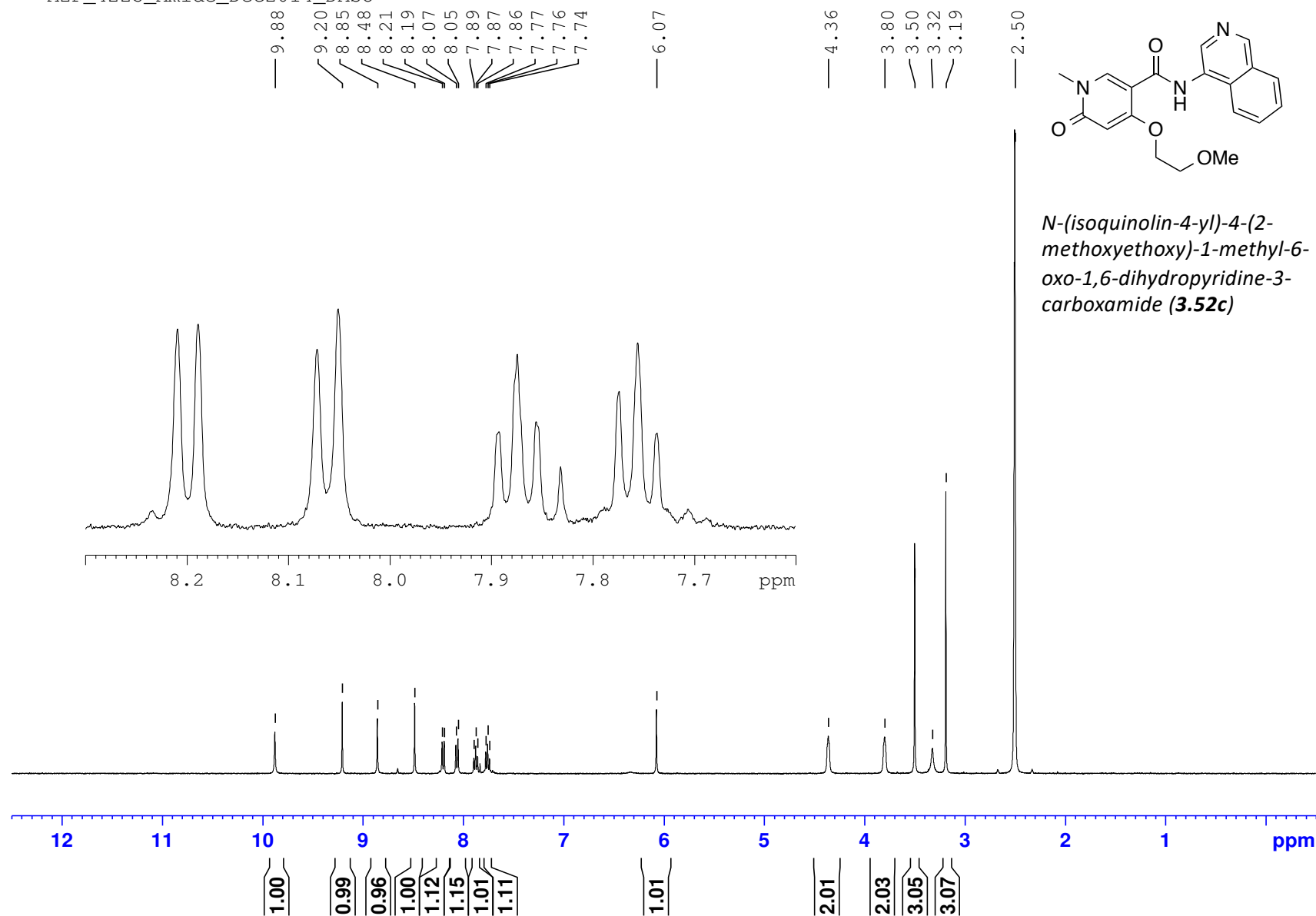


*4-(2-methoxyethoxy)-1-methyl-N-(5-methylisoxazol-3-yl)-6-oxo-1,6-dihydropyridine-3-carboxamide (3.52b)*



MZP\_4225\_Amide\_Dec2014\_DMSO

(400 MHz, 297.2 K, DMSO-d6)



(100 MHz, 297.2 K, DMSO-d6)

MZP-Amide-4225-Sep02-2014-10mg-13CBB DMSO

163.59  
162.79  
161.75

149.46  
145.34

138.39  
130.66  
129.99  
128.40  
128.30  
127.89  
127.68  
121.29

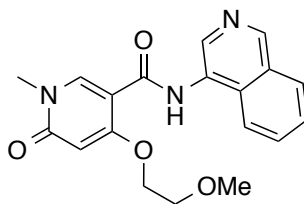
105.76

96.46

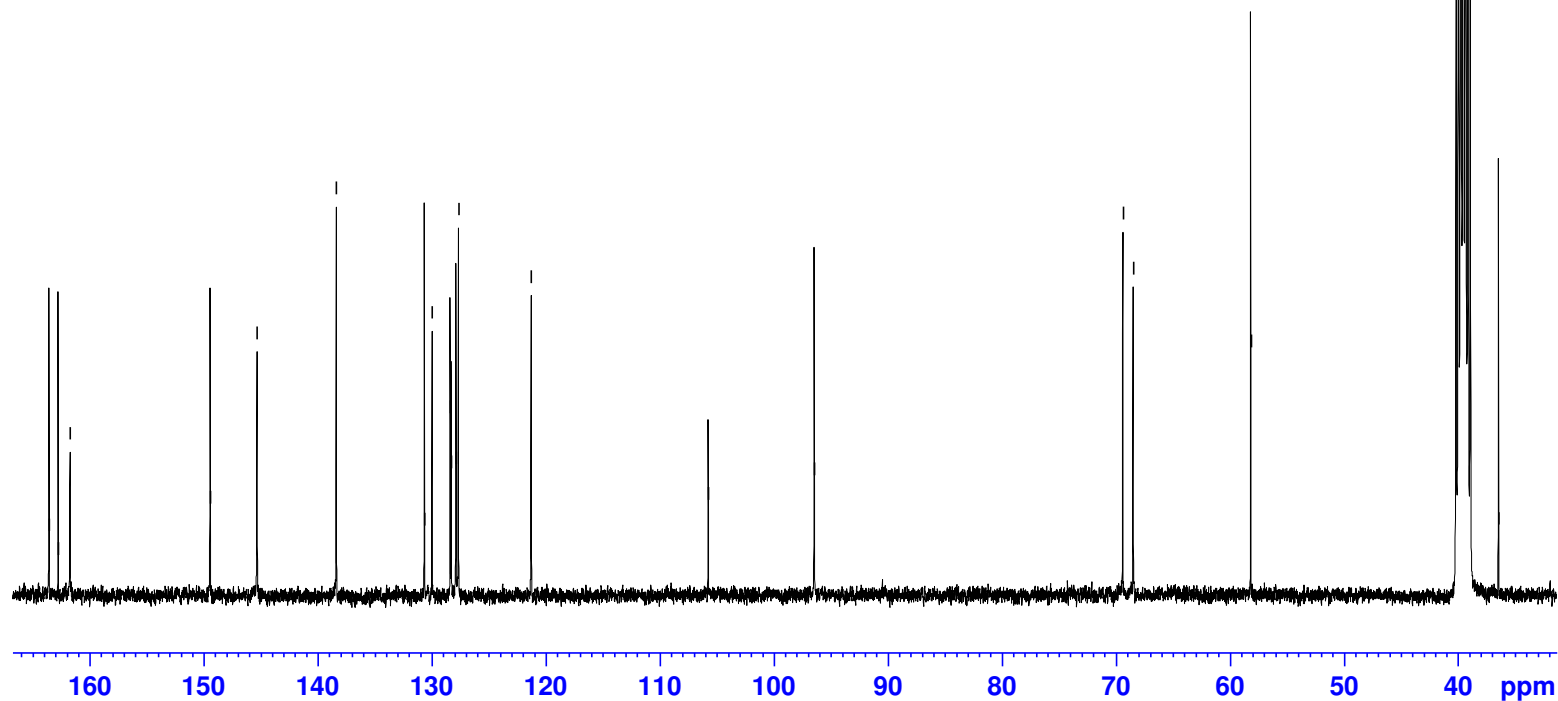
69.39  
68.48

58.17

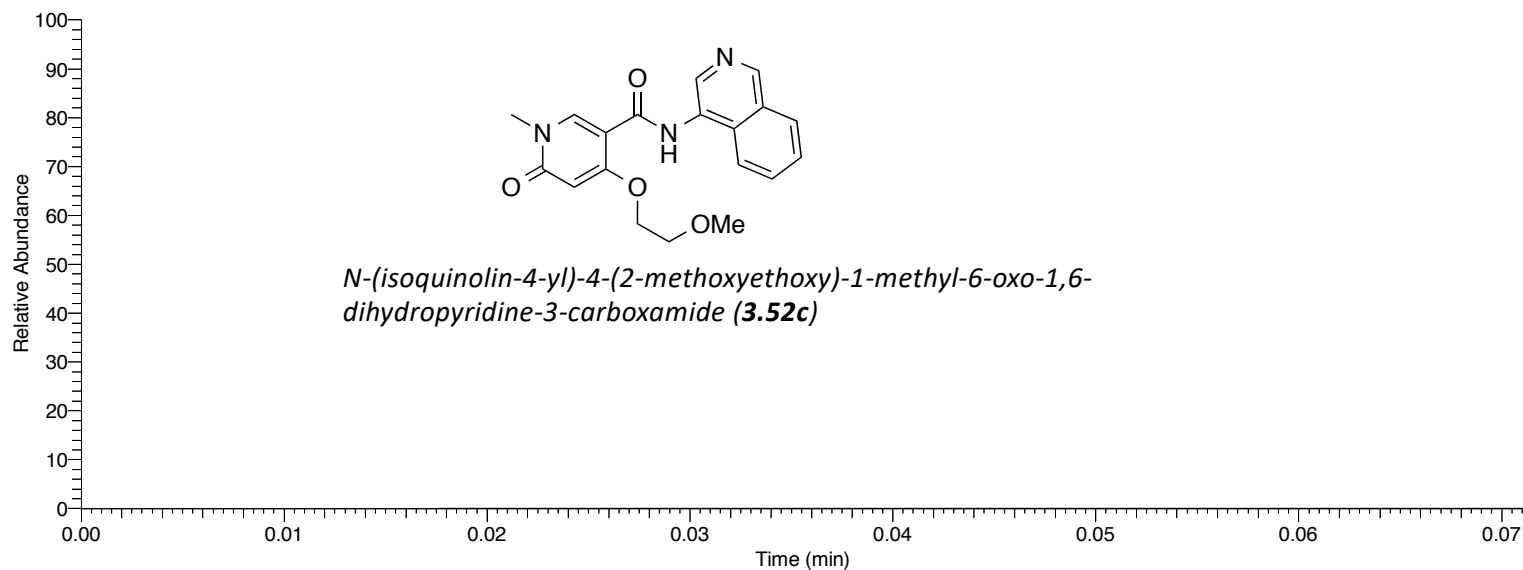
39.94  
39.73  
39.52  
39.31  
39.10  
36.43



*N*-(isoquinolin-4-yl)-4-(2-methoxyethoxy)-1-methyl-6-oxo-1,6-dihydropyridine-3-carboxamide (**3.52c**)

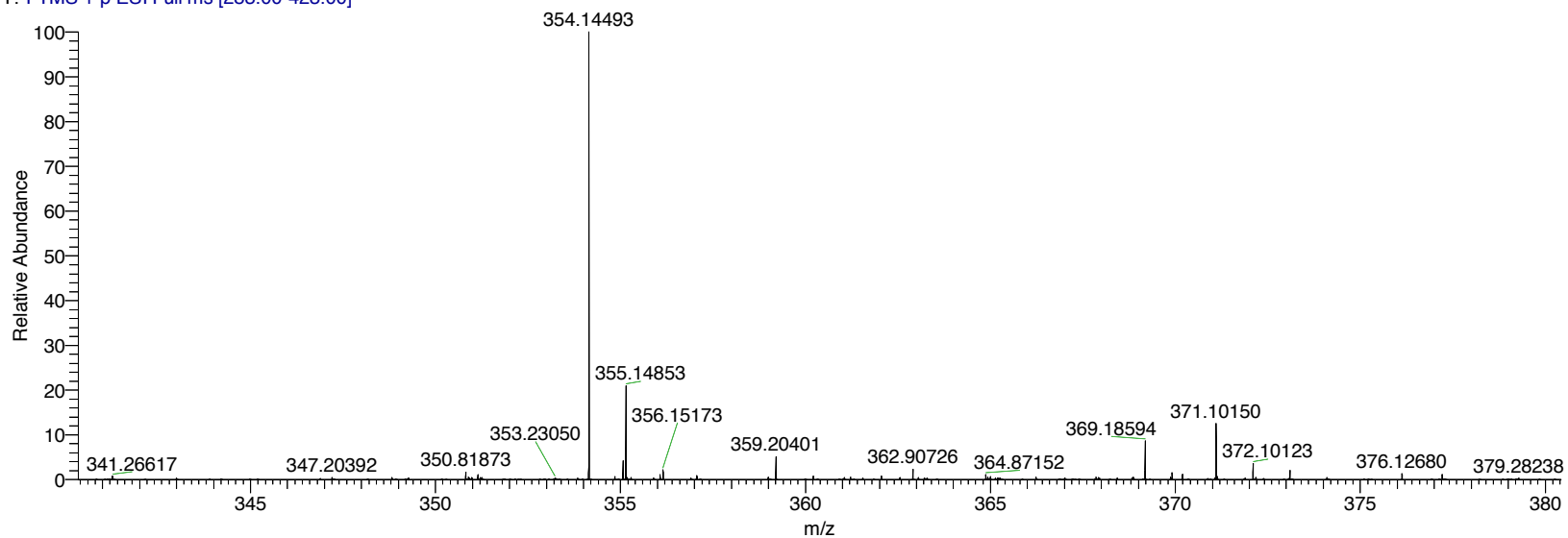


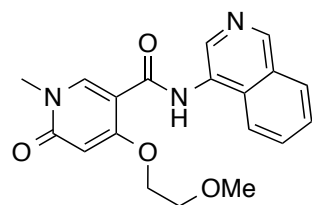
RT: 0.00 - 0.07



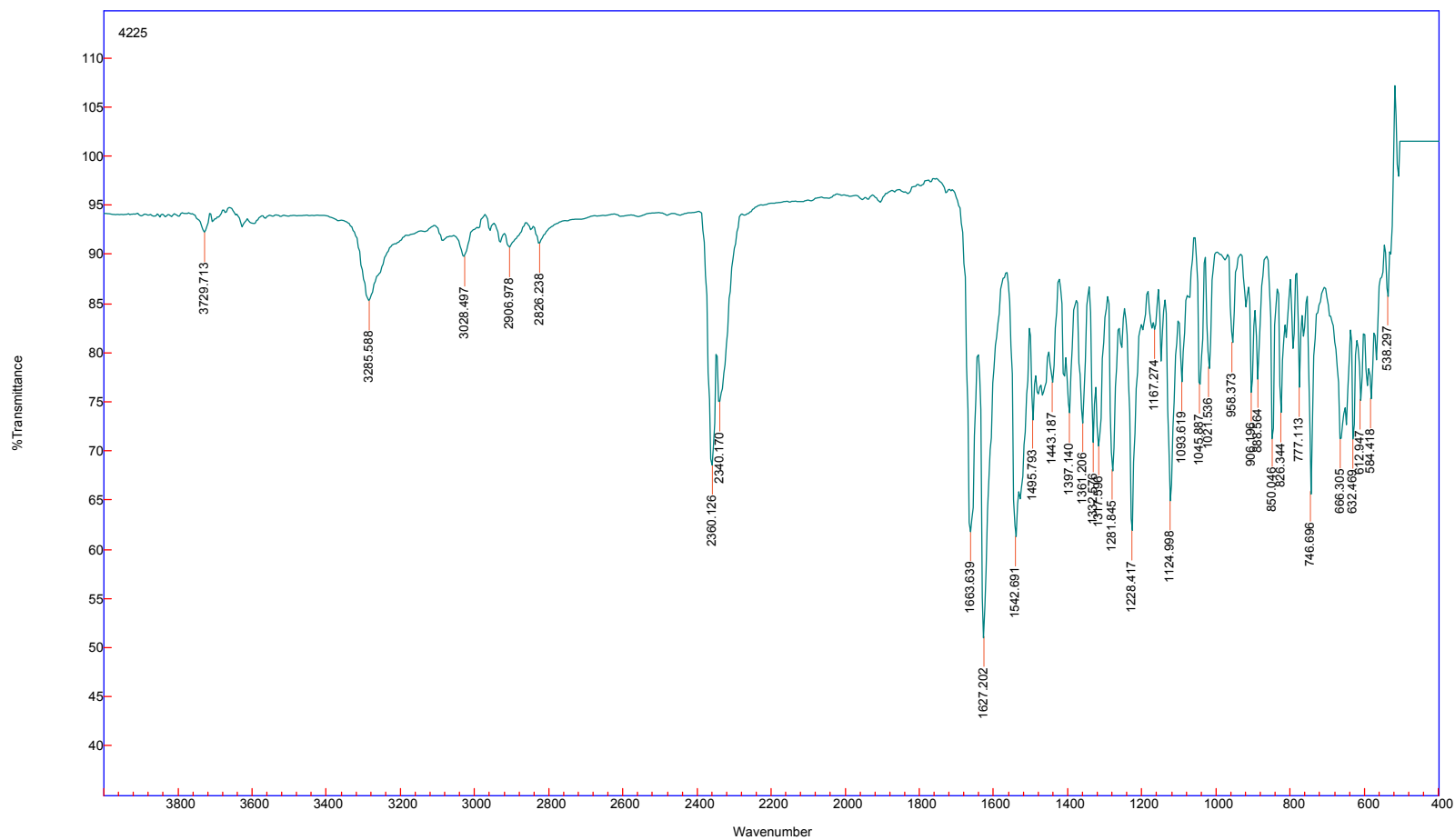
NL:  
0  
m/z=  
350.48998-  
350.49699  
MS  
MZP\_Amide\_  
4225\_020914  
\_pos

MZP\_Amide\_4225\_020914\_pos #1 RT: 0.02 AV: 1 NL: 4.11E7  
T: FTMS + p ESI Full ms [283.00-423.00]



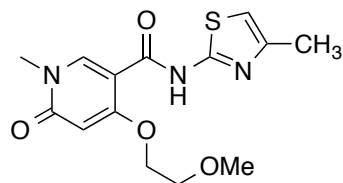


*N*-(isoquinolin-4-yl)-4-(2-methoxyethoxy)-1-methyl-6-oxo-1,6-dihydropyridine-3-carboxamide (**3.52c**)

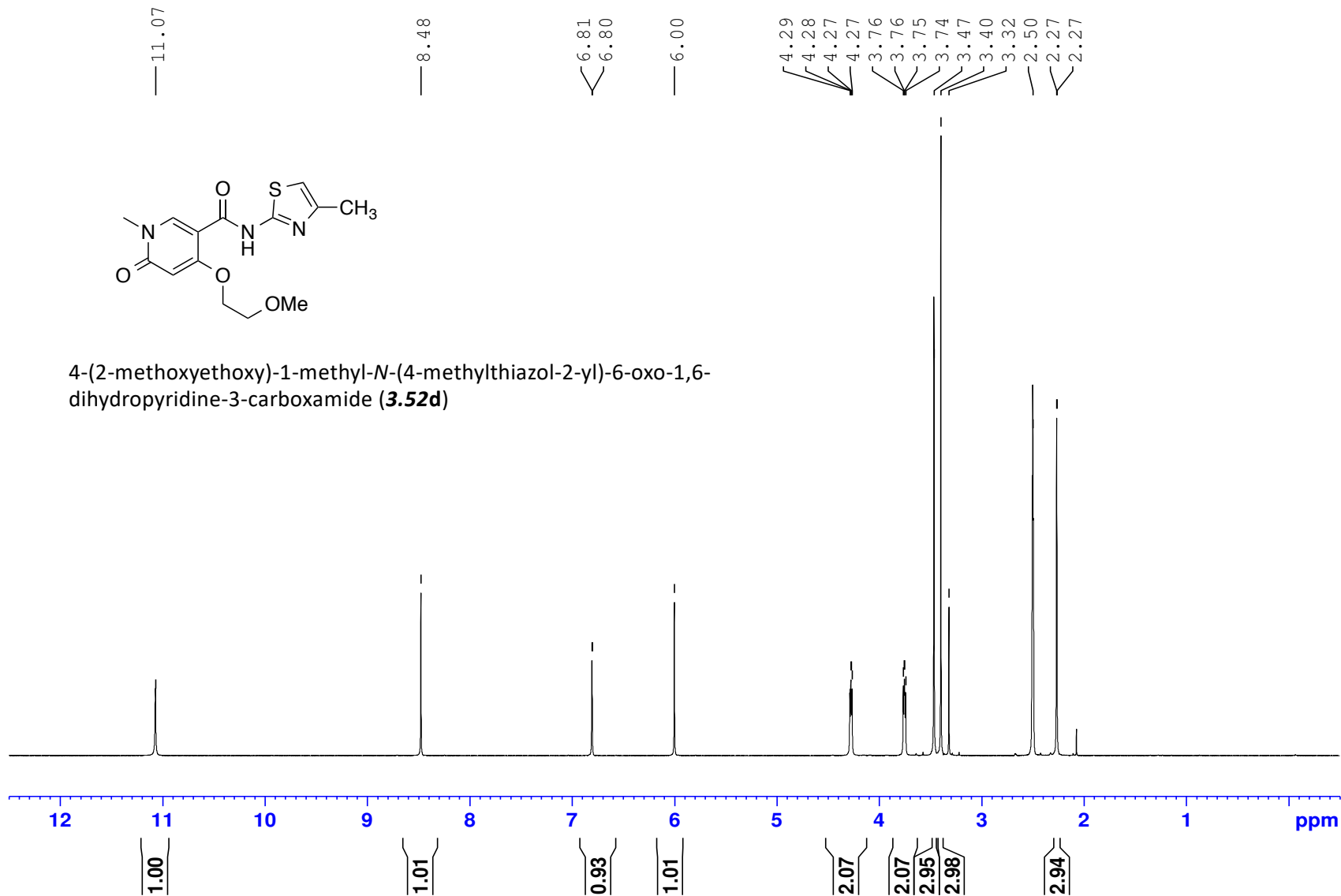


MZP\_A17\_Amide\_Dec2014\_DMSO

(400 MHz, 297.2 K, DMSO-d6)



4-(2-methoxyethoxy)-1-methyl-*N*-(4-methylthiazol-2-yl)-6-oxo-1,6-dihydropyridine-3-carboxamide (**3.52d**)





(100 MHz, 297.2 K, DMSO-d6)

MZP-amide-17-10mg-13CBB-DMSO

163.30  
162.70  
160.34  
156.52

146.99  
145.75

108.38  
104.02

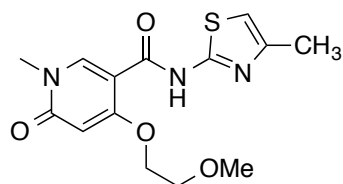
96.43

69.44  
68.50

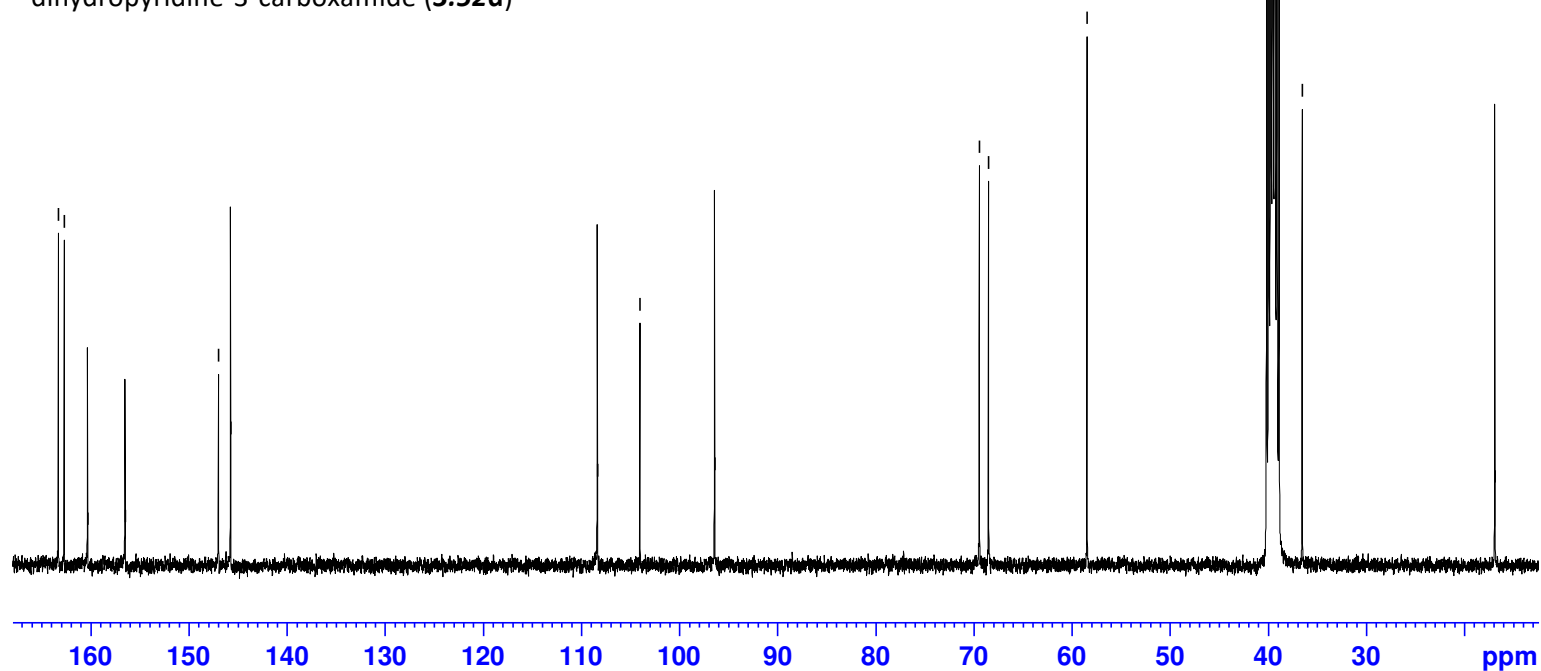
58.46

40.15  
39.94  
39.73  
39.52  
39.31  
39.10  
38.90  
36.53

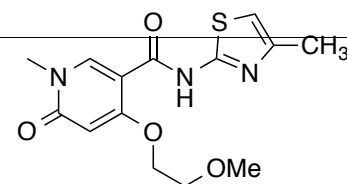
16.91



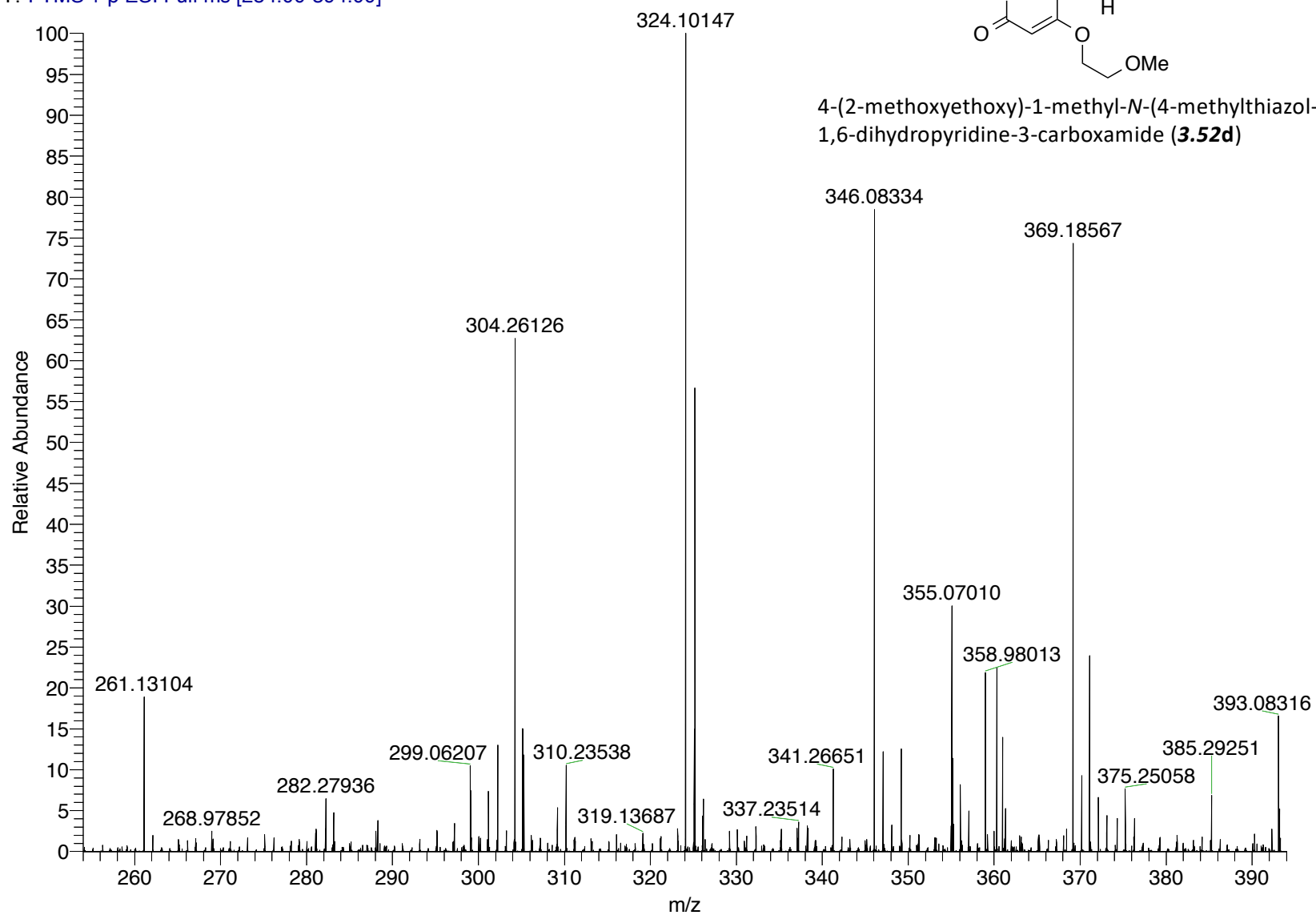
4-(2-methoxyethoxy)-1-methyl-*N*-(4-methylthiazol-2-yl)-6-oxo-1,6-dihydropyridine-3-carboxamide (**3.52d**)

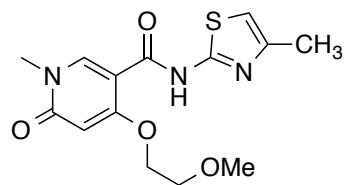


MZP-Amide-A17-Dec14-2014-pos #14 RT: 0.25 AV: 1 NL: 3.46E6  
T: FTMS + p ESI Full ms [254.00-394.00]

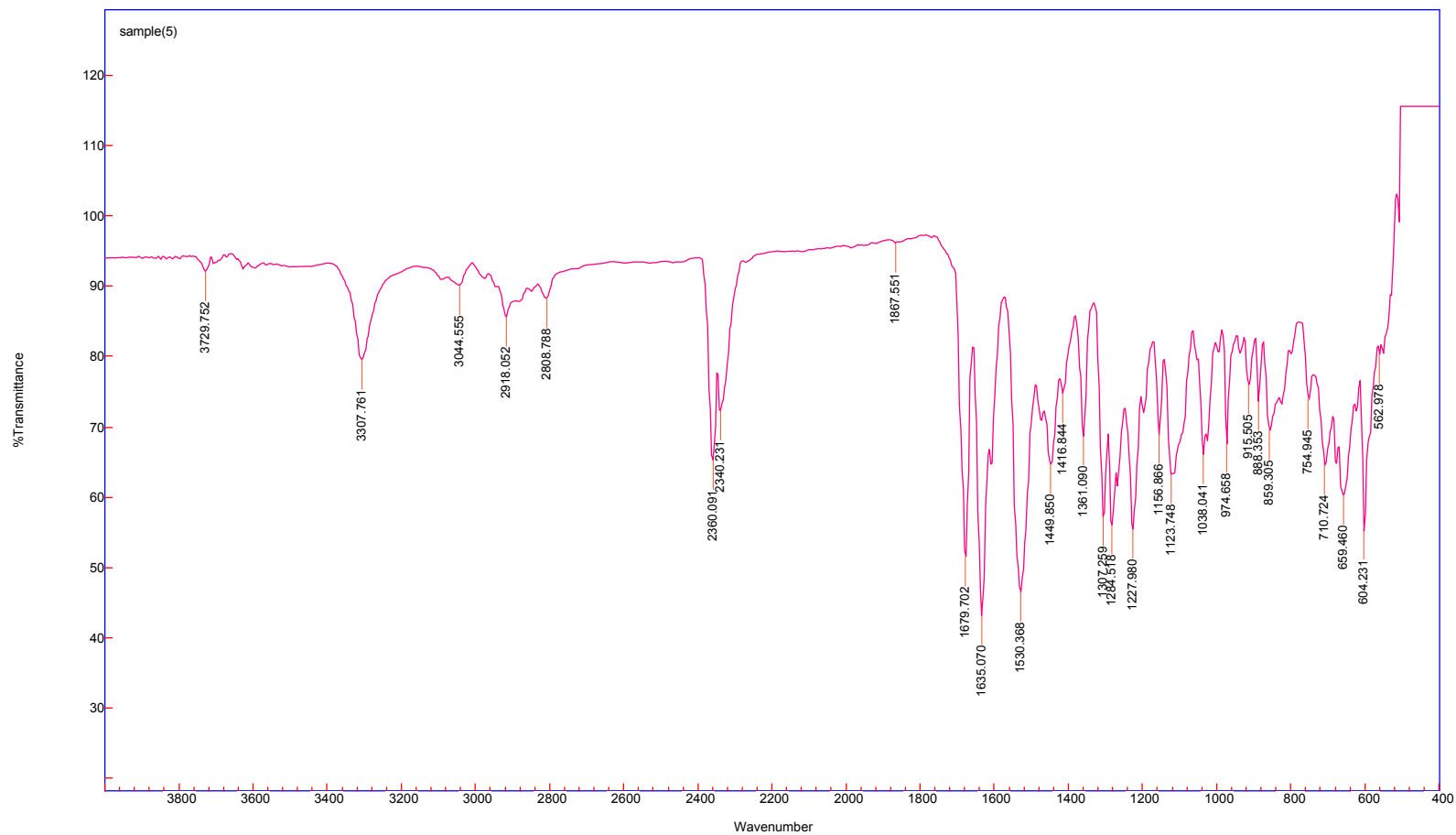


4-(2-methoxyethoxy)-1-methyl-*N*-(4-methylthiazol-2-yl)-6-oxo-1,6-dihydropyridine-3-carboxamide (**3.52d**)



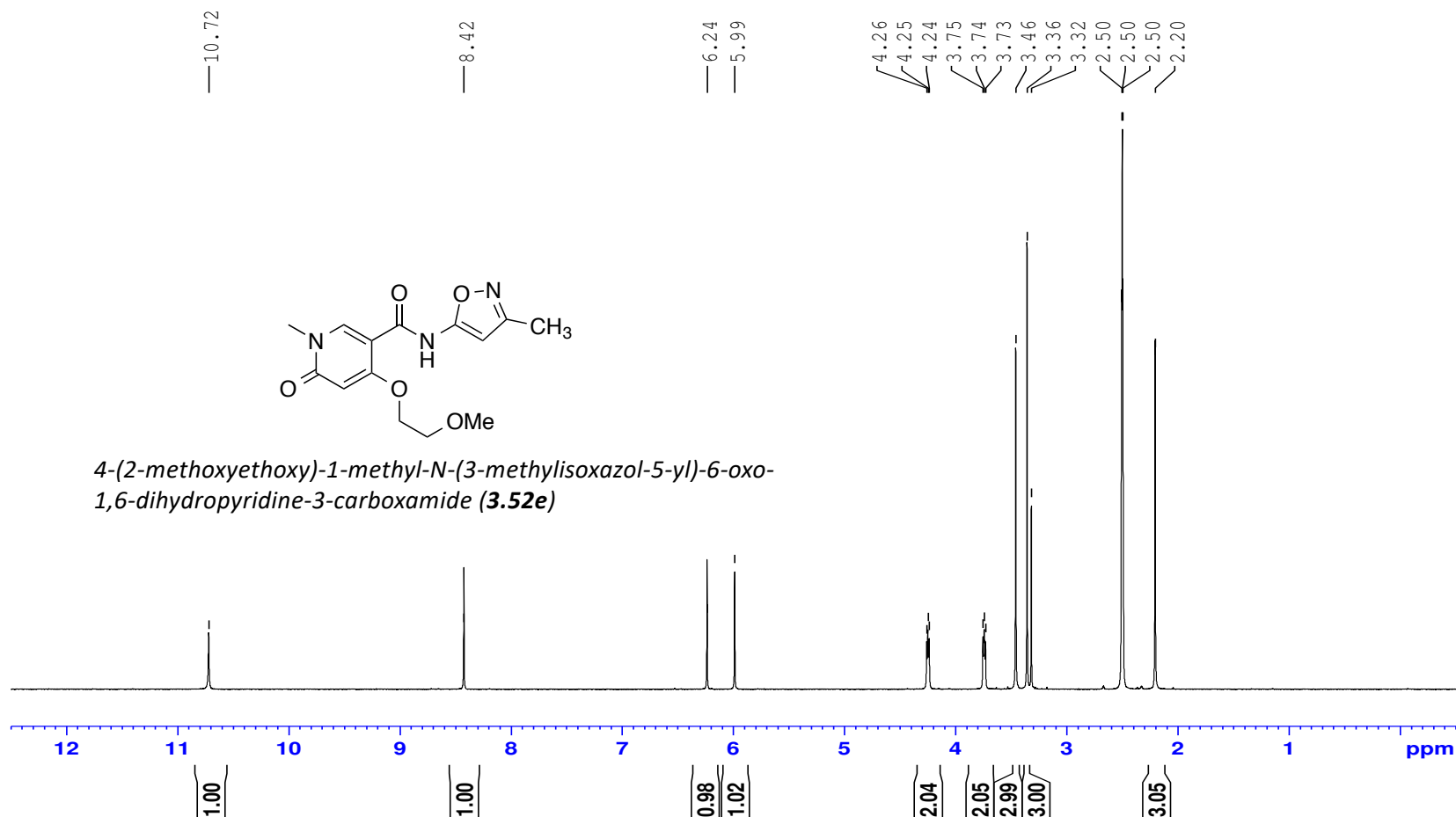


4-(2-methoxyethoxy)-1-methyl-*N*-(4-methylthiazol-2-yl)-6-oxo-1,6-dihydropyridine-3-carboxamide (**3.52d**)



(400 MHz, 297.2 K, DMSO-d6)

MZP31\_Amide\_Dec2014\_DMSO



MZP-Amide-A31-Dec-2014-13CBB-DMSO

(100 MHz, 297.2 K, DMSO-d6)

162.68  
160.83  
160.42  
159.06

145.67

104.62

96.39

89.25

69.37

68.29

58.28

40.15

39.94

39.73

39.52

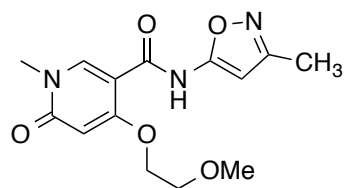
39.31

39.10

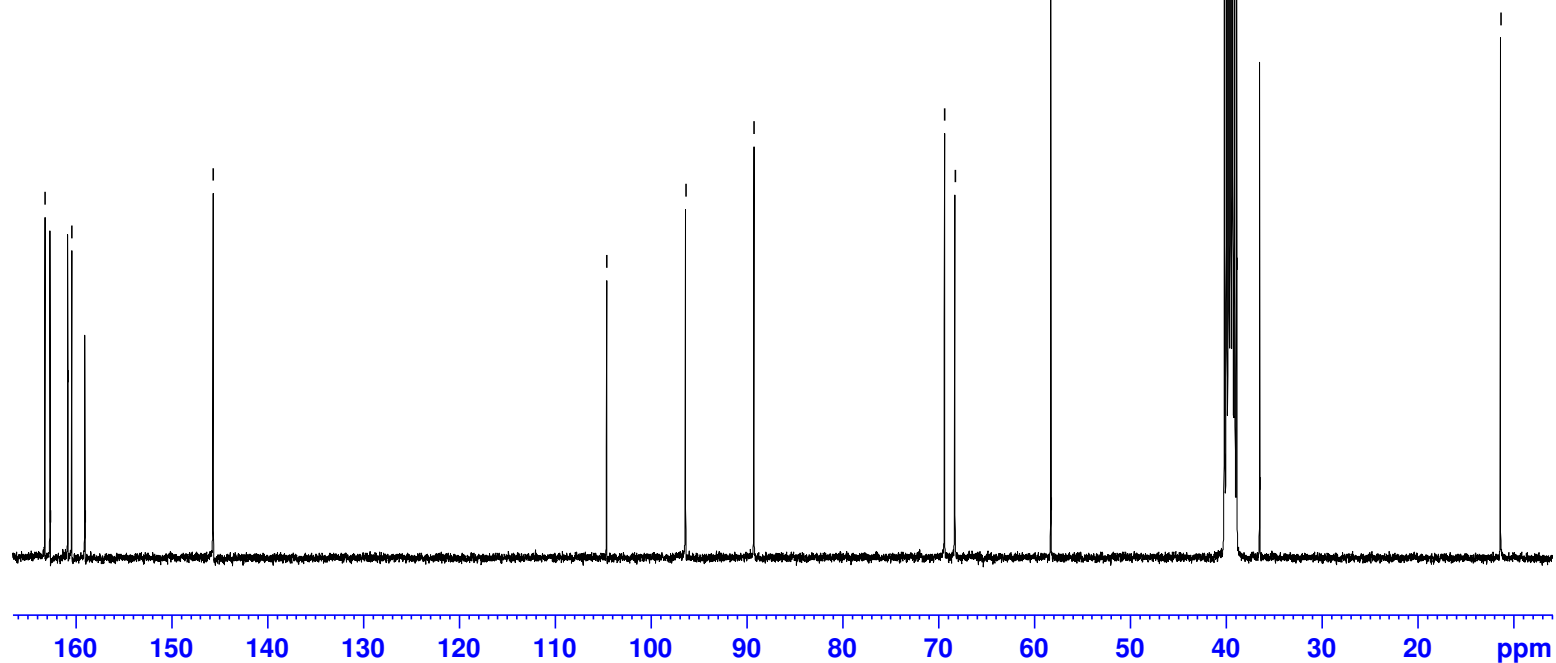
38.90

36.49

11.37

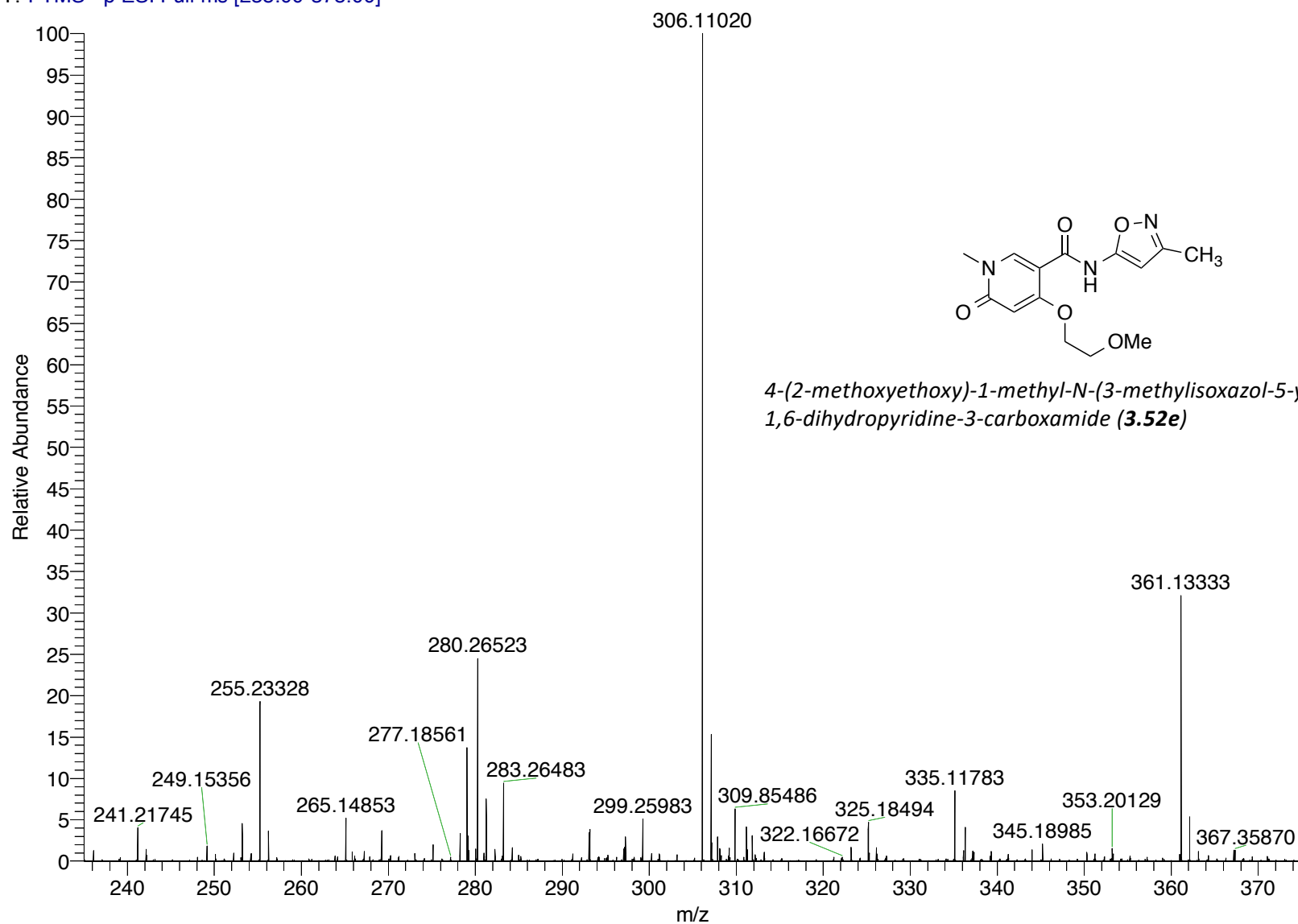


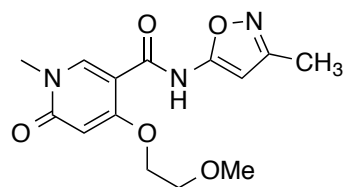
4-(2-methoxyethoxy)-1-methyl-N-(3-methylisoxazol-5-yl)-6-oxo-1,6-dihydropyridine-3-carboxamide (**3.52e**)



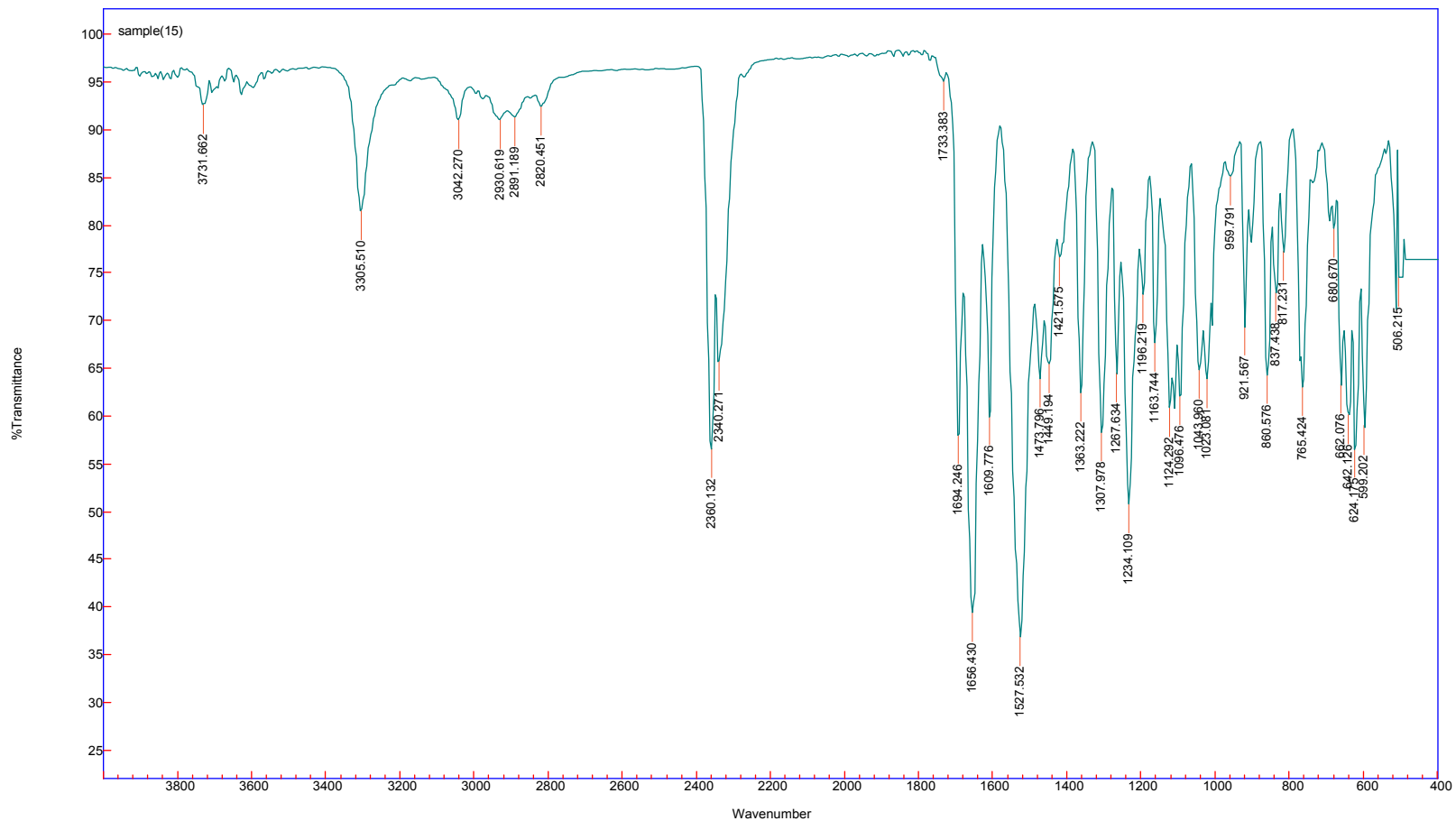
MZIP-Amide-A31-Dec14-2014-neg #11 RT: 0.20 AV: 1 NL: 9.33E6

T: FTMS - p ESI Full ms [235.00-375.00]



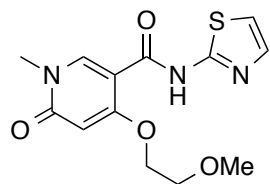


4-(2-methoxyethoxy)-1-methyl-N-(3-methylisoxazol-5-yl)-6-oxo-1,6-dihydropyridine-3-carboxamide (**3.52e**)

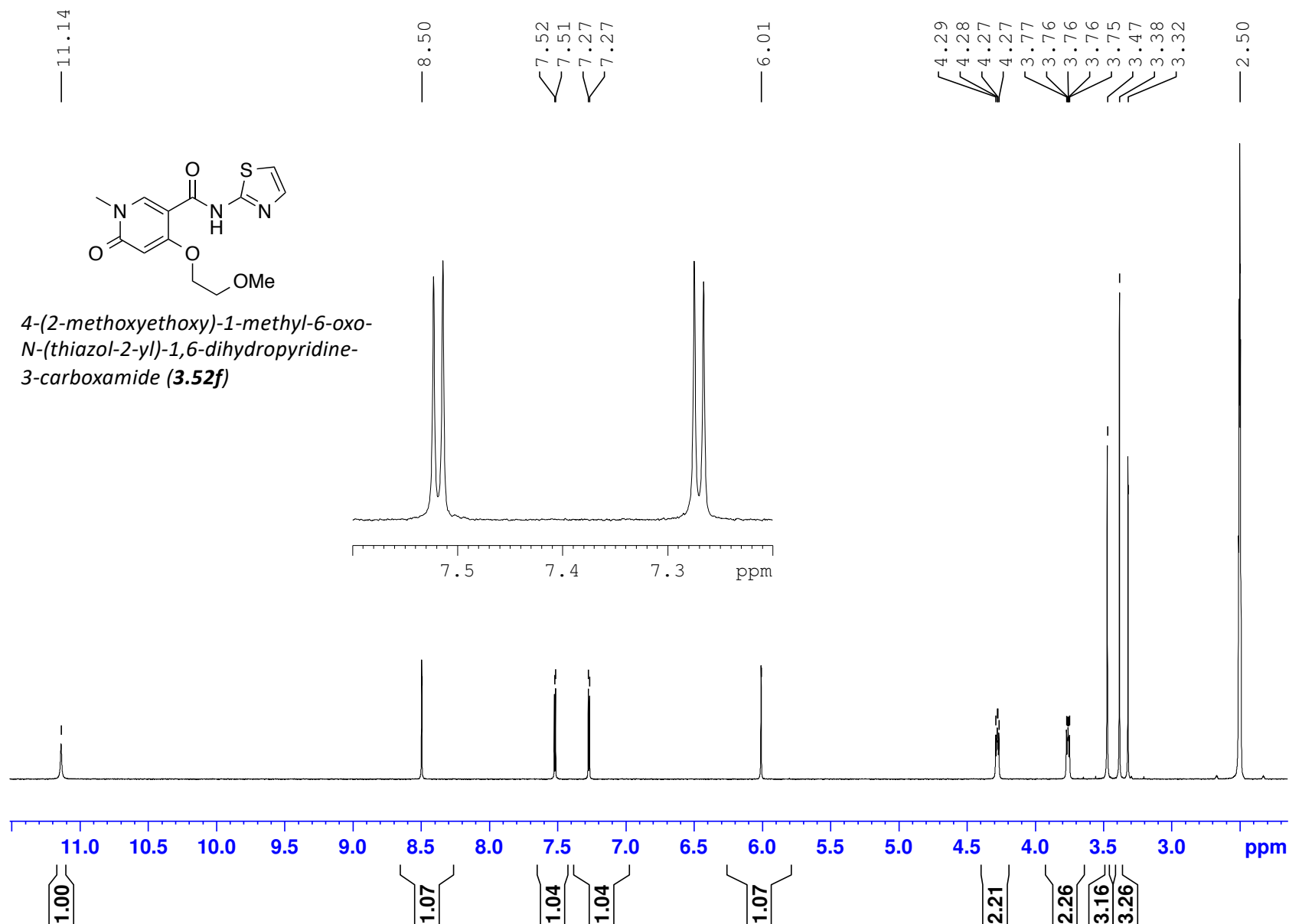


MZP\_3129\_Amide\_Feb2015\_DMSO

(400 MHz, 297.2 K, DMSO-d6)



4-(2-methoxyethoxy)-1-methyl-6-oxo-  
N-(thiazol-2-yl)-1,6-dihydropyridine-  
3-carboxamide (**3.52f**)





(100 MHz, 297.2 K, DMSO-d6)

MZP\_3129\_Amide\_Feb\_2015\_DMSO

163.32  
162.70  
160.44  
157.29

145.79

137.96

114.15

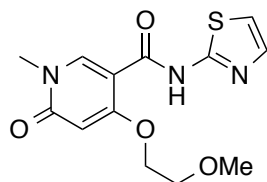
103.95

96.42

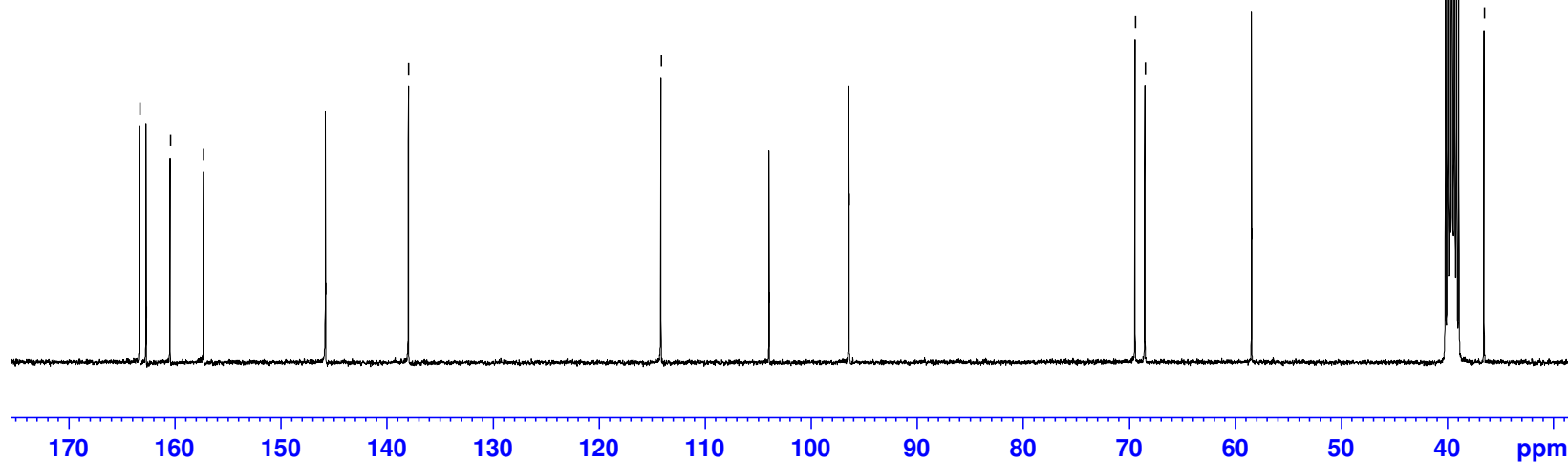
69.44  
68.52

58.45

39.52  
36.52

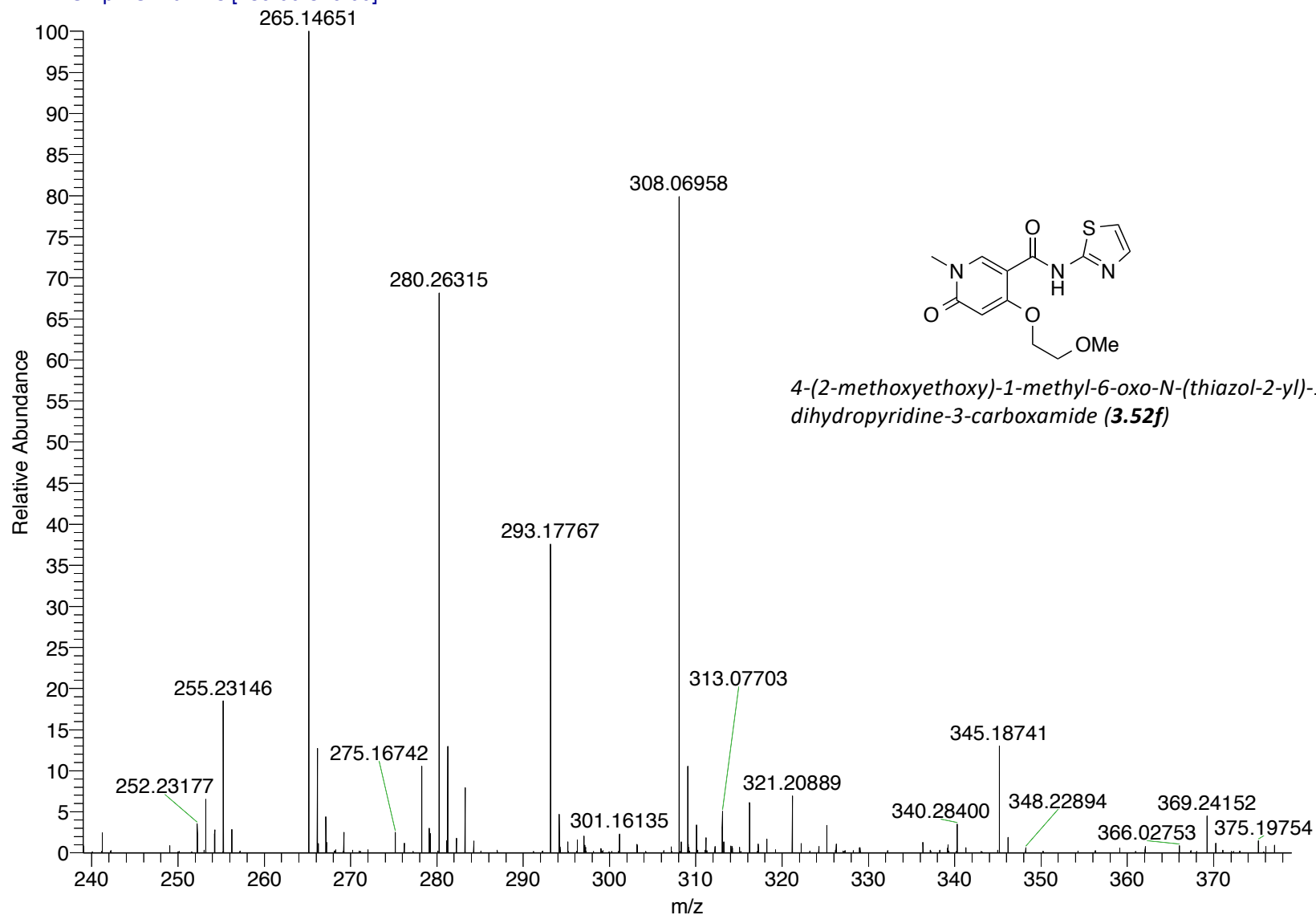


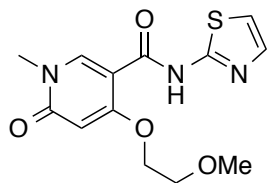
4-(2-methoxyethoxy)-1-methyl-6-oxo-N-(thiazol-2-yl)-1,6-dihydropyridine-3-carboxamide (**3.52f**)



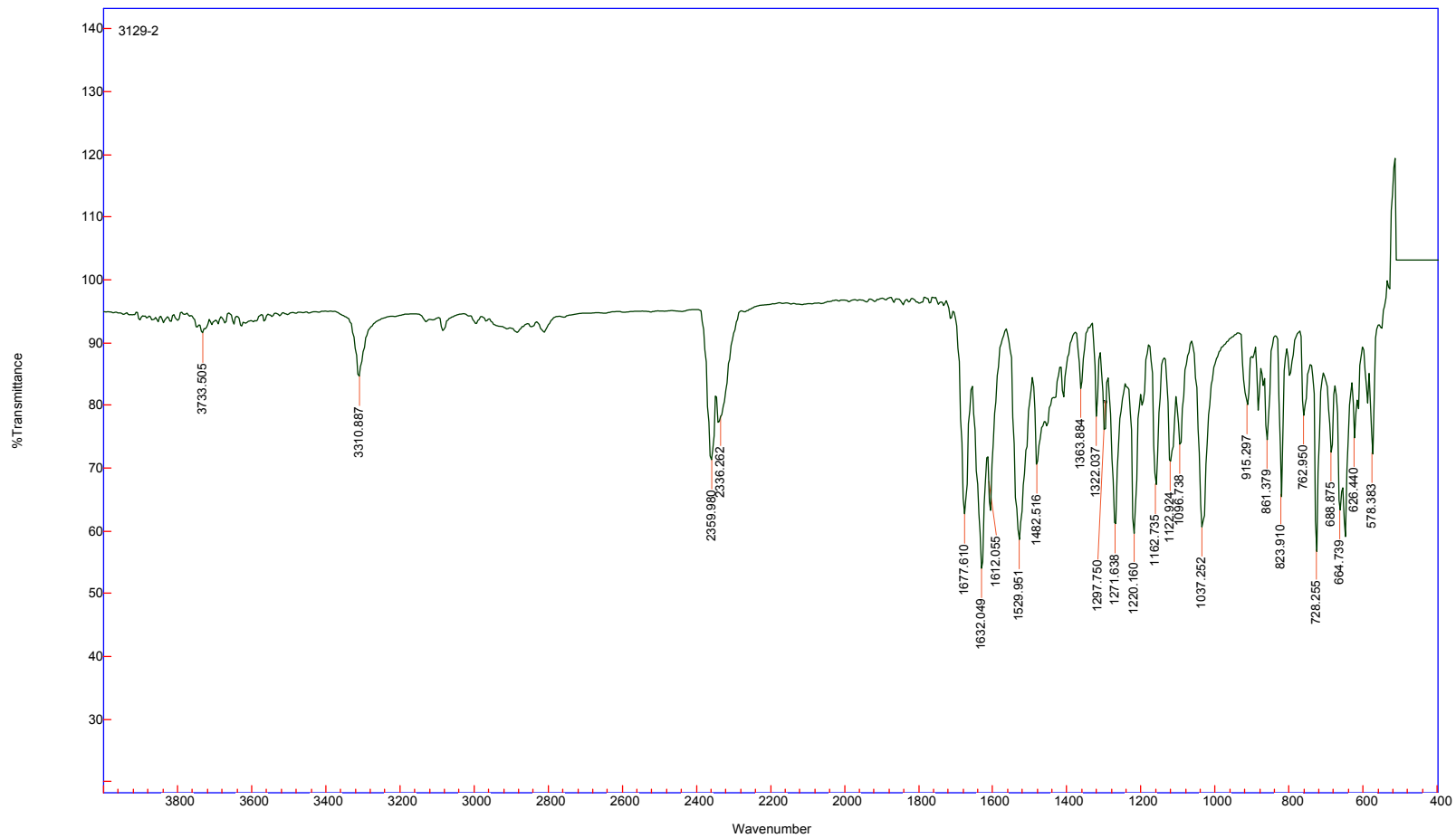
MMP-Amide-3129-HRMS-neg #11 RT: 0.20 AV: 1 NL: 1.54E7

T: FTMS - p ESI Full ms [239.00-379.00]



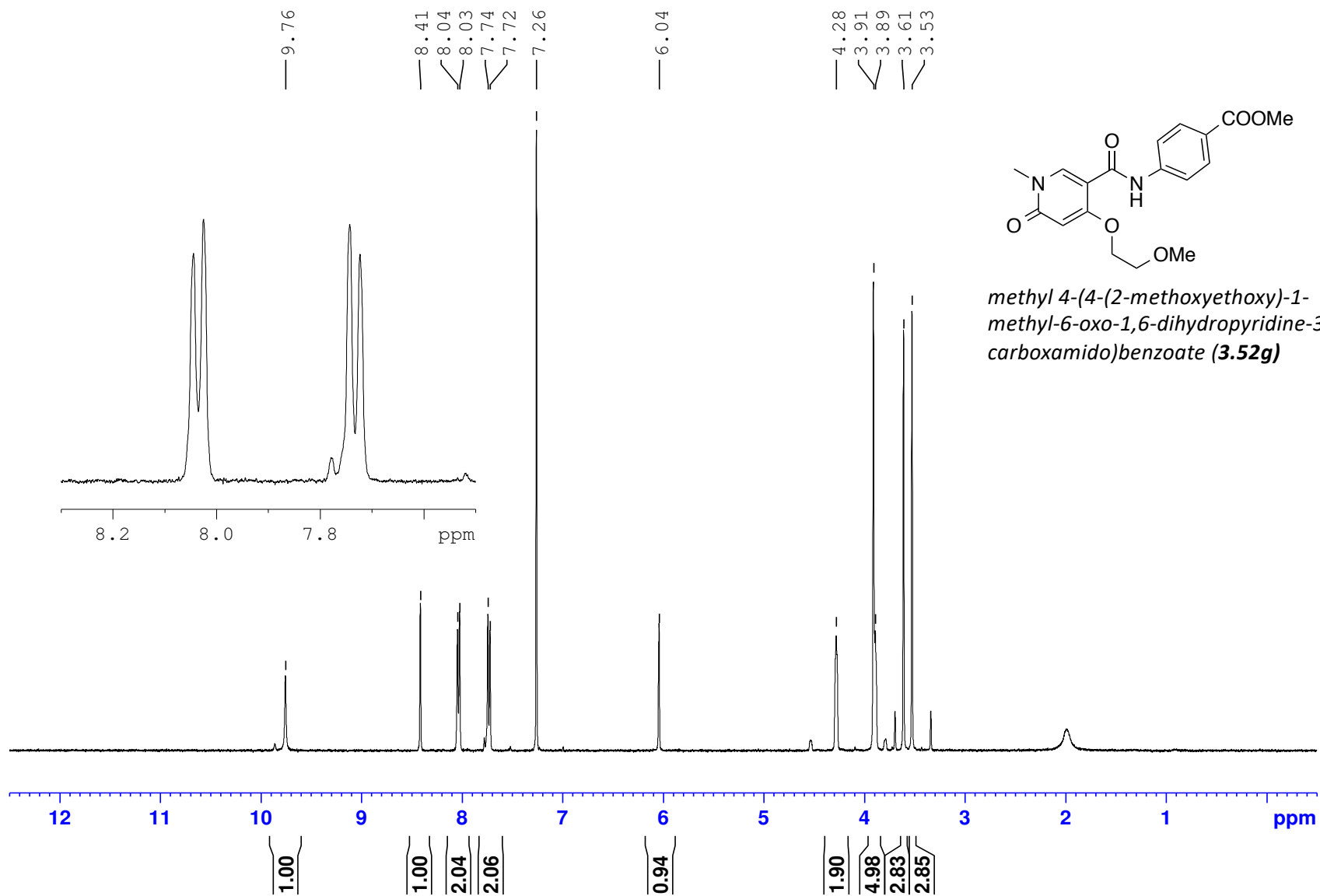


4-(2-methoxyethoxy)-1-methyl-6-oxo-N-(thiazol-2-yl)-1,6-dihydropyridine-3-carboxamide (**3.52f**)



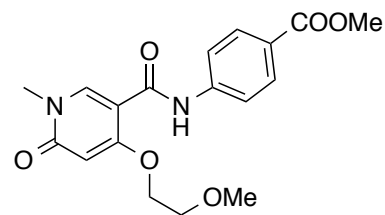
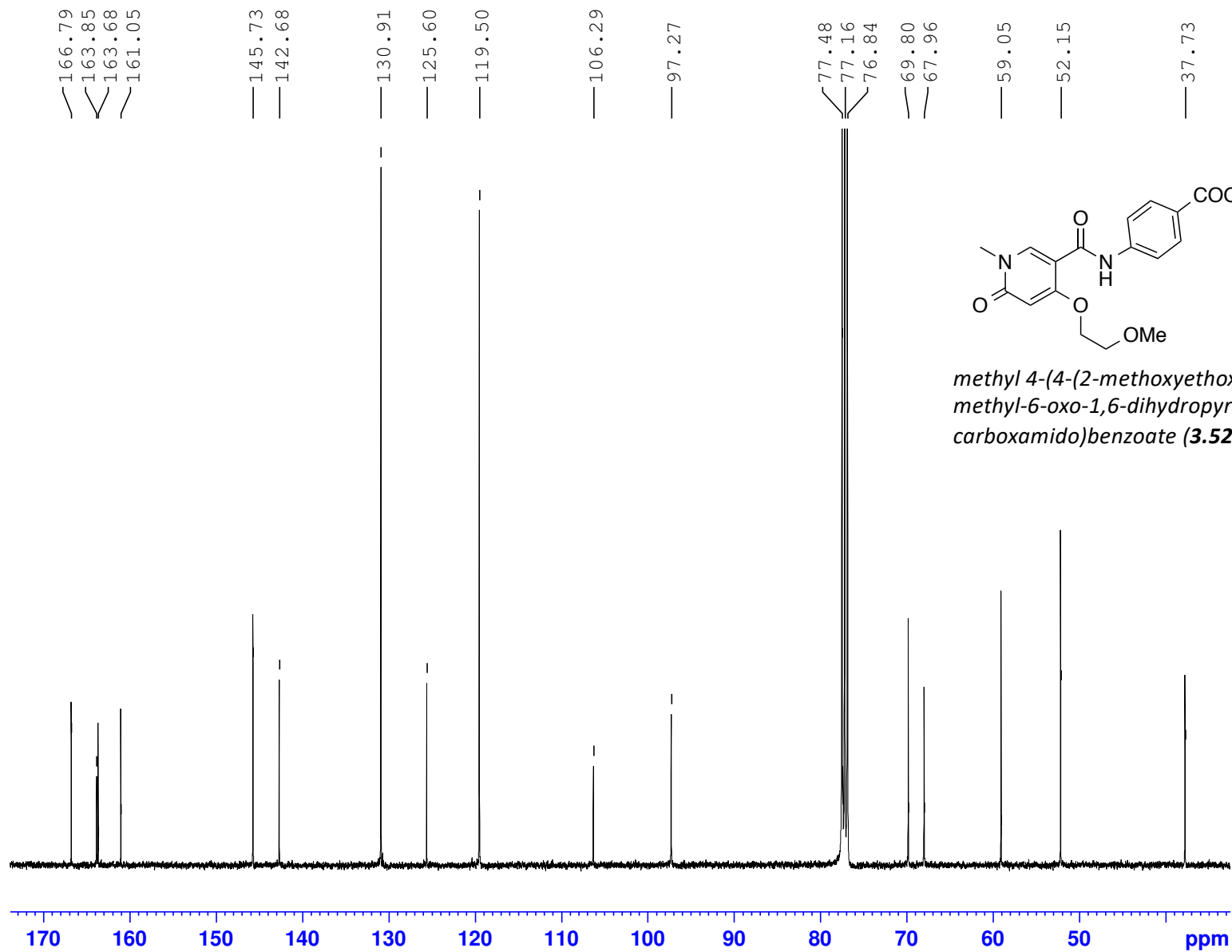
MZP\_A109B\_Amide\_Dec2014\_CDCL3

(400 MHz, 297.2 K, CDCl<sub>3</sub>)



MZP-Amide-A109-13CBB-CDCl<sub>3</sub>

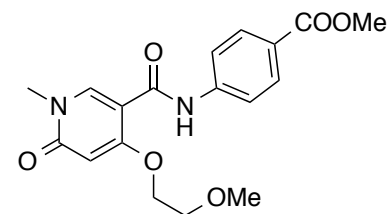
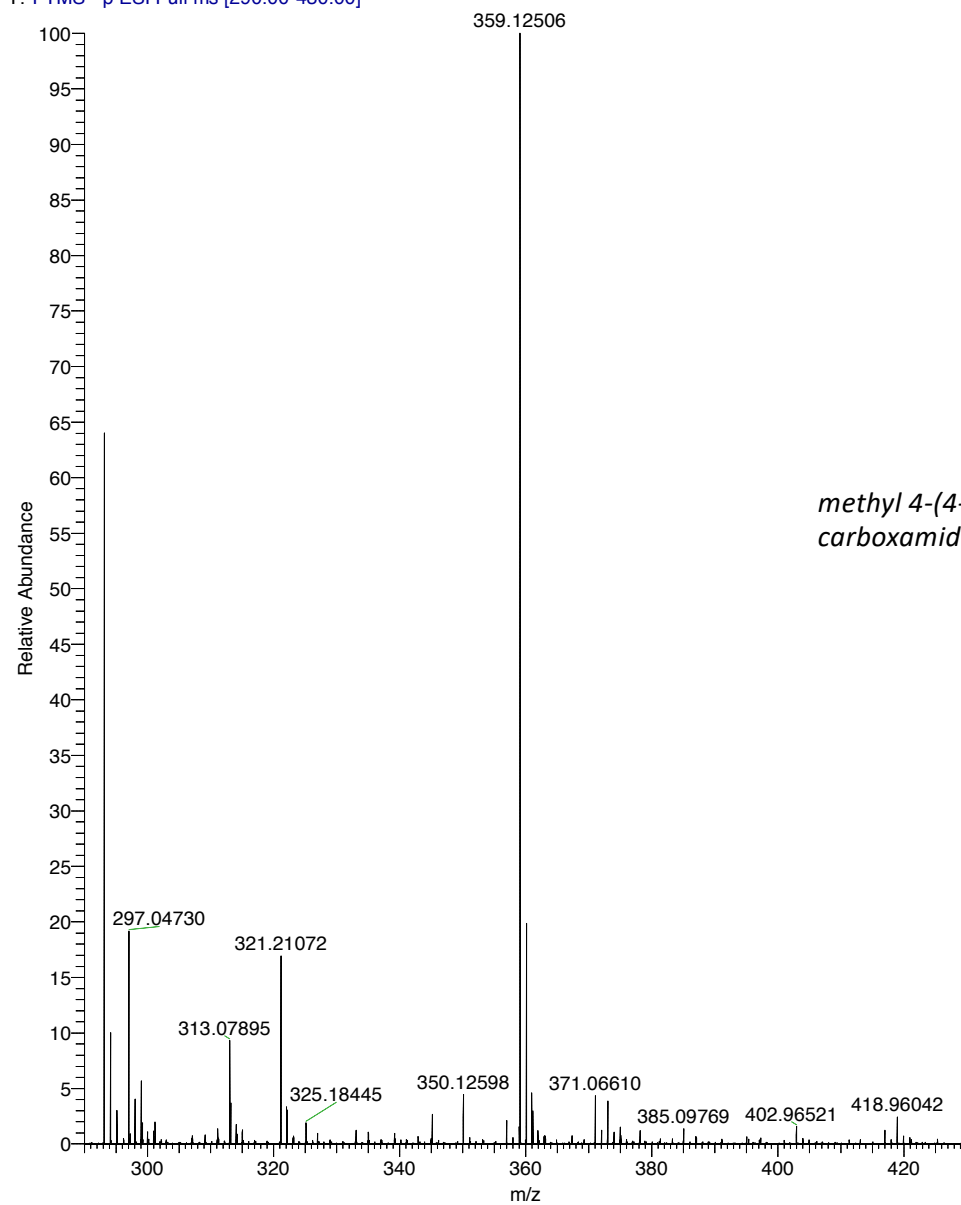
(100 MHz, 297.2 K, CDCl<sub>3</sub>)



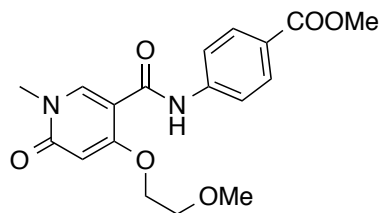
*methyl 4-(4-(2-methoxyethoxy)-1-methyl-6-oxo-1,6-dihydropyridine-3-carboxamido)benzoate (3.52g)*

MZP\_Amide\_109A+B\_Neg\_HRMS #1 RT: 0.02 AV: 1 NL: 1.24E7

T: FTMS - p ESI Full ms [290.00-430.00]



*methyl 4-(4-(2-methoxyethoxy)-1-methyl-6-oxo-1,6-dihydropyridine-3-carboxamido)benzoate (3.52g)*

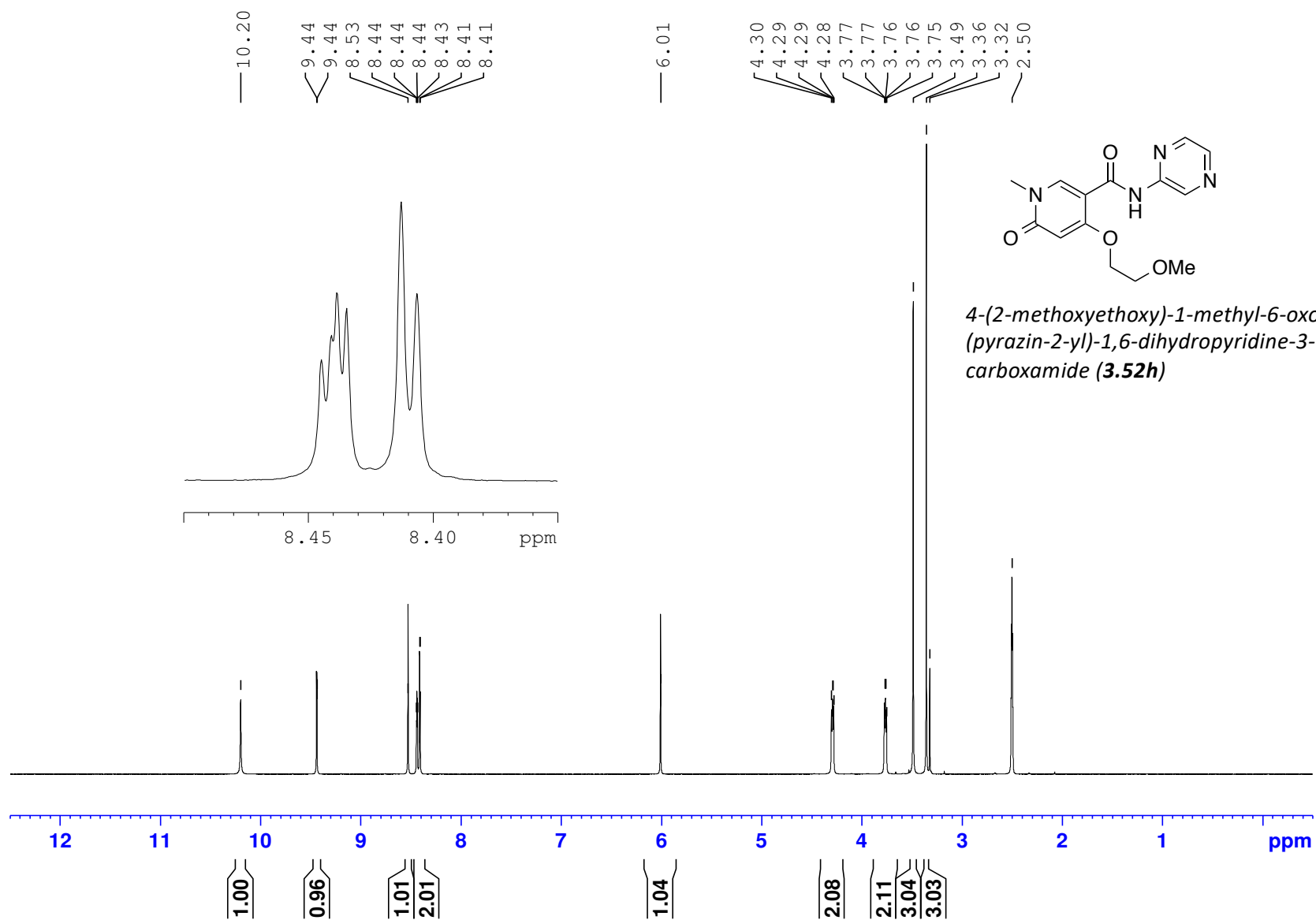


*methyl 4-(4-(2-methoxyethoxy)-1-methyl-6-oxo-1,6-dihydropyridine-3-carboxamido)benzoate (3.52g)*



MZP\_6958\_Amide\_Dec2014\_DMSO

(400 MHz, 297.2 K, DMSO-d6)





MZP-6958-Amide-Dec2014-13CBB-DMSO

(100 MHz, 297.2 K, DMSO-d6)

163.27  
162.73  
161.13

148.26  
146.15  
142.94  
140.19  
136.33

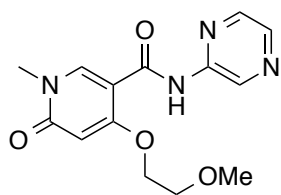
104.45

96.36

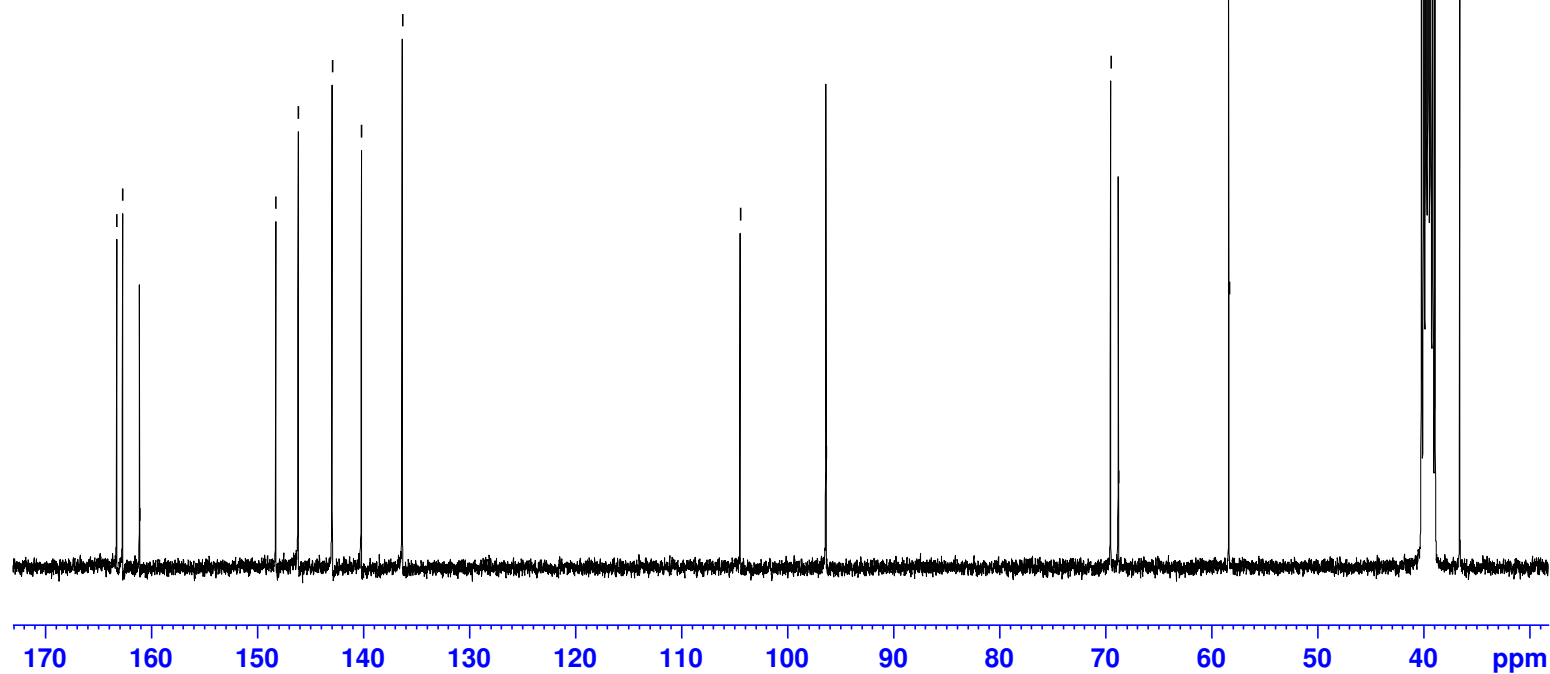
69.50  
68.78

58.35

40.15  
39.94  
39.73  
39.52  
39.31  
39.10  
38.90  
36.56

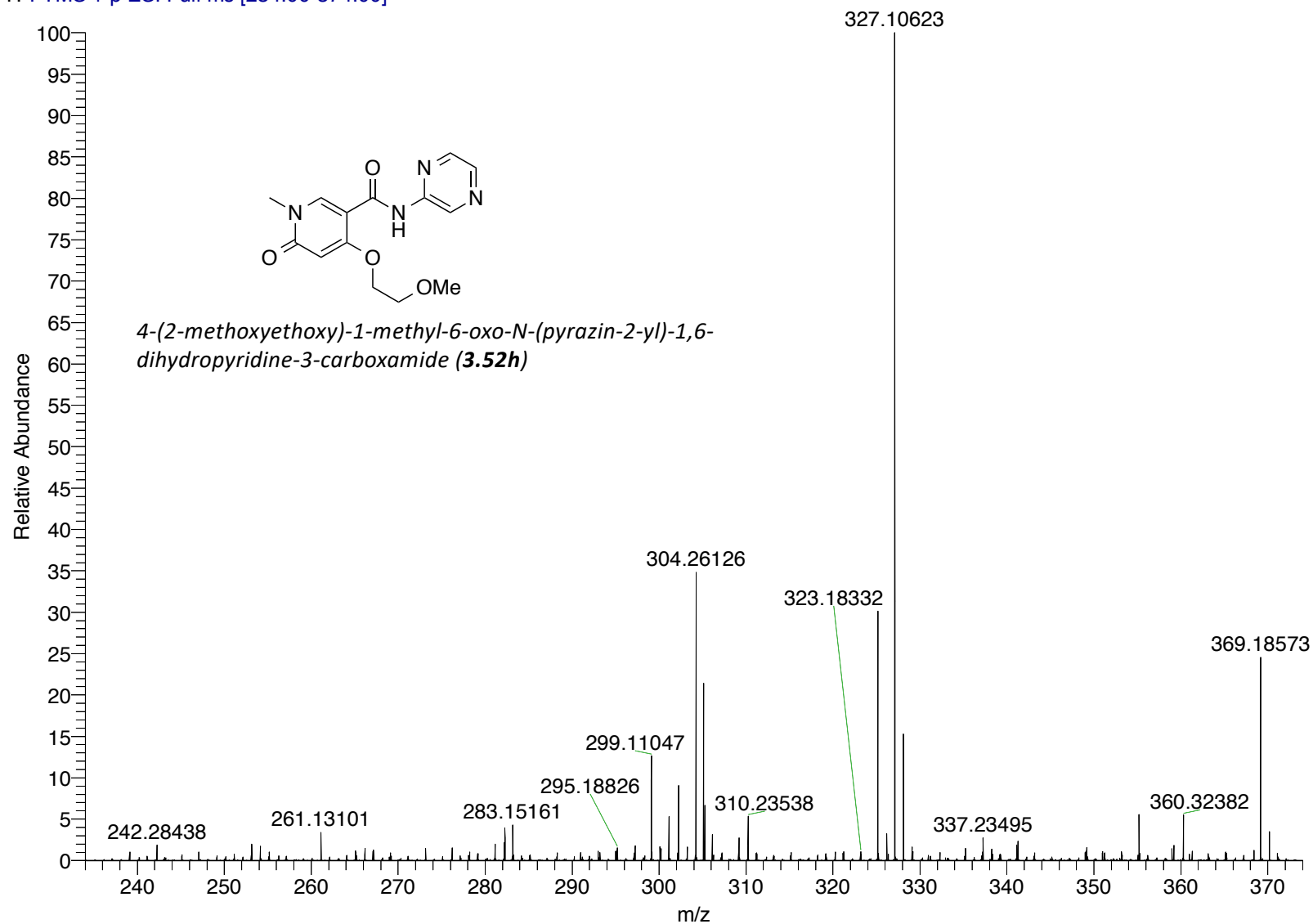


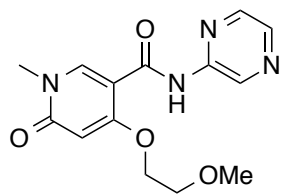
4-(2-methoxyethoxy)-1-methyl-6-oxo-N-(pyrazin-2-yl)-1,6-dihydropyridine-3-carboxamide (**3.52h**)



MZP-Amide-6958-Dec14-2014-pos #21 RT: 0.37 AV: 1 NL: 5.47E6

T: FTMS + p ESI Full ms [234.00-374.00]



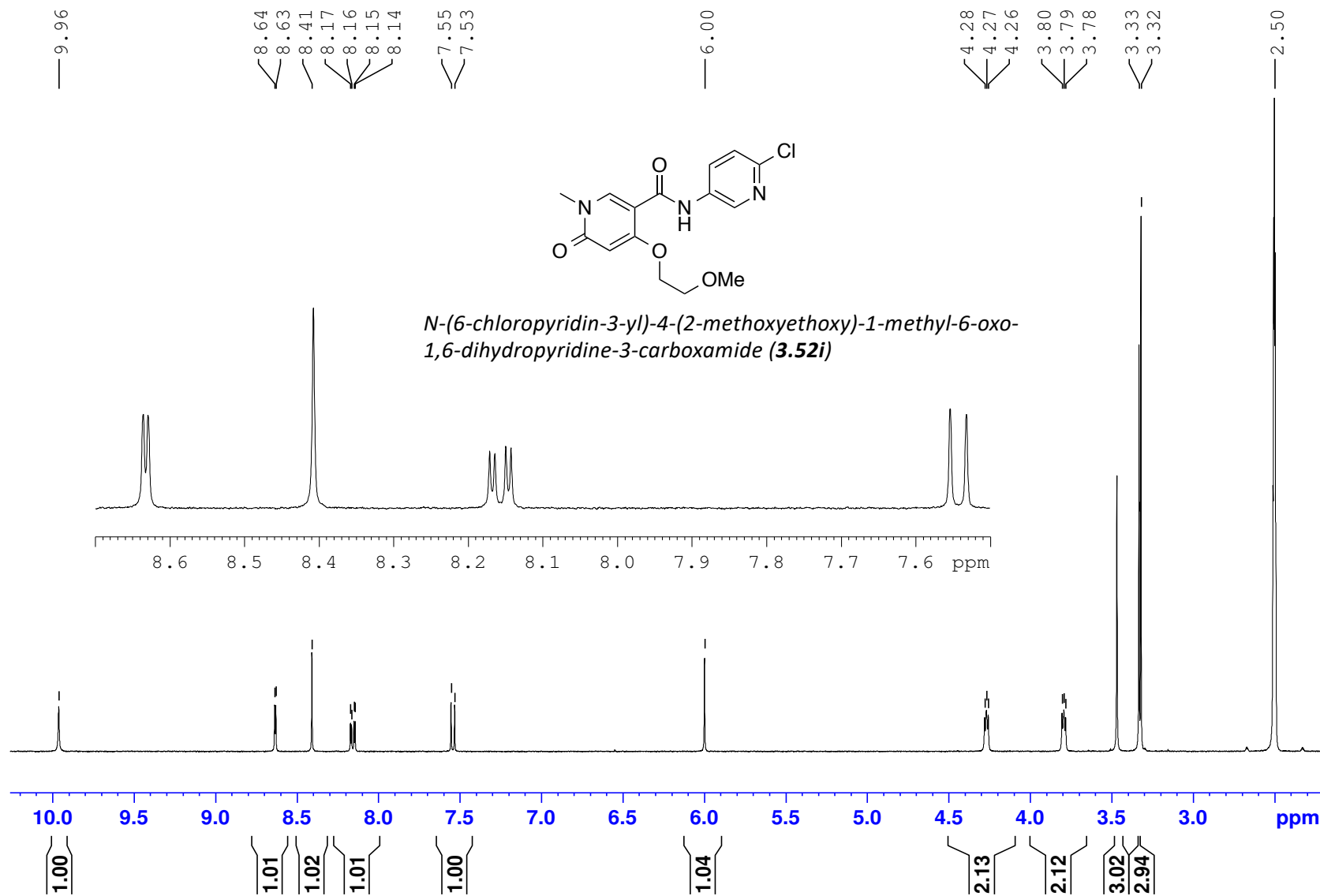


*4-(2-methoxyethoxy)-1-methyl-6-oxo-N-(pyrazin-2-yl)-1,6-dihydropyridine-3-carboxamide (3.52h)*



MZP\_A100B\_Amide\_Feb2015\_DMSO

(400 MHz, 297.2 K, DMSO-d6)



MZP-Amide-A100B-Feb2015-10mg-13CBB-DMSO

(100 MHz, 297.2 K, DMSO-d6)

163.25  
162.70  
161.38

145.17  
143.94  
140.76

134.91  
130.16  
124.34

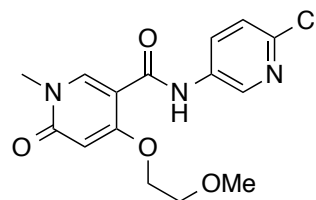
105.60

96.29

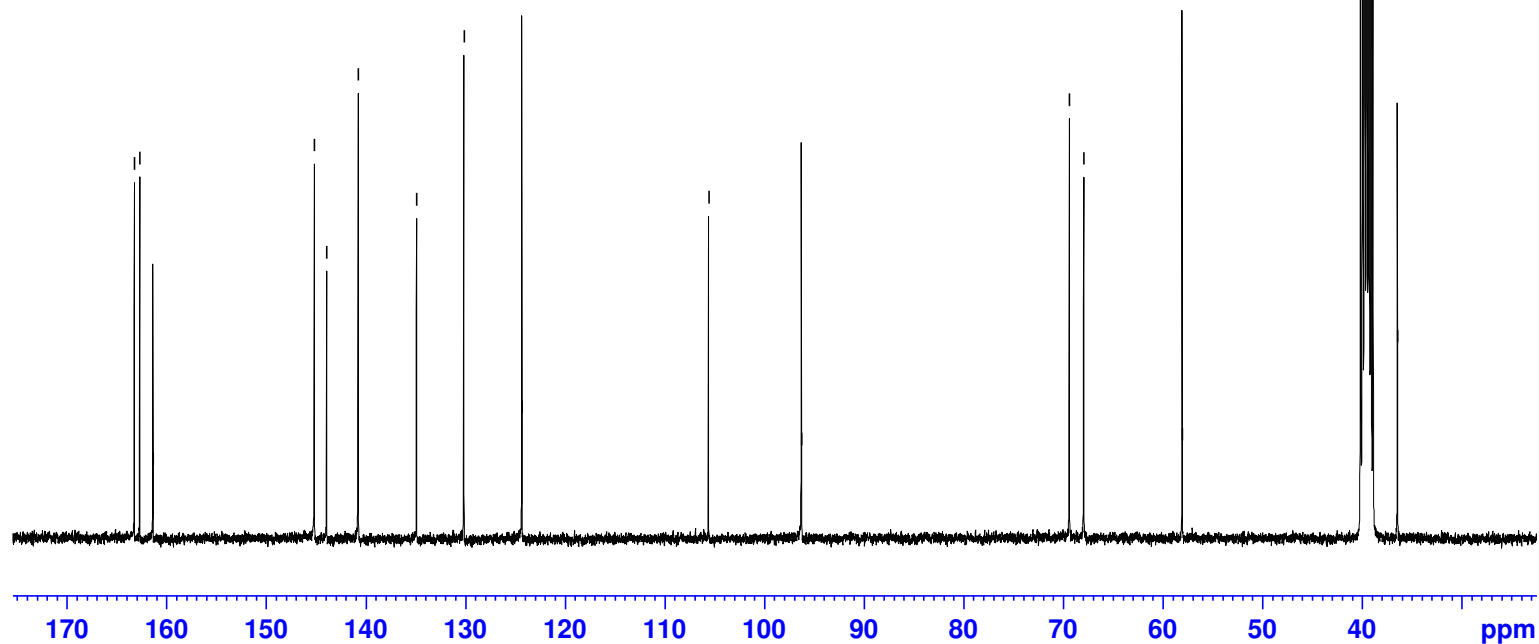
69.38  
67.94

58.06

40.15  
39.94  
39.73  
39.52  
39.31  
39.10  
38.89  
36.45

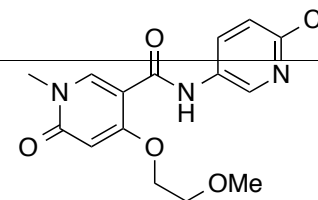


*N*-(6-chloropyridin-3-yl)-4-(2-methoxyethoxy)-1-methyl-6-oxo-1,6-dihydropyridine-3-carboxamide (**3.52i**)

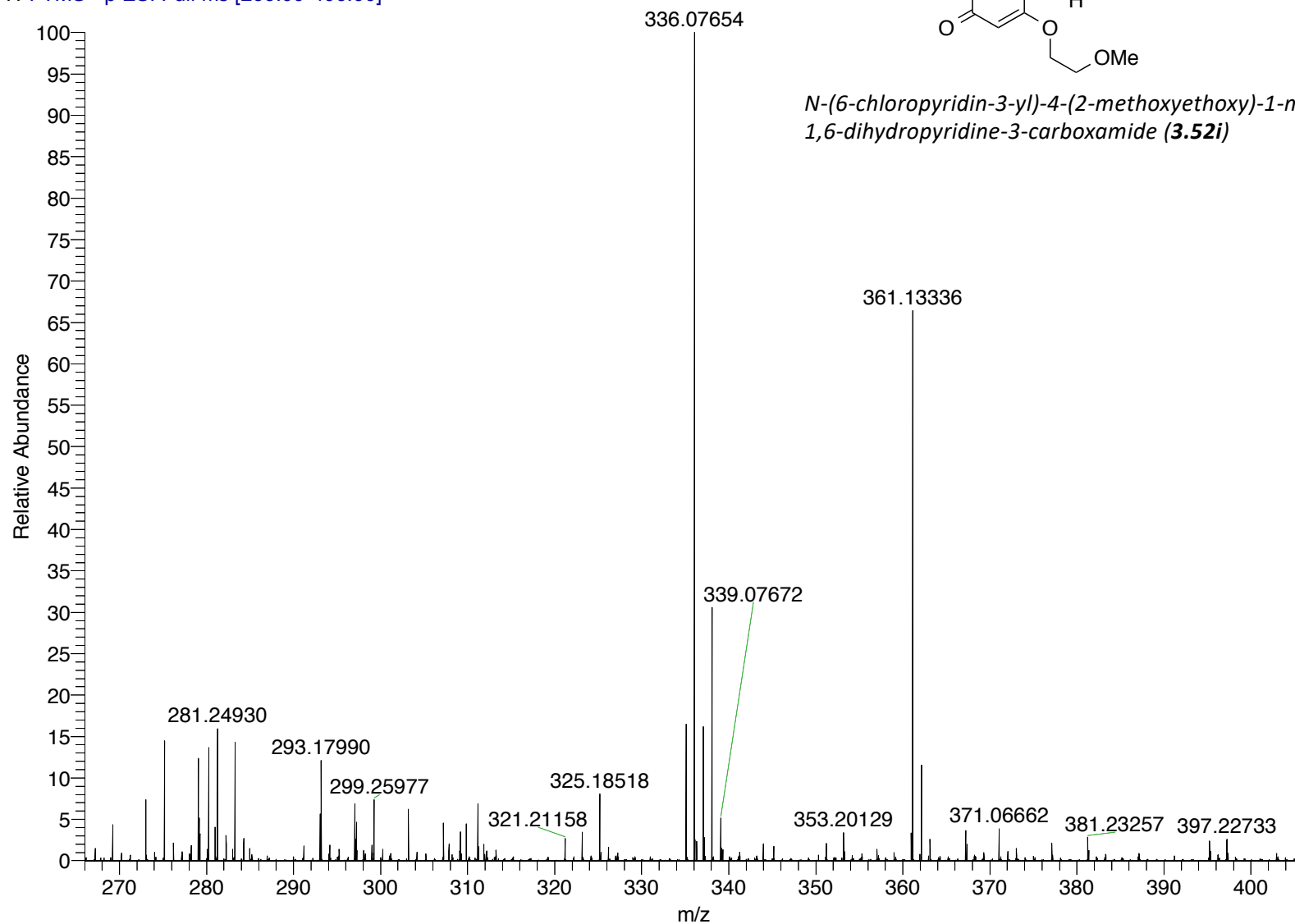


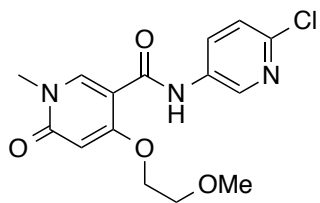
MZP-Amide-A100B-Feb15-2015-neg #22 RT: 0.39 AV: 1 NL: 3.37E6

T: FTMS - p ESI Full ms [266.00-406.00]

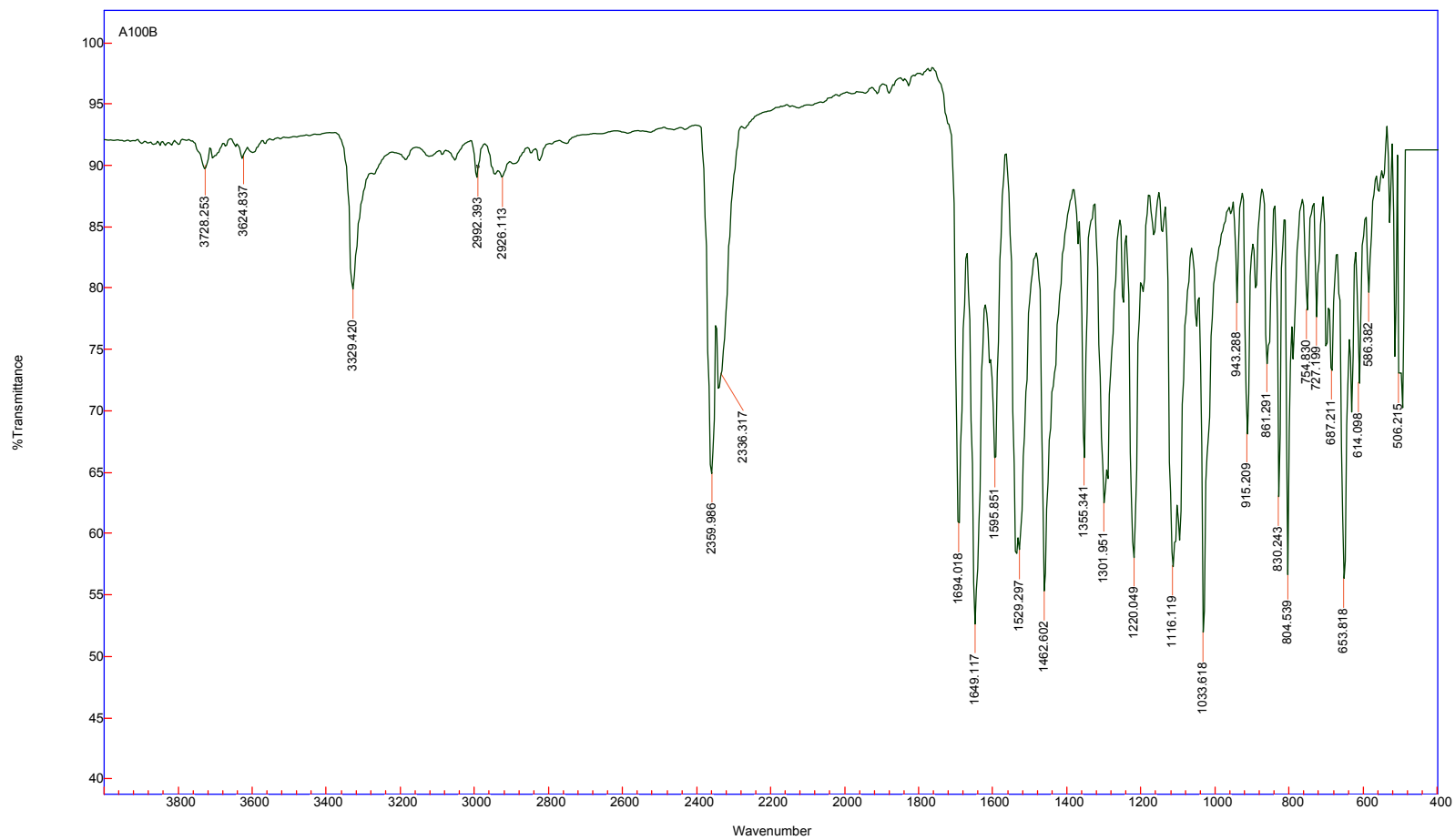


*N*-(6-chloropyridin-3-yl)-4-(2-methoxyethoxy)-1-methyl-6-oxo-1,6-dihydropyridine-3-carboxamide (**3.52i**)



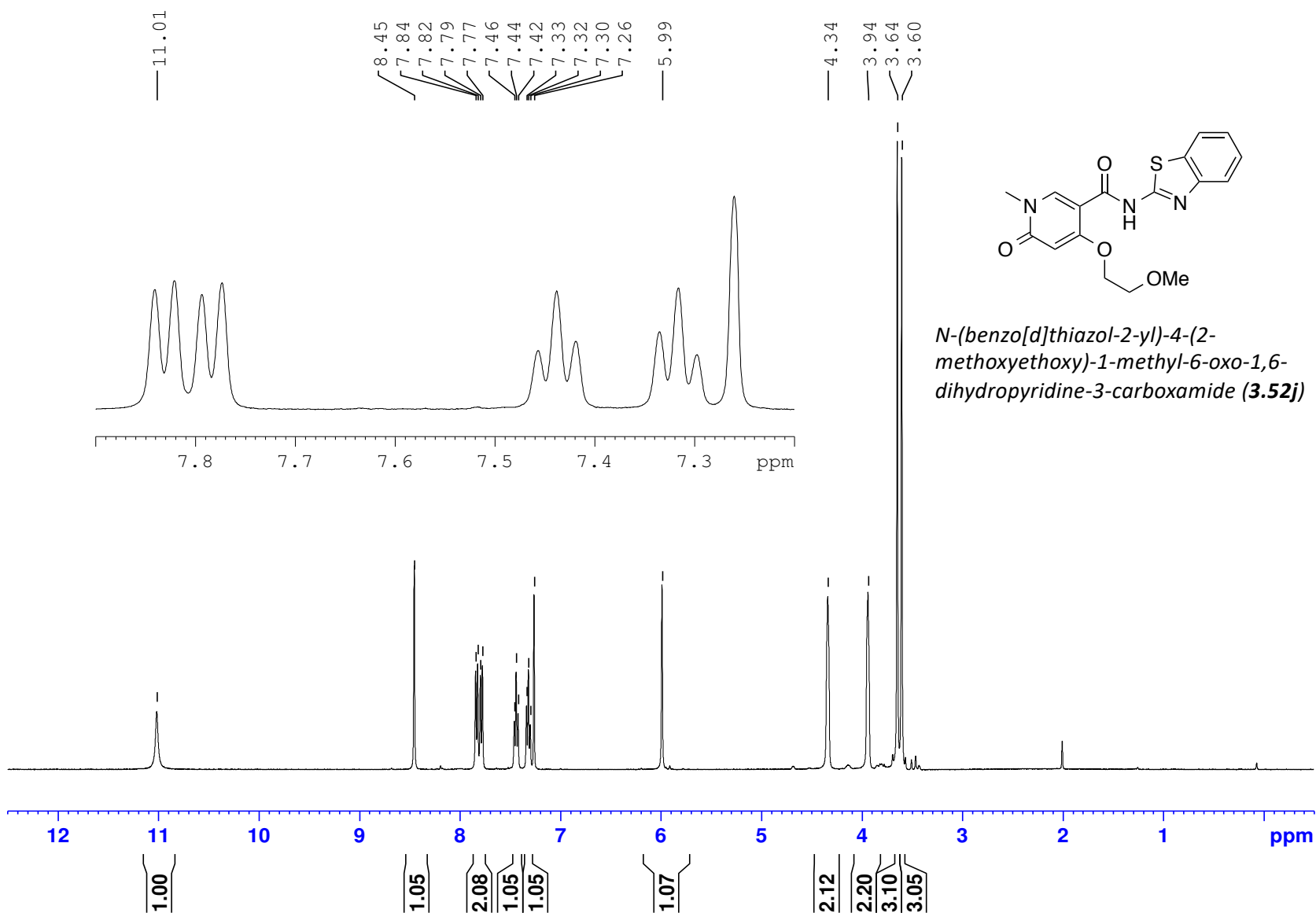


*N*-(6-chloropyridin-3-yl)-4-(2-methoxyethoxy)-1-methyl-6-oxo-1,6-dihydropyridine-3-carboxamide (**3.52i**)



MZP\_8812\_Amide\_Dec2014\_CDC13

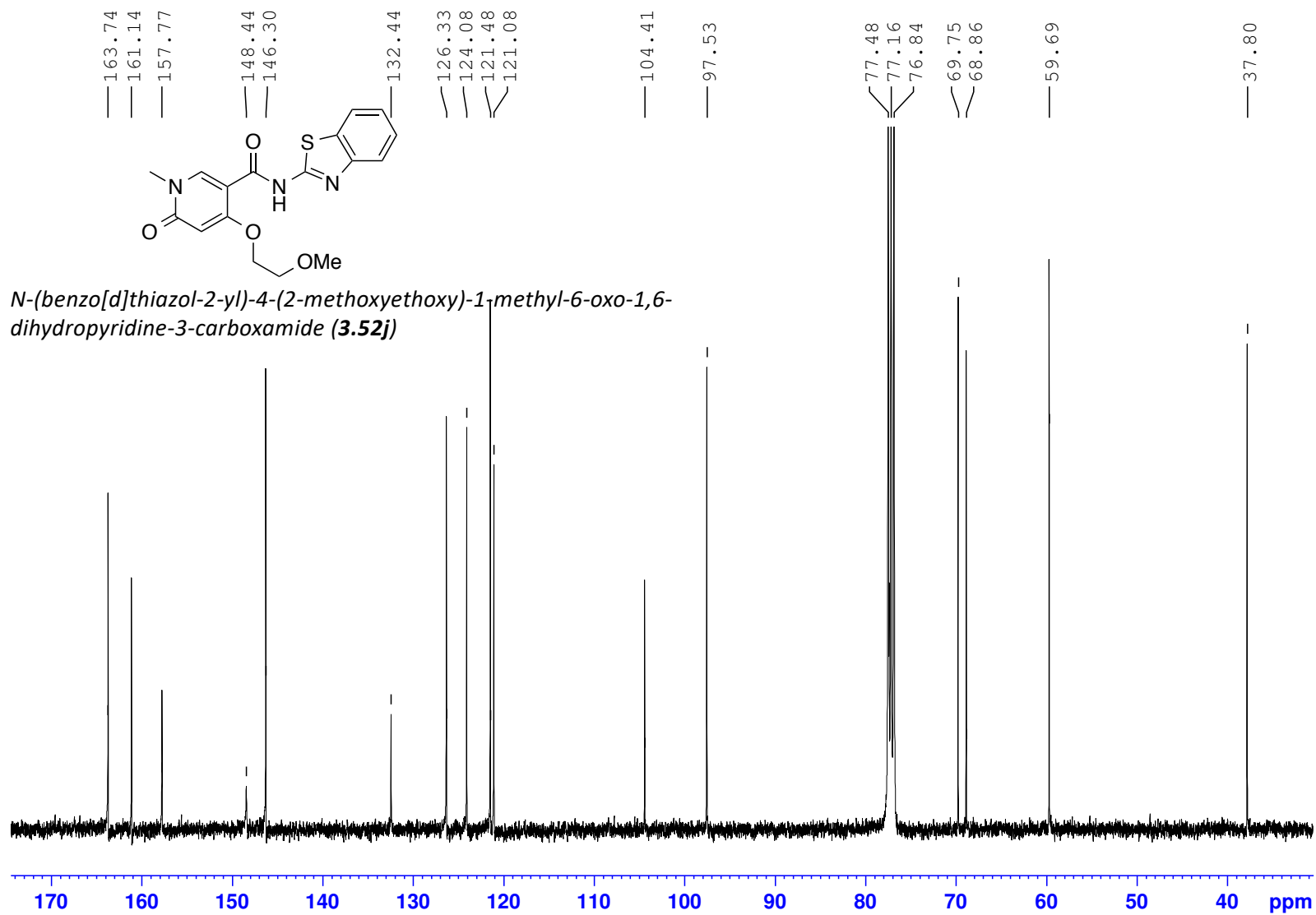
(400 MHz, 297.2 K, CDCl<sub>3</sub>)



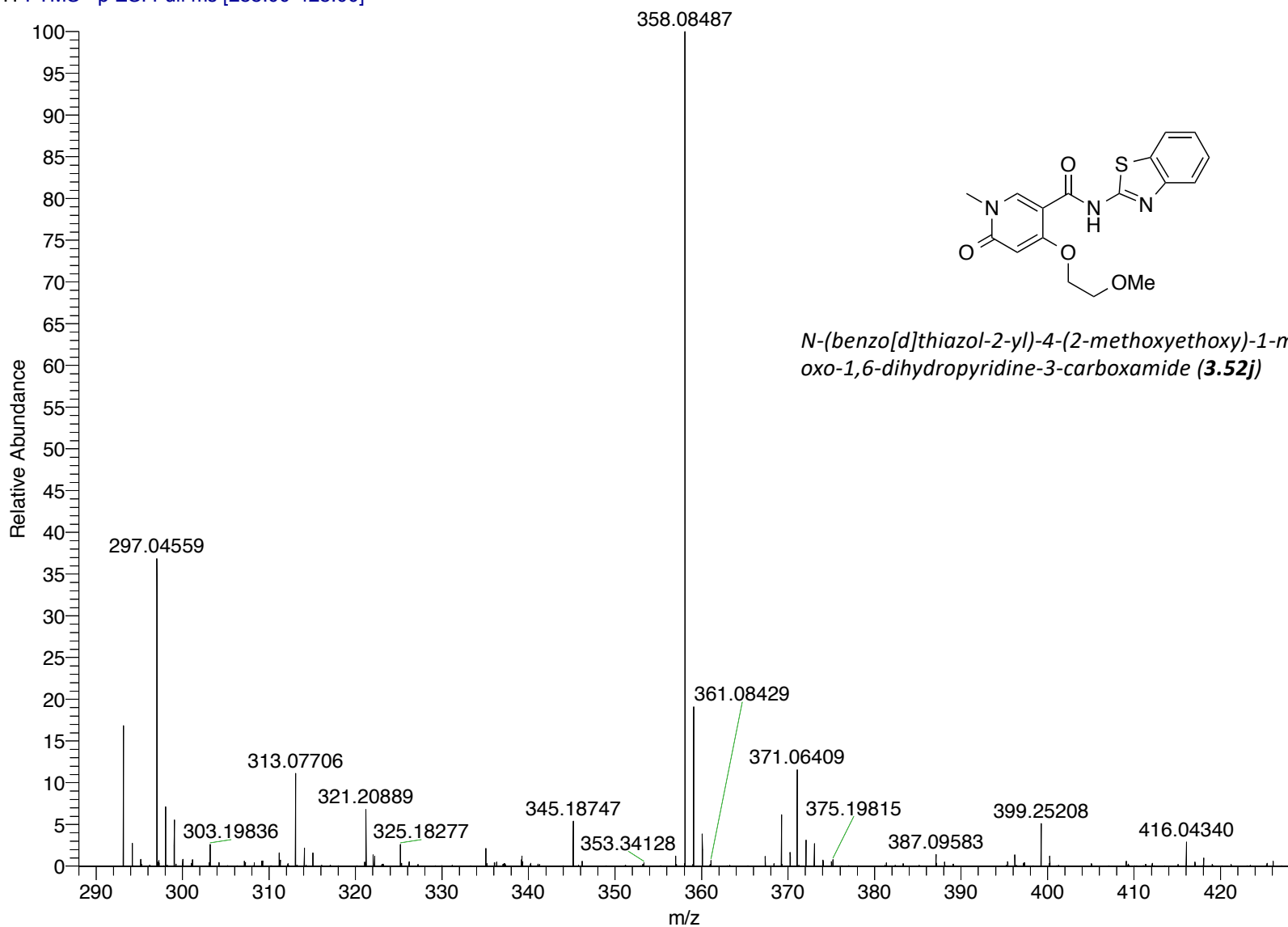


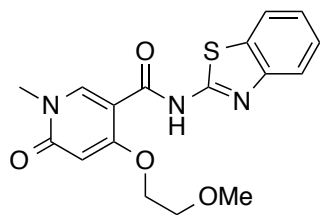
MZP-amide-8812-Dec-2014-13CBB-CDCL3

(100 MHz, 297.2 K, CDCl<sub>3</sub>)

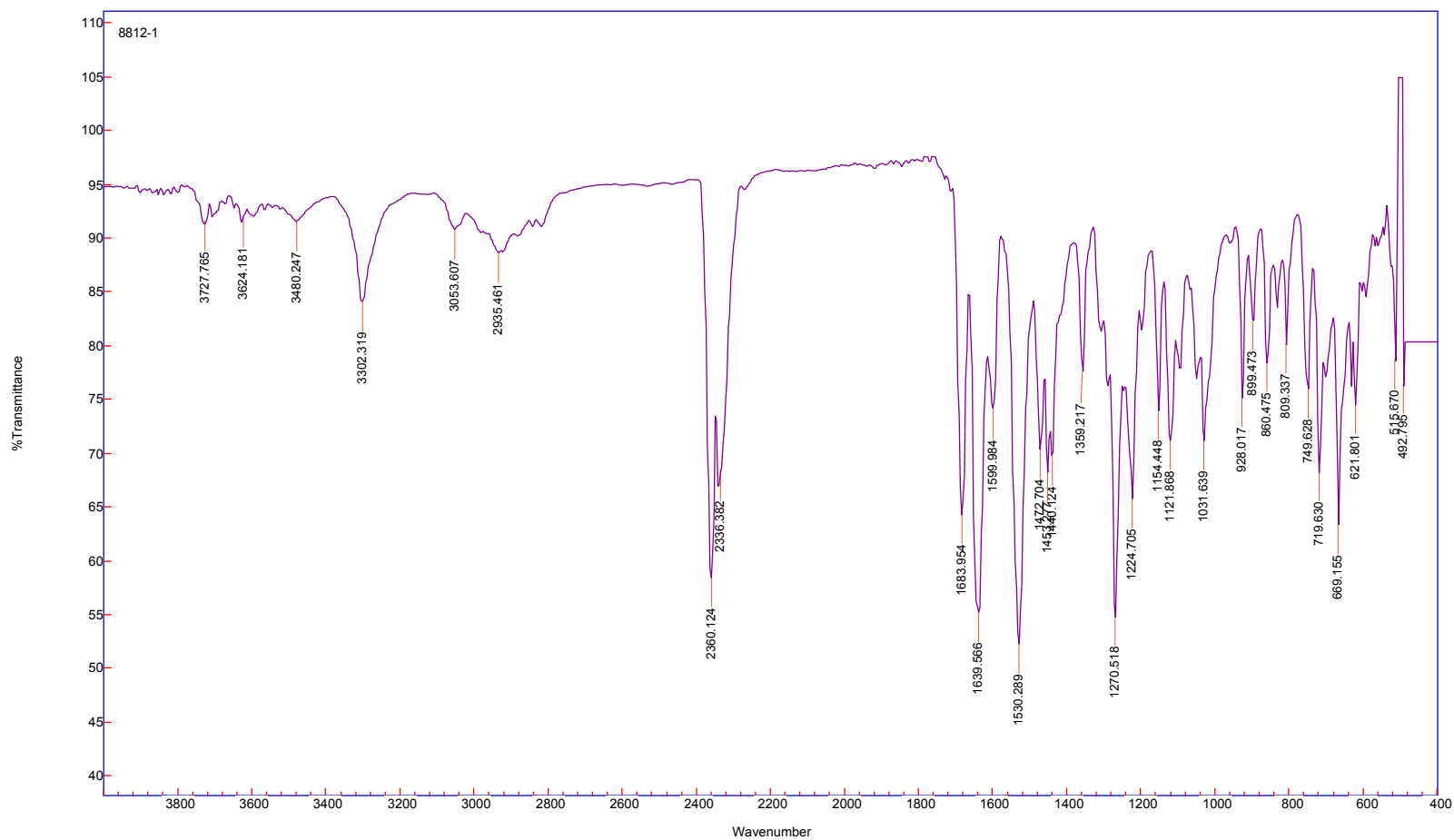


MZP-Amide-8812-HRMS-neg #21 RT: 0.37 AV: 1 NL: 1.62E7  
T: FTMS - p ESI Full ms [288.00-428.00]



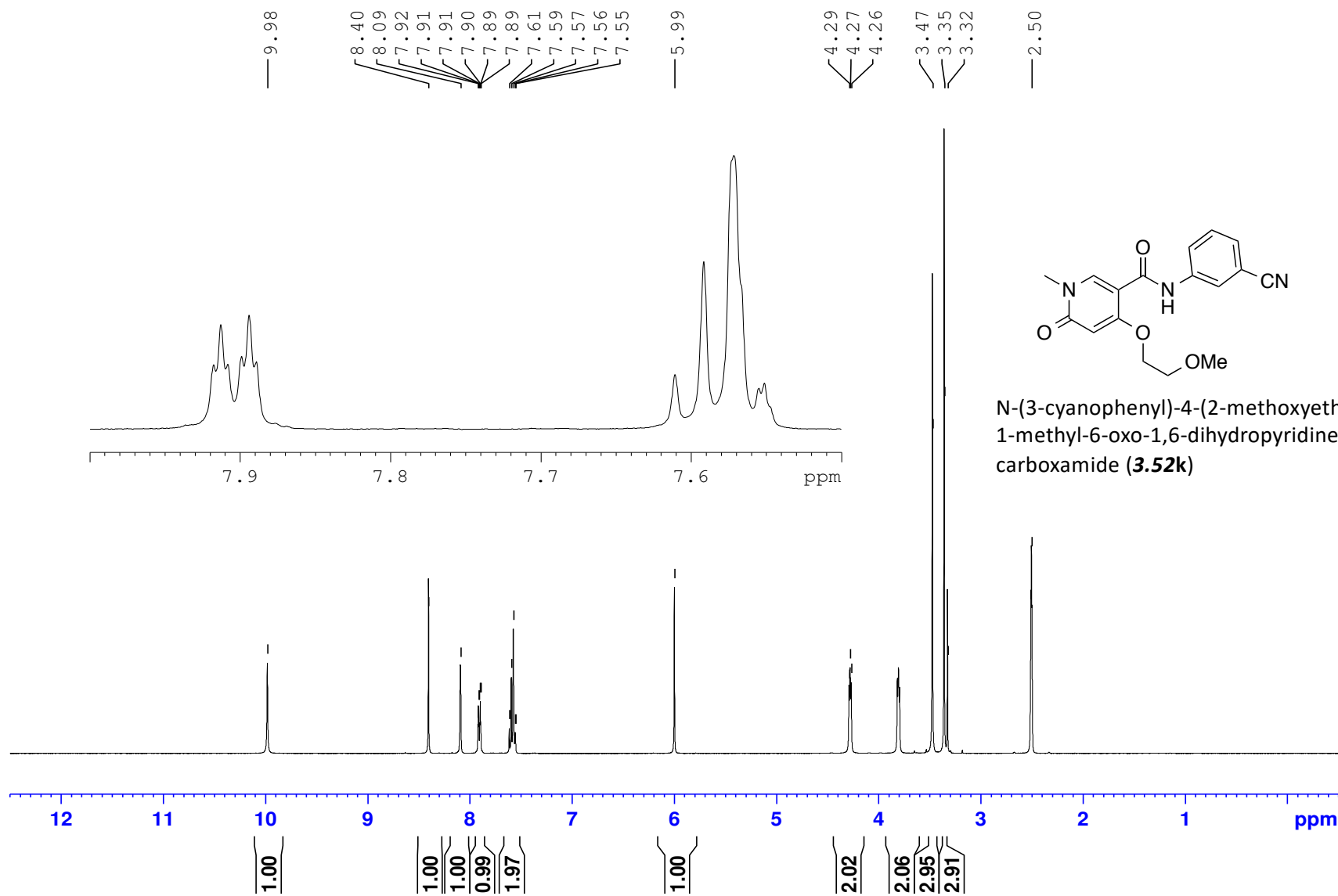


*N*-(benzo[d]thiazol-2-yl)-4-(2-methoxyethoxy)-1-methyl-6-oxo-1,6-dihydropyridine-3-carboxamide (**3.52j**)



MZP\_A14\_Amide\_Dec2014\_DMSO

(400 MHz, 297.2 K, DMSO-d6)



MZP-amide-A14-Dec-2014-13CBB-DMSO

(100 MHz, 297.2 K, DMSO-d6)

163.25  
162.70  
161.29

145.17

139.37

130.42

127.15

124.08

122.28

118.63

111.71

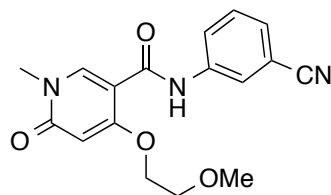
105.69

96.30

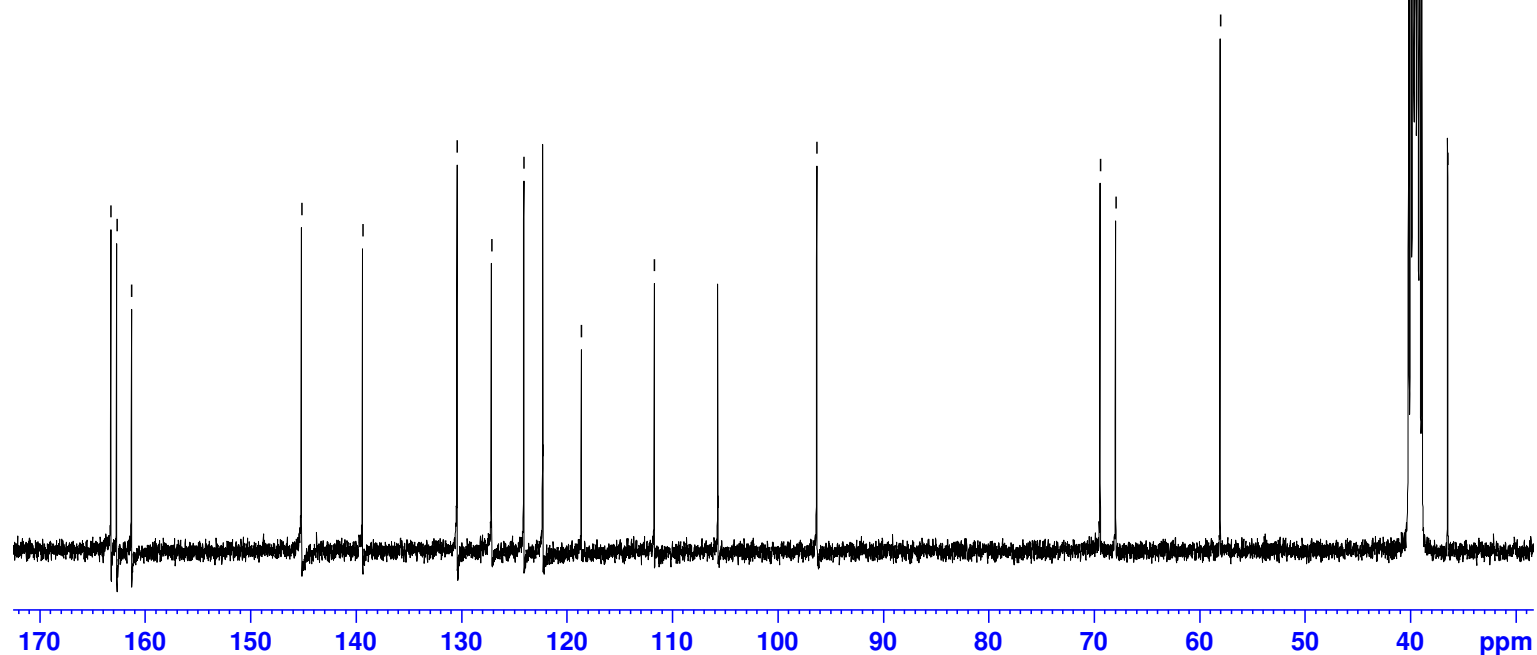
69.42  
67.96

58.04

39.52  
36.46

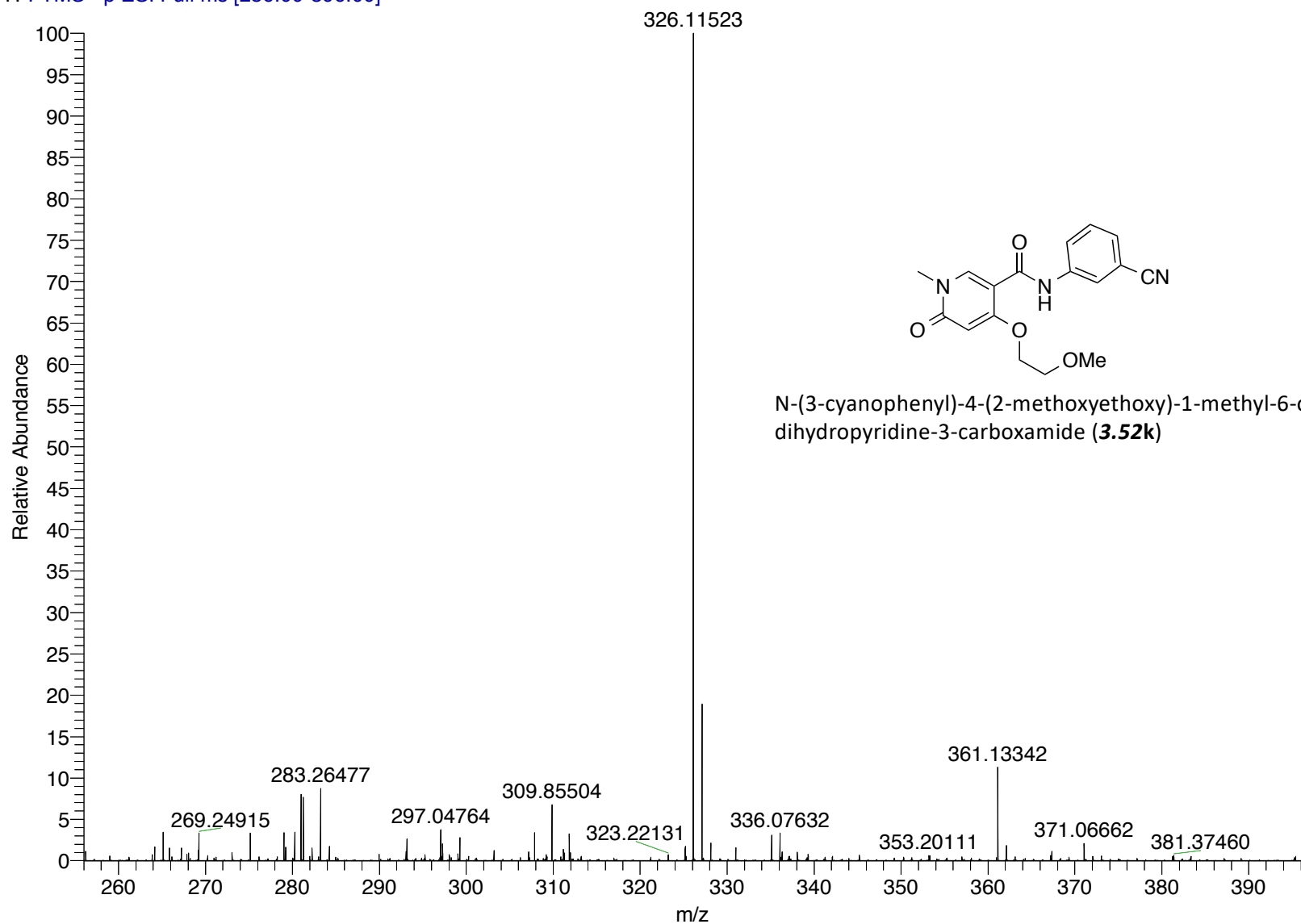


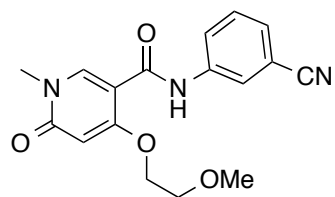
N-(3-cyanophenyl)-4-(2-methoxyethoxy)-1-methyl-6-oxo-1,6-dihydropyridine-3-carboxamide (**3.52k**)



MZIP-Amide-A14-Dec14-2014-neg #19 RT: 0.34 AV: 1 NL: 3.70E6

T: FTMS - p ESI Full ms [256.00-396.00]



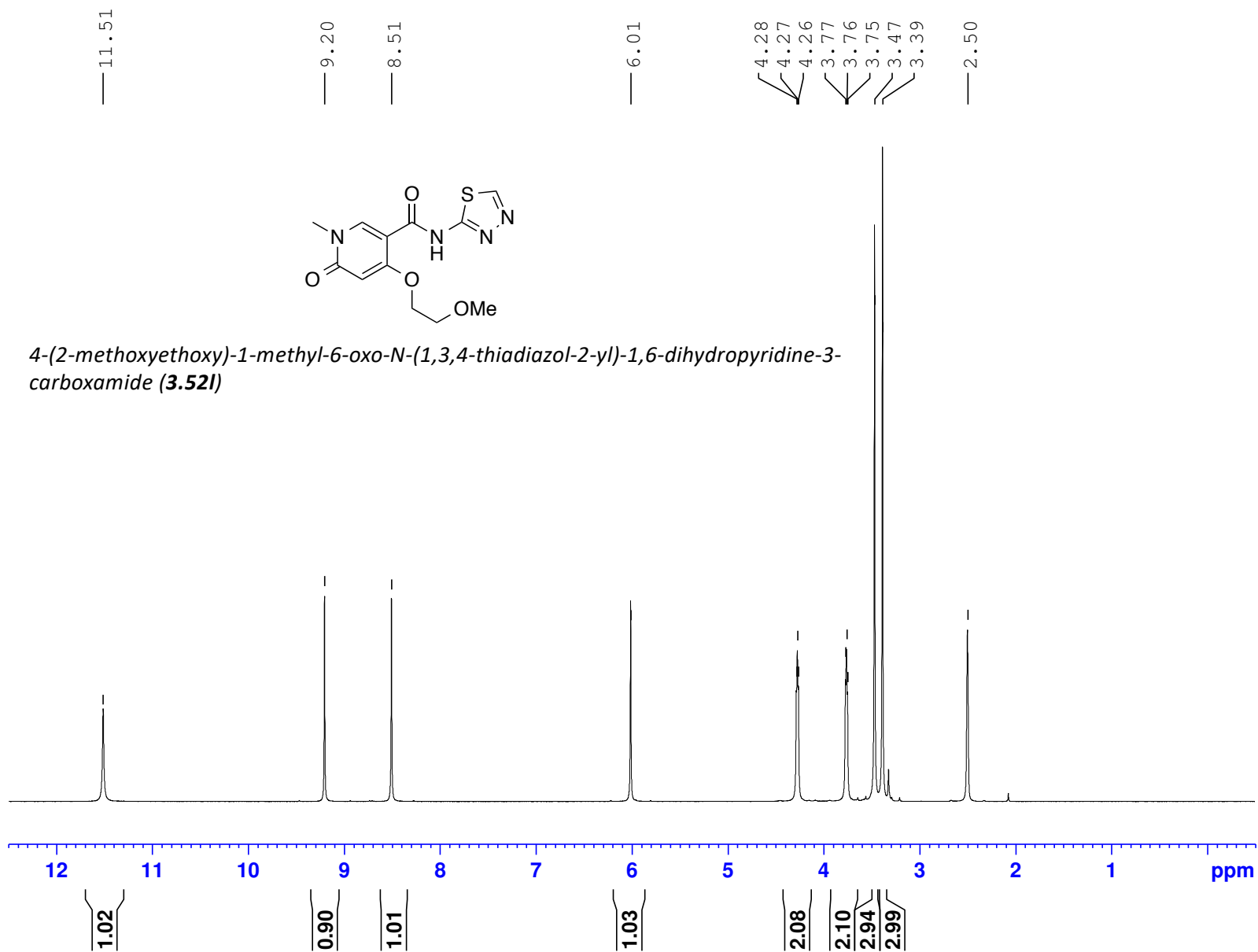


N-(3-cyanophenyl)-4-(2-methoxyethoxy)-1-methyl-6-oxo-1,6-dihydropyridine-3-carboxamide (**3.52k**)



MZP\_8881\_Amide\_Dec2014\_DMSO

(400 MHz, 297.2 K, DMSO-d6)





MZP-amide-8881-Dec-2014-13CBB-DMSO

(100 MHz, 297.2 K, DMSO-d6)

163.38  
162.68  
160.85  
158.21

149.20  
146.04

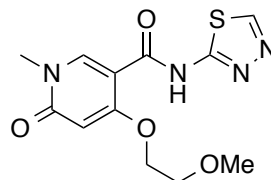
103.77

96.41

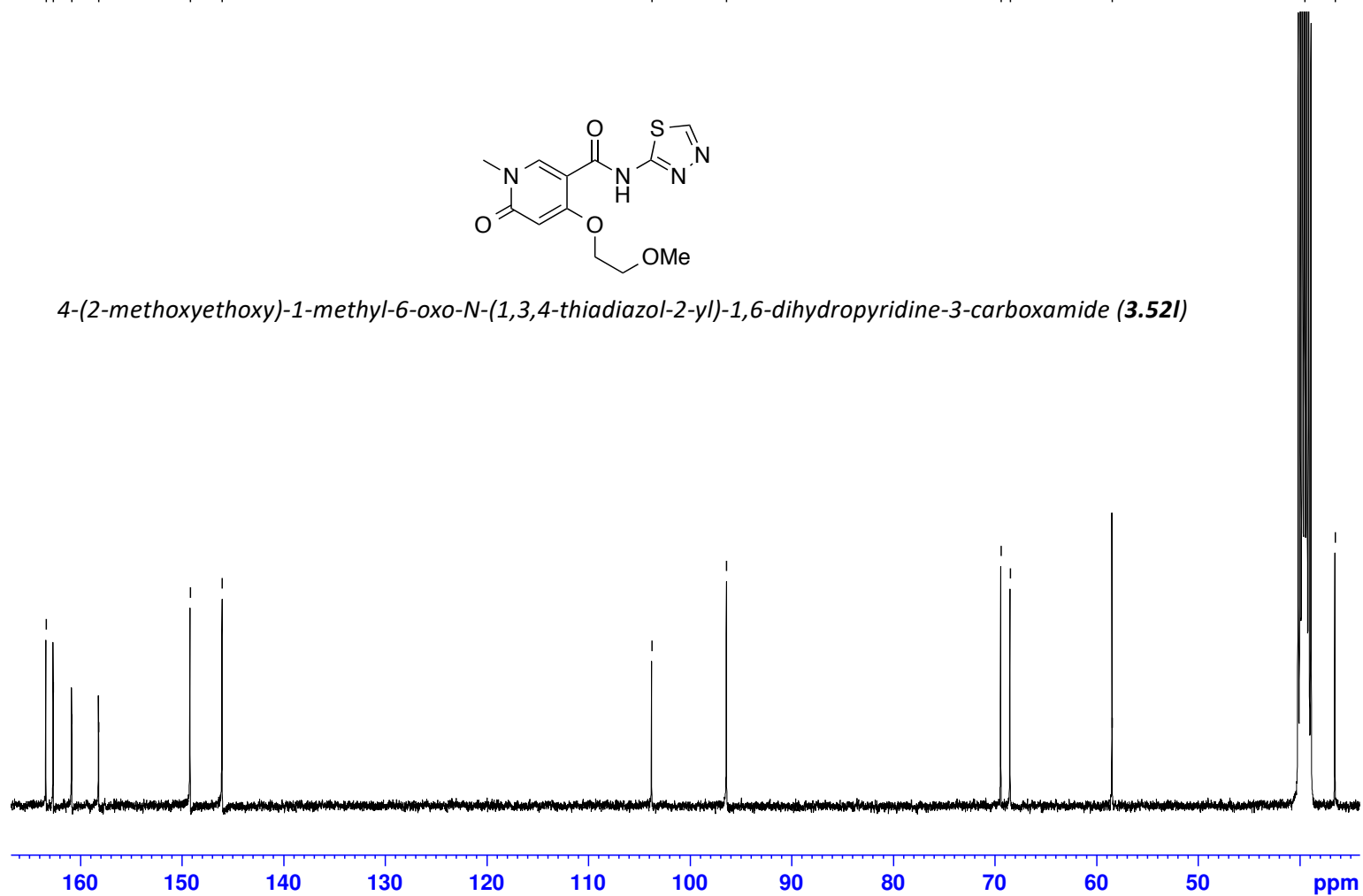
69.41  
68.50

58.46

39.50  
36.52

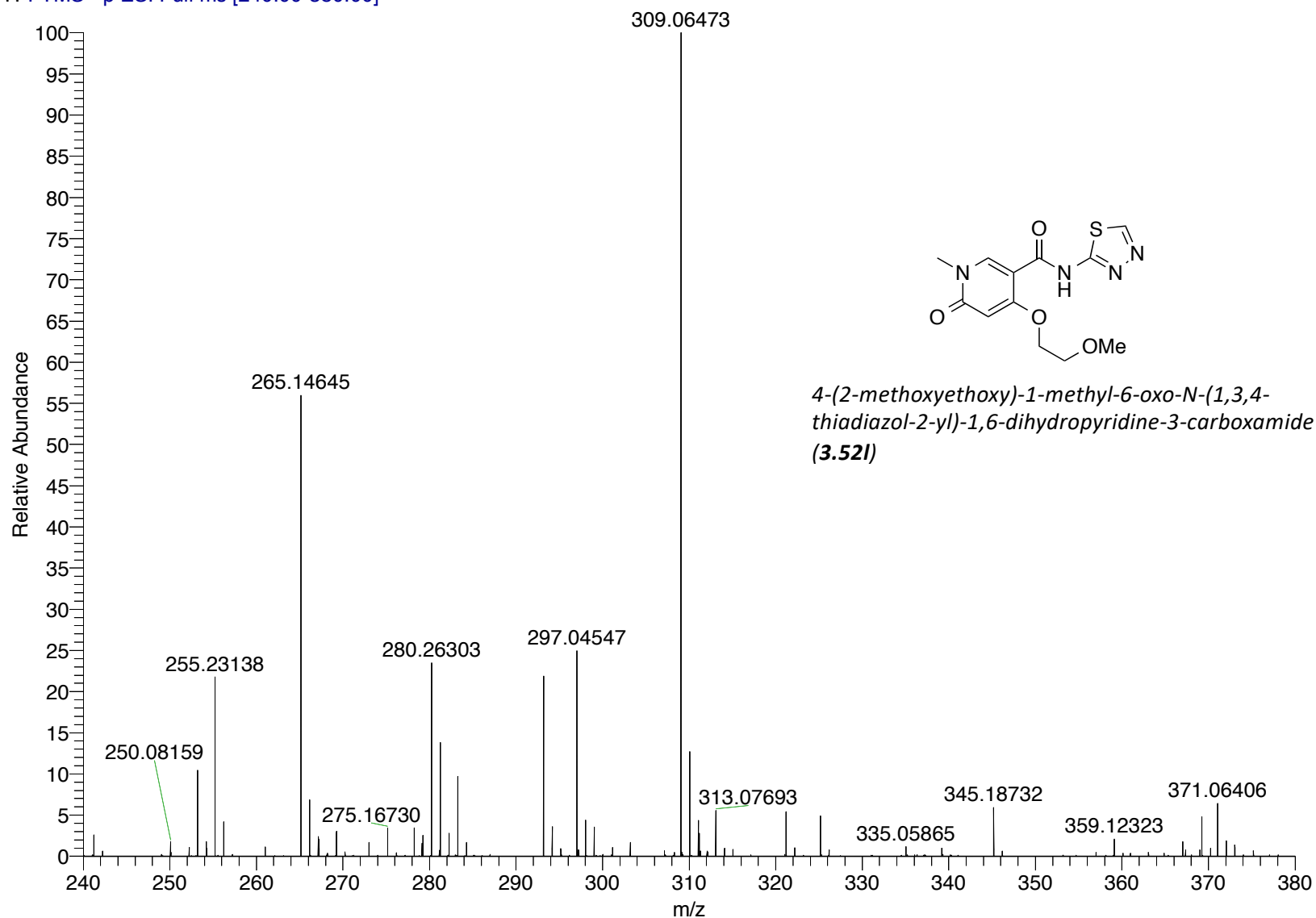


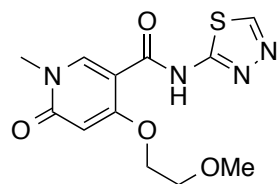
4-(2-methoxyethoxy)-1-methyl-6-oxo-N-(1,3,4-thiadiazol-2-yl)-1,6-dihydropyridine-3-carboxamide (**3.52I**)



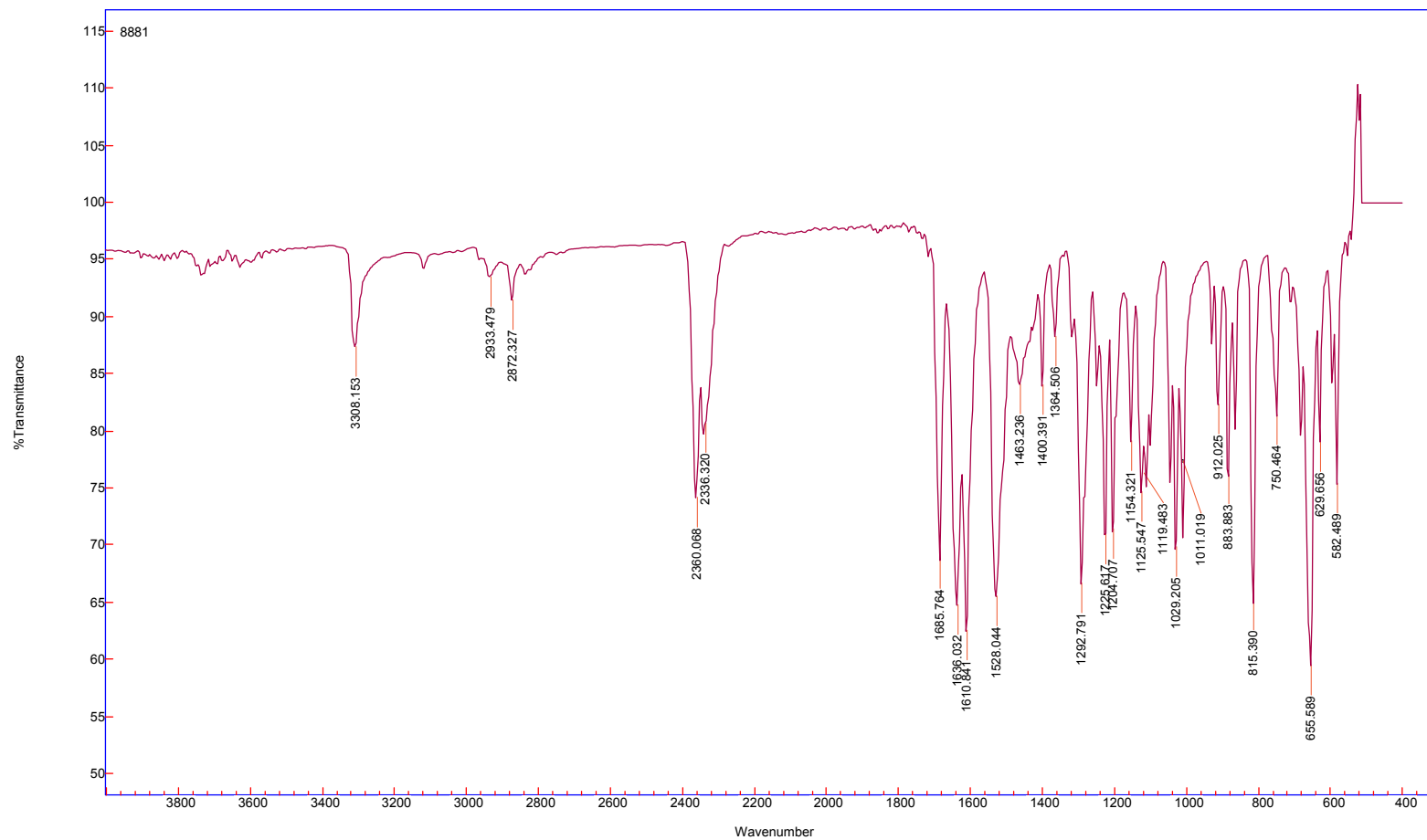
MZP-Amide-8881-HRMS-neg #16 RT: 0.28 AV: 1 NL: 2.50E7

T: FTMS - p ESI Full ms [240.00-380.00]



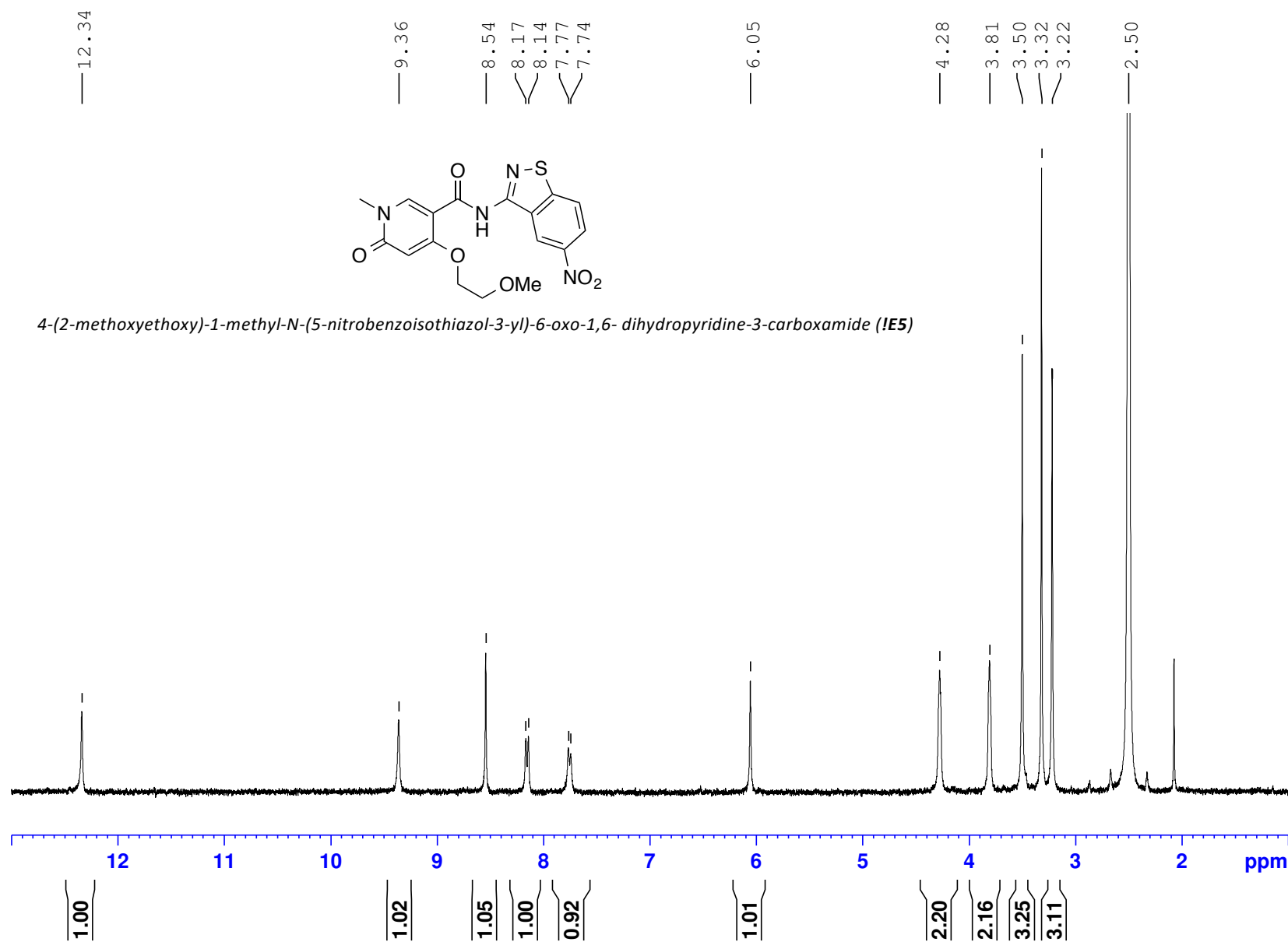


4-(2-methoxyethoxy)-1-methyl-6-oxo-N-(1,3,4-thiadiazol-2-yl)-1,6-dihydropyridine-3-carboxamide (**3.52I**)



MZP\_C20\_Amide\_Dec2014\_DMSO

(400 MHz, 297.2 K, DMSO-d6)



MZP-E5-13CBB-DMSO

(100 MHz, 297.2 K, DMSO-d6)

163.43  
162.93  
162.71  
161.83  
157.79

145.62  
141.62

122.27  
122.03  
119.95  
119.38

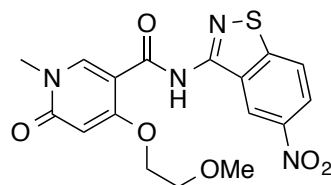
104.40

96.15

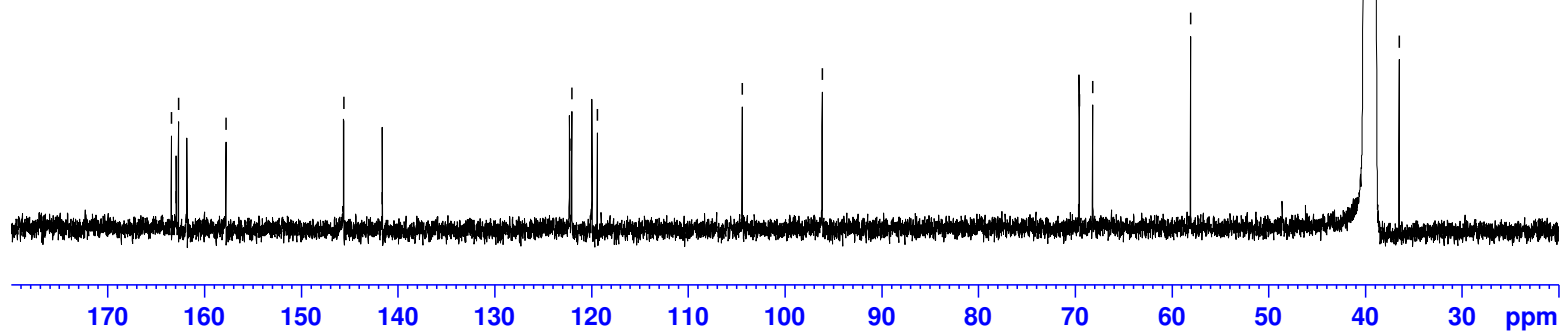
69.58  
68.18

58.06

40.15  
39.94  
39.73  
39.52  
39.31  
39.10  
38.90  
36.50

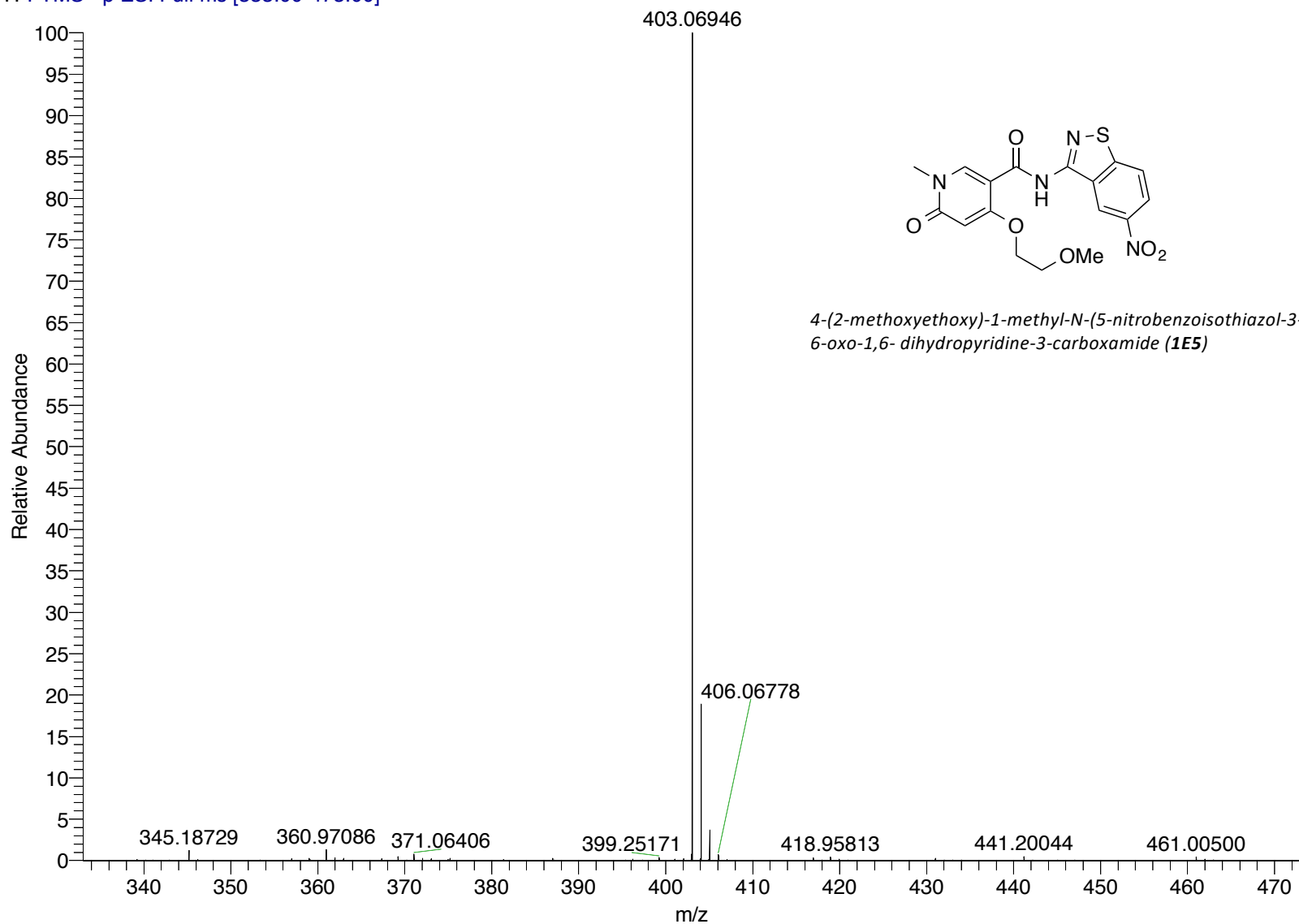


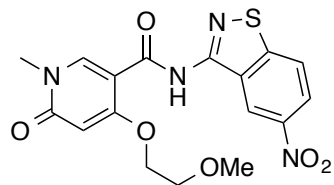
4-(2-methoxyethoxy)-1-methyl-N-(5-nitrobenzothiazol-3-yl)-6-oxo-1,6-dihydropyridine-3-carboxamide (**1E5**)



MZP-Amide-C20-HRMS-neg #10 RT: 0.18 AV: 1 NL: 2.56E8

T: FTMS - p ESI Full ms [333.00-473.00]



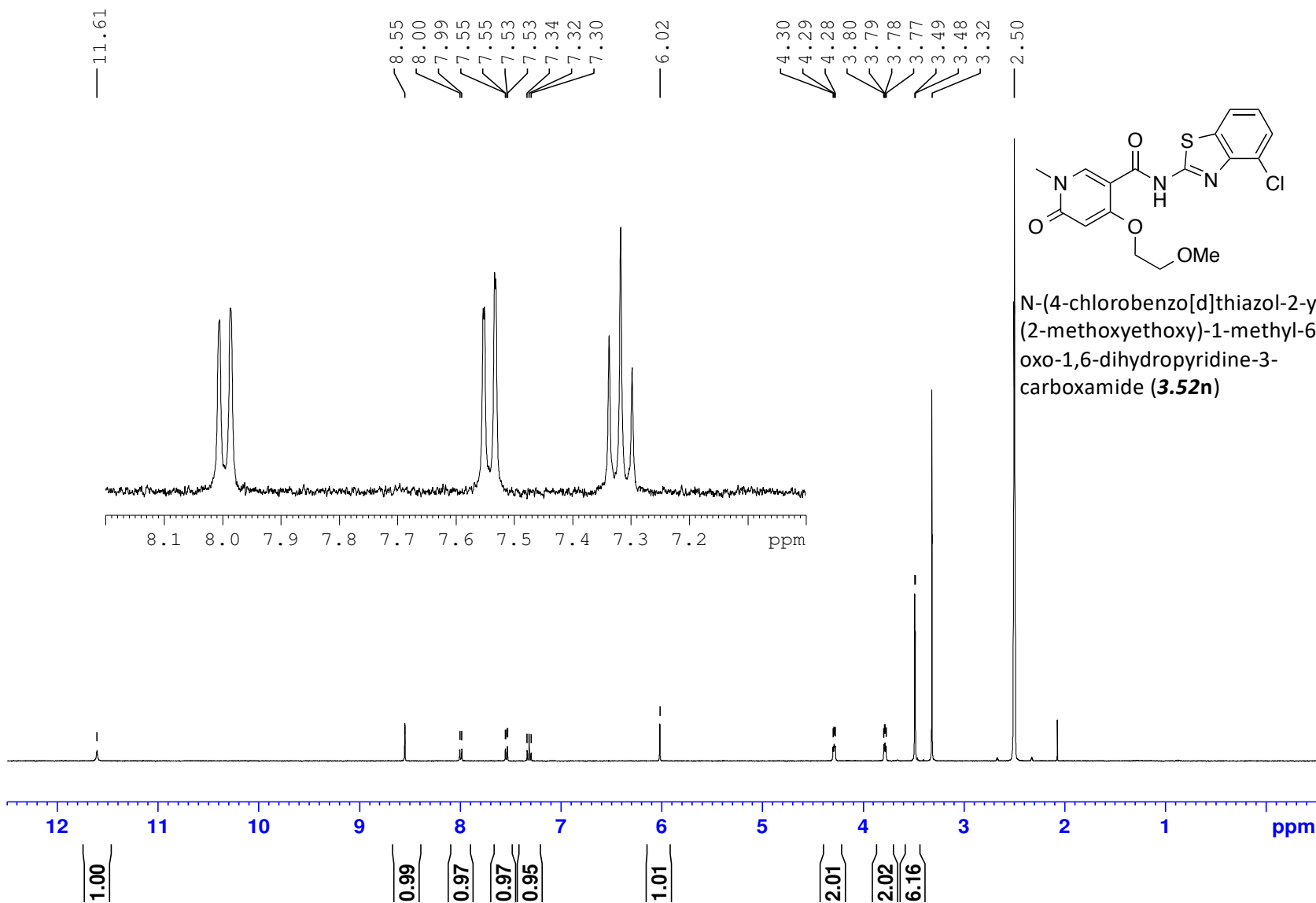


4-(2-methoxyethoxy)-1-methyl-N-(5-nitrobenzothiazol-3-yl)-6-oxo-1,6-dihydropyridine-3-carboxamide (**1E5**)



MZP\_A42\_Amide\_Dec2014\_DMSO

(400 MHz, 297.2 K, DMSO-d6)





(100 MHz, 297.2 K, DMSO-d6)

MZP-Amide-A42-13CBB-NMR-DMSO-50h

163.36  
162.70  
161.66  
158.42

146.21  
145.43

133.36

126.32  
124.54  
124.47  
120.90

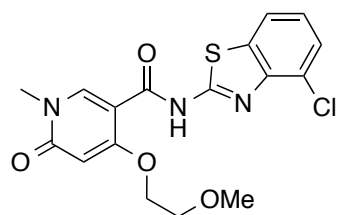
103.75

96.37

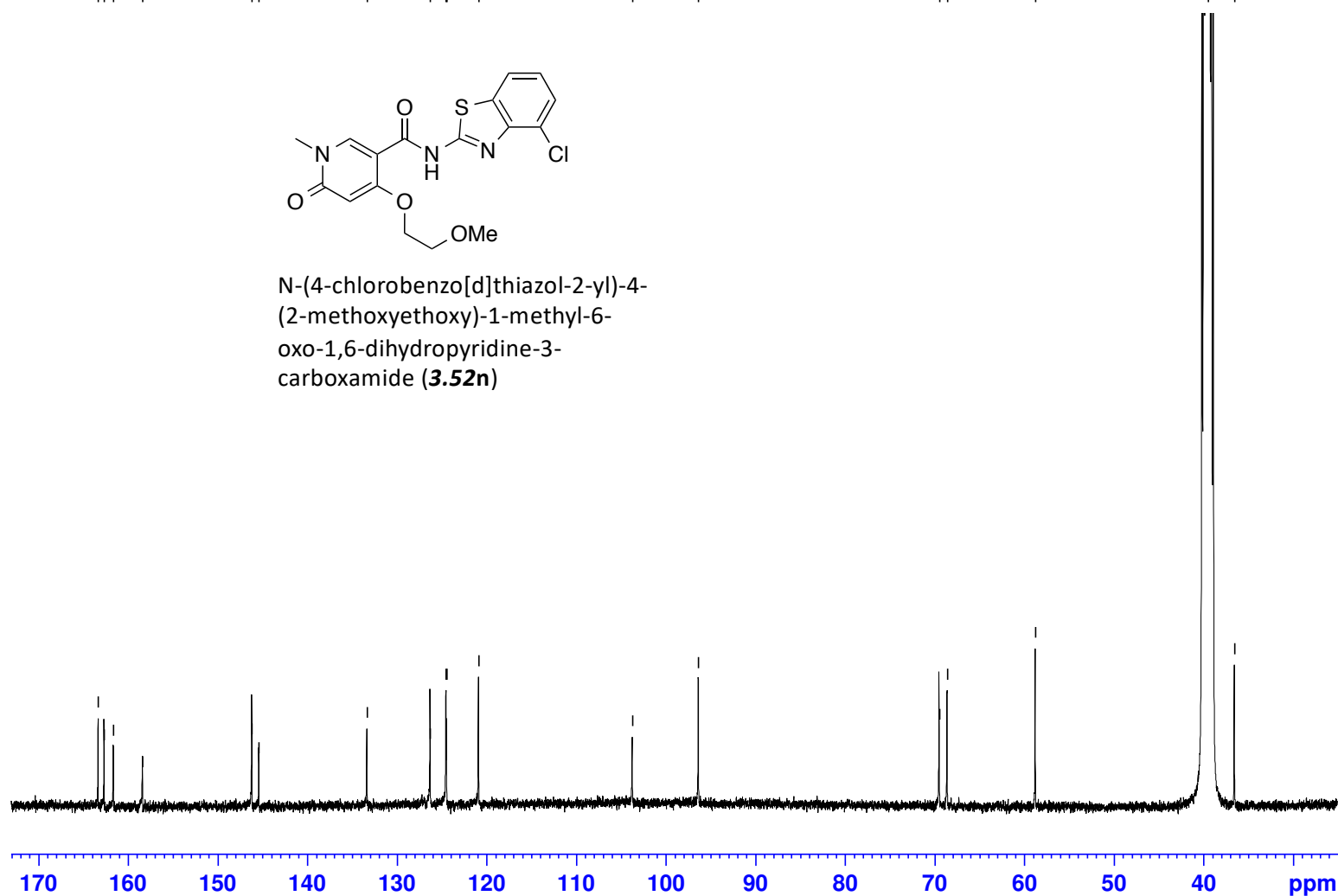
69.50  
68.61

58.77

39.52  
36.54

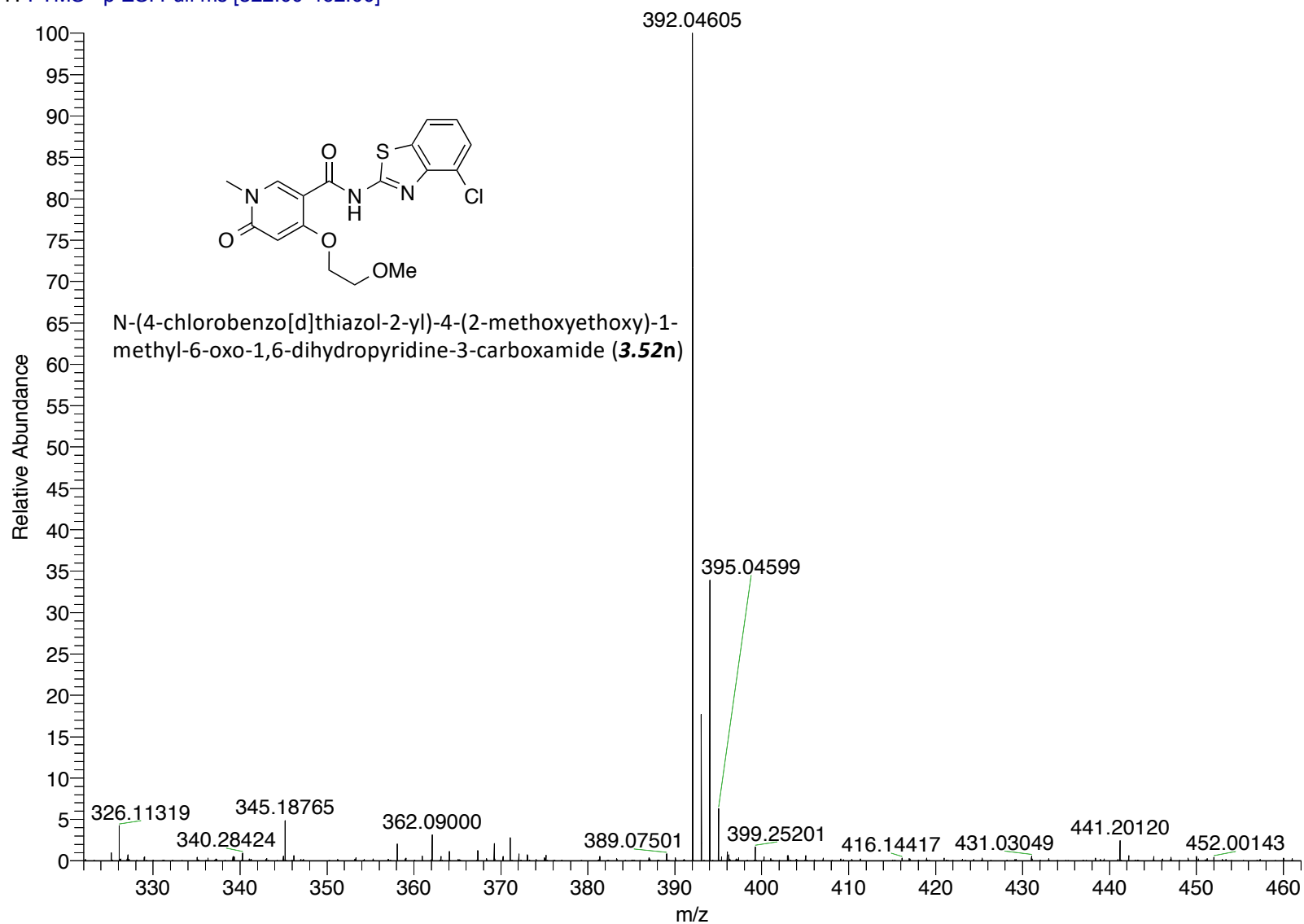


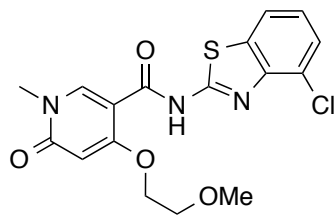
N-(4-chlorobenzo[d]thiazol-2-yl)-4-(2-methoxyethoxy)-1-methyl-6-oxo-1,6-dihydropyridine-3-carboxamide (**3.52n**)



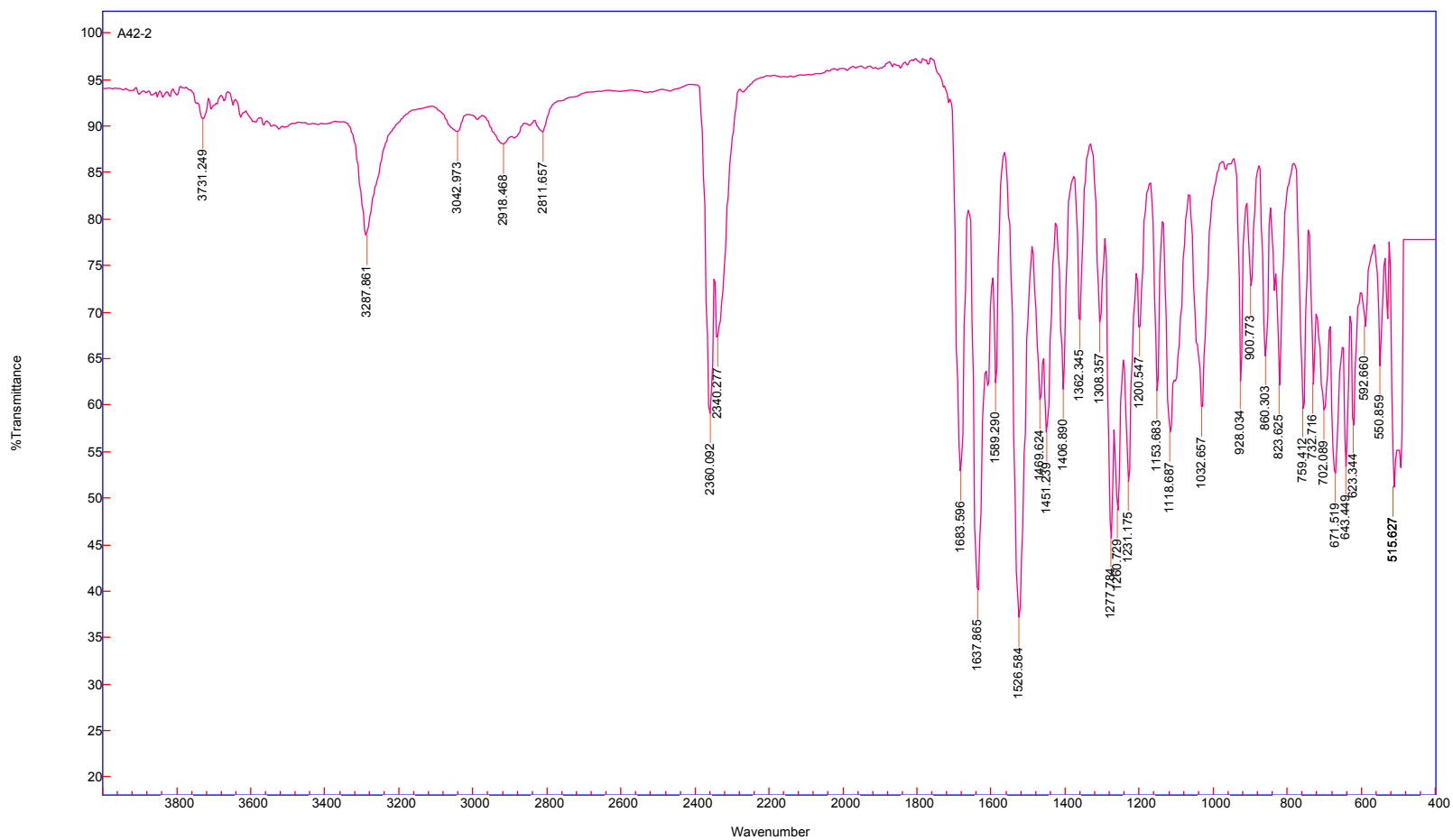
MZP-Amide-A42-HRMS-neg #24 RT: 0.43 AV: 1 NL: 3.77E7

T: FTMS - p ESI Full ms [322.00-462.00]



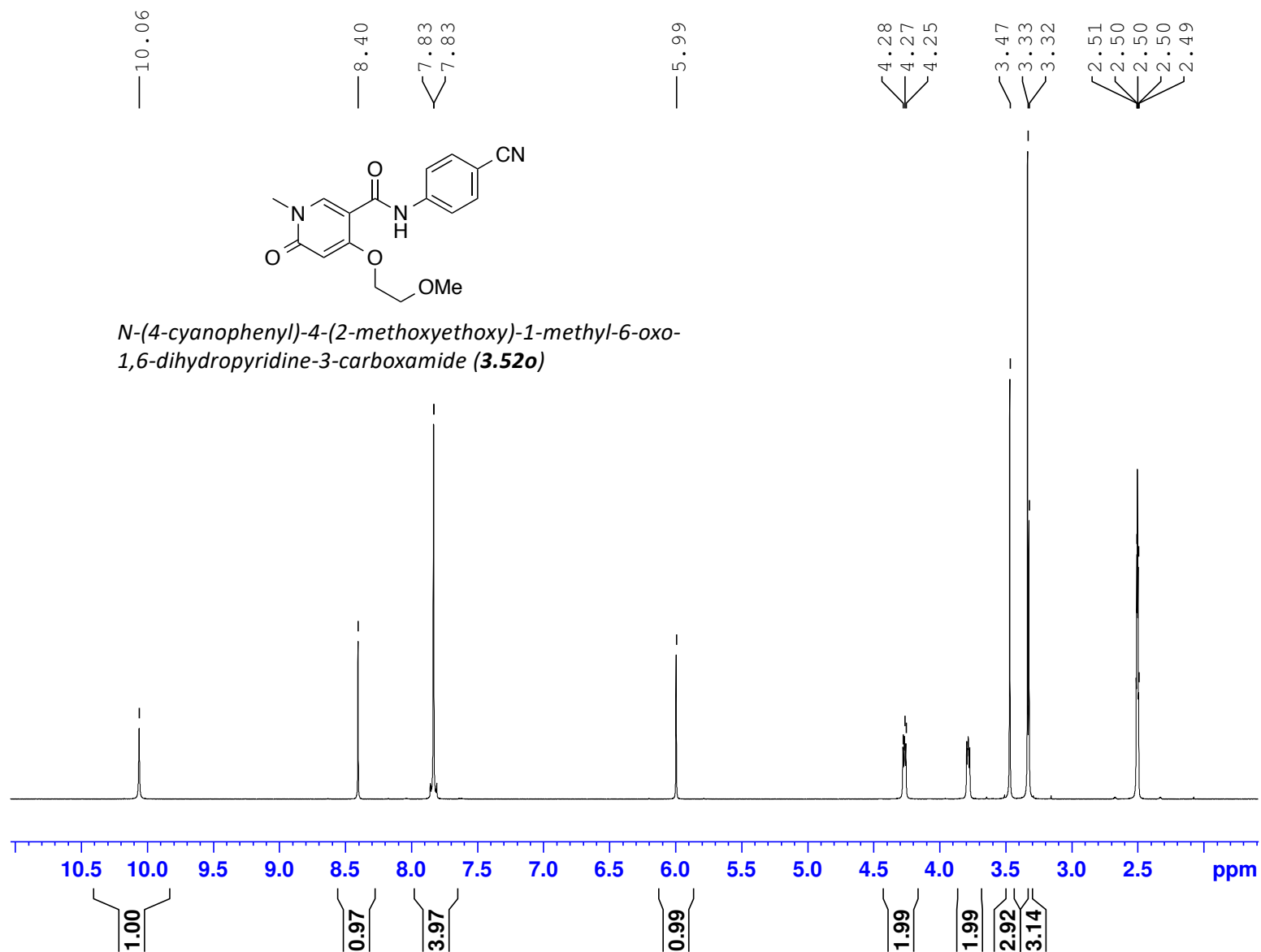


N-(4-chlorobenzo[d]thiazol-2-yl)-4-(2-methoxyethoxy)-1-methyl-6-oxo-1,6-dihydropyridine-3-carboxamide (**3.52n**)



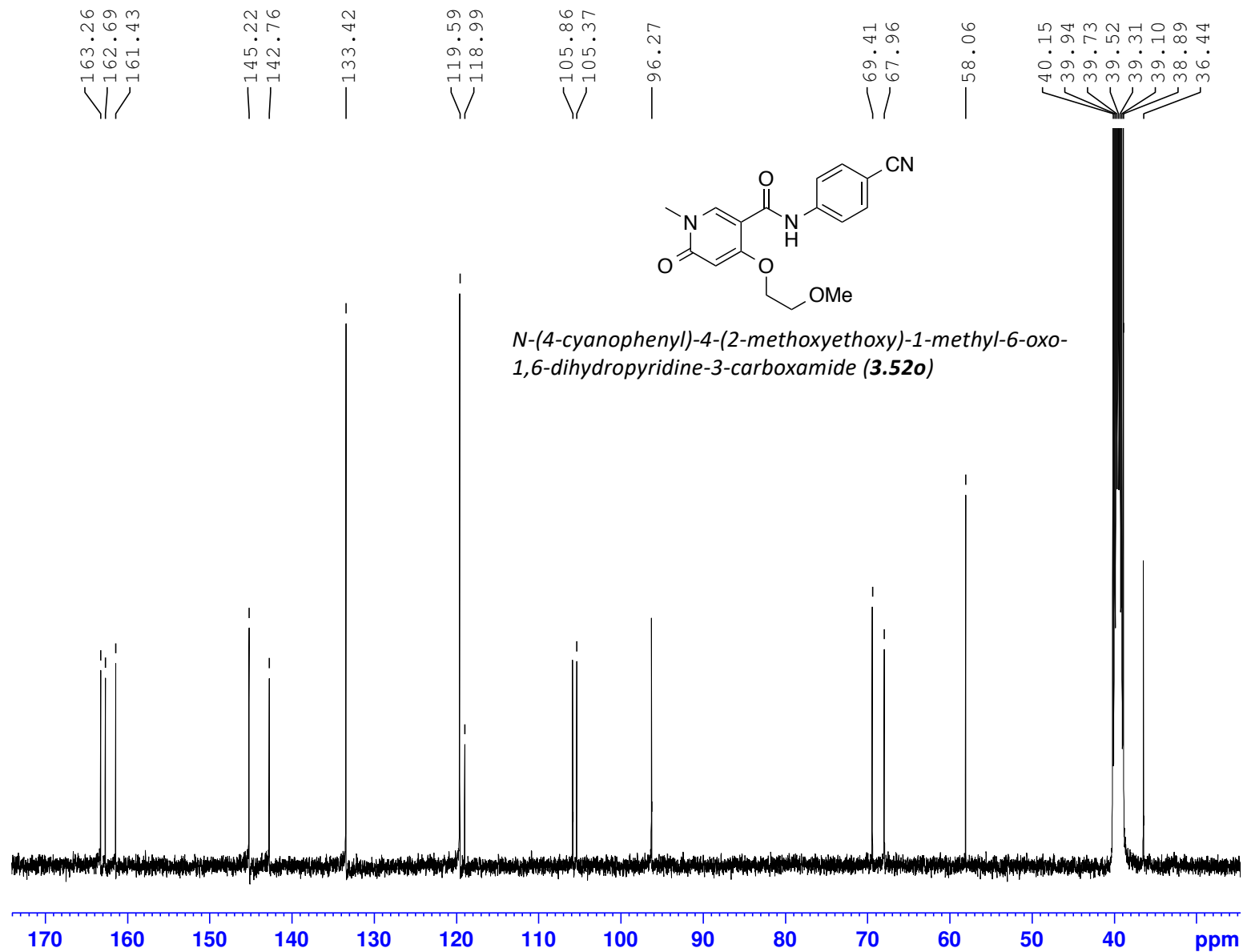
MZP-Amide-A112C-Feb2015-10mg-1H-NMR- DMSO

(400 MHz, 297.2 K, DMSO-d6)



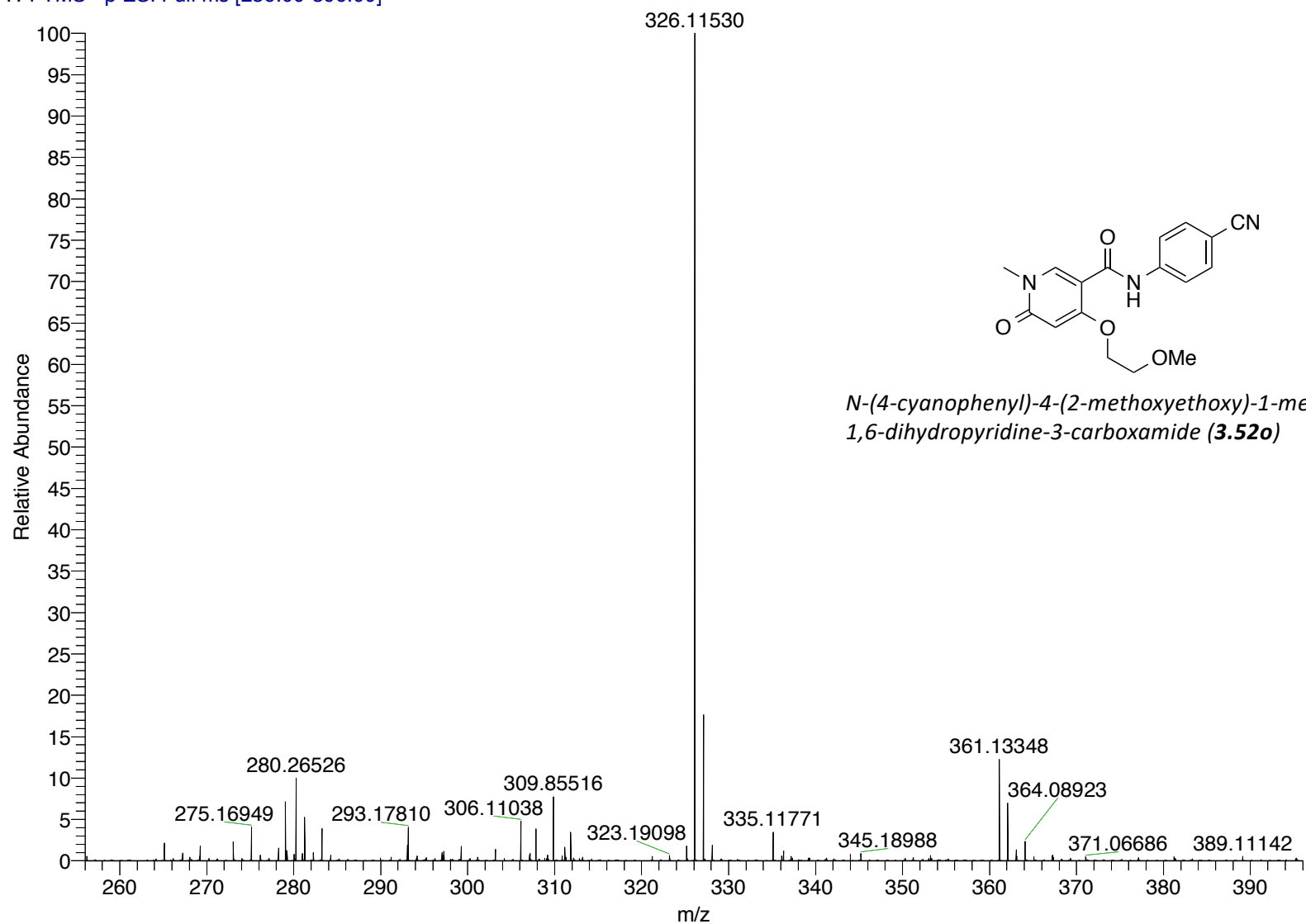
(100 MHz, 297.2 K, DMSO-d6)

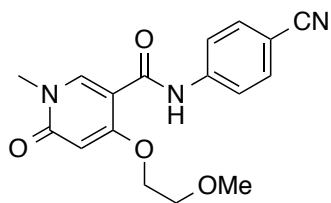
MZP-Amide-A112C-Feb2015-10mg-13CBB-DMSO



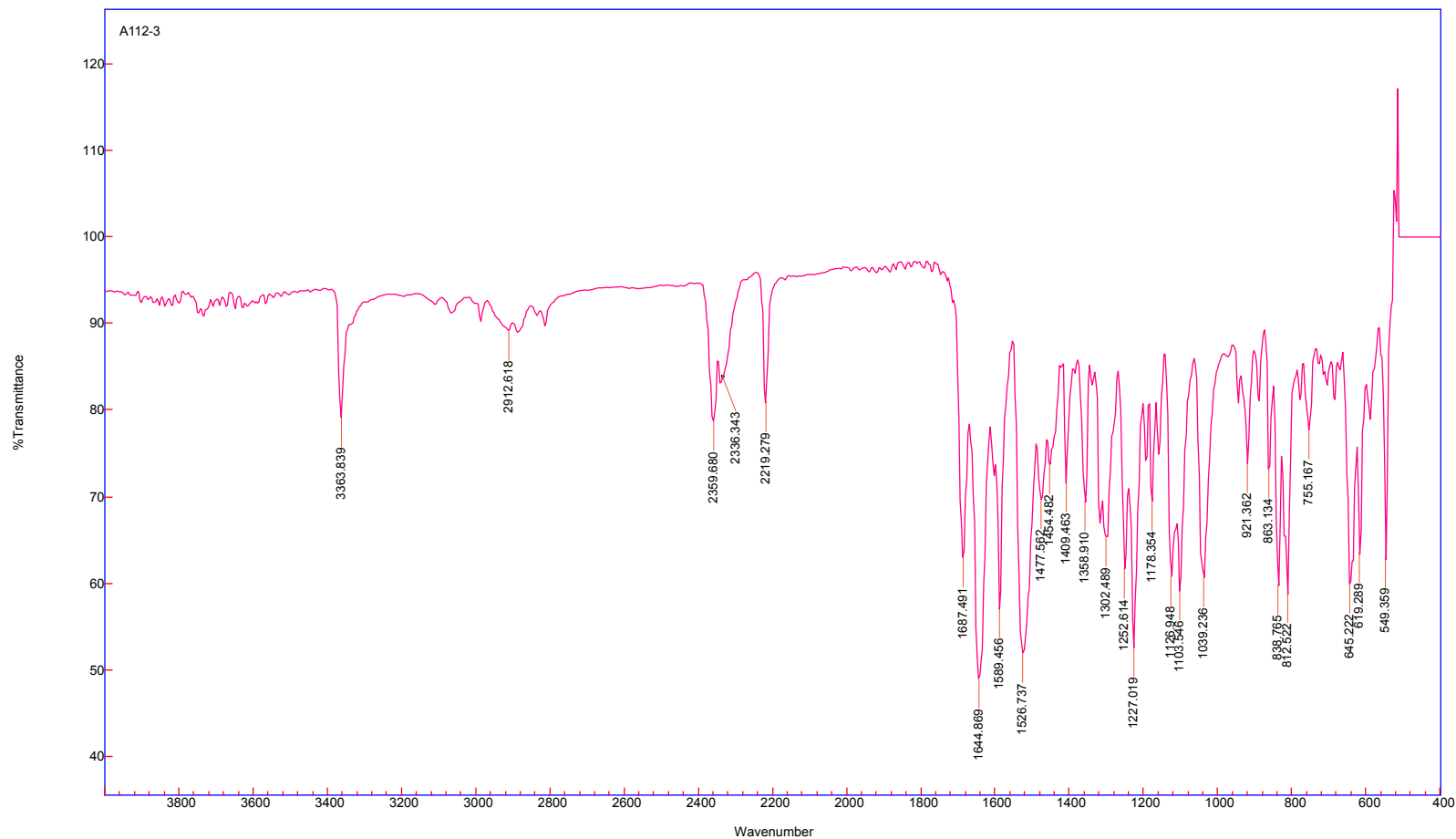
MZIP-Amide-A112C-Feb15-2015-neg #10 RT: 0.18 AV: 1 NL: 3.20E7

T: FTMS - p ESI Full ms [256.00-396.00]



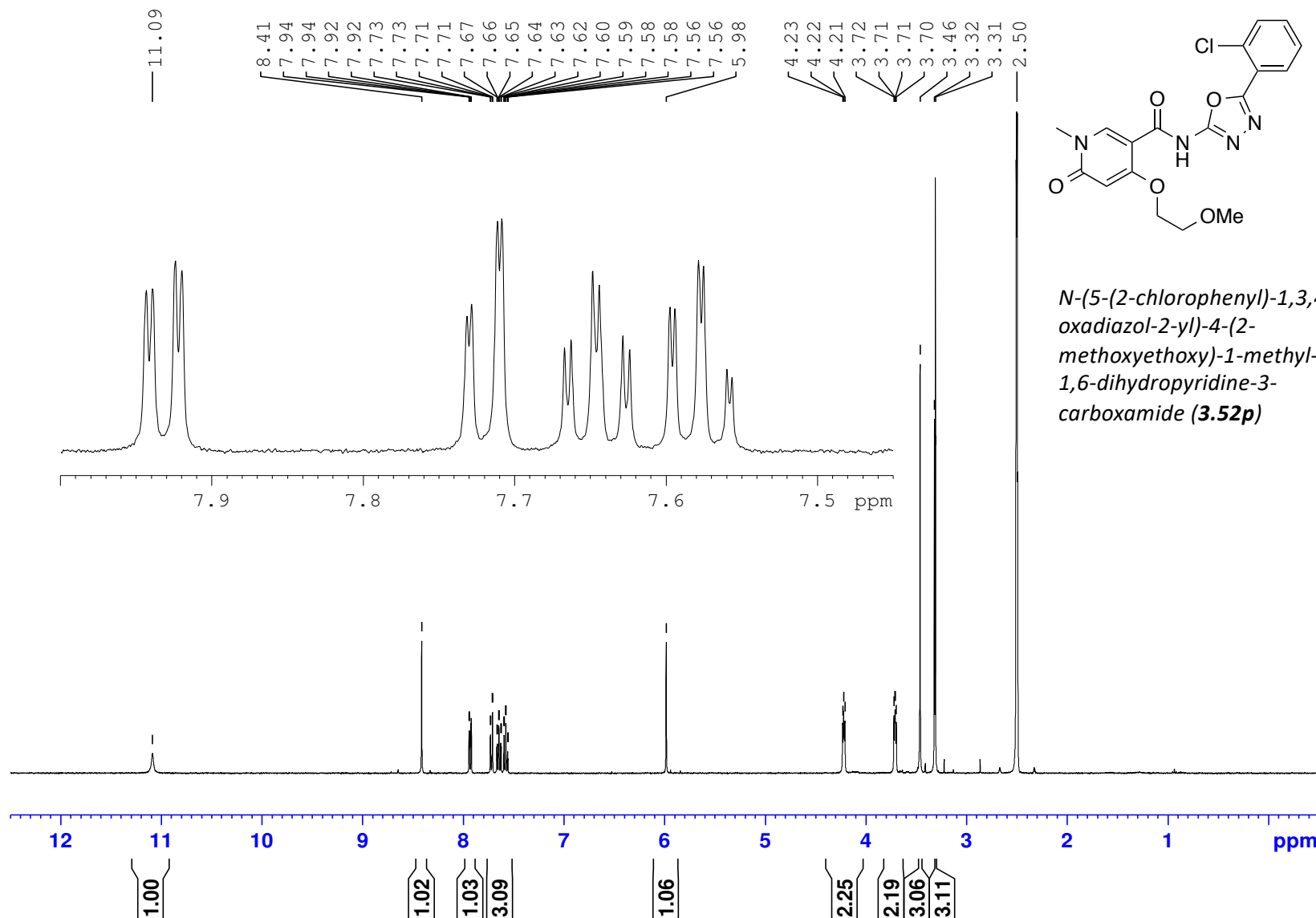


*N*-(4-cyanophenyl)-4-(2-methoxyethoxy)-1-methyl-6-oxo-1,6-dihydropyridine-3-carboxamide (**3.52o**)



MZP-A30\_Amide\_Dec2014\_DMSO

(400 MHz, 297.2 K, DMSO-d6)





MZP-Amide-A30-Dec-2014-13CBB-DMSO

(100 MHz, 297.2 K, DMSO-d6)

163.33  
162.71  
160.44  
158.90  
157.59

145.58

133.08  
131.64  
131.12  
131.00  
127.92  
122.54

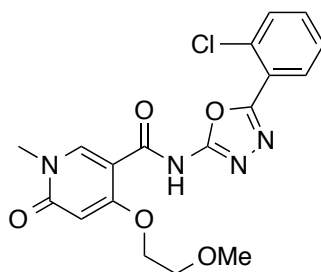
105.12

96.33

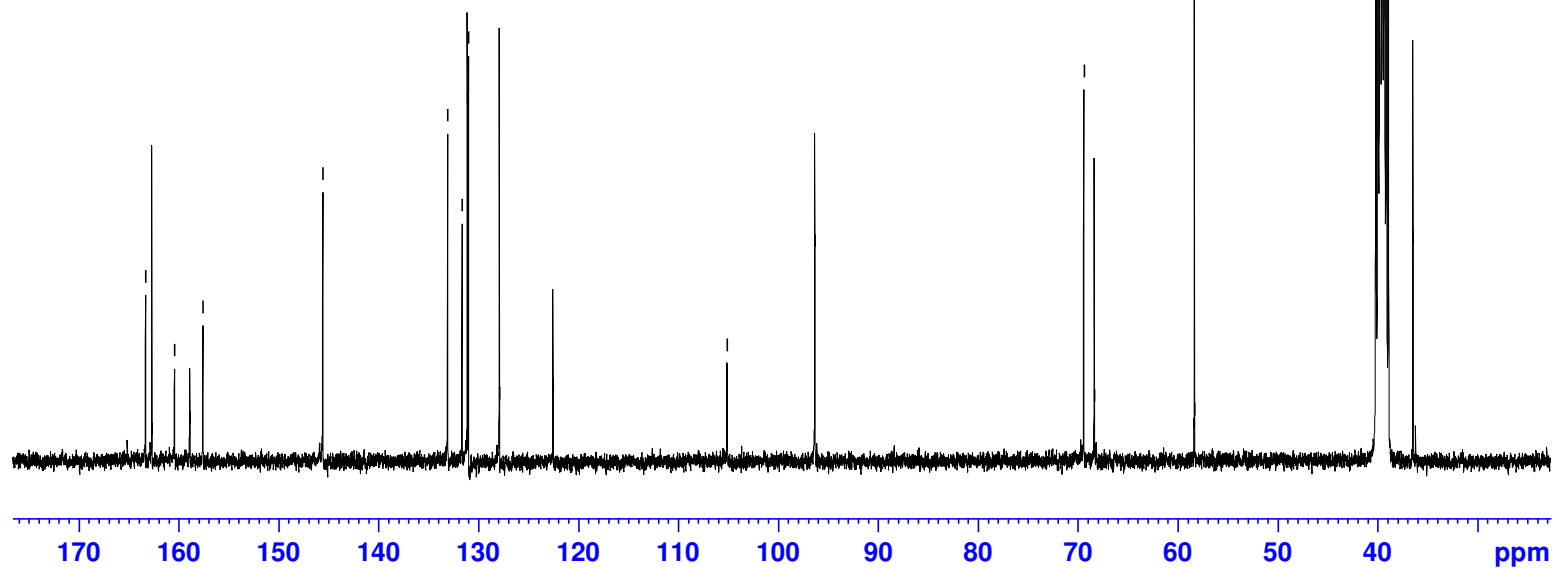
69.41  
68.36

58.34

40.15  
39.94  
39.73  
39.52  
39.31  
39.10  
38.90  
36.45

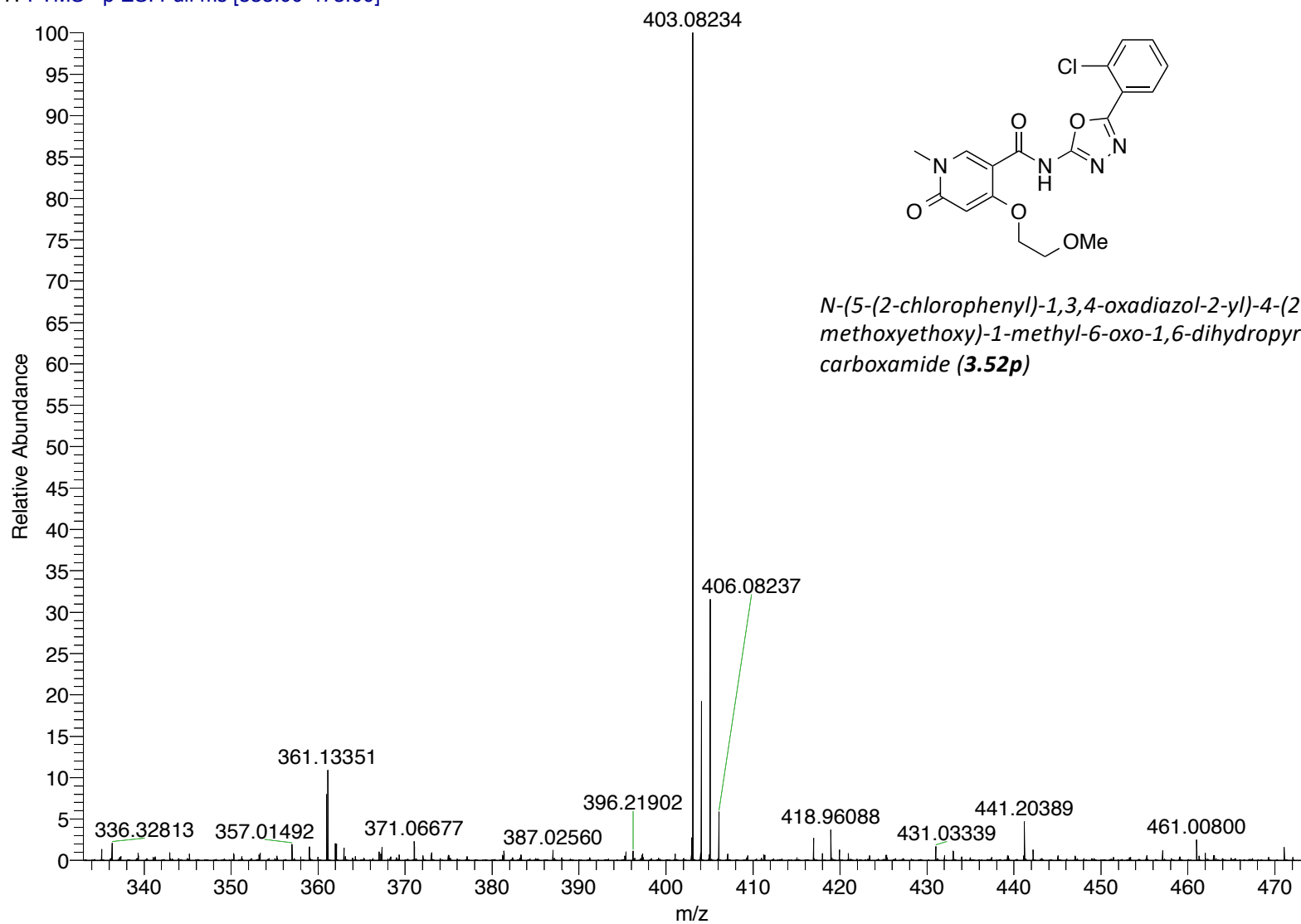


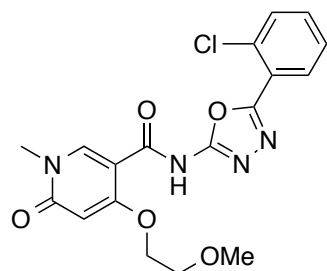
*N*-(5-(2-chlorophenyl)-1,3,4-oxadiazol-2-yl)-4-(2-methoxyethoxy)-1-methyl-6-oxo-1,6-dihydropyridine-3-carboxamide (**3.52p**)



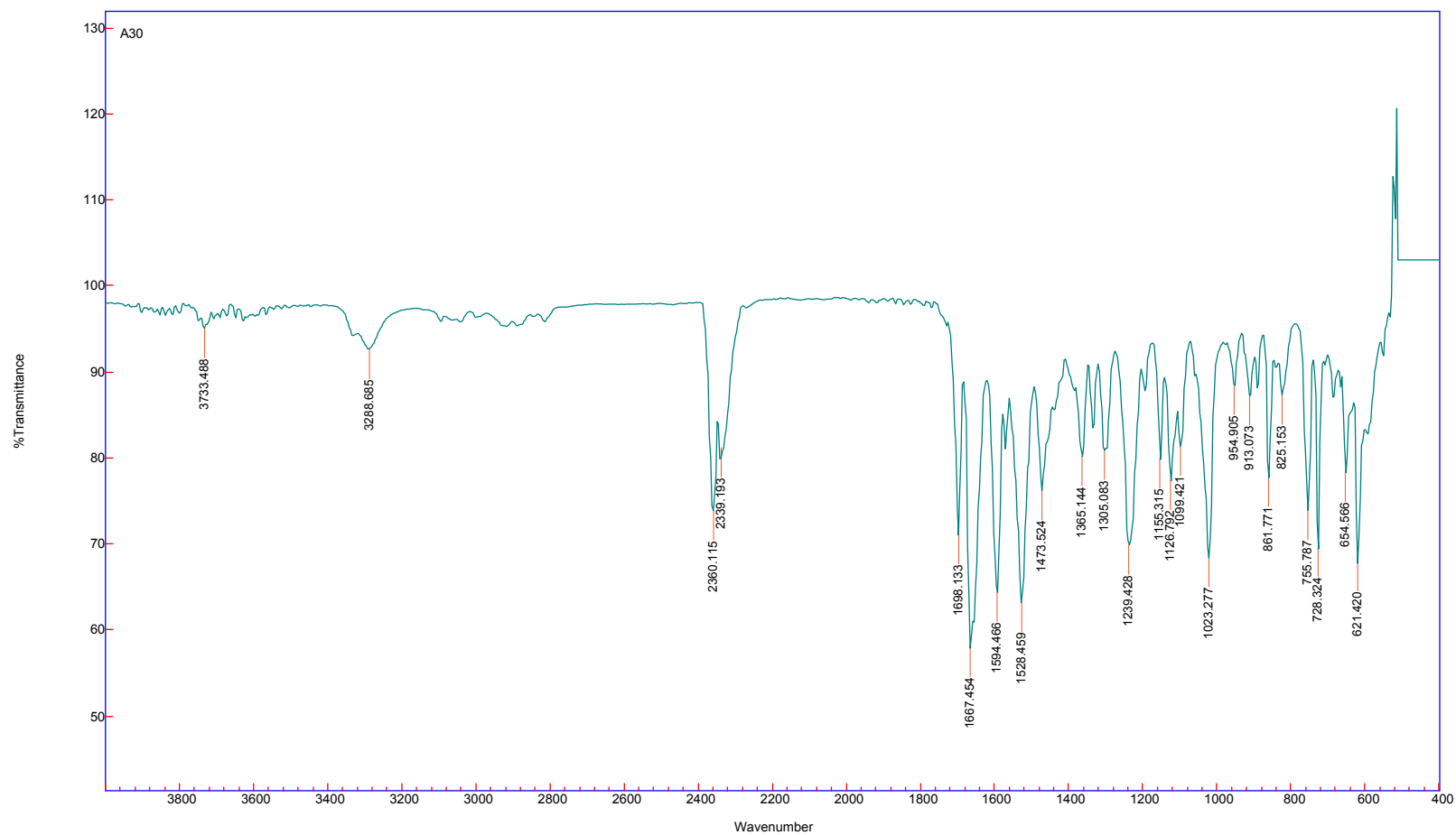
MZIP-Amide-A30-Dec14-2014-neg #22 RT: 0.39 AV: 1 NL: 1.02E7

T: FTMS - p ESI Full ms [333.00-473.00]



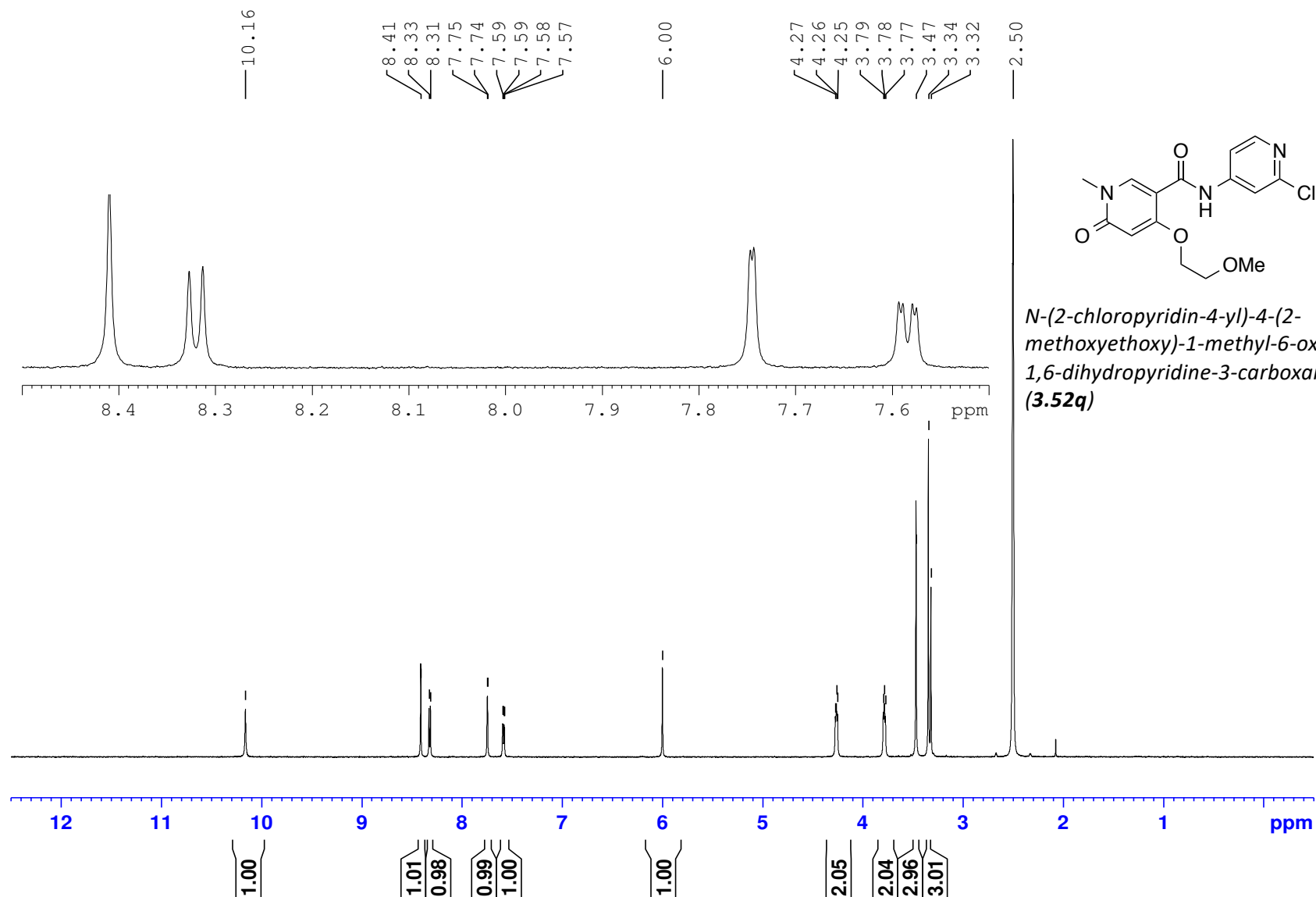


*N*-(5-(2-chlorophenyl)-1,3,4-oxadiazol-2-yl)-4-(2-methoxyethoxy)-1-methyl-6-oxo-1,6-dihydropyridine-3-carboxamide (**3.52p**)



MZP\_A13\_Amide\_Dec2014\_DMSO

(400 MHz, 297.2 K, DMSO-d6)



(100 MHz, 297.2 K, DMSO-d6)

MZP-Amide-A13-Dec-2014-13CBB-DMSO

163.65  
163.14  
162.49

151.45  
151.02  
148.20  
145.96

113.45  
113.32

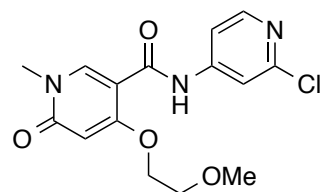
106.01

96.73

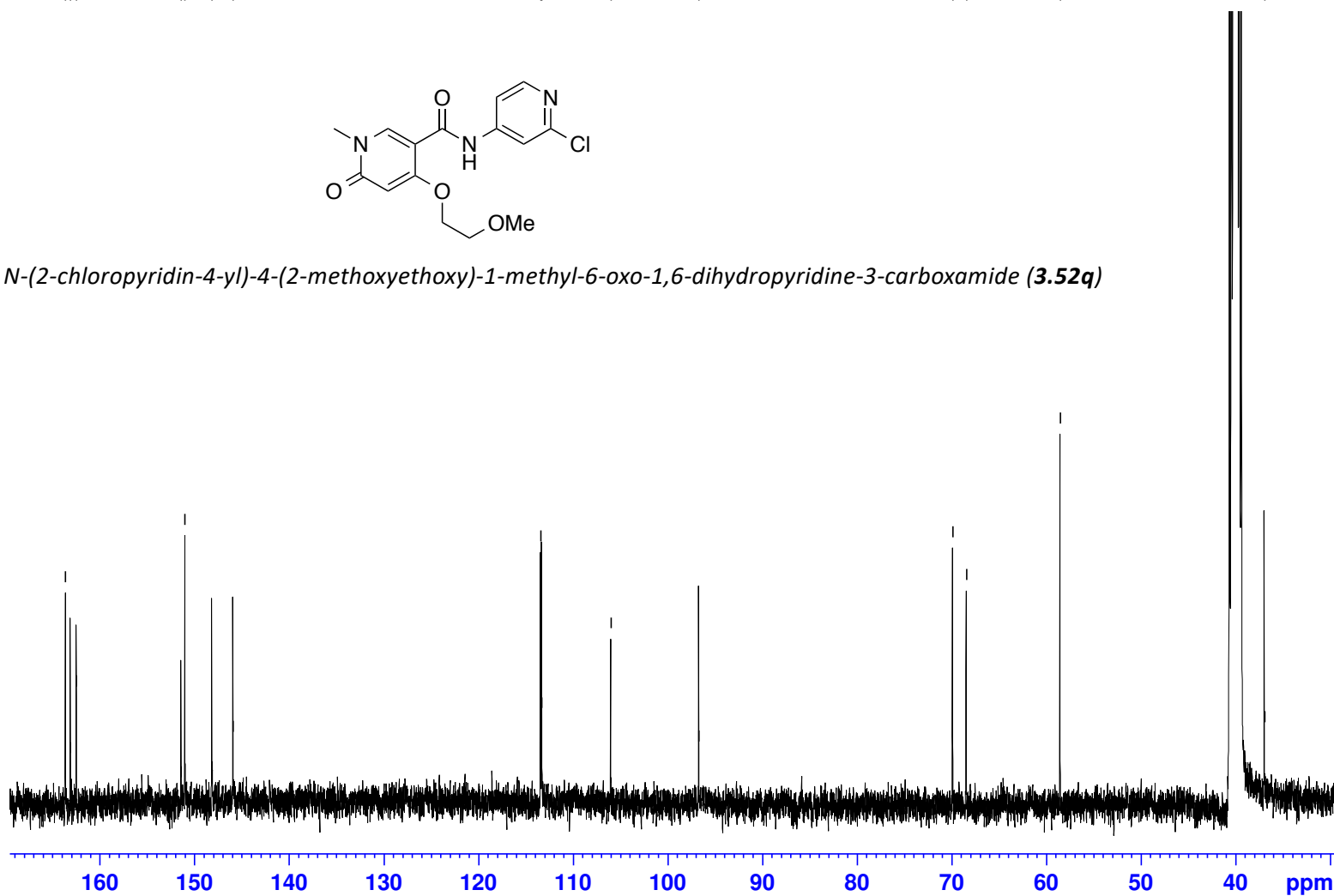
69.89  
68.45

58.53

36.95

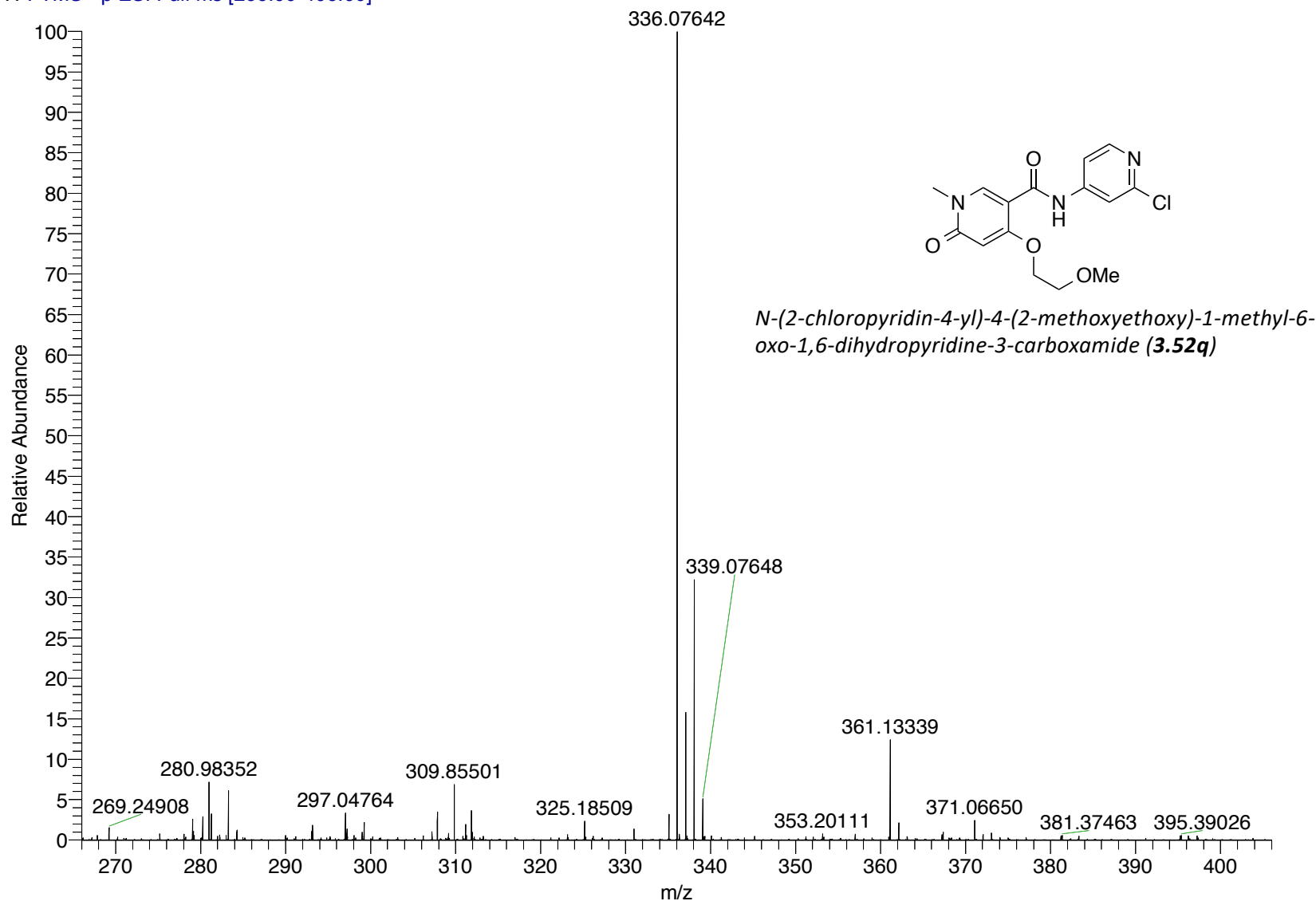


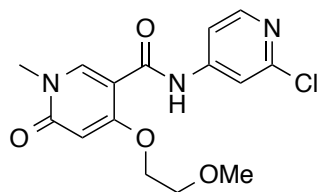
*N*-(2-chloropyridin-4-yl)-4-(2-methoxyethoxy)-1-methyl-6-oxo-1,6-dihydropyridine-3-carboxamide (**3.52q**)



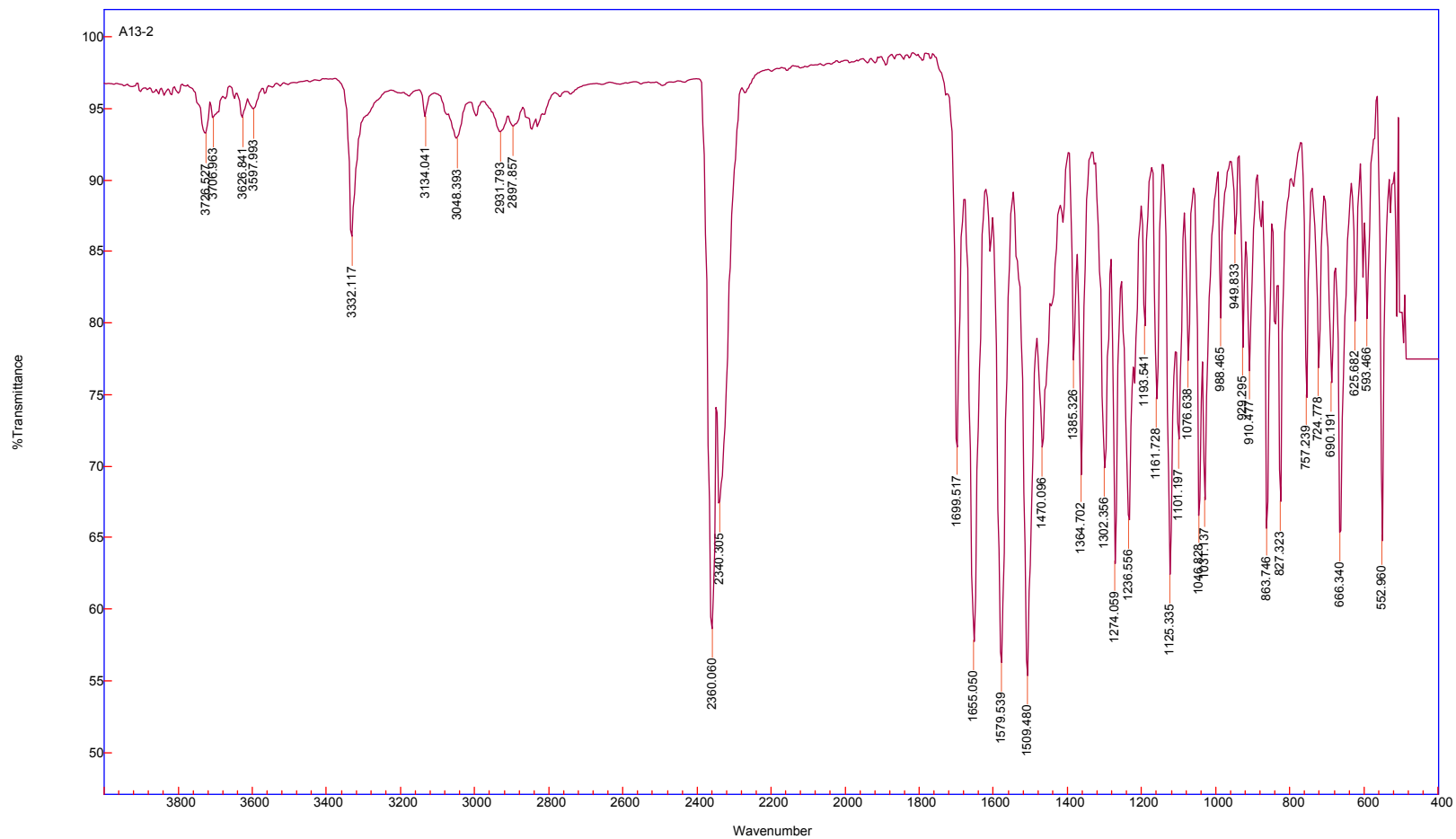
MZIP-Amide-A13-Dec14-2014-neg #17 RT: 0.30 AV: 1 NL: 3.36E6

T: FTMS - p ESI Full ms [266.00-406.00]



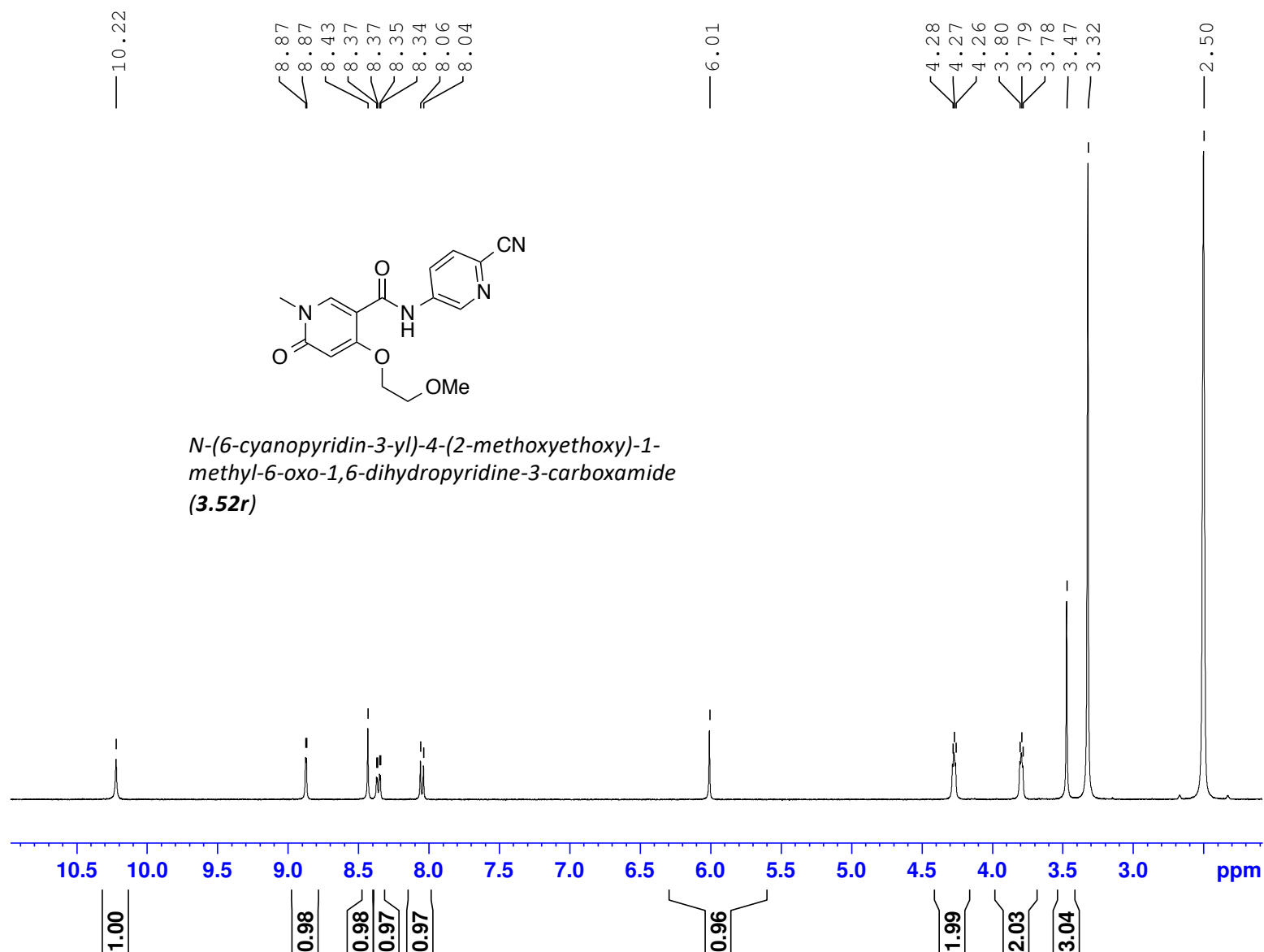


*N*-(2-chloropyridin-4-yl)-4-(2-methoxyethoxy)-1-methyl-6-oxo-1,6-dihydropyridine-3-carboxamide (**3.52q**)



MZP-Amide-A101-Feb2015-1H-NMR-DMSO

(400 MHz, 297.2 K, DMSO-d6)





(100 MHz, 297.2 K, DMSO-d6)

MZP101-13CBB-NMR-DMSO-57h

163.21  
162.68  
161.90

145.43  
142.30  
138.52

129.77  
126.23  
126.19

117.65

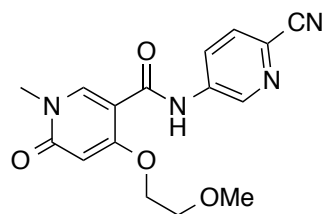
105.52

96.27

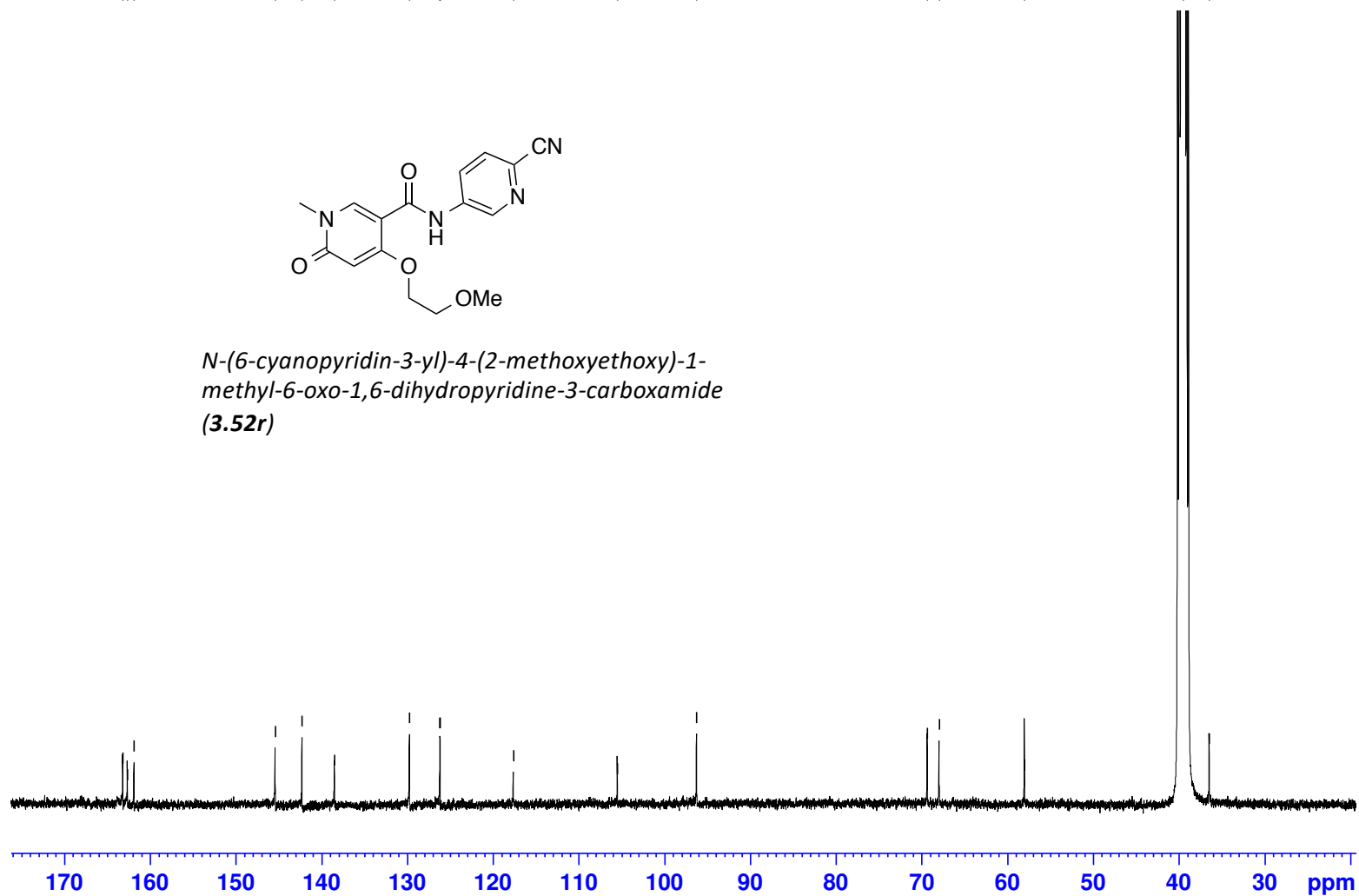
69.37  
67.97

58.03

39.51  
36.47

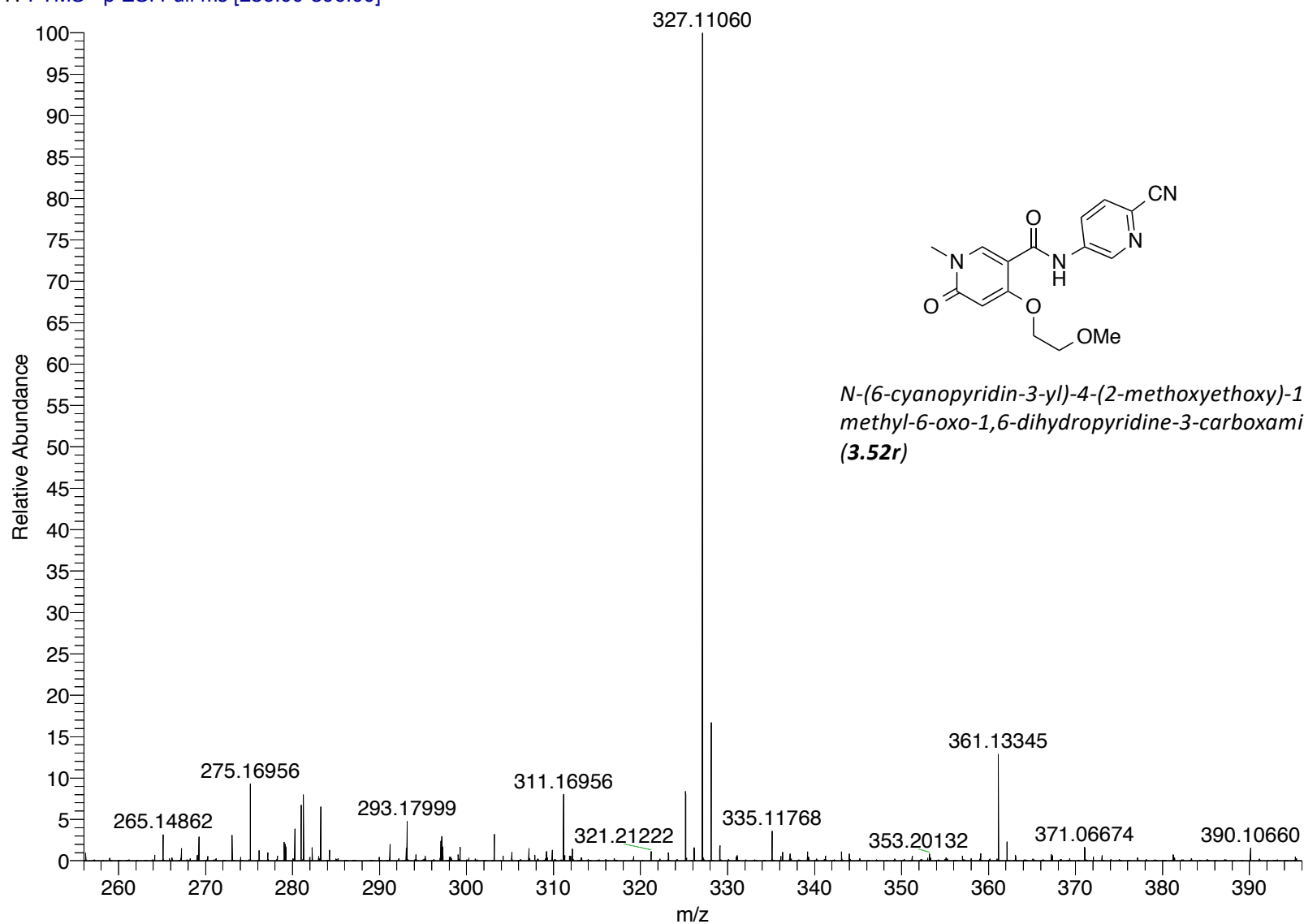


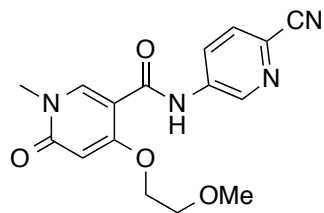
*N*-(6-cyanopyridin-3-yl)-4-(2-methoxyethoxy)-1-methyl-6-oxo-1,6-dihydropyridine-3-carboxamide  
**(3.52r)**



MZP-Amide-A101-Feb15-2015-neg #7 RT: 0.12 AV: 1 NL: 7.97E6

T: FTMS - p ESI Full ms [256.00-396.00]

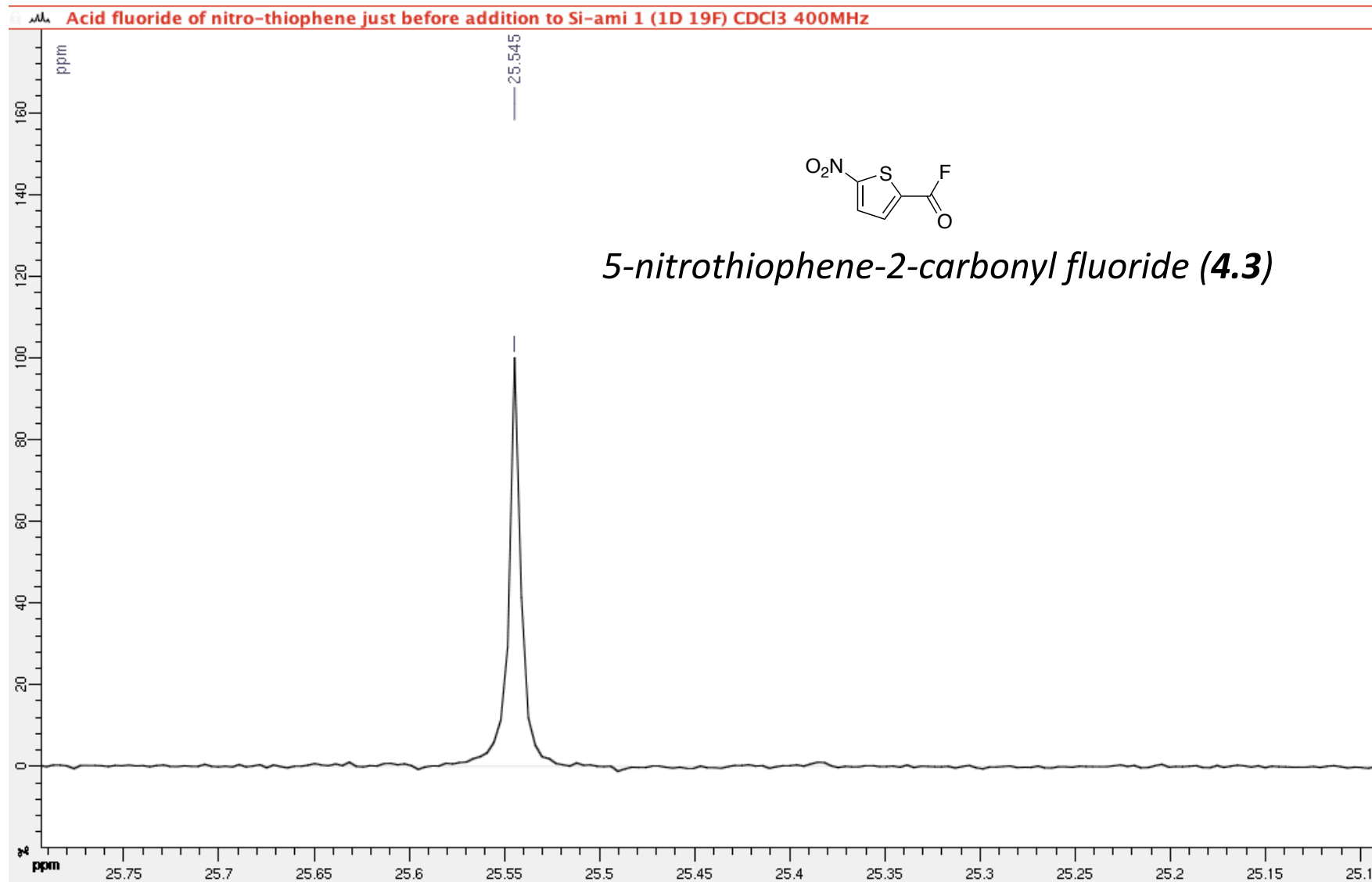




*N*-(6-cyanopyridin-3-yl)-4-(2-methoxyethoxy)-1-methyl-6-oxo-1,6-dihydropyridine-3-carboxamide (**3.52r**)



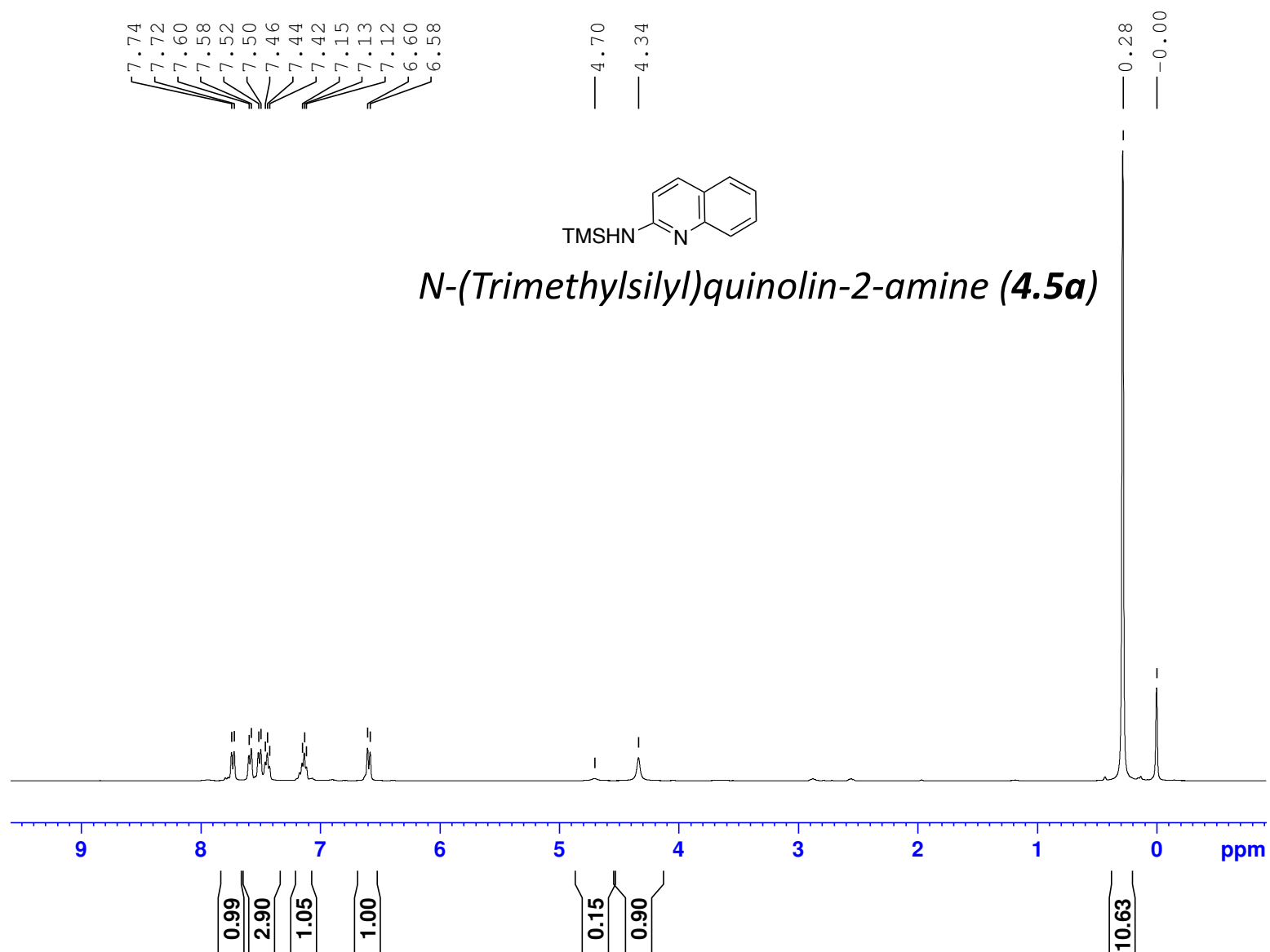
(400 MHz, 297.2 K, CDCl<sub>3</sub>)



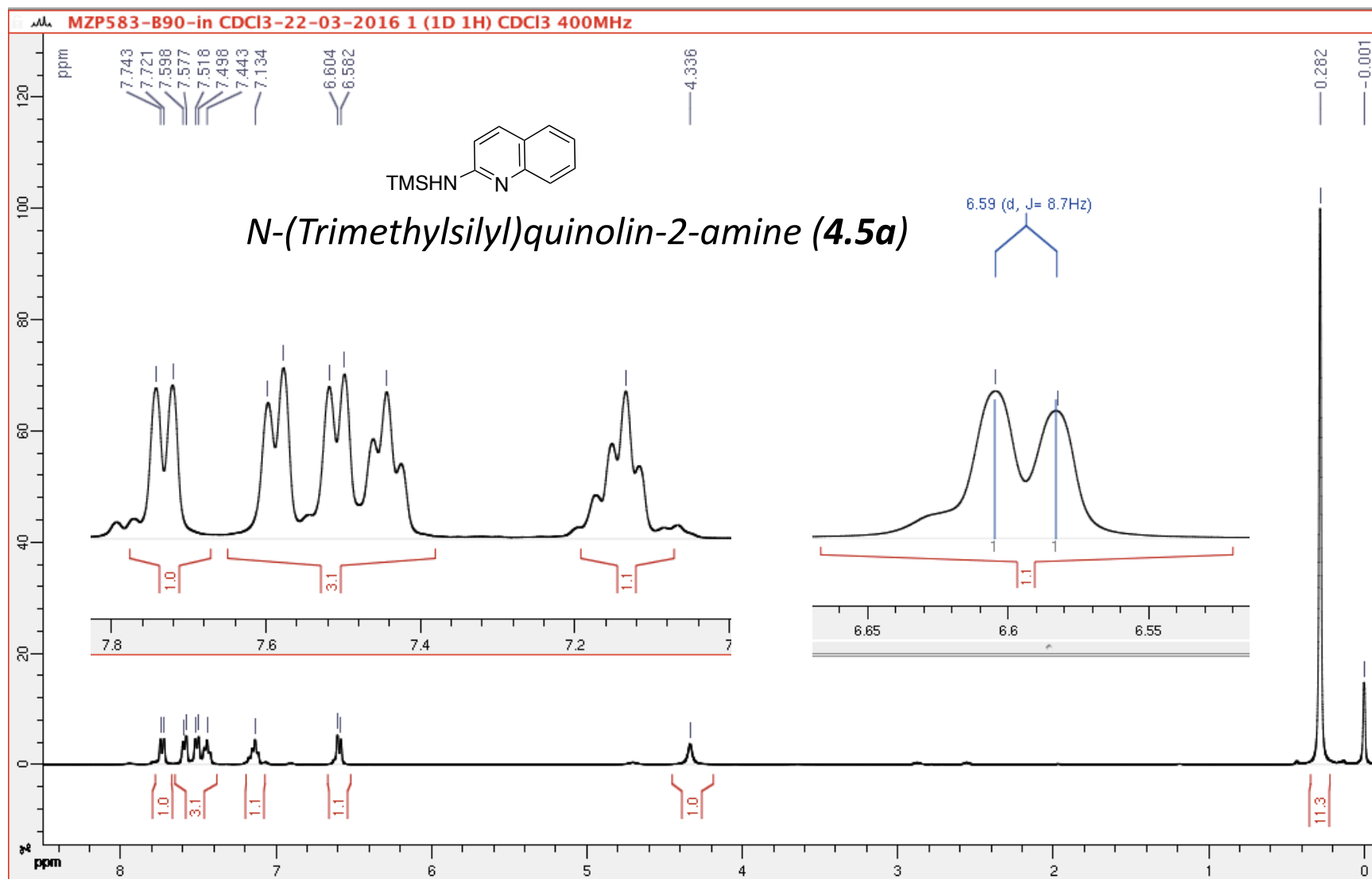
MZP583-B90-4h-90% conversion-in CDCl<sub>3</sub>-22-03-2016

(400 MHz, 297.2 K, CDCl<sub>3</sub>)

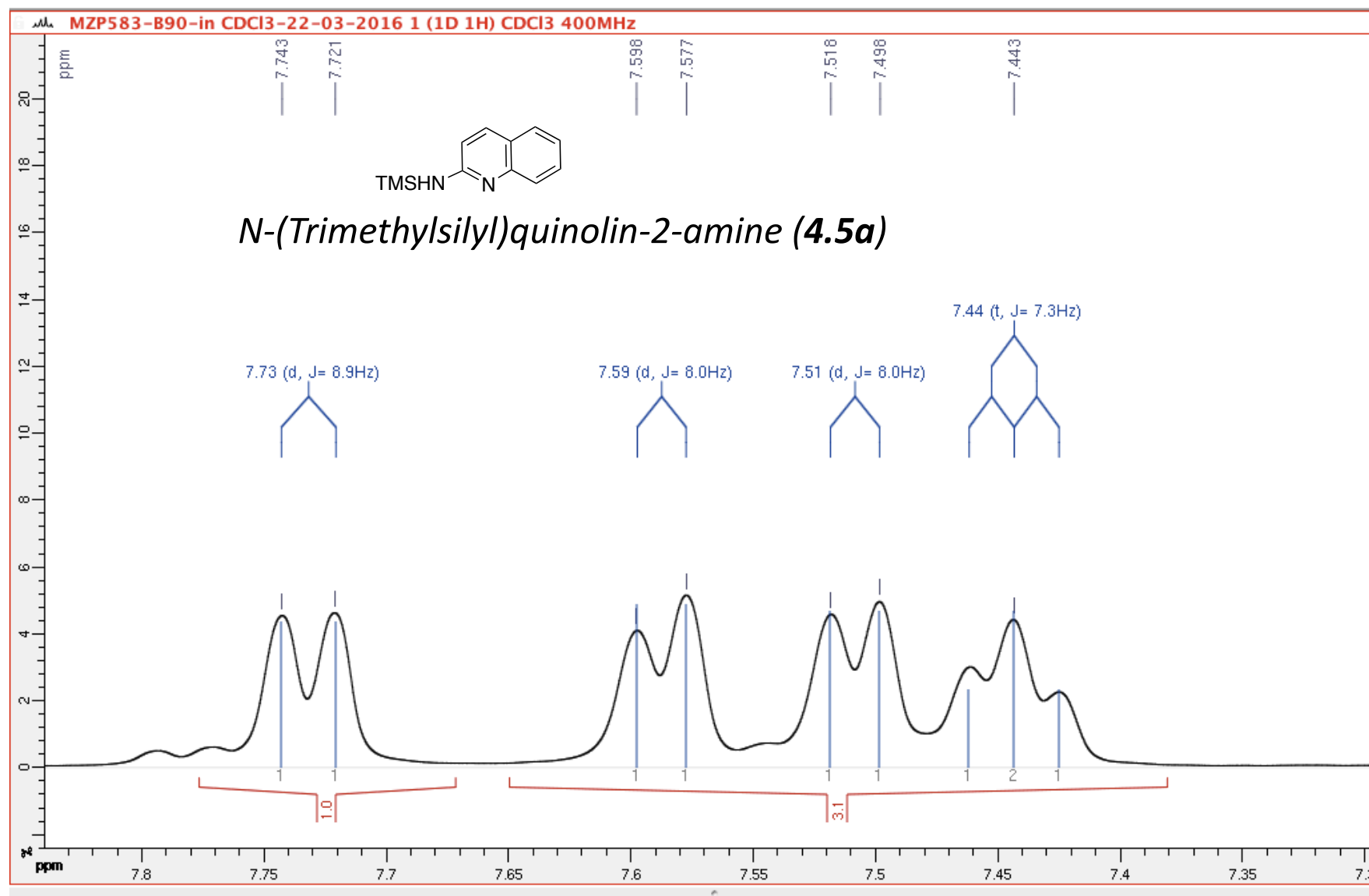
TMS-GPS439



(400 MHz, 297.2 K, CDCl<sub>3</sub>) TMS-GPS439



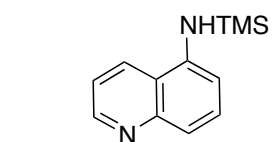
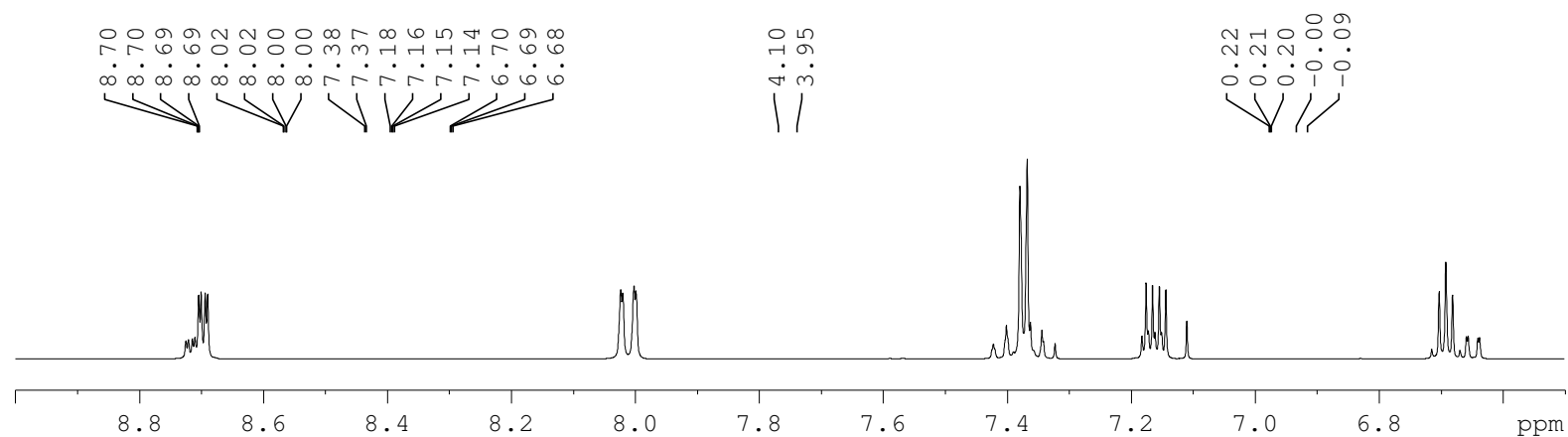
(400 MHz, 297.2 K, CDCl<sub>3</sub>) TMS-GPS439



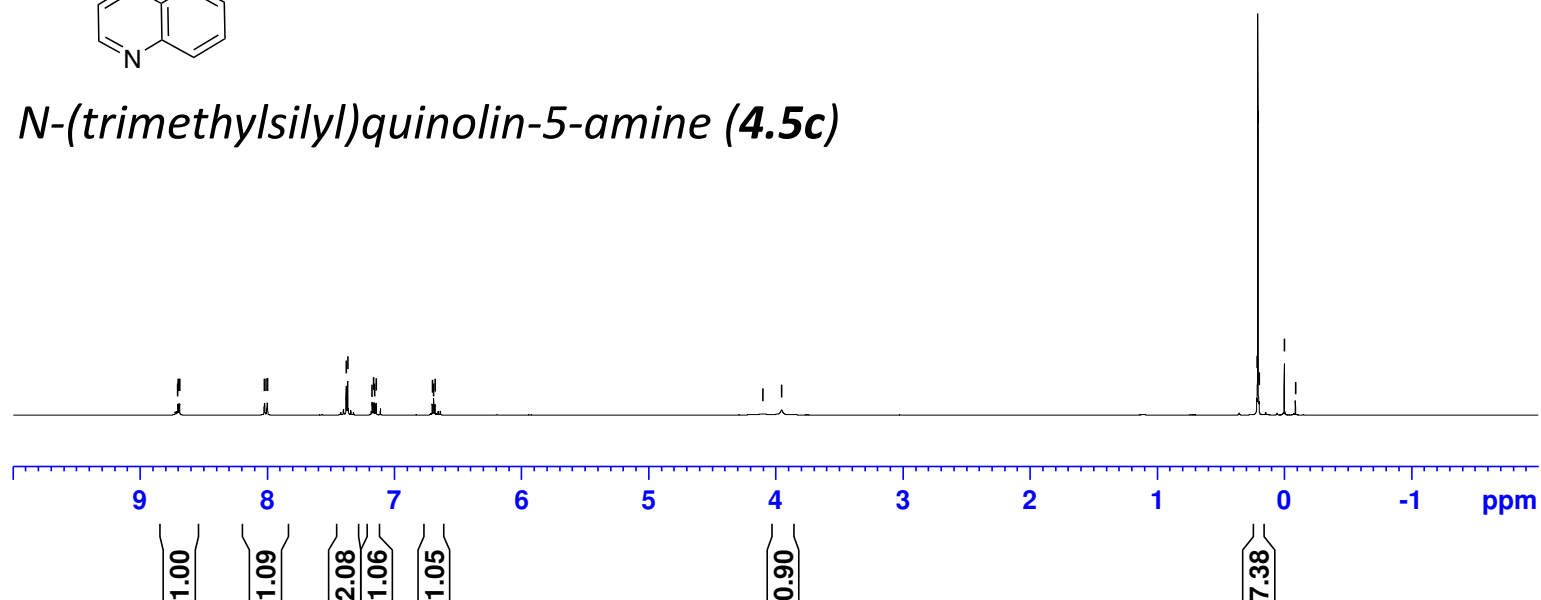
TMS-GPS466-MZP593-B99-1H-NMR-Aug-10-2016

(400 MHz, 297.2 K, CDCl<sub>3</sub>)

TMS-GPS466



*N*-(trimethylsilyl)quinolin-5-amine (**4.5c**)

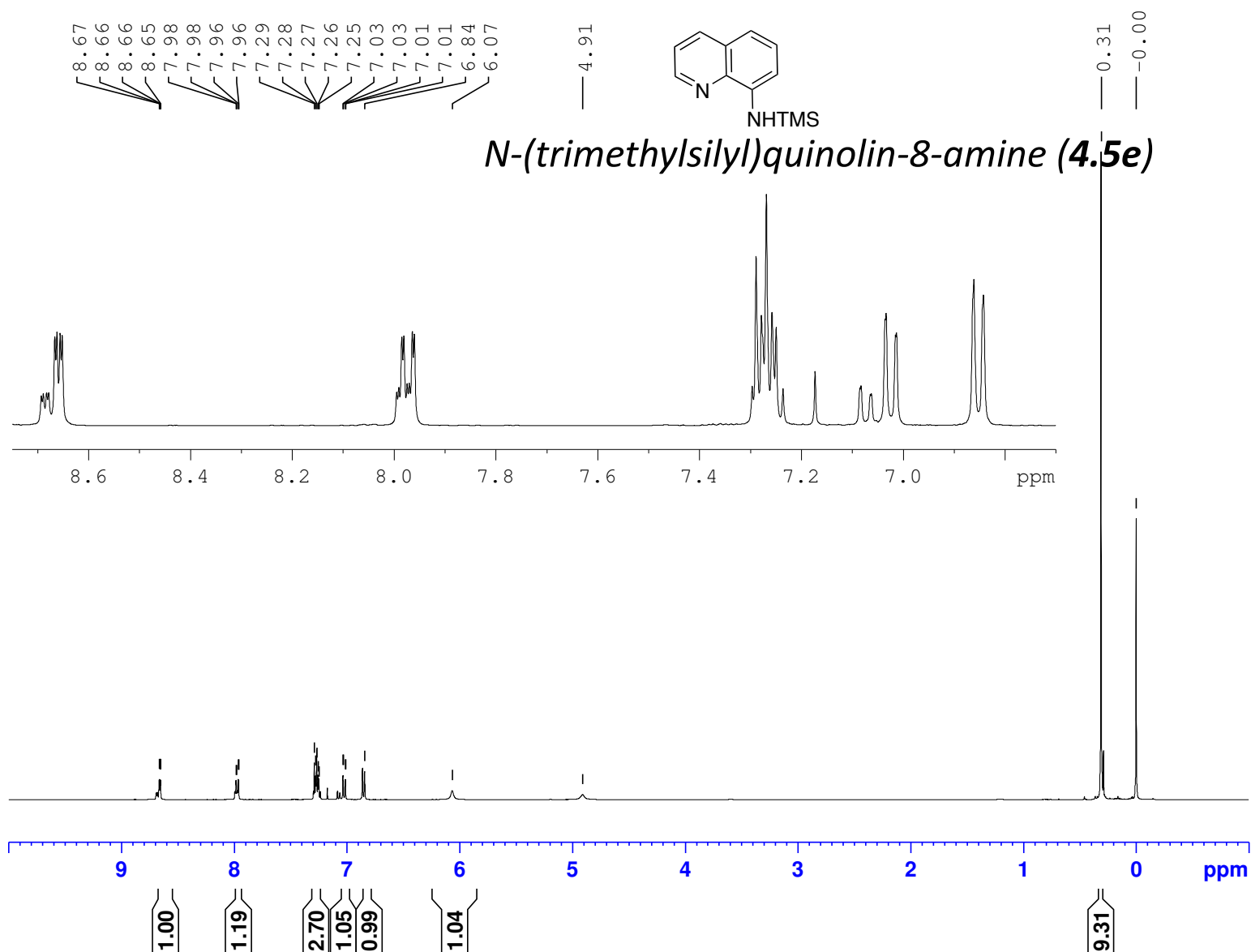




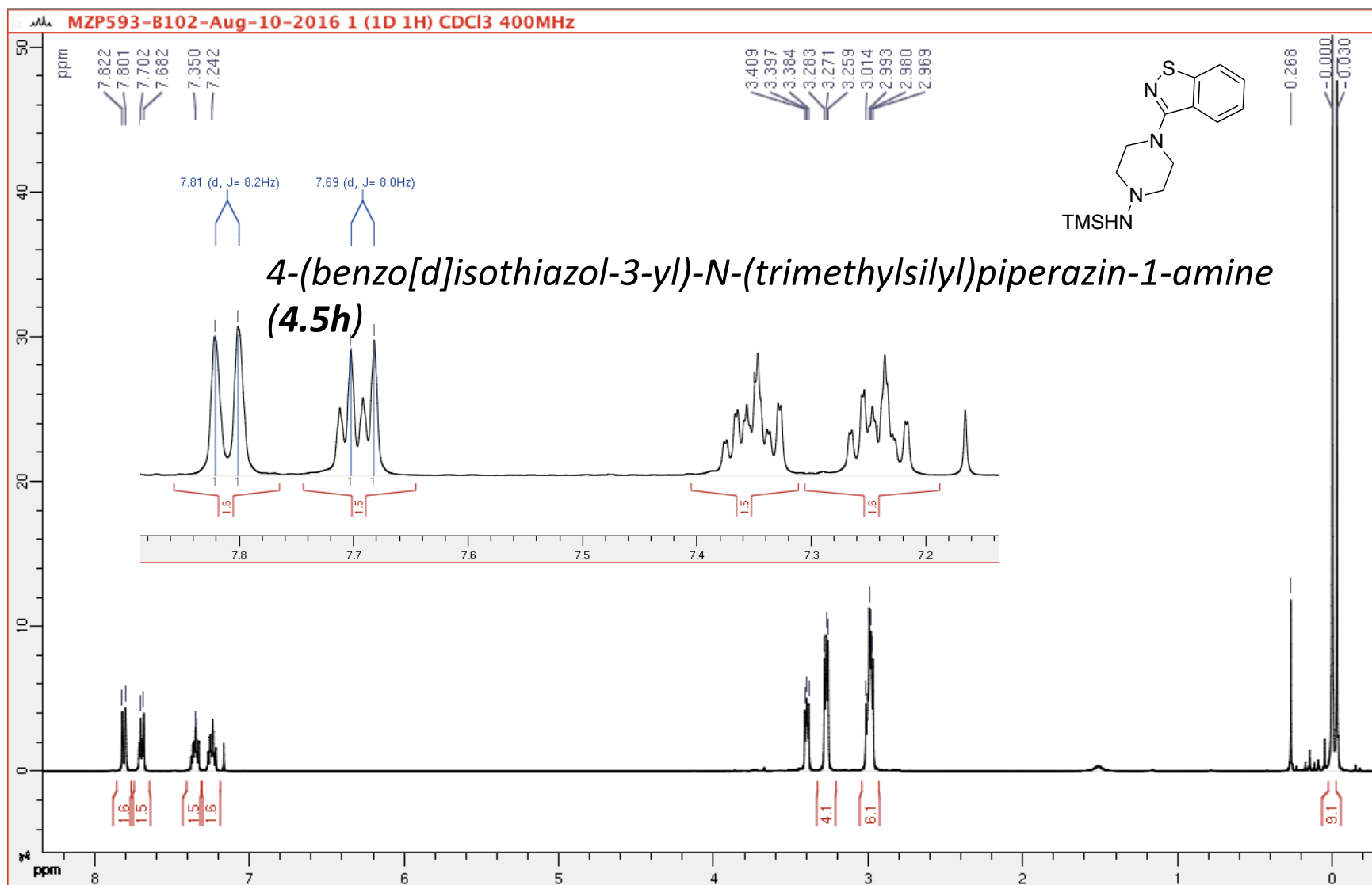
TMS-GPS468-MZP593-B100-1H-NMR-Aug-10-2016

(400 MHz, 297.2 K, CDCl<sub>3</sub>)

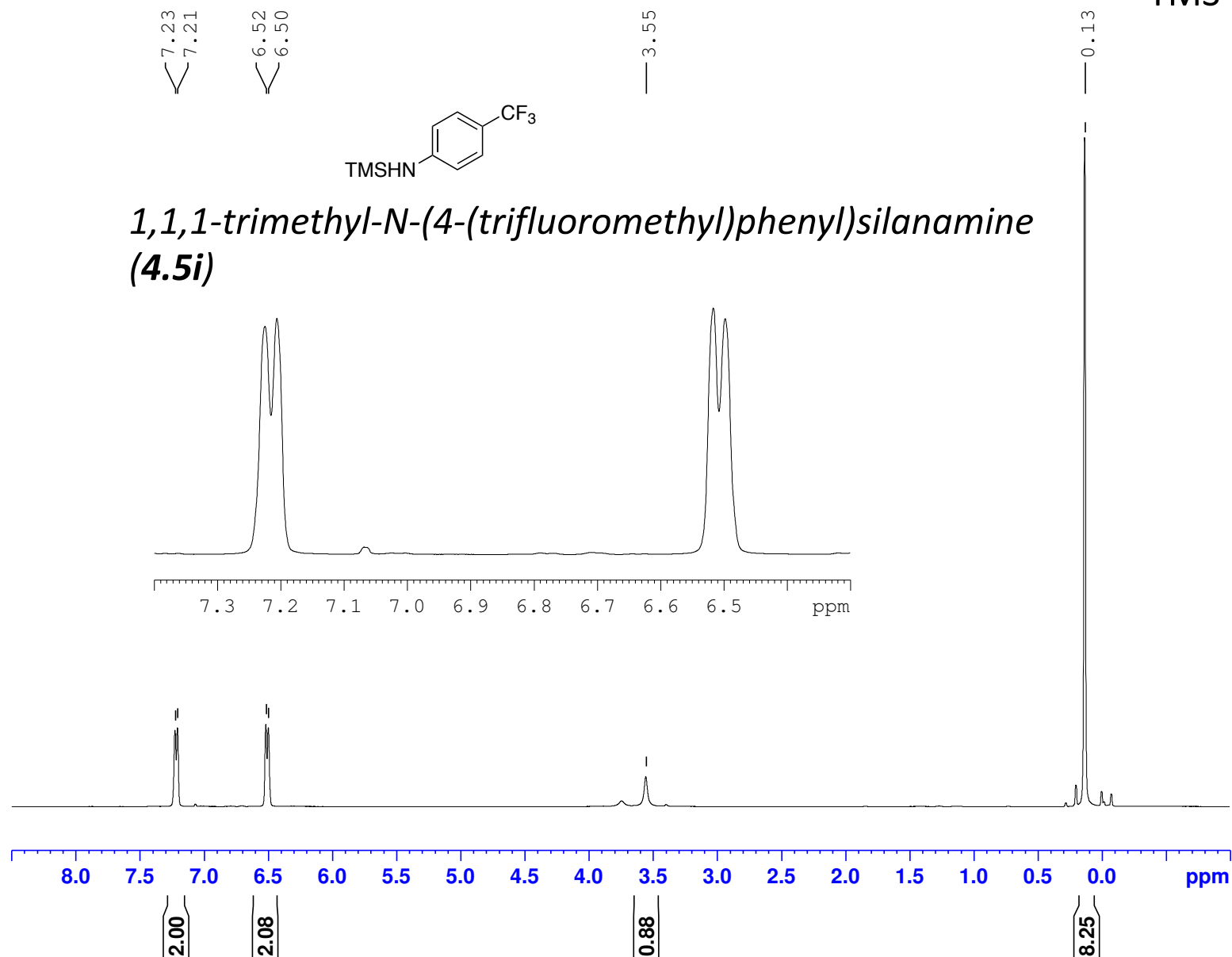
TMS-GPS468



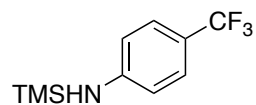
(400 MHz, 297.2 K, CDCl<sub>3</sub>) TMS-GPS431



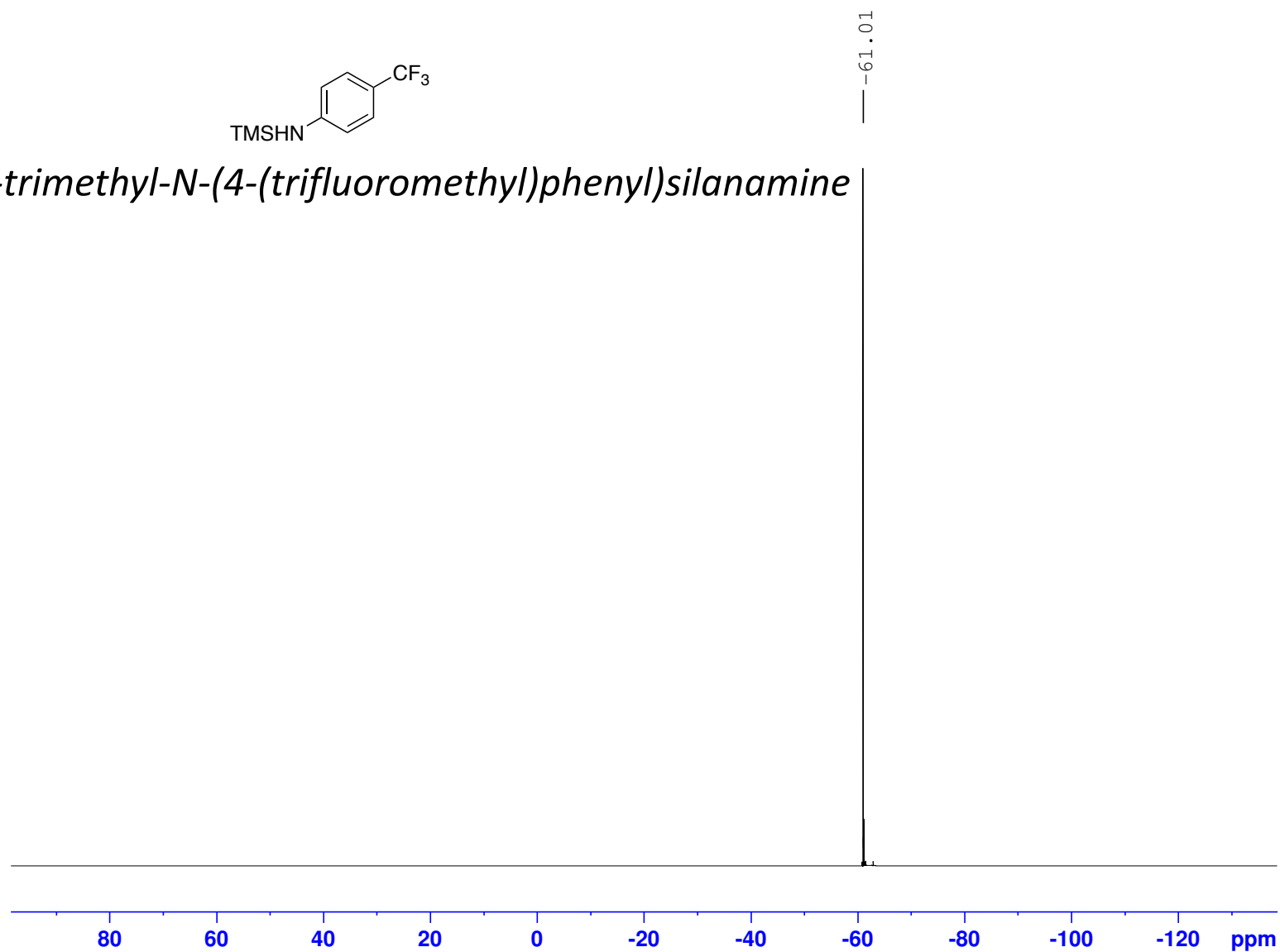
MZP570-B81-88% conversion-ON-in CDCl<sub>3</sub>-1H-NMR-07-03-2016 (400 MHz, 297.2 K, CDCl<sub>3</sub>) TMS-GPS431



MZP570-B81-88% conversion-ON-in CDCl<sub>3</sub>-19F-NMR-07-03-2016 (400 MHz, 297.2 K, CDCl<sub>3</sub>)TMS-GPS431



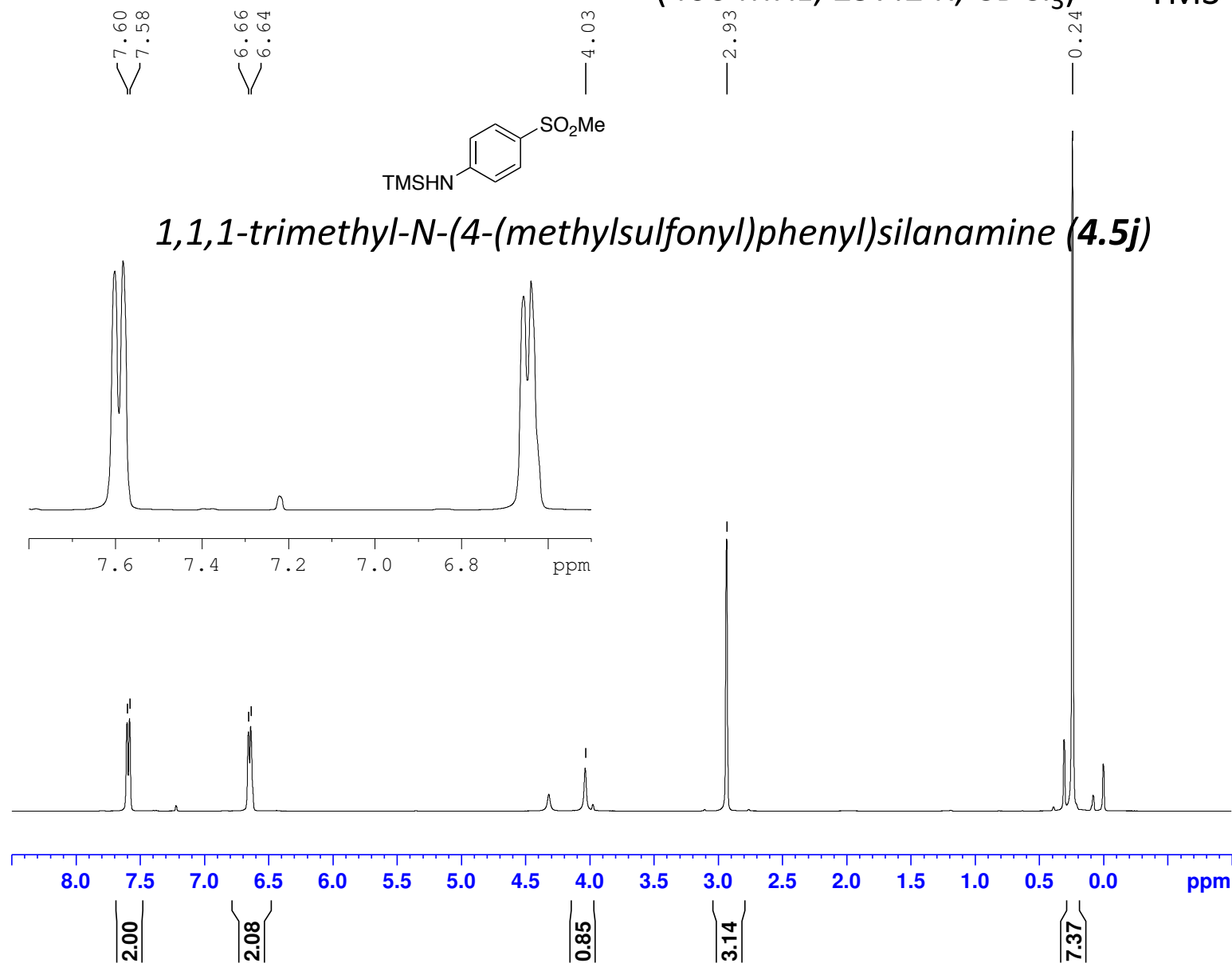
*1,1,1-trimethyl-N-(4-(trifluoromethyl)phenyl)silanamine*  
**(4.5i)**



MZP569-B89-ON-1H-NMR-in CDC13-04-03-2016

(400 MHz, 297.2 K, CDCl<sub>3</sub>)

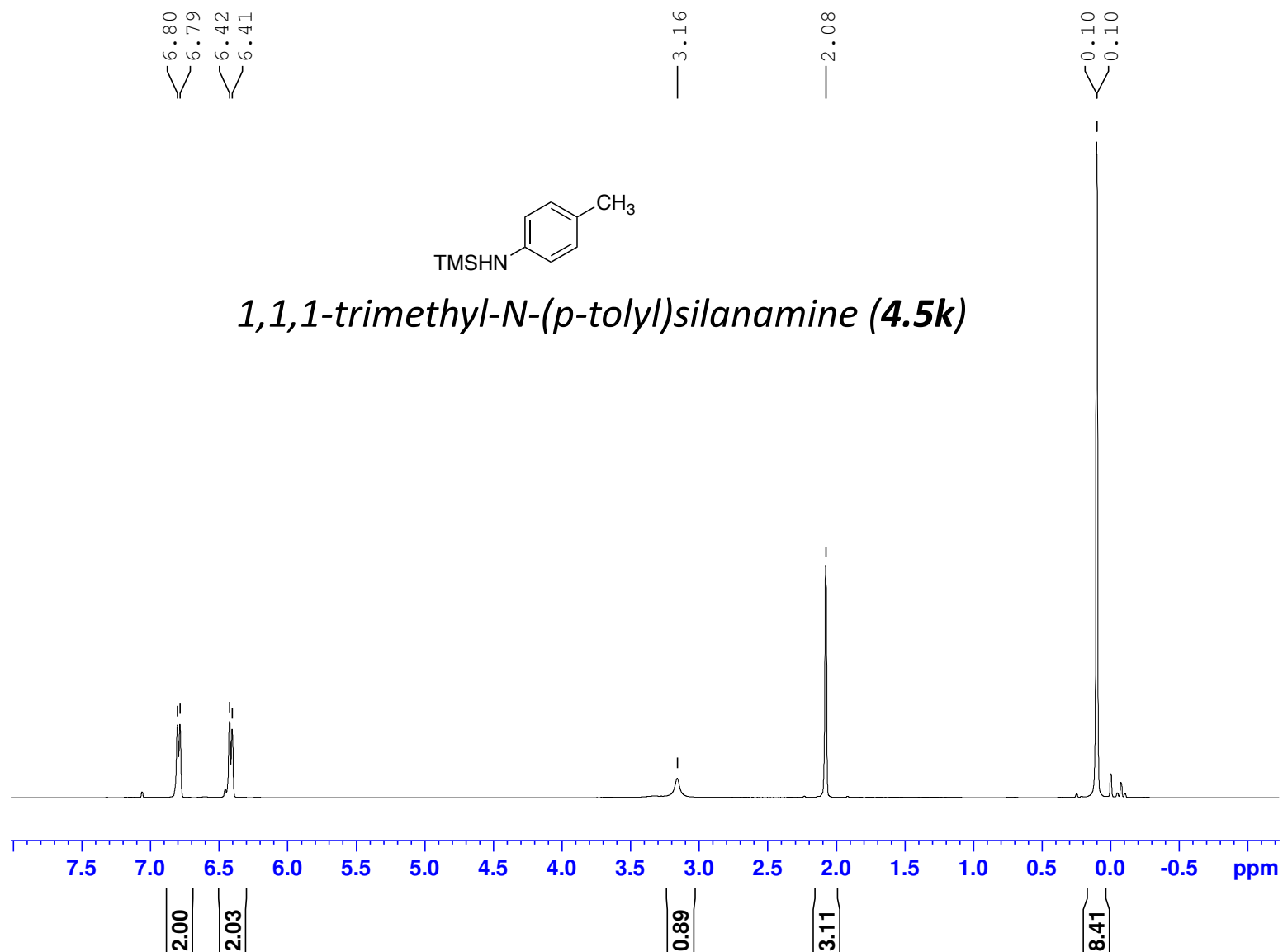
TMS-GPS438



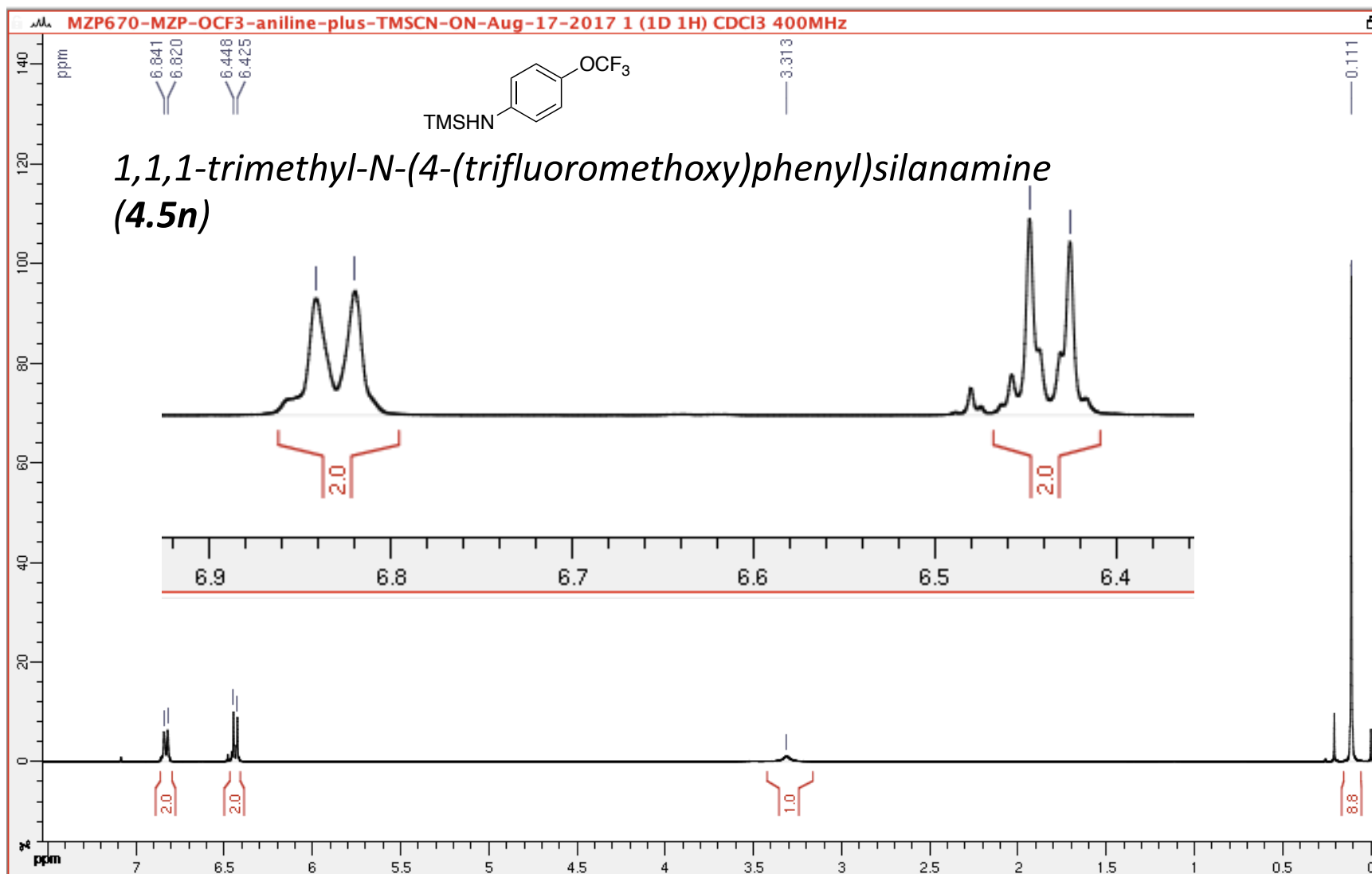
MZP568-B85-2h-1H-NMR-in CDCl3-03-03-2016

(400 MHz, 297.2 K, CDCl<sub>3</sub>)

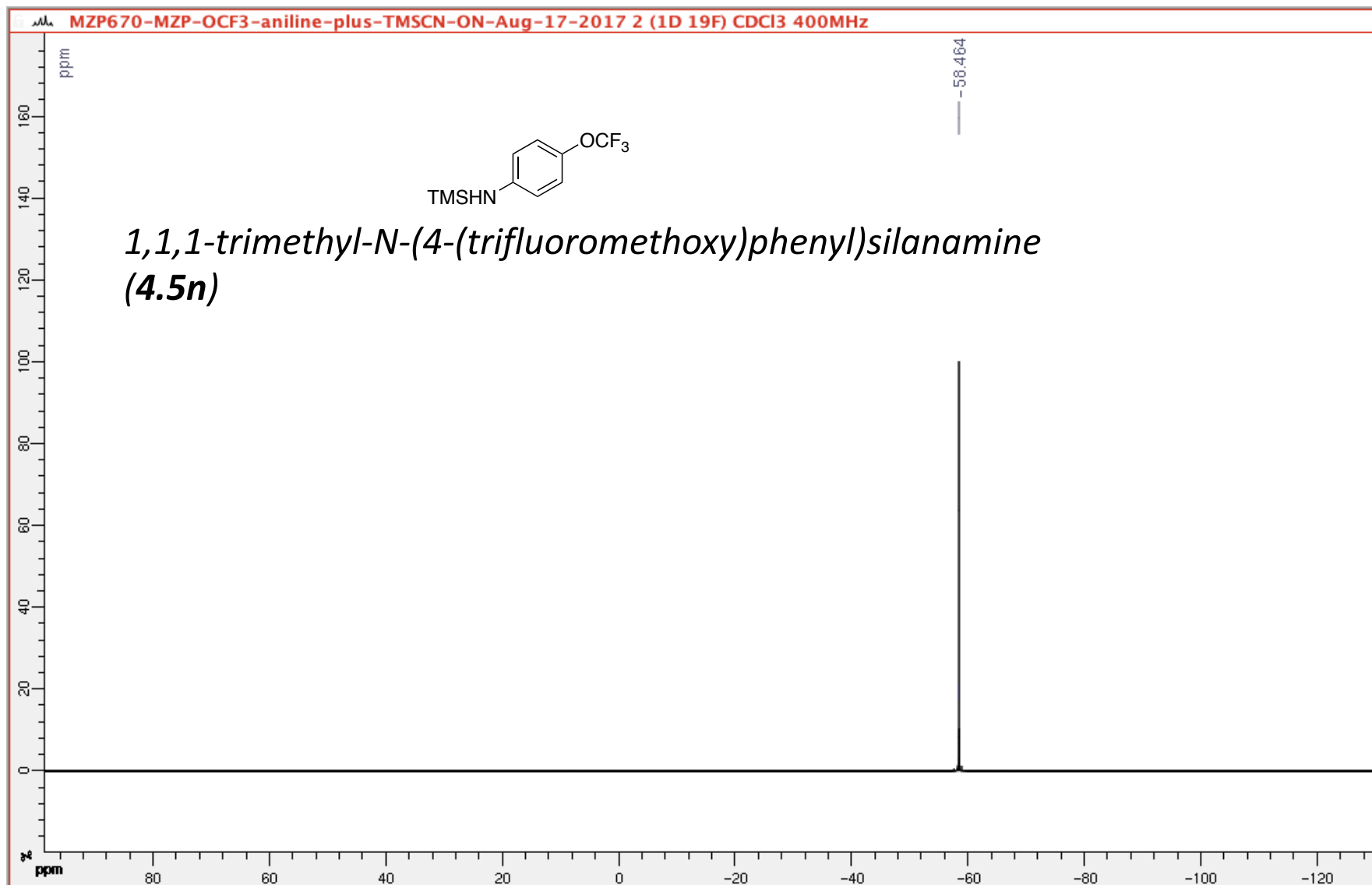
TMS-GPS434



(400 MHz, 297.2 K, CDCl<sub>3</sub>) TMS-GPS514



(400 MHz, 297.2 K, CDCl<sub>3</sub>) TMS-GPS514





TMS-GPS495-MZP593-B105-1H-NMR

(400 MHz, 297.2 K, CDCl<sub>3</sub>)

TMS-GPS495

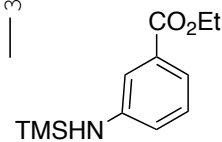
7.25  
7.24  
7.24  
7.23  
7.22  
7.20  
7.19  
7.19  
7.05  
7.03  
7.01  
6.69  
6.69  
6.68  
6.68  
6.67  
6.66  
6.66

4.22  
4.20  
4.18  
4.16

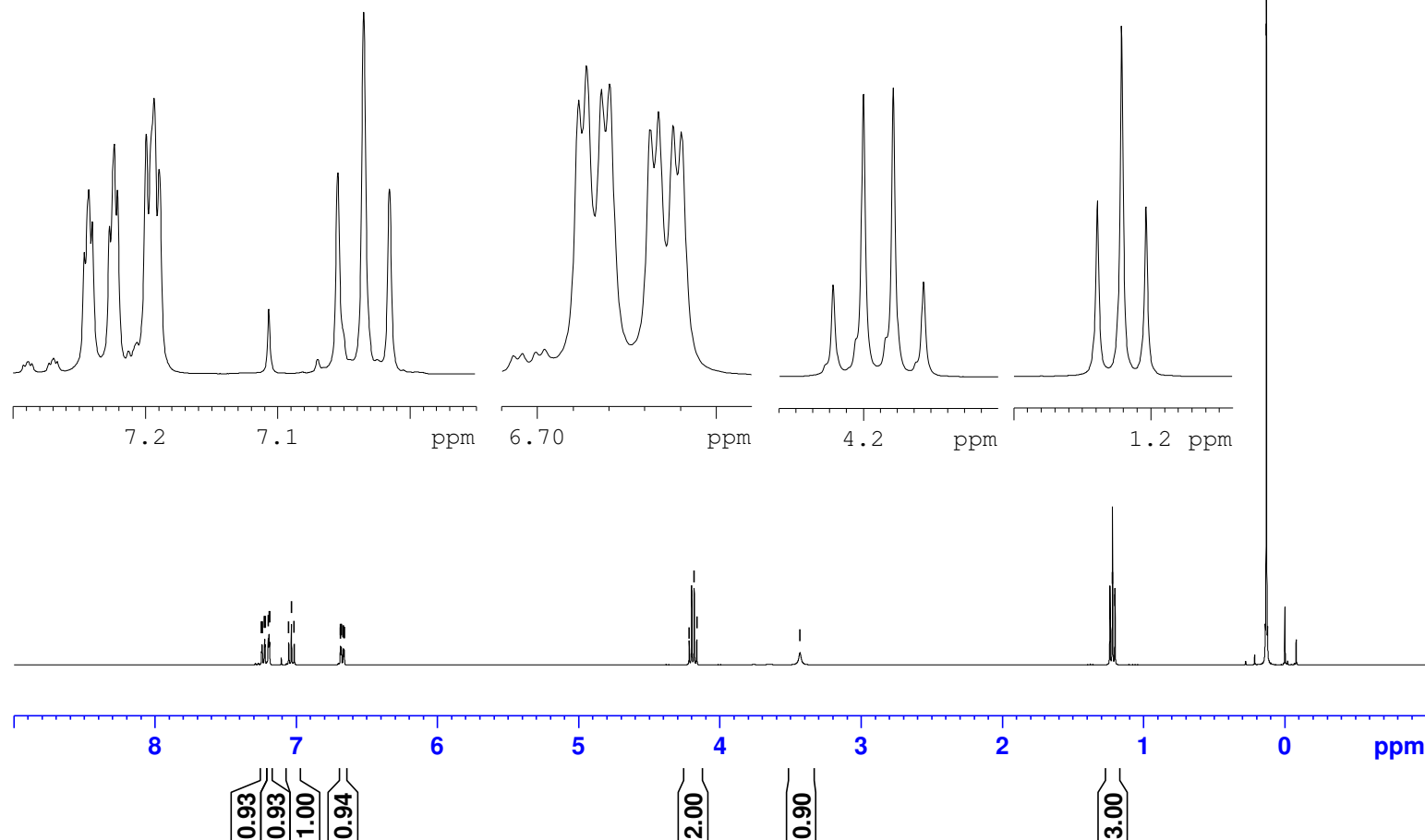
3.44

1.24  
1.22  
1.20

0.13

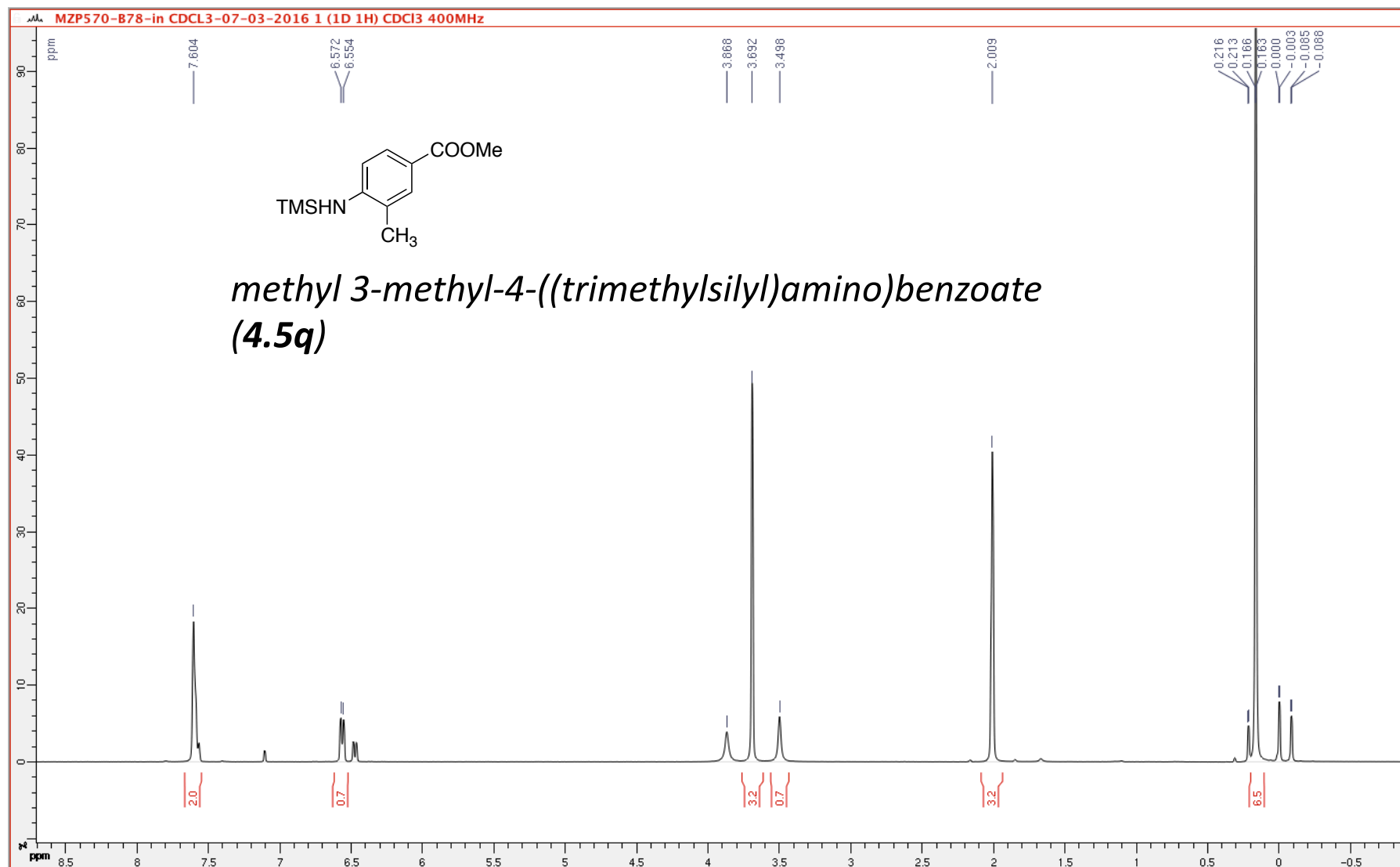


*ethyl 3-((trimethylsilyl)amino)benzoate (4.5p)*



(400 MHz, 297.2 K, CDCl<sub>3</sub>)

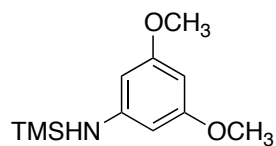
TMS-GPS429



MZP133\_Si-0001\_CDCl3

(400 MHz, 297.2 K, CDCl<sub>3</sub>)

TMS-GPS400

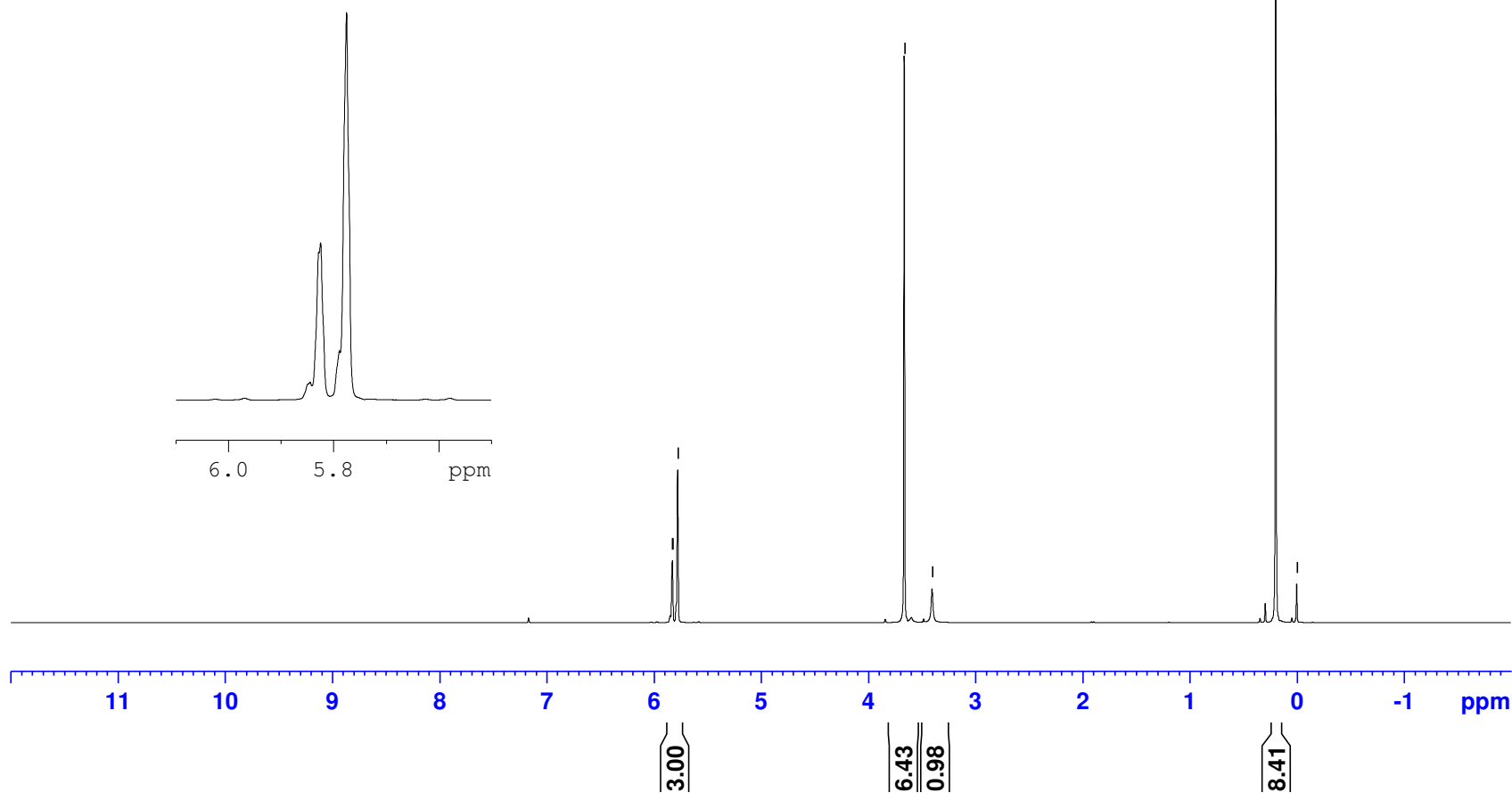


5.83  
5.82  
5.78

3.66  
3.40

0.20  
-0.00

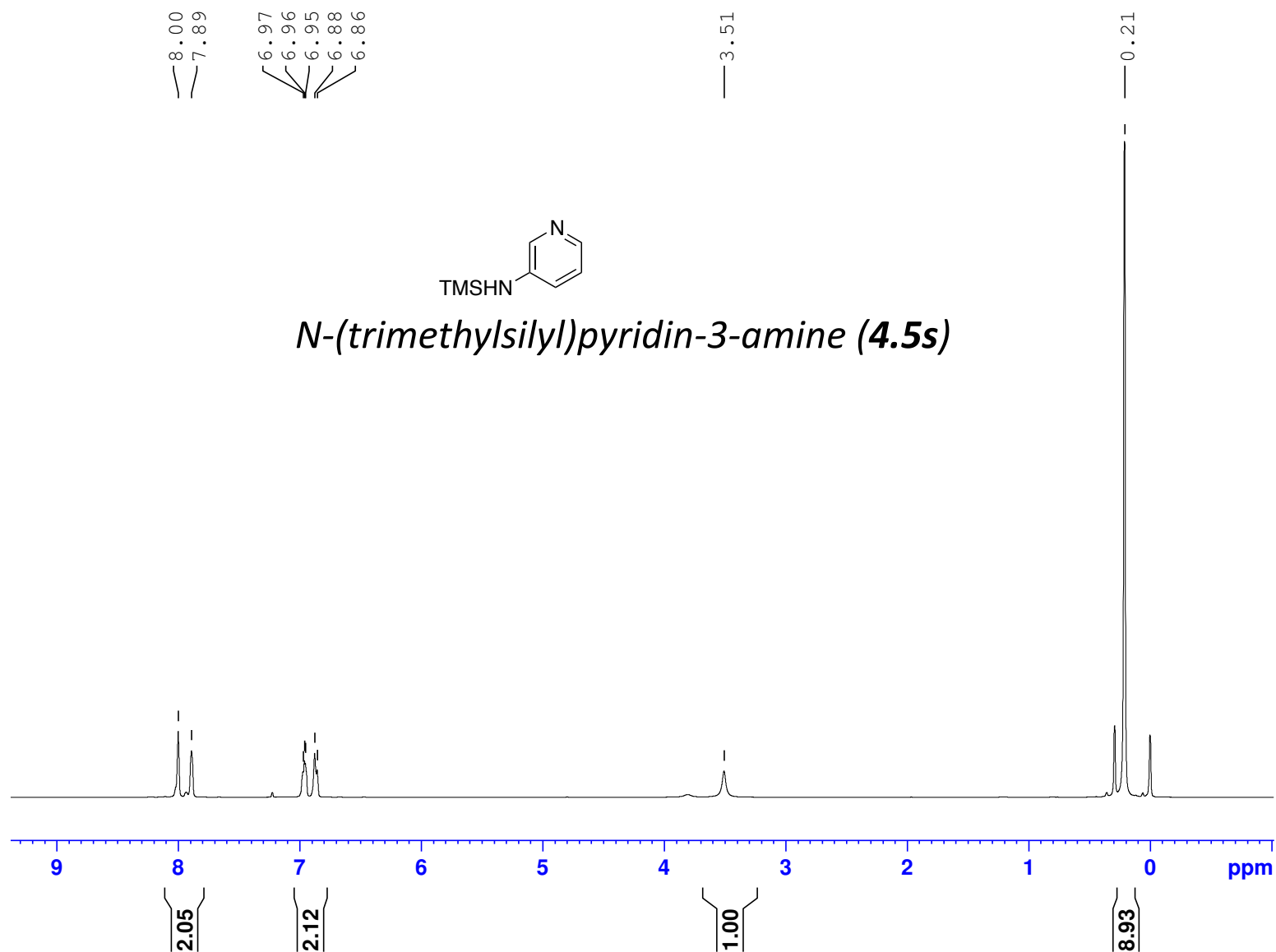
*N*-(3,5-dimethoxyphenyl)-1,1,1-trimethylsilanamine (**4.5r**)



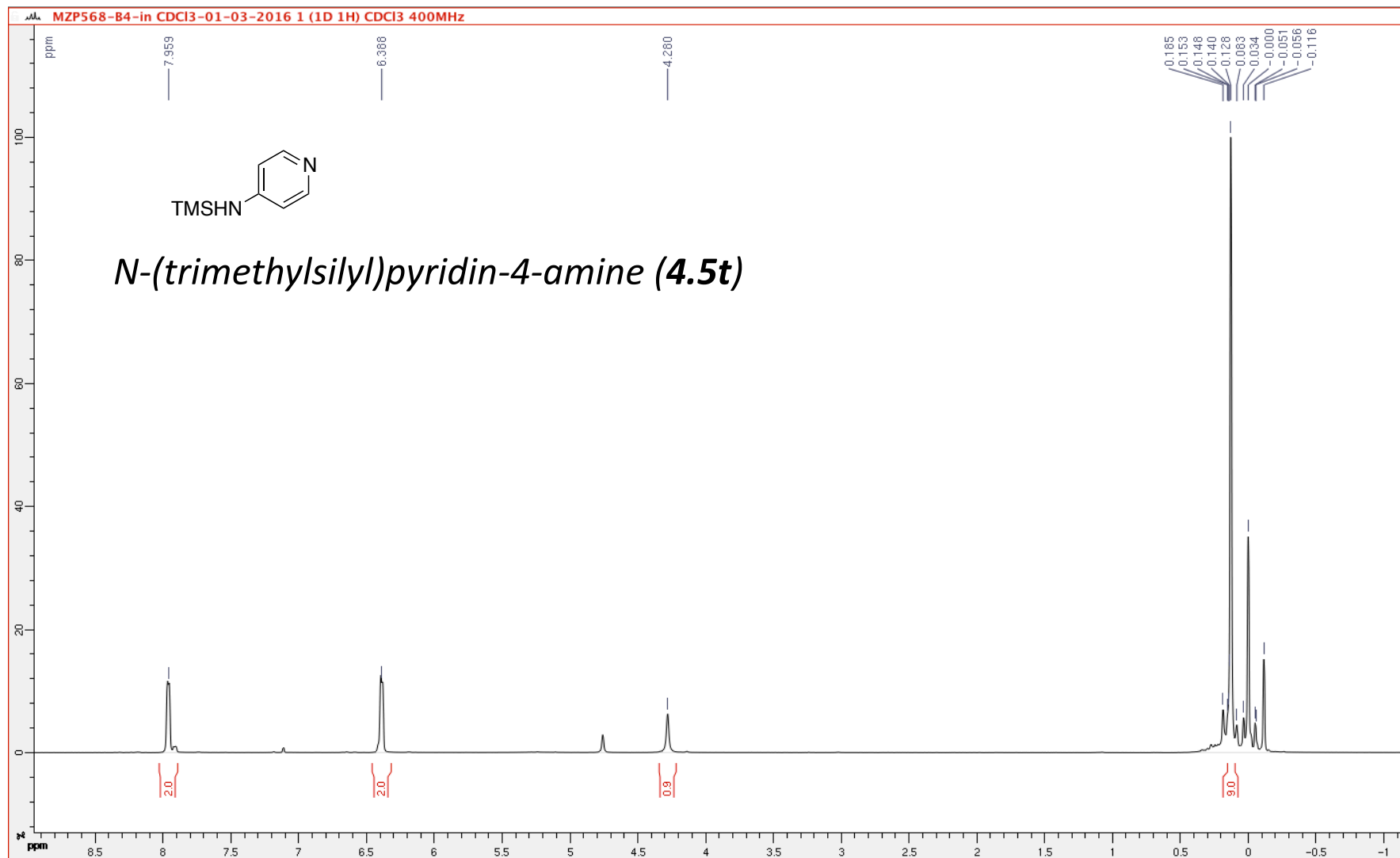
MZP569-B3-4h-1H-NMR-in CDCl<sub>3</sub>-03-03-2016

(400 MHz, 297.2 K, CDCl<sub>3</sub>)

TMS-GPS424



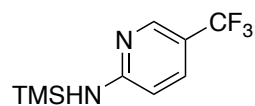
(400 MHz, 297.2 K, CDCl<sub>3</sub>) TMS-GPS425



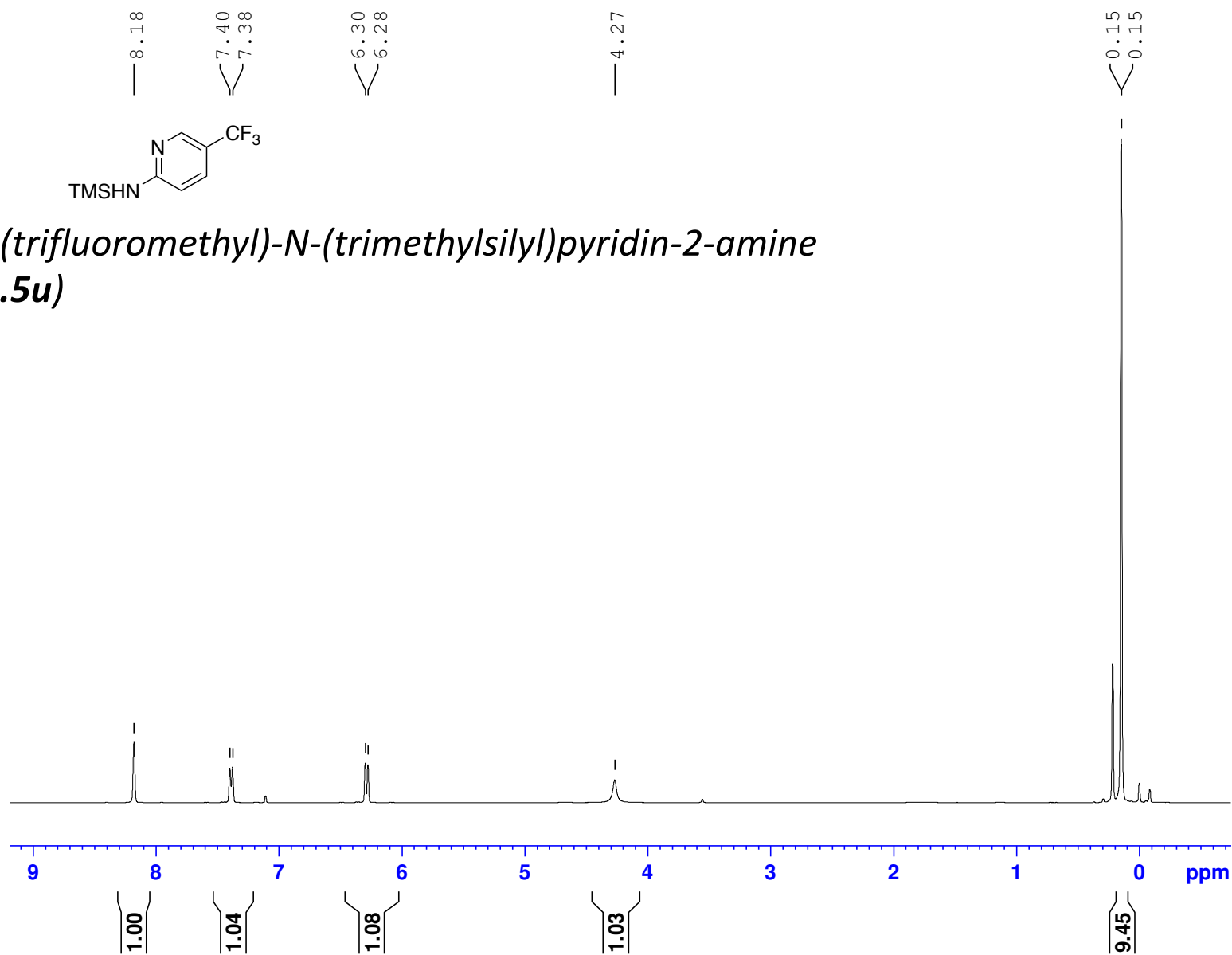
MZP569-B83-4h-1H-NMR-in CDCl<sub>3</sub>-03-03-2016

(400 MHz, 297.2 K, CDCl<sub>3</sub>)

TMS-GPS432



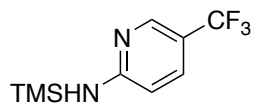
*5-(trifluoromethyl)-N-(trimethylsilyl)pyridin-2-amine*  
**(4.5u)**



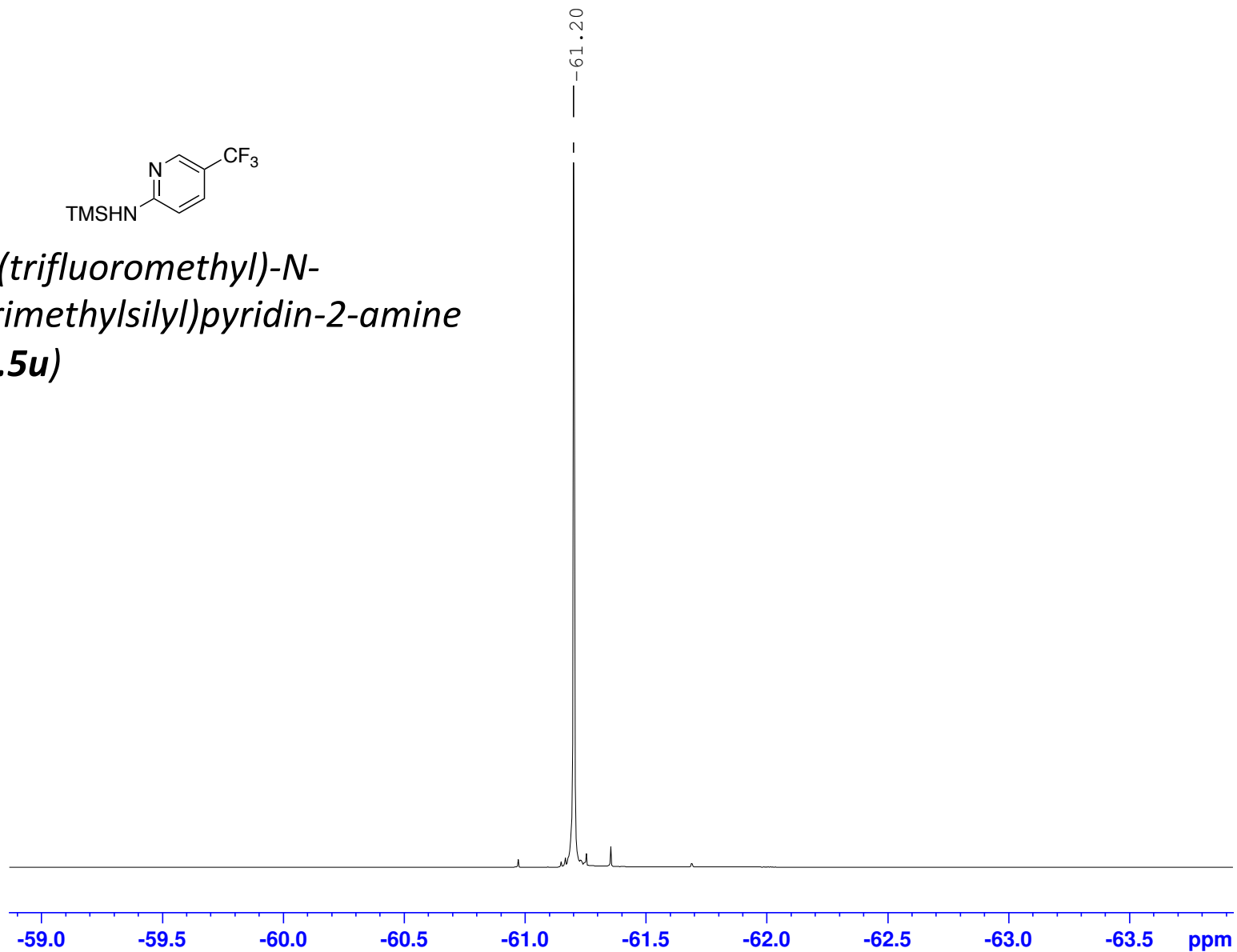
MZP569-B83-4h-19F-NMR-in CDCl<sub>3</sub>-03-03-2016

(400 MHz, 297.2 K, CDCl<sub>3</sub>)

TMS-GPS432



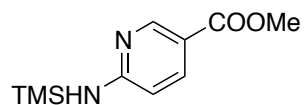
*5-(trifluoromethyl)-N-(trimethylsilyl)pyridin-2-amine*  
**(4.5u)**



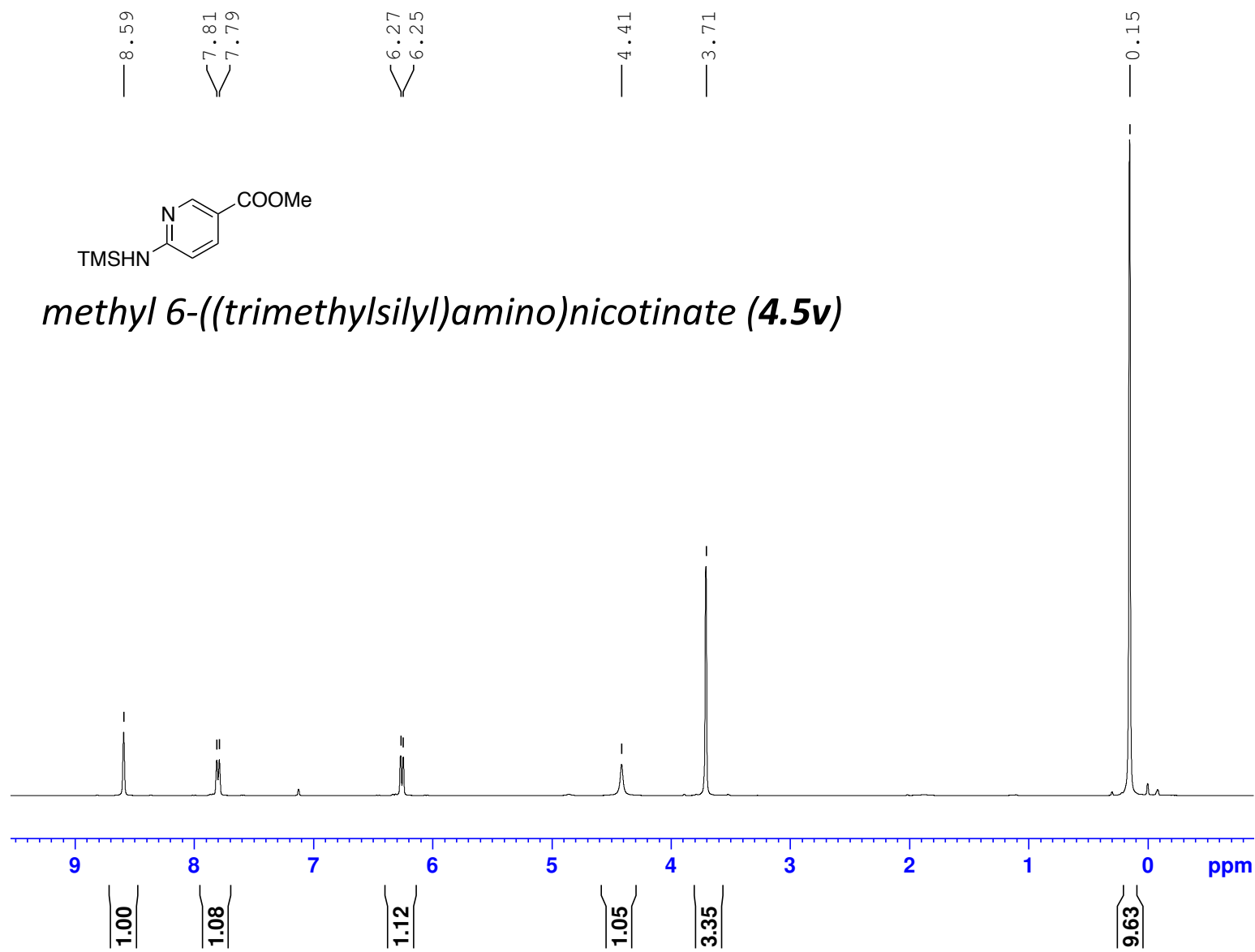
MZP568-B80-2h-1H-NMR-in CDCl3-03-03-2016

(400 MHz, 297.2 K, CDCl<sub>3</sub>)

TMS-GPS430



*methyl 6-((trimethylsilyl)amino)nicotinate (4.5v)*

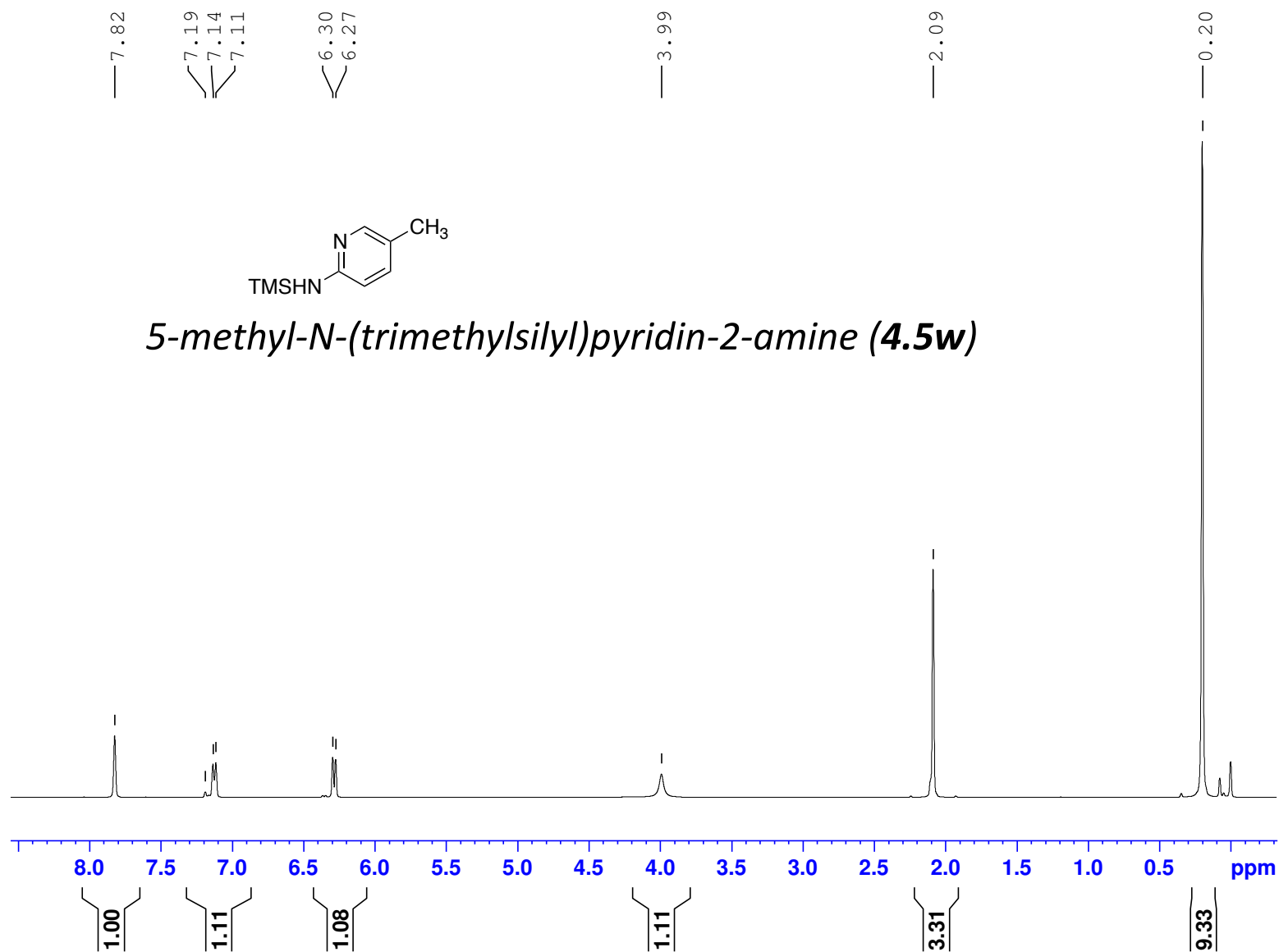




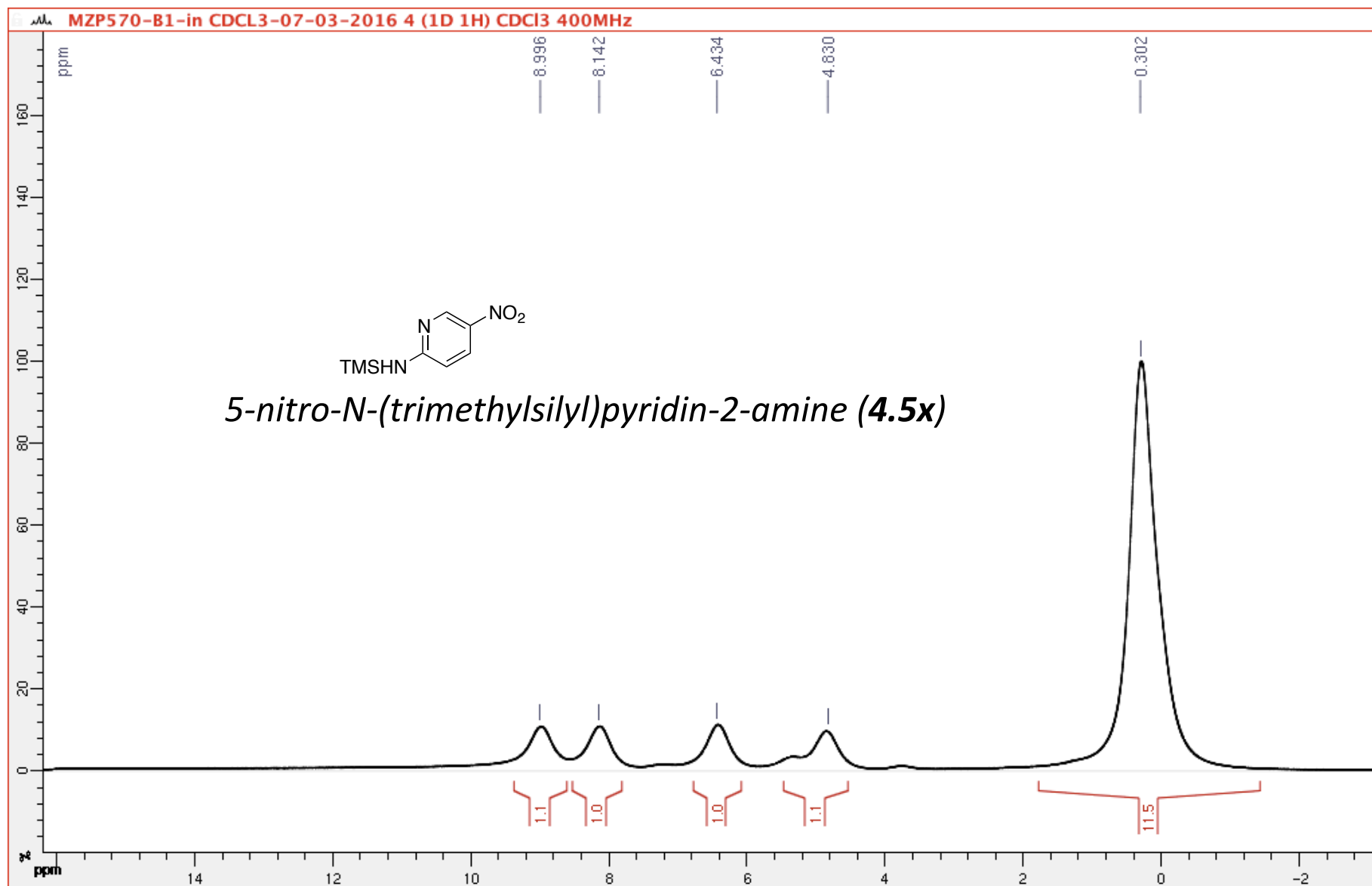
MZP567-B86-30 min-1H-NMR-in DMSO-26-02-2016

(400 MHz, 297.2 K, CDCl<sub>3</sub>)

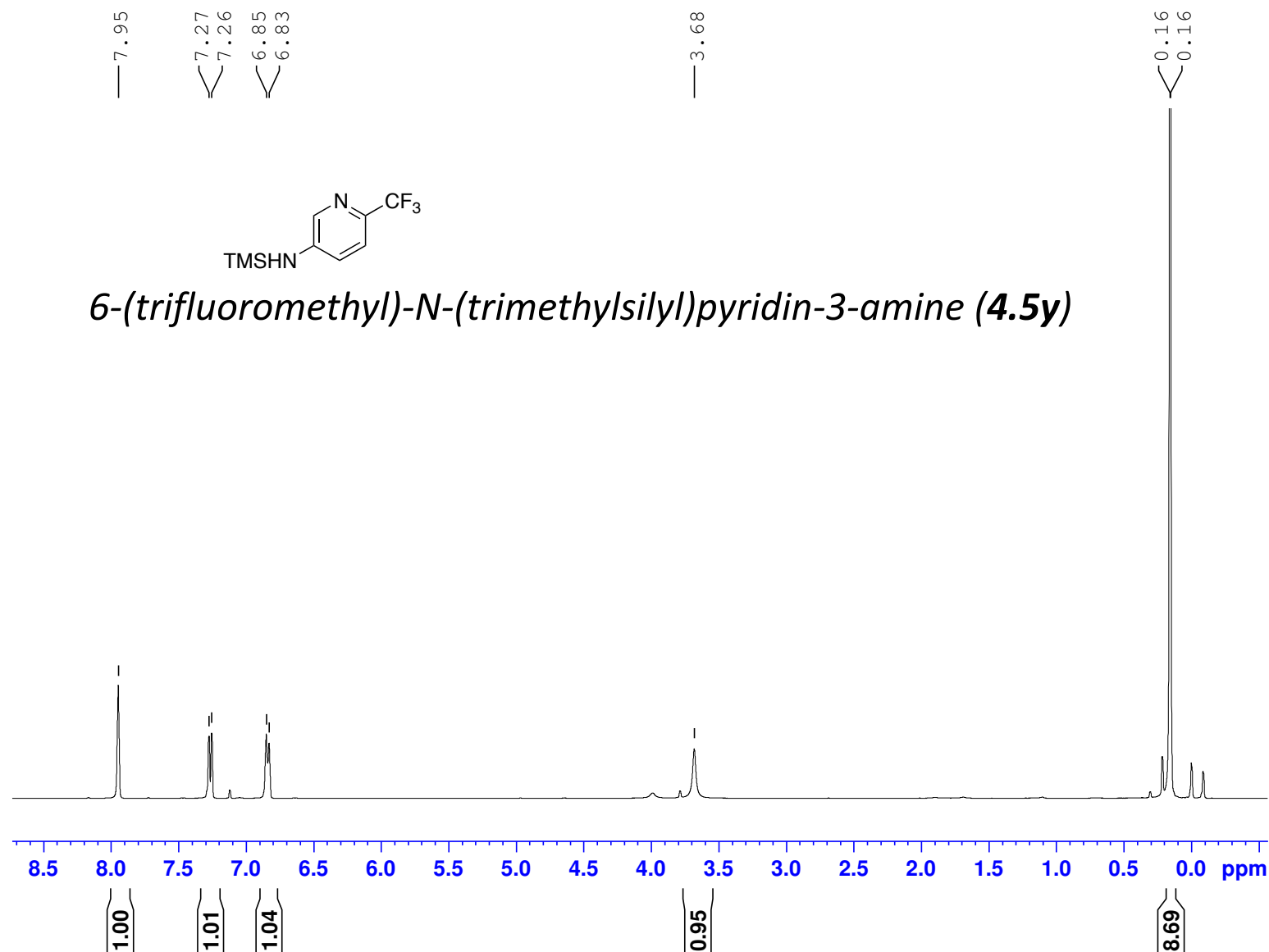
TMS-GPS435



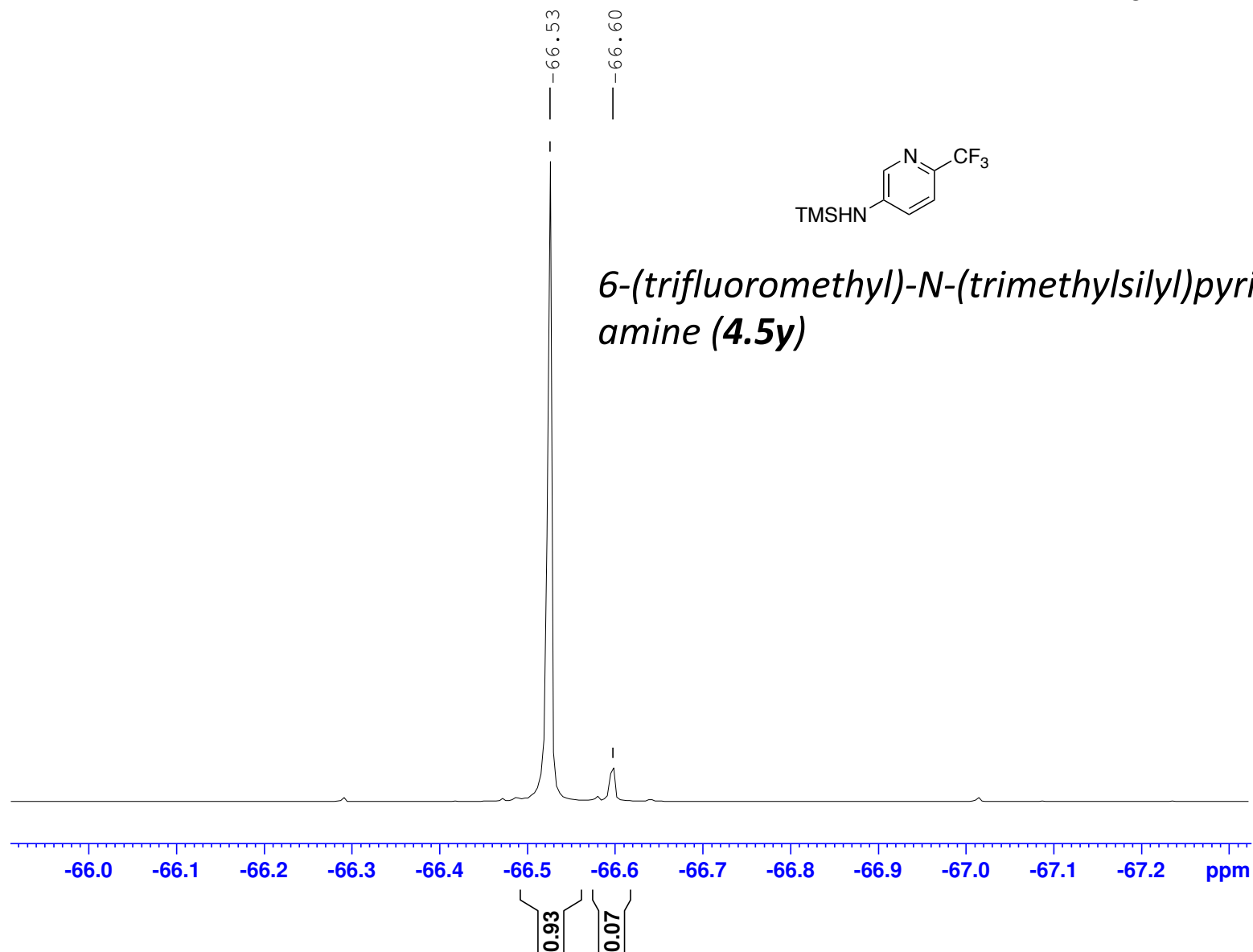
(400 MHz, 297.2 K, CDCl<sub>3</sub>) TMS-GPS422



MZP570-B84-ON-93% conversion-in CDCl<sub>3</sub>-1H-NMR-07-03-2016 (400 MHz, 297.2 K, CDCl<sub>3</sub>) TMS-GPS433



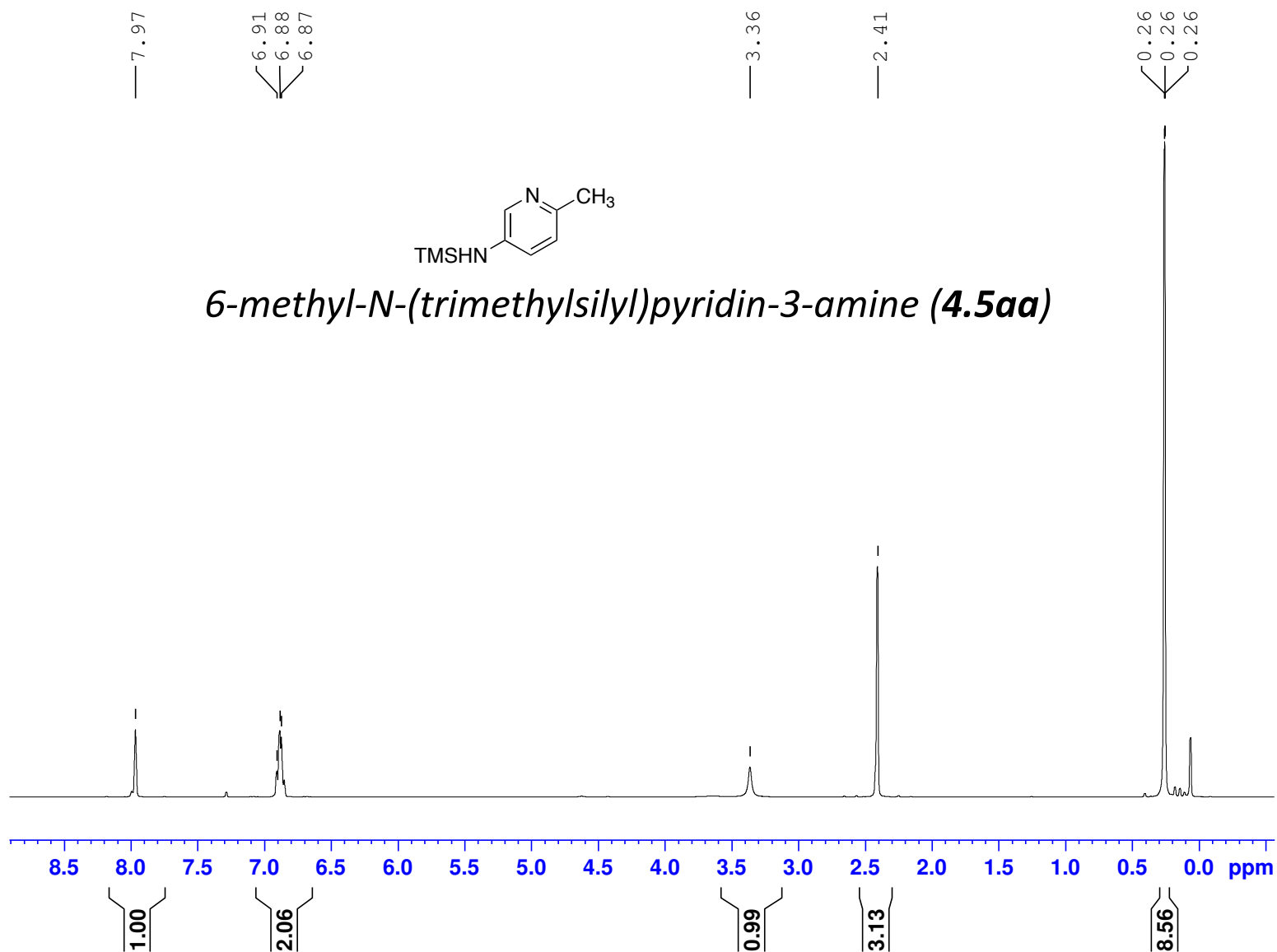
MZP570-B84-ON-93% conversion-in CDCl<sub>3</sub>-19F-NMR-07-03-2016 (400 MHz, 297.2 K, CDCl<sub>3</sub>) TMS-GPS433



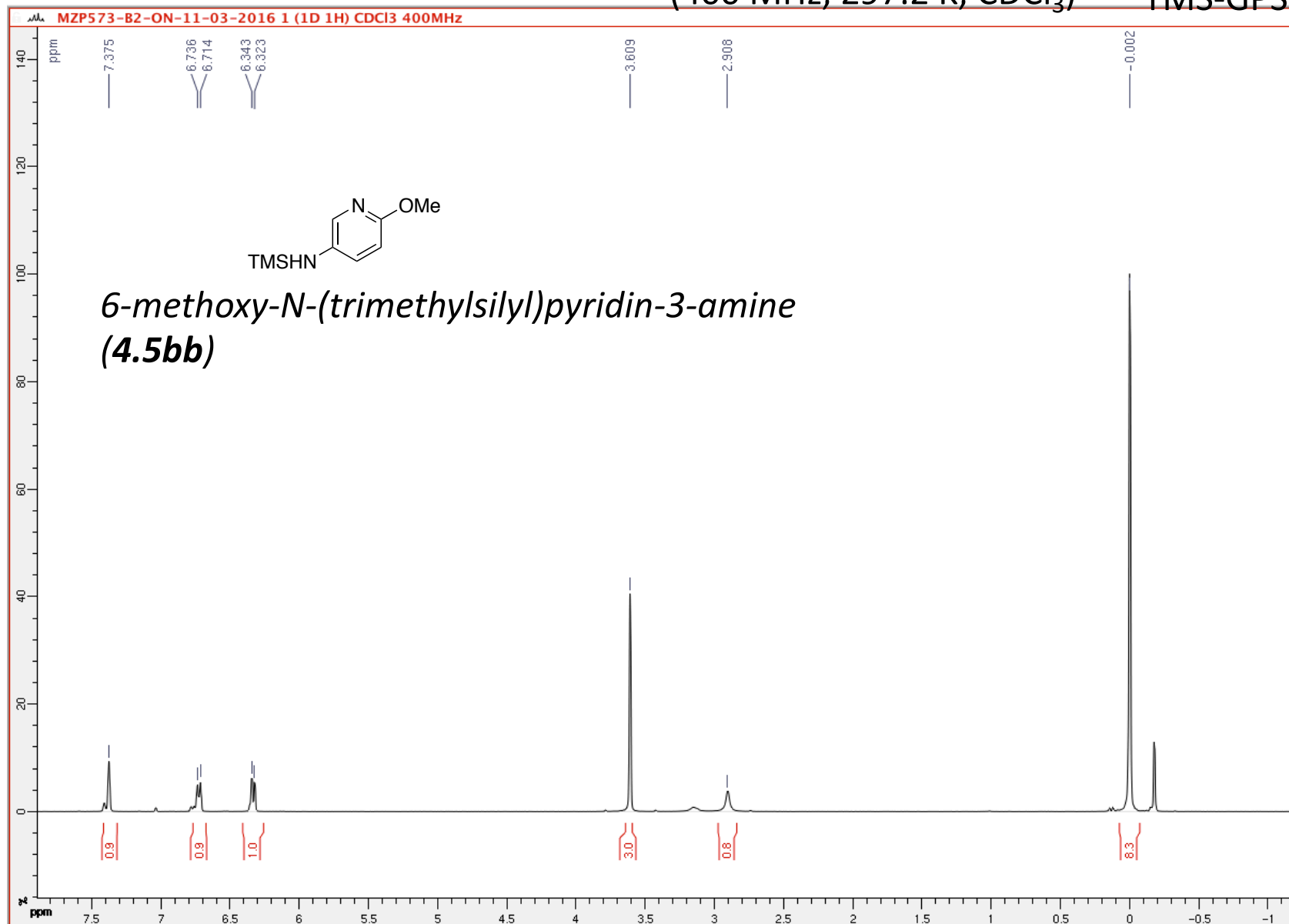
MZP568-B87-2h-1H-NMR-in CDCl<sub>3</sub>-03-03-2016

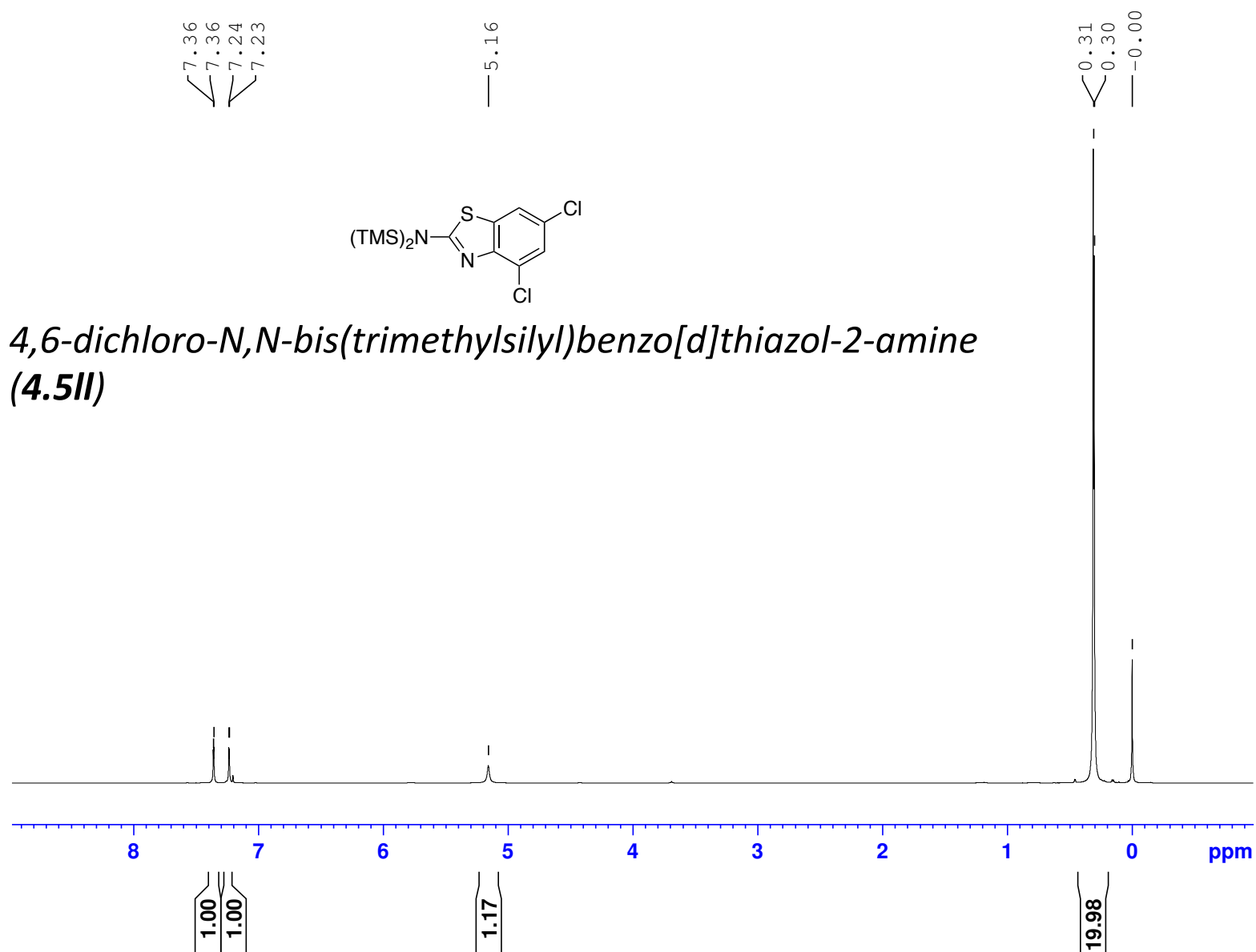
(400 MHz, 297.2 K, CDCl<sub>3</sub>)

TMS-GPS436



(400 MHz, 297.2 K, CDCl<sub>3</sub>) TMS-GPS423





TMS-GPS515





MZP570-B77-ON-in CDCl<sub>3</sub>-1H-NMR-07-03-2016

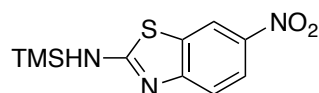
(400 MHz, 297.2 K, CDCl<sub>3</sub>)

TMS-GPS428

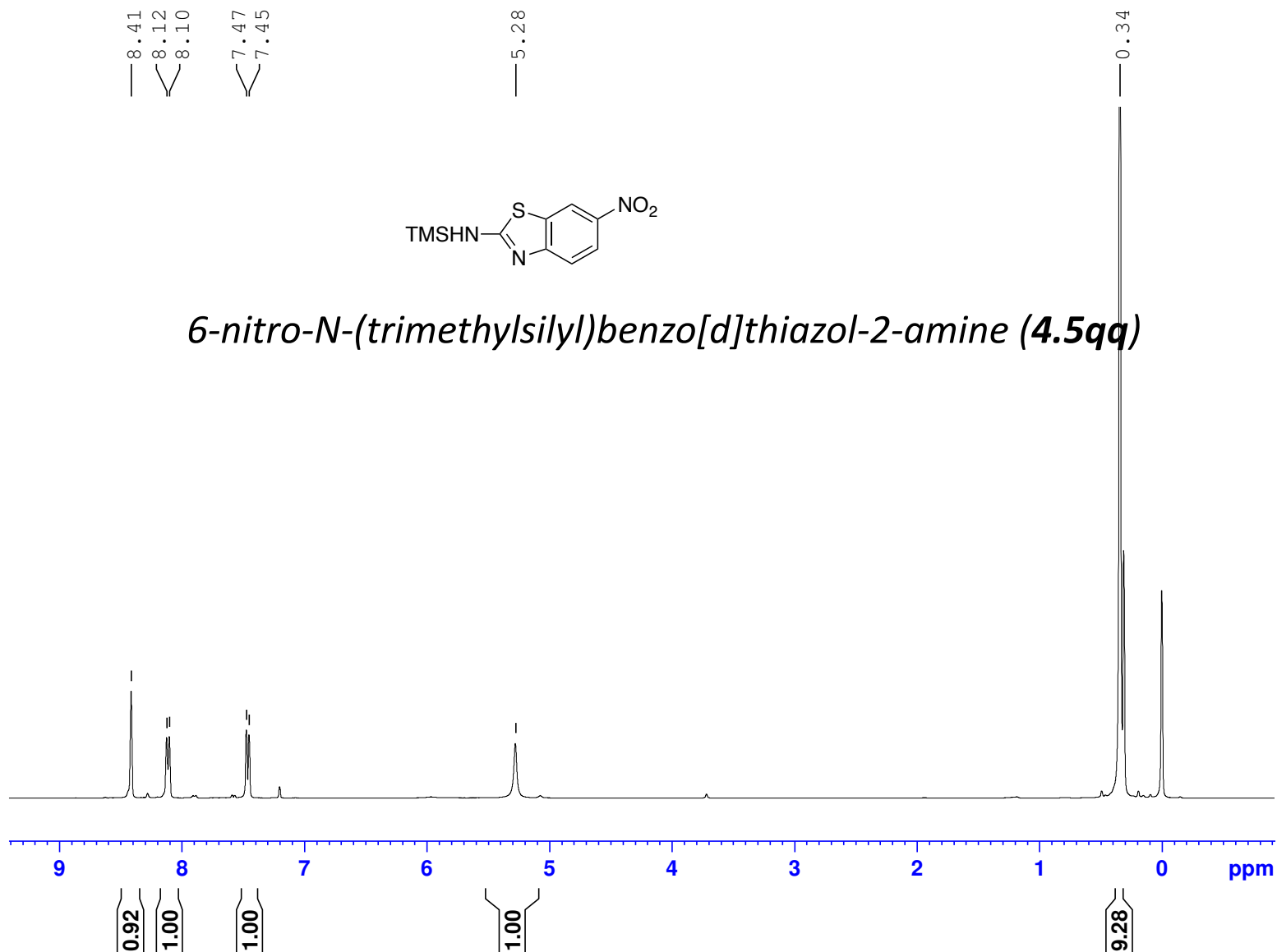
8.41  
8.12  
8.10  
7.47  
7.45

5.28

0.34

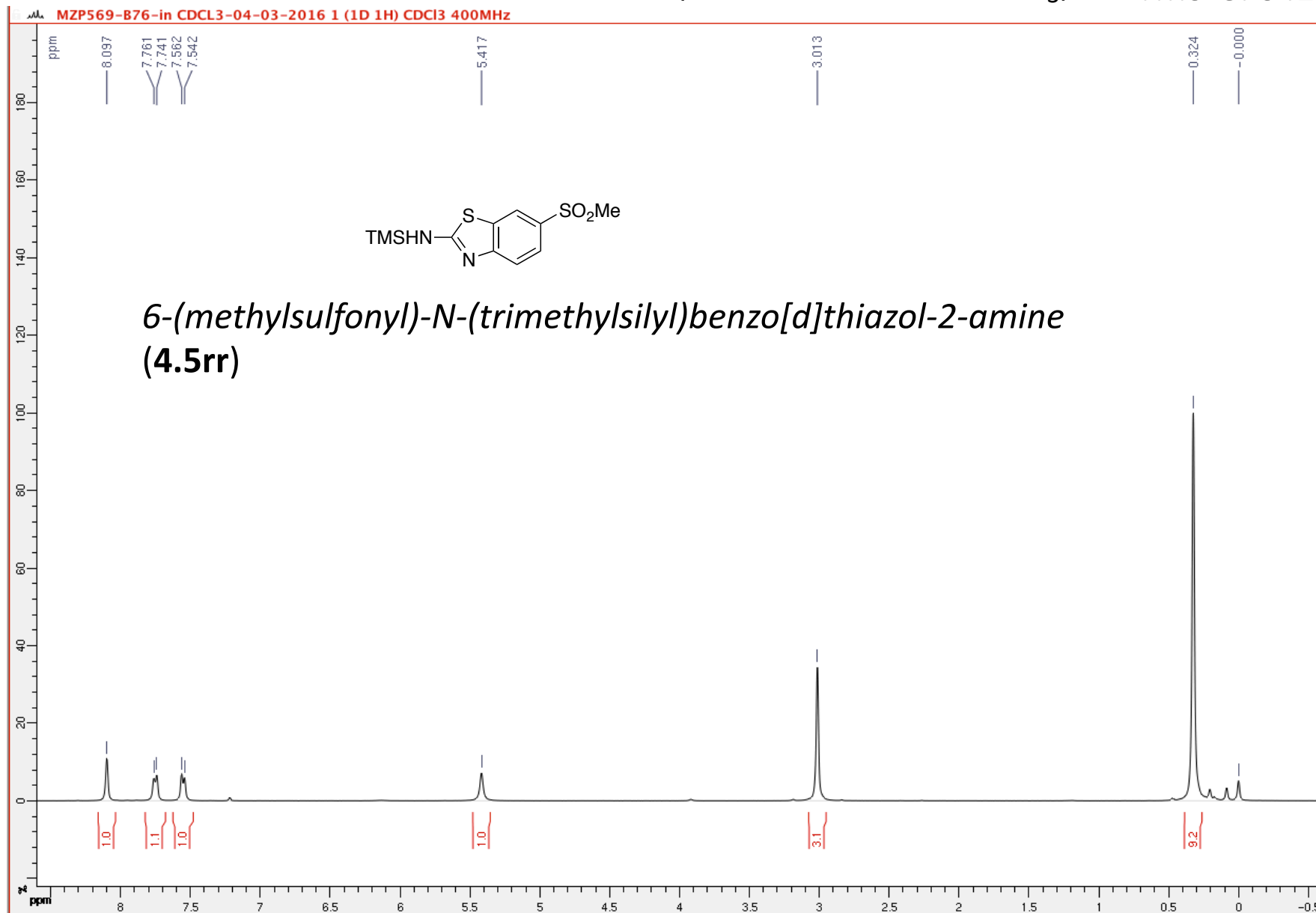


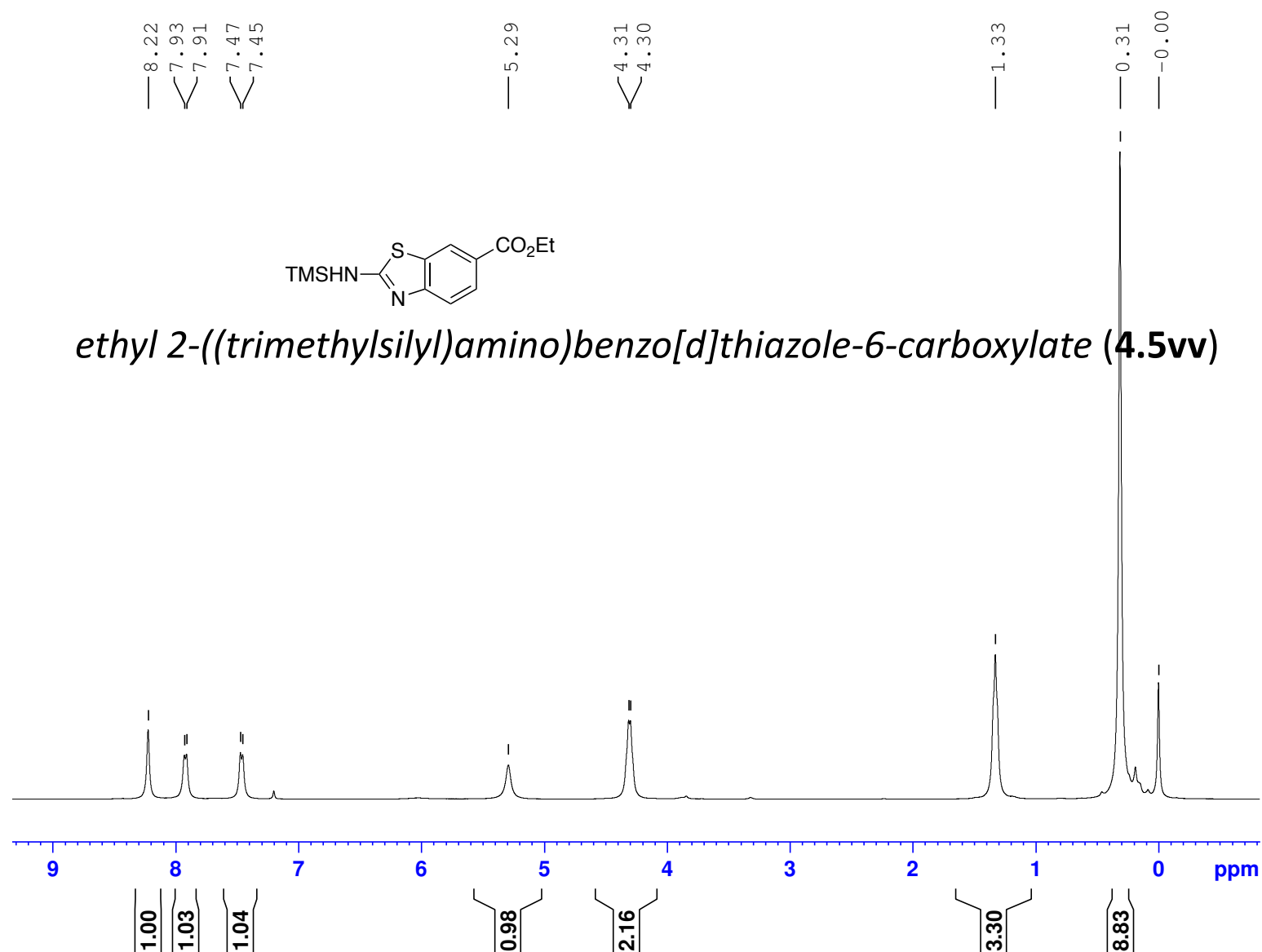
*6-nitro-N-(trimethylsilyl)benzo[d]thiazol-2-amine (4.5qq)*



(400 MHz, 297.2 K, CDCl<sub>3</sub>)

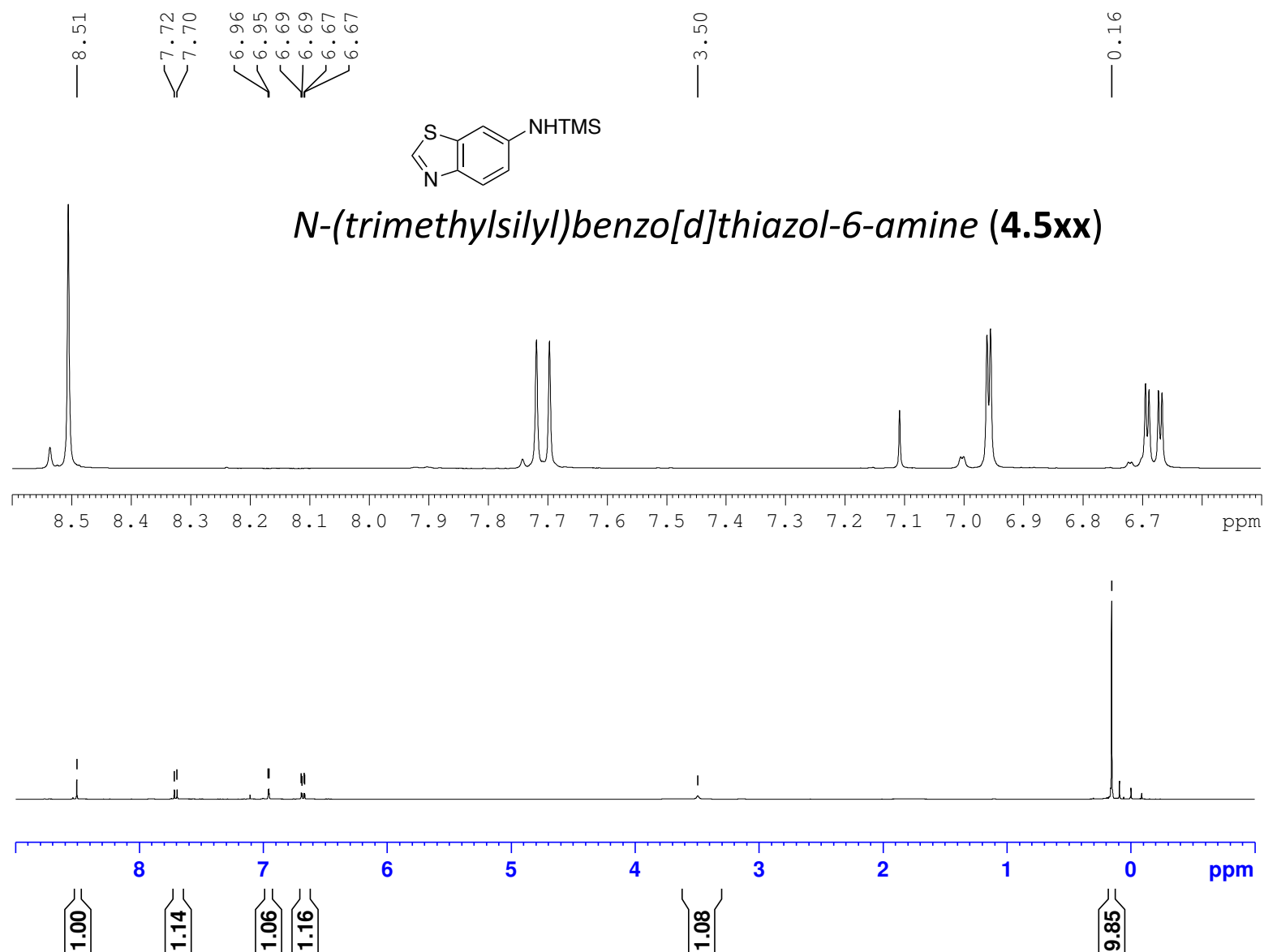
TMS-GPS427





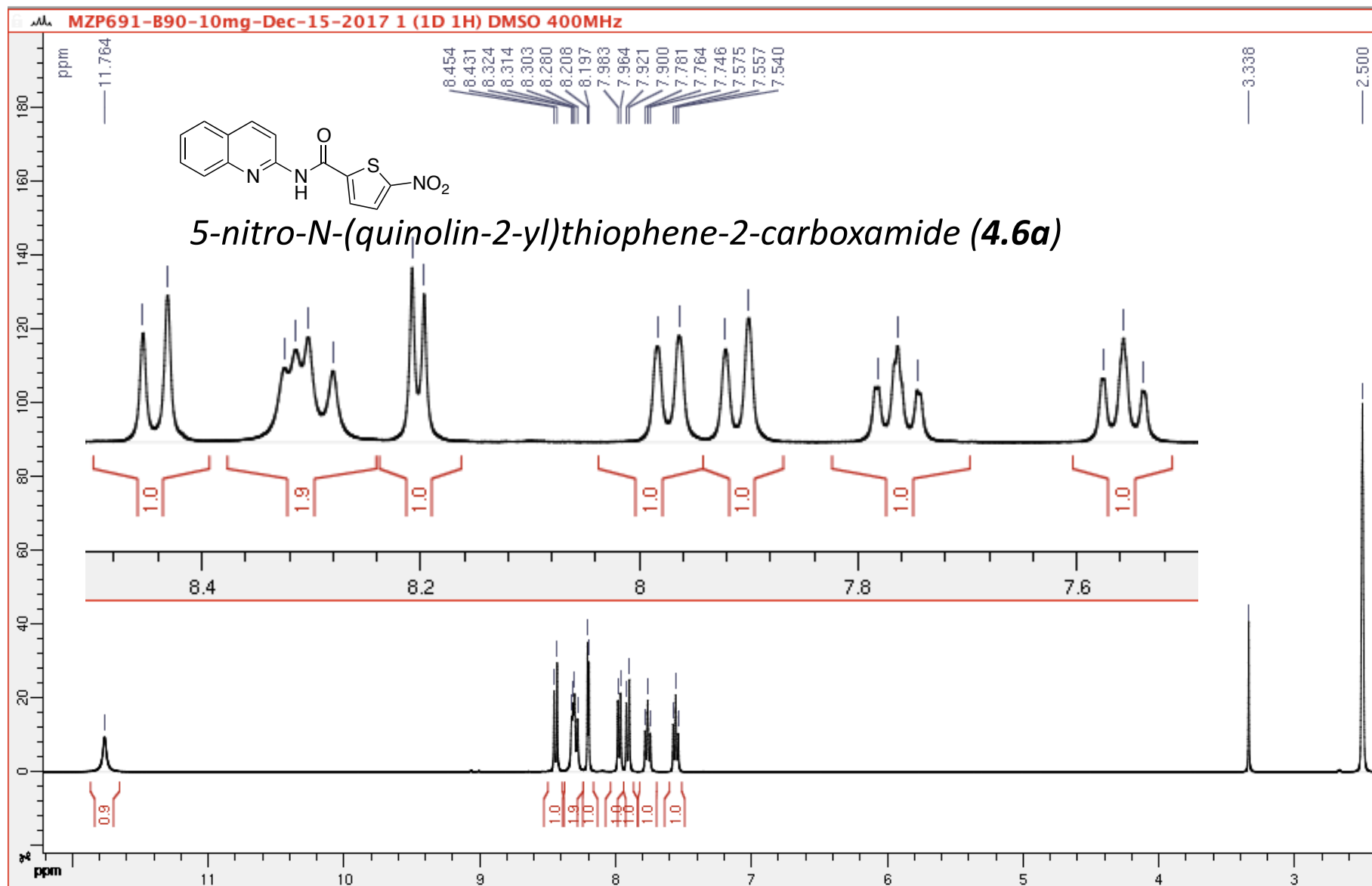
GPS480-MZP601-1H-NMR-Aug-11-2016

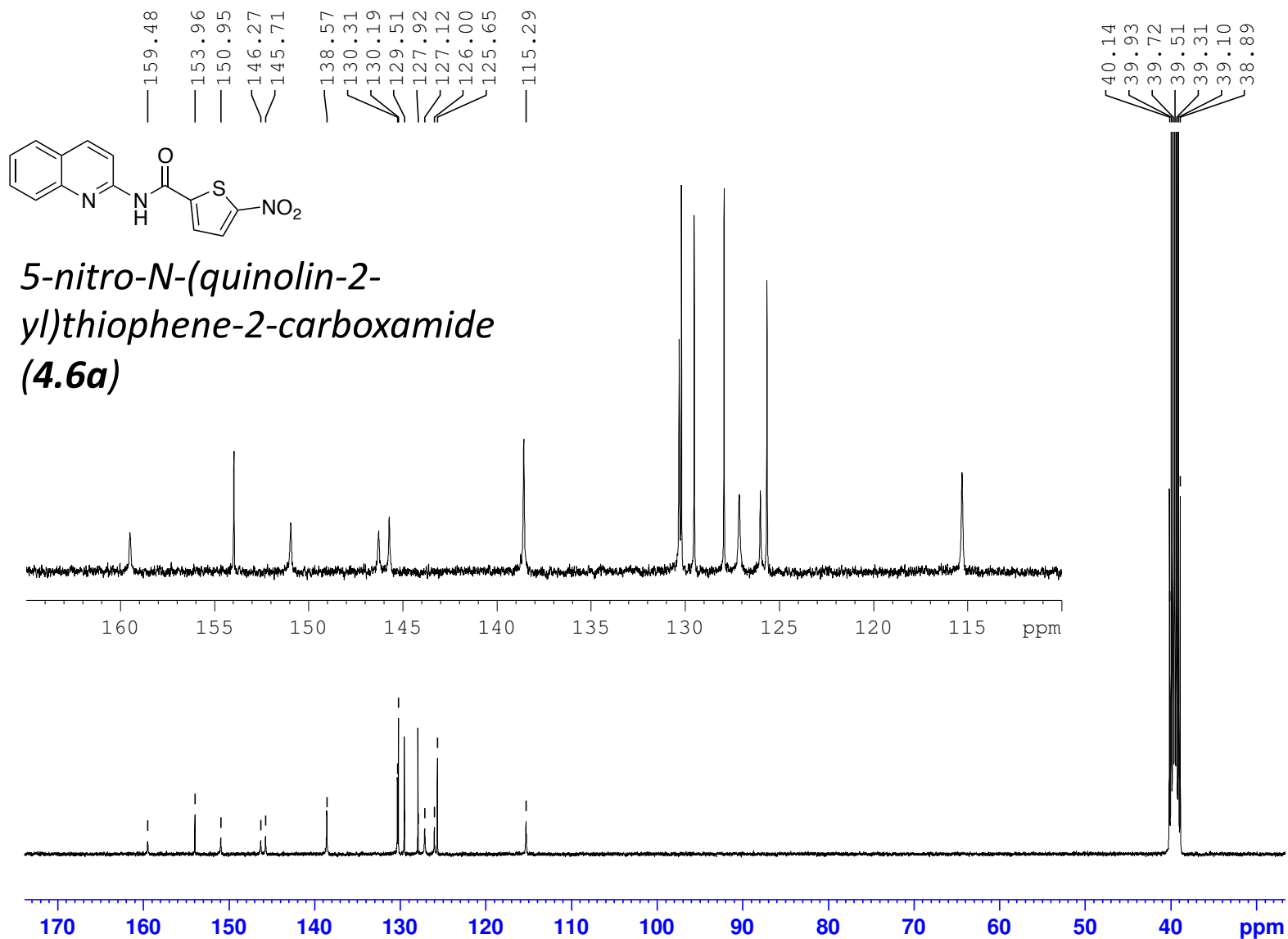
(400 MHz, 297.2 K, CDCl<sub>3</sub>) TMS-GPS480



(400 MHz, 297.2 K, DMSO-d6)

GPS439

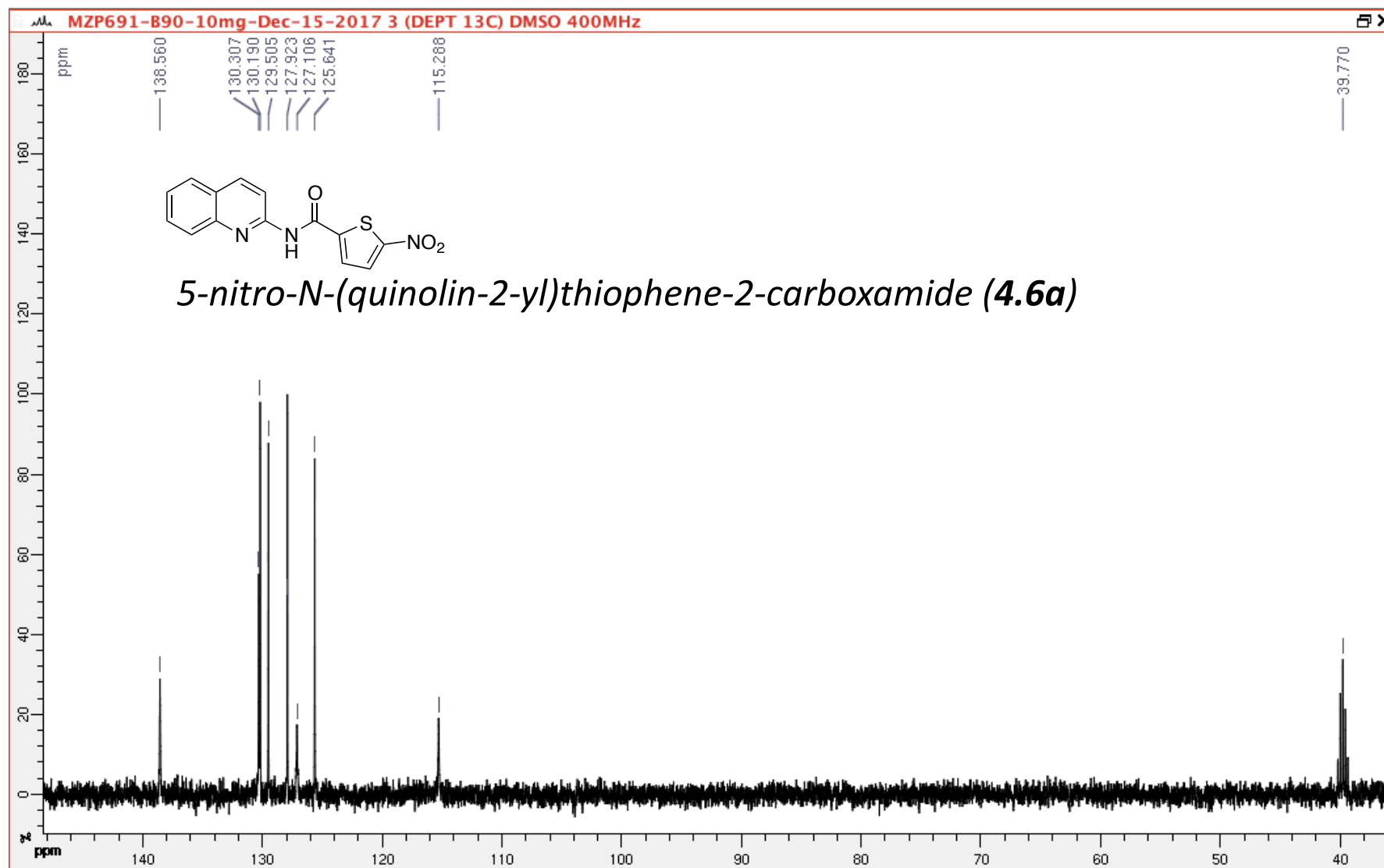




DEPT 90

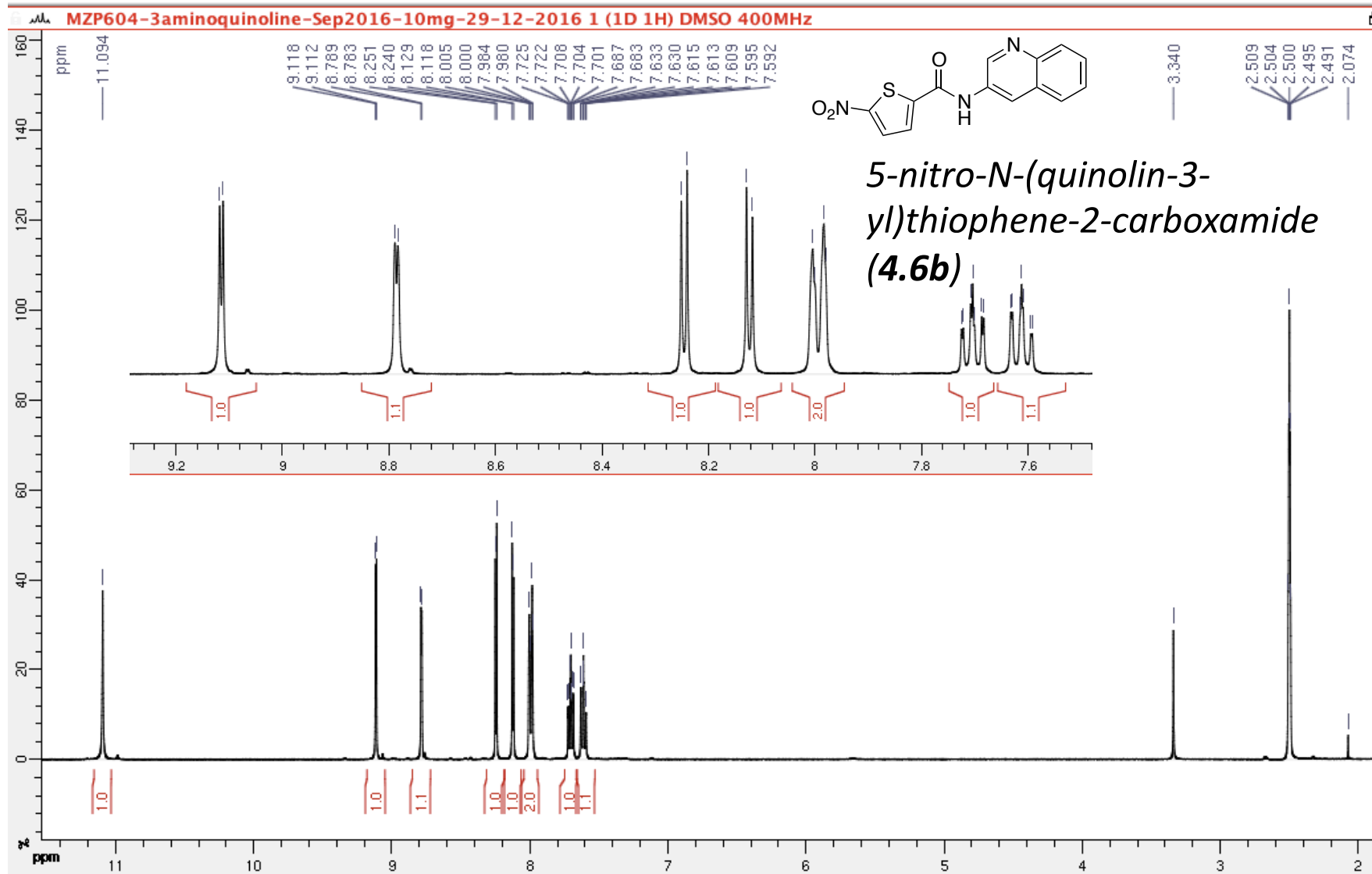
(100 MHz, 297.2 K, DMSO-d6)

GPS439



(400 MHz, 297.2 K, DMSO-d6)

GPS387

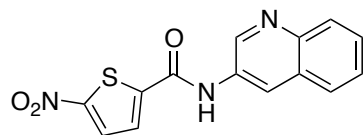




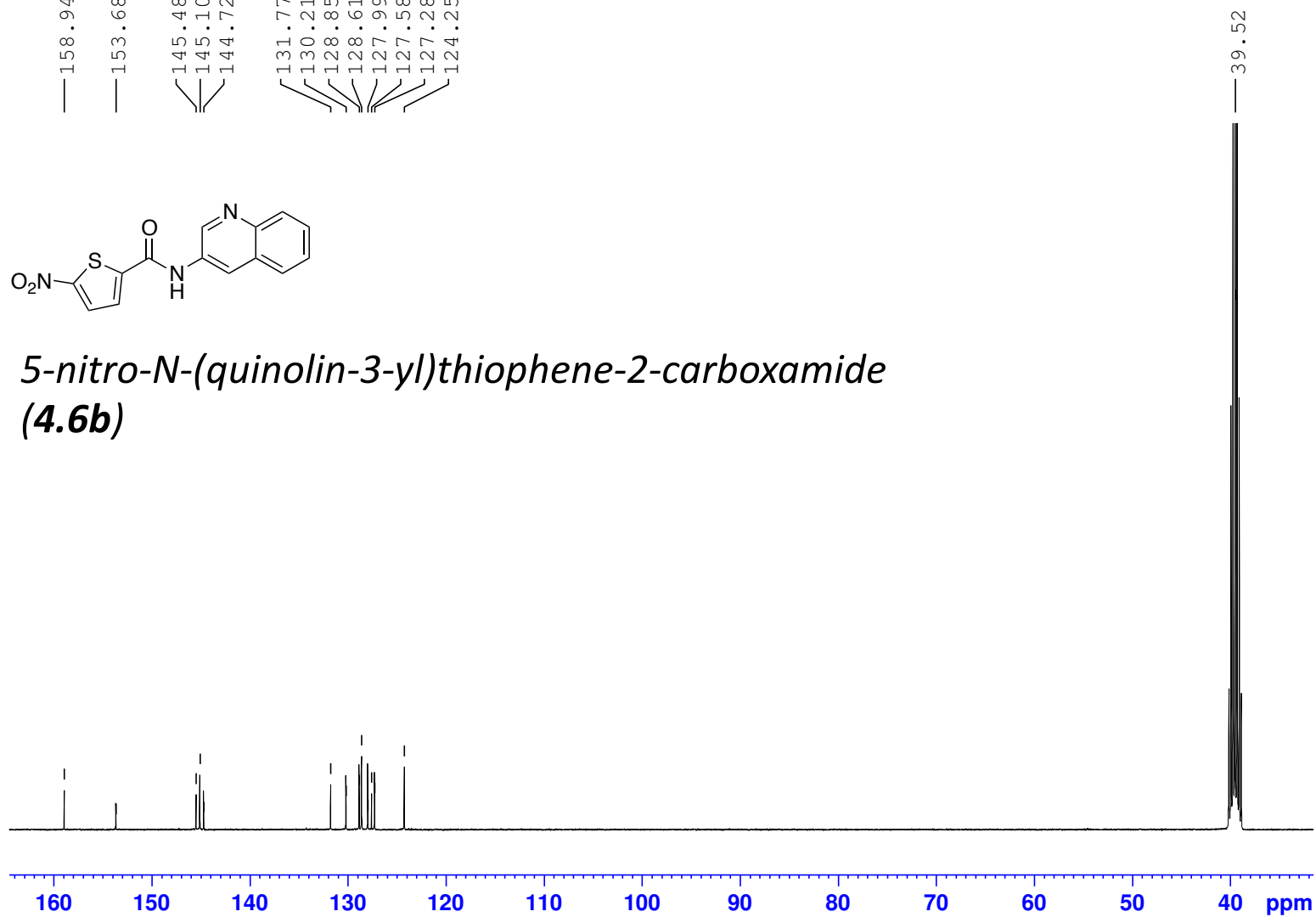
MZP604-3-aminoquinoline-Sep2016-10mg-13C-NMR-29-12-2016

(100 MHz, 297.2 K, DMSO-d6) GPS387

— 158.94  
— 153.68  
145.48  
145.10  
144.72  
131.77  
130.21  
128.85  
128.61  
127.99  
127.58  
127.28  
124.25



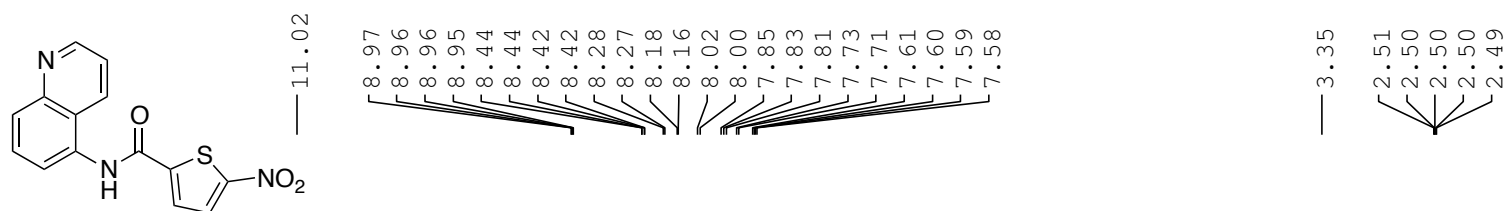
*5-nitro-N-(quinolin-3-yl)thiophene-2-carboxamide*  
**(4.6b)**



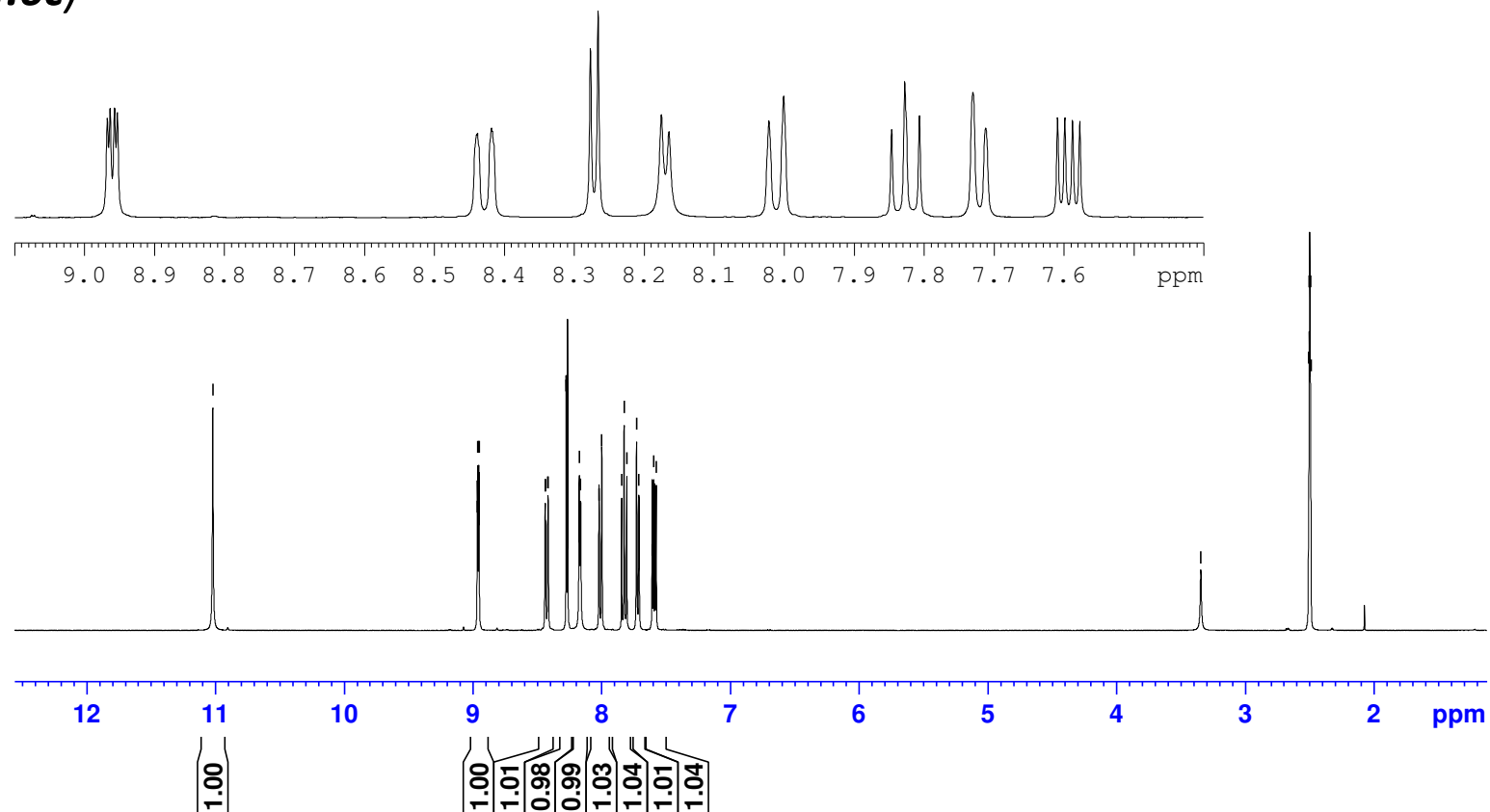
GPS466-MZP594-B99-Amide-13mg-1H-NMR-Oct-18-2016

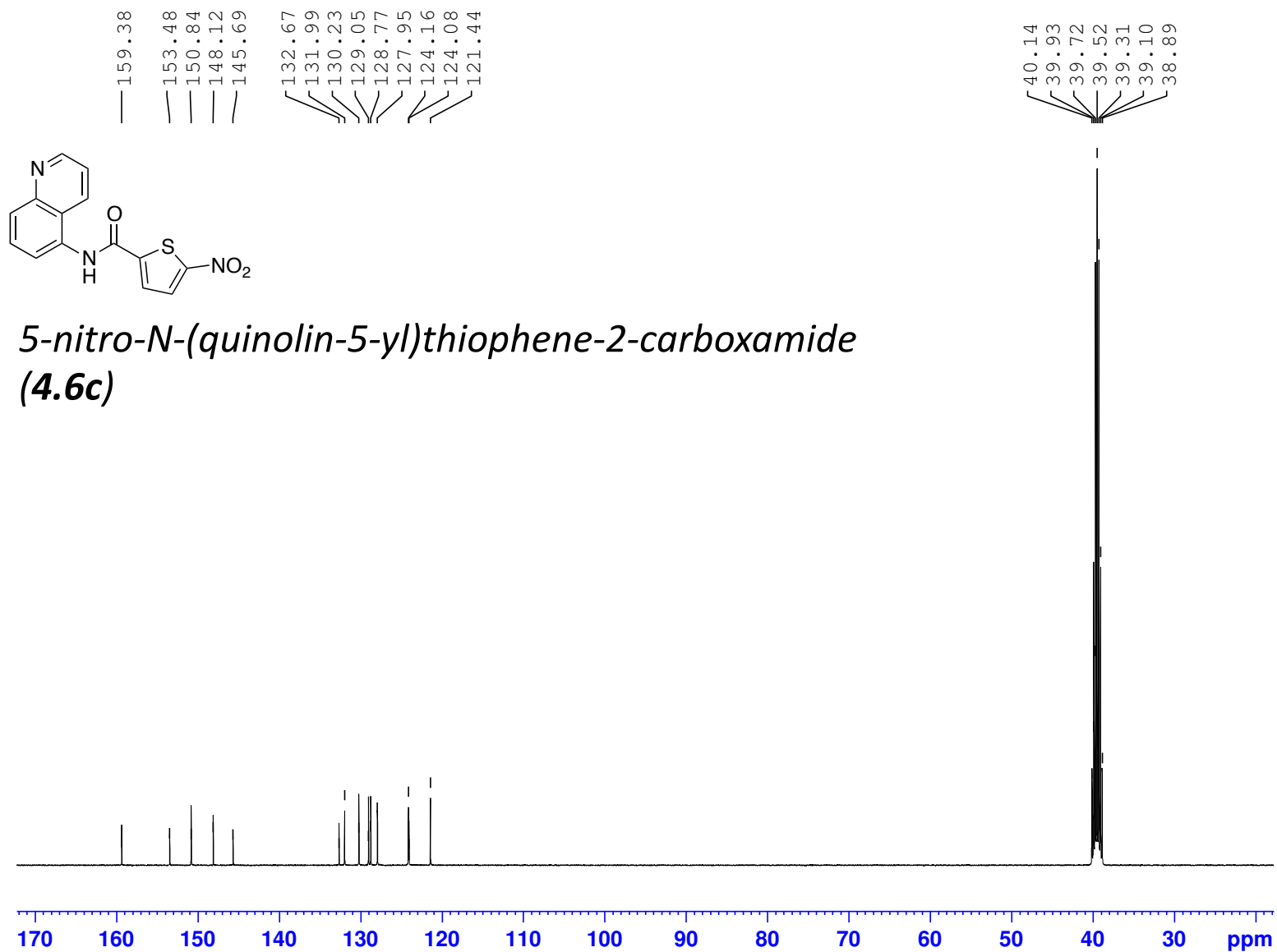
(400 MHz, 297.2 K, DMSO-d6)

GPS466



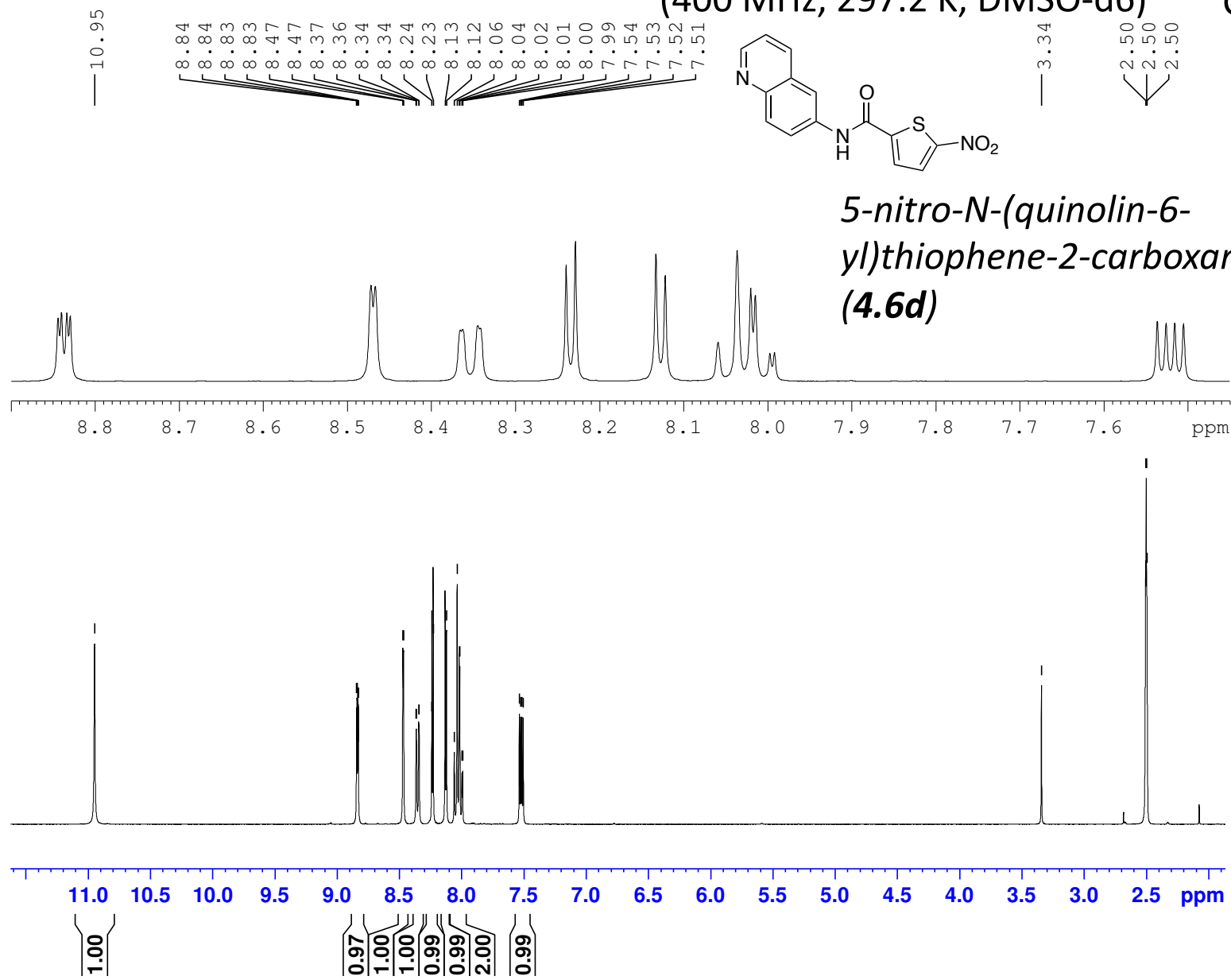
**5-nitro-N-(quinolin-5-yl)thiophene-2-carboxamide  
(4.6c)**





(400 MHz, 297.2 K, DMSO-d<sub>6</sub>)

GPS467

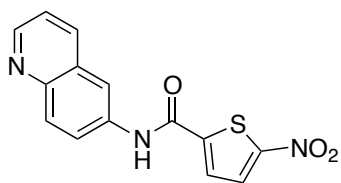


MZP594-B101-10mg-<sup>13</sup>C-NMR-May-16-2017

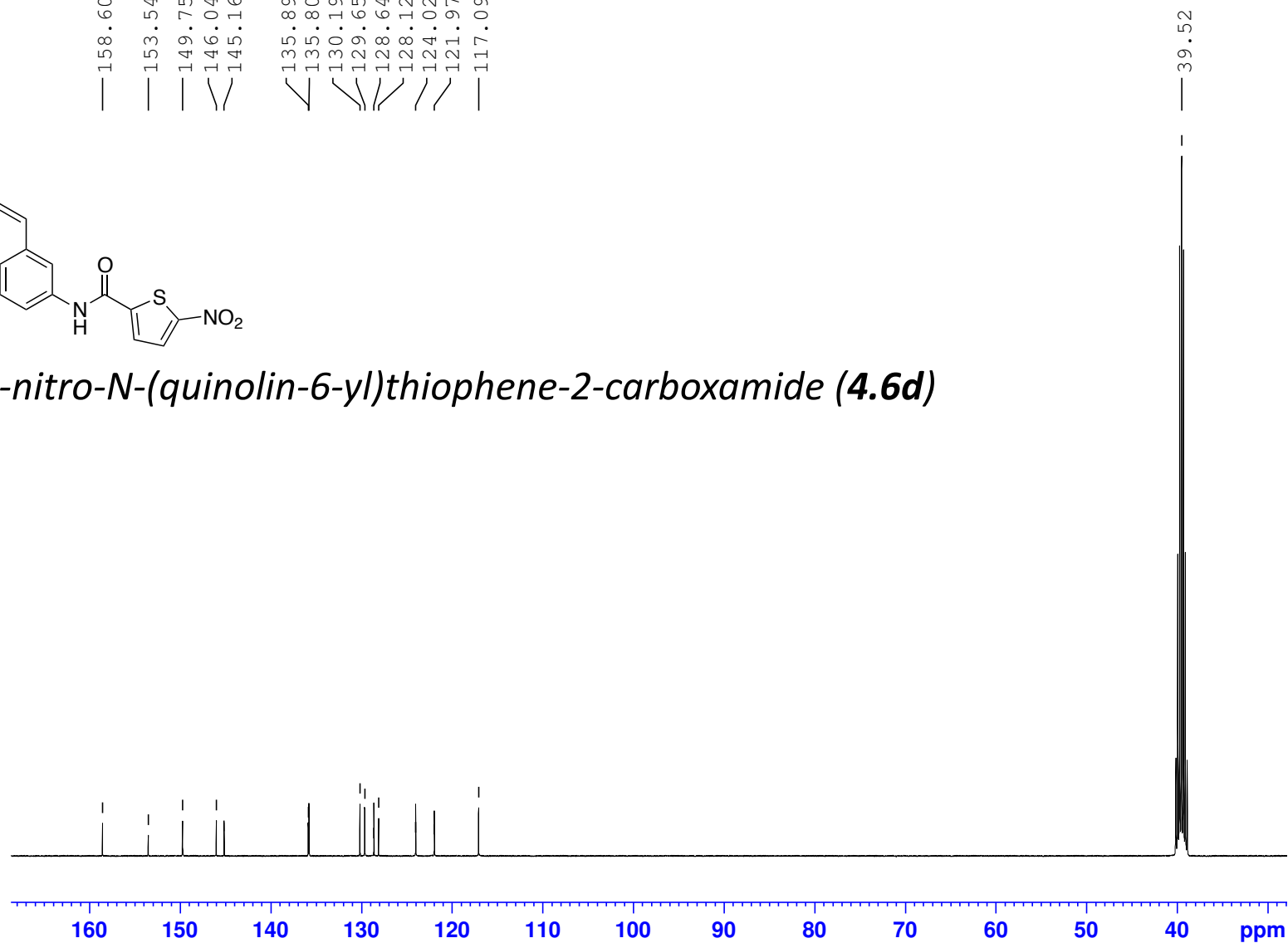
(100 MHz, 297.2 K, DMSO-d<sub>6</sub>)

GPS467

— 158.60  
— 153.54  
— 149.75  
— 146.04  
— 145.16  
  
— 135.89  
— 135.80  
— 130.19  
— 129.65  
— 128.64  
— 128.12  
— 124.02  
— 121.97  
— 117.09



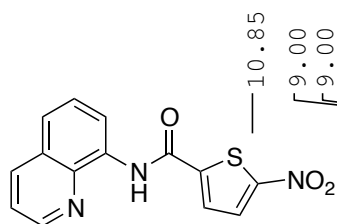
*5-nitro-N-(quinolin-6-yl)thiophene-2-carboxamide (4.6d)*



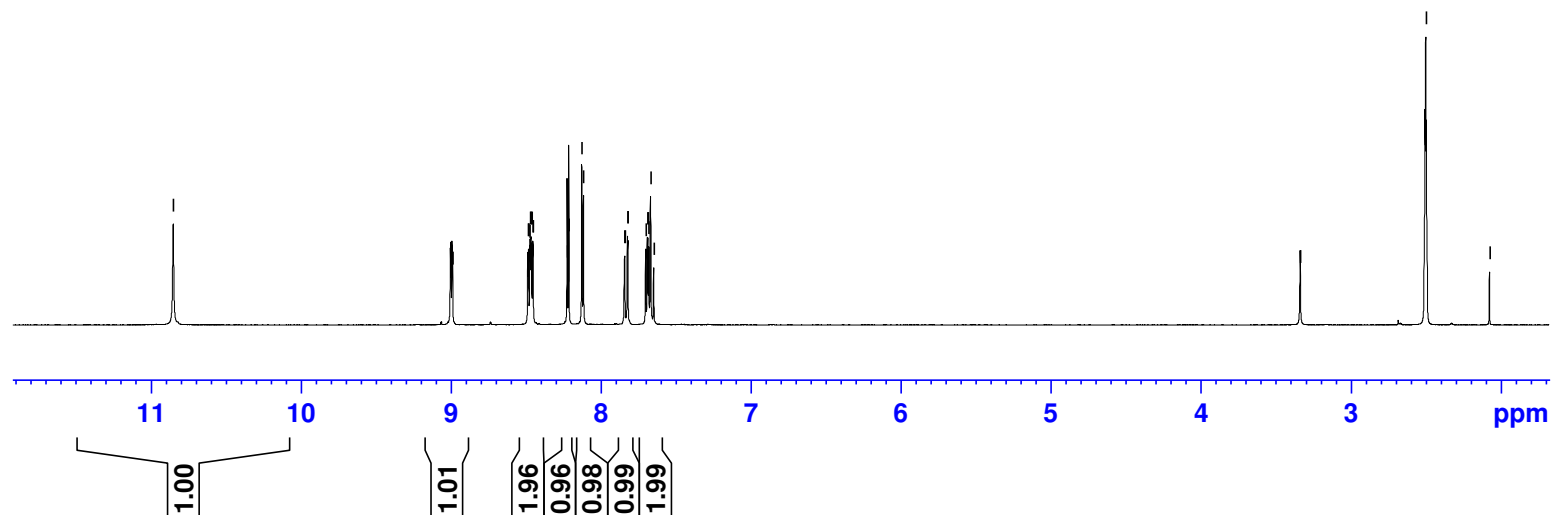
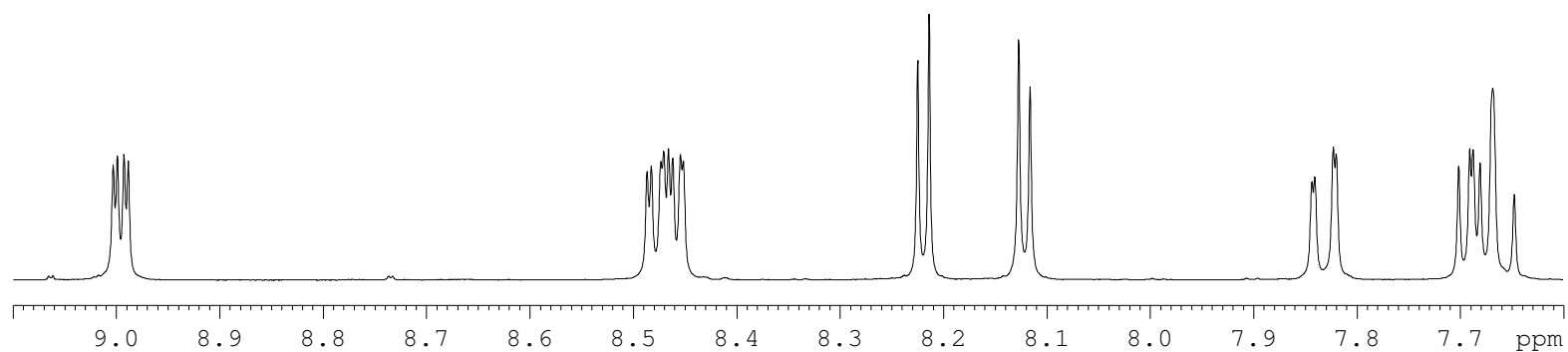
GPS468-MZP594-B100-10mg-1H-NMR-May-17-2017

(400 MHz, 297.2 K, DMSO-d<sub>6</sub>)

GPS468



**5-nitro-N-(quinolin-8-yl)thiophene-2-carboxamide (4.6e)**



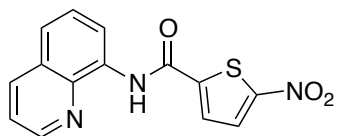
GPS468-MZP594-B100-10mg-13C-NMR-May-17-2017

(100 MHz, 297.2 K, DMSO-d6)

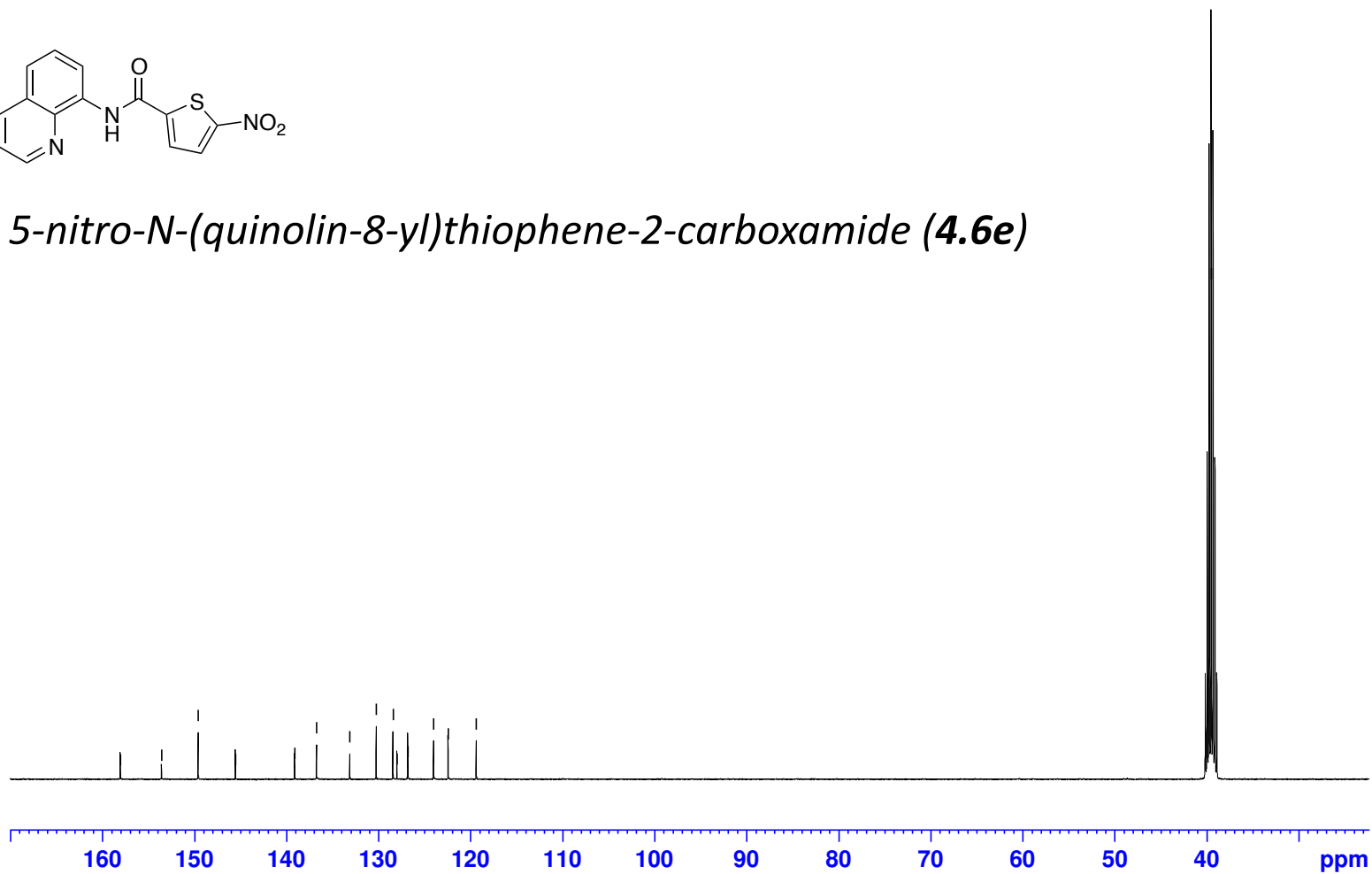
GPS468

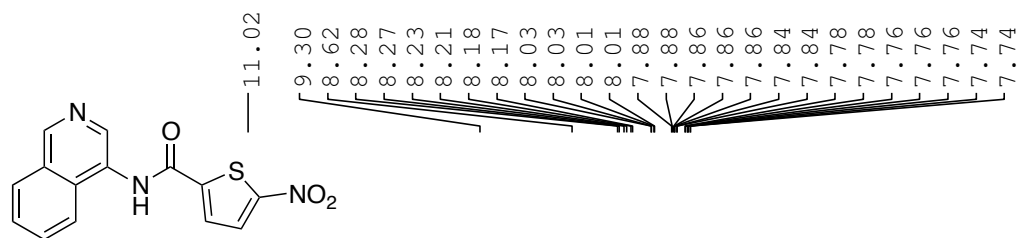
158.08  
153.59  
149.60  
145.57  
139.12  
136.74  
133.13  
130.26  
128.44  
128.02  
126.82  
124.02  
122.44  
119.39

39.52

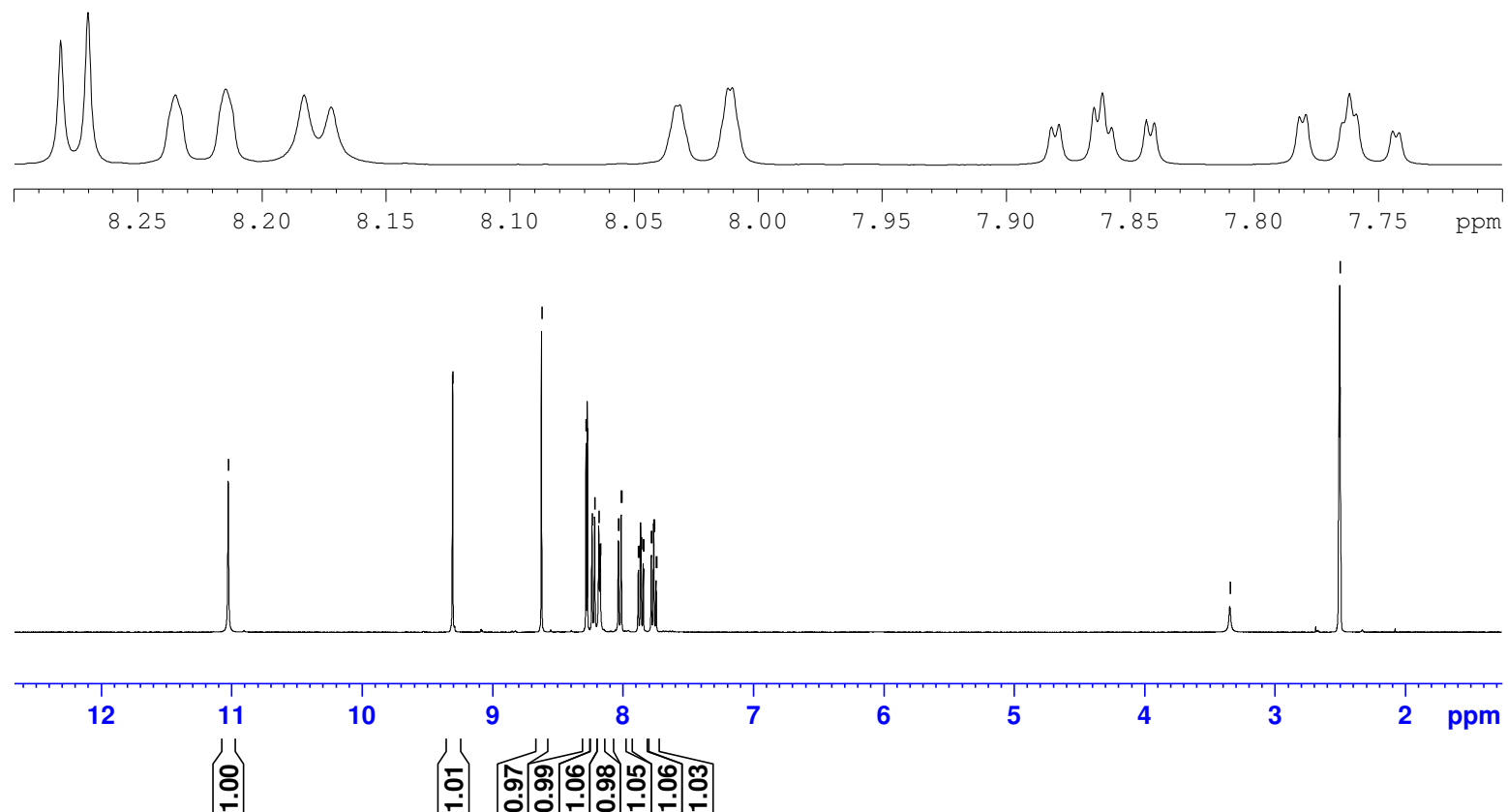


*5-nitro-N-(quinolin-8-yl)thiophene-2-carboxamide (4.6e)*





*N*-(isoquinolin-4-yl)-5-nitrothiophene-2-carboxamide (**4.6f**)



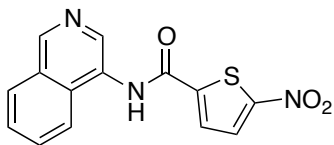


MZP604-4225-Amide-10mg-13C-NMR-Nov-18-2016

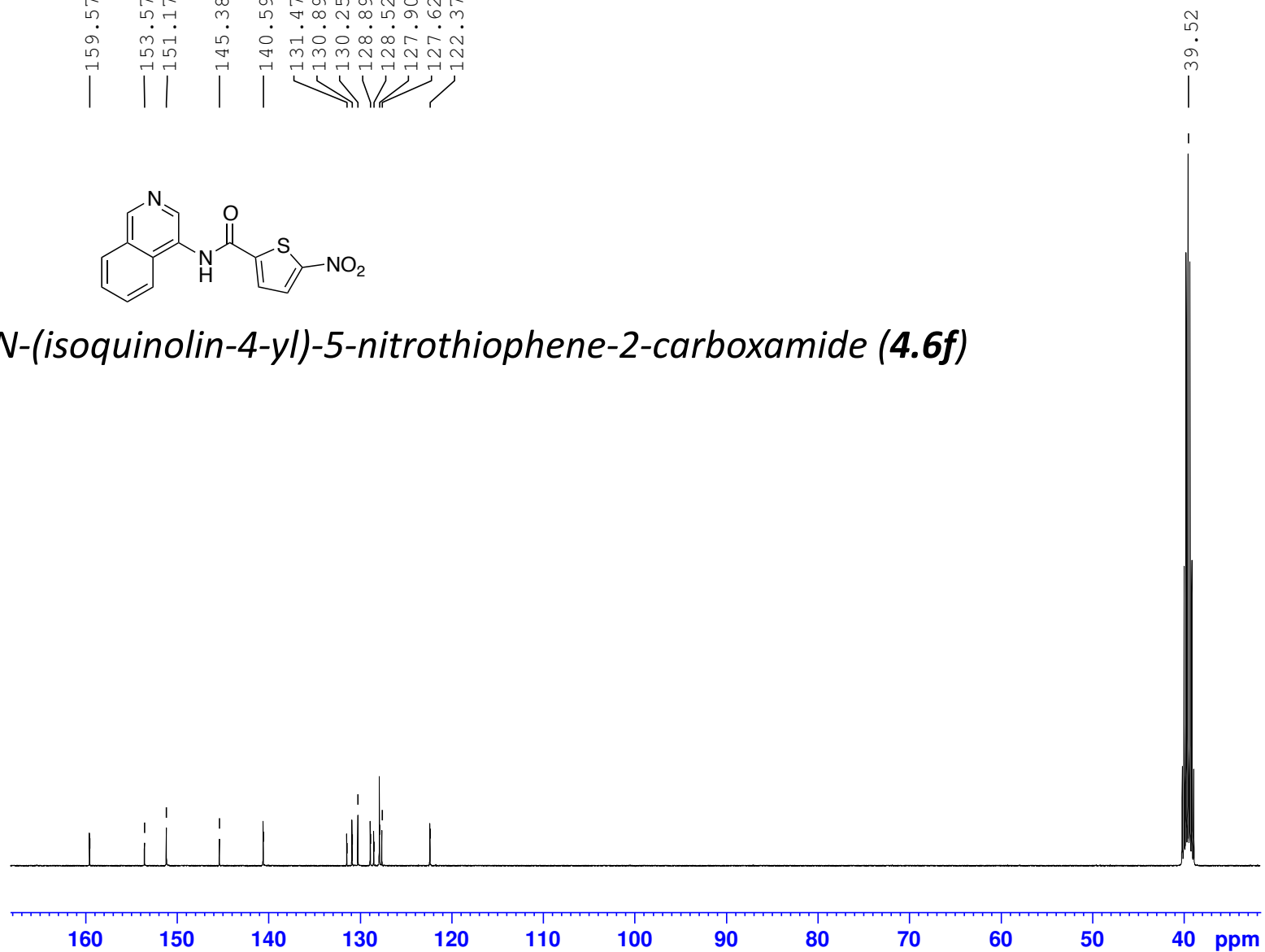
(100 MHz, 297.2 K, DMSO-d6)

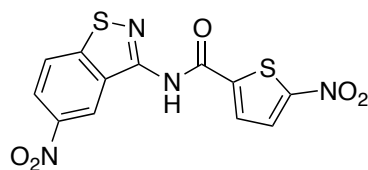
GPS469

— 159.57  
— 153.57  
— 151.17  
— 145.38  
— 140.59  
131.47  
130.89  
130.25  
128.89  
128.52  
127.90  
127.62  
122.37

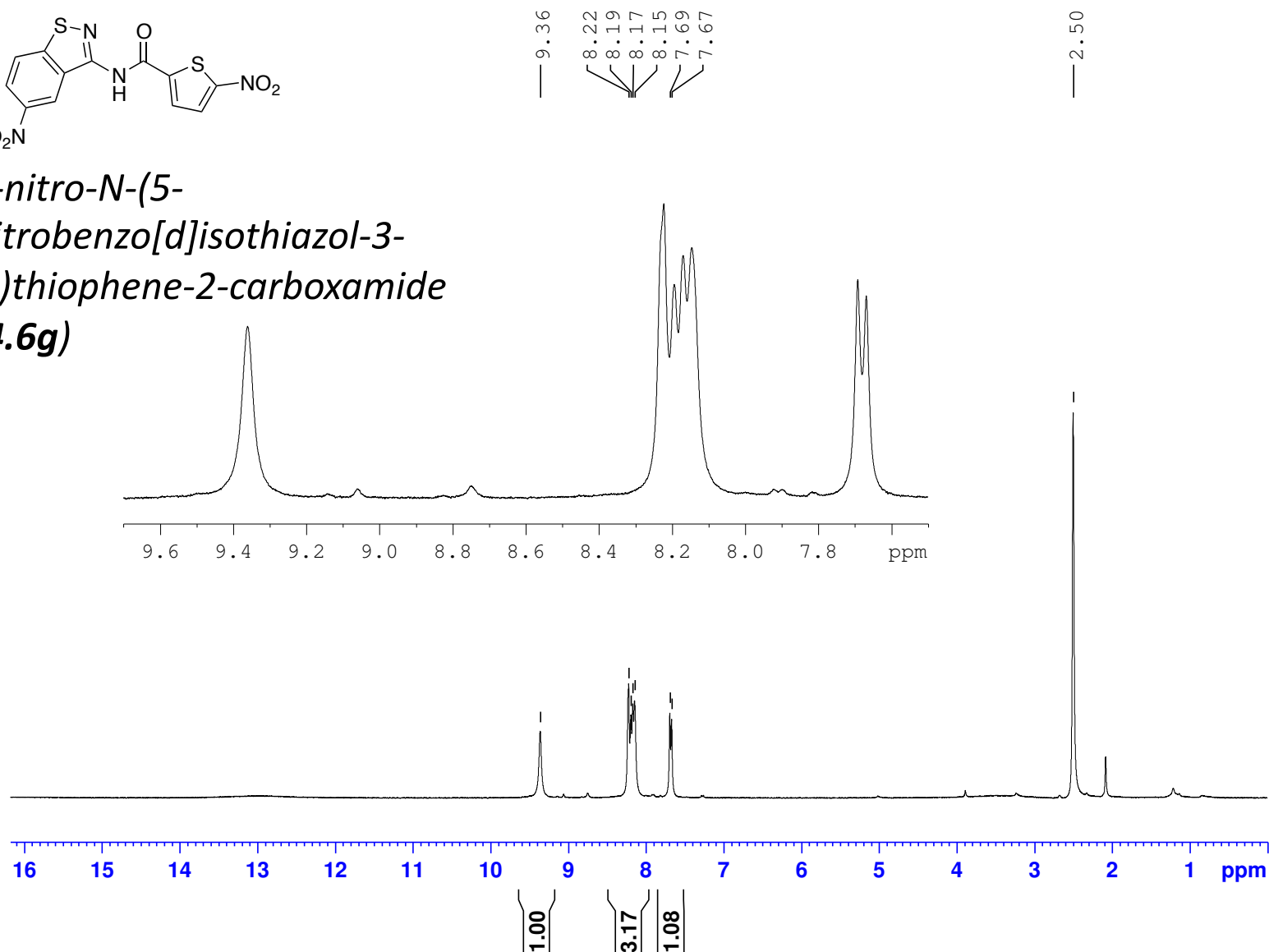


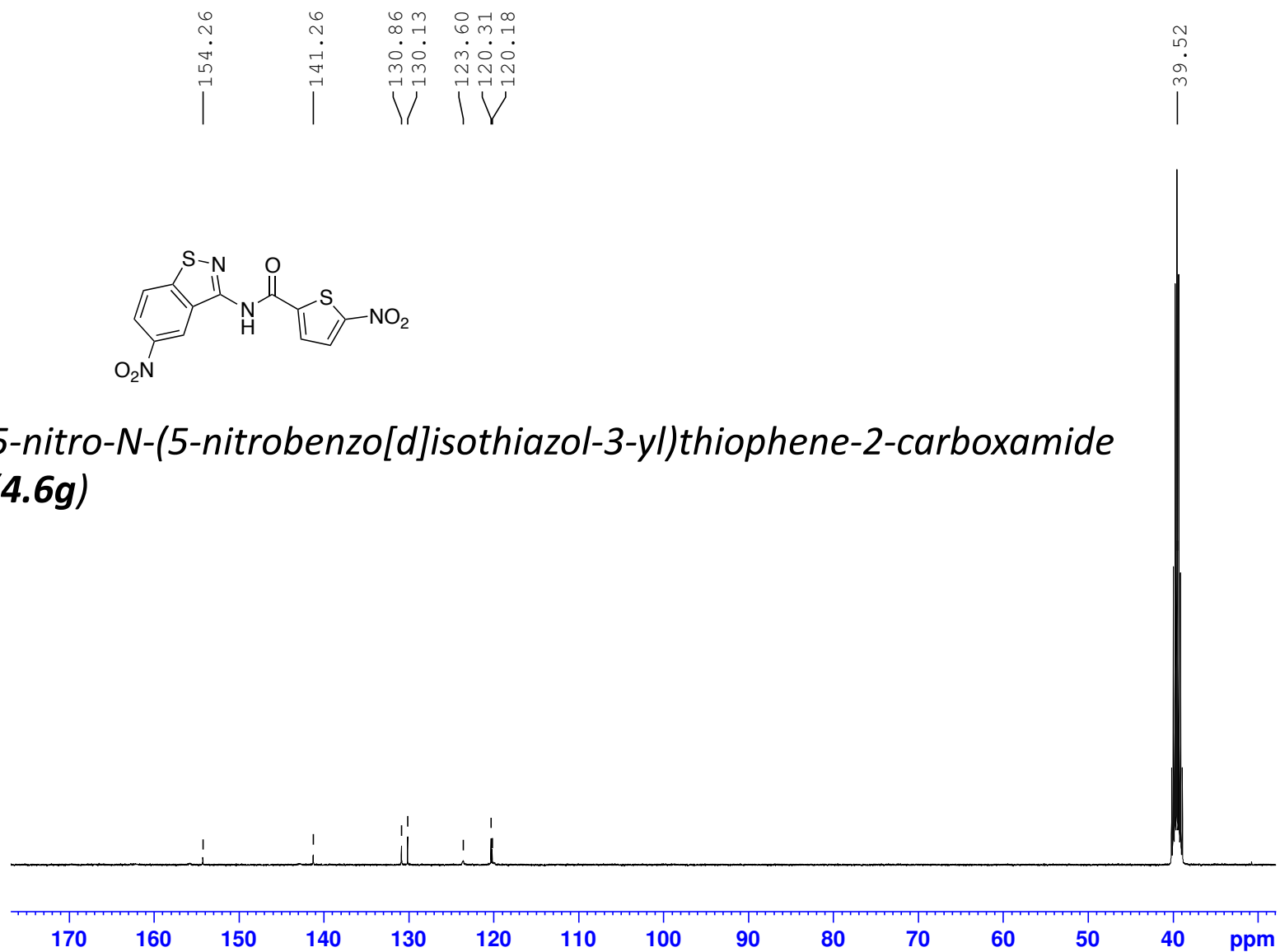
*N*-(isoquinolin-4-yl)-5-nitrothiophene-2-carboxamide (**4.6f**)





*5-nitro-N-(5-nitrobenzo[d]isothiazol-3-yl)thiophene-2-carboxamide*  
**(4.6g)**

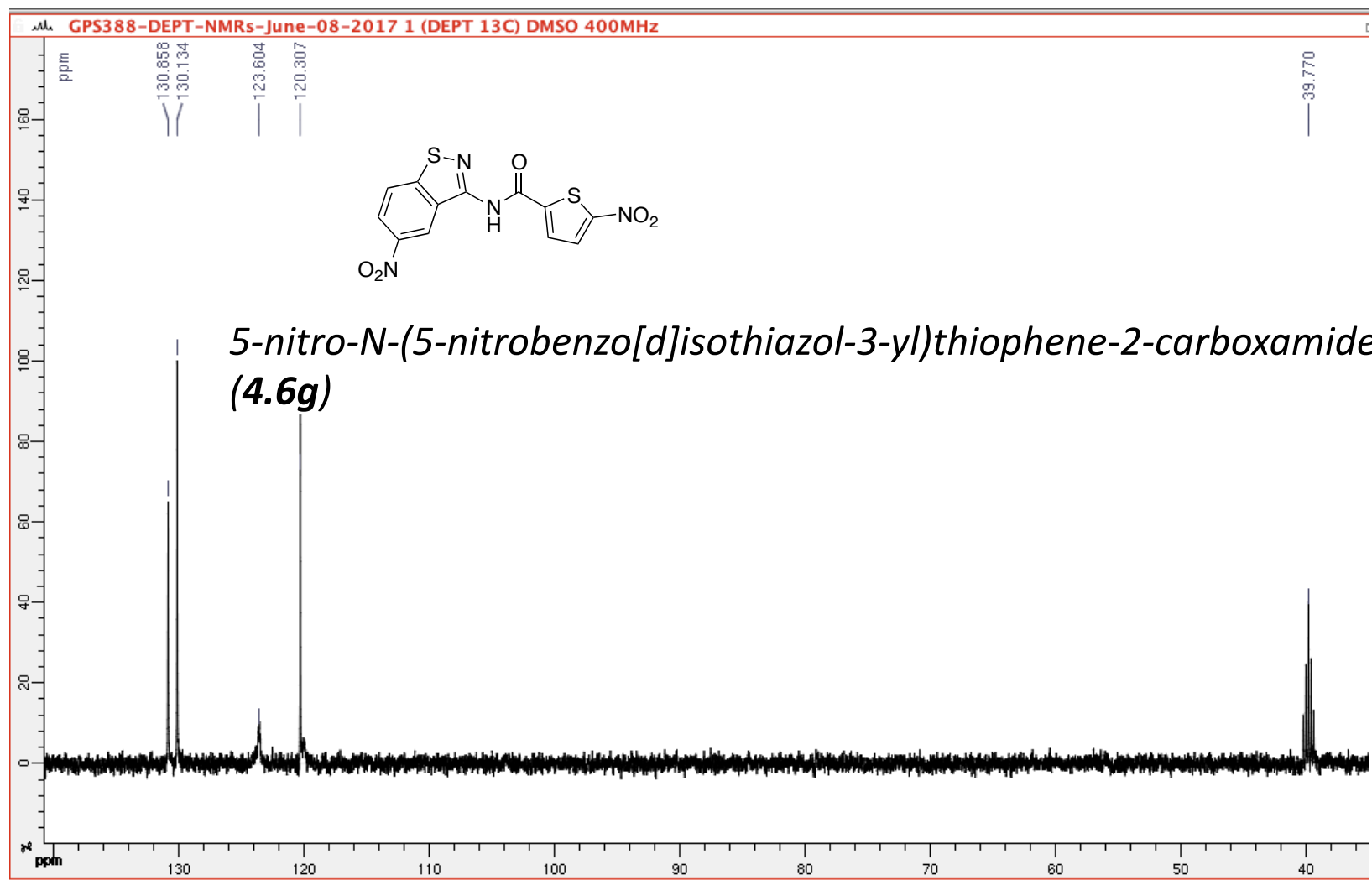




## DEPT135 NMR

(100 MHz, 297.2 K, DMSO-d<sub>6</sub>)

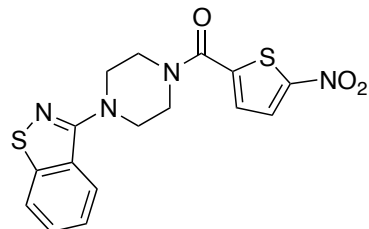
GPS388



GPS494-MZP594-B102-10mg-1H-NMR-June-03-2017

(400 MHz, 297.2 K, DMSO-d6)

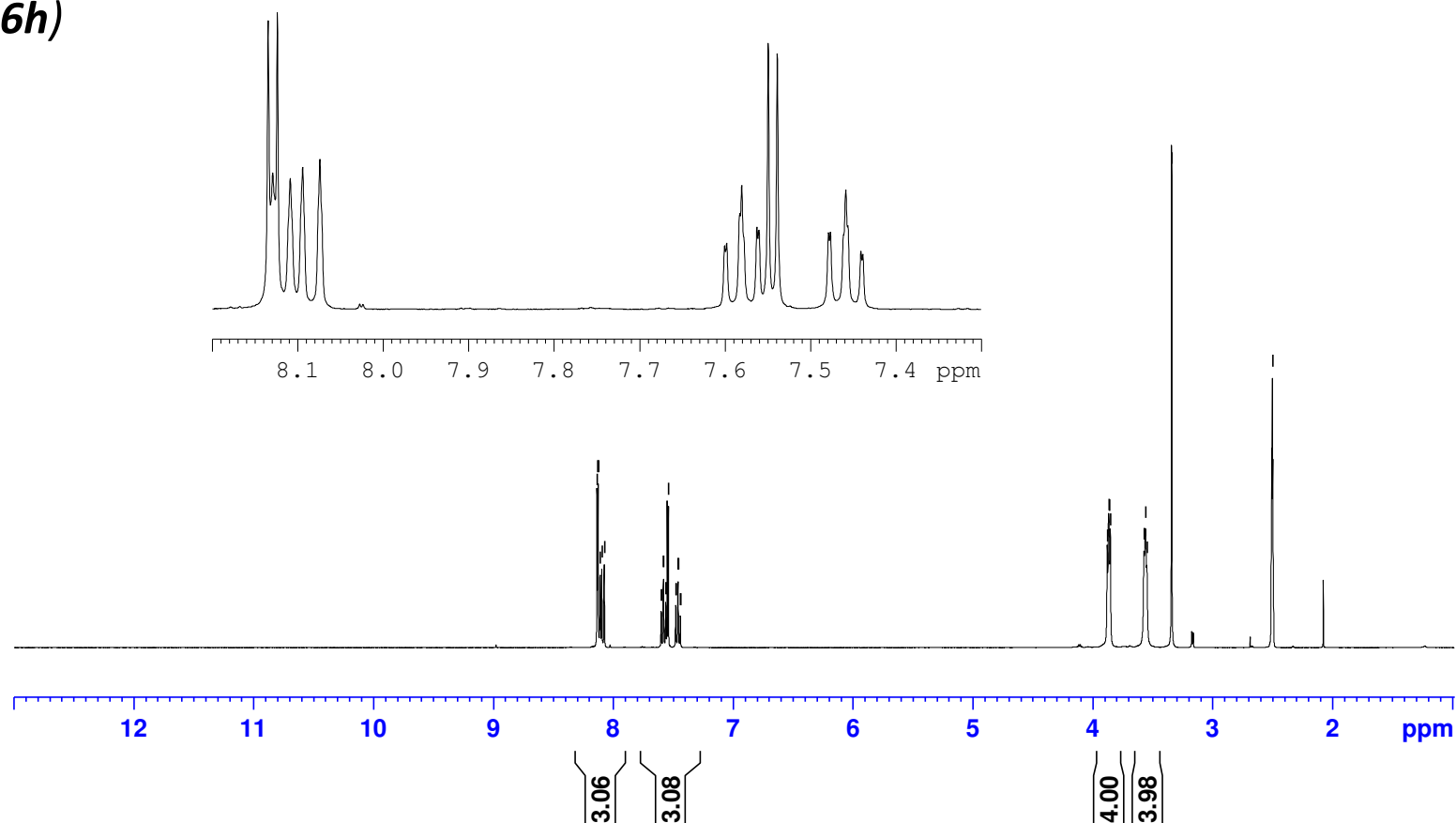
GPS494

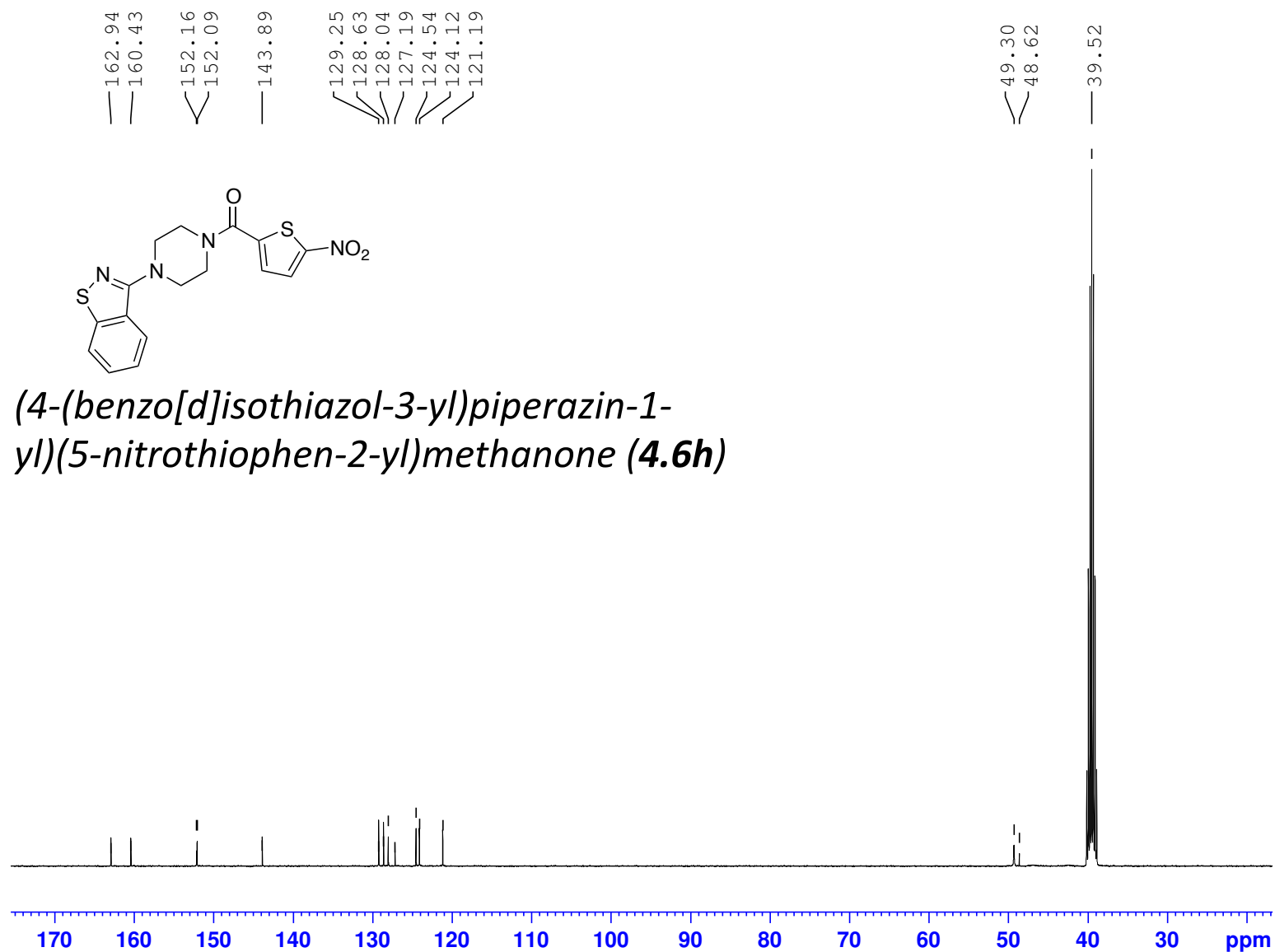


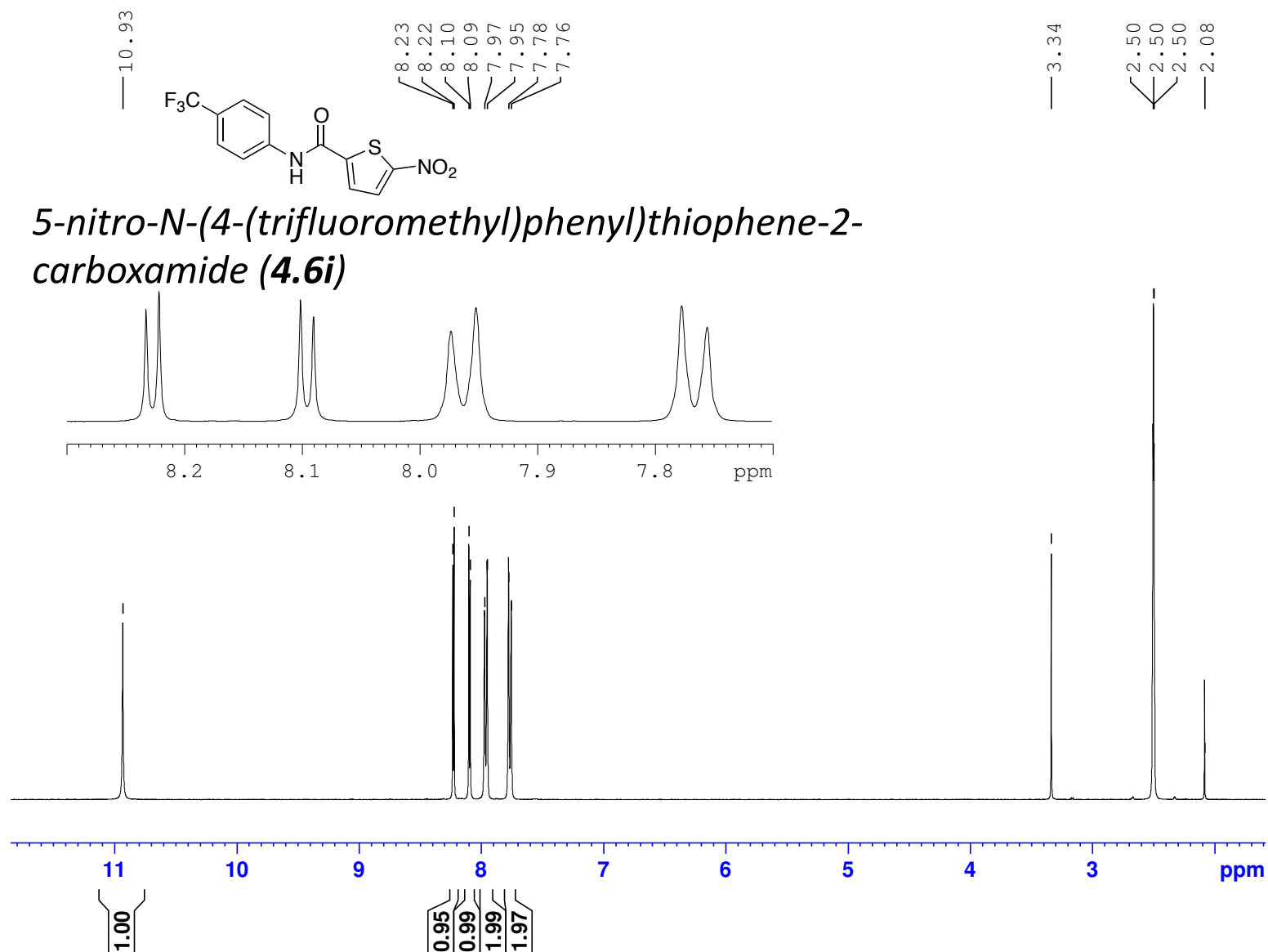
8.13  
8.13  
8.12  
8.11  
8.09  
8.07  
7.60  
7.60  
7.58  
7.58  
7.56  
7.56  
7.55  
7.54  
7.48  
7.48  
7.46  
7.46  
7.46  
7.44  
7.44

3.88  
3.87  
3.86  
3.85  
3.57  
3.56  
3.55  
3.34  
— 2.50

**(4-(benzo[d]isothiazol-3-yl)piperazin-1-yl)(5-nitrothiophen-2-yl)methanone**  
**(4.6h)**

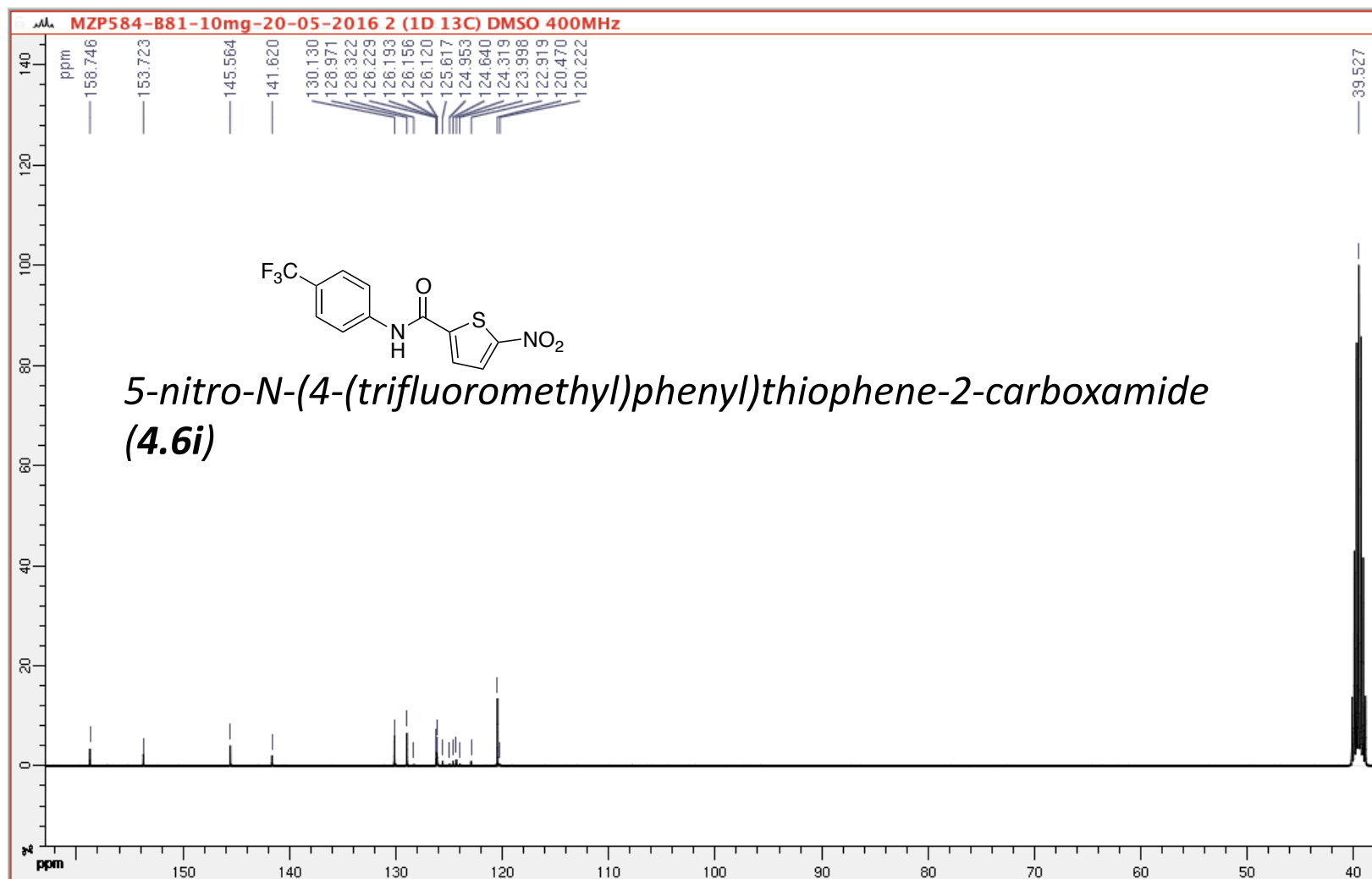




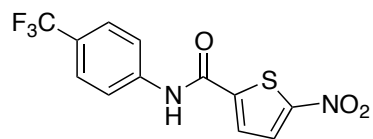


(100 MHz, 297.2 K, DMSO-d6)

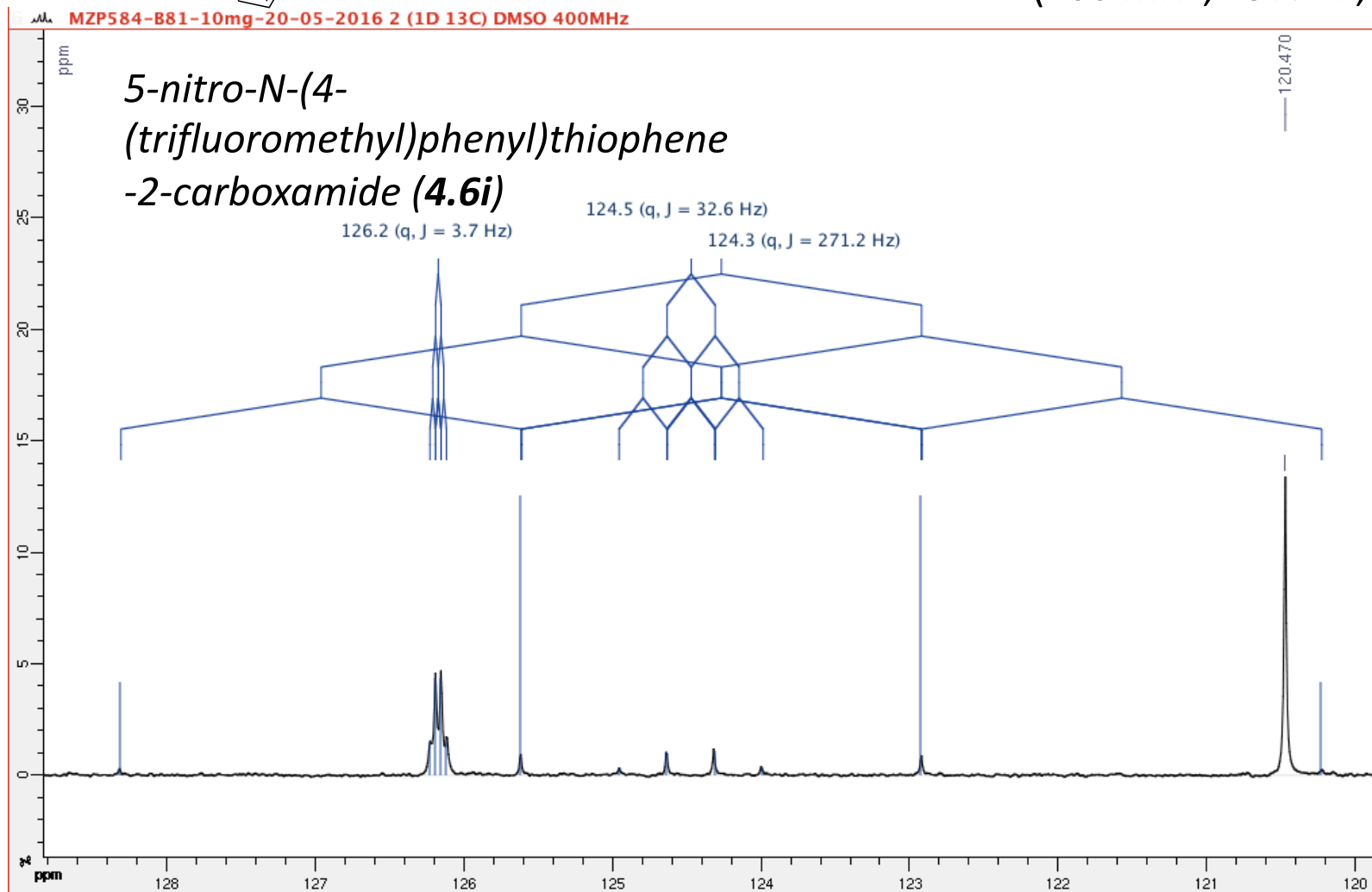
GPS431

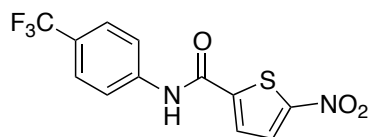




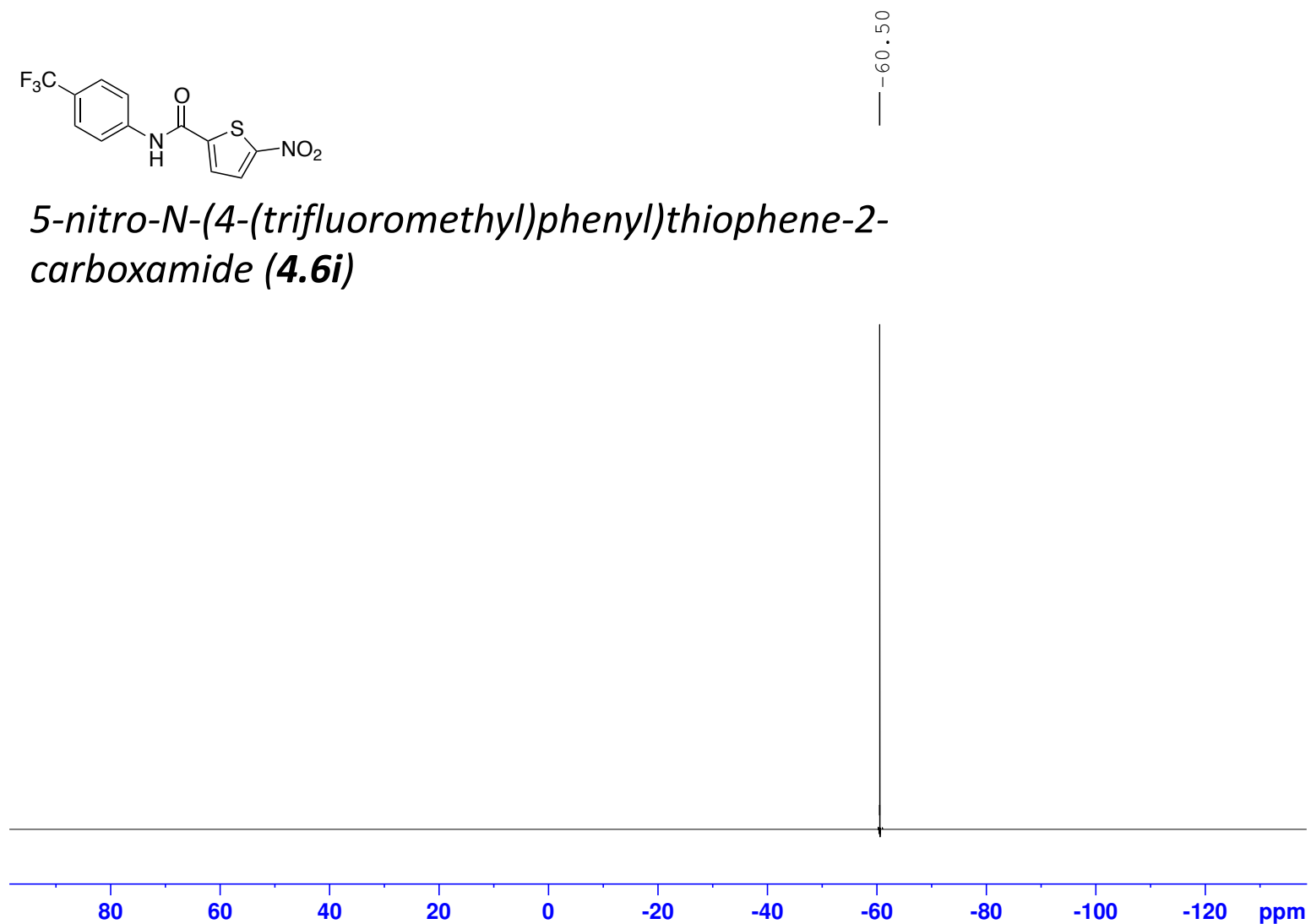


GPS431  
(100 MHz, 297.2 K, DMSO-d6)





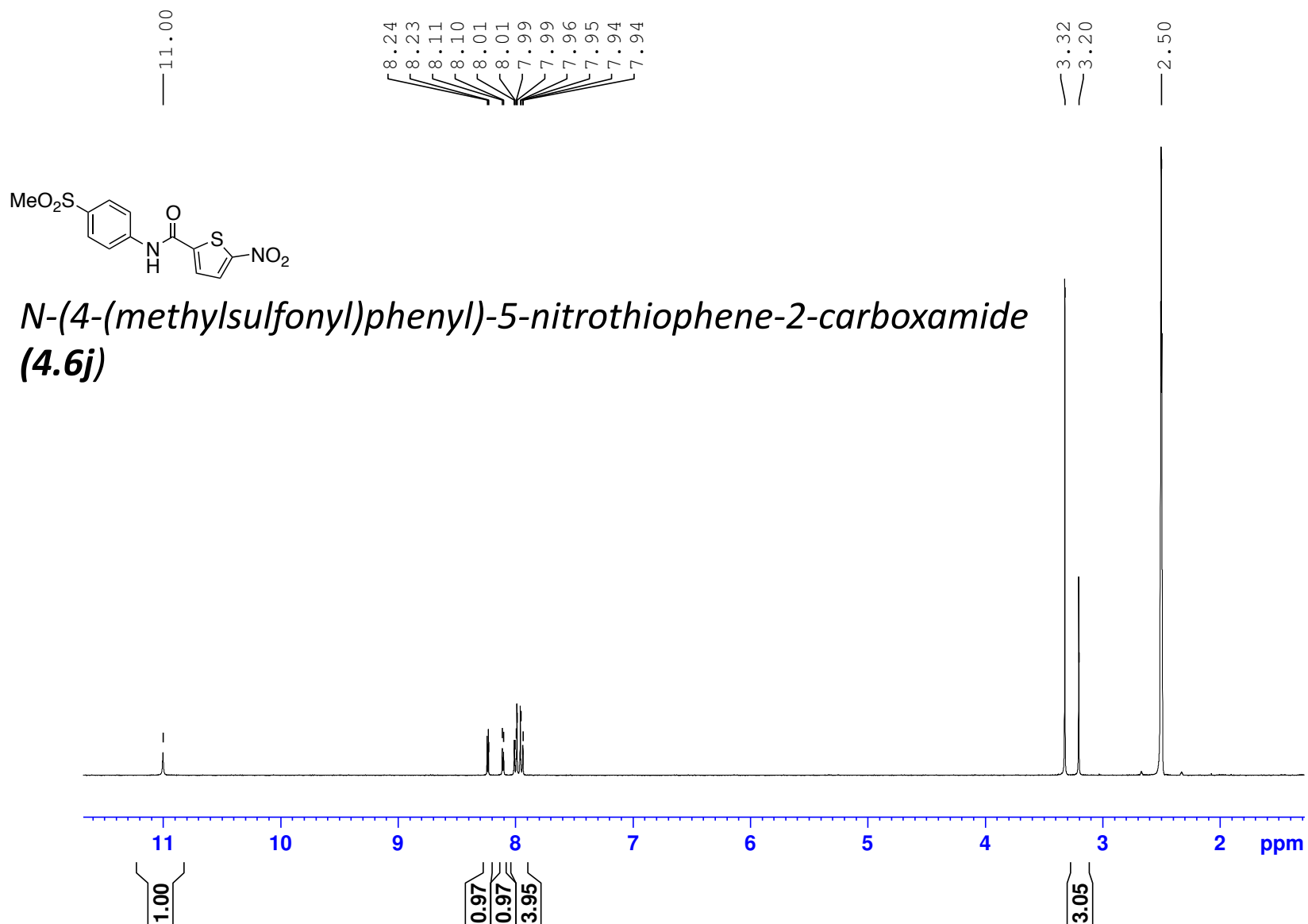
*5-nitro-N-(4-(trifluoromethyl)phenyl)thiophene-2-carboxamide (4.6i)*



MZP573-B89-1H-NMR-14-03-2016

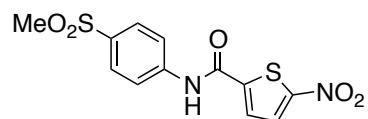
(400 MHz, 297.2 K, DMSO-d6)

GPS438

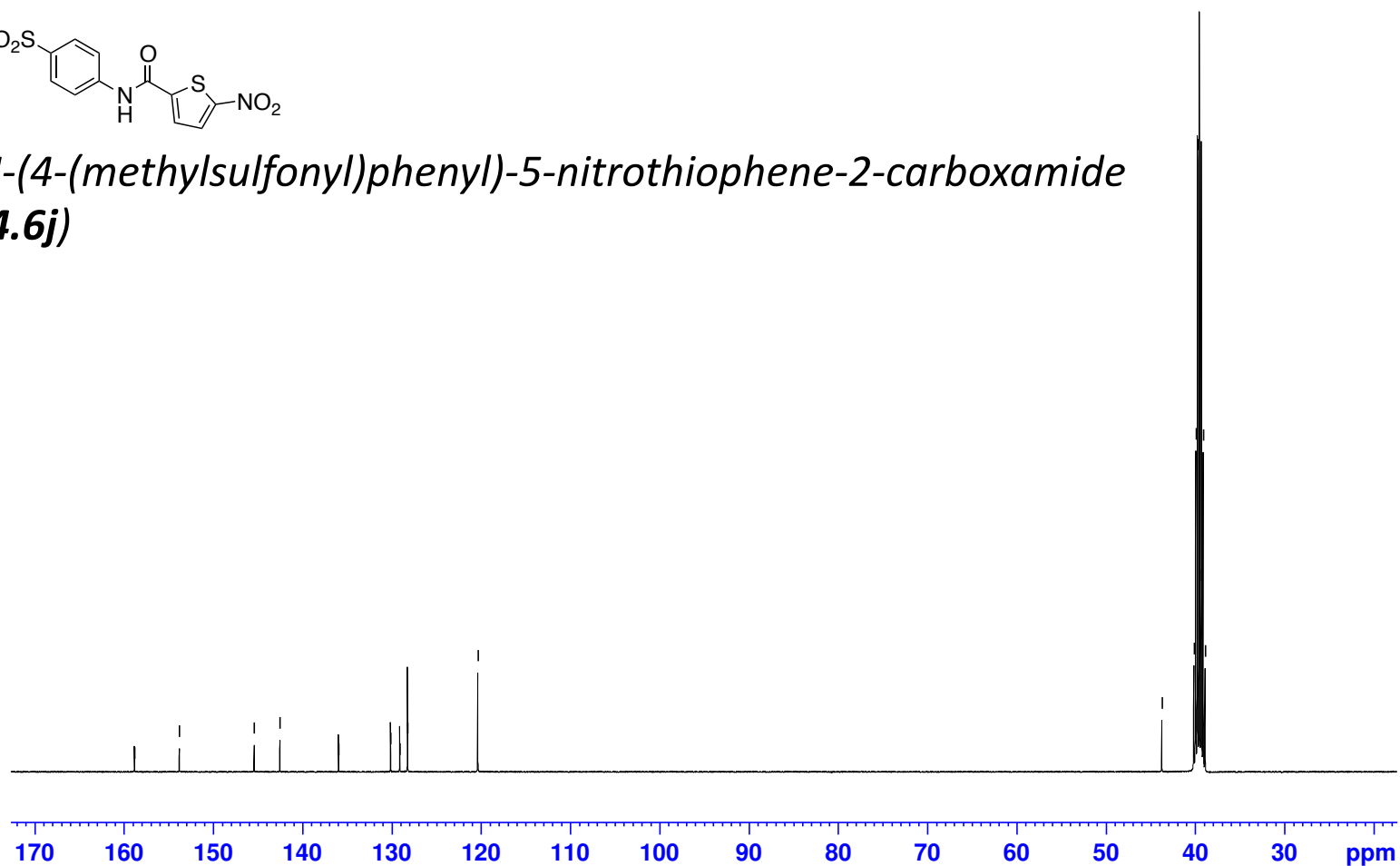


— 158.84  
— 153.81  
— 145.42  
— 142.53  
— 135.96  
— 130.14  
— 129.11  
— 128.24  
— 120.37

43.73  
40.14  
39.93  
39.72  
39.52  
39.31  
39.10  
38.89



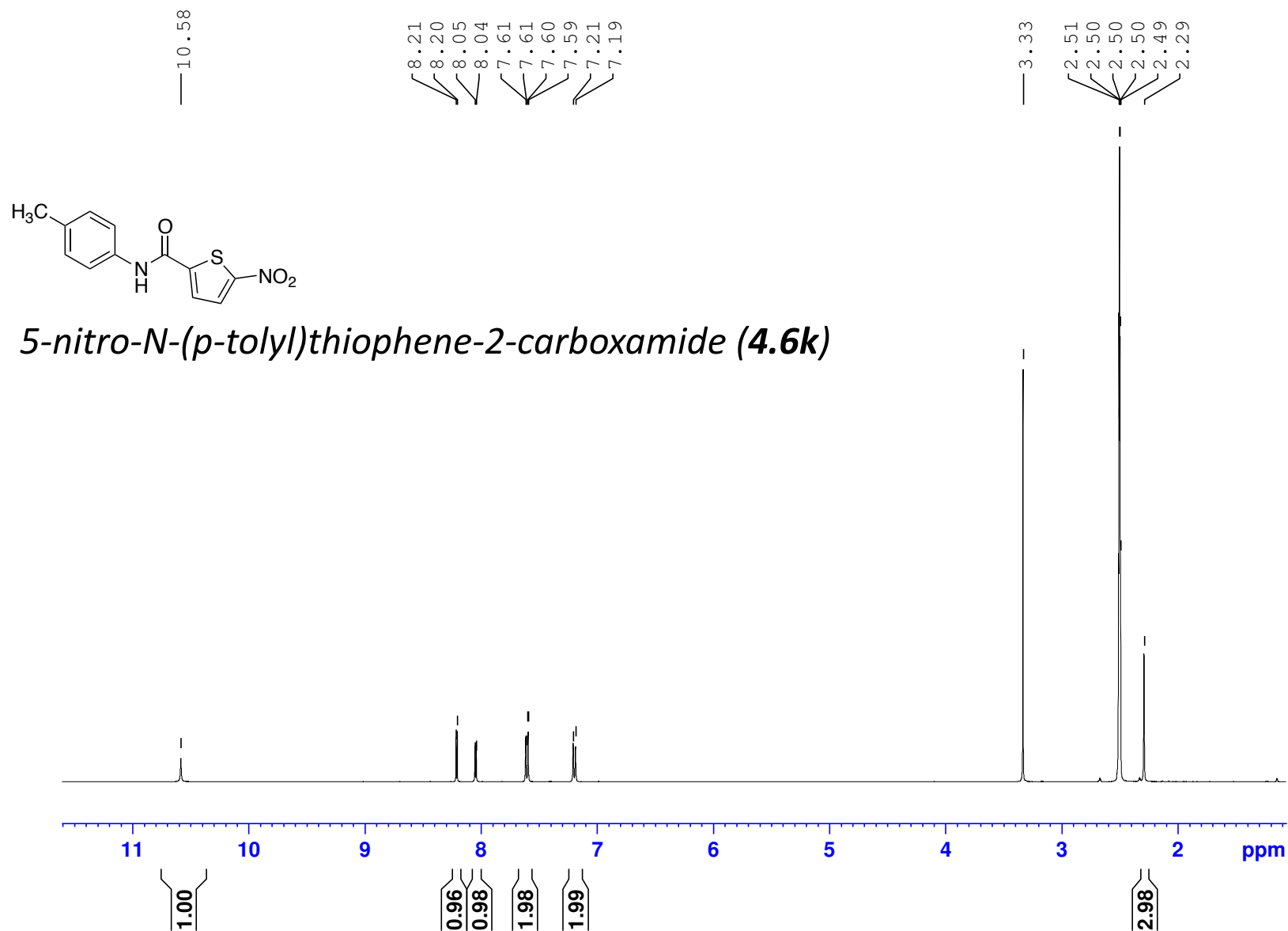
*N*-(4-(methylsulfonyl)phenyl)-5-nitrothiophene-2-carboxamide  
**(4.6j)**

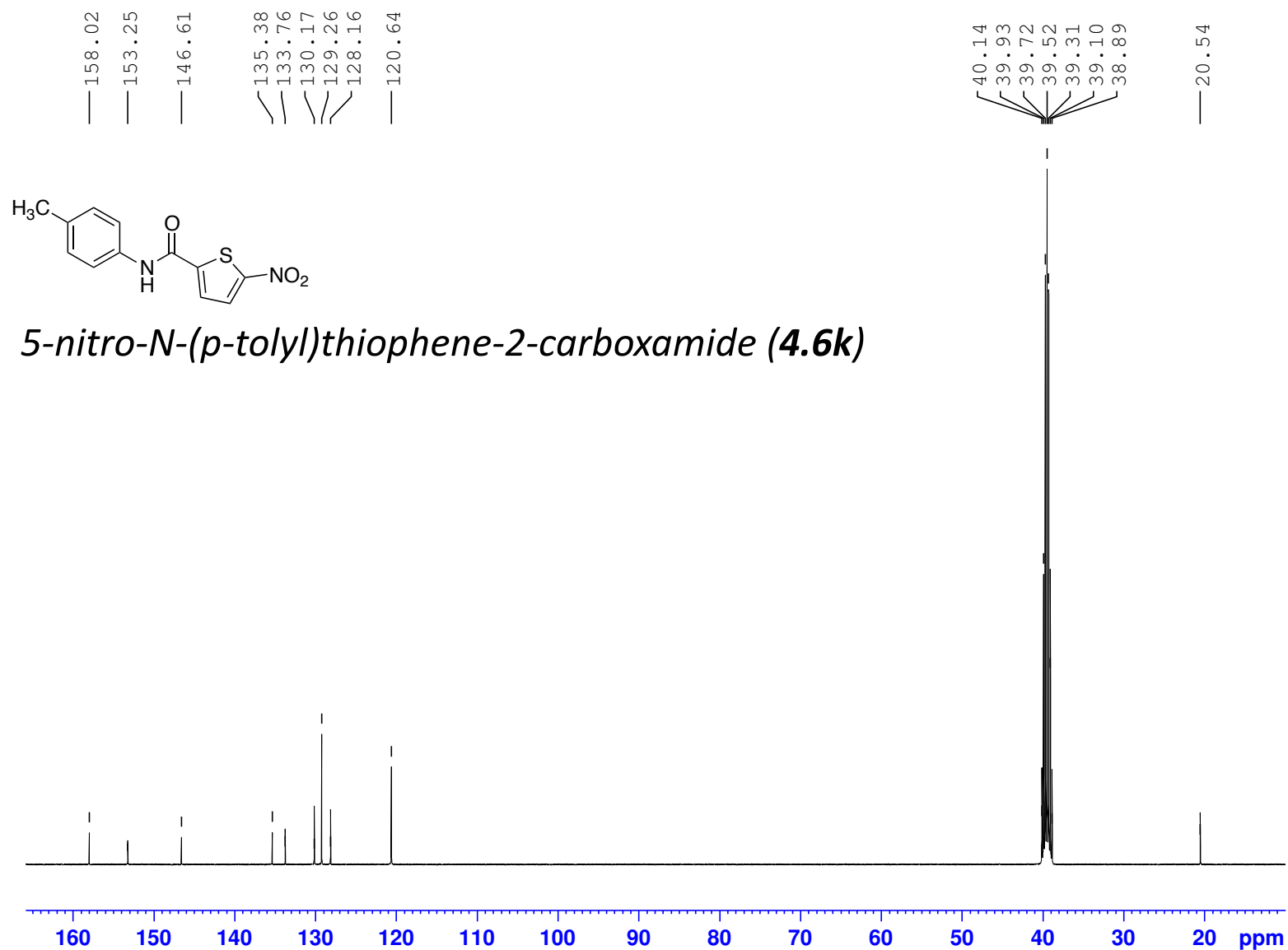


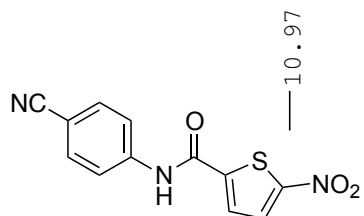
MZP584-B85-1H-NMR-04-04-2016

(400 MHz, 297.2 K, DMSO-d6)

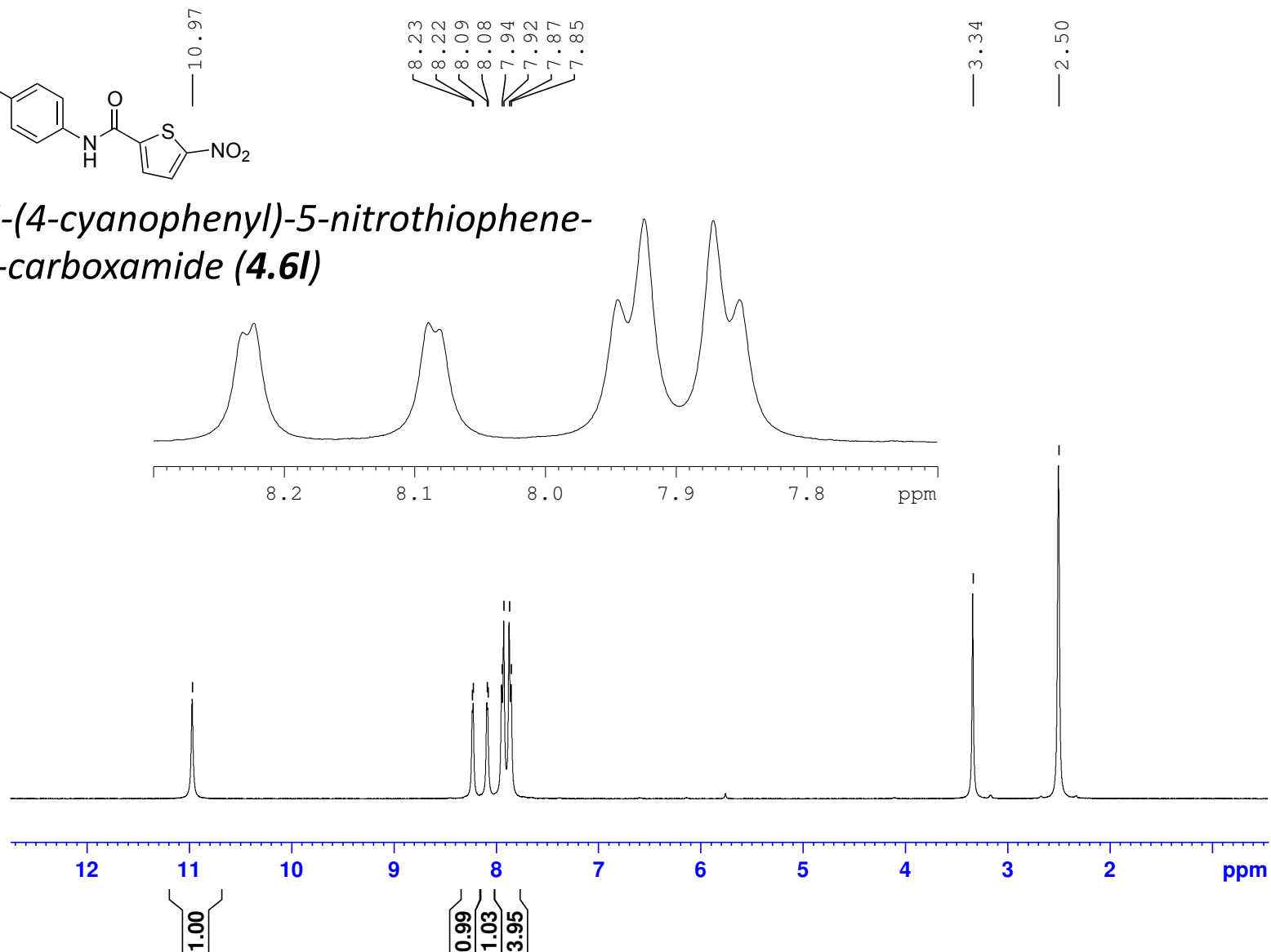
GPS434

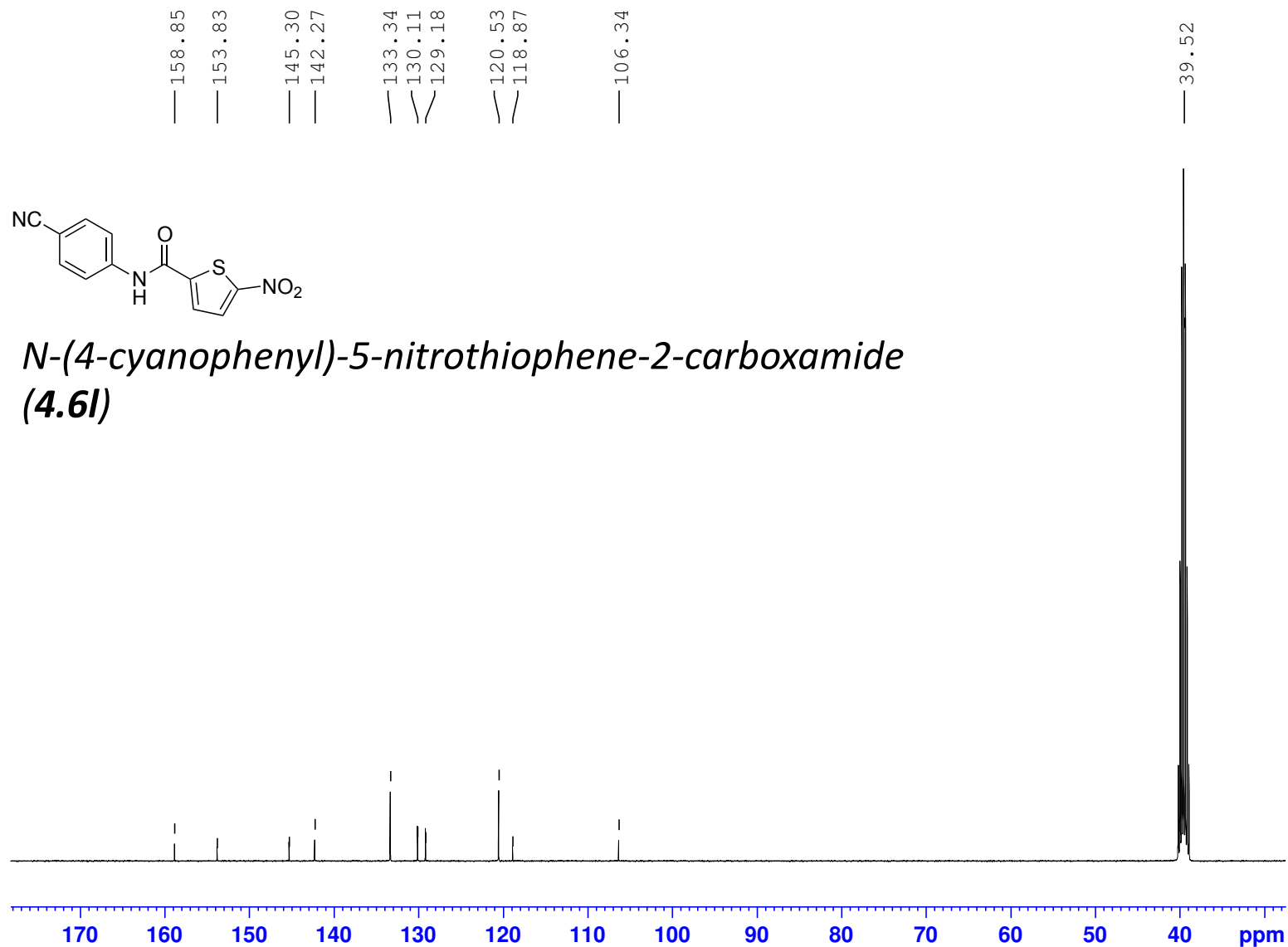




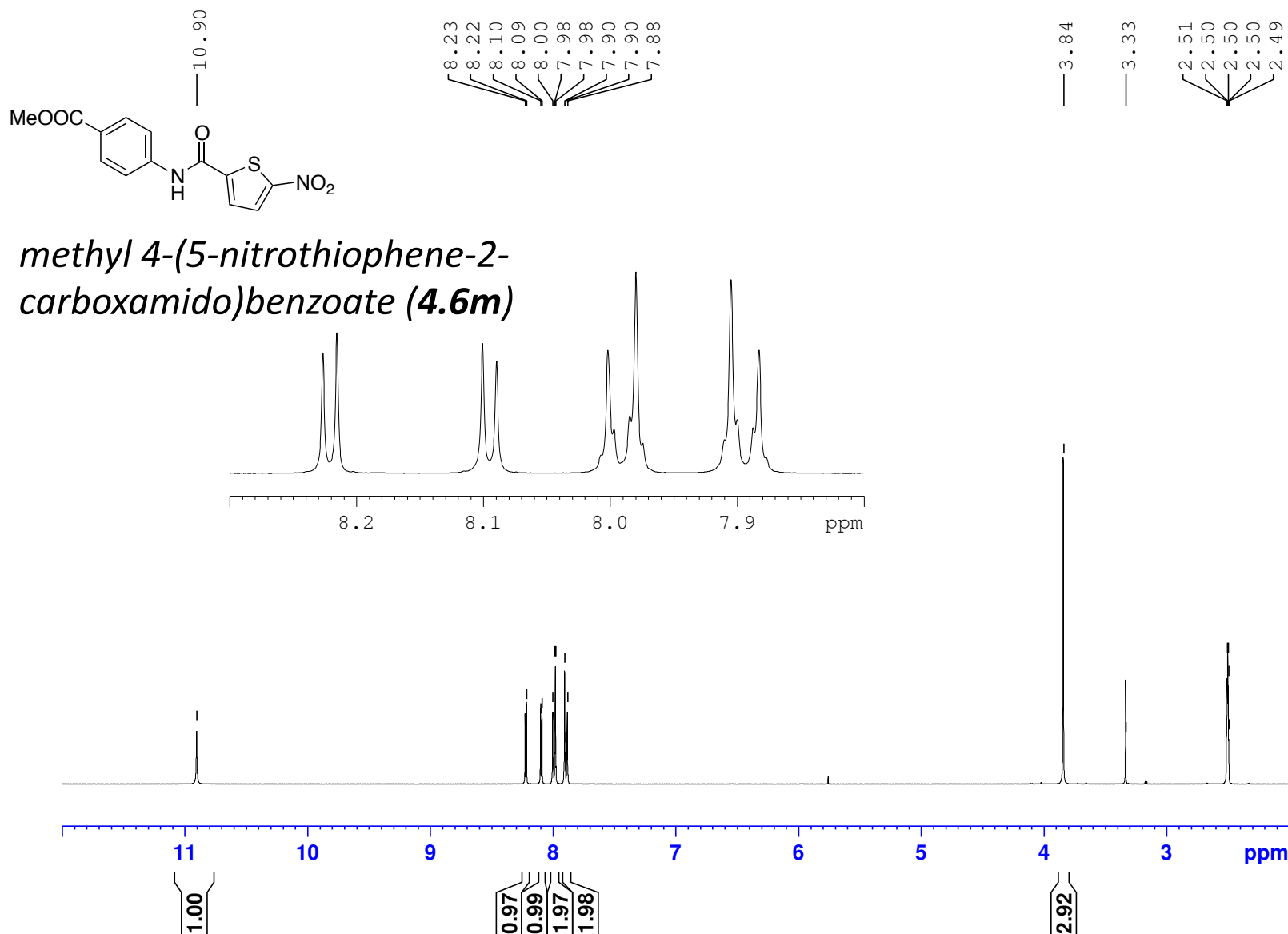


*N*-(4-cyanophenyl)-5-nitrothiophene-2-carboxamide (**4.6I**)





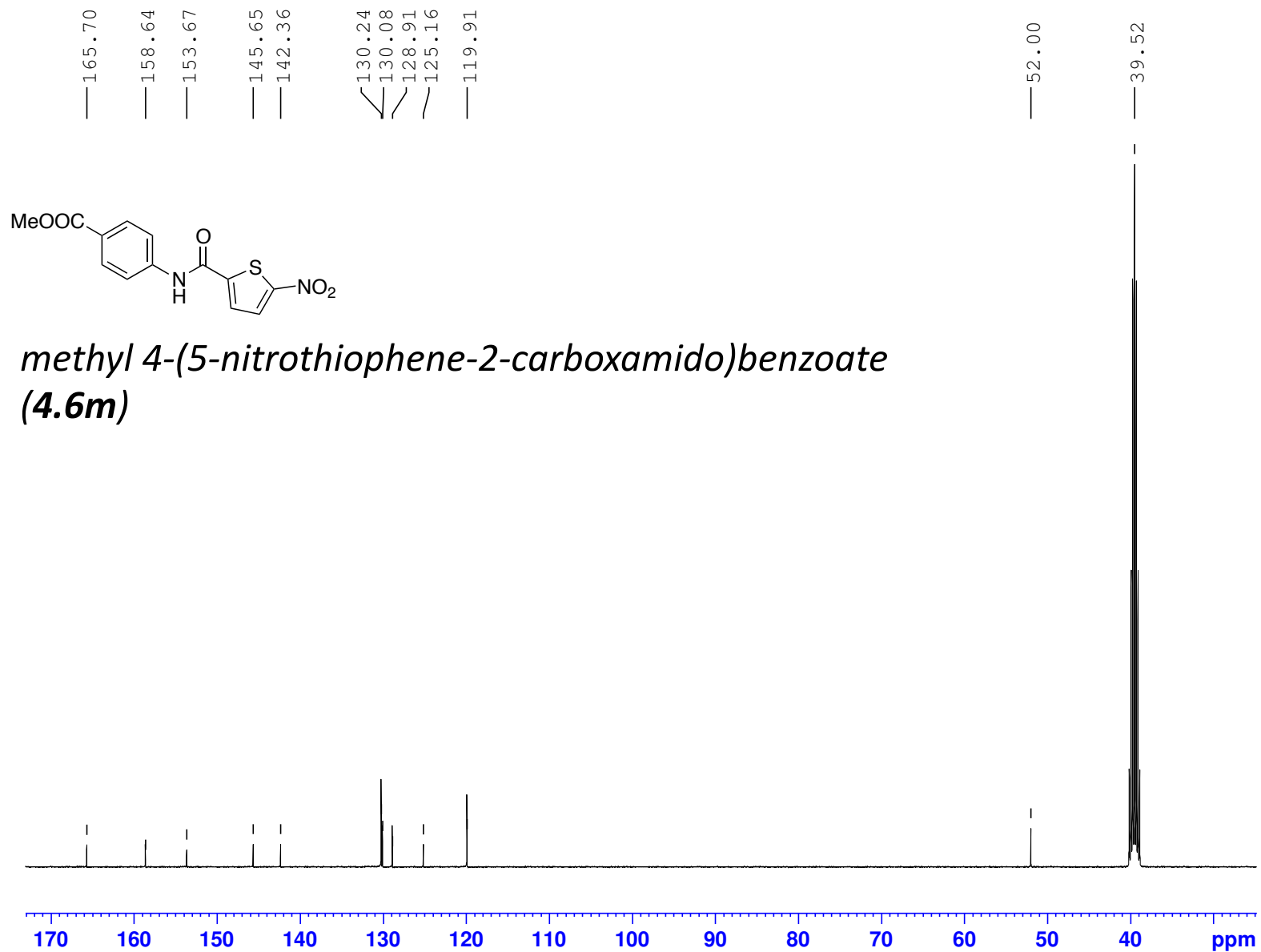




GPS420-MZP109-13C-NMR-May-24-2017

(100 MHz, 297.2 K, DMSO-d6)

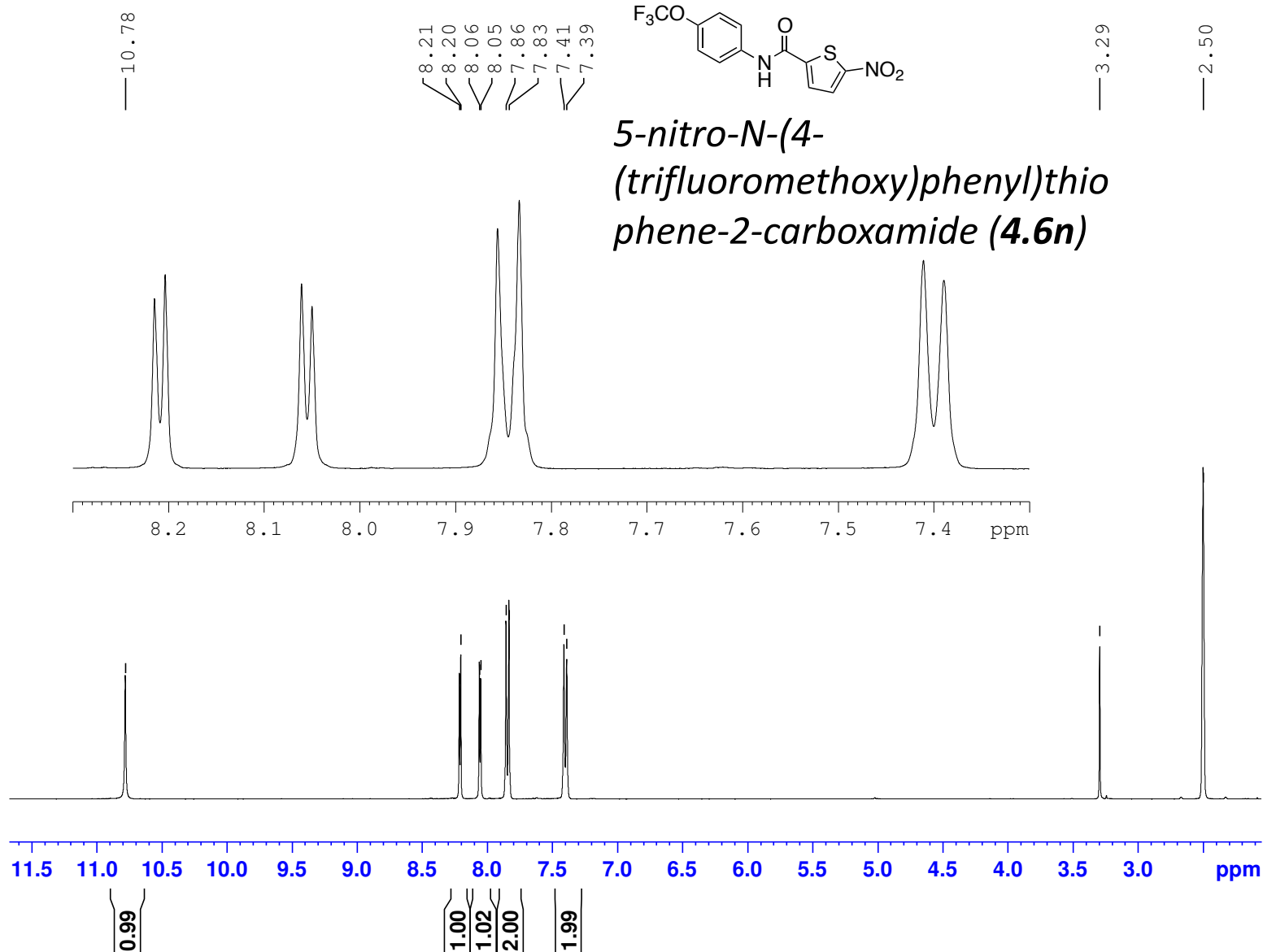
GPS420



MZP692-ABX-amine-C2-10mg-1H-NMR-April-06-2018

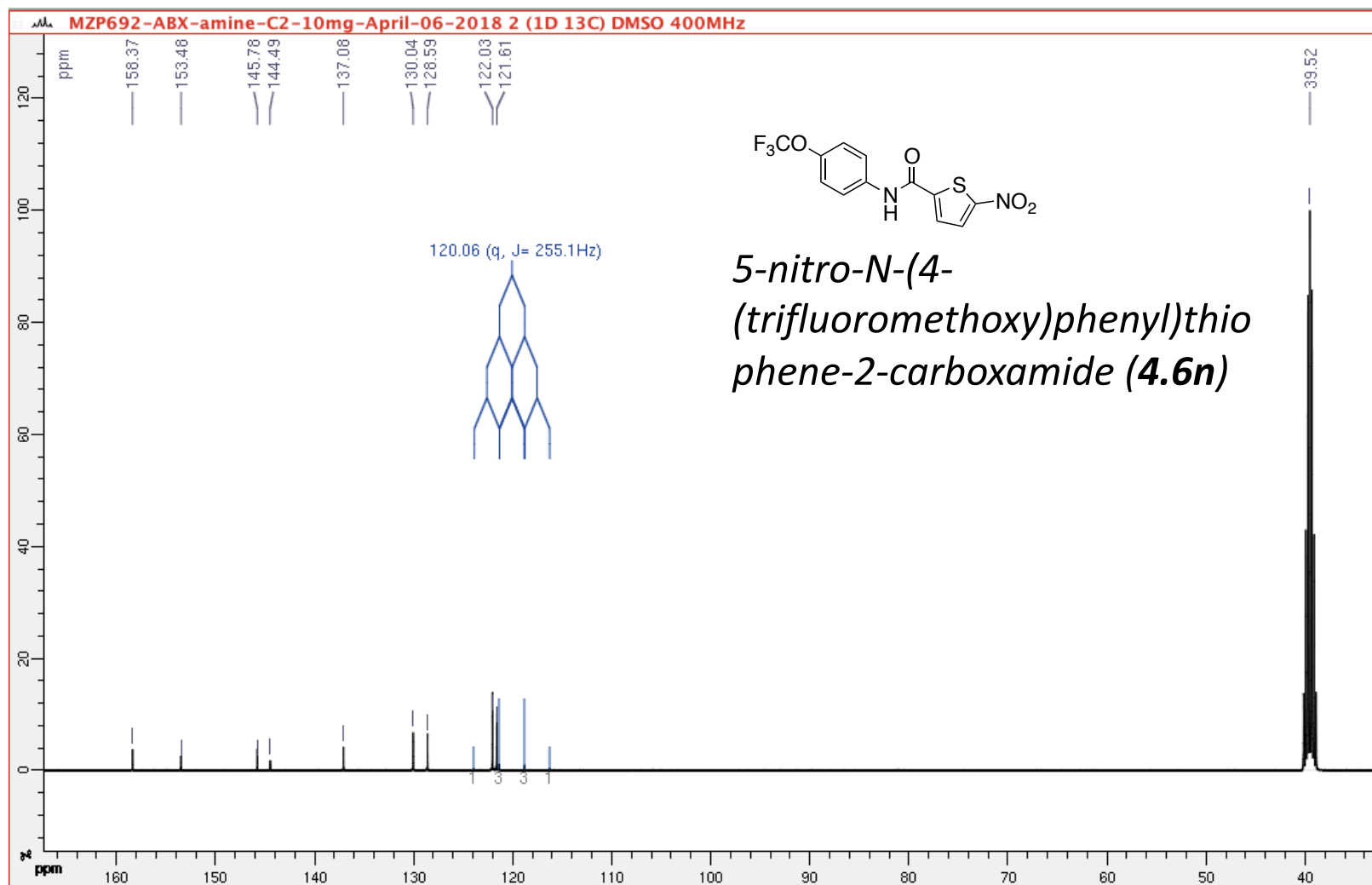
(400 MHz, 297.2 K, DMSO-d6)

GPS514



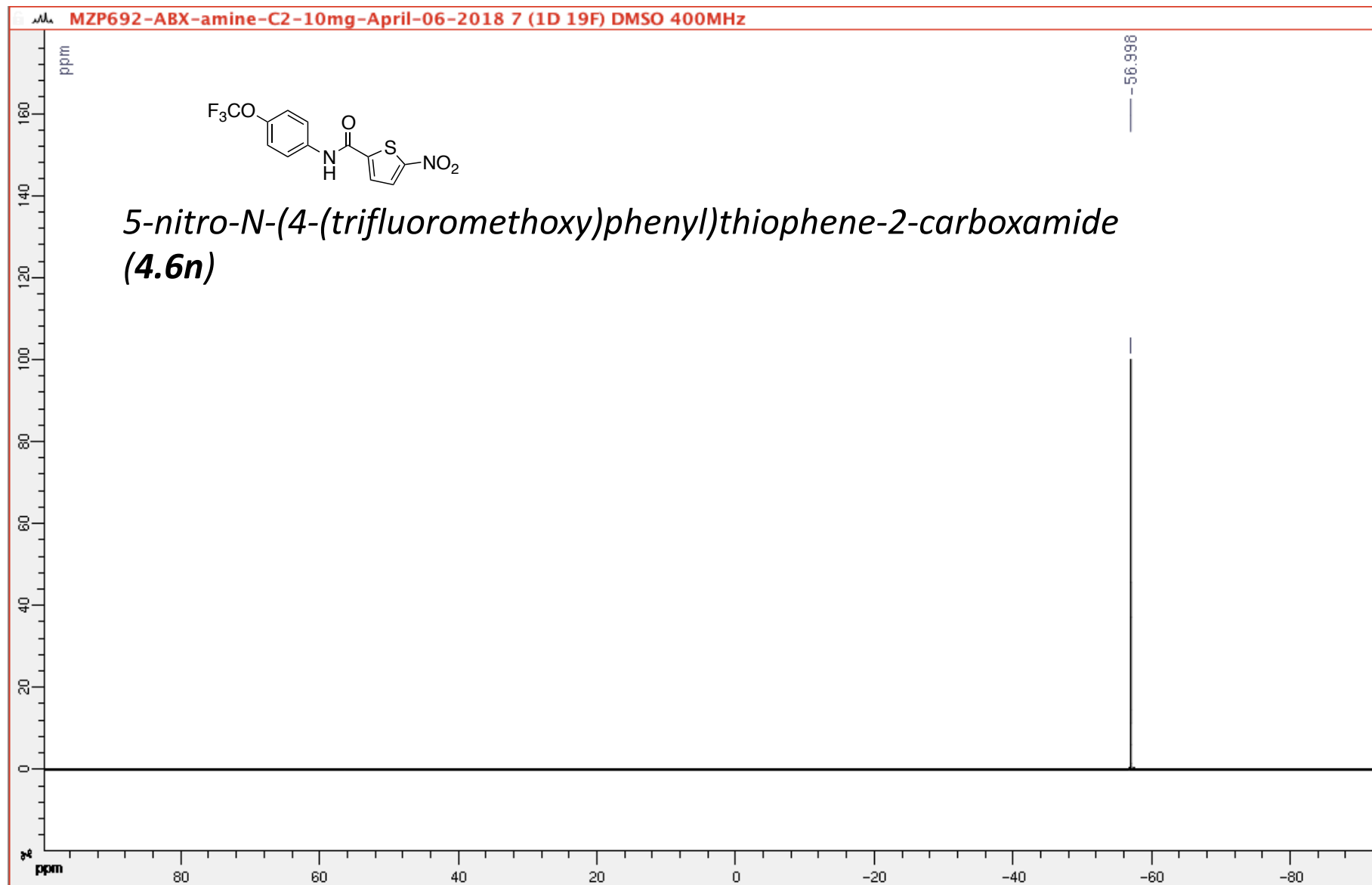
(100 MHz, 297.2 K, DMSO-d6)

GPS514



(400 MHz, 297.2 K, DMSO-d6)

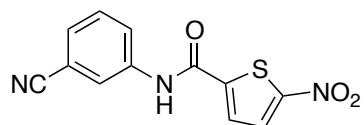
GPS514



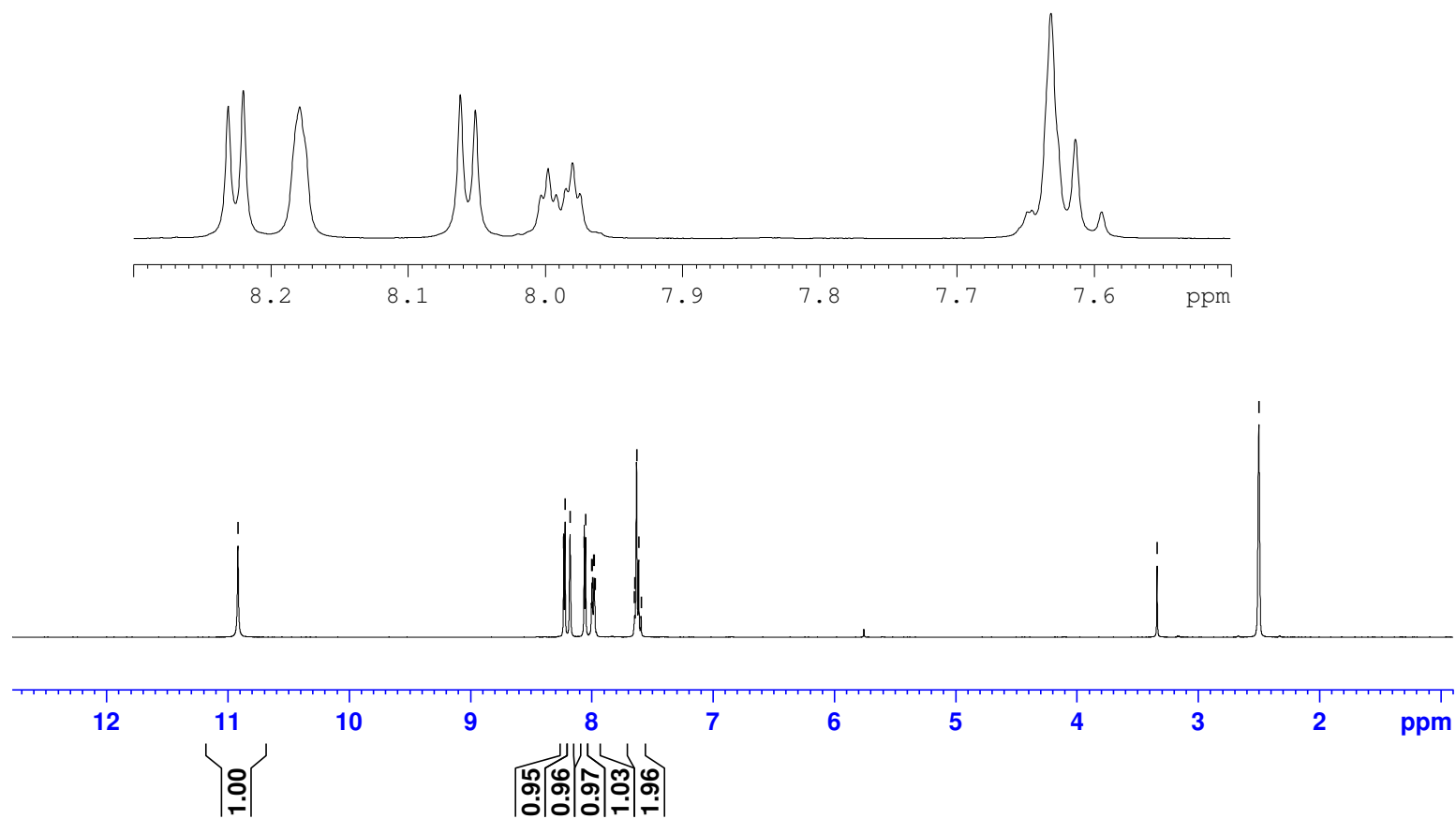
GPS419-A14-1H-NMR-May-30-2017

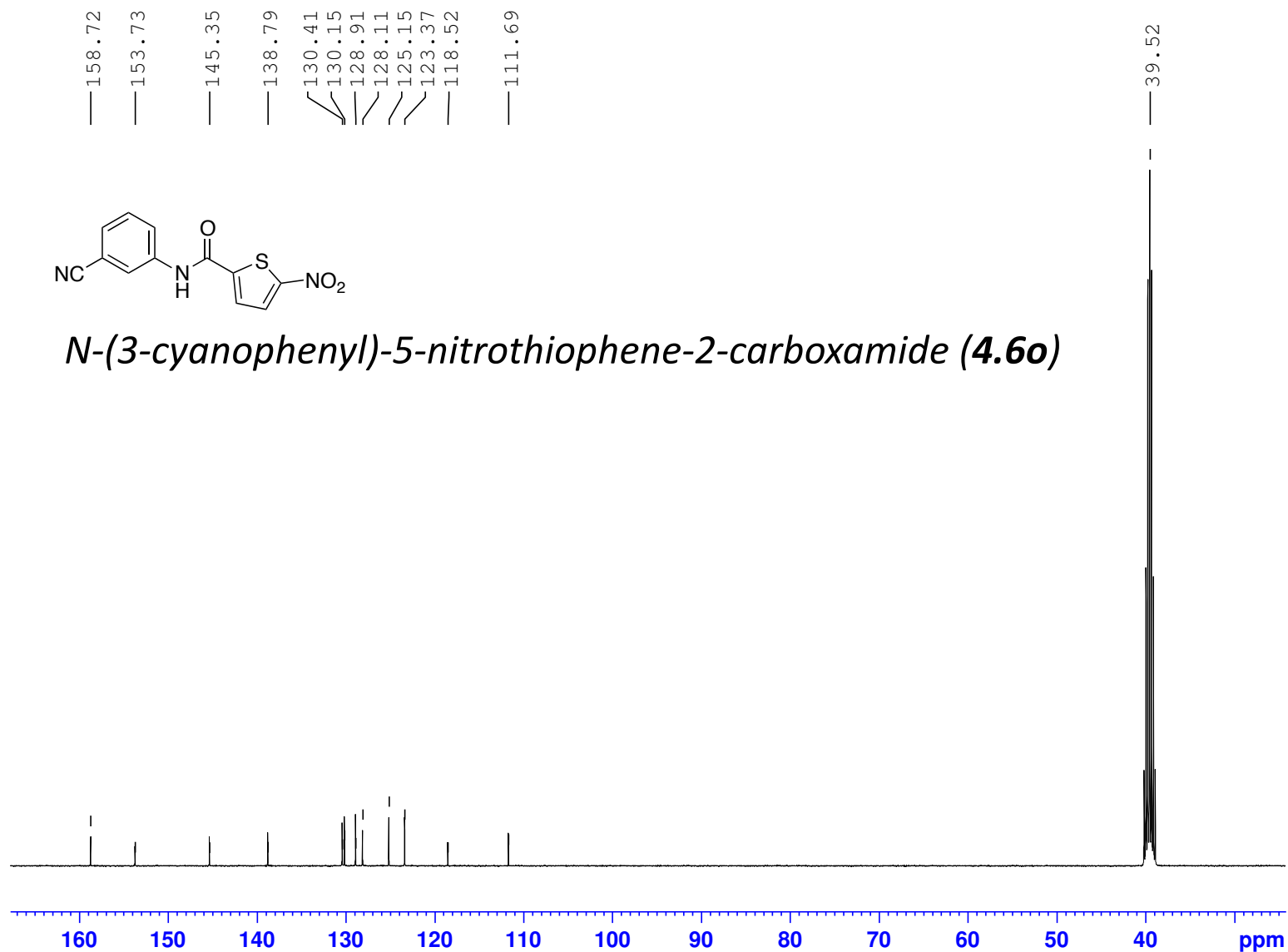
(400 MHz, 297.2 K, DMSO-d6)

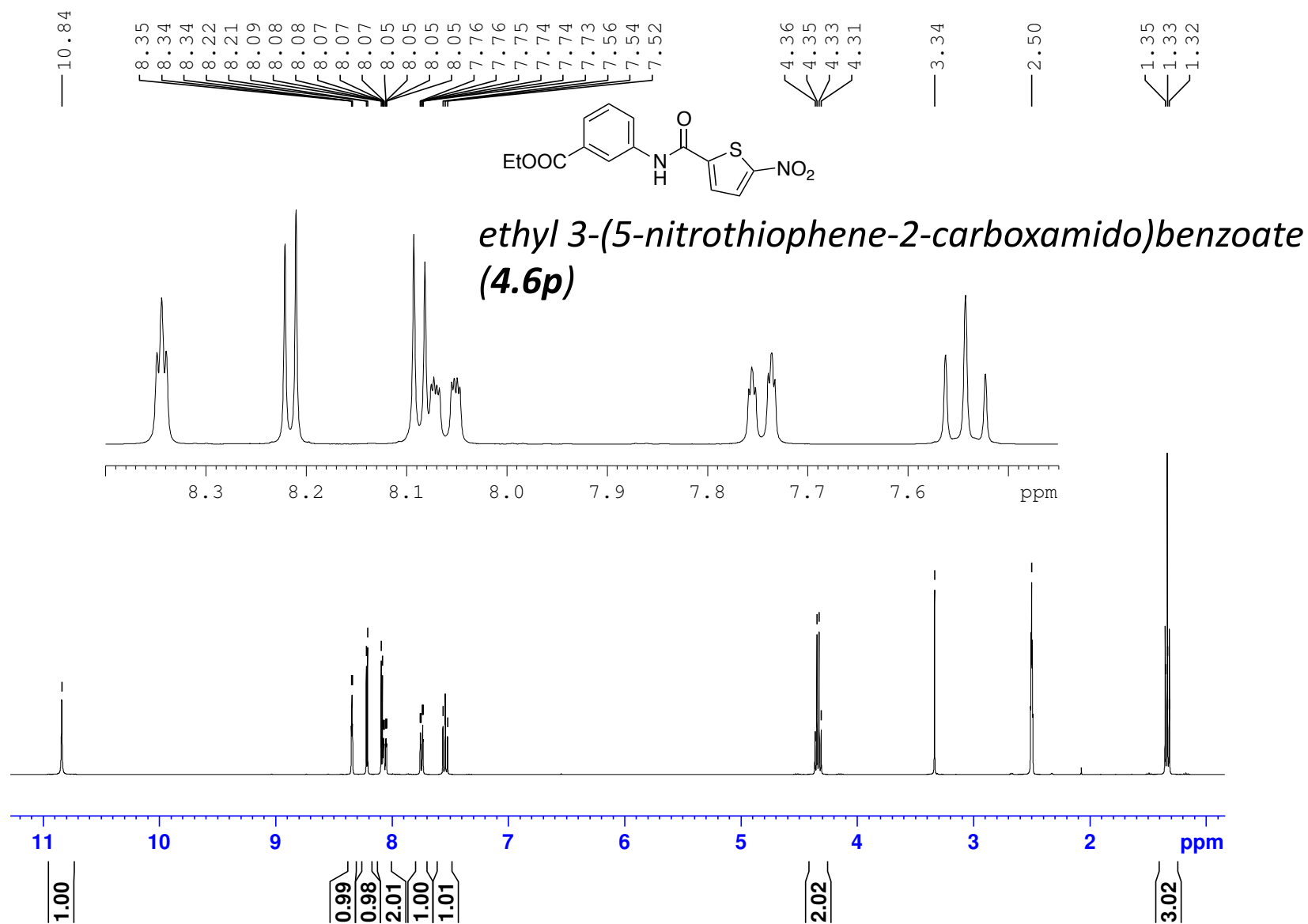
GPS419



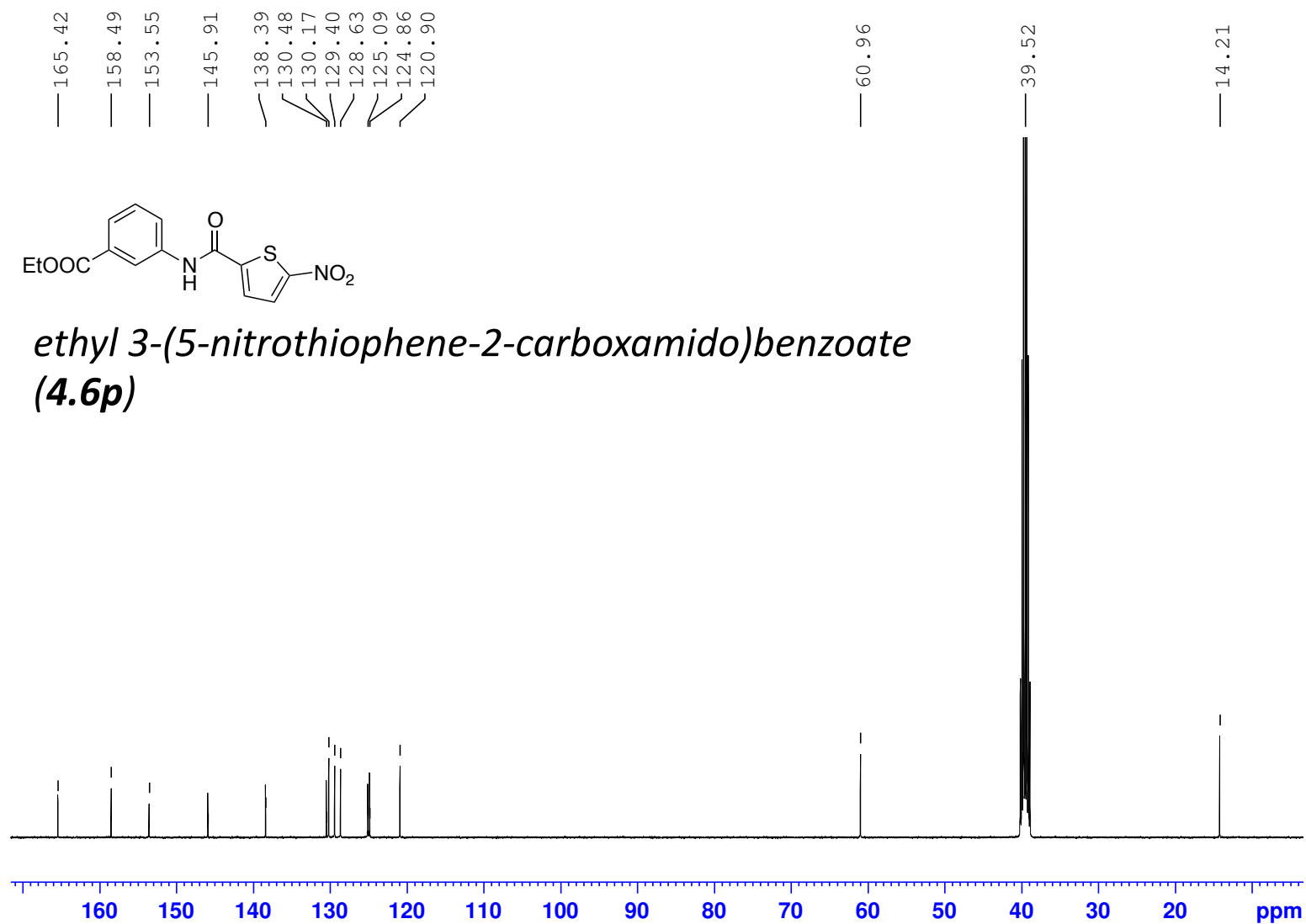
*N*-(3-cyanophenyl)-5-nitrothiophene-2-carboxamide (**4.6o**)

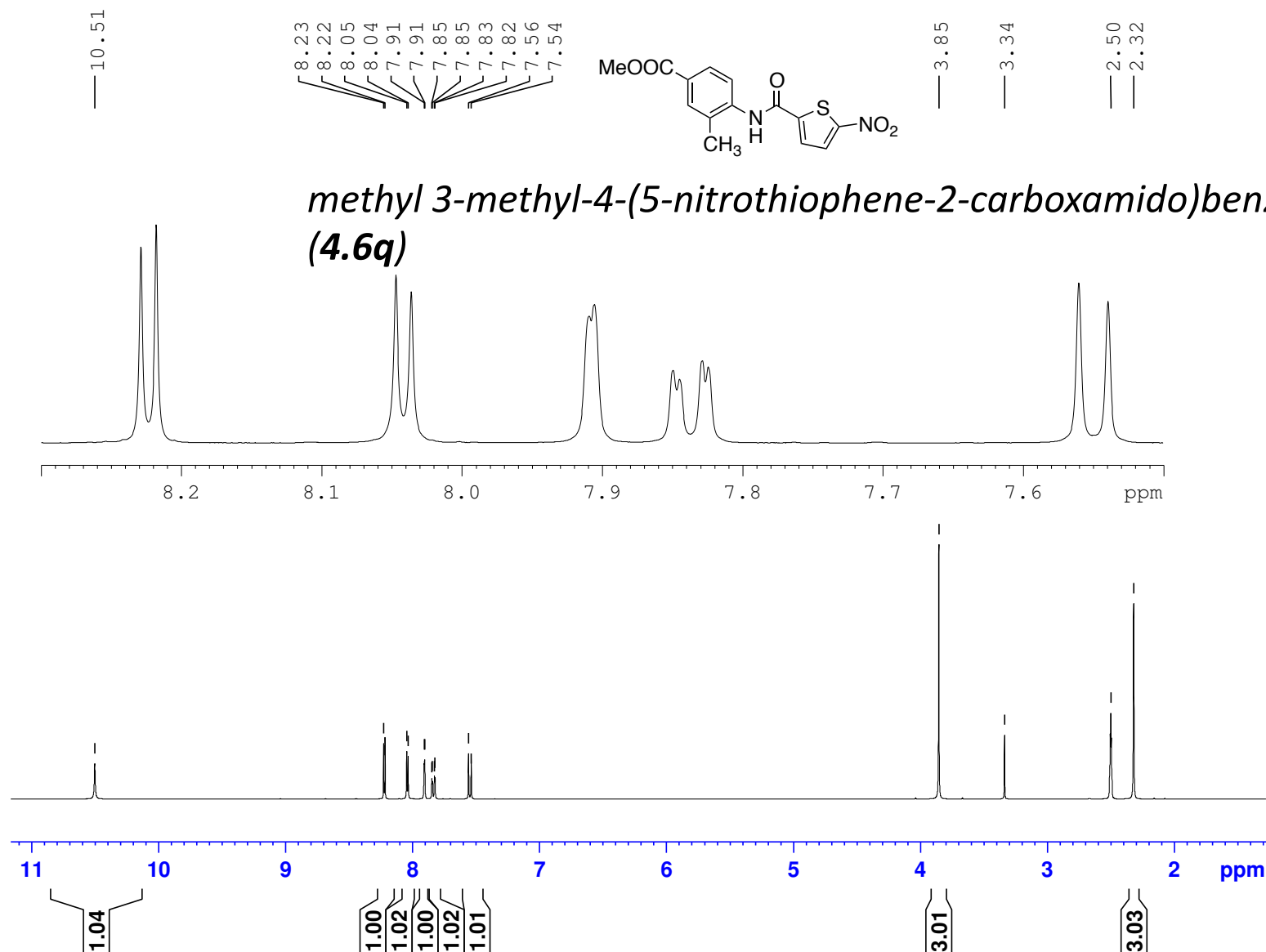








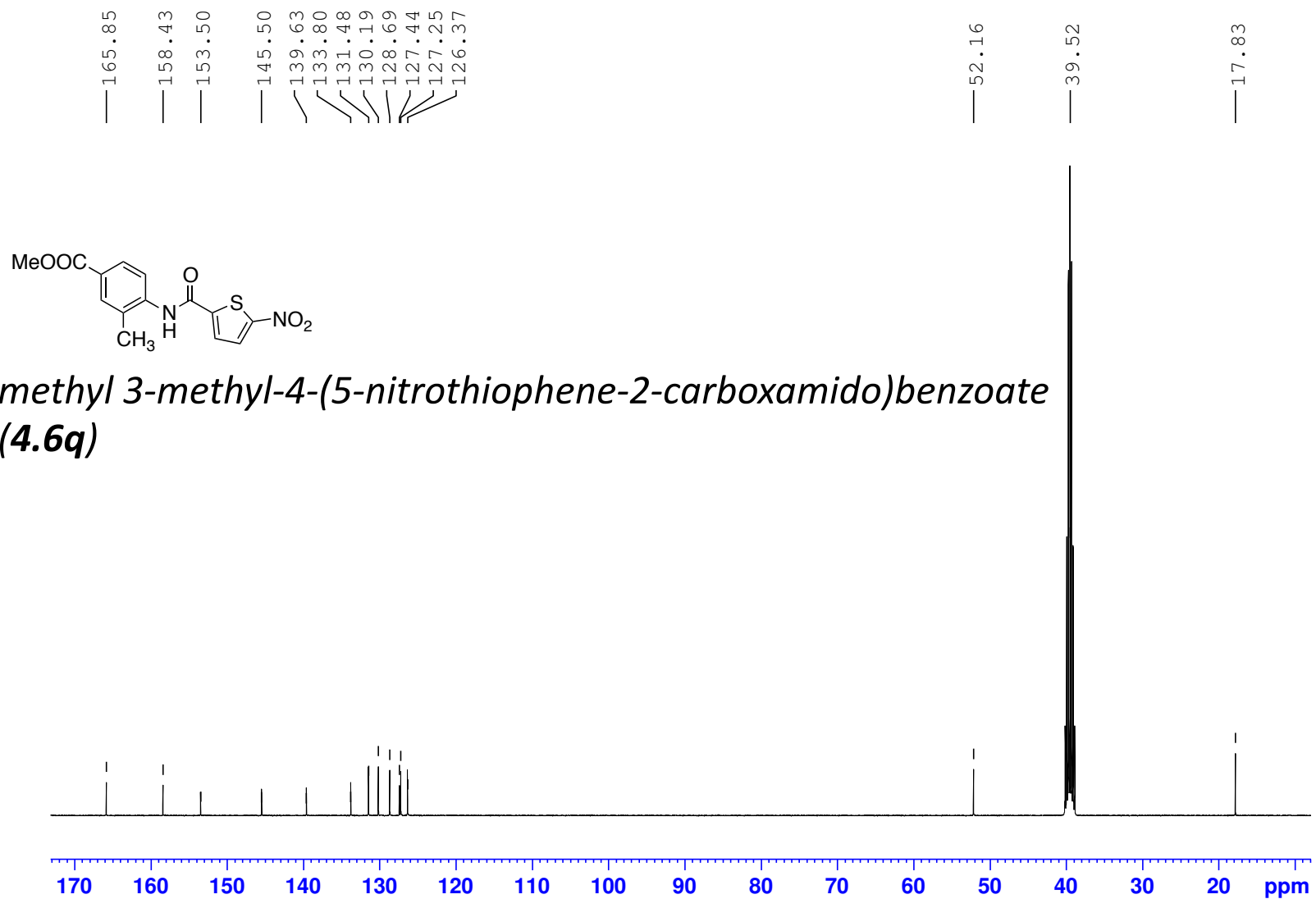




(100 MHz, 297.2 K, DMSO-d6)

GPS429

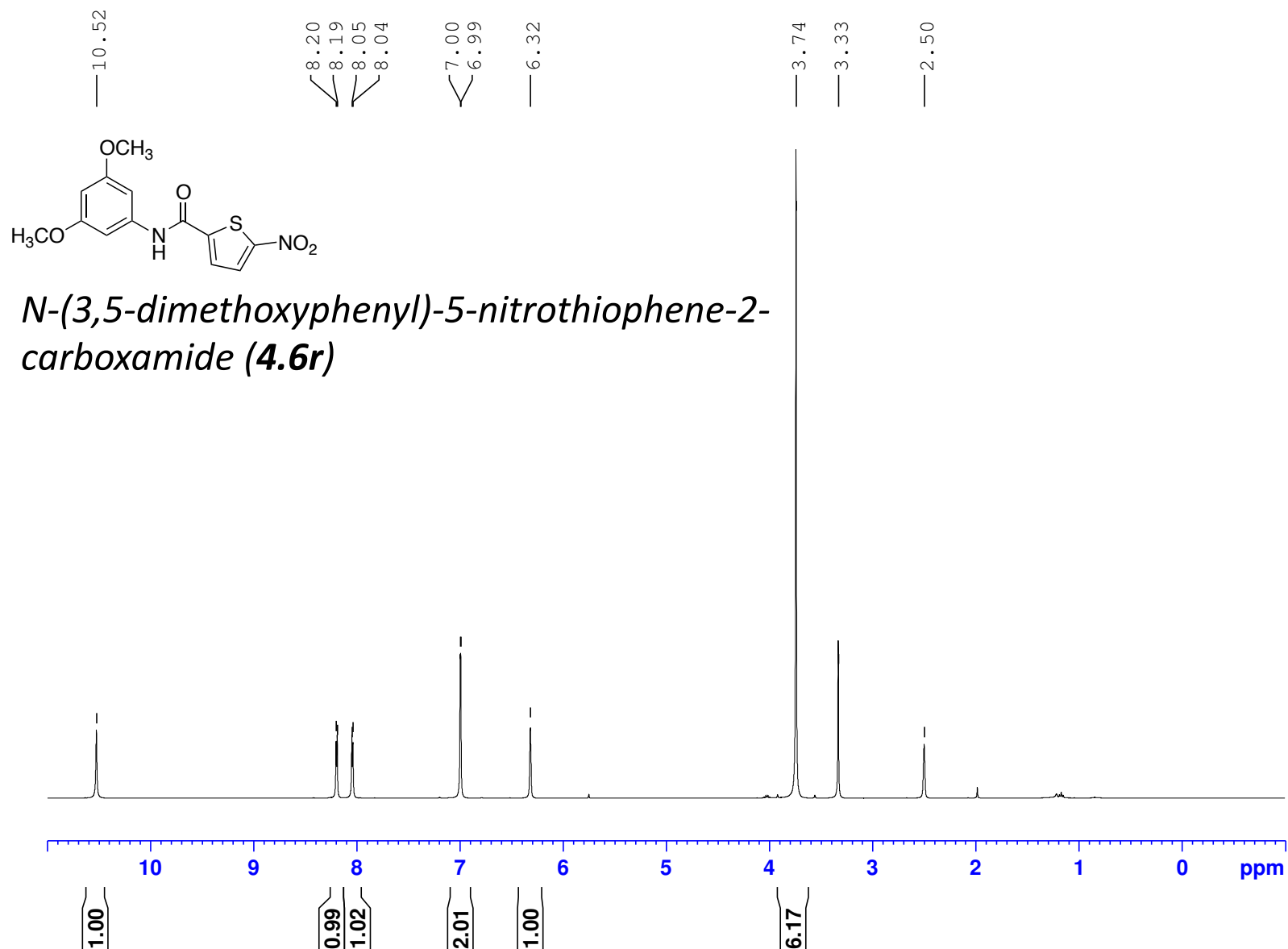
phar\_13CBB DMSO {C:\Bruker\TopSpin3.2} Maryam 15



GPS400-MZP-Amide-NT-0001-1H-NMR

(400 MHz, 297.2 K, DMSO-d6)

GPS400



GPS400-MZP-Amide-NT-0001-13C-NMR

(100 MHz, 297.2 K, DMSO-d6)

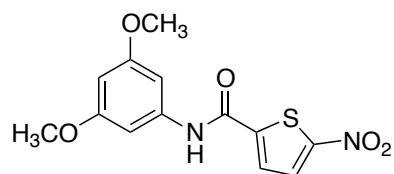
GPS400

160.46  
158.24  
153.42  
146.30  
139.60  
130.09  
128.32

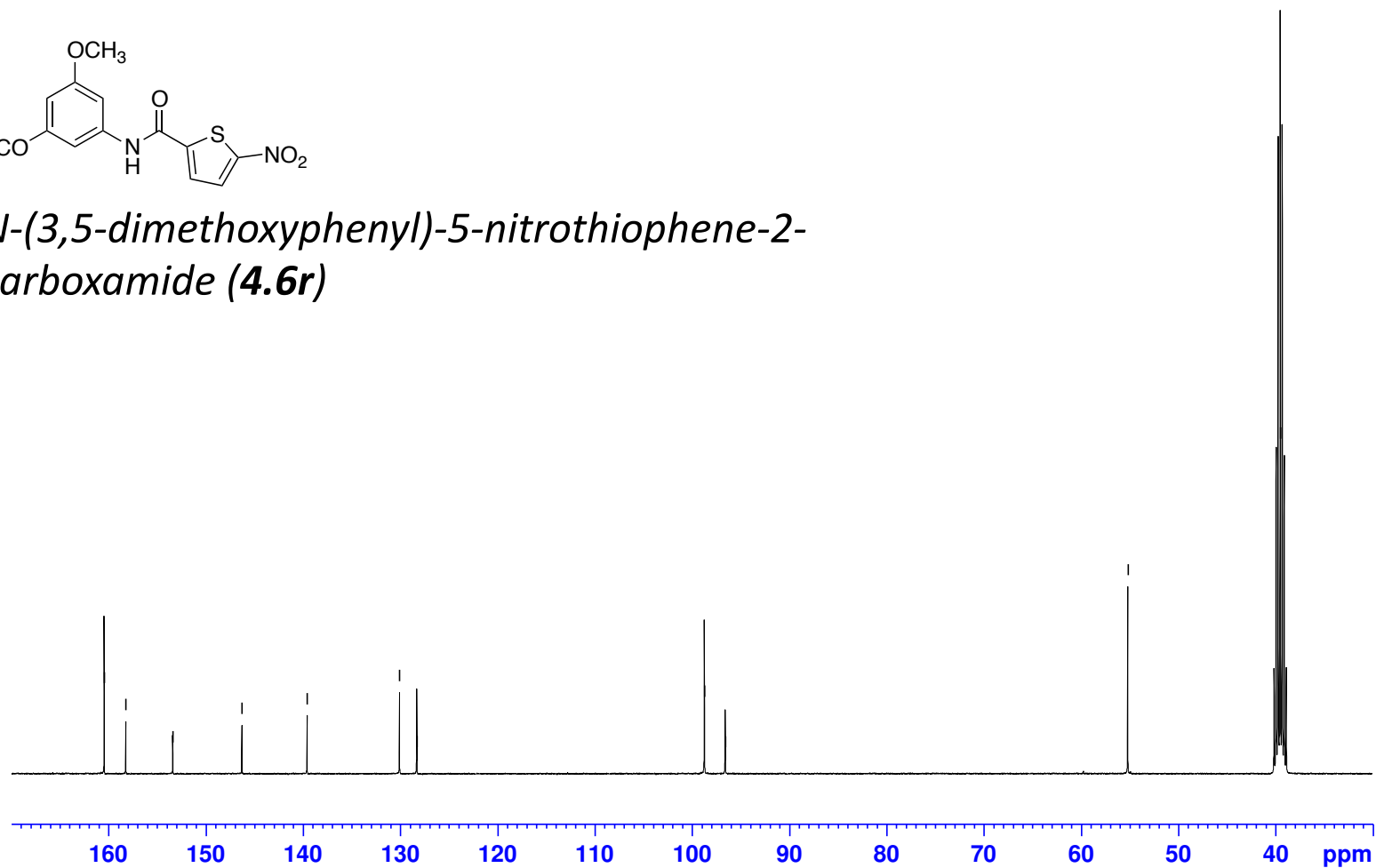
98.74  
96.60

55.20

39.52



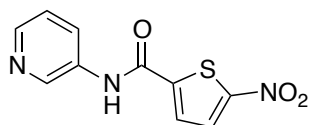
*N*-(3,5-dimethoxyphenyl)-5-nitrothiophene-2-carboxamide (**4.6r**)



MZP571-B3-10mg-1H-NMR-Nov-16-2016

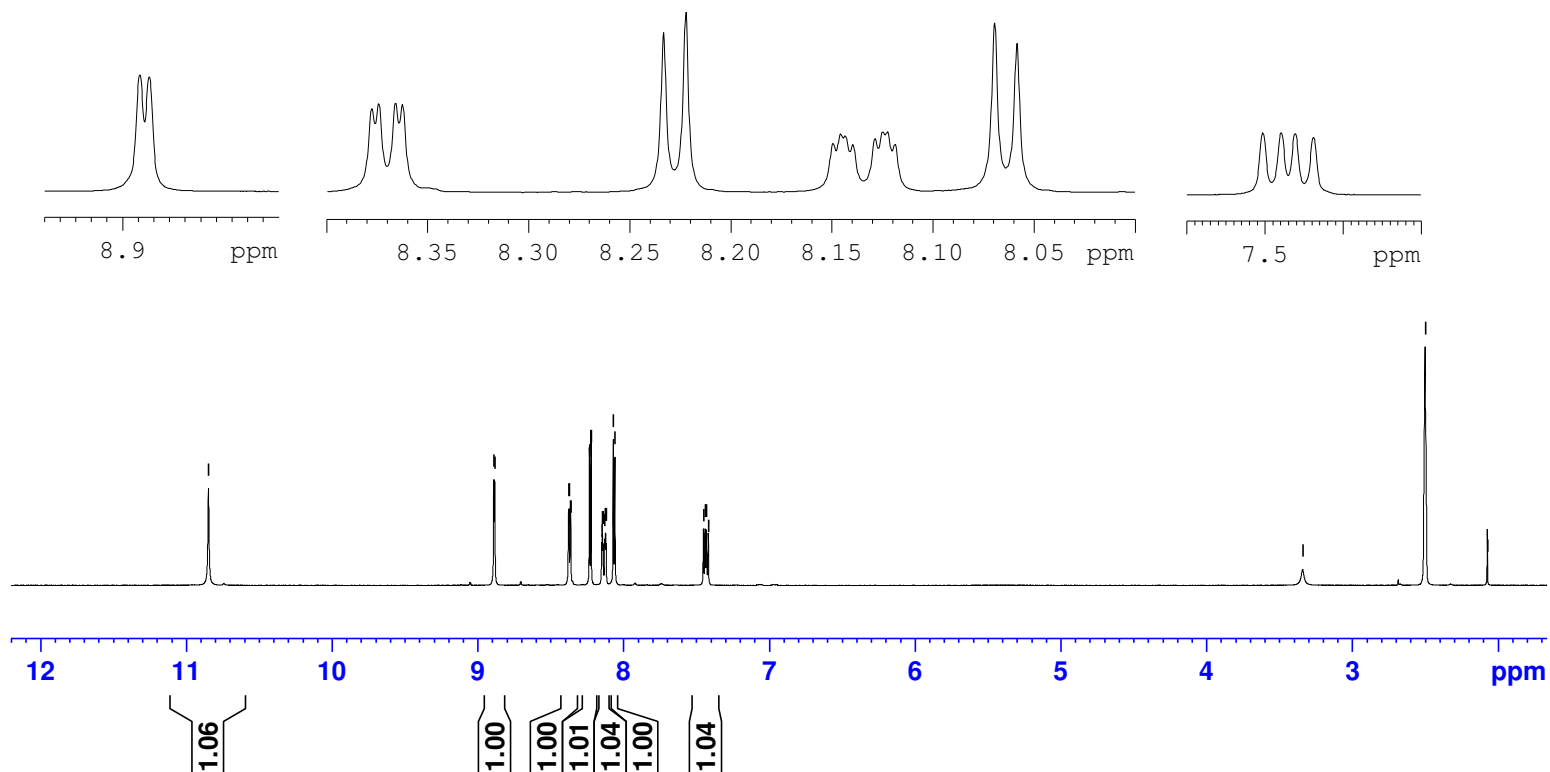
(400 MHz, 297.2 K, DMSO-d6)

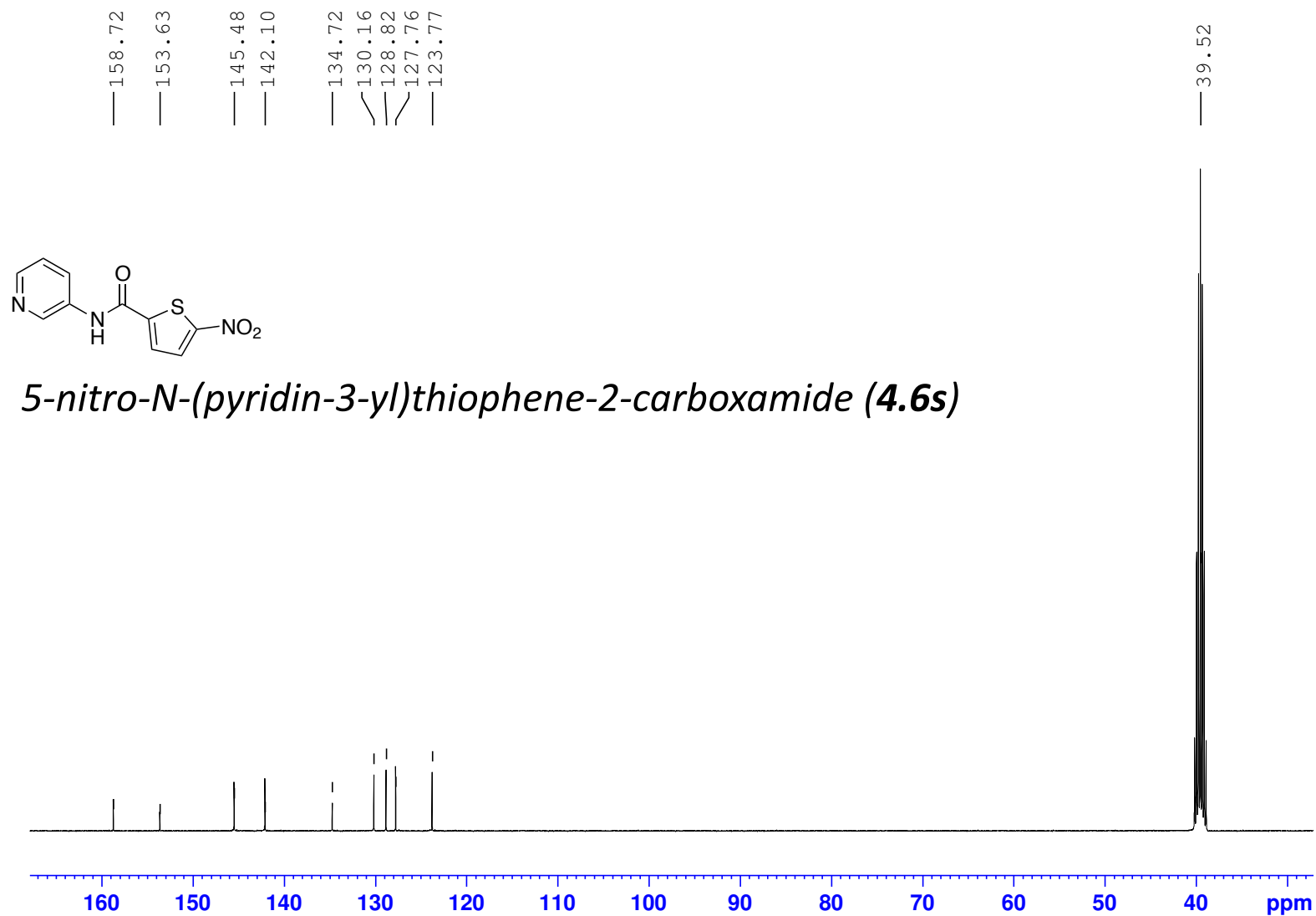
GPS424



10.85  
8.89  
8.88  
8.38  
8.37  
8.37  
8.36  
8.23  
8.22  
8.15  
8.15  
8.14  
8.14  
8.13  
8.12  
8.12  
8.12  
8.07  
8.06  
7.45  
7.44  
7.43  
7.42  
3.34  
2.50  
2.07

*5-nitro-N-(pyridin-3-yl)thiophene-2-carboxamide (4.6s)*

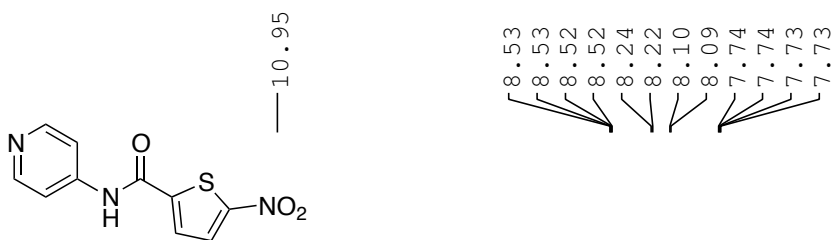




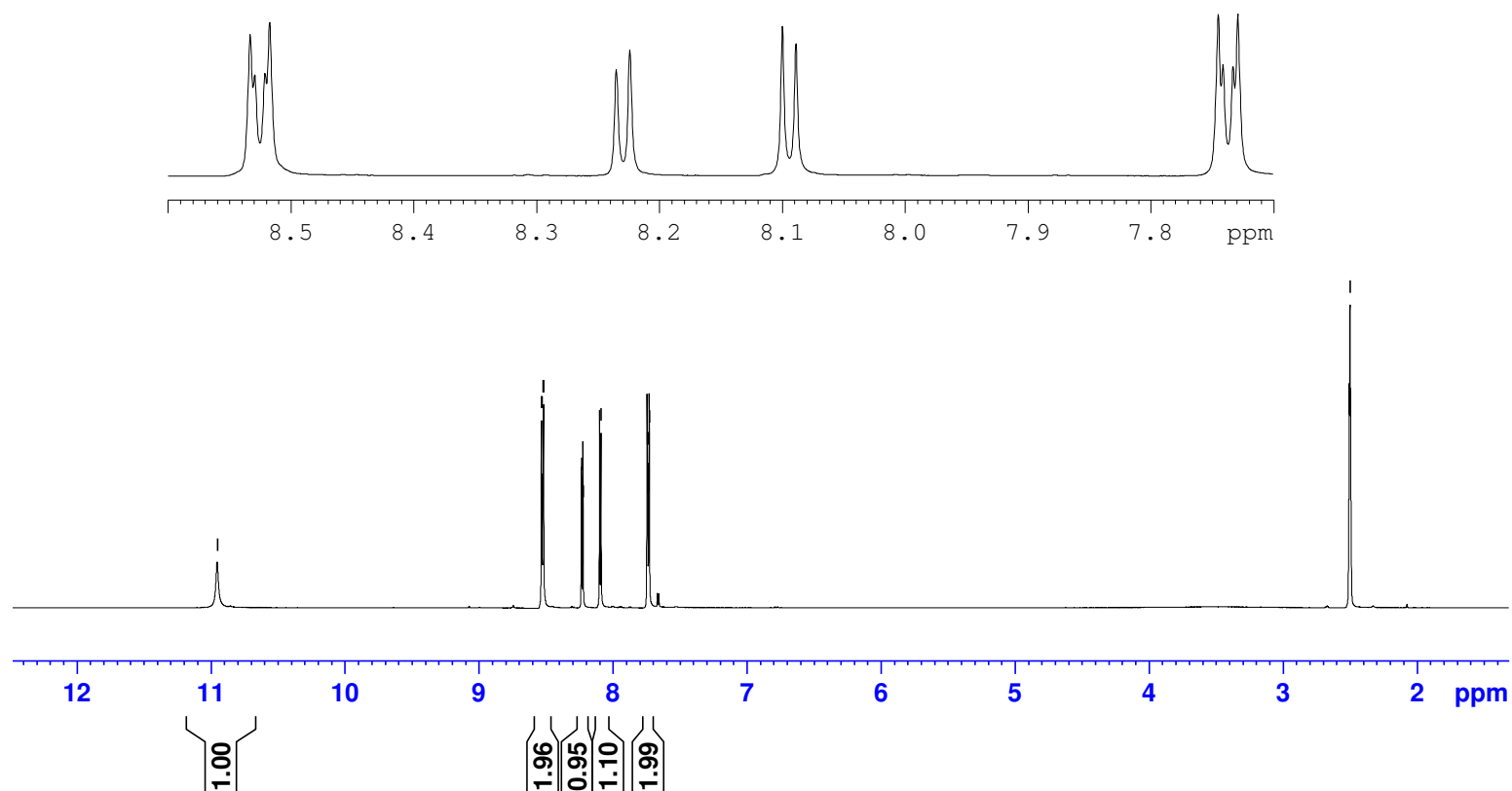
MZP584-B4-Amide-10mg-1H-NMR-09072016

(400 MHz, 297.2 K, DMSO-d6)

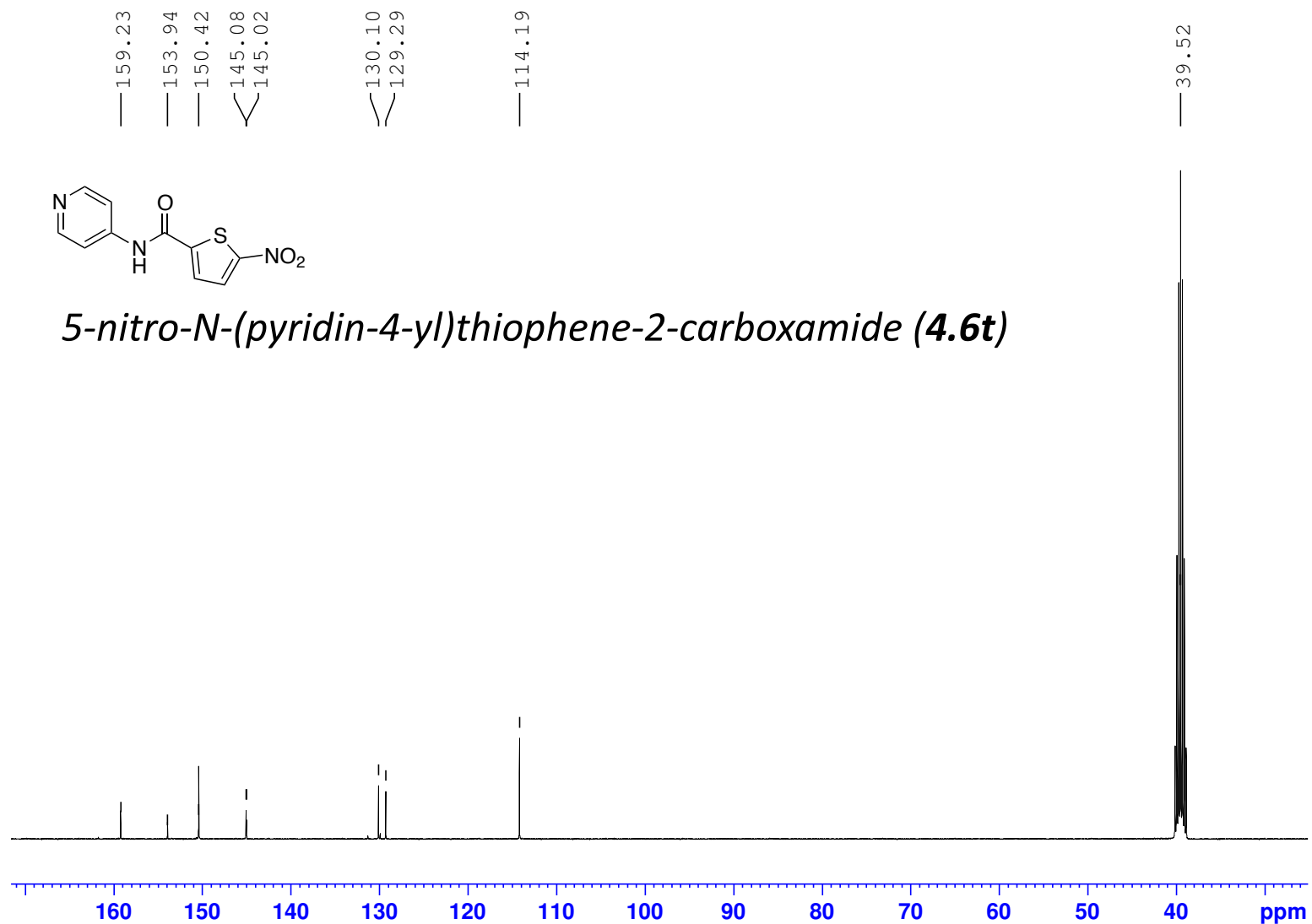
GPS425



**5-nitro-N-(pyridin-4-yl)thiophene-2-carboxamide (4.6t)**



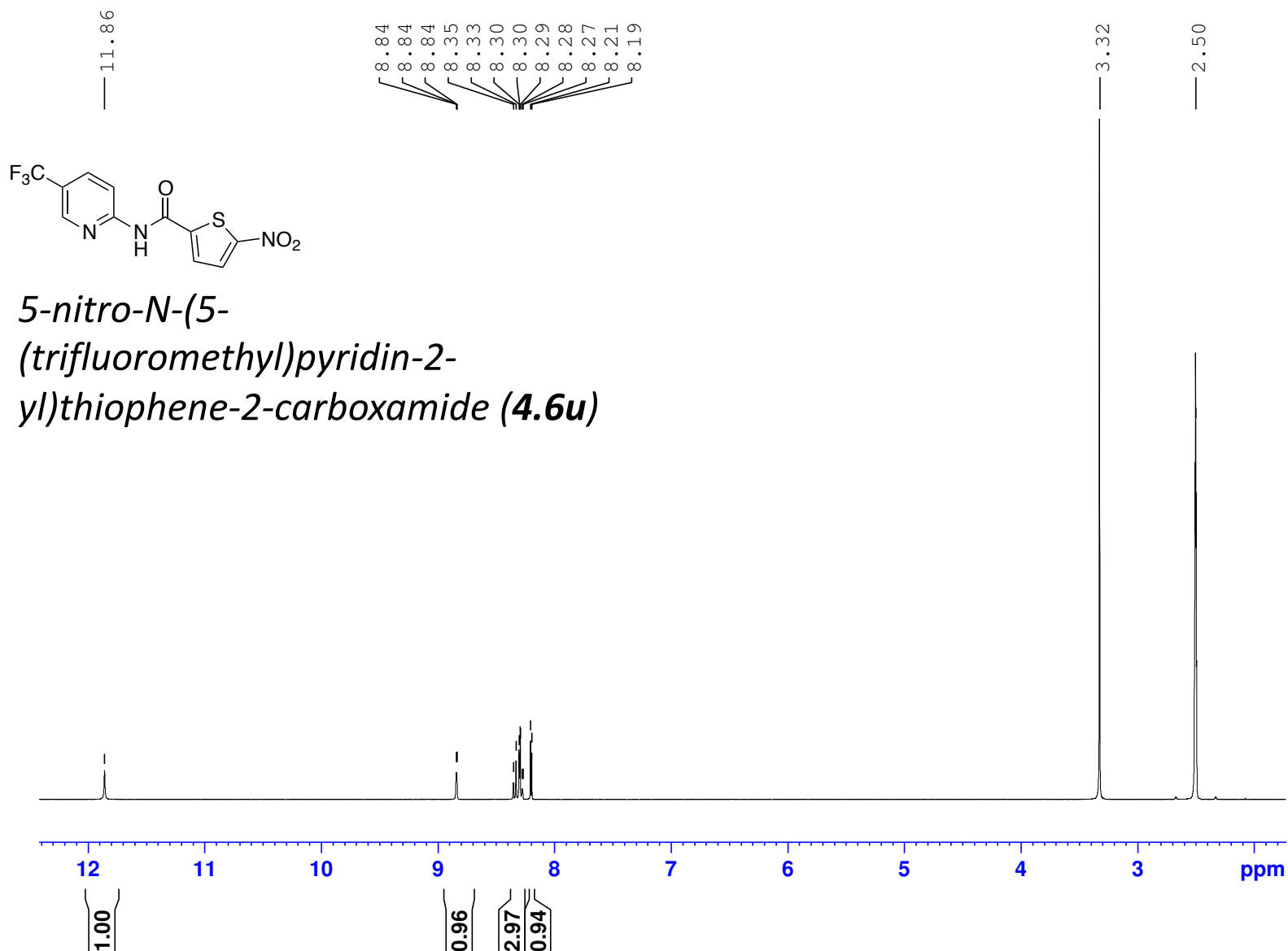




MZP573-B83-1H-NMR-14-03-2016

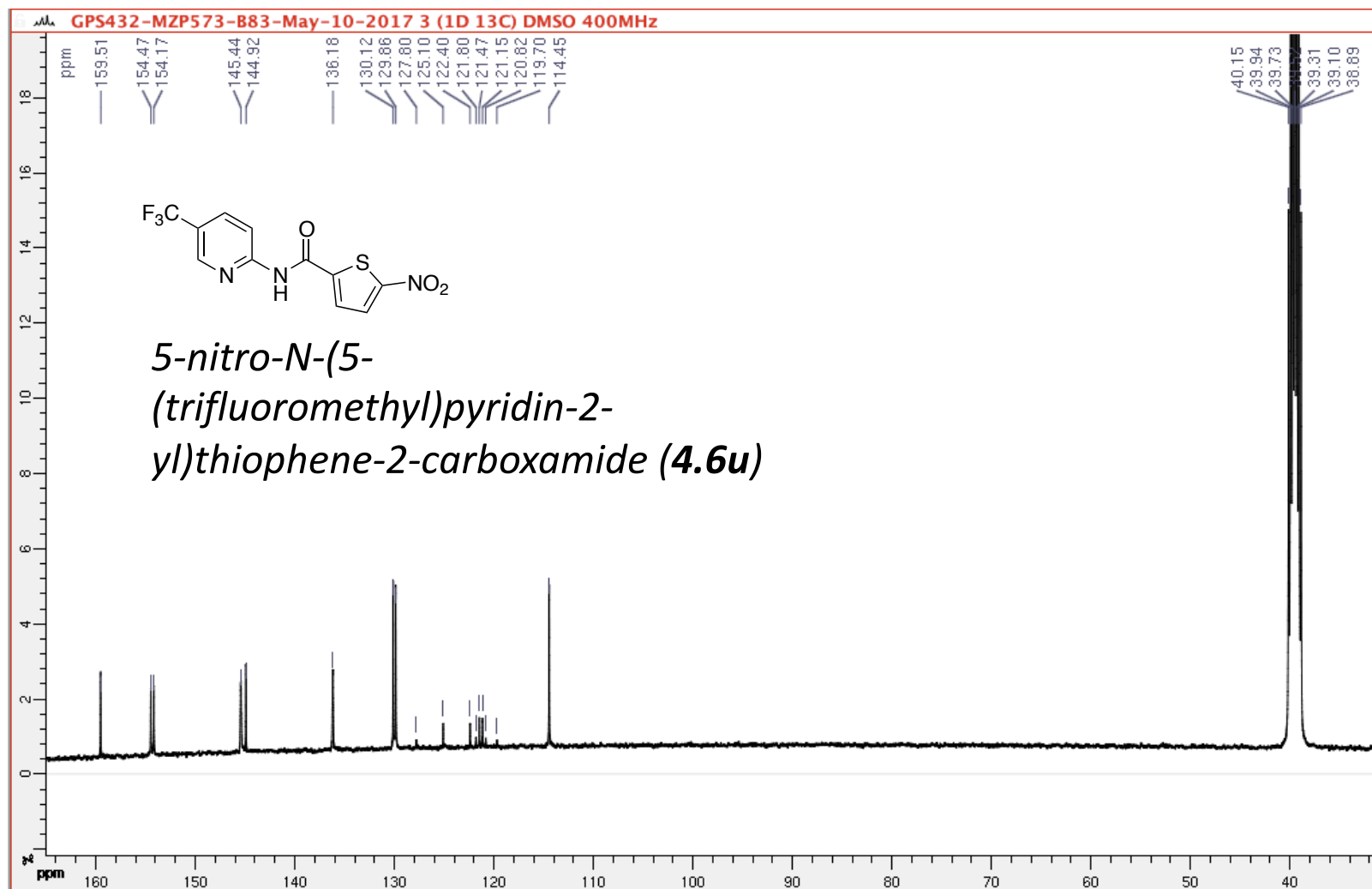
(400 MHz, 297.2 K, DMSO-d6)

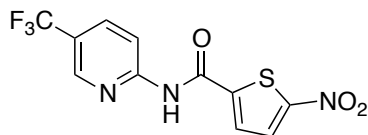
GPS432



(100 MHz, 297.2 K, DMSO-d6)

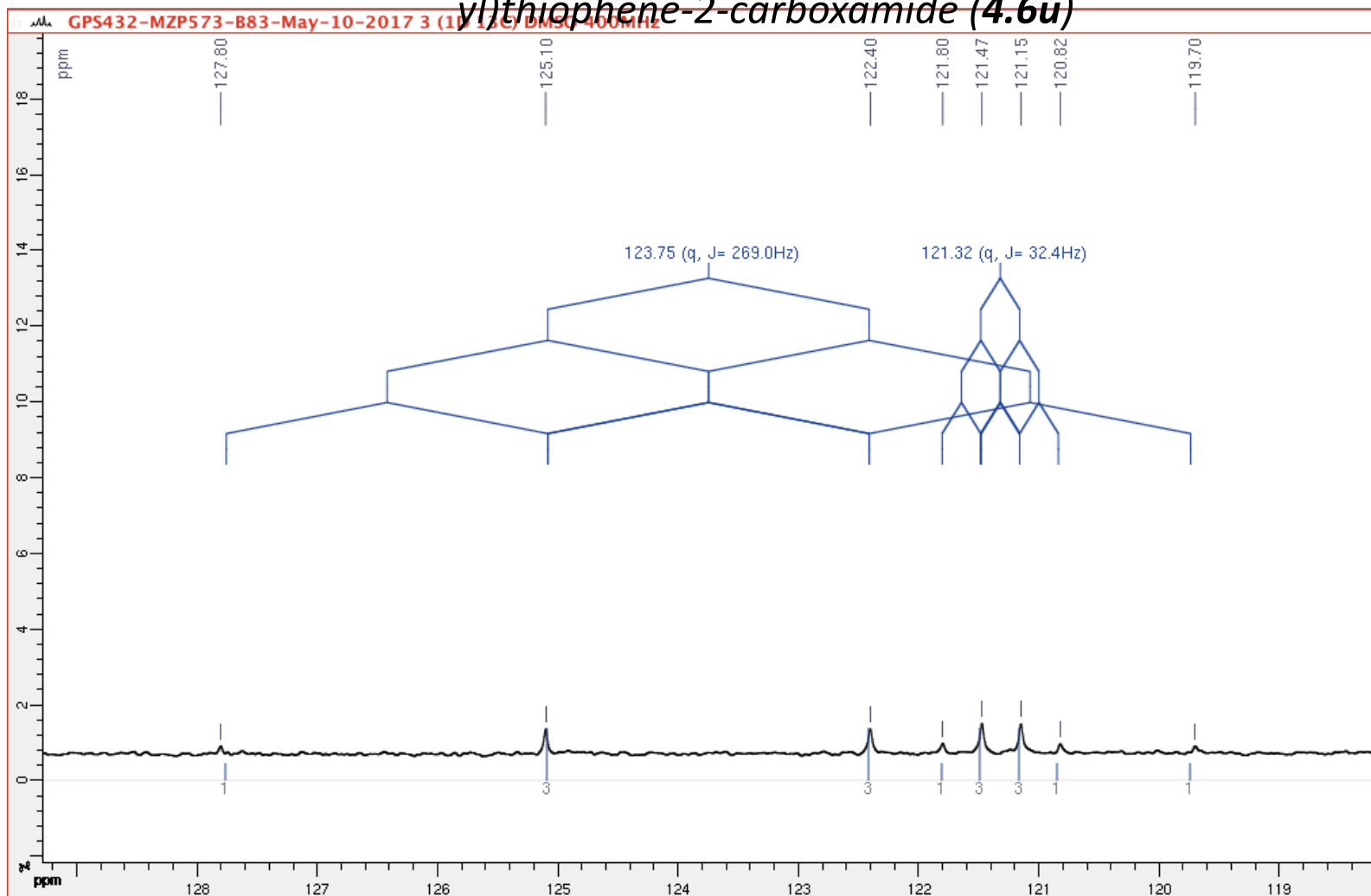
GPS432





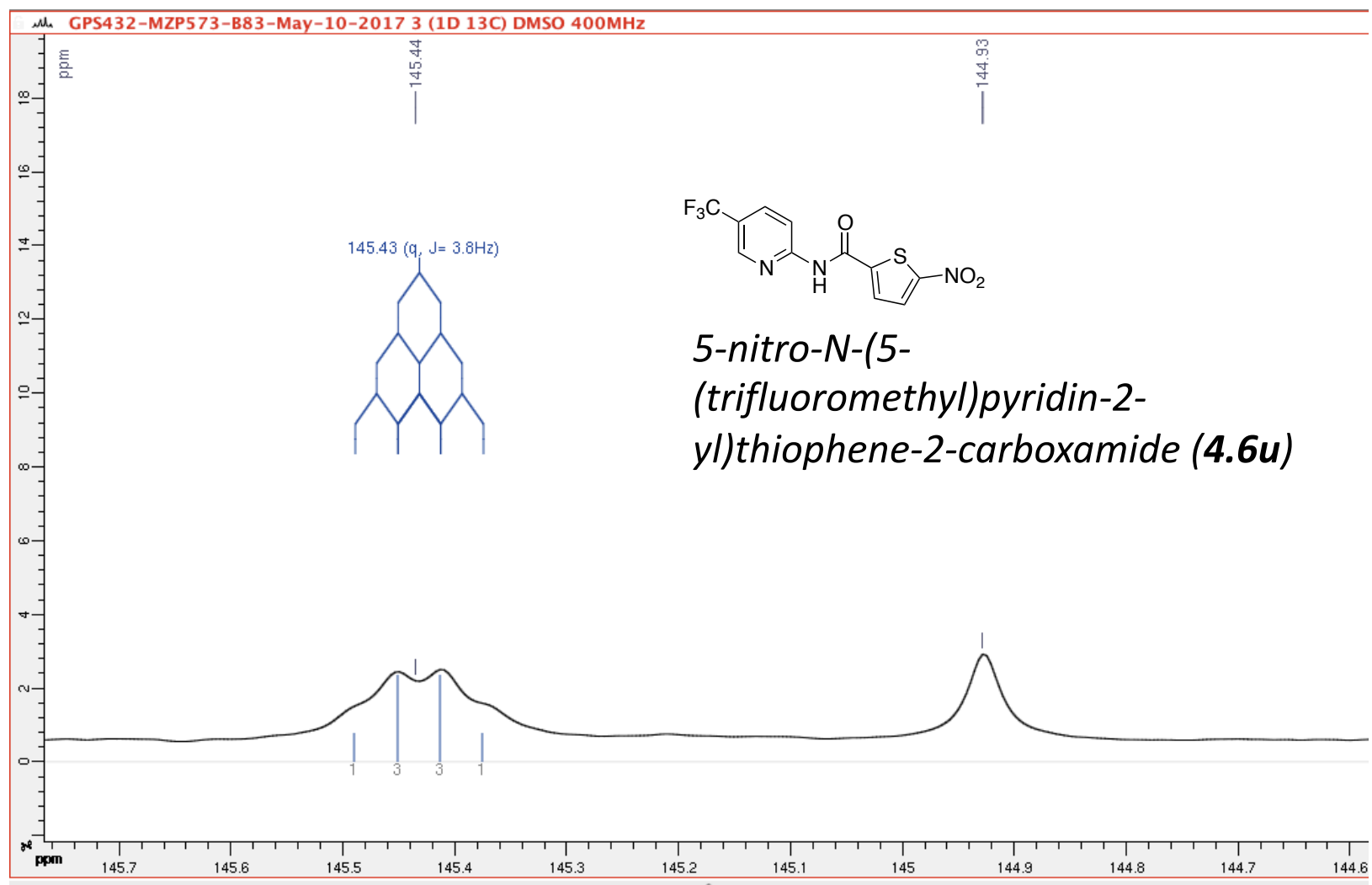
5-nitro-N-(5-(trifluoromethyl)pyridin-2-yl)thiophene-2-carboxamide (**4.6u**)

GPS432  
(100 MHz, 297.2 K, DMSO-d6)



(100 MHz, 297.2 K, DMSO-d6)

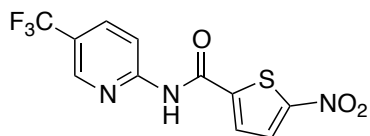
GPS432



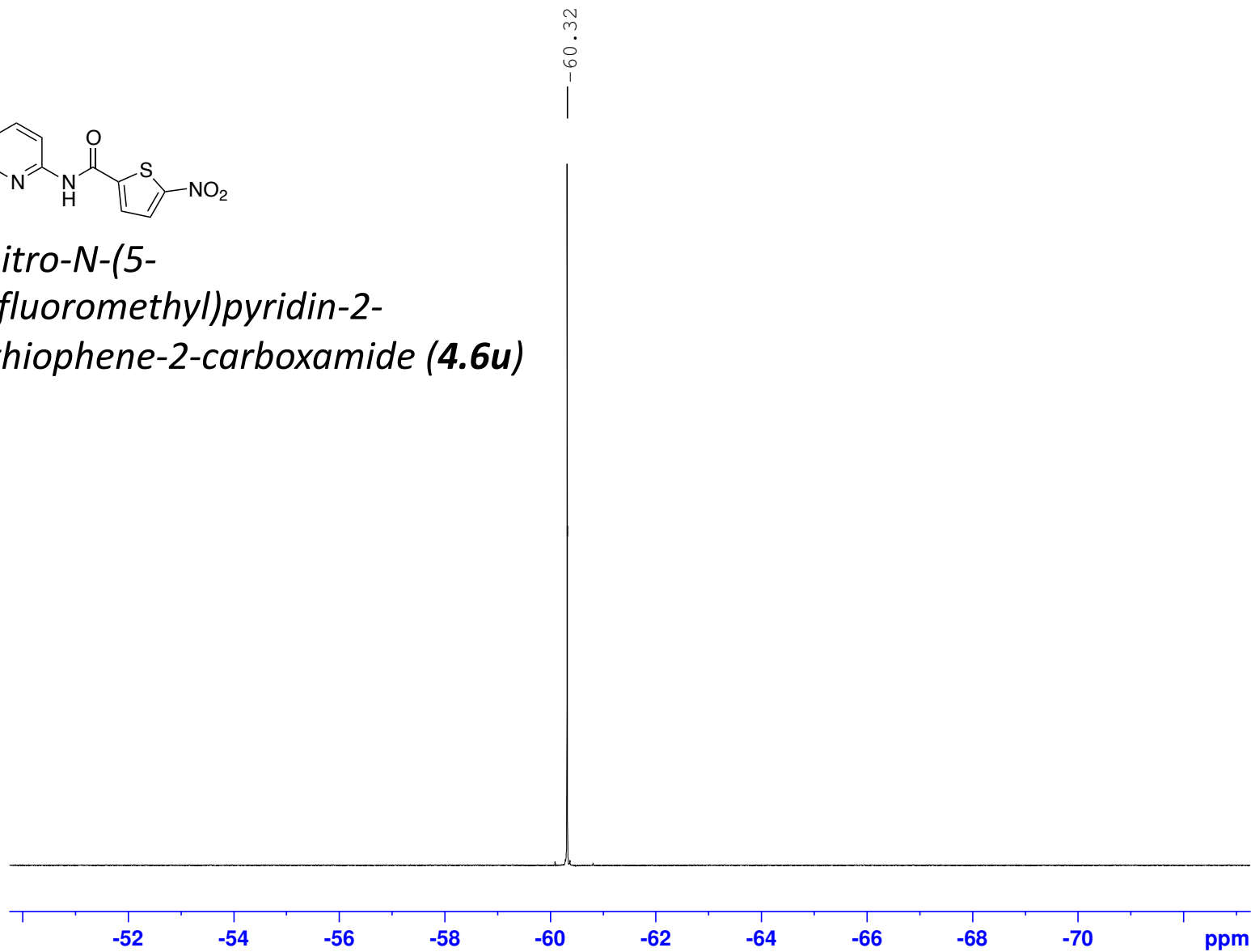
MZP573-B83-19F-NMR-14-03-2016

(400 MHz, 297.2 K, DMSO-d6)

GPS432



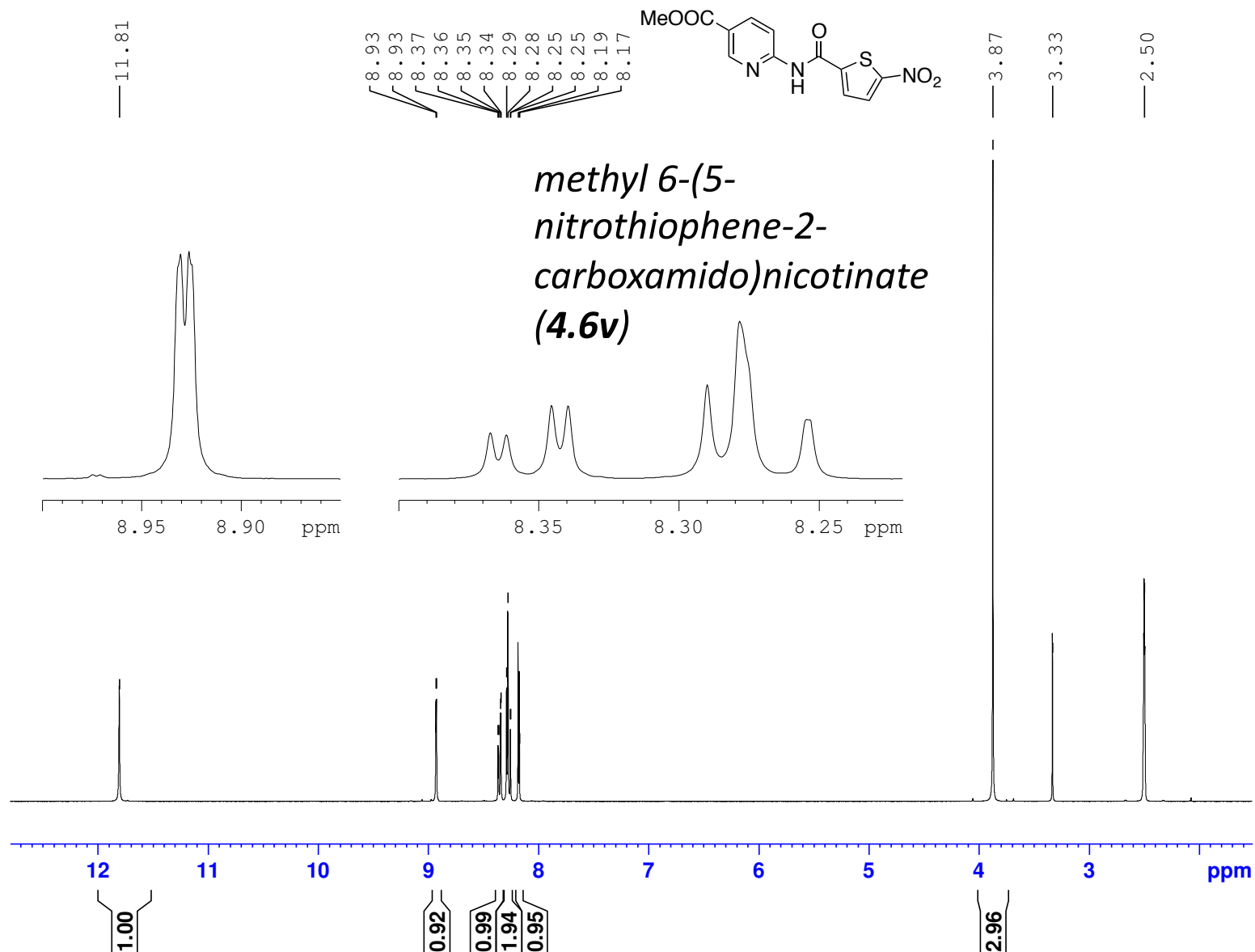
*5-nitro-N-(5-(trifluoromethyl)pyridin-2-yl)thiophene-2-carboxamide (4.6u)*

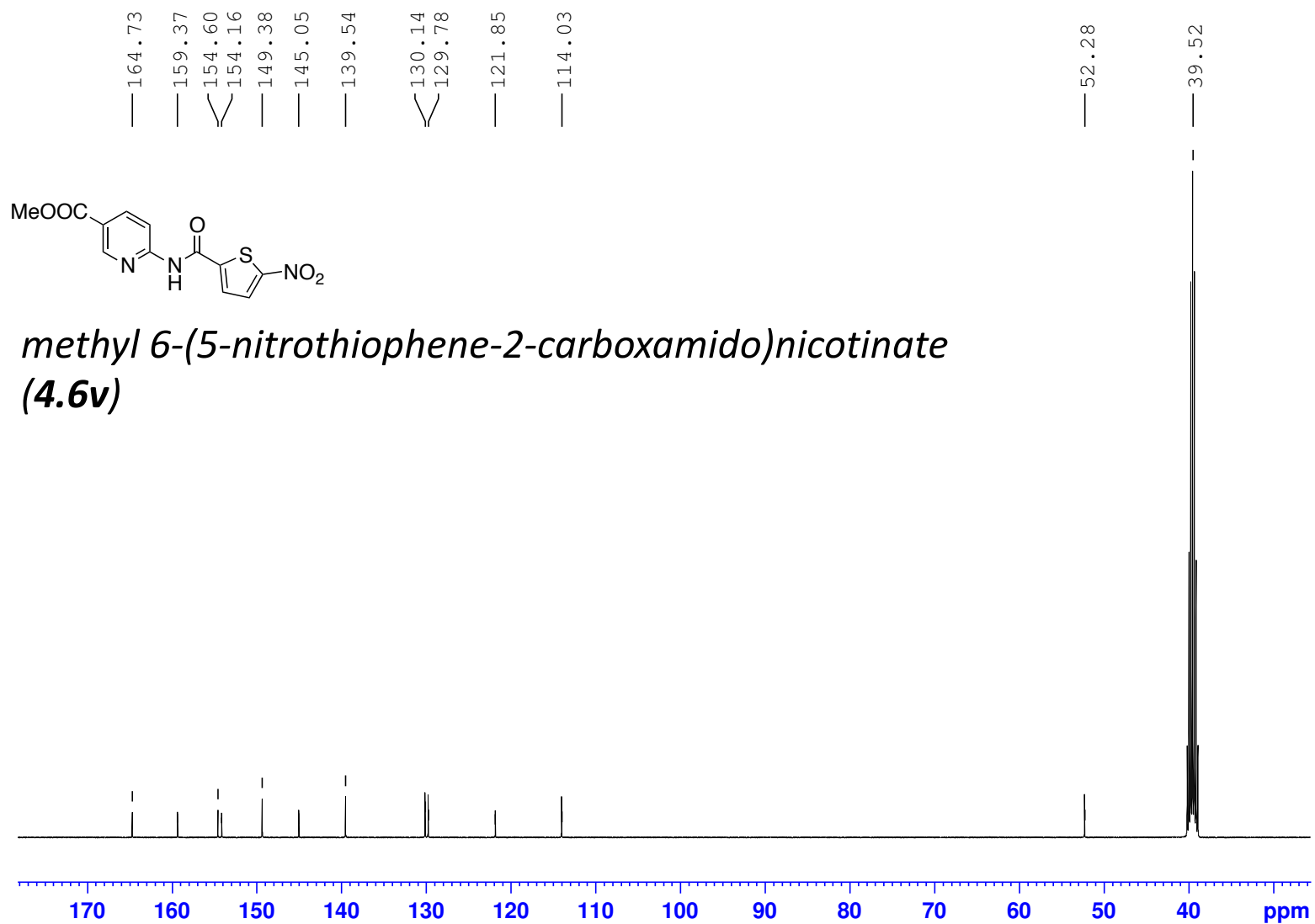


MZP584-B80-Amide-10mg-1H-NMR-Oct-31-2016

(400 MHz, 297.2 K, DMSO-d6)

GPS430



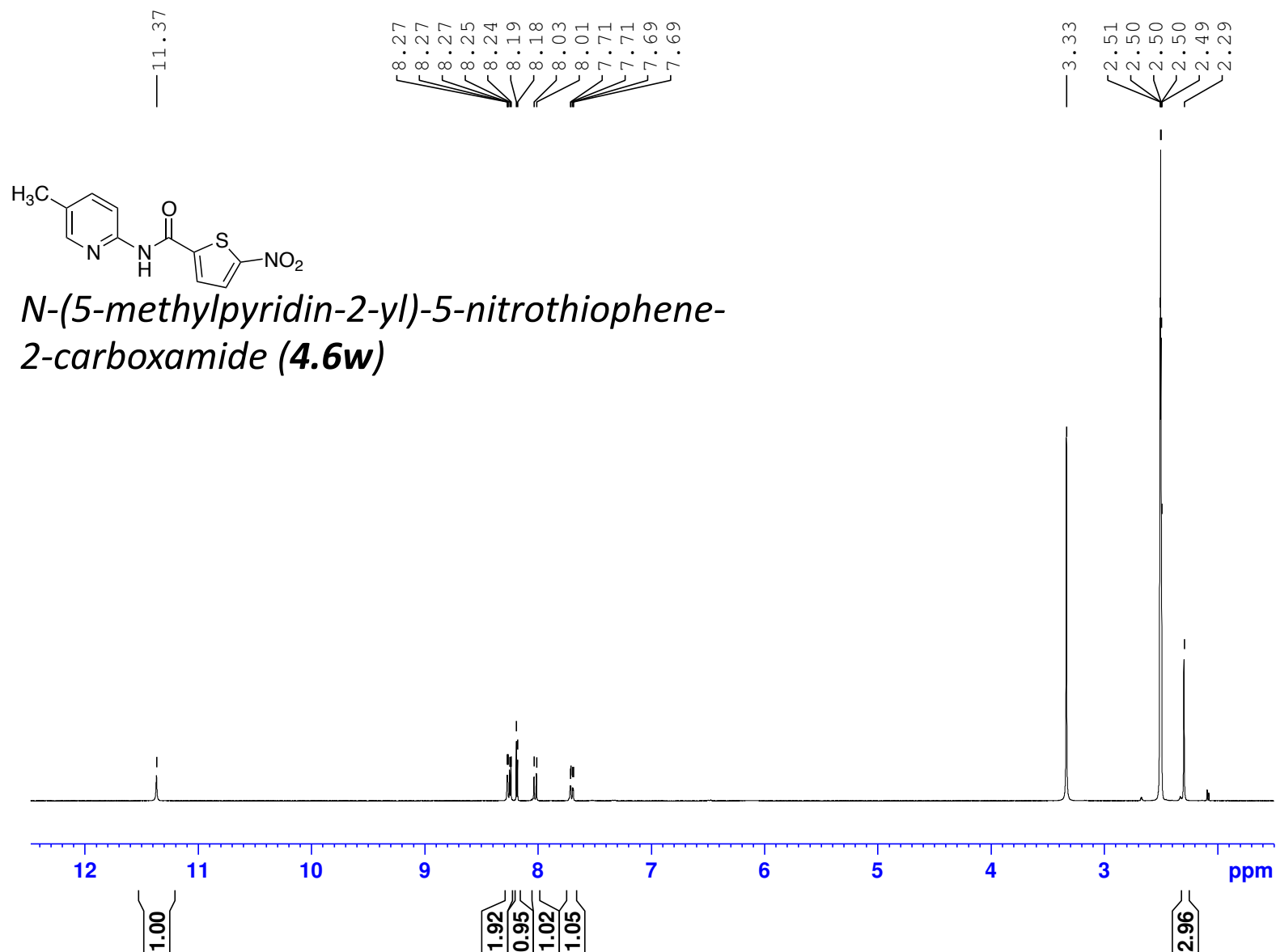




MZP584-B86-1H-NMR-04-04-2016

(400 MHz, 297.2 K, DMSO-d6)

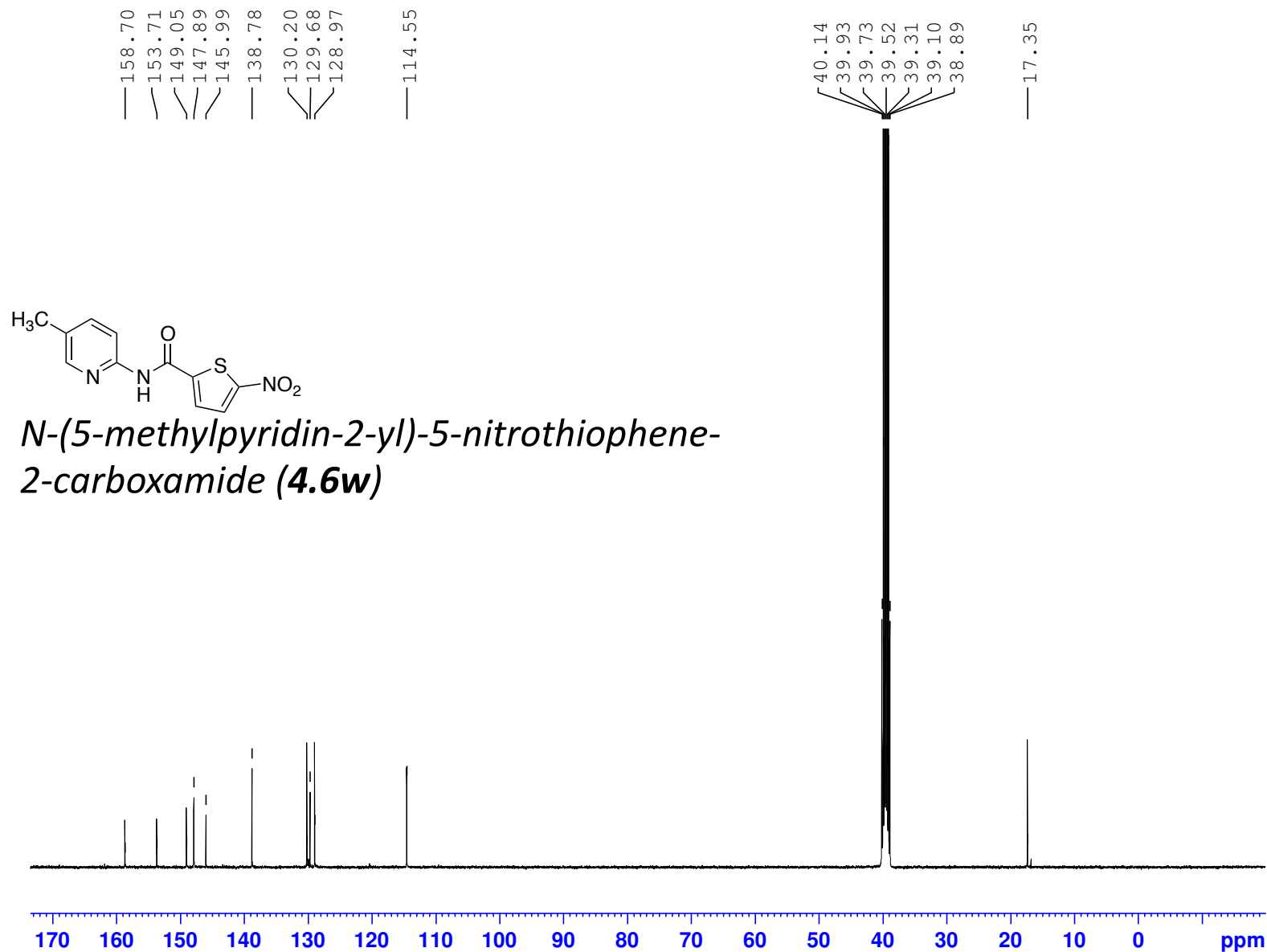
GPS435



GPS435-MZP584-B86-Amide-10mg-13C-NMR-Nov-09-2016

(100 MHz, 297.2 K, DMSO-d6)

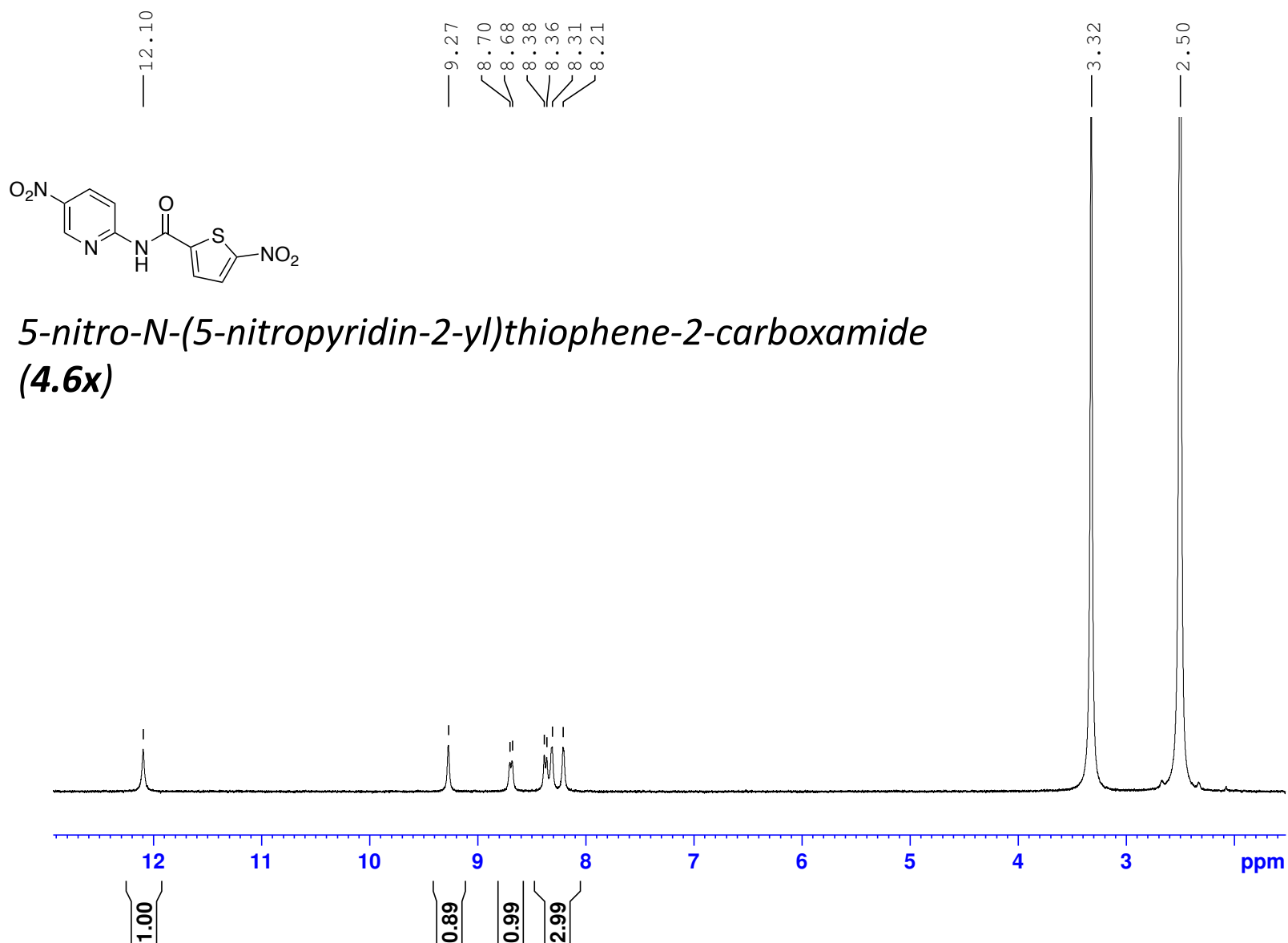
GPS435



MZP572-B1-1H-NMR-14-03-2016

(400 MHz, 297.2 K, DMSO-d6)

GPS422



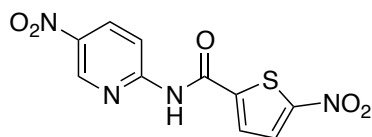
MZP572-B1-Amide-10mg-13C-NMR-Nov-18-2016

(100 MHz, 297.2 K, DMSO-d6)

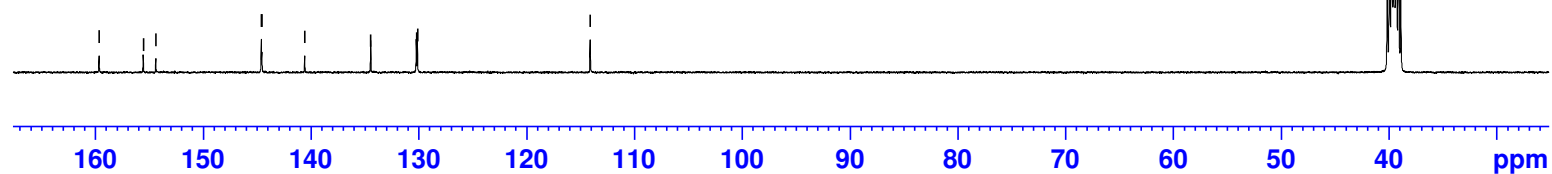
GPS422

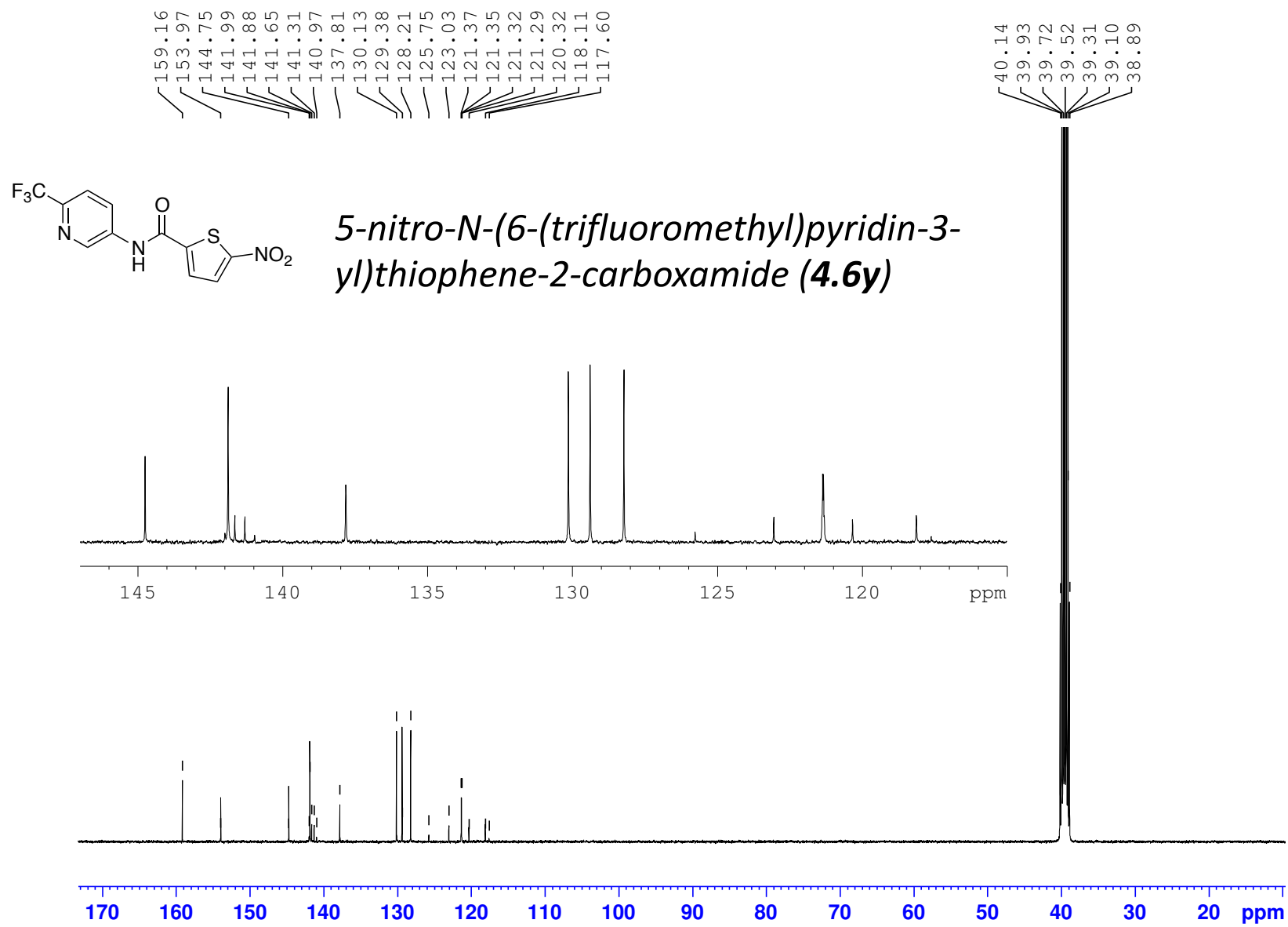
— 159.65  
— 155.56  
— 154.39  
  
— 144.60  
— 144.55  
— 140.58  
  
— 134.46  
— 130.23  
— 130.13  
  
— 114.10

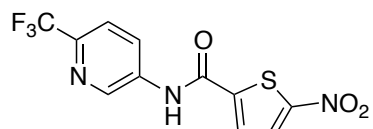
— 39.52



*5-nitro-N-(5-nitropyridin-2-yl)thiophene-2-carboxamide*  
**(4.6x)**

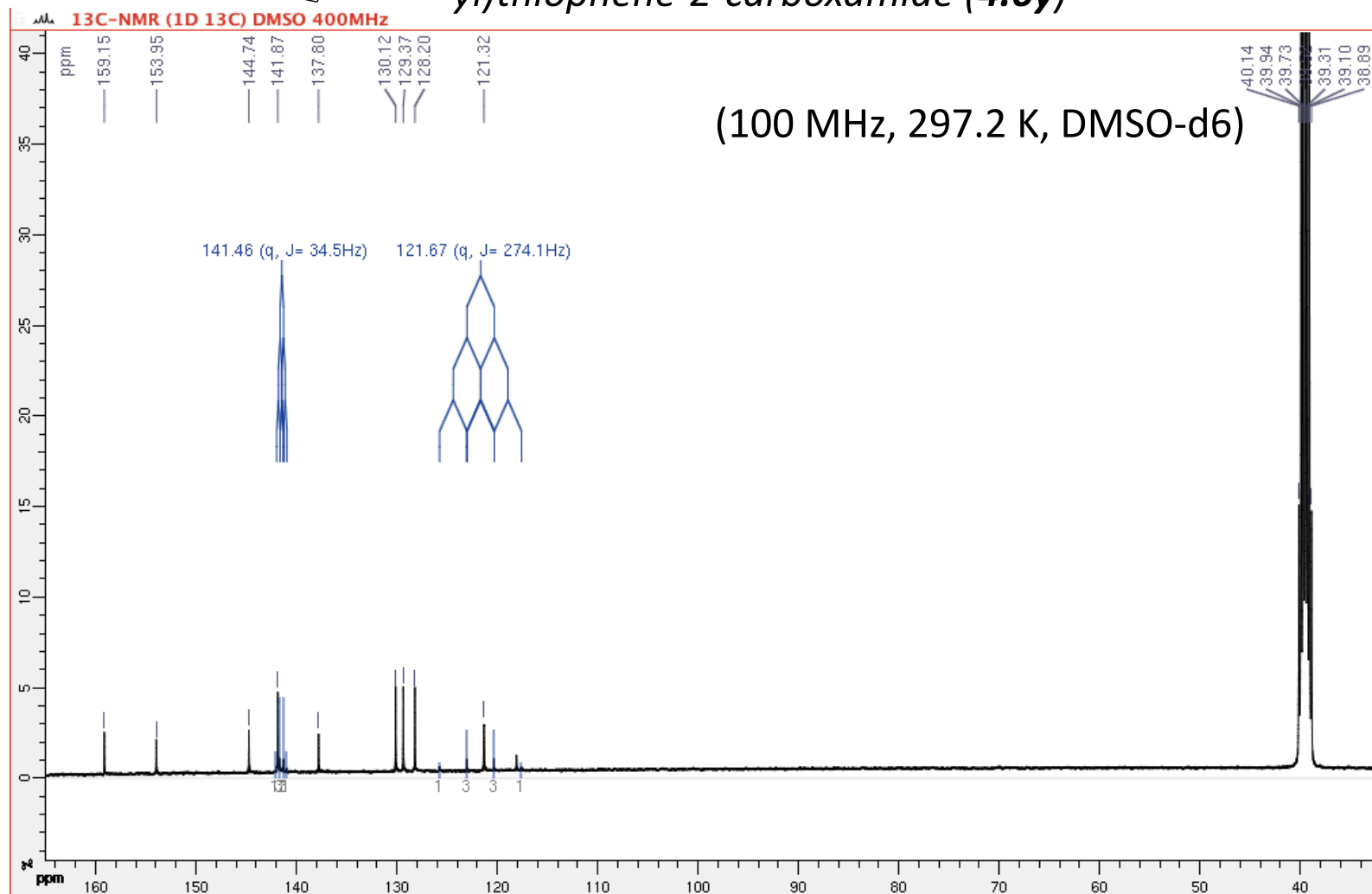






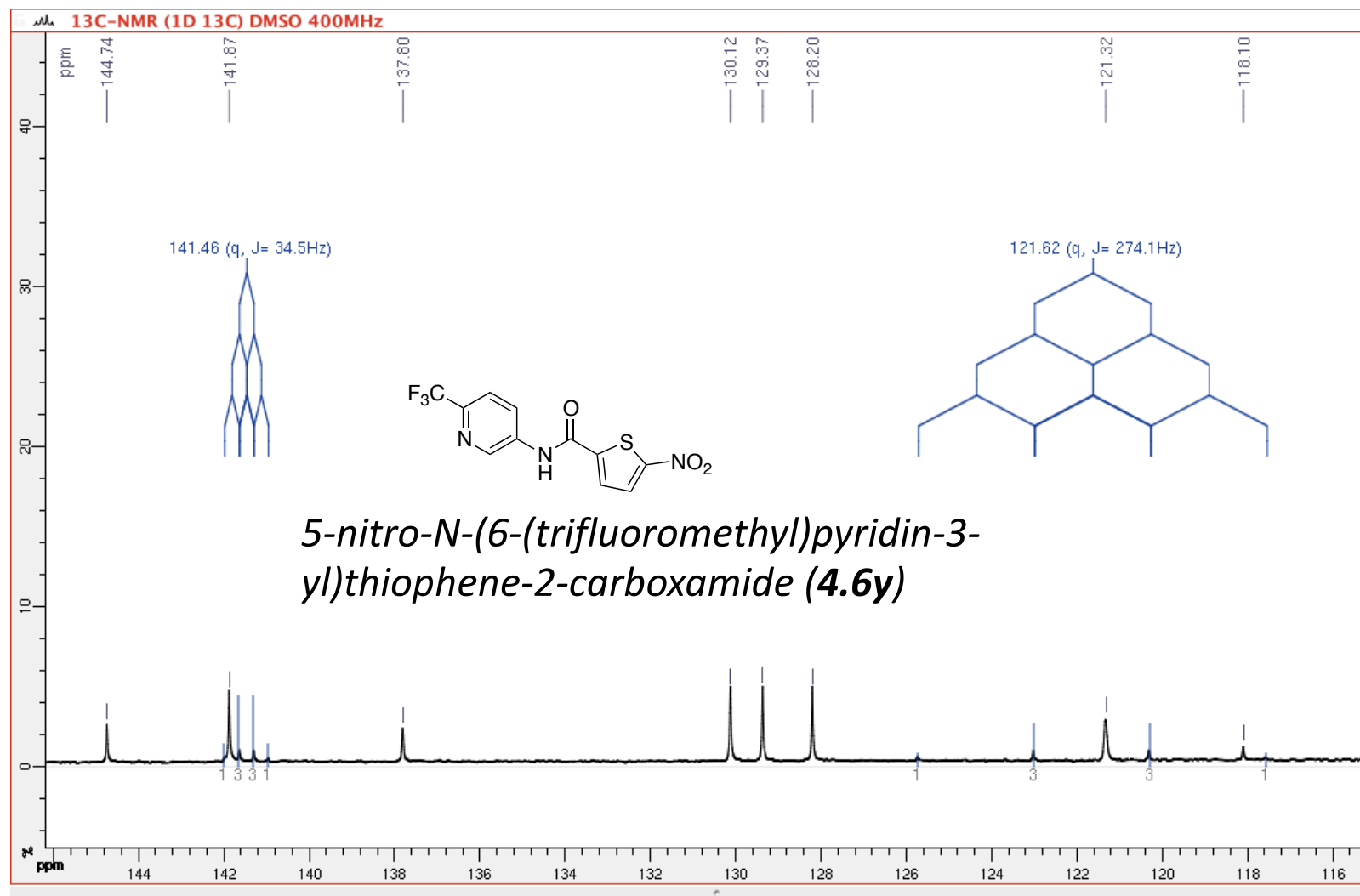
*5-nitro-N-(6-(trifluoromethyl)pyridin-3-yl)thiophene-2-carboxamide (4.6y)*

GPS433



(100 MHz, 297.2 K, DMSO-d6)

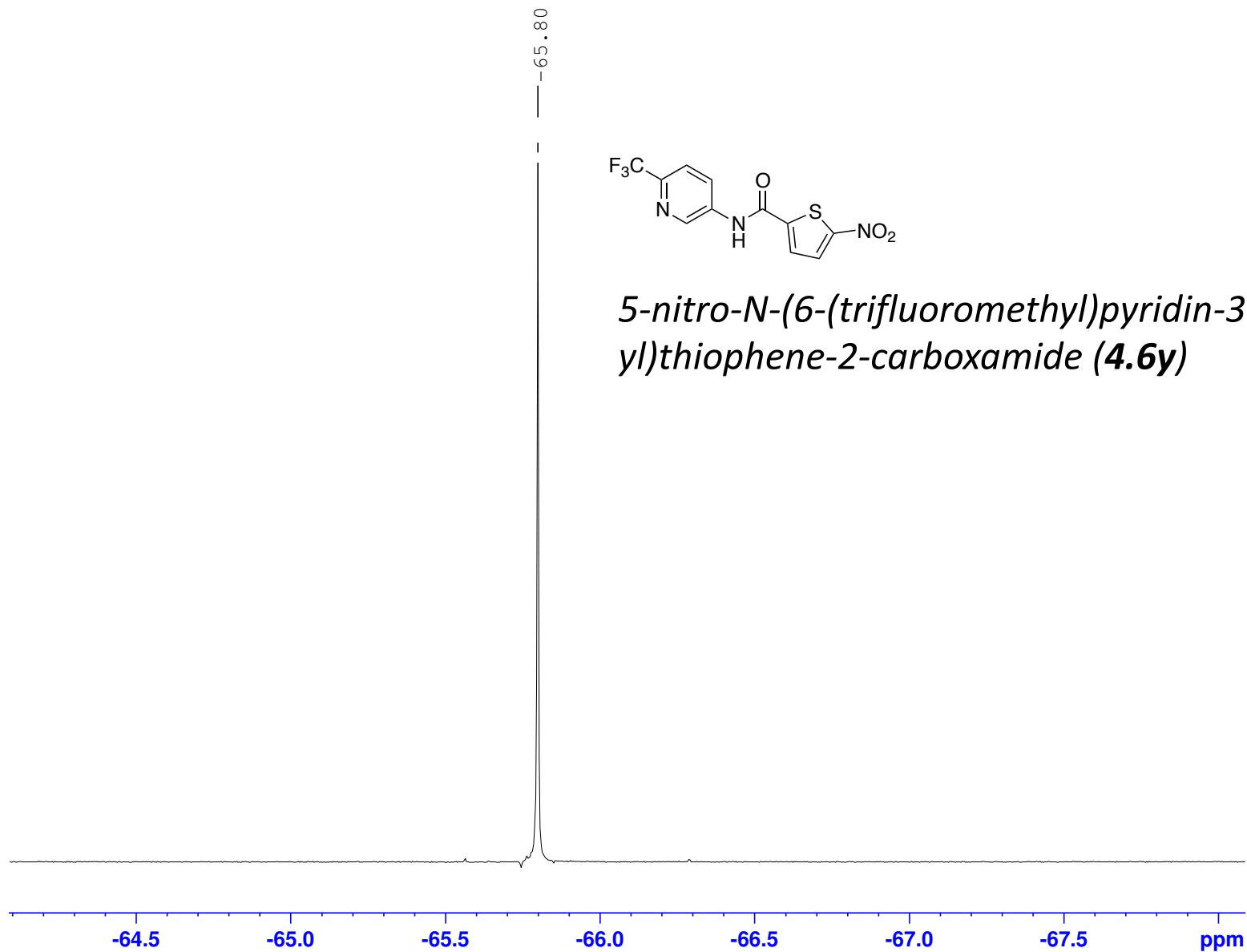
GPS433



MZP572-B84-Amide-in DMSO-19F-NMR-11-03-2016

(400 MHz, 297.2 K, DMSO-d6)

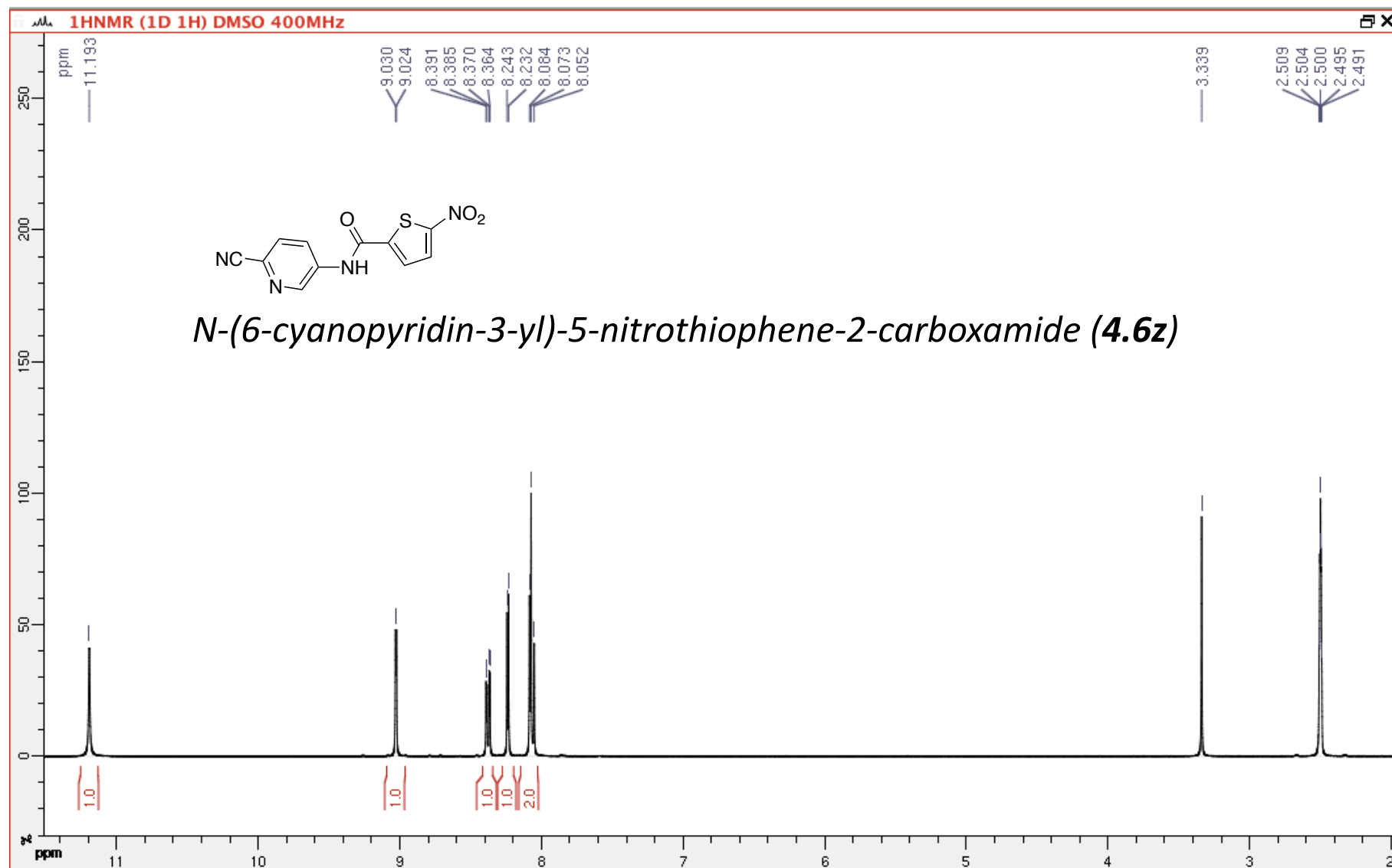
GPS433





(400 MHz, 297.2 K, DMSO-d6)

GPS444

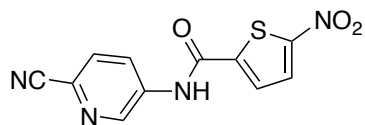


MZP564-A101-Amide-10mg-13C-NMR-Nov-03-2016

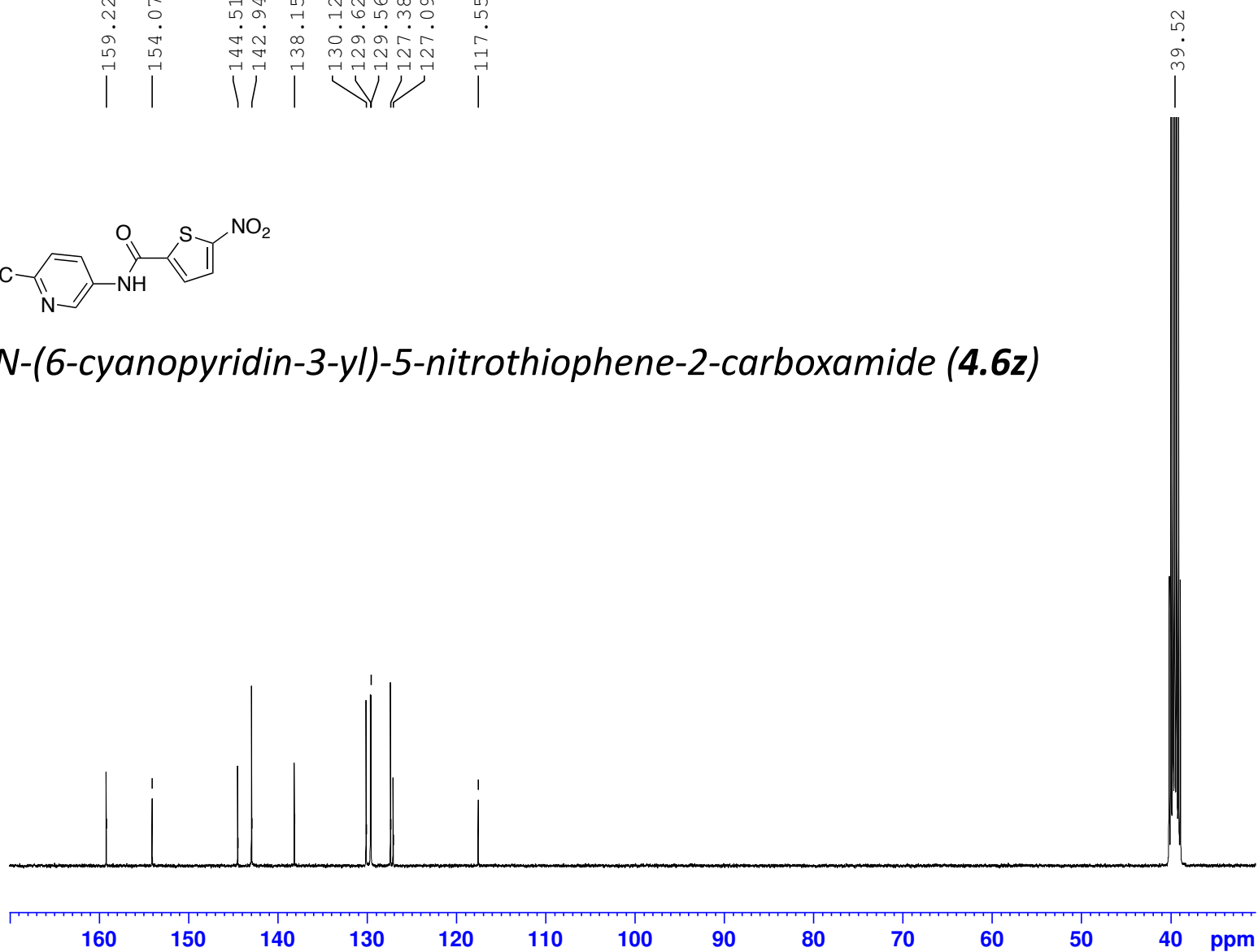
(100 MHz, 297.2 K, DMSO-d6)

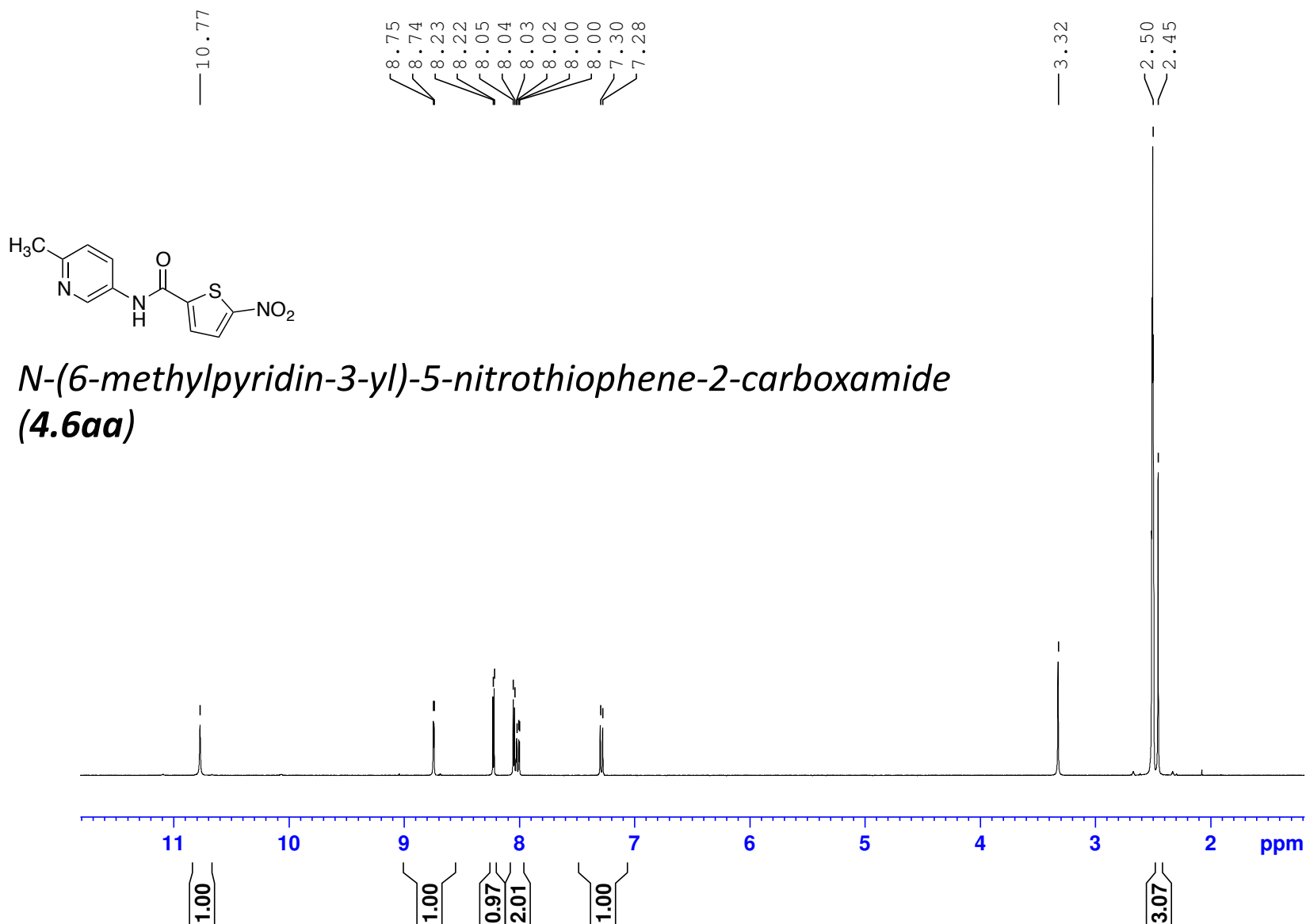
GPS444

— 159.22  
— 154.07  
— 144.51  
— 142.94  
— 138.15  
— 130.12  
— 129.62  
— 129.56  
— 127.38  
— 127.09  
— 117.55



*N*-(6-cyanopyridin-3-yl)-5-nitrothiophene-2-carboxamide (**4.6z**)





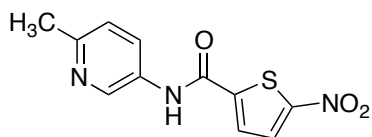
GPS436-MZP571-B87-Amide-10mg-13C-NMR-09072016

(100 MHz, 297.2 K, DMSO-d6)

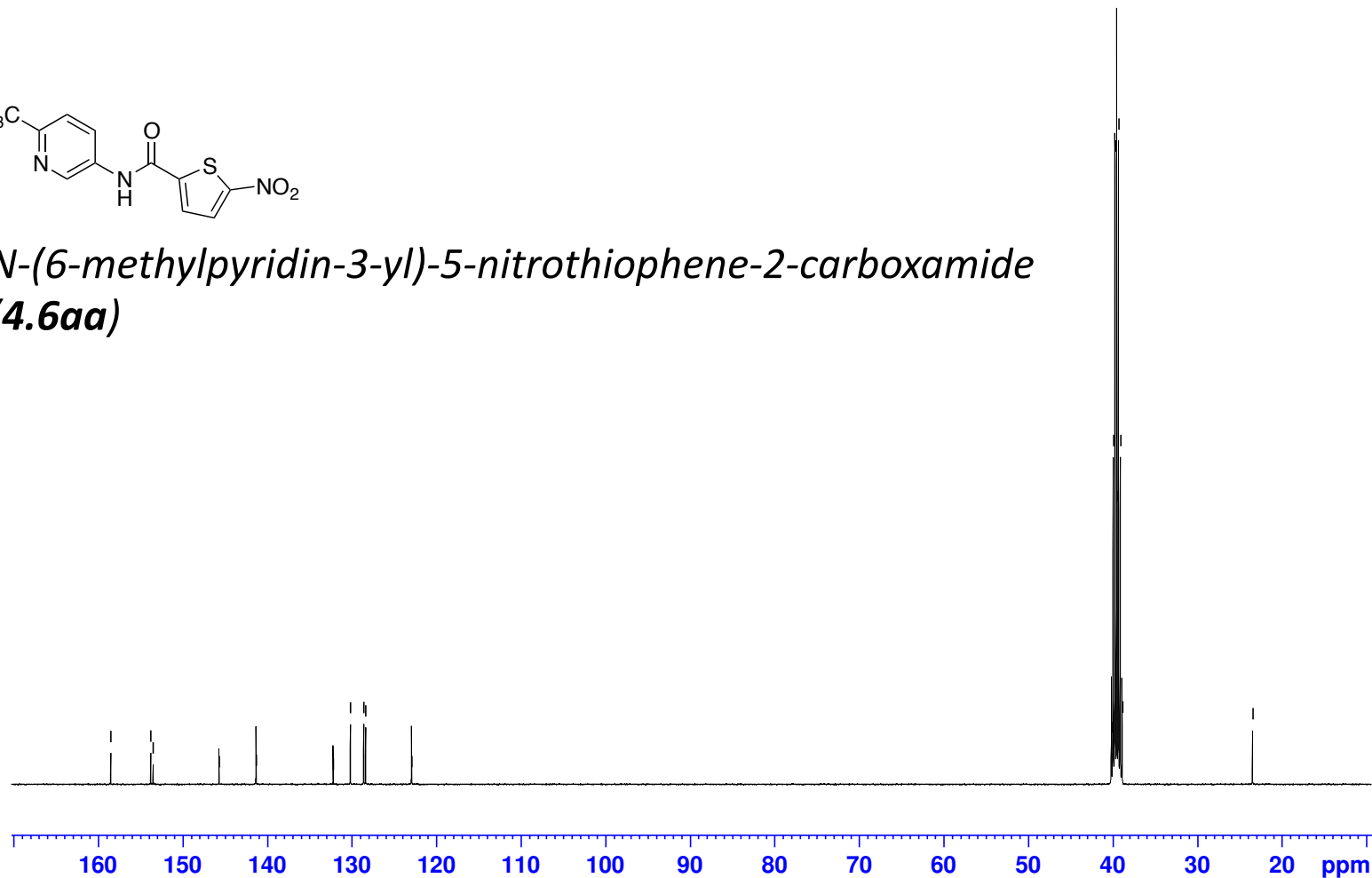
GPS436

158.52  
153.79  
153.51  
145.71  
141.34  
132.22  
130.18  
128.60  
128.37  
122.95

40.14  
39.93  
39.72  
39.52  
39.31  
39.10  
38.89  
23.45



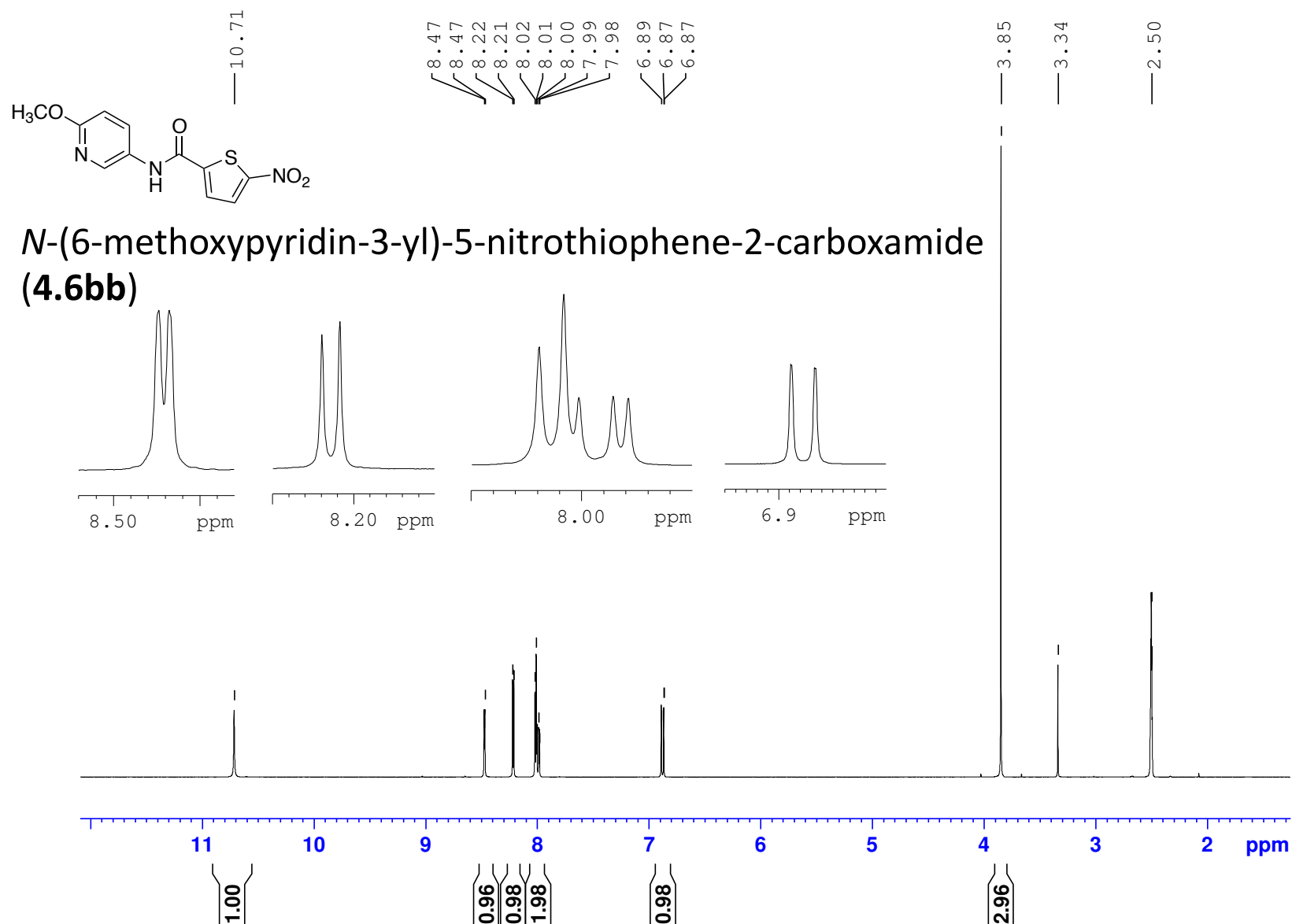
*N*-(6-methylpyridin-3-yl)-5-nitrothiophene-2-carboxamide  
**(4.6aa)**



MZP584-B2-Amide-10mg-1H-NMR-Nov-18-2016

(400 MHz, 297.2 K, DMSO-d6)

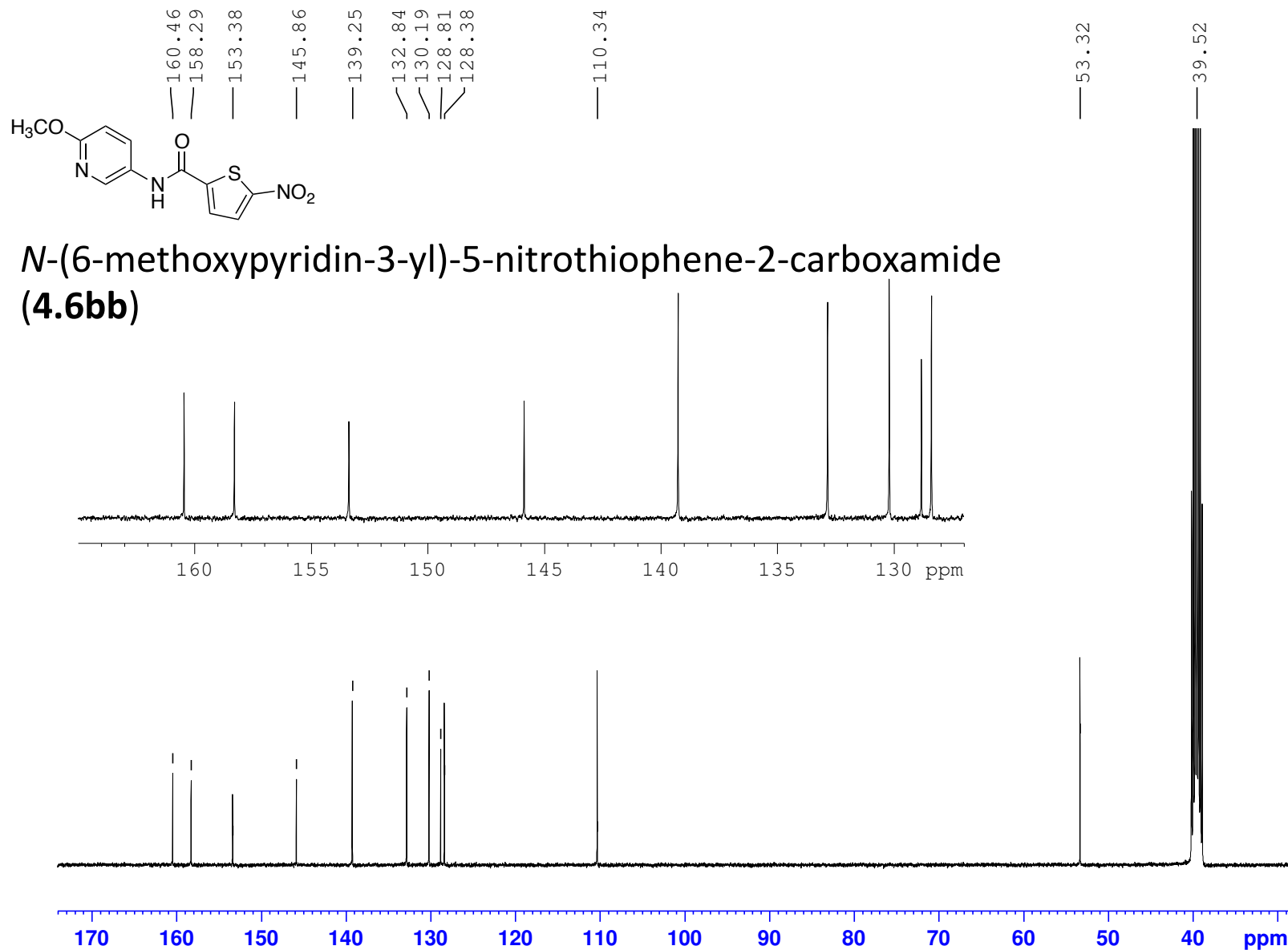
GPS423

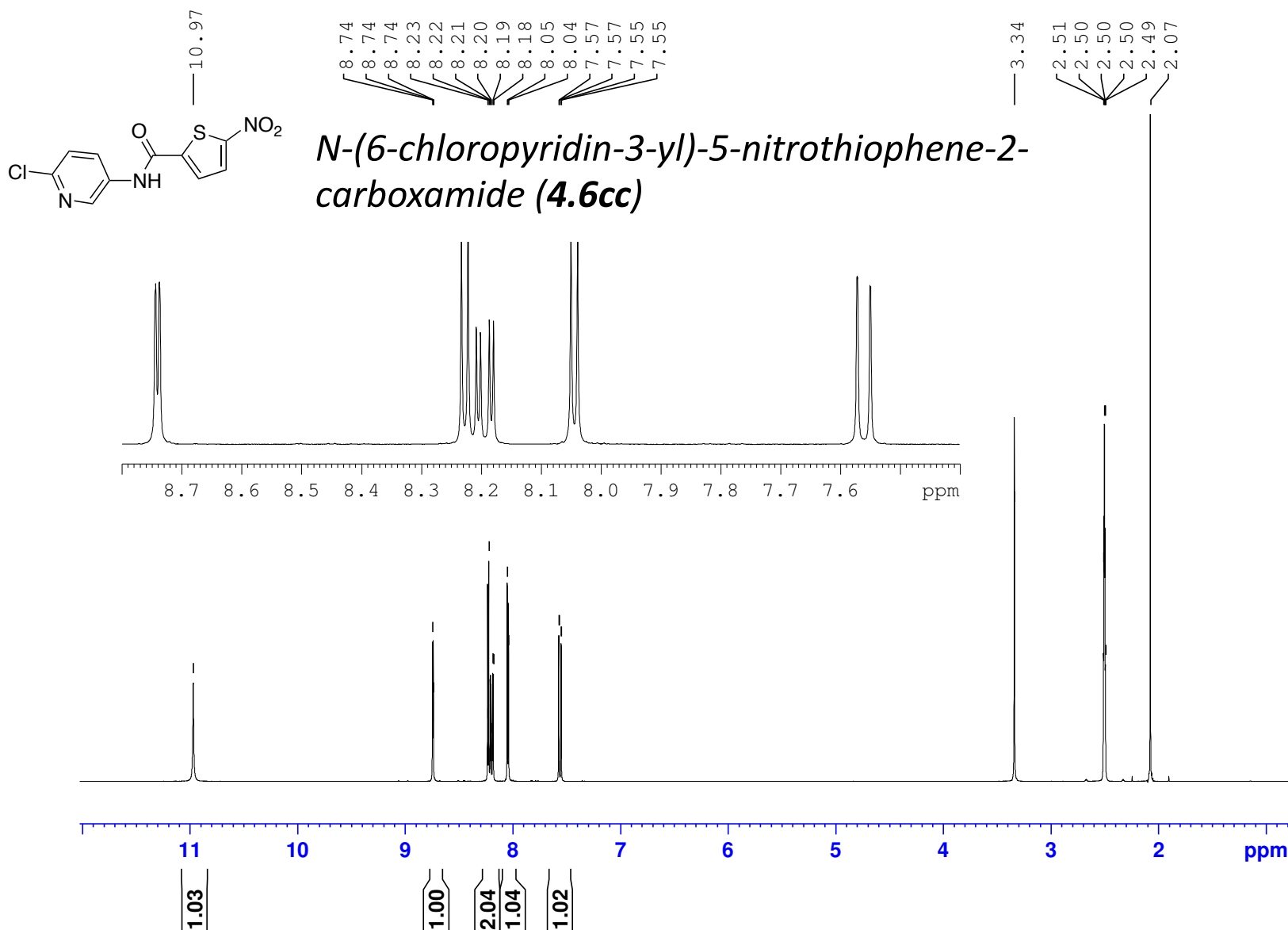


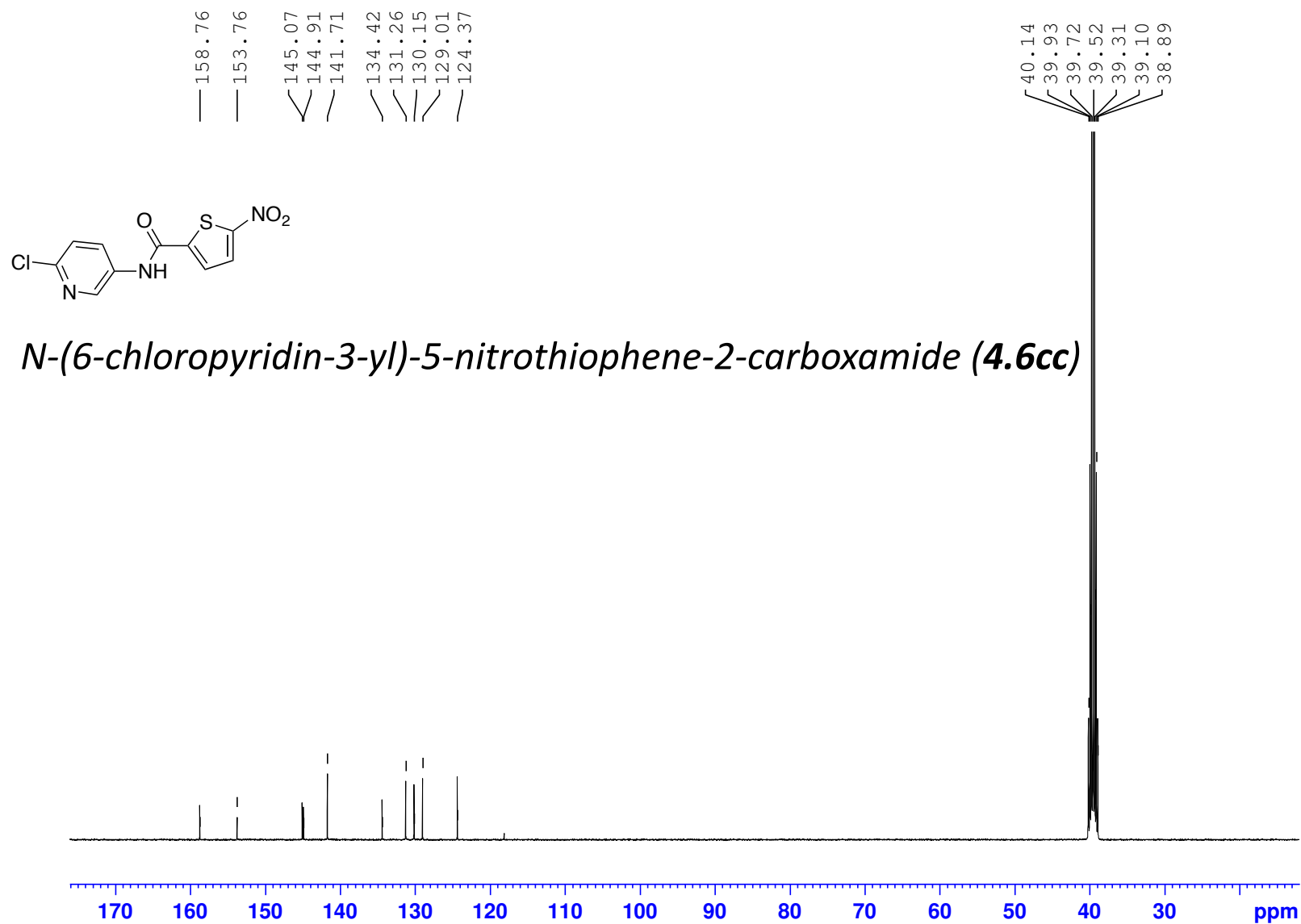
MZP584-B2-Amide-10mg-13C-NMR-Nov-18-2016

(100 MHz, 297.2 K, DMSO-d6)

GPS423



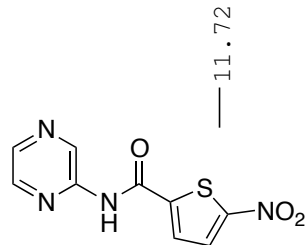






(400 MHz, 297.2 K, DMSO-d<sub>6</sub>)

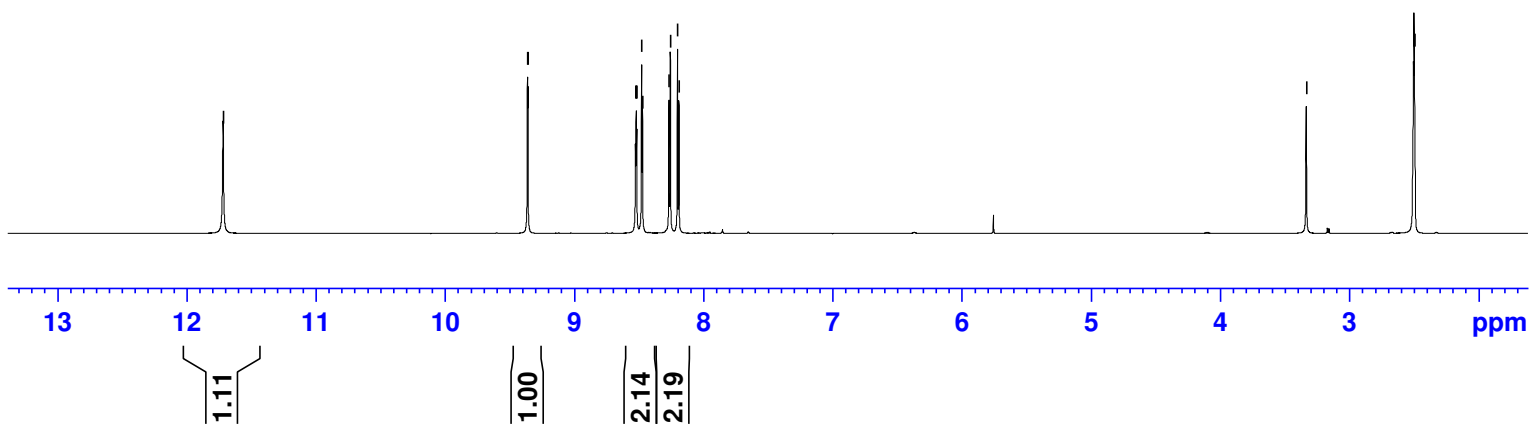
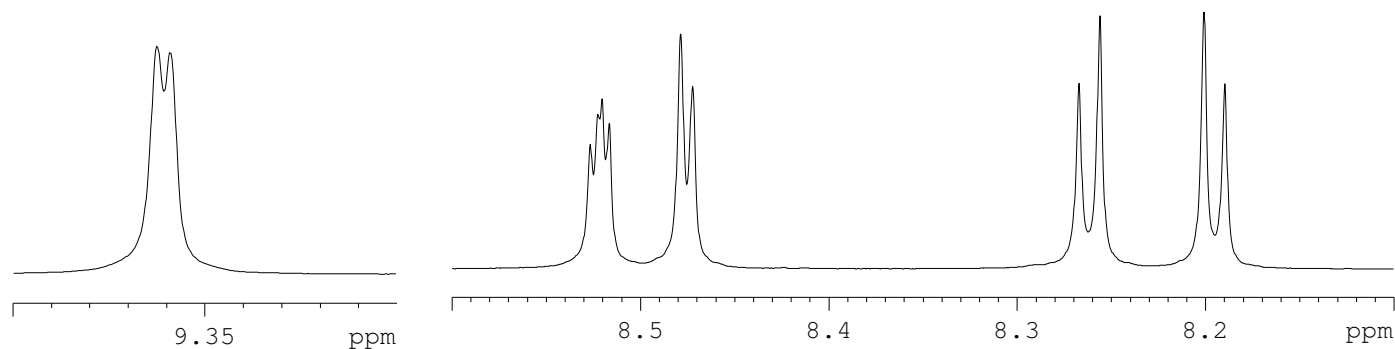
GPS421

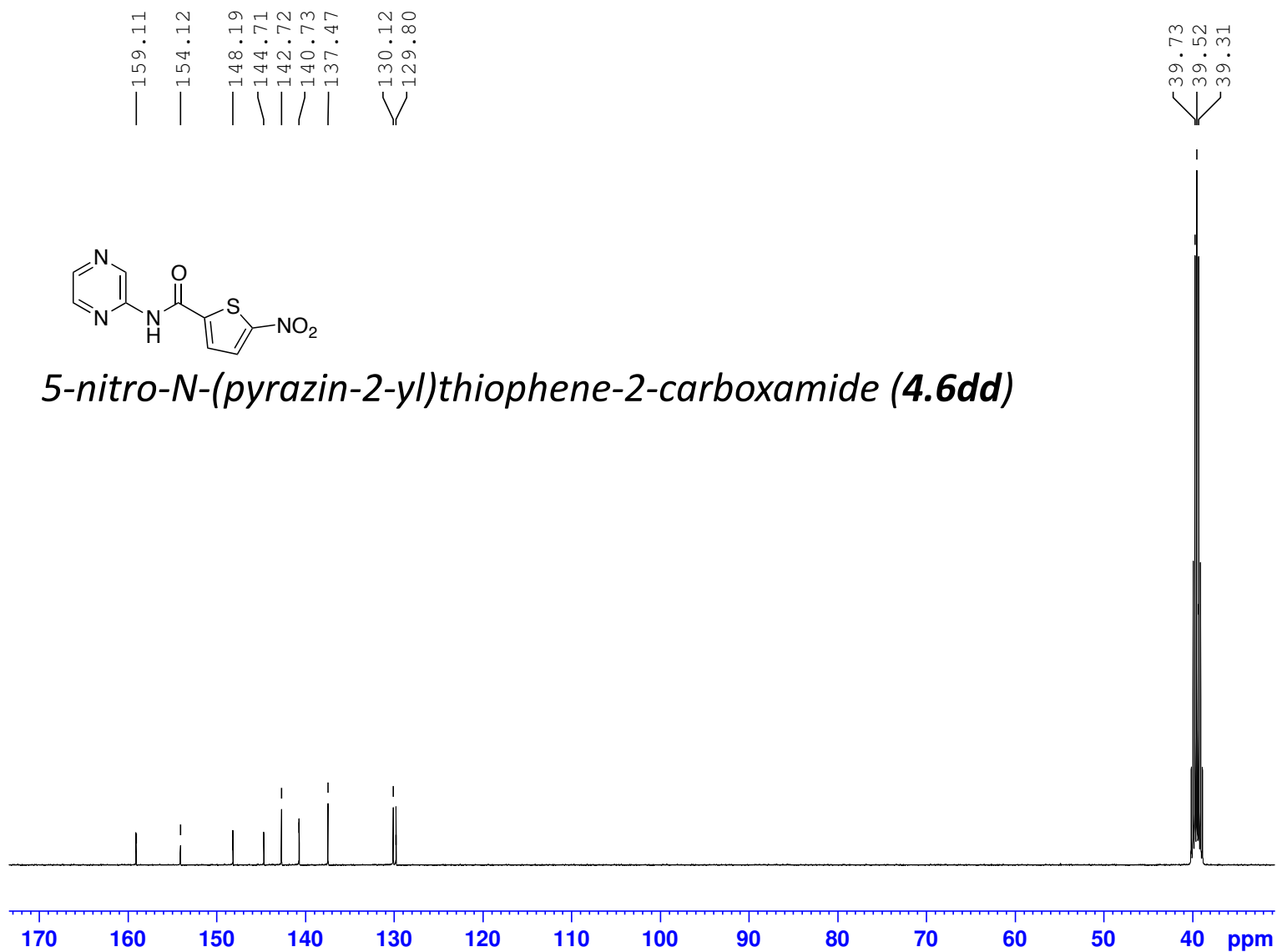


9.36  
9.36  
8.53  
8.52  
8.52  
8.48  
8.47  
8.27  
8.26  
8.20  
8.19

3.33

2.50  
2.50  
2.50

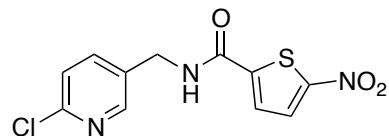
**5-nitro-N-(pyrazin-2-yl)thiophene-2-carboxamide (4.6dd)**



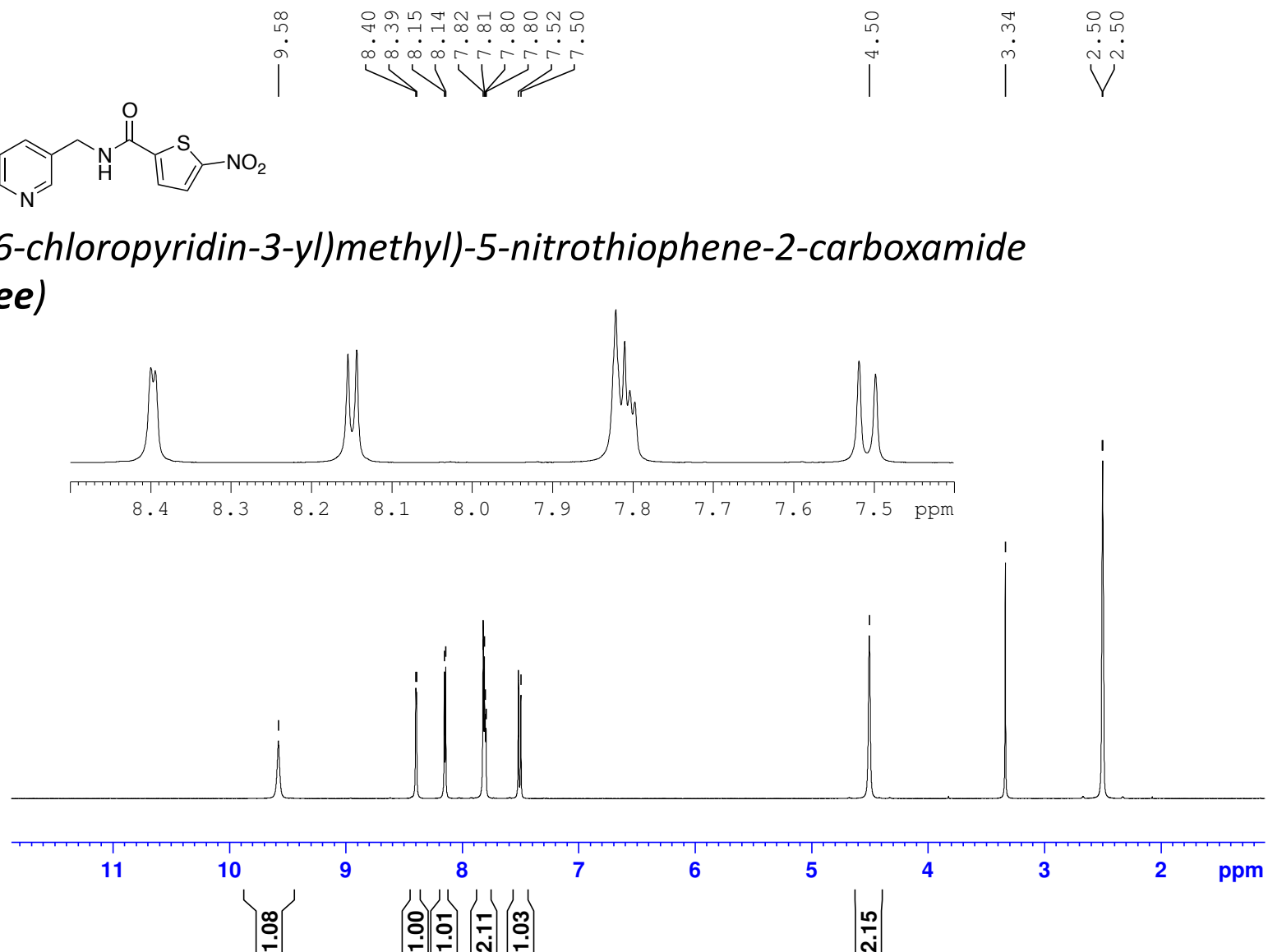
GPS441-MZP564-A18-Amide-10mg-1H-NMR-Nov-05-2016

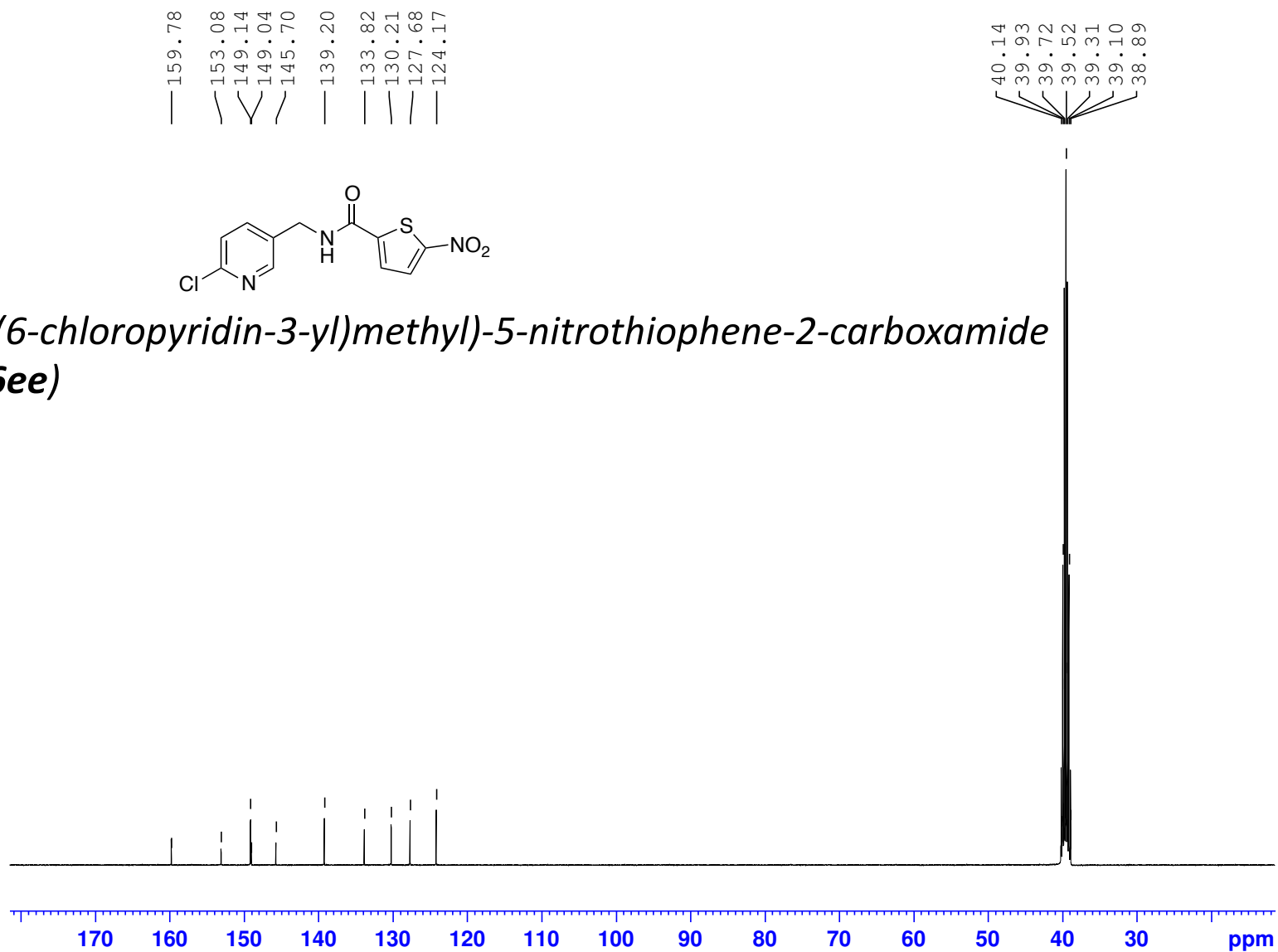
(400 MHz, 297.2 K, DMSO-d6)

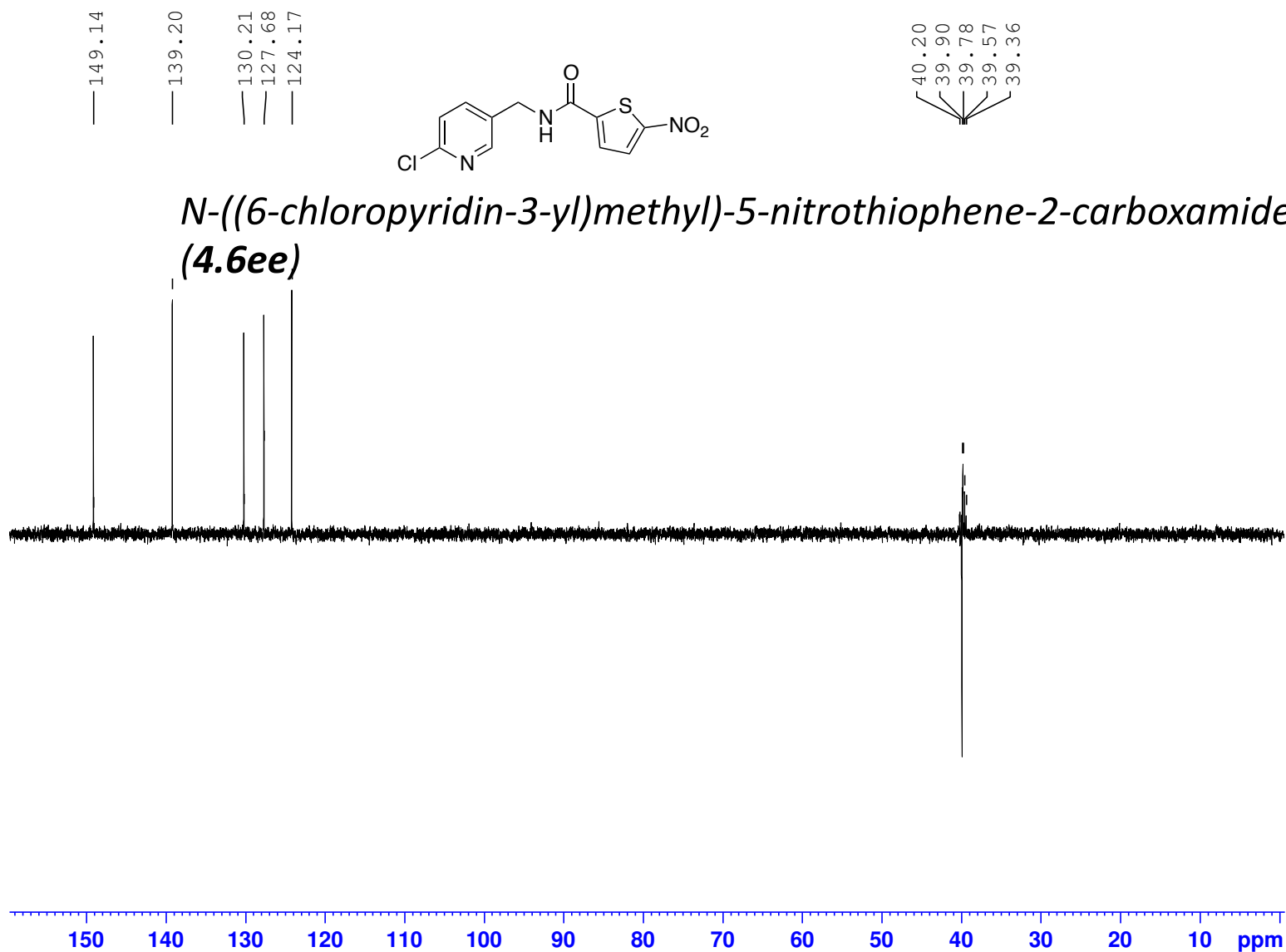
GPS441

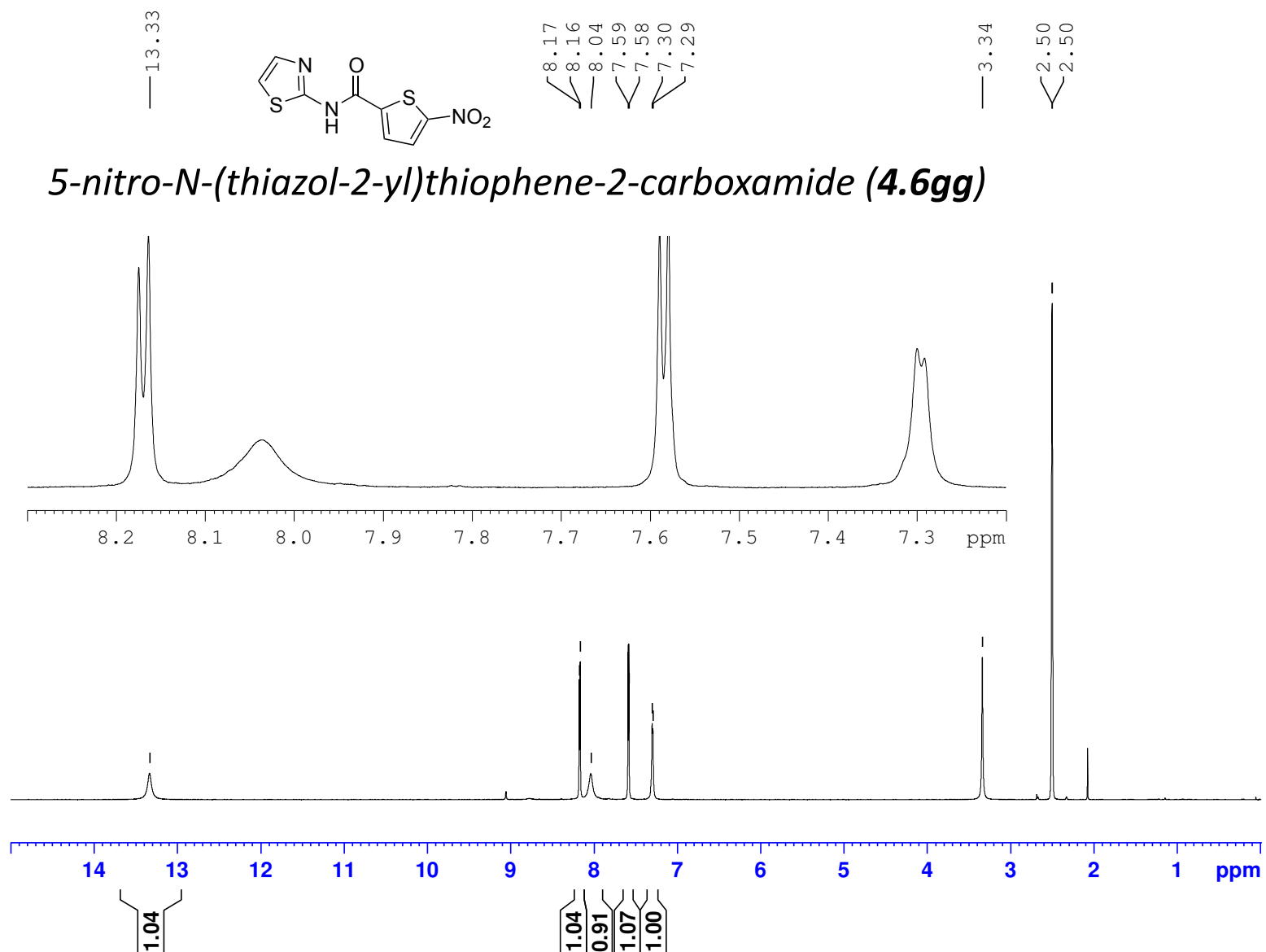


*N*-((6-chloropyridin-3-yl)methyl)-5-nitrothiophene-2-carboxamide  
(4.6ee)





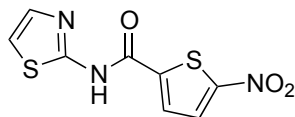




GPS390-MZP690-3129-13C-NMR-Jan-29-2018

(100 MHz, 297.2 K, DMSO-d6)

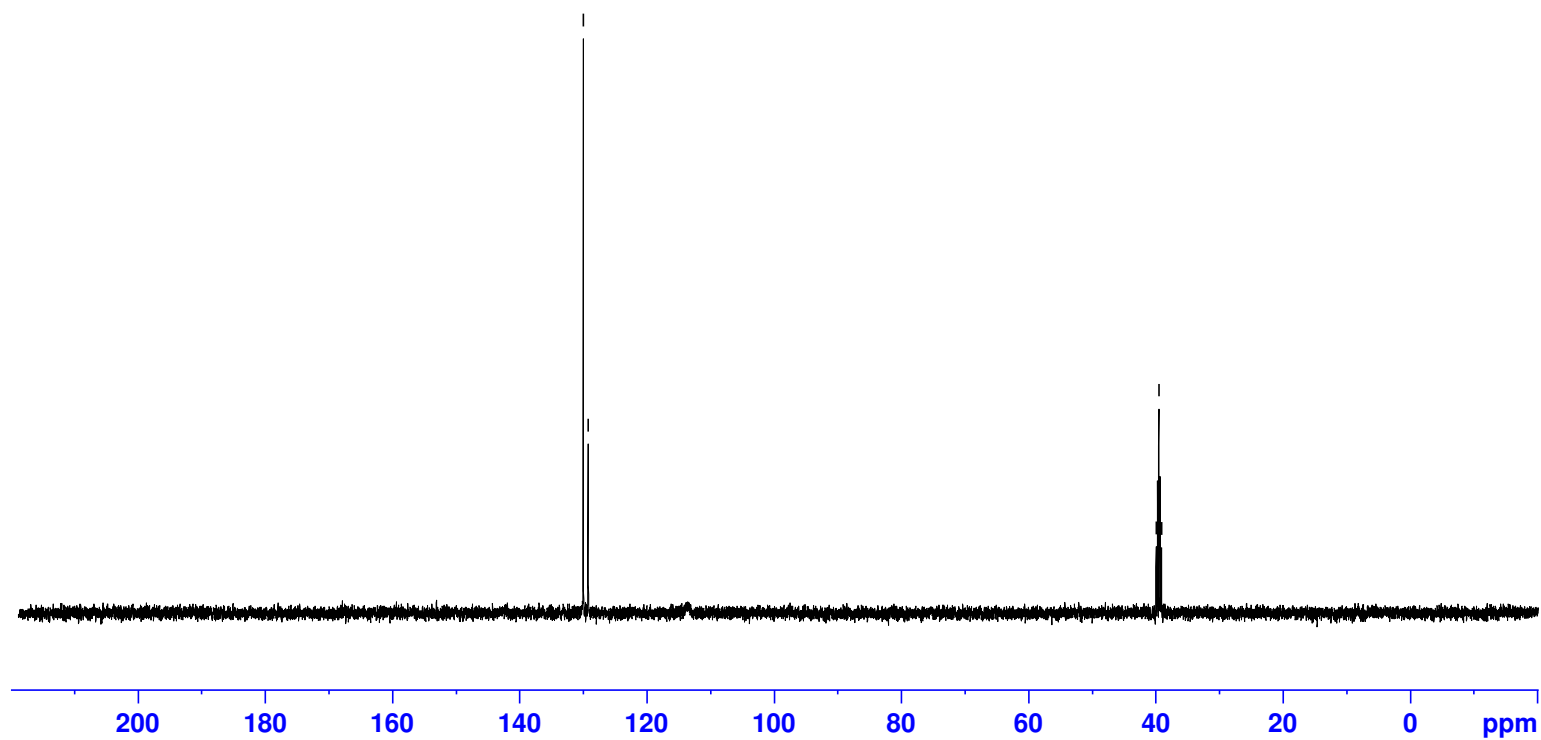
GPS390



129.98  
129.23

39.93  
39.72  
39.52  
39.31  
39.10

*5-nitro-N-(thiazol-2-yl)thiophene-2-carboxamide (4.6gg)*



MZP566-A17-Amide-10mg-1H-NMR-Nov-05-2016

(400 MHz, 297.2 K, DMSO-d6)

GPS443

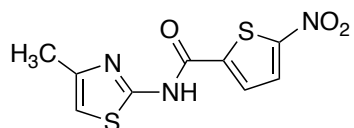
—13.27

8.15  
8.14  
7.93

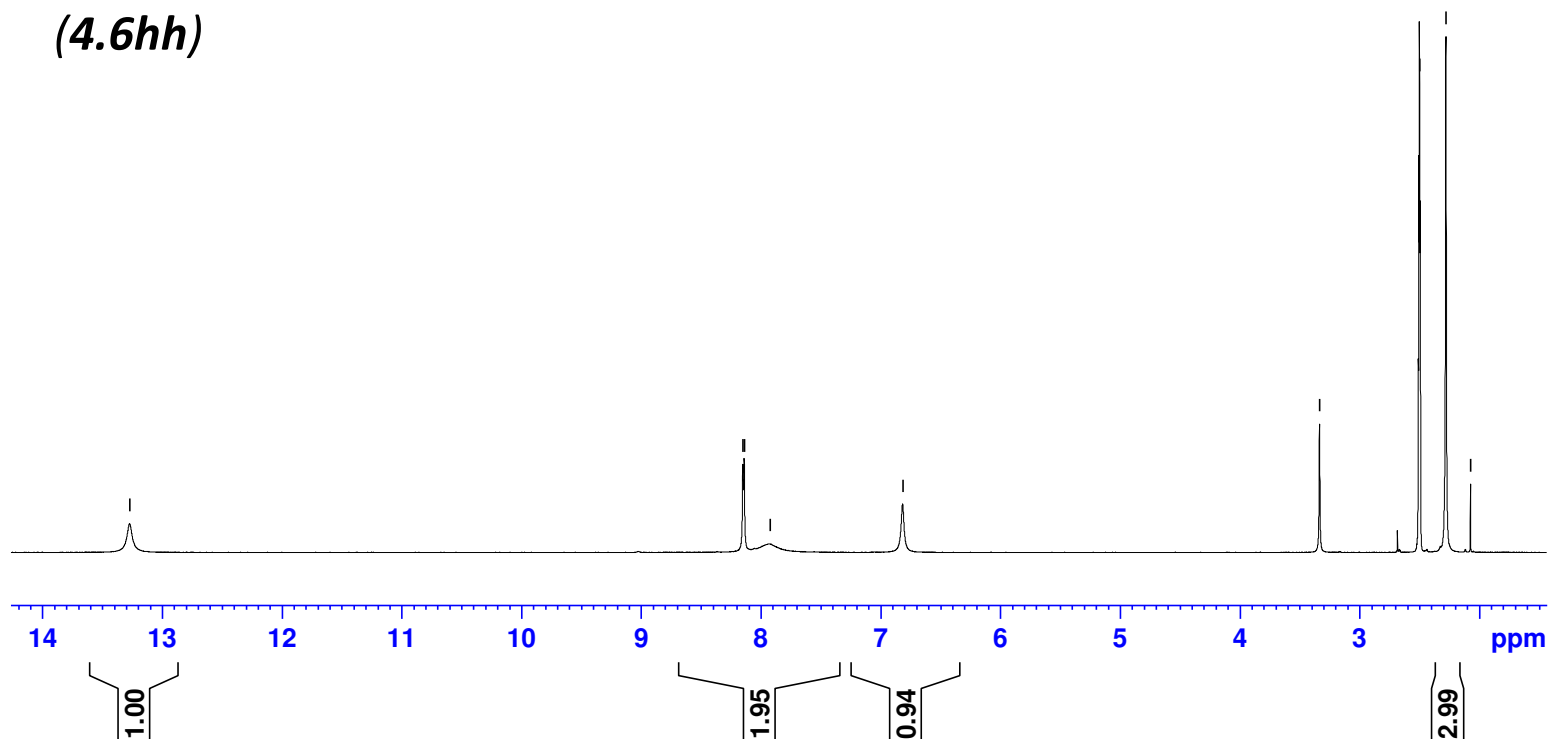
—6.82

—3.33

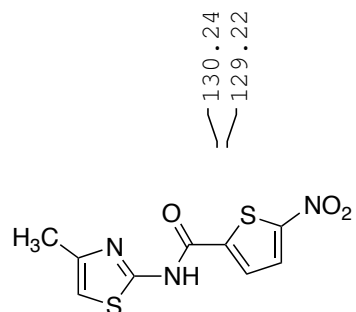
2.50  
2.28  
2.07



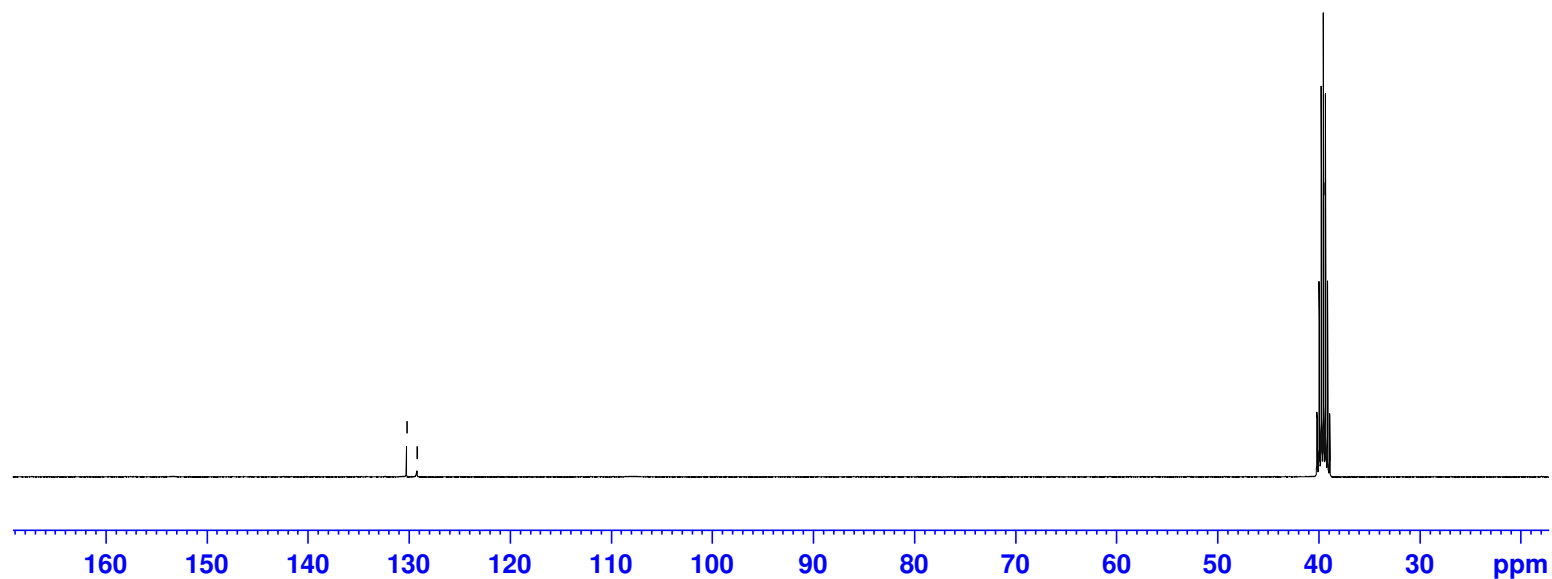
*N*-(4-methylthiazol-2-yl)-5-nitrothiophene-2-carboxamide  
**(4.6hh)**

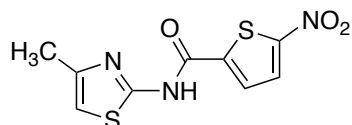






*N*-(4-methylthiazol-2-yl)-5-nitrothiophene-2-carboxamide  
**(4.6hh)**

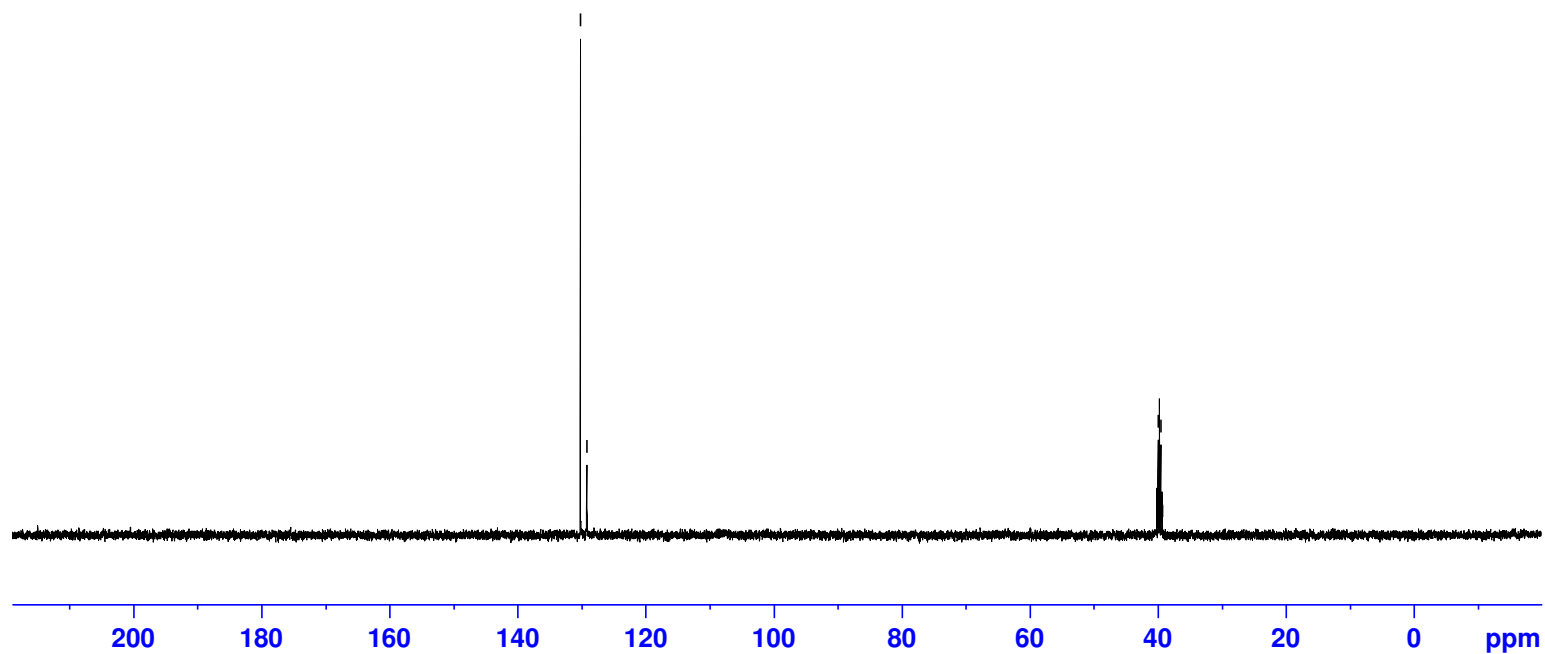




130.24  
129.21

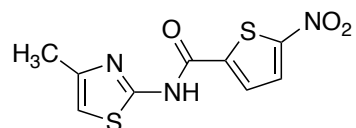
40.18  
39.97  
39.76  
39.56  
39.35

*N*-(4-methylthiazol-2-yl)-5-nitrothiophene-2-carboxamide  
(4.6hh)

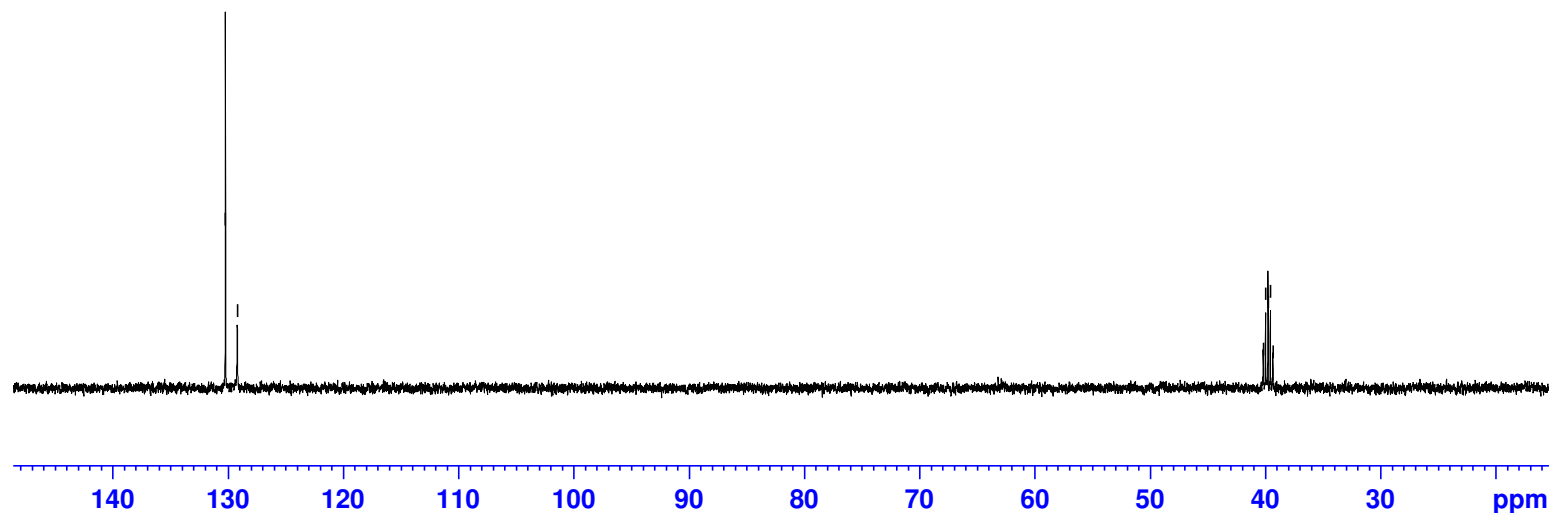


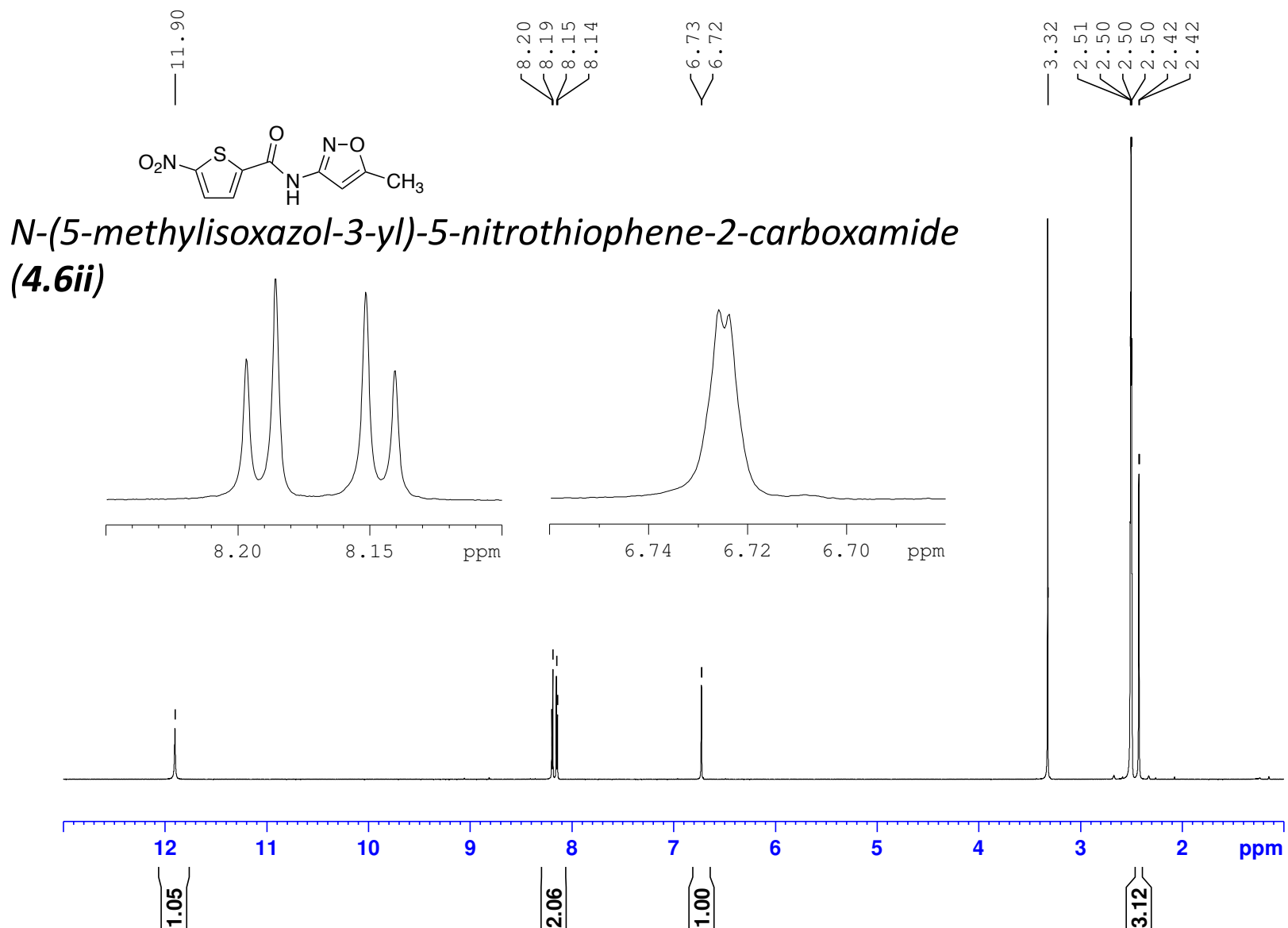
130.24  
129.22

40.18  
39.98  
39.77  
39.56  
39.35



*N*-(4-methylthiazol-2-yl)-5-nitrothiophene-2-carboxamide  
**(4.6hh)**

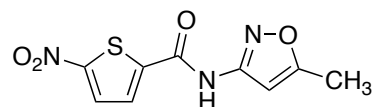




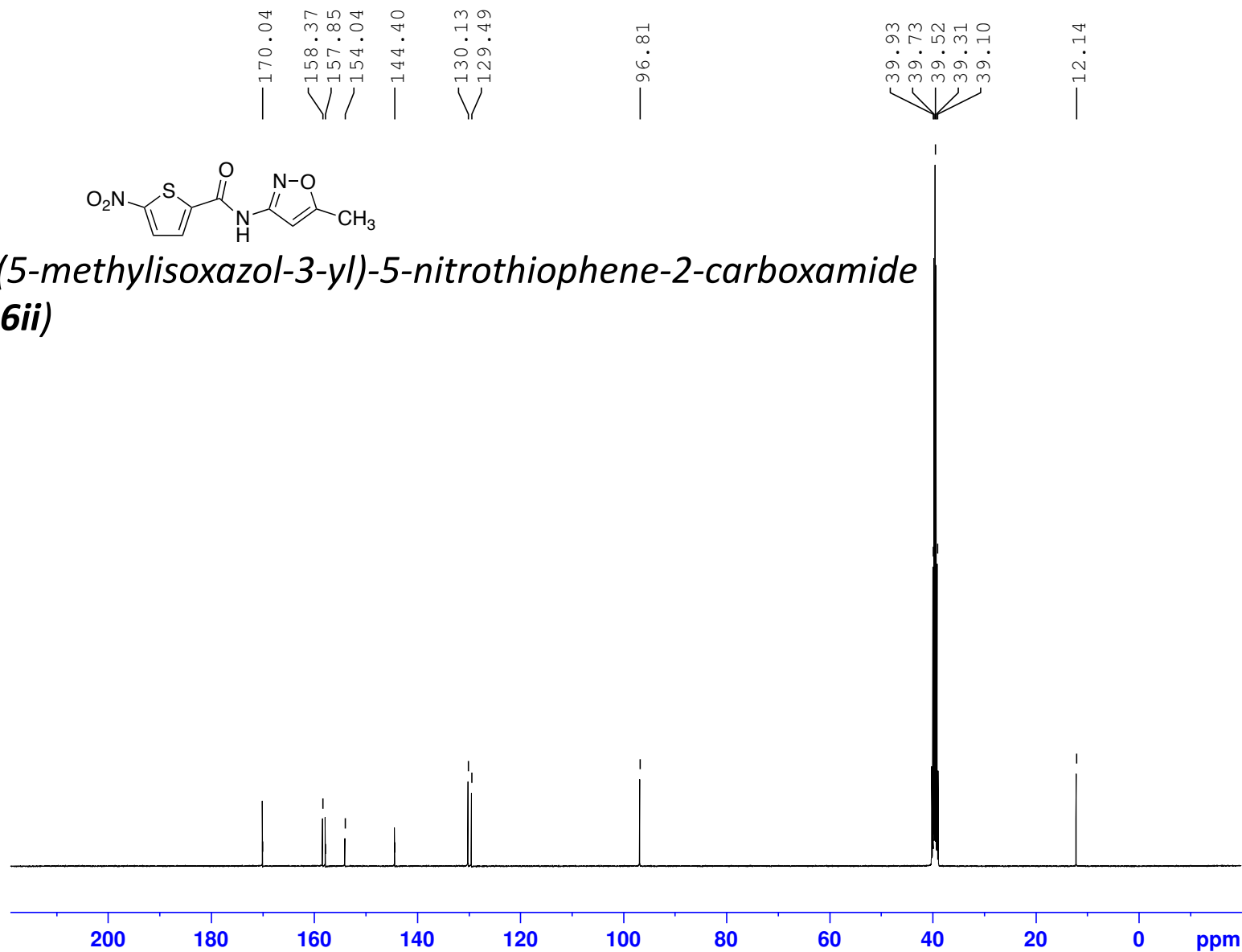
GPS401-MZP-Amide-NT-A16-13C-NMR-Feb-2015

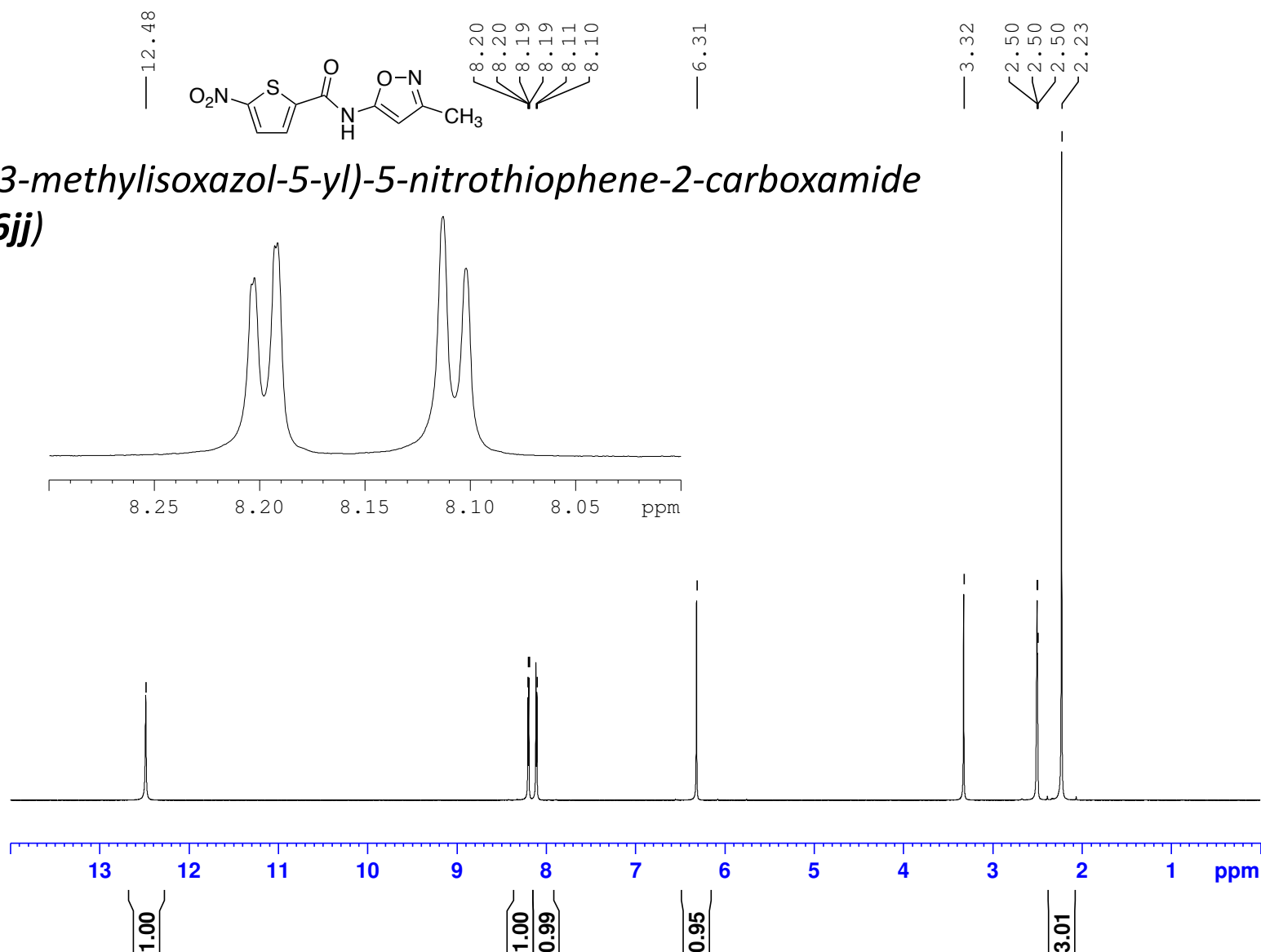
(100 MHz, 297.2 K, DMSO-d6)

GPS401



*N*-(5-methylisoxazol-3-yl)-5-nitrothiophene-2-carboxamide  
(4.6ii)





GPS402-MZP-NT-Amide-A31-13C-NMR-March-19-2015

(100 MHz, 297.2 K, DMSO-d6)

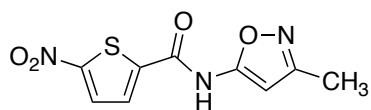
GPS402

160.90  
160.41  
156.75  
154.25  
143.50  
130.13  
129.73

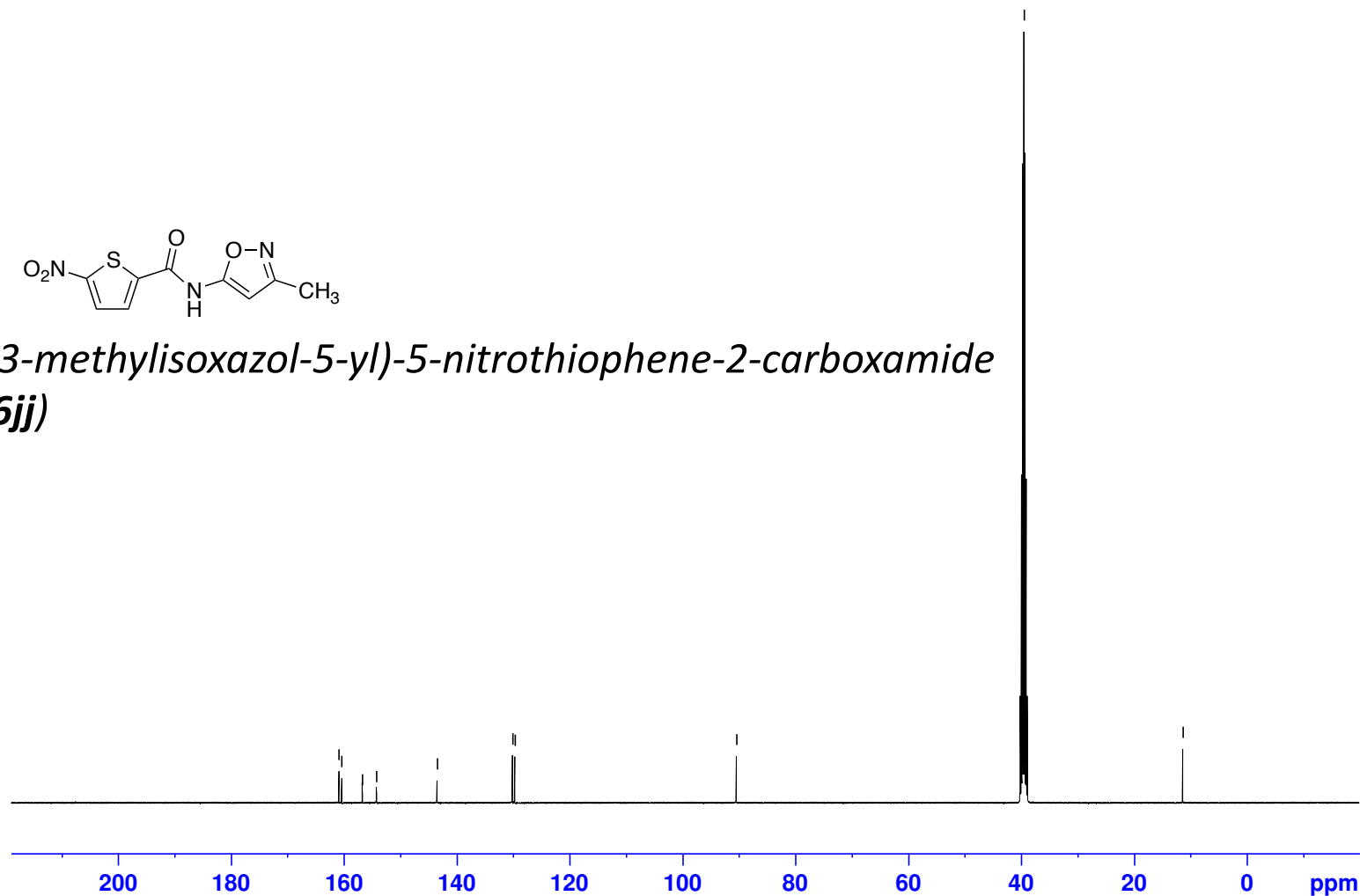
90.47

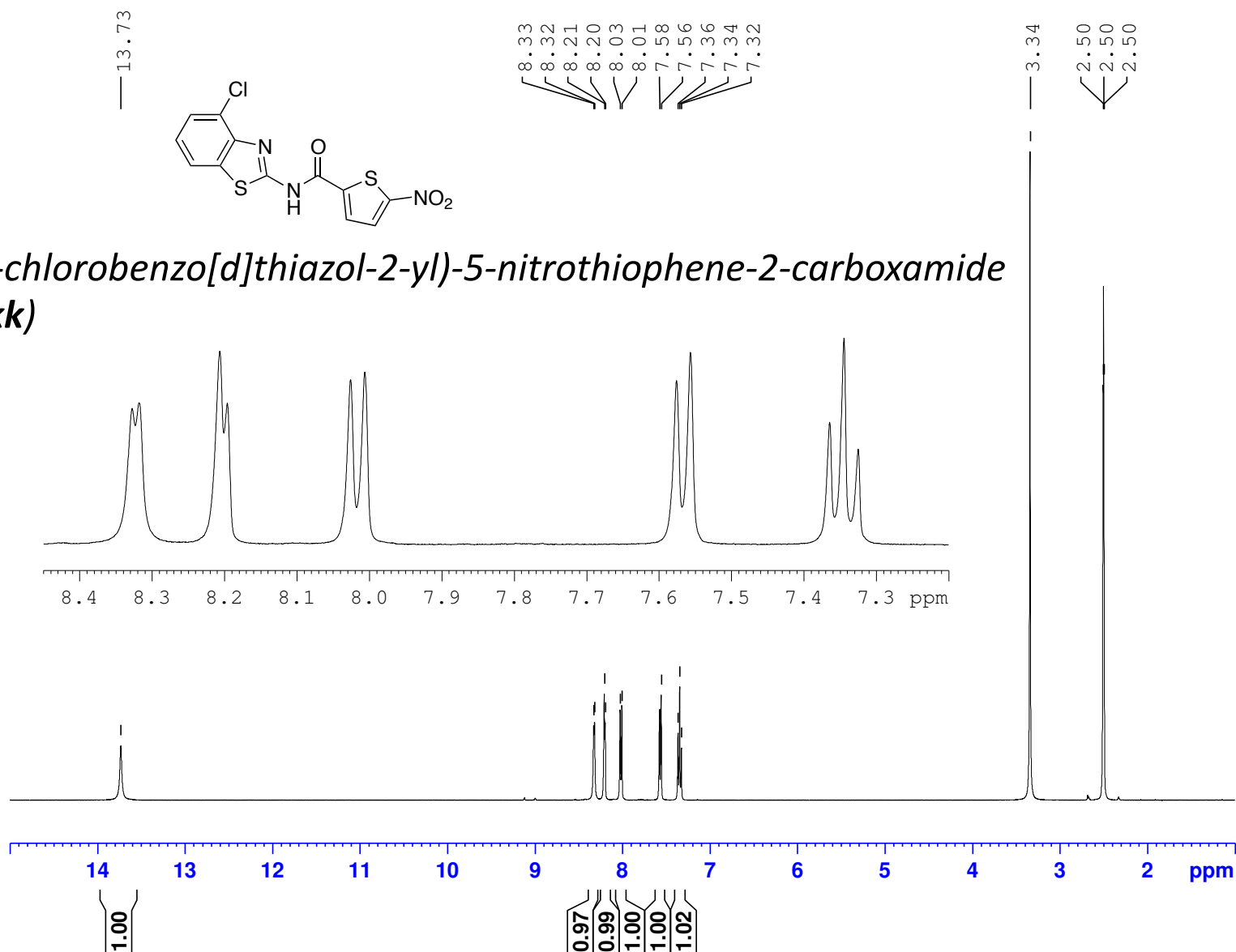
39.72  
39.52  
39.31

11.36



*N*-(3-methylisoxazol-5-yl)-5-nitrothiophene-2-carboxamide  
(4.6jj)



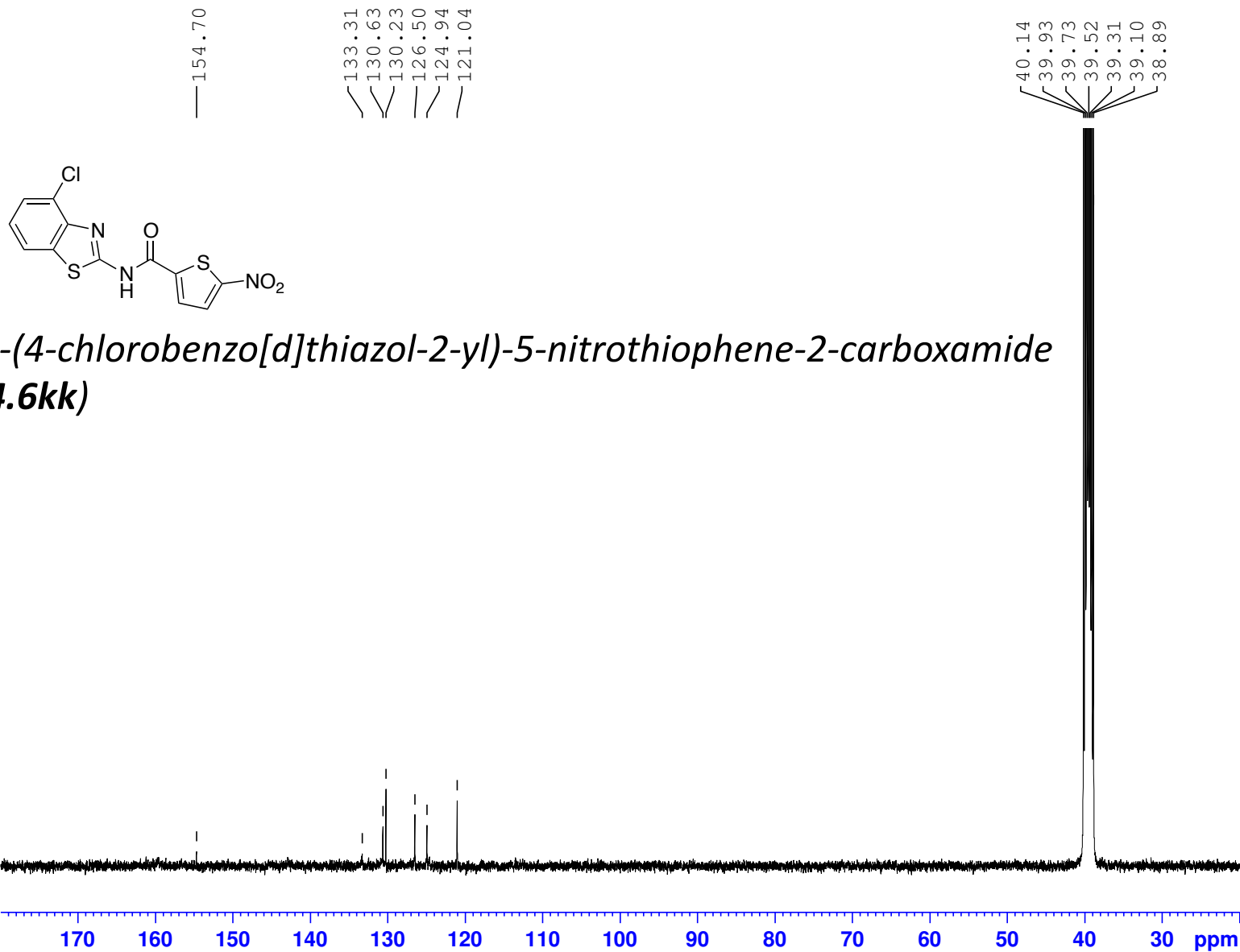




GPS389-MZP566-A42-13C-NMR-June-14-2017

(100 MHz, 297.2 K, DMSO-d6)

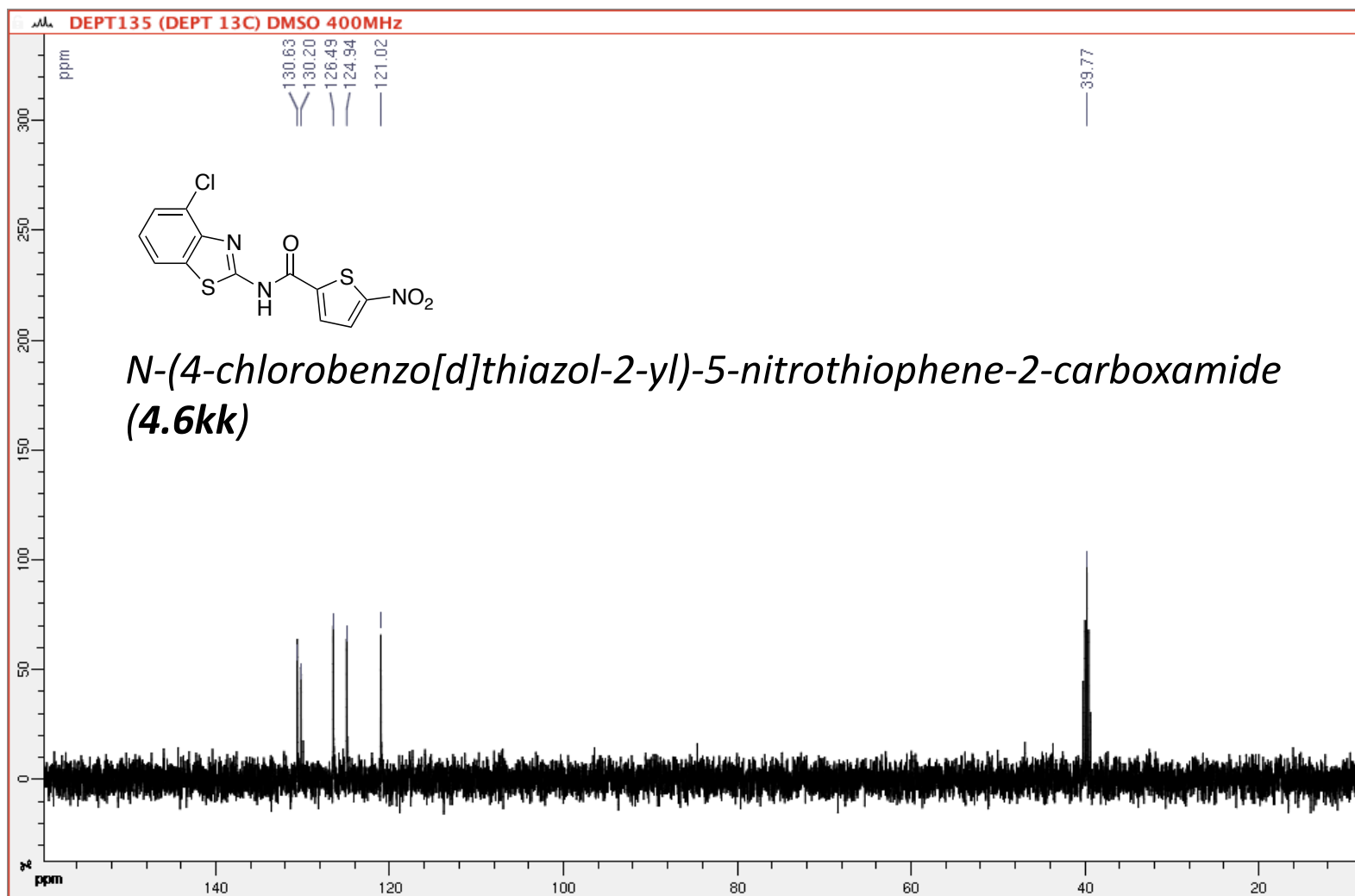
GPS389



(100 MHz, 297.2 K, DMSO-d6)

GPS389

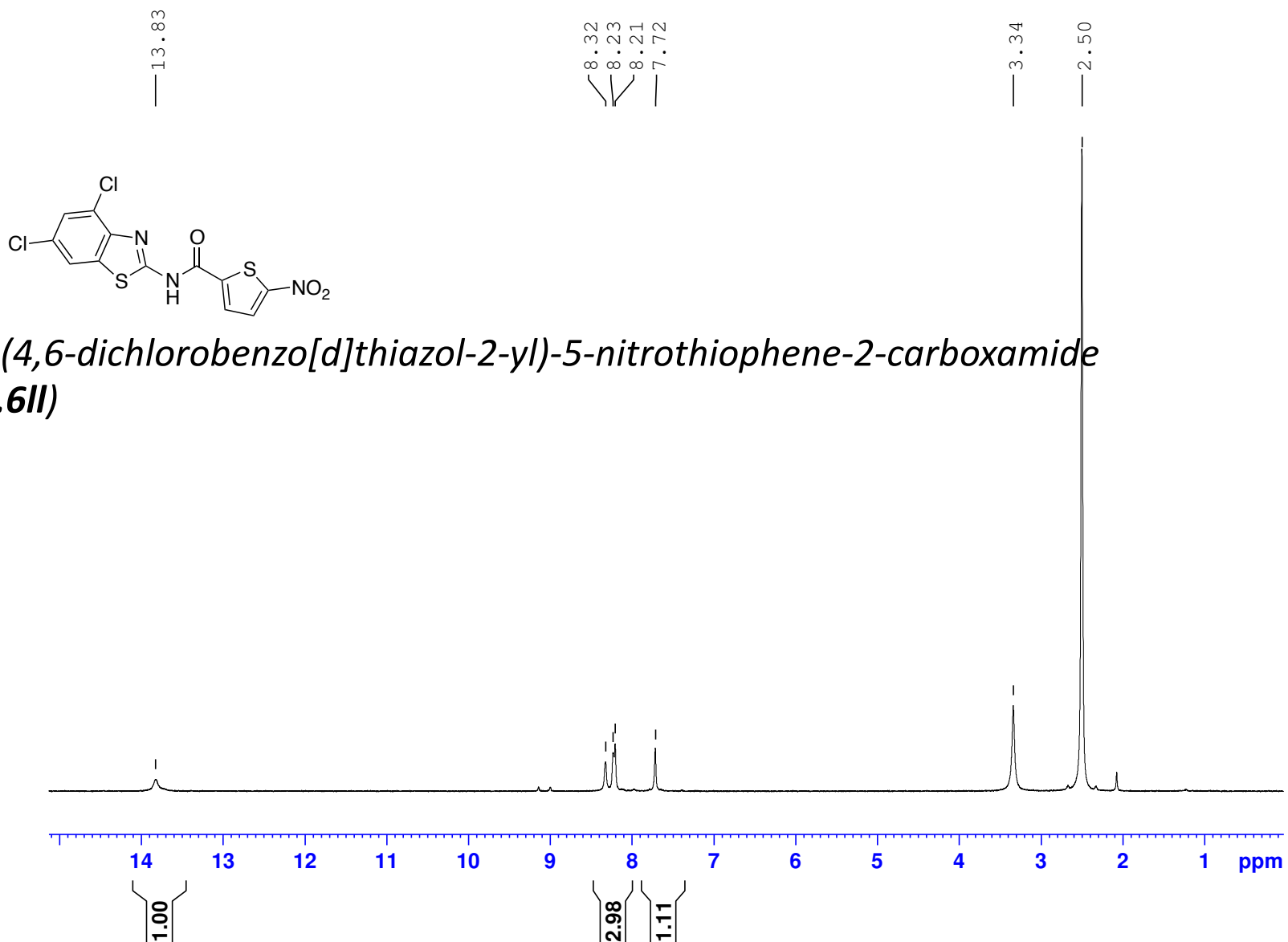
DEPT 135



MZP594-B96-Amide-10mg-Sep-29-2016

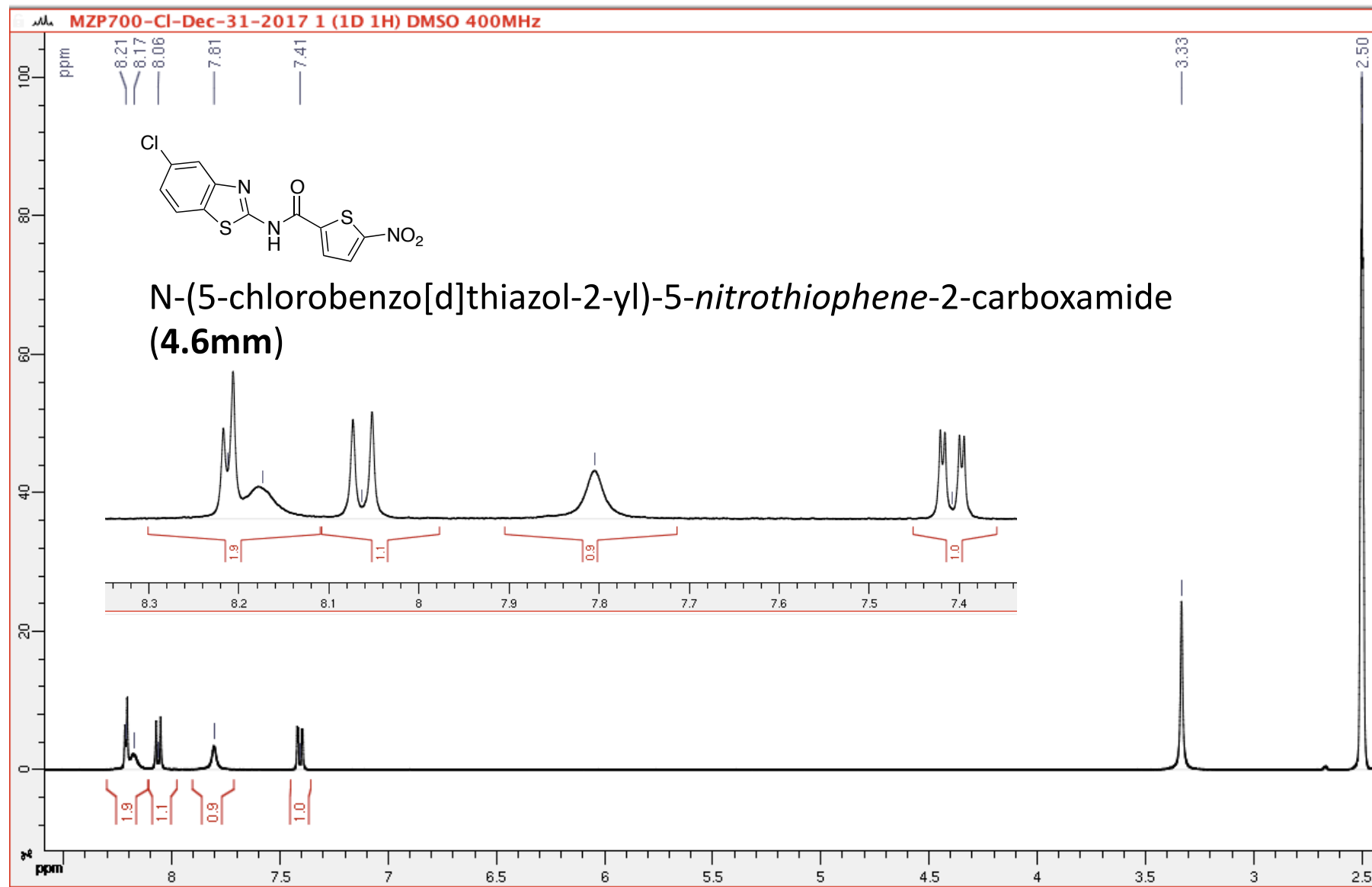
(400 MHz, 297.2 K, DMSO-d6)

GPS476



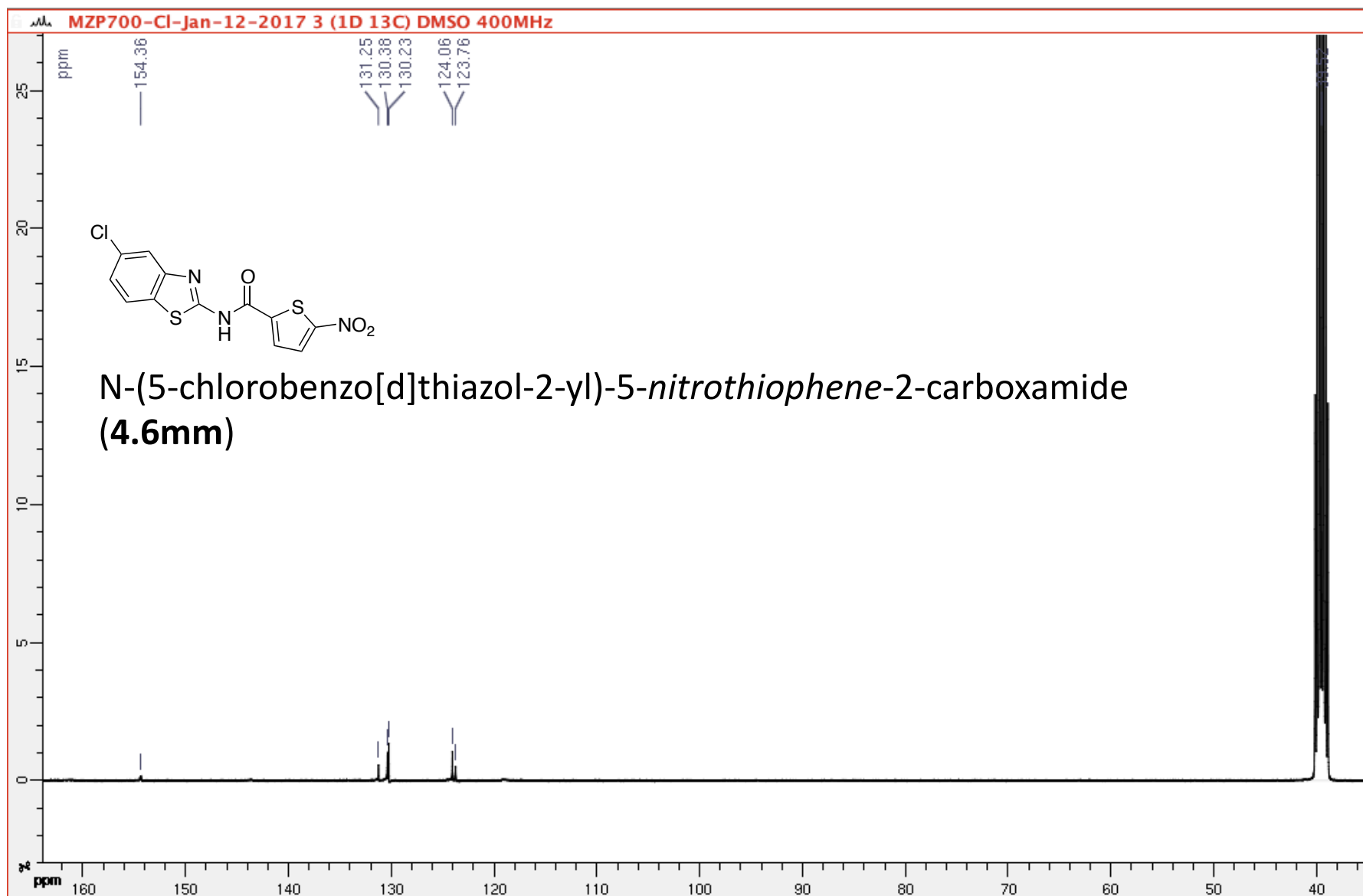
(400 MHz, 297.2 K, DMSO-d6)

GPS515



(100 MHz, 297.2 K, DMSO-d6)

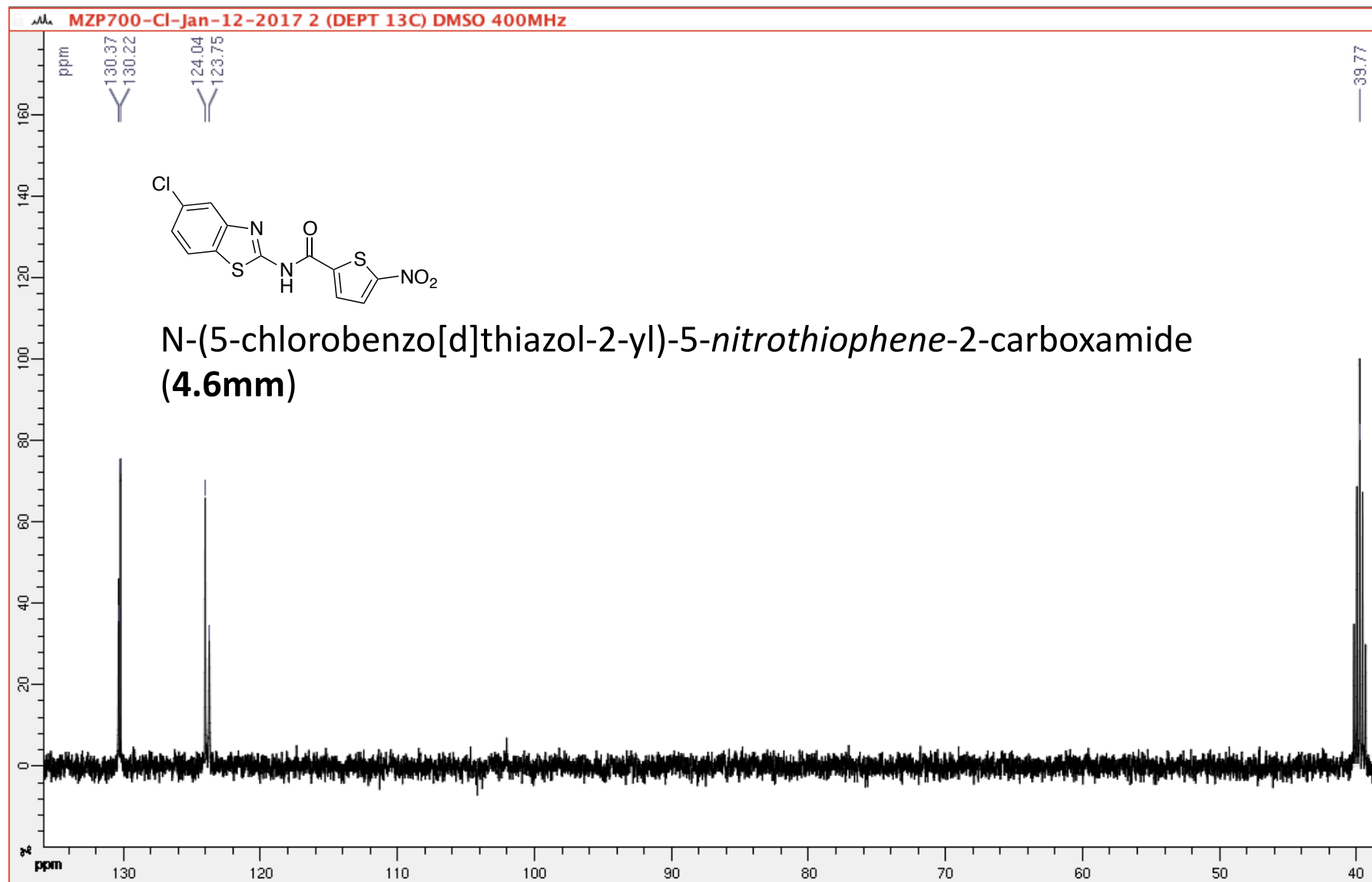
GPS515

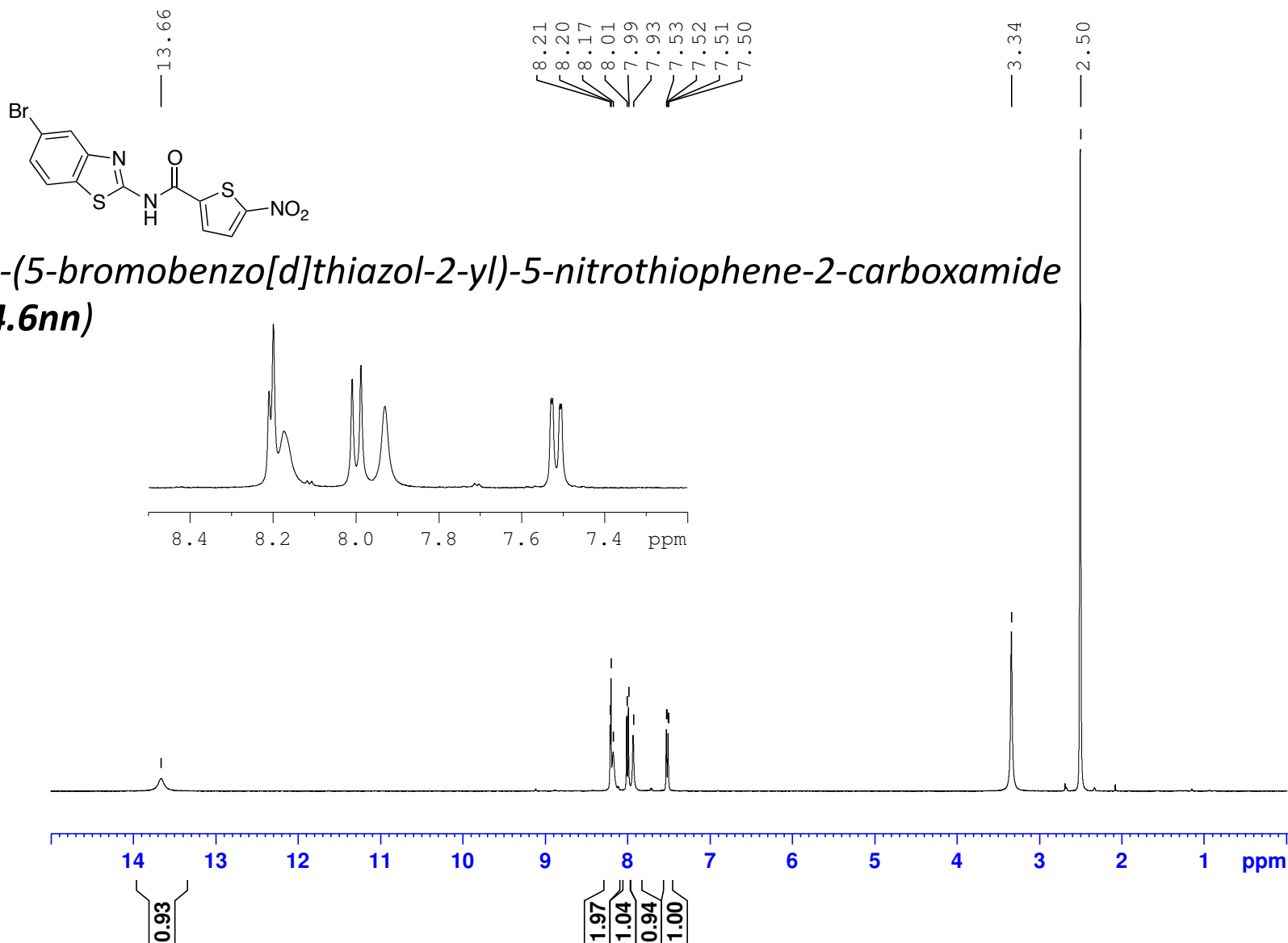


DEPT 90

(100 MHz, 297.2 K, DMSO-d6)

GPS515

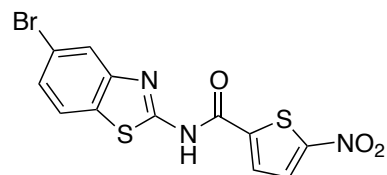




GPS478-13C-DEPT90-NMR-Jan-31-2018

(100 MHz, 297.2 K, DMSO-d6)

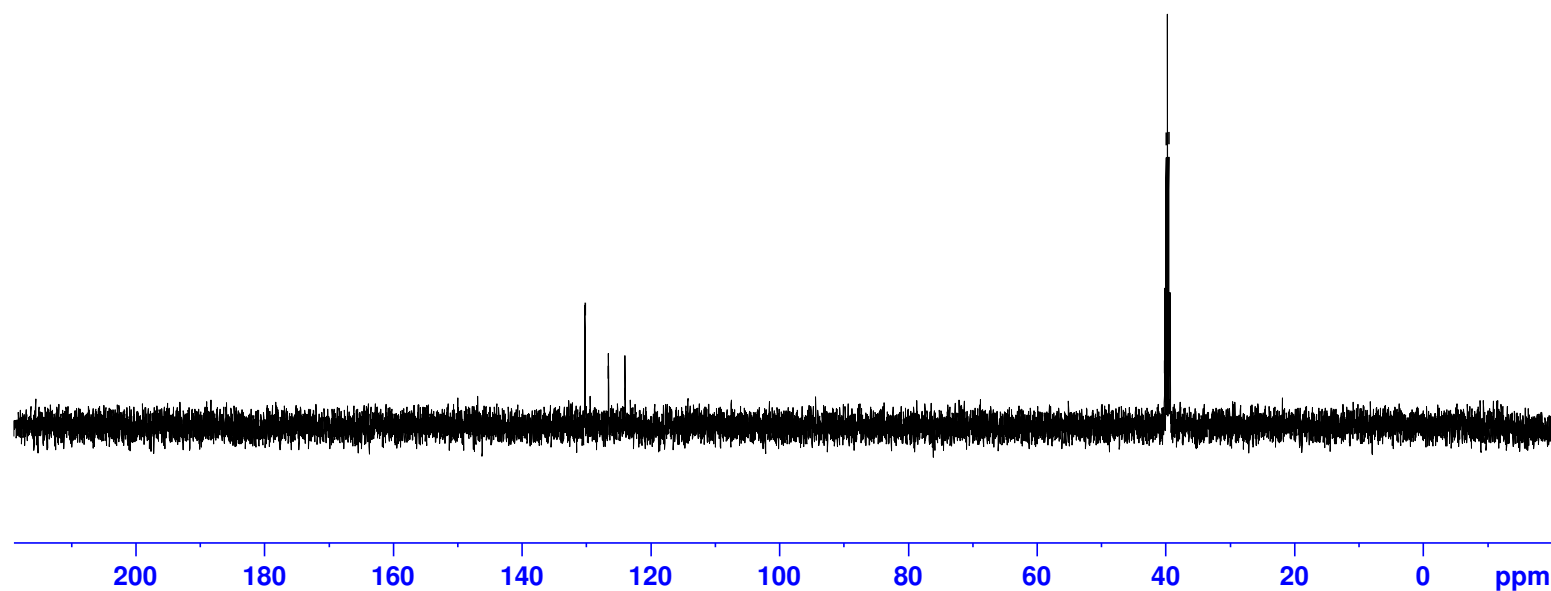
GPS478



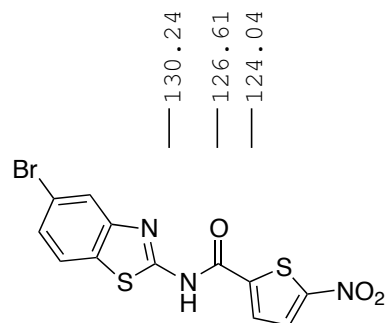
130.24  
126.61  
124.04

40.18  
39.97  
39.76  
39.55  
39.34

*N*-(5-bromobenzo[d]thiazol-2-yl)-5-nitrothiophene-2-carboxamide  
(4.6nn)

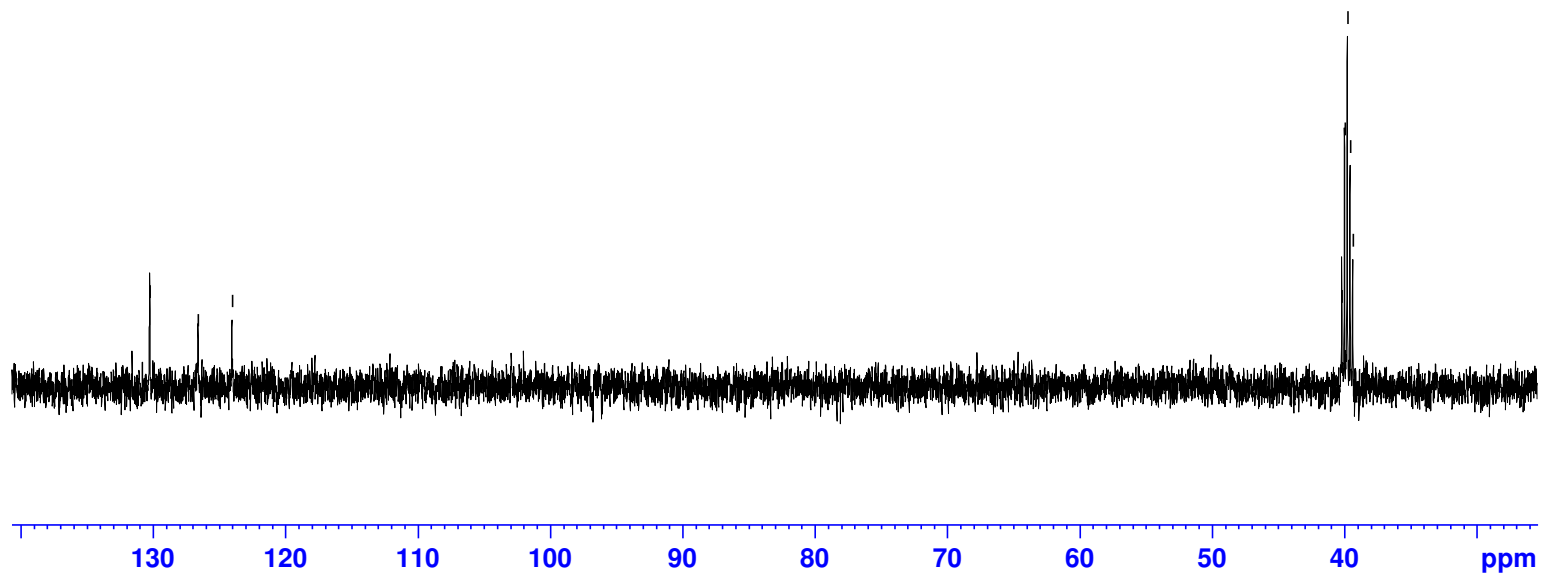






40.19  
39.98  
39.77  
39.56  
39.36

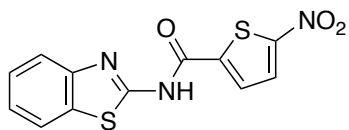
*N*-(5-bromobenzo[d]thiazol-2-yl)-5-nitrothiophene-2-carboxamide  
(4.6nn)



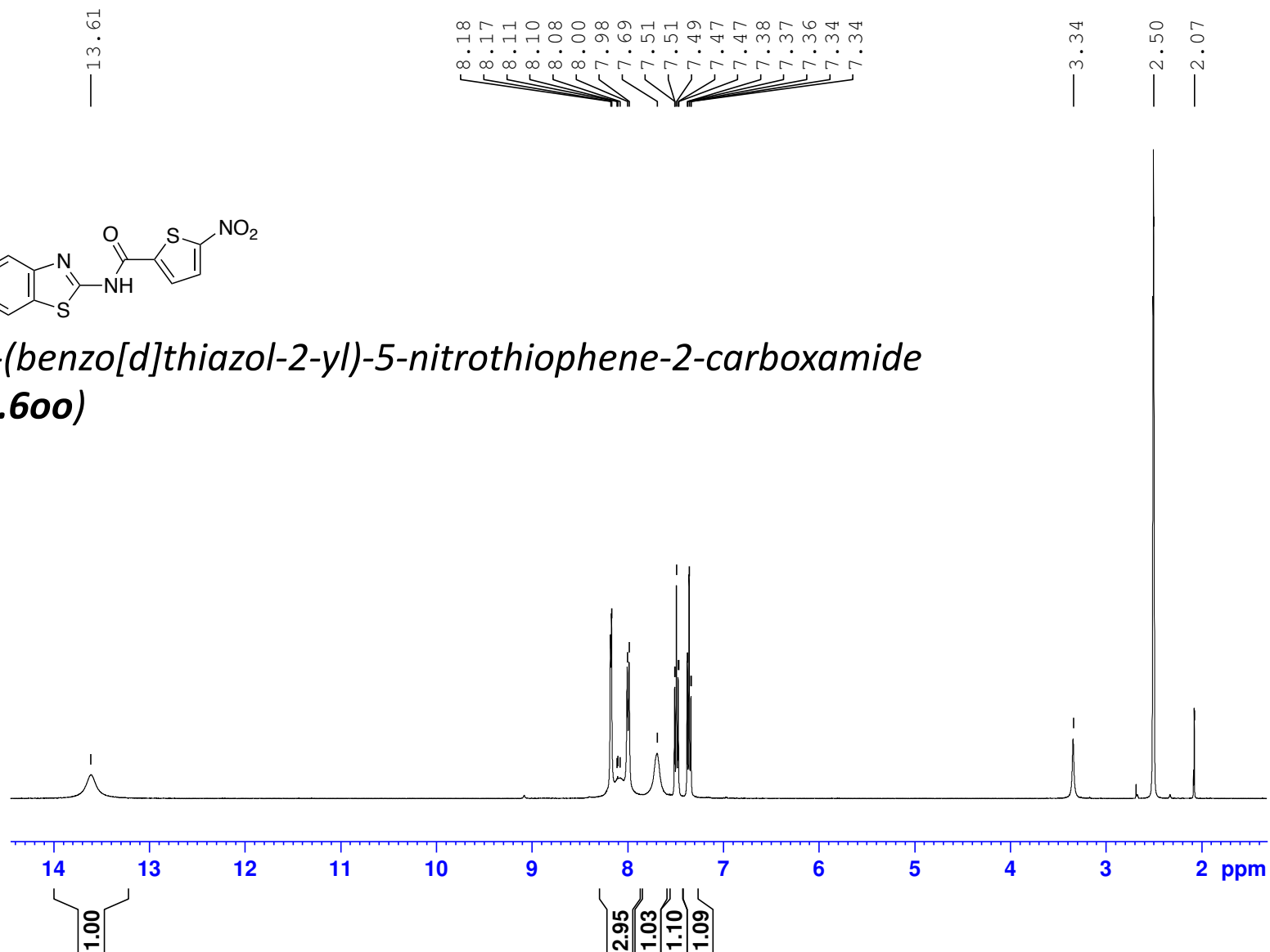
MZP584-8812-10mg-18-05-2016-1H-NMR-DMSO

(400 MHz, 297.2 K, DMSO-d6)

GPS445



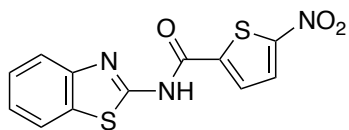
*N*-(benzo[d]thiazol-2-yl)-5-nitrothiophene-2-carboxamide  
(4.600)



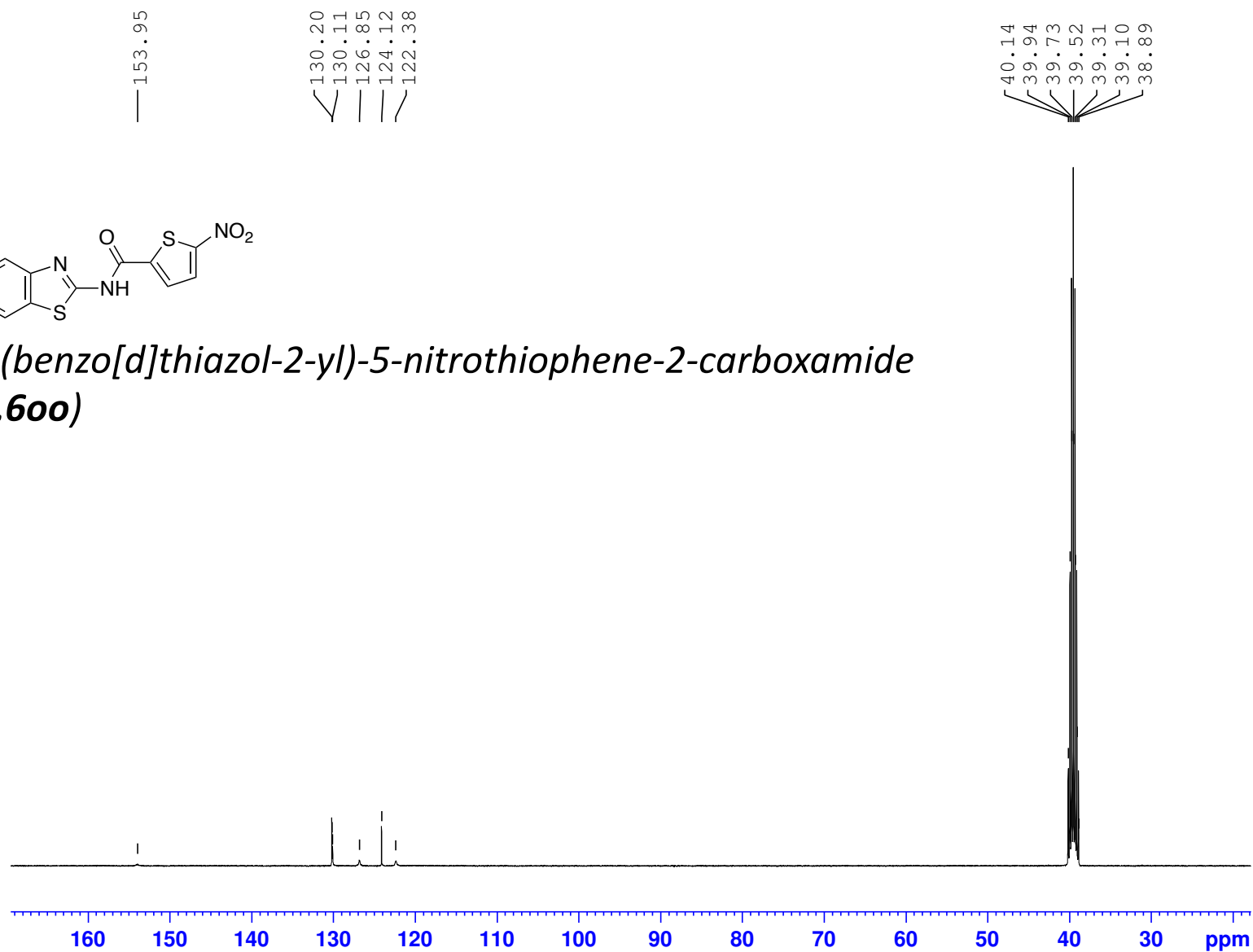
GPS445-MZP584-8812-Amide-10mg-13C-NMR-Oct-25-2016

(100 MHz, 297.2 K, DMSO-d6)

GPS445



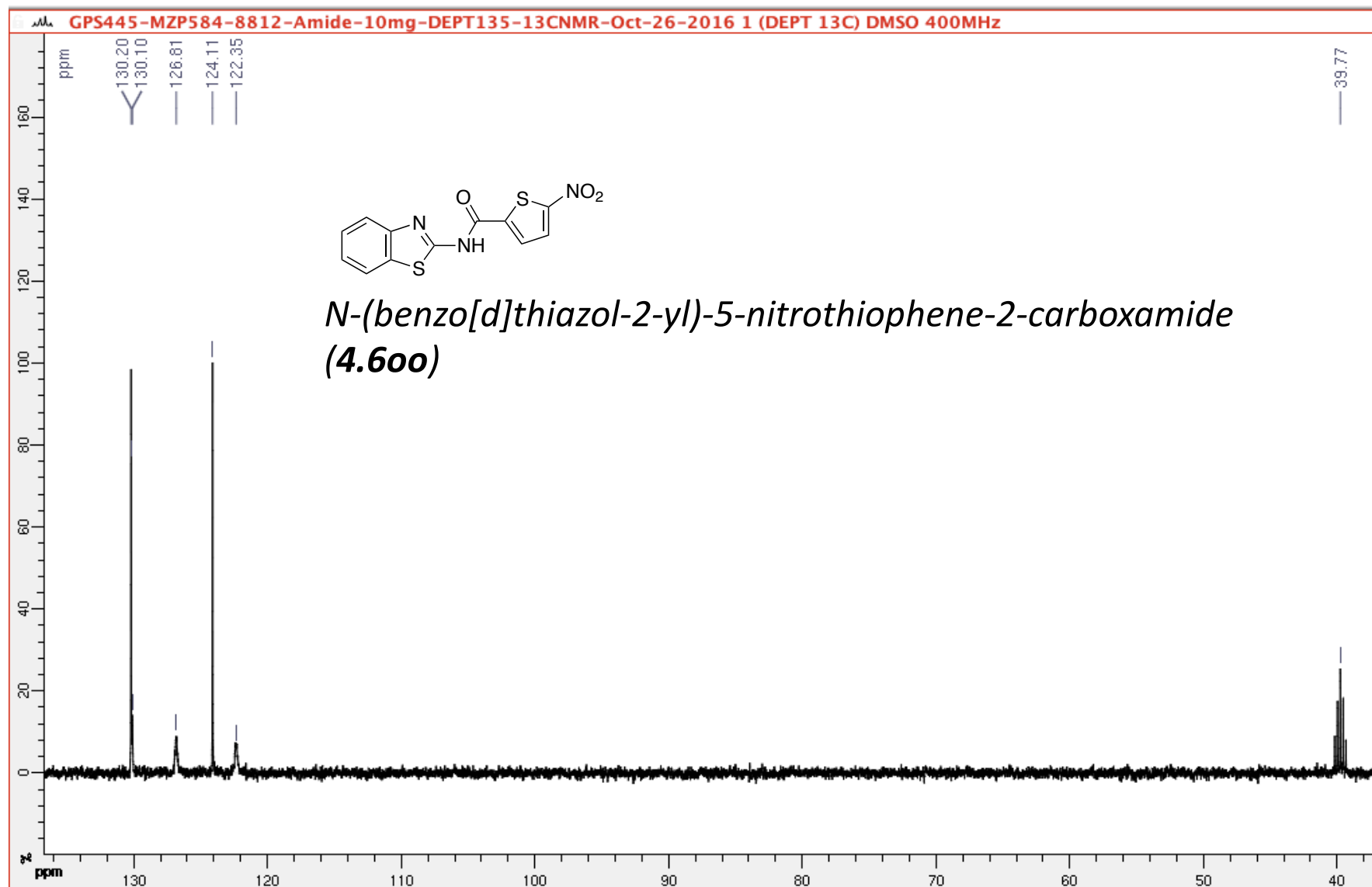
*N*-(benzo[d]thiazol-2-yl)-5-nitrothiophene-2-carboxamide  
**(4.600)**



DEPT135

(100 MHz, 297.2 K, DMSO-d6)

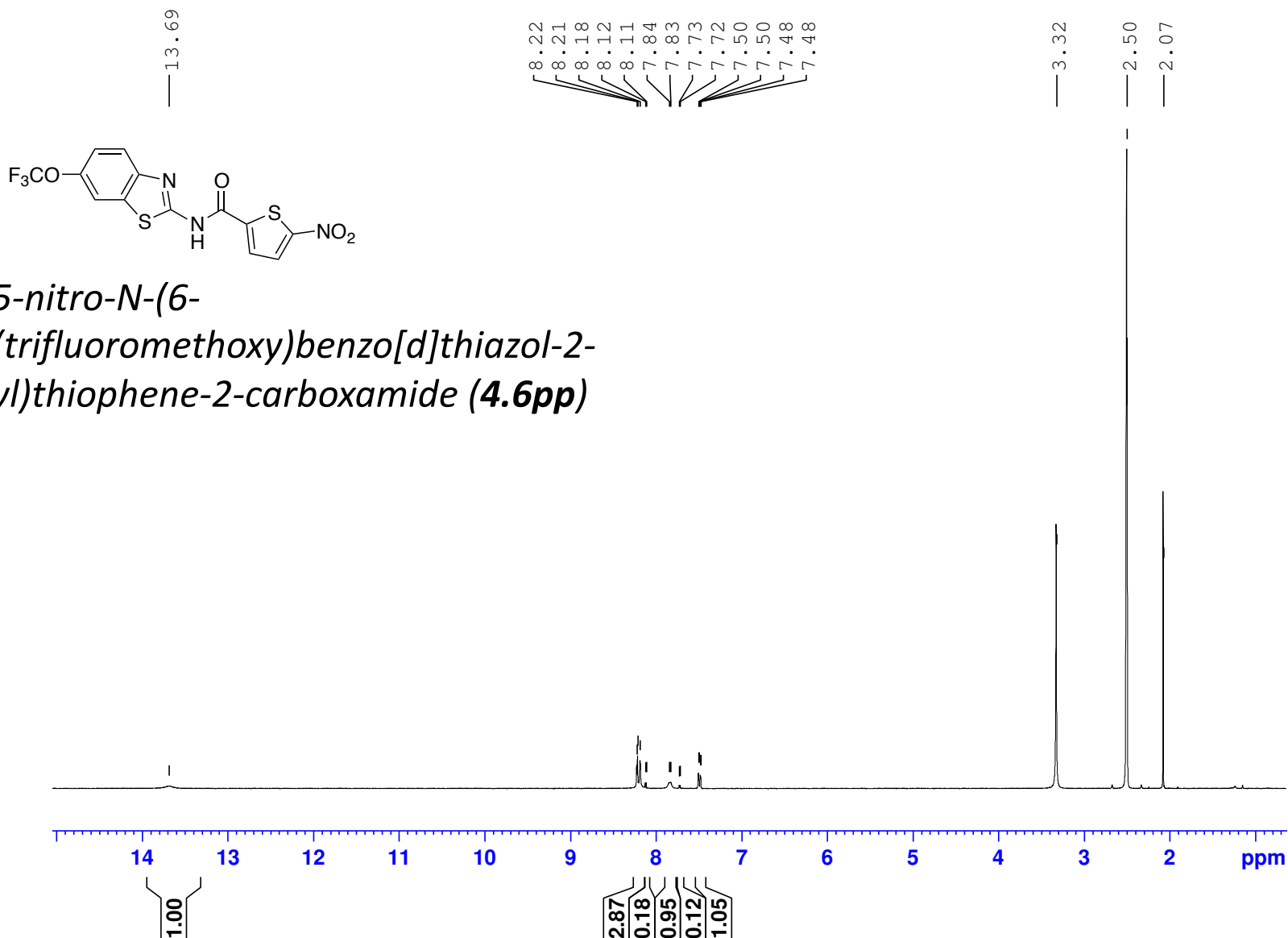
GPS445



MZP573-B74-1H-NMR-14-03-2016

(400 MHz, 297.2 K, DMSO-d6)

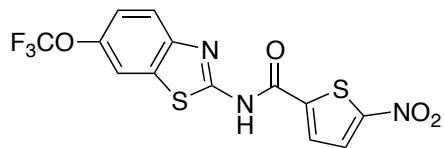
GPS426



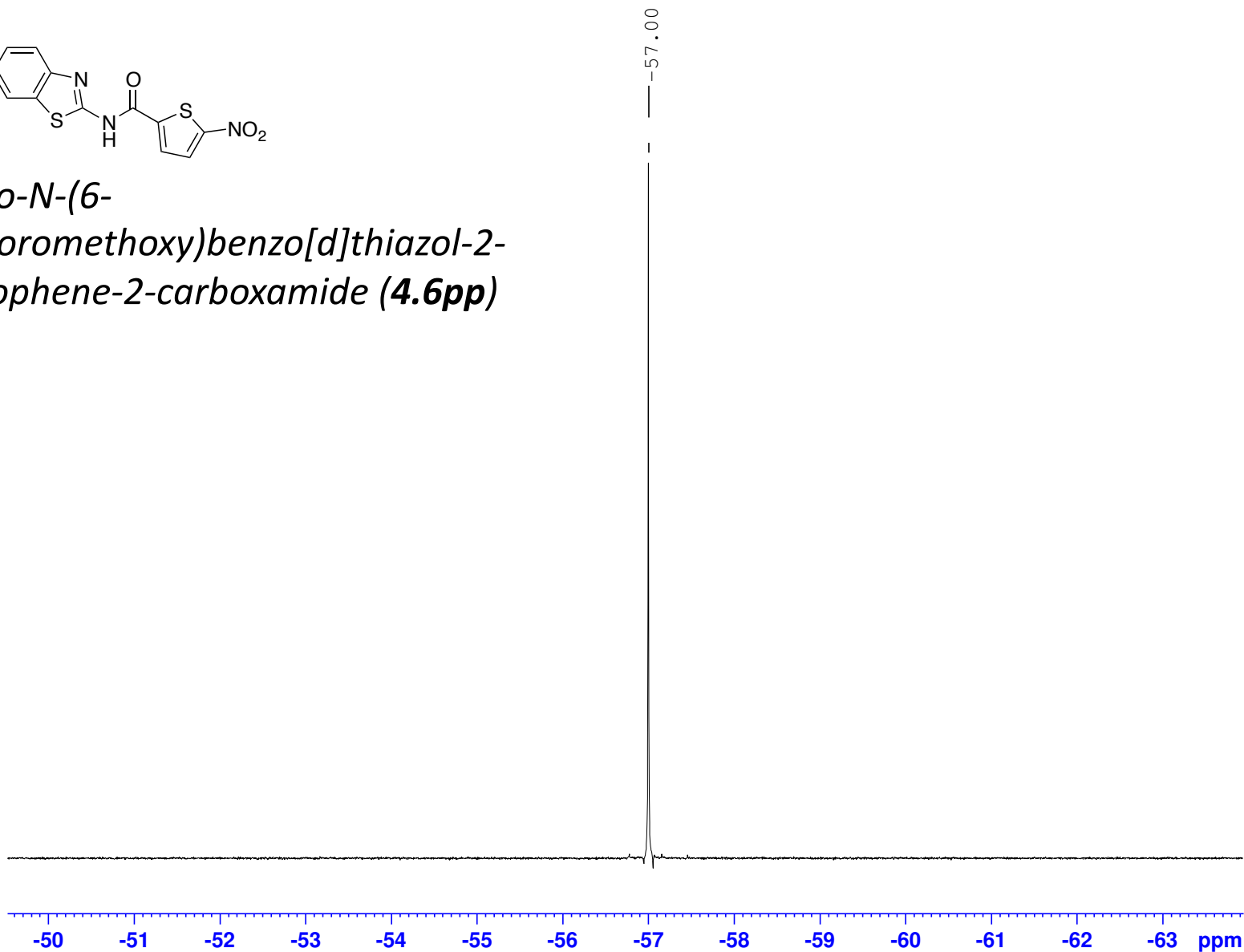
MZP573-B74-19F-NMR-14-03-2016

(400 MHz, 297.2 K, DMSO-d6)

GPS426

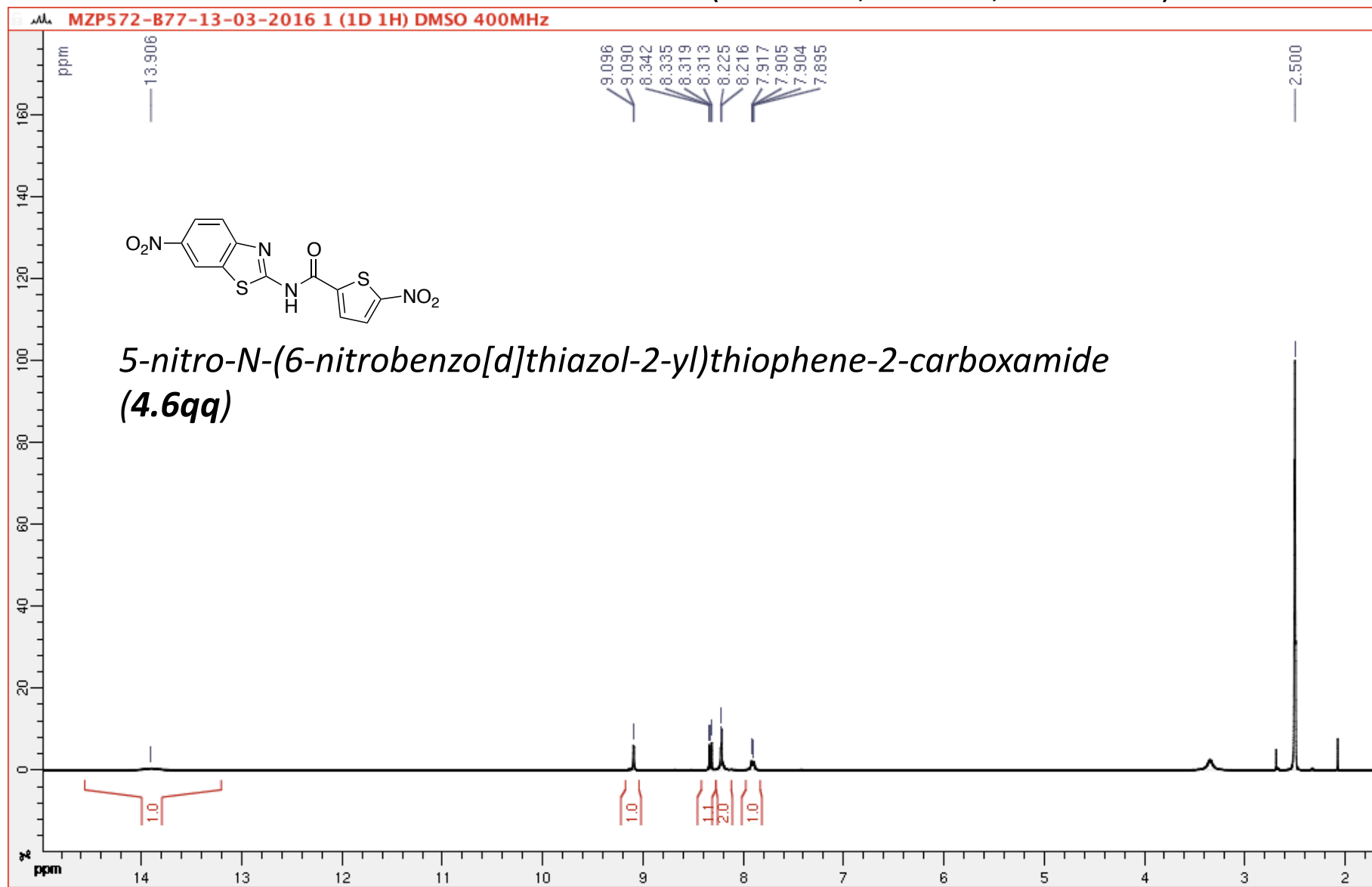


*5-nitro-N-(6-(trifluoromethoxy)benzo[d]thiazol-2-yl)thiophene-2-carboxamide (4.6pp)*



(400 MHz, 297.2 K, DMSO-d6)

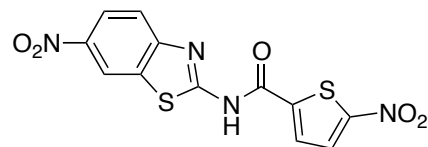
GPS428



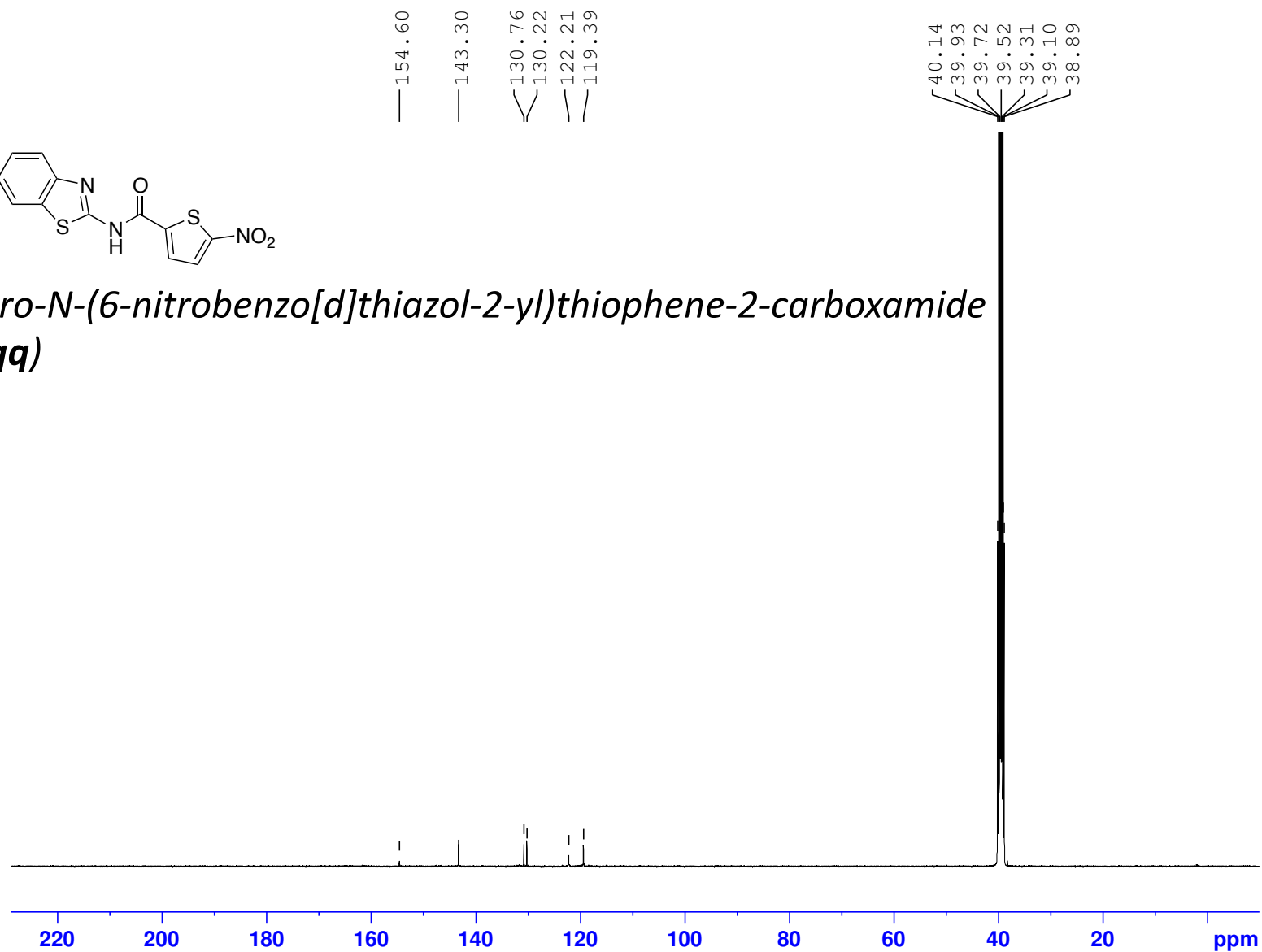
GPS428-5mg-13C-NMR-Dec-22-2017

(100 MHz, 297.2 K, DMSO-d6)

GPS428



*5-nitro-N-(6-nitrobenzo[d]thiazol-2-yl)thiophene-2-carboxamide*  
**(4.6qq)**

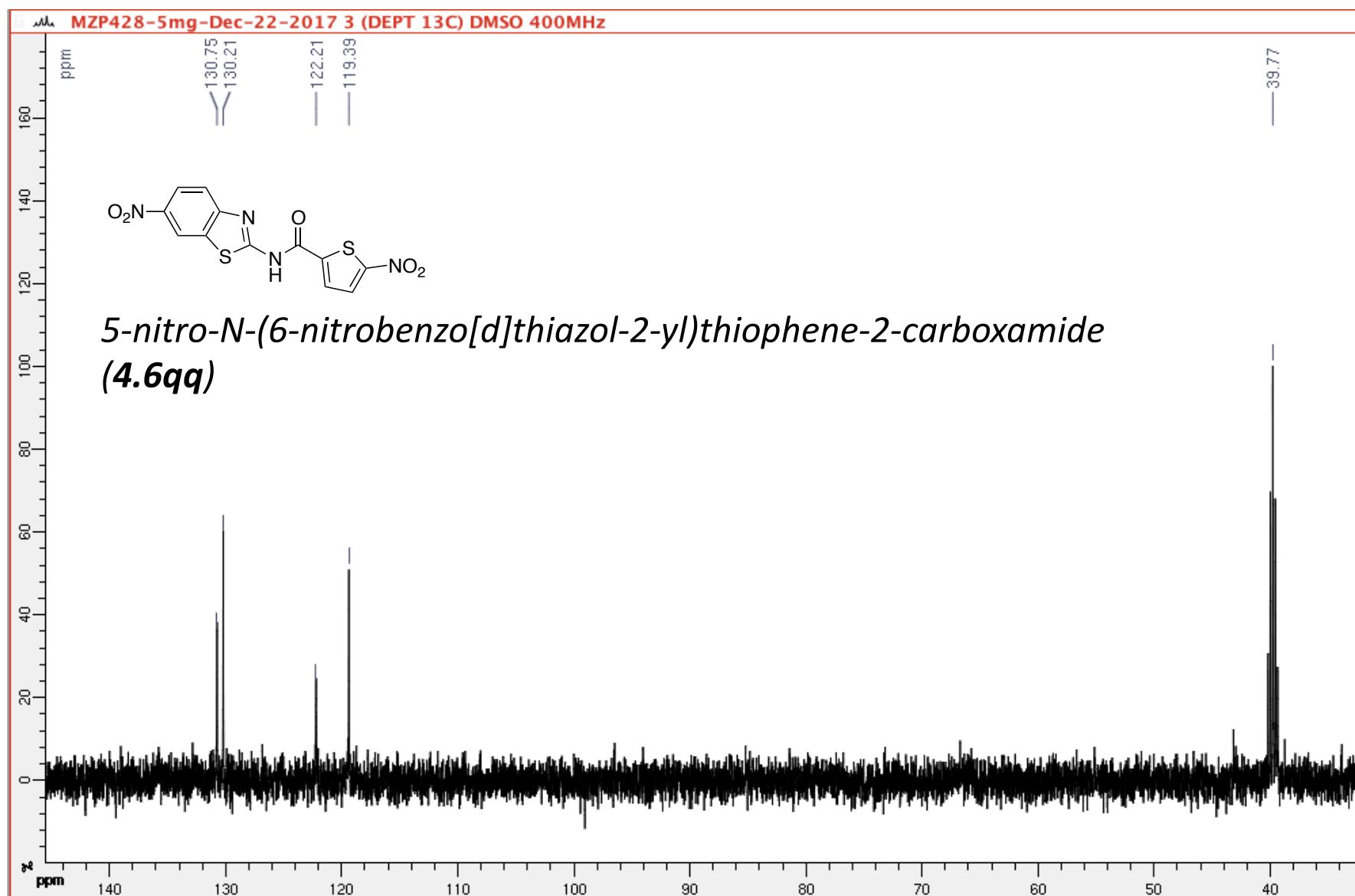




DEPT90

(100 MHz, 297.2 K, DMSO-d6)

GPS428



MZP573-B76-1H-NMR-14-03-2016

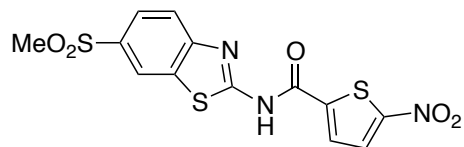
(400 MHz, 297.2 K, DMSO-d6)

GPS427

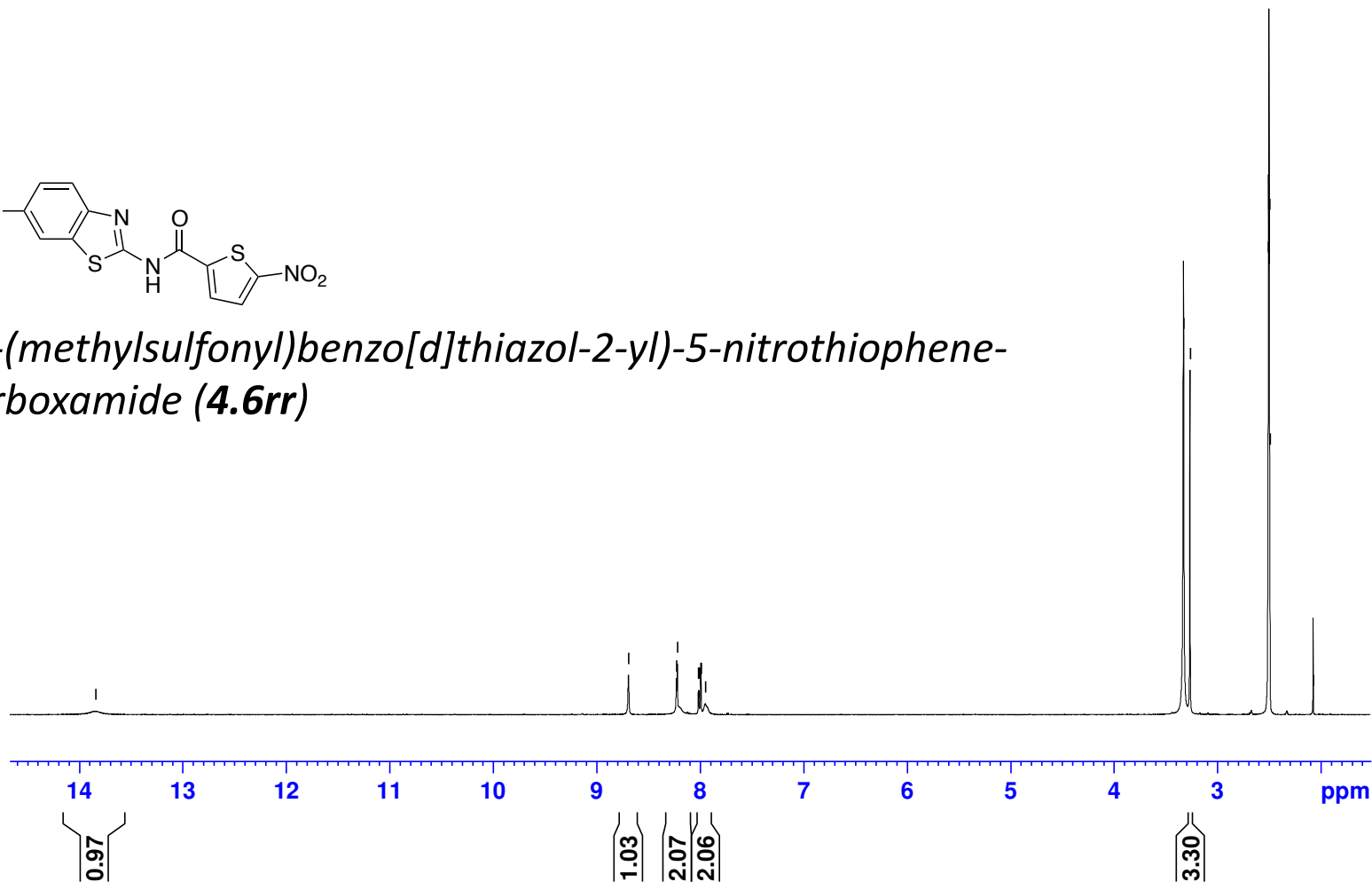
— 13.84

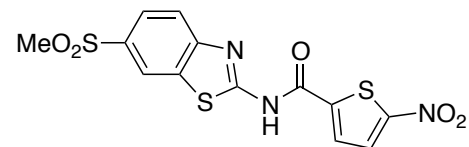
8.69  
8.23  
8.22  
8.02  
8.01  
7.99  
7.99  
7.95

3.33  
3.26  
2.51  
2.50  
2.50  
2.50  
2.49  
2.07

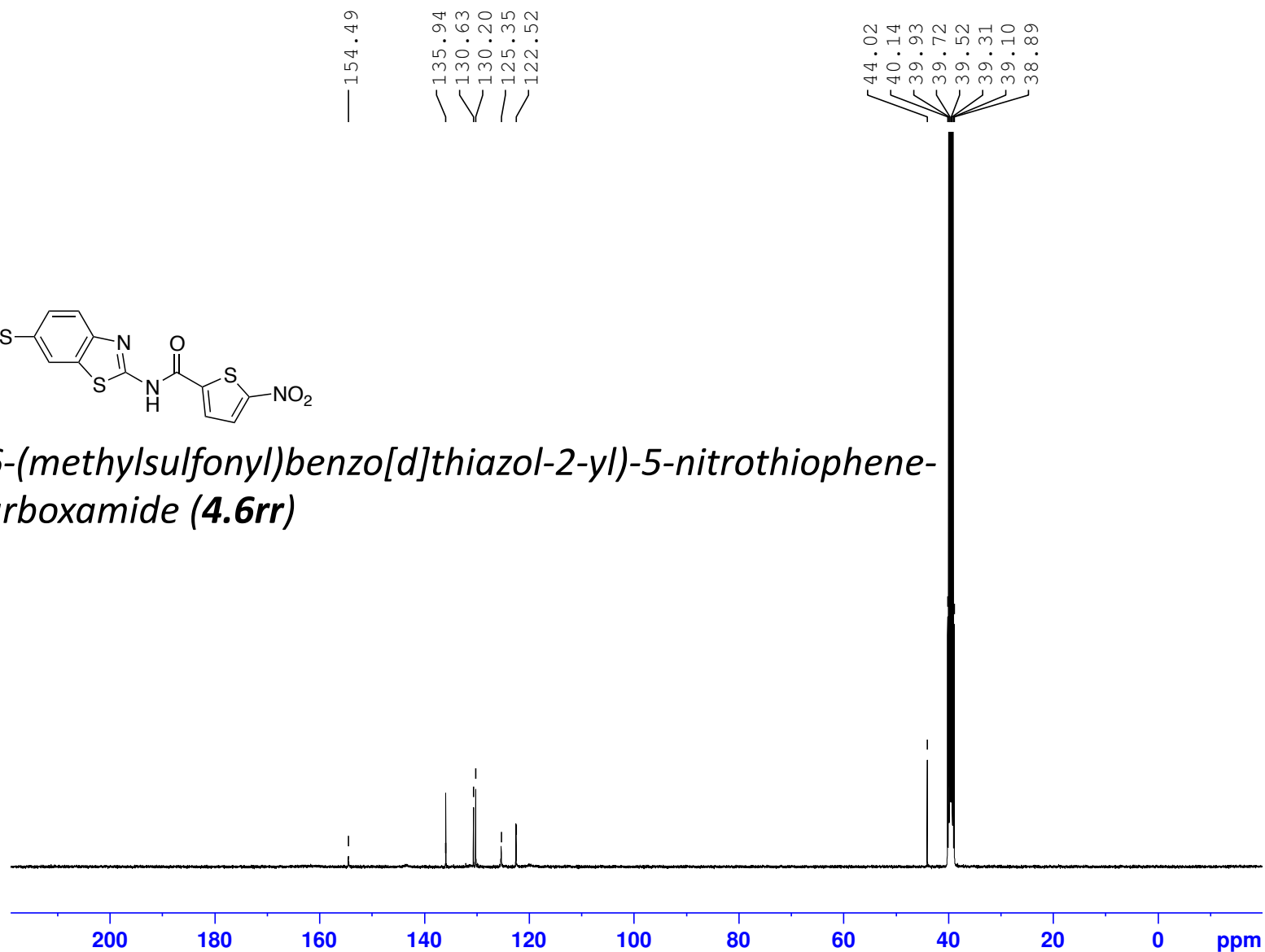


*N*-(6-(methylsulfonyl)benzo[d]thiazol-2-yl)-5-nitrothiophene-2-carboxamide (**4.6rr**)





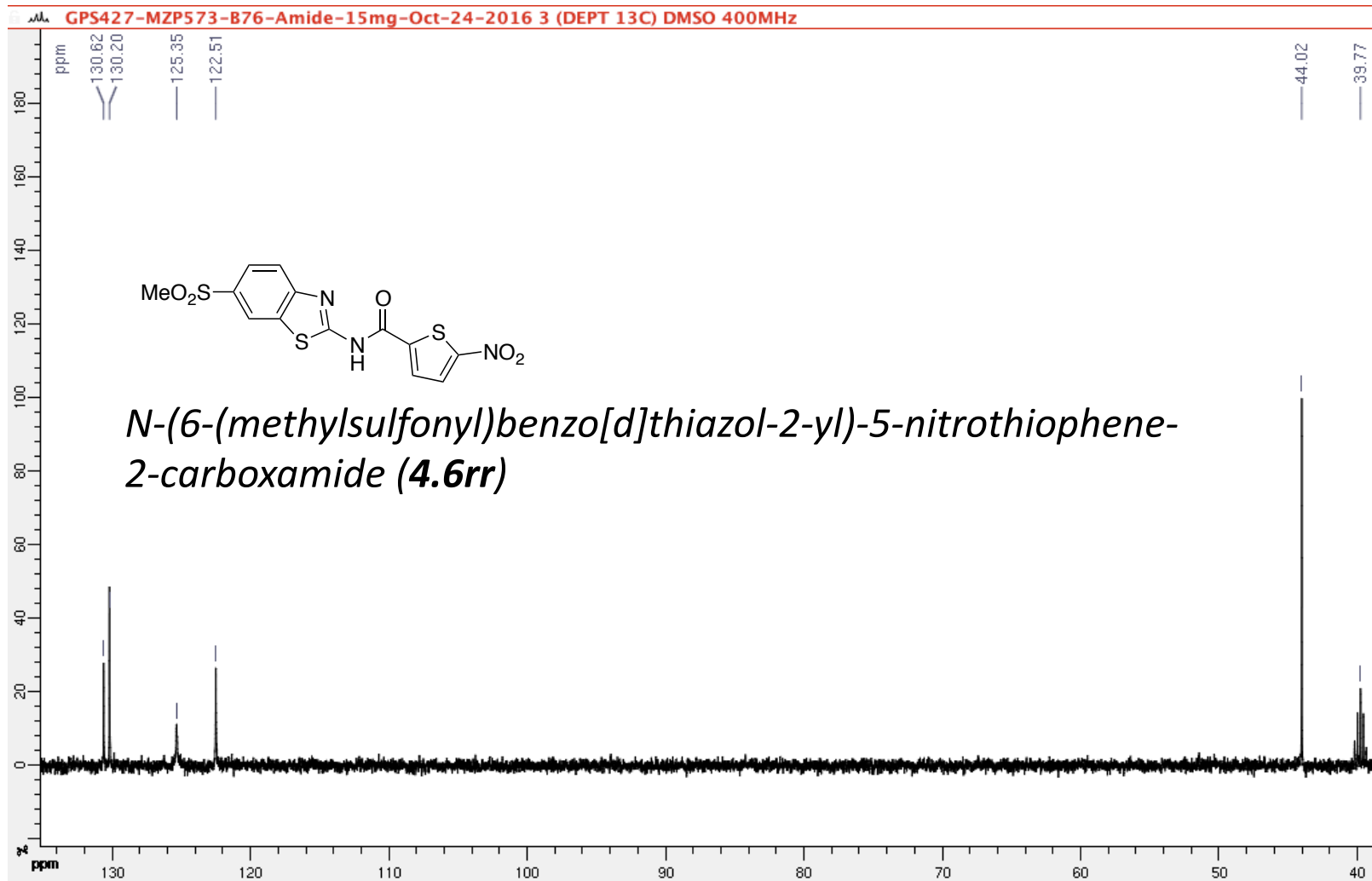
*N*-(6-(methylsulfonyl)benzo[d]thiazol-2-yl)-5-nitrothiophene-2-carboxamide (**4.6rr**)



DEPT 135

(100 MHz, 297.2 K, DMSO-d6)

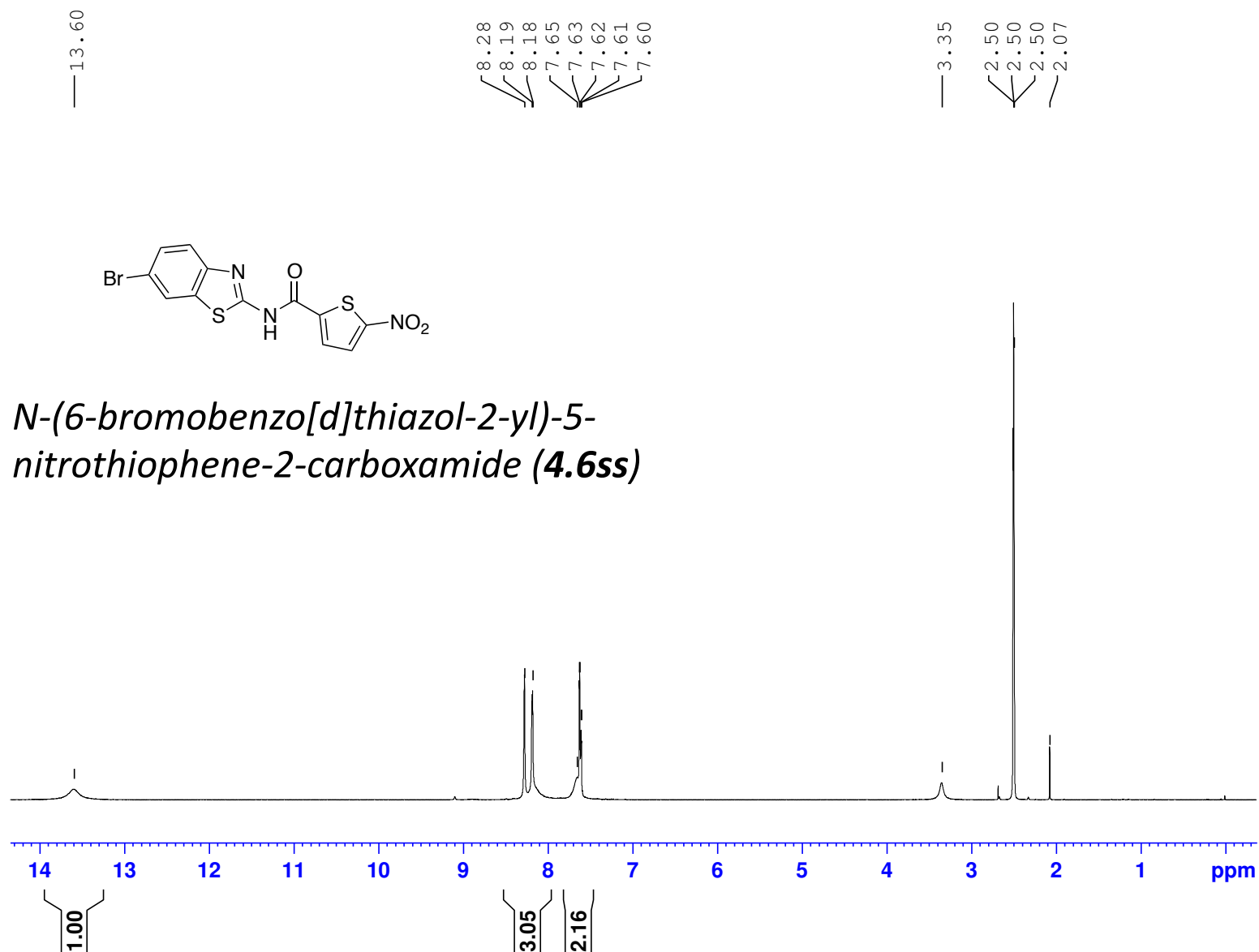
GPS427



MZP594-B92-Amide-10mg-1H NMR-Sep-23-2016

(400 MHz, 297.2 K, DMSO-d6)

GPS473

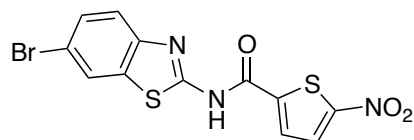


MZP594-B92-Amide-10mg-13C NMR-Sep-23-2016

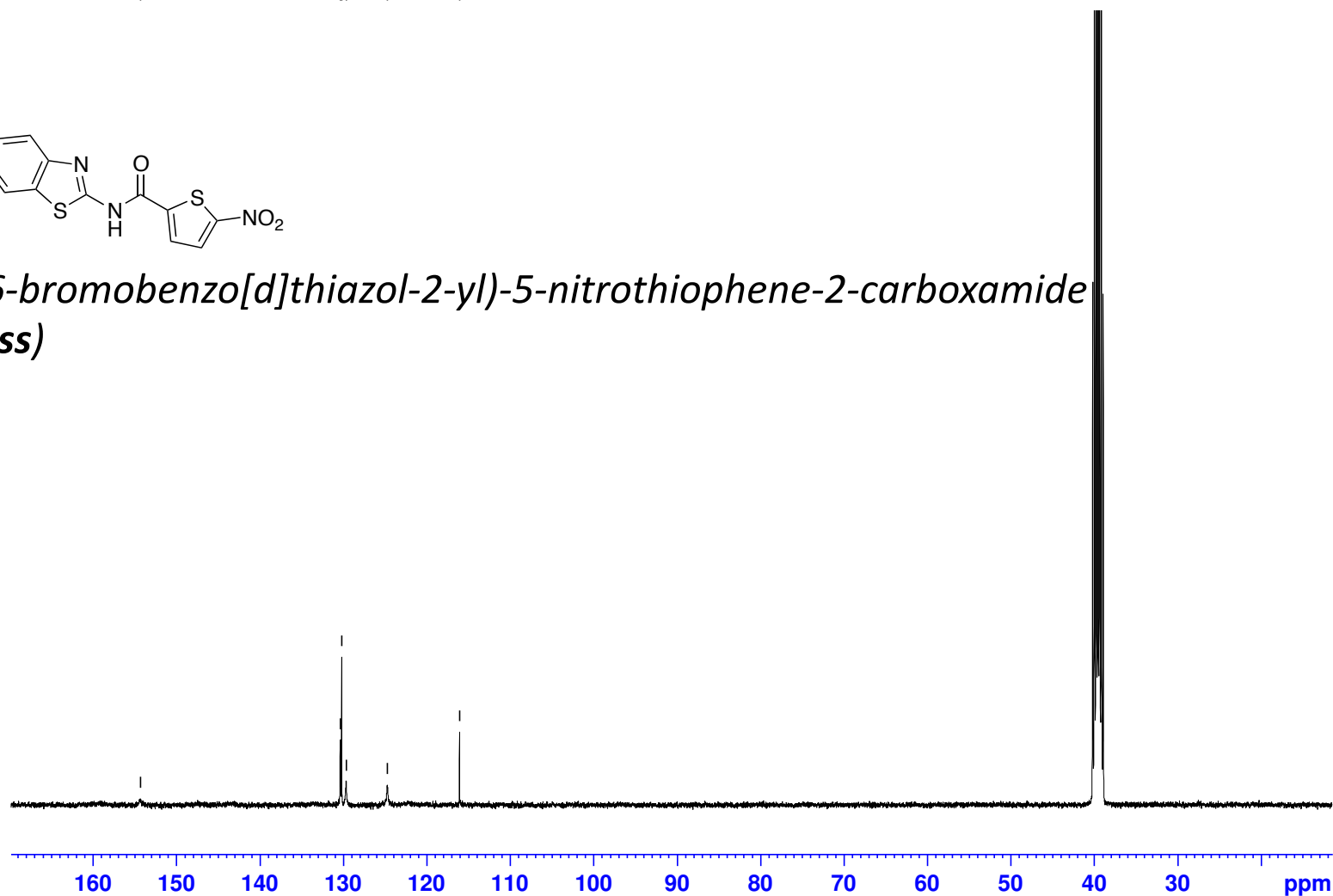
(100 MHz, 297.2 K, DMSO-d6)

GPS473

—154.32  
130.35  
130.19  
129.67  
124.72  
—116.06



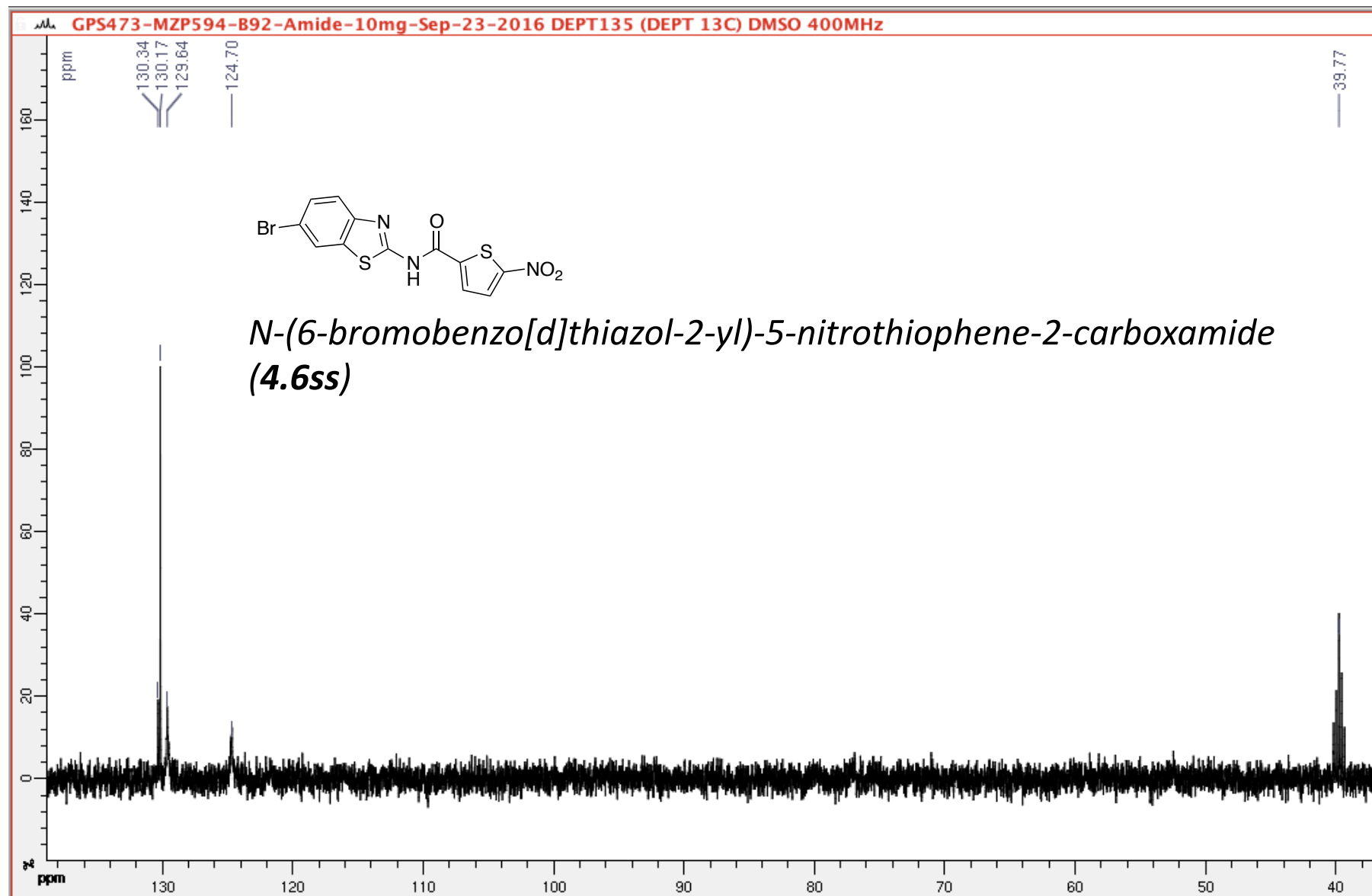
*N*-(6-bromobenzo[d]thiazol-2-yl)-5-nitrothiophene-2-carboxamide  
(4.6ss)

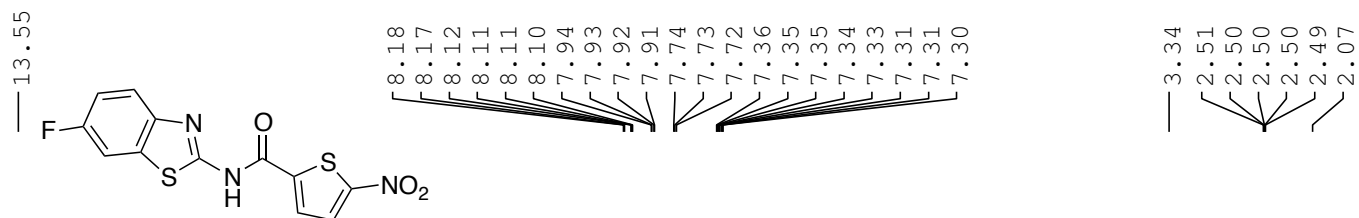


DEPT 135

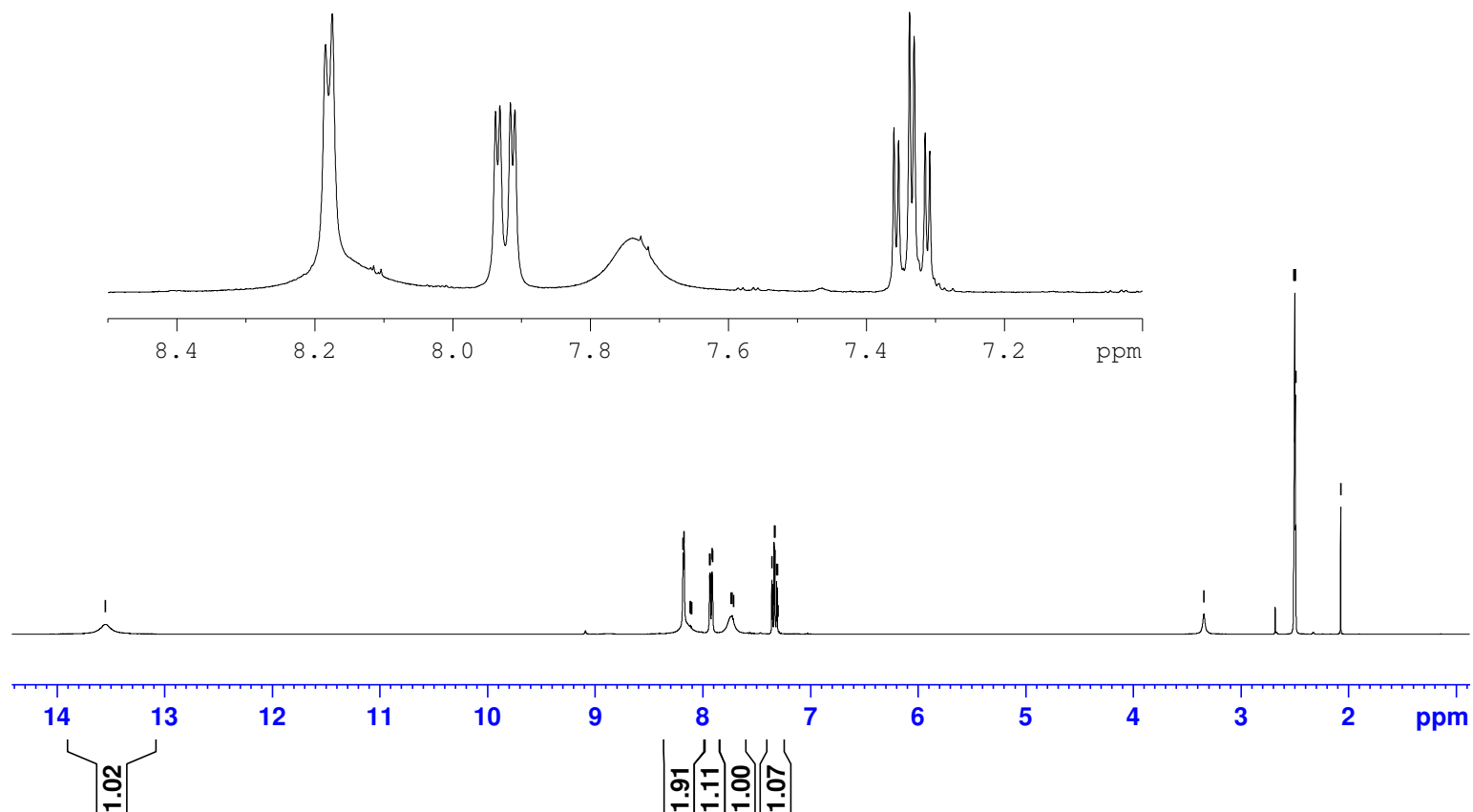
(100 MHz, 297.2 K, DMSO-d6)

GPS473





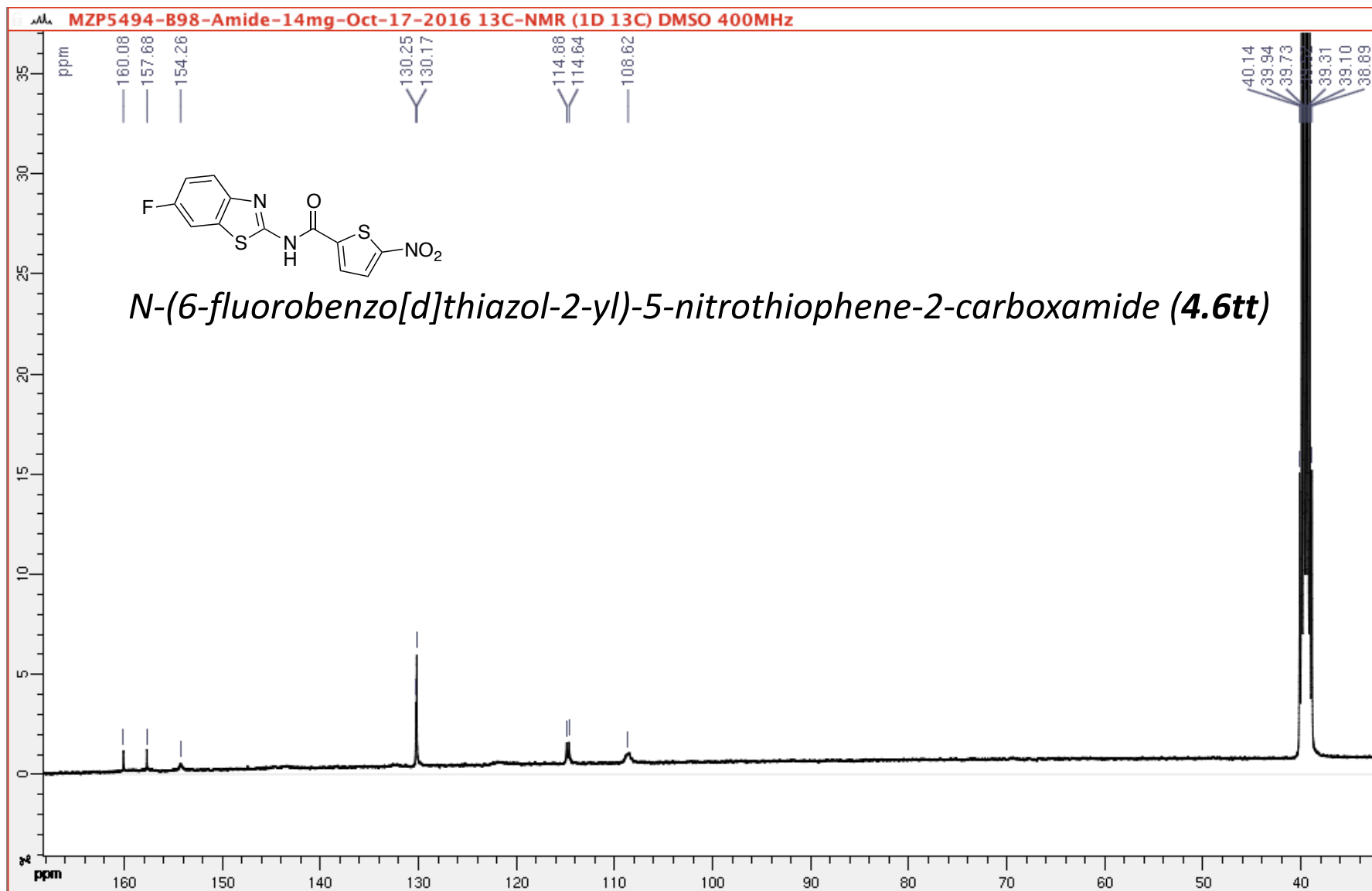
*N*-(6-fluorobenzo[d]thiazol-2-yl)-5-nitrothiophene-2-carboxamide (**4.6tt**)





(100 MHz, 297.2 K, DMSO-d6)

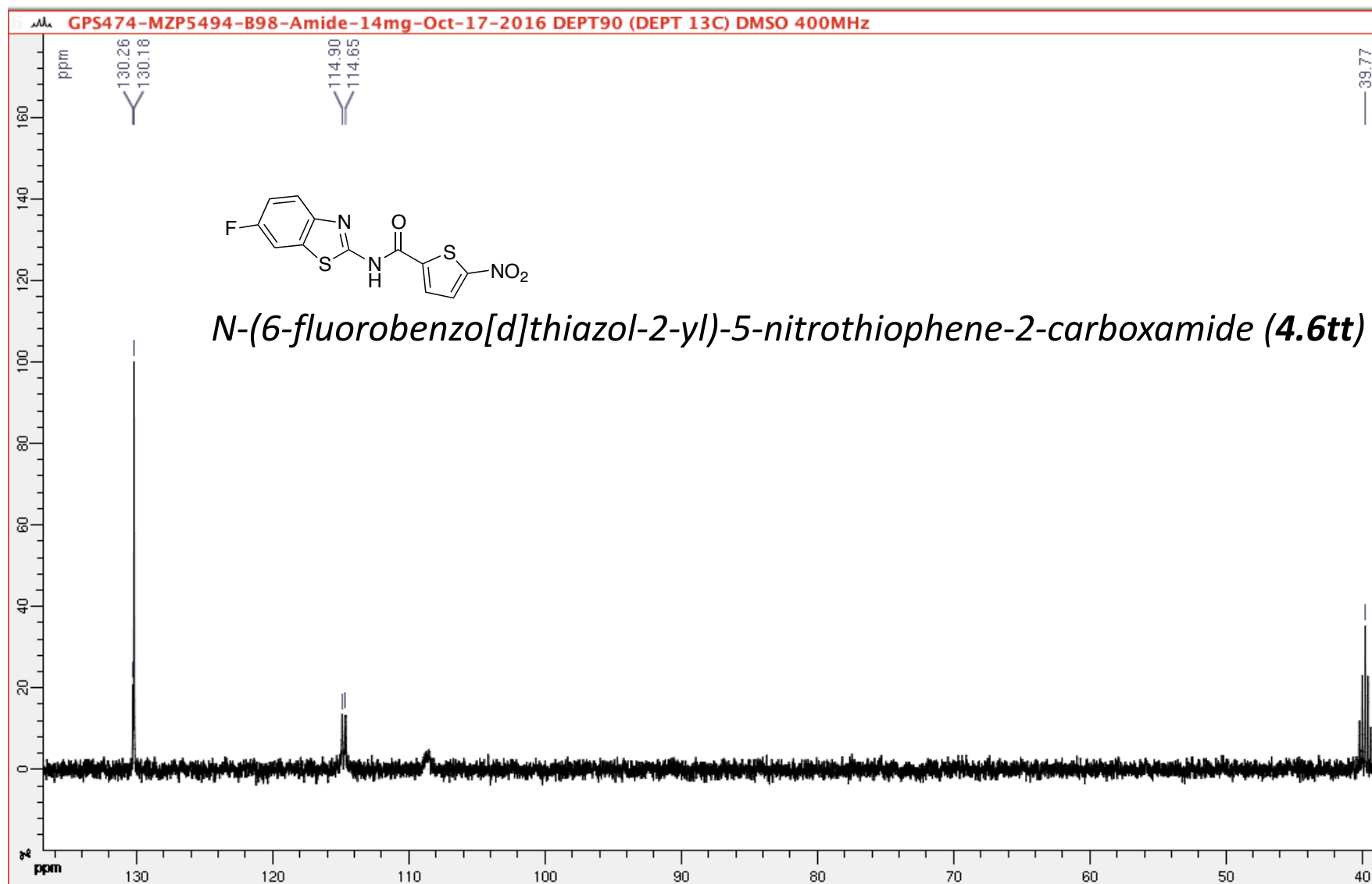
GPS474



DEPT 90

(100 MHz, 297.2 K, DMSO-d6)

GPS474

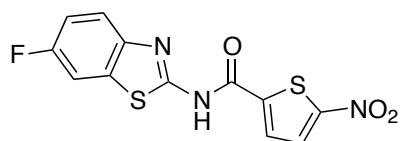


GPS474-MZP594-B98-Amide-14mg-19F-NMR-Oct-17-2016

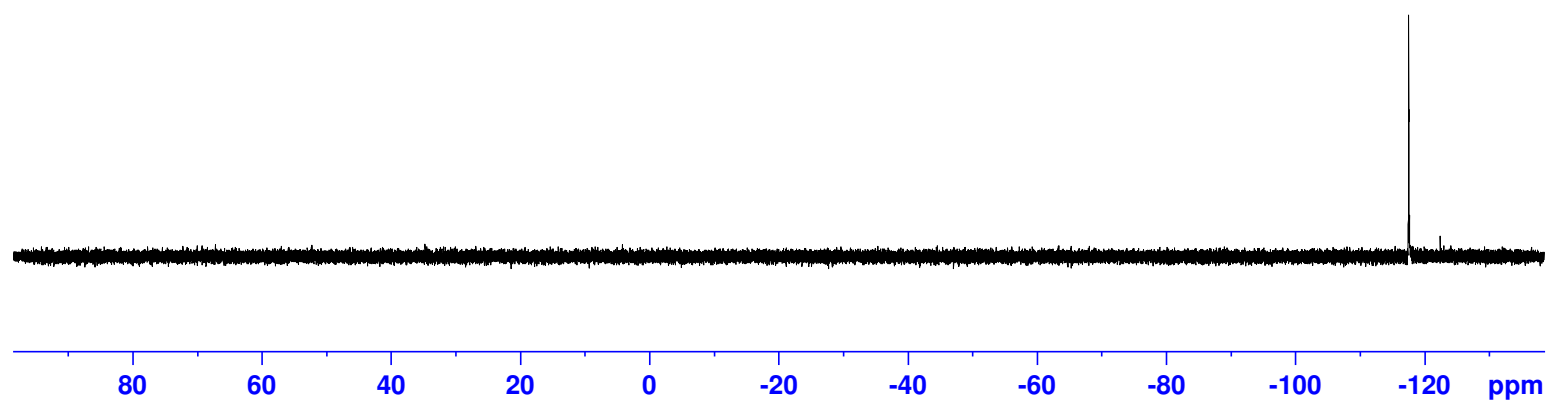
(400 MHz, 297.2 K, DMSO-d<sub>6</sub>)

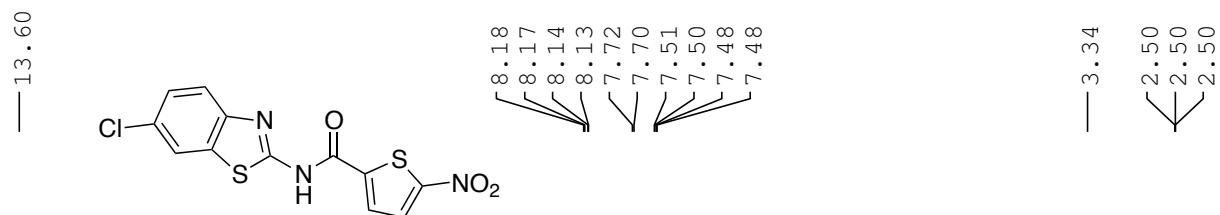
GPS474

— -117.57

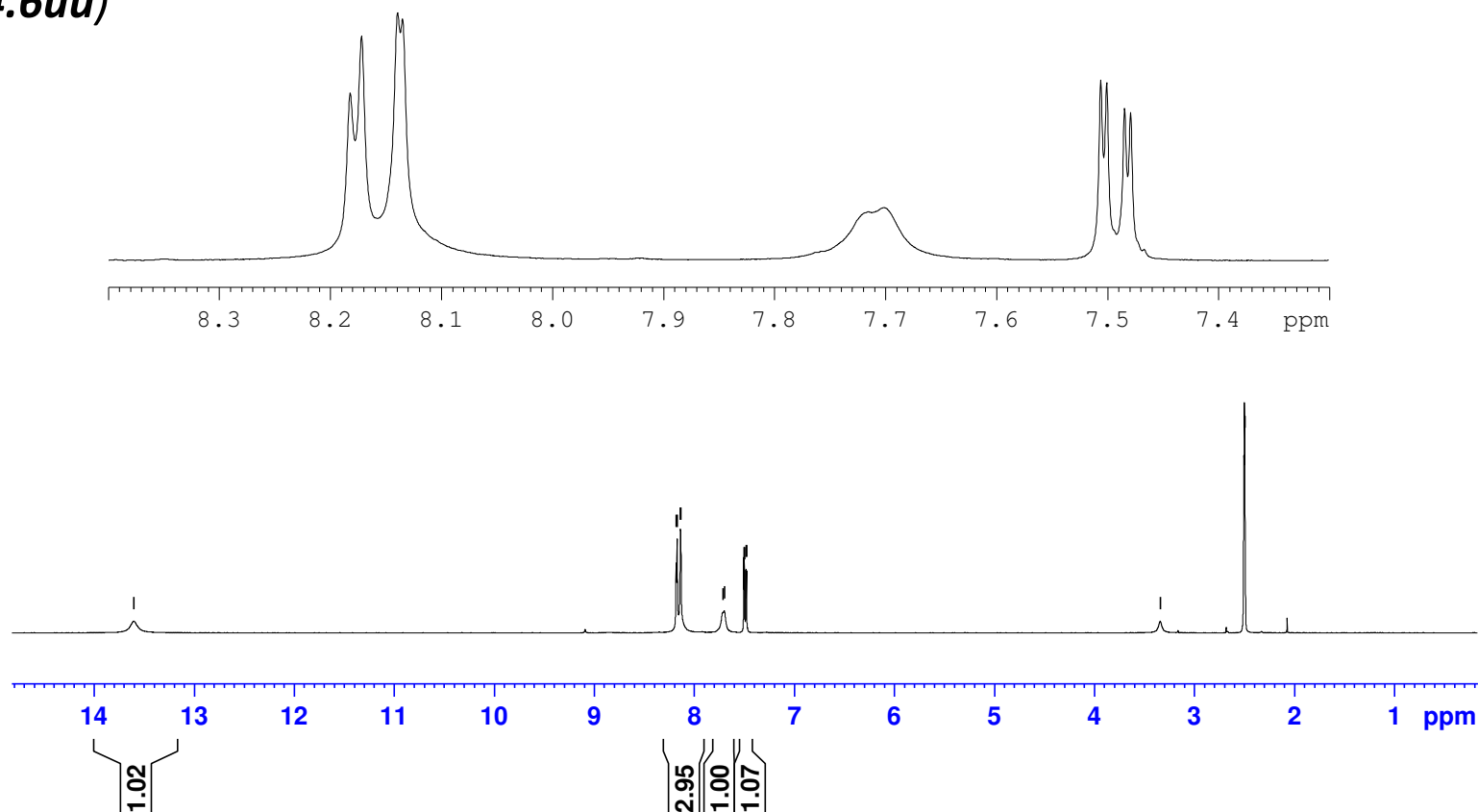


*N*-(6-fluorobenzo[d]thiazol-2-yl)-5-nitrothiophene-2-carboxamide (**4.6tt**)





*N*-(6-chlorobenzo[d]thiazol-2-yl)-5-nitrothiophene-2-carboxamide  
(4.6uu)



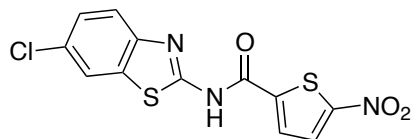
MZP594-B94-Amide-10mg-13C-NMR-8h-26-09-2016

(100 MHz, 297.2 K, DMSO-d6)

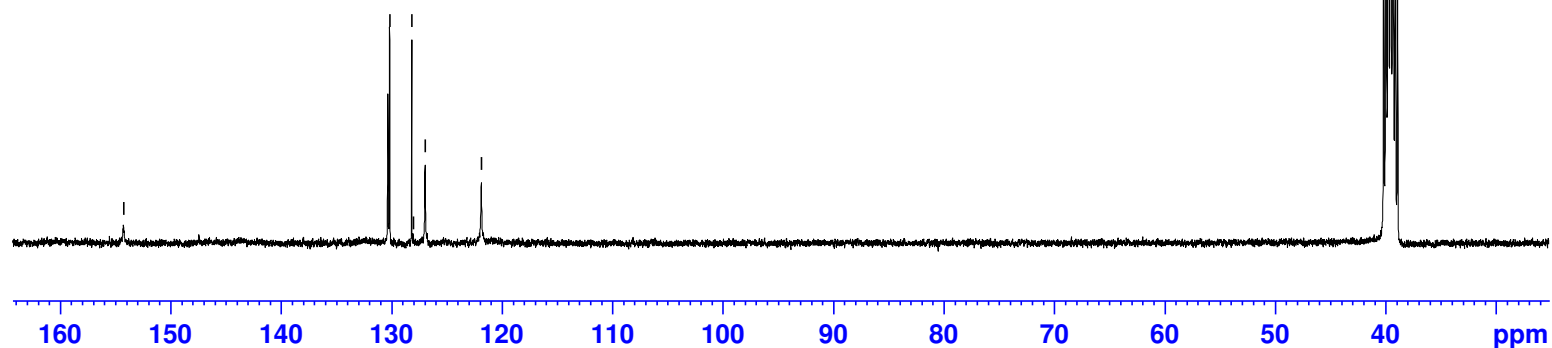
GPS475

154.28  
130.33  
130.17  
128.17  
128.04  
126.96  
121.87

39.52



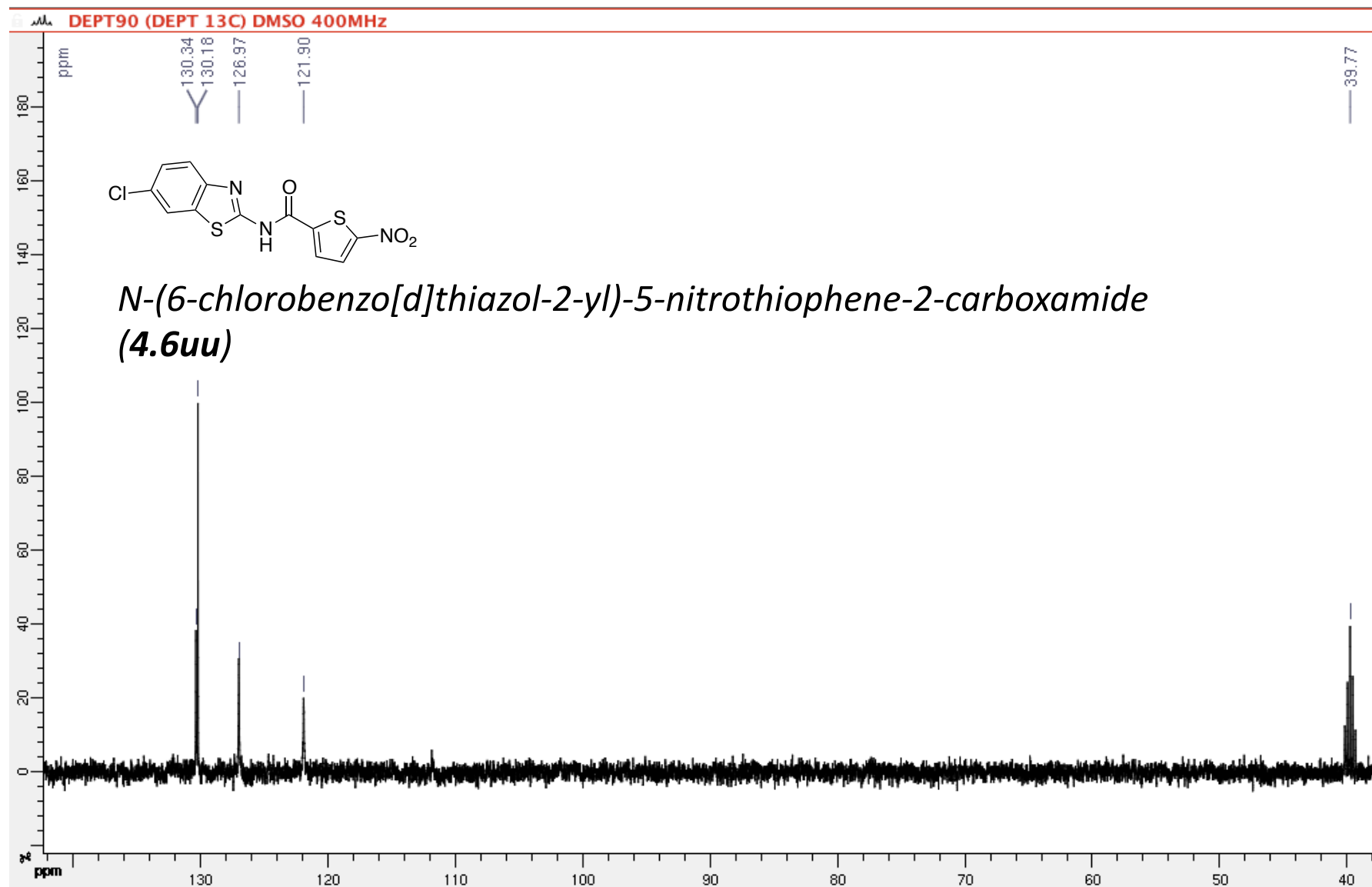
*N*-(6-chlorobenzo[d]thiazol-2-yl)-5-nitrothiophene-2-carboxamide  
**(4.6uu)**



DEPT90

(100 MHz, 297.2 K, DMSO-d6)

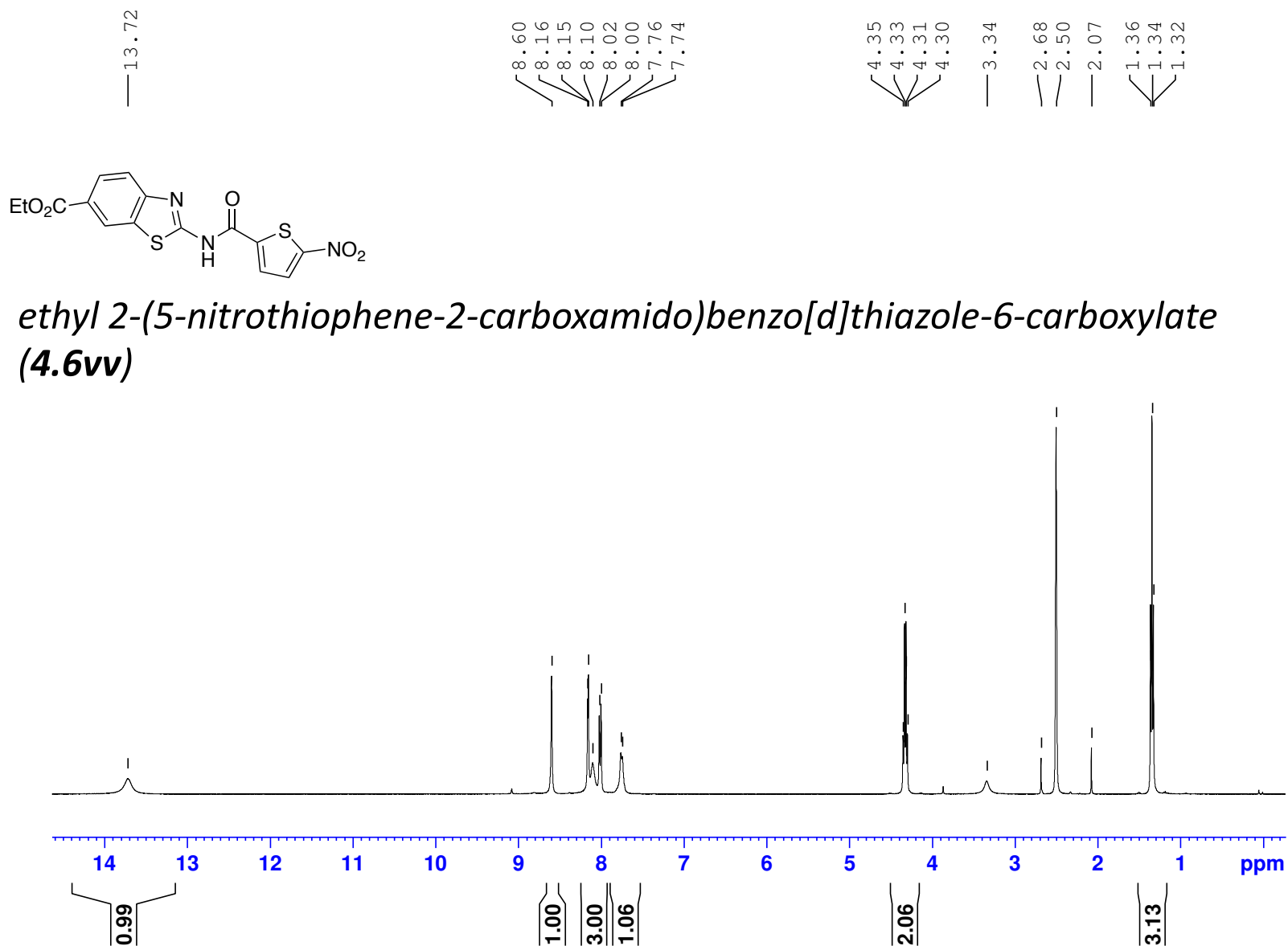
GPS475



MZP594-B93-Amide-10mg-1H-NMR-Sep-25-2016

(400 MHz, 297.2 K, DMSO-d6)

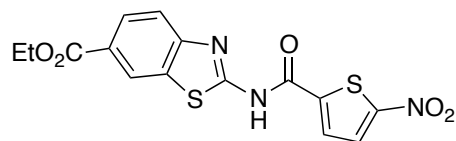
GPS477



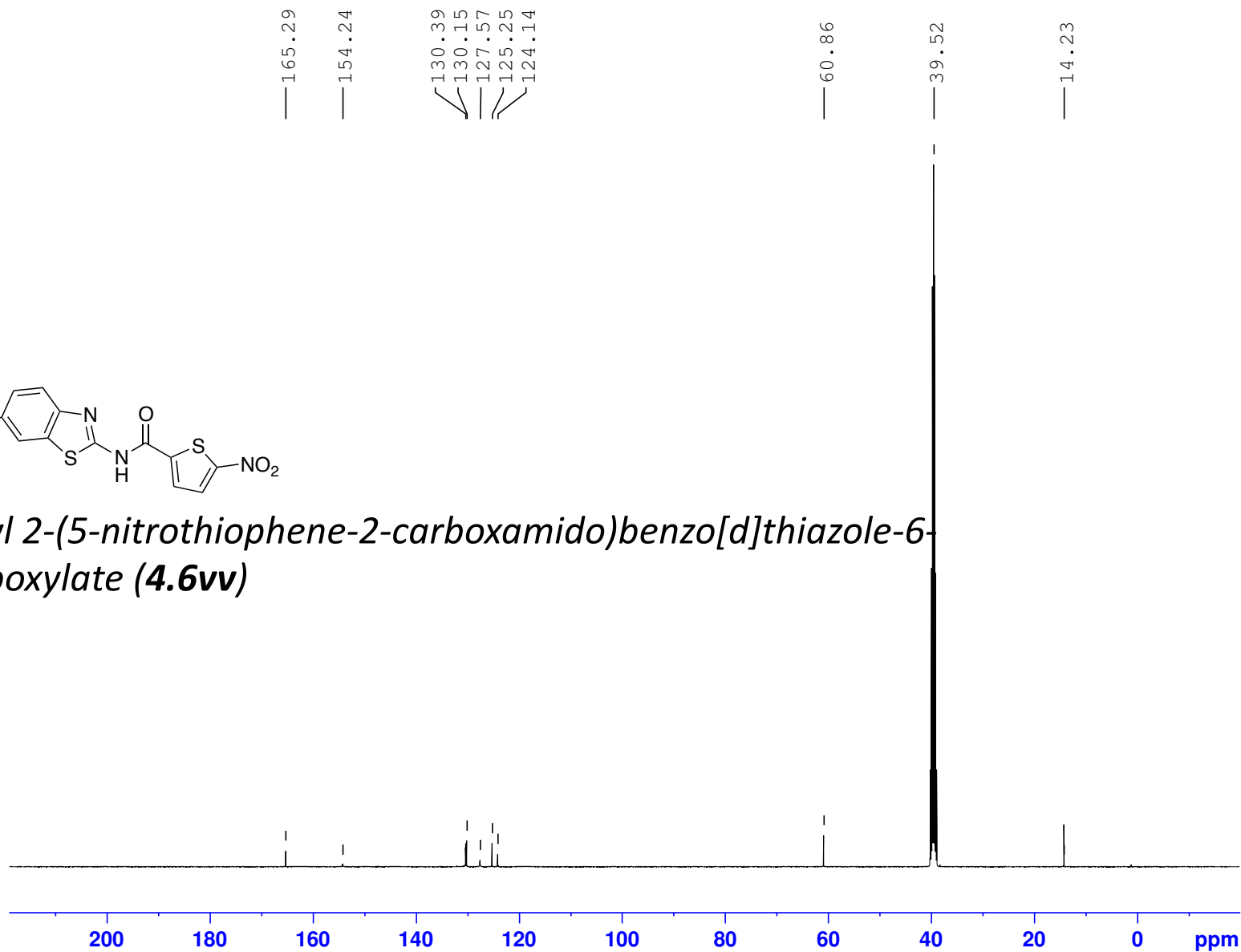
MZP594-B93-Amide-10mg-23h-13C-NMR-Oct-08-2016

(100 MHz, 297.2 K, DMSO-d6)

GPS477



*ethyl 2-(5-nitrothiophene-2-carboxamido)benzo[d]thiazole-6-carboxylate (4.6vv)*

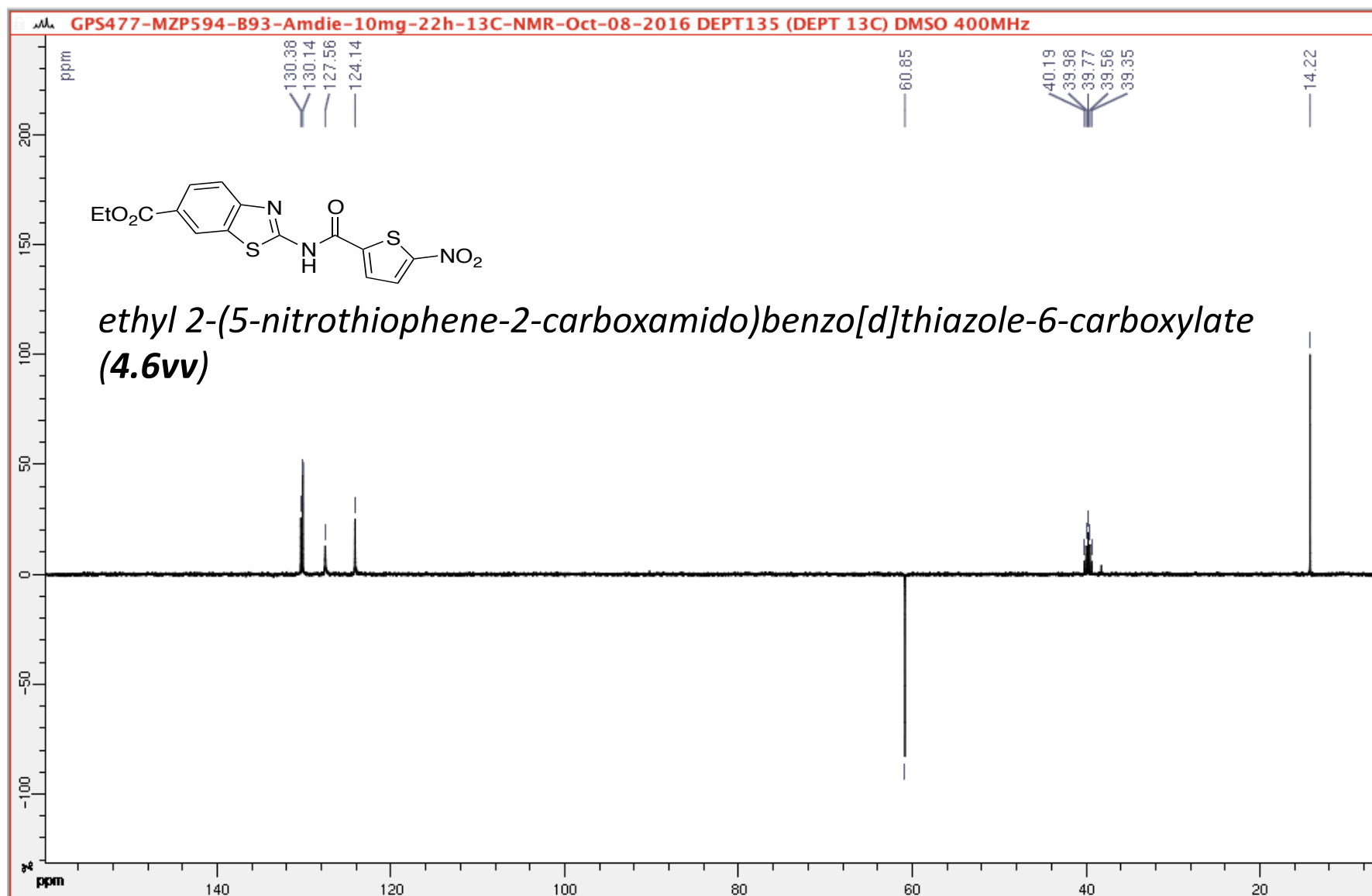




DEPT 135

(100 MHz, 297.2 K, DMSO-d6)

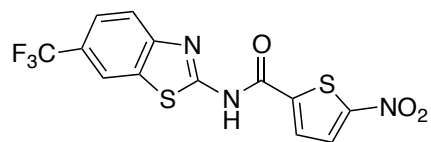
GPS477



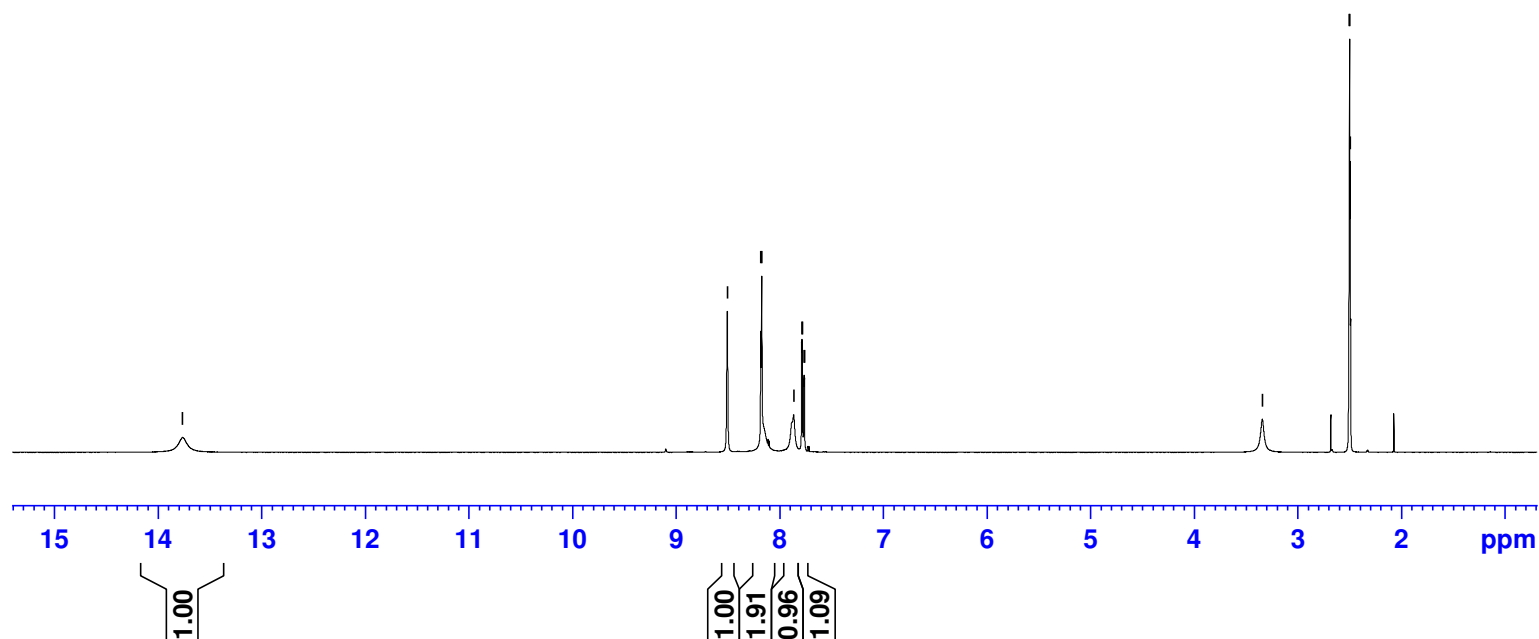
— 13.77

8.51  
8.18  
8.17  
7.87  
7.79  
7.79  
7.77  
7.76

— 3.34

2.50  
2.50  
2.50

*5-nitro-N-(6-(trifluoromethyl)benzo[d]thiazol-2-yl)thiophene-2-carboxamide (4.6ww)*

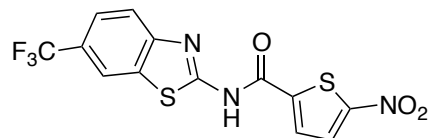


MZP594-B95-Amide-10mg-13C-NMR-8h-28-09-2016

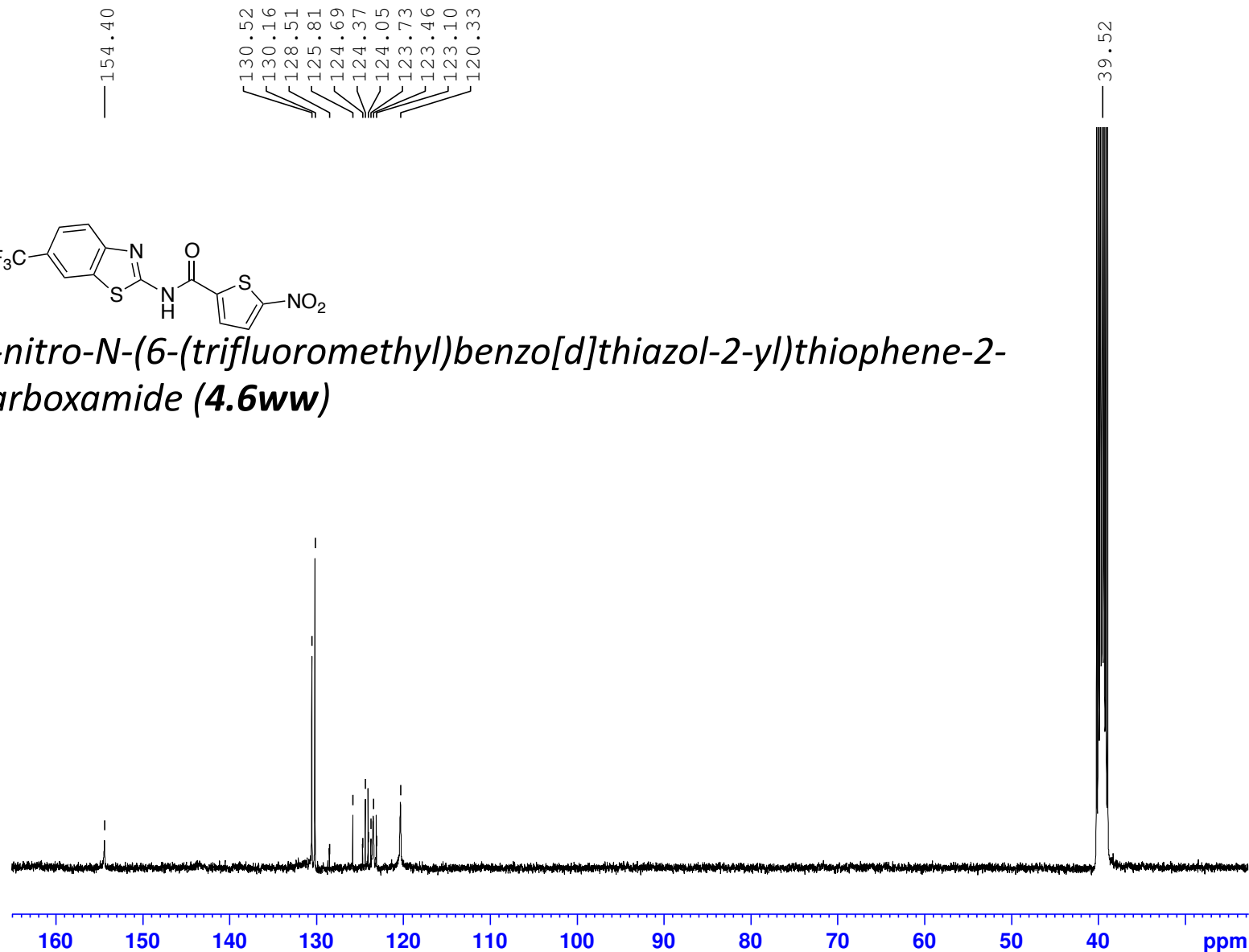
(100 MHz, 297.2 K, DMSO-d6)

GPS484

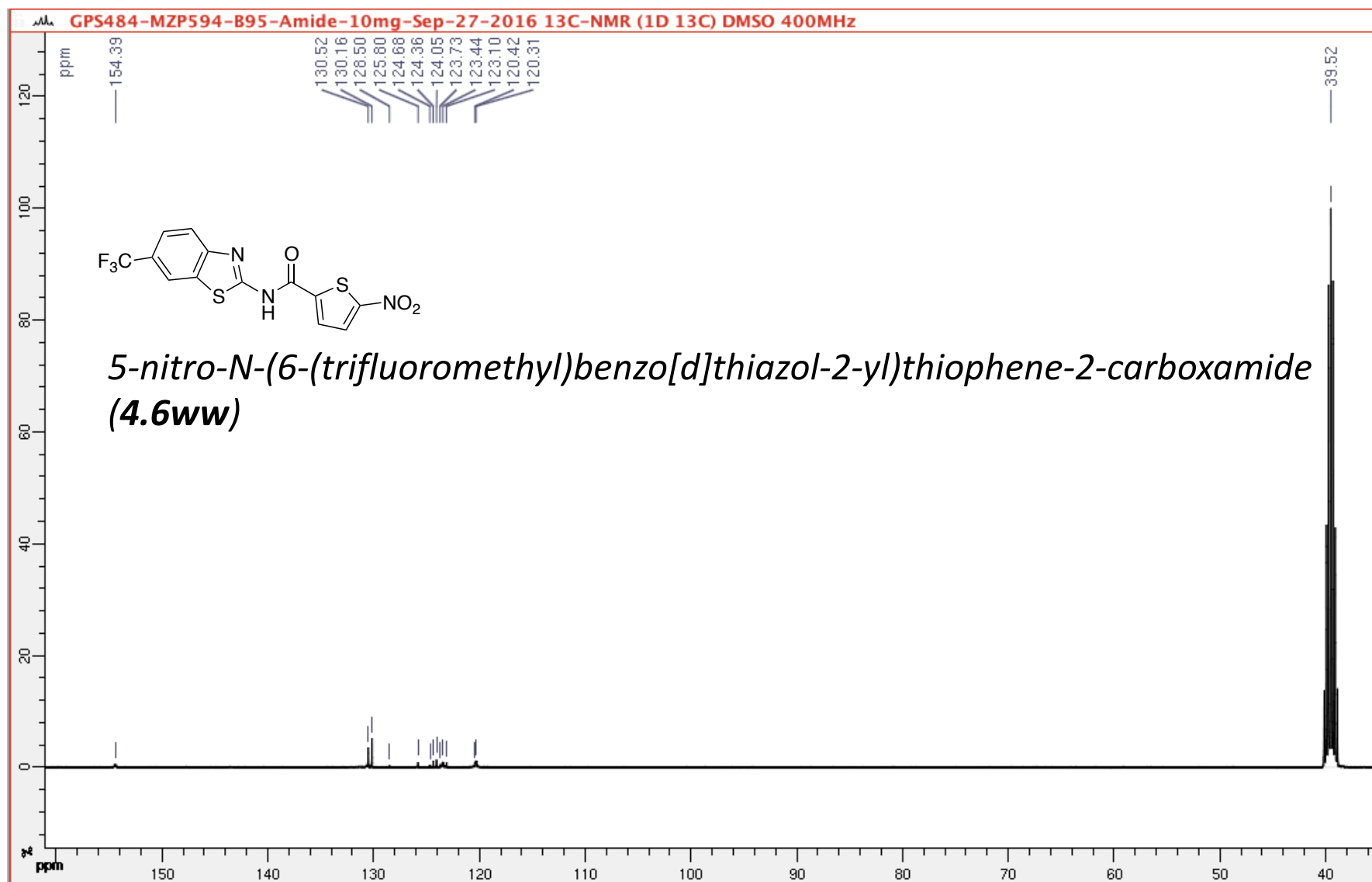
154.40  
130.52  
130.16  
128.51  
125.81  
124.69  
124.37  
124.05  
123.73  
123.46  
123.10  
120.33

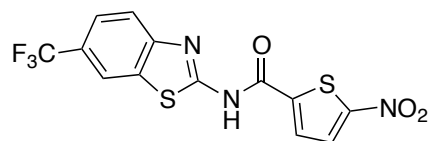


*5-nitro-N-(6-(trifluoromethyl)benzo[d]thiazol-2-yl)thiophene-2-carboxamide (4.6ww)*



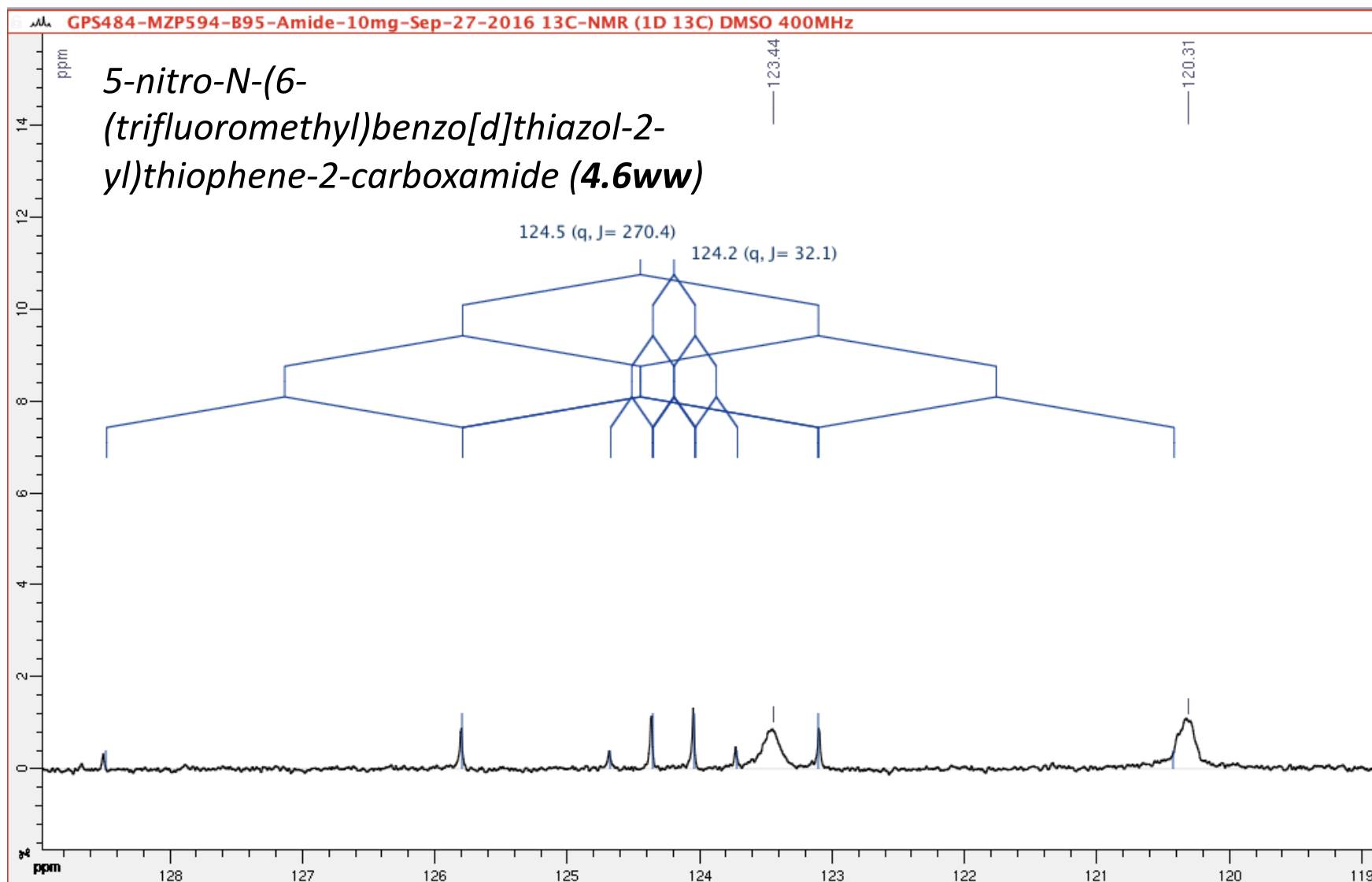
(100 MHz, 297.2 K, DMSO-d6) GPS484





(100 MHz, 297.2 K, DMSO-d6)

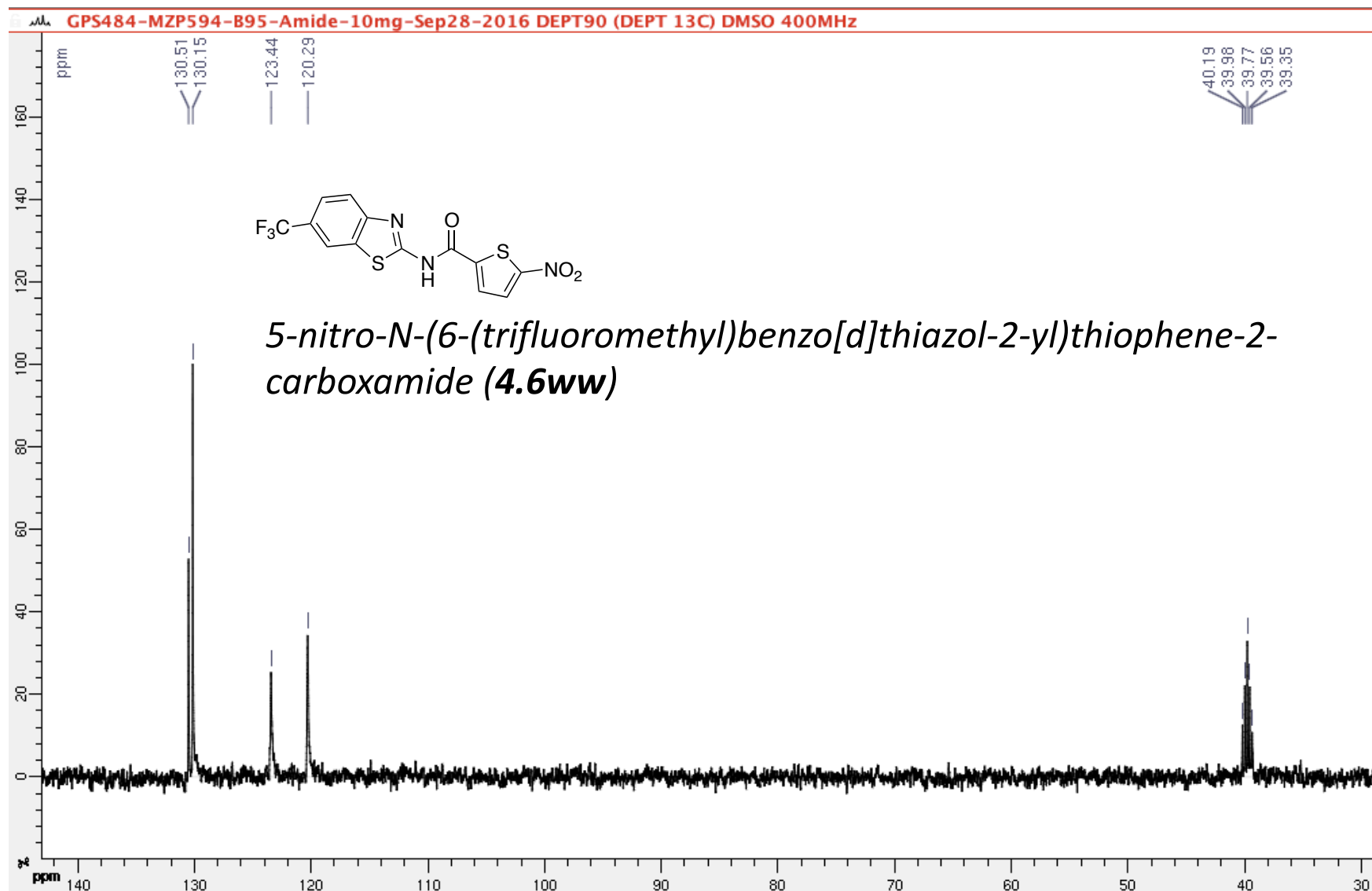
GPS484

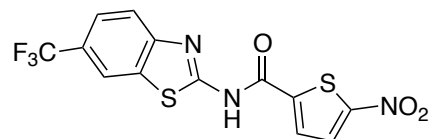


DEPT 90

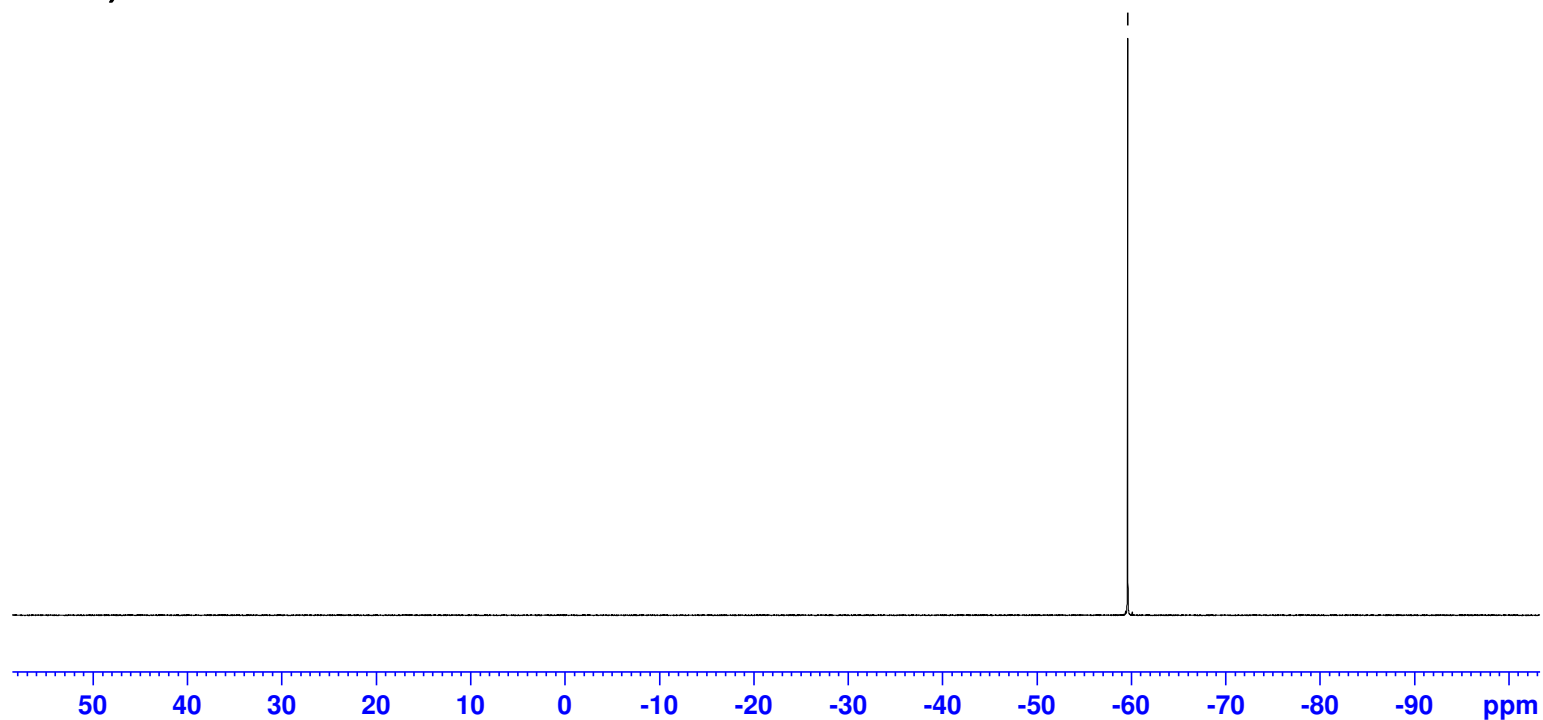
(100 MHz, 297.2 K, DMSO-d6)

GPS484





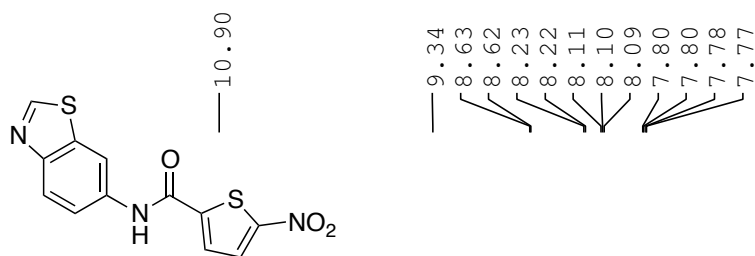
*5-nitro-N-(6-(trifluoromethyl)benzo[d]thiazol-2-yl)thiophene-2-carboxamide*  
**(4.6ww)**



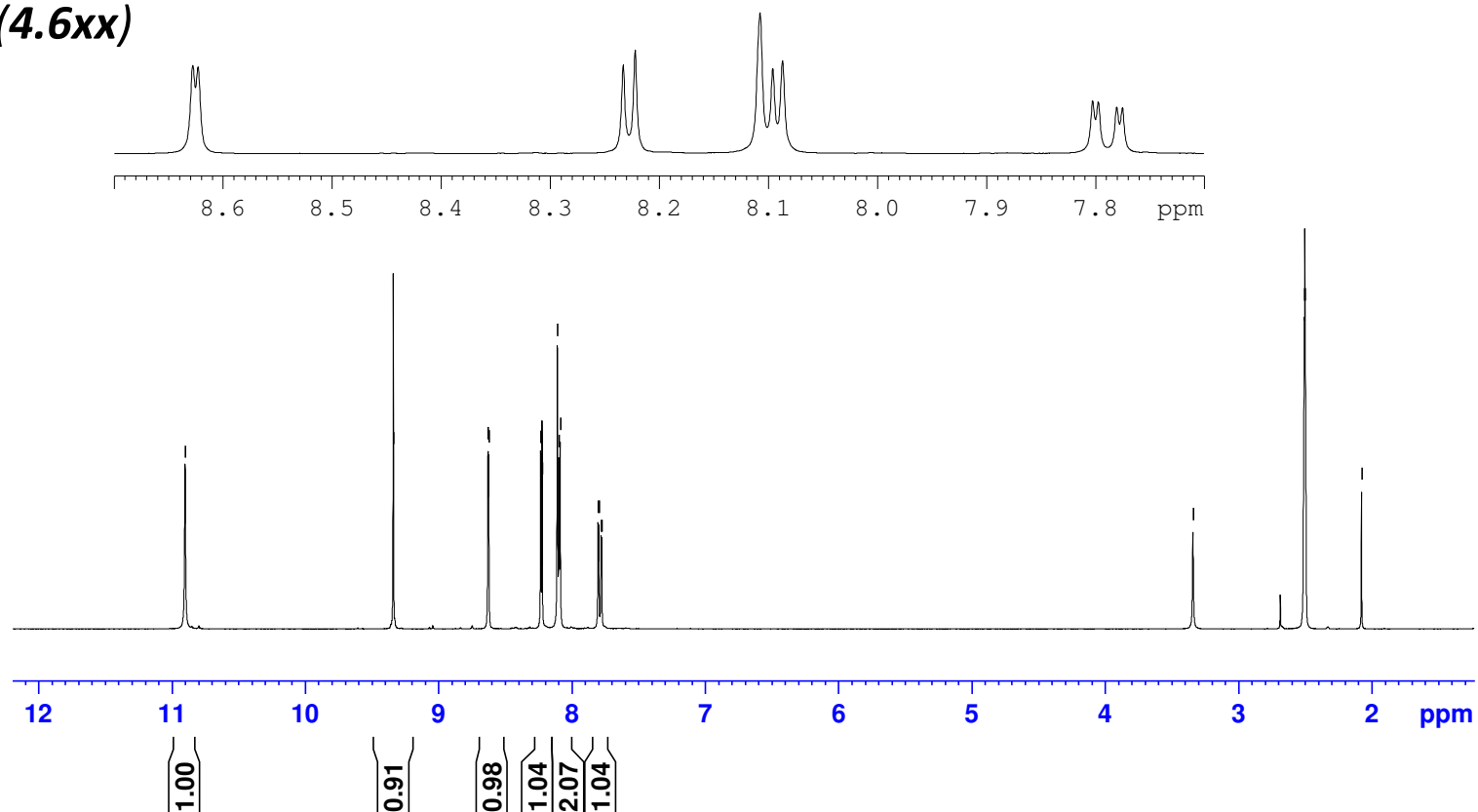
GPS480-MZP604-B103-11mg-1H-NMR-May-17-2017

(400 MHz, 297.2 K, DMSO-d6)

GPS480



*N*-(benzo[d]thiazol-6-yl)-5-nitrothiophene-2-carboxamide  
(4.6xx)



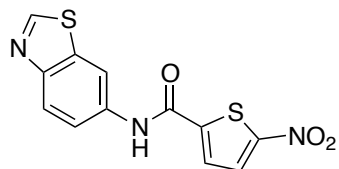


GPS480-MZP604-B103-11mg-13C-NMR-May-17-2017

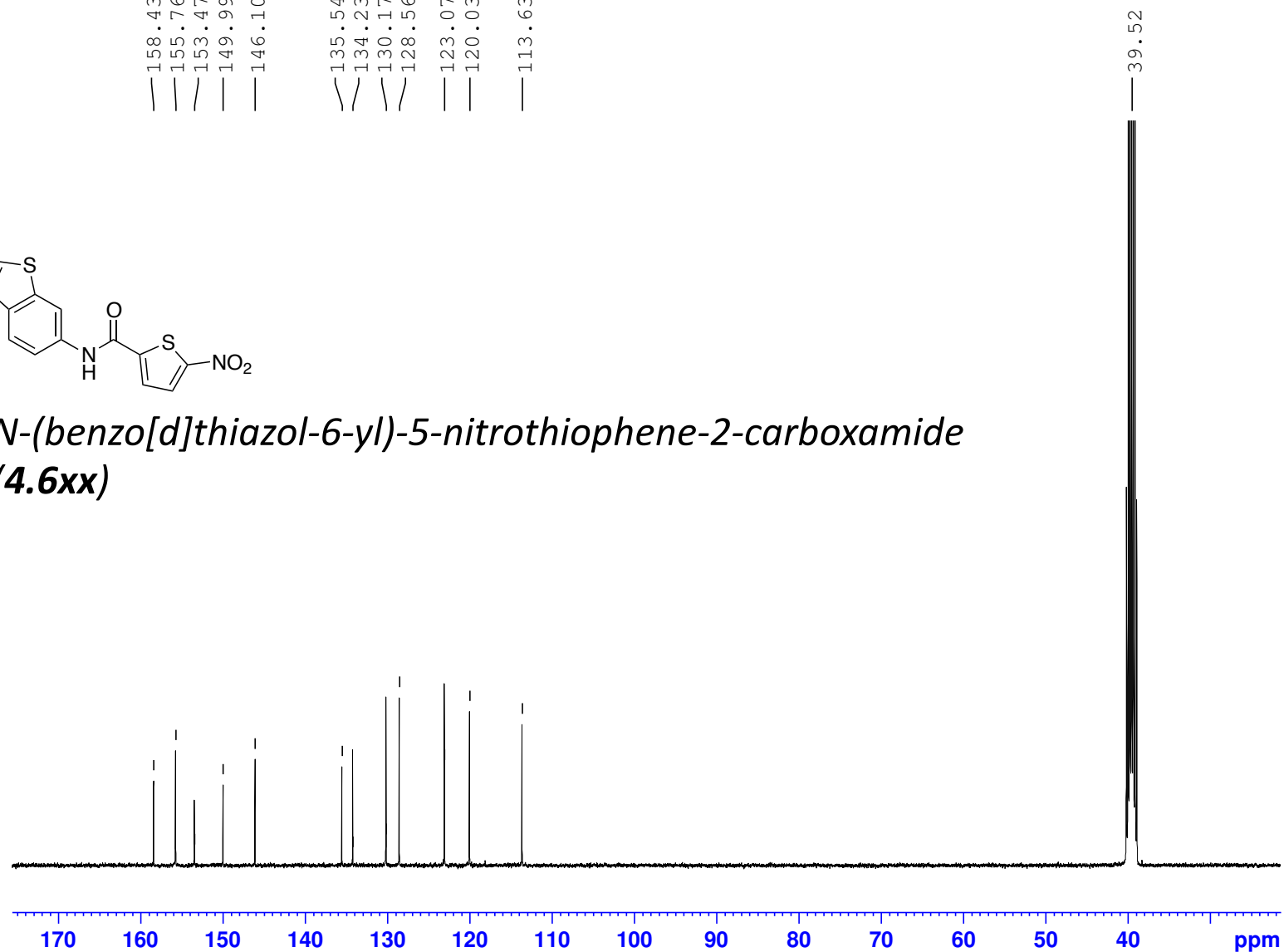
(100 MHz, 297.2 K, DMSO-d6)

GPS480

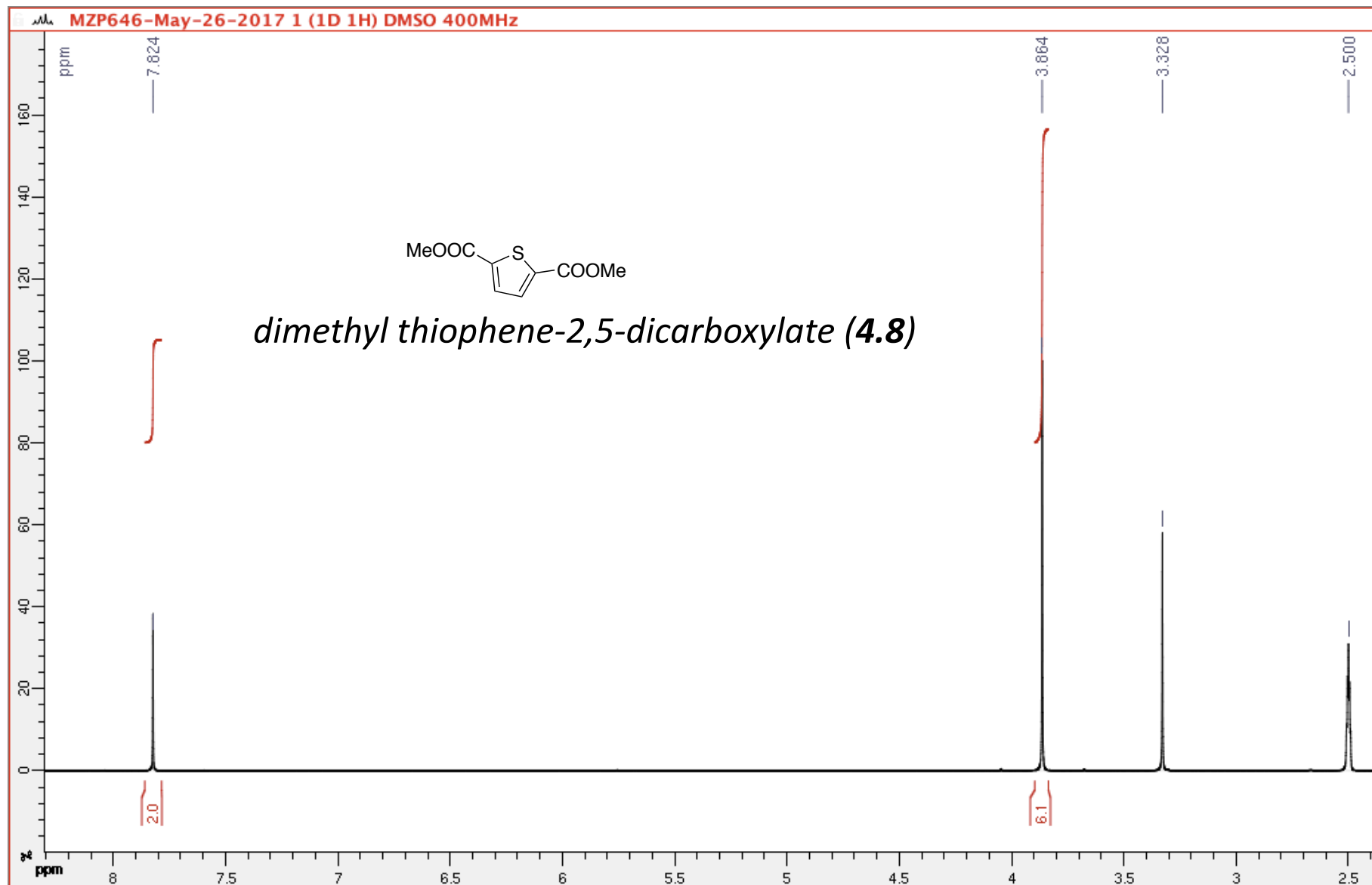
158.43  
155.76  
153.47  
149.99  
146.10  
135.54  
134.23  
130.17  
128.56  
123.07  
120.03  
113.63



*N*-(benzo[d]thiazol-6-yl)-5-nitrothiophene-2-carboxamide  
**(4.6xx)**

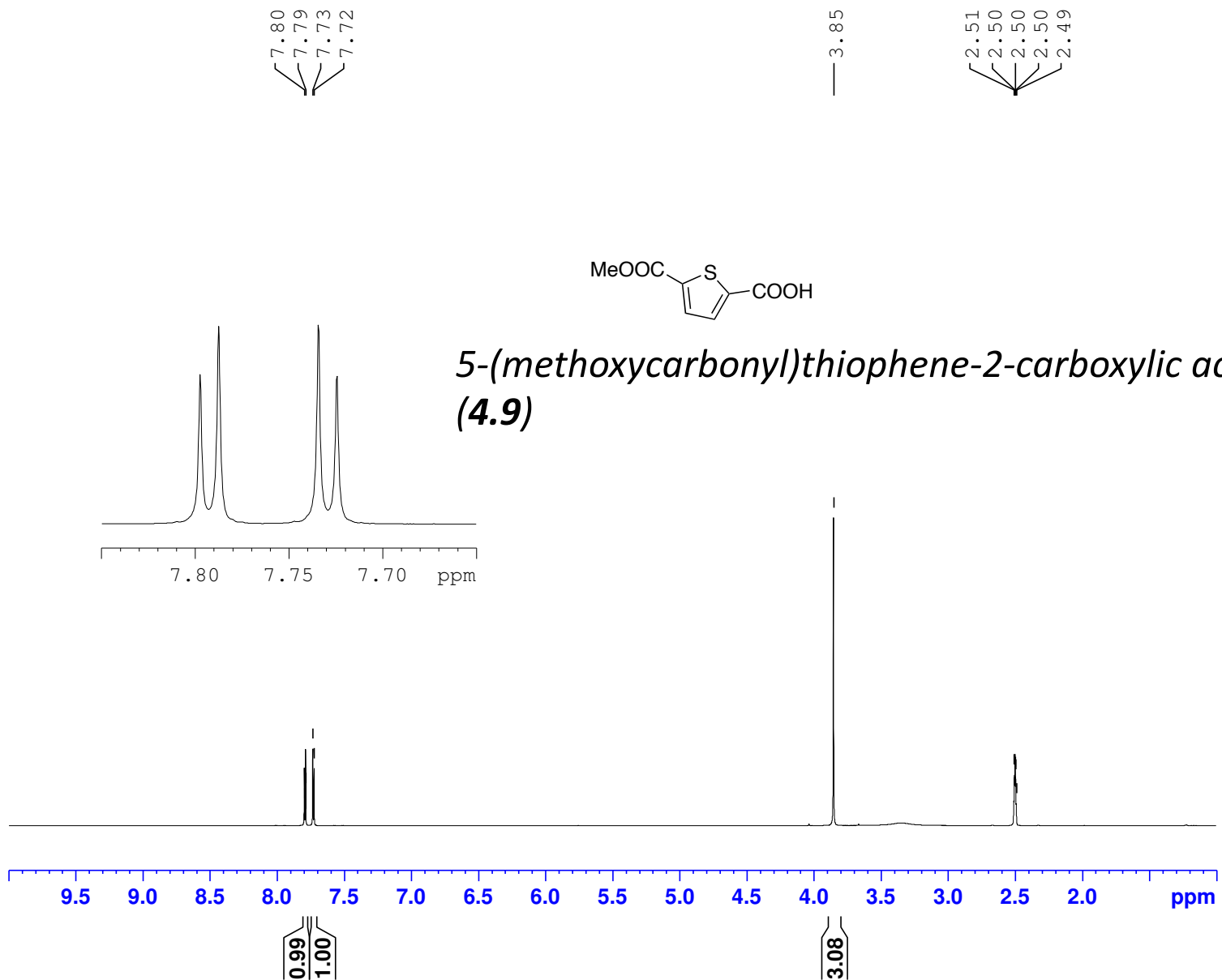


(400 MHz, 297.2 K, DMSO-d6)



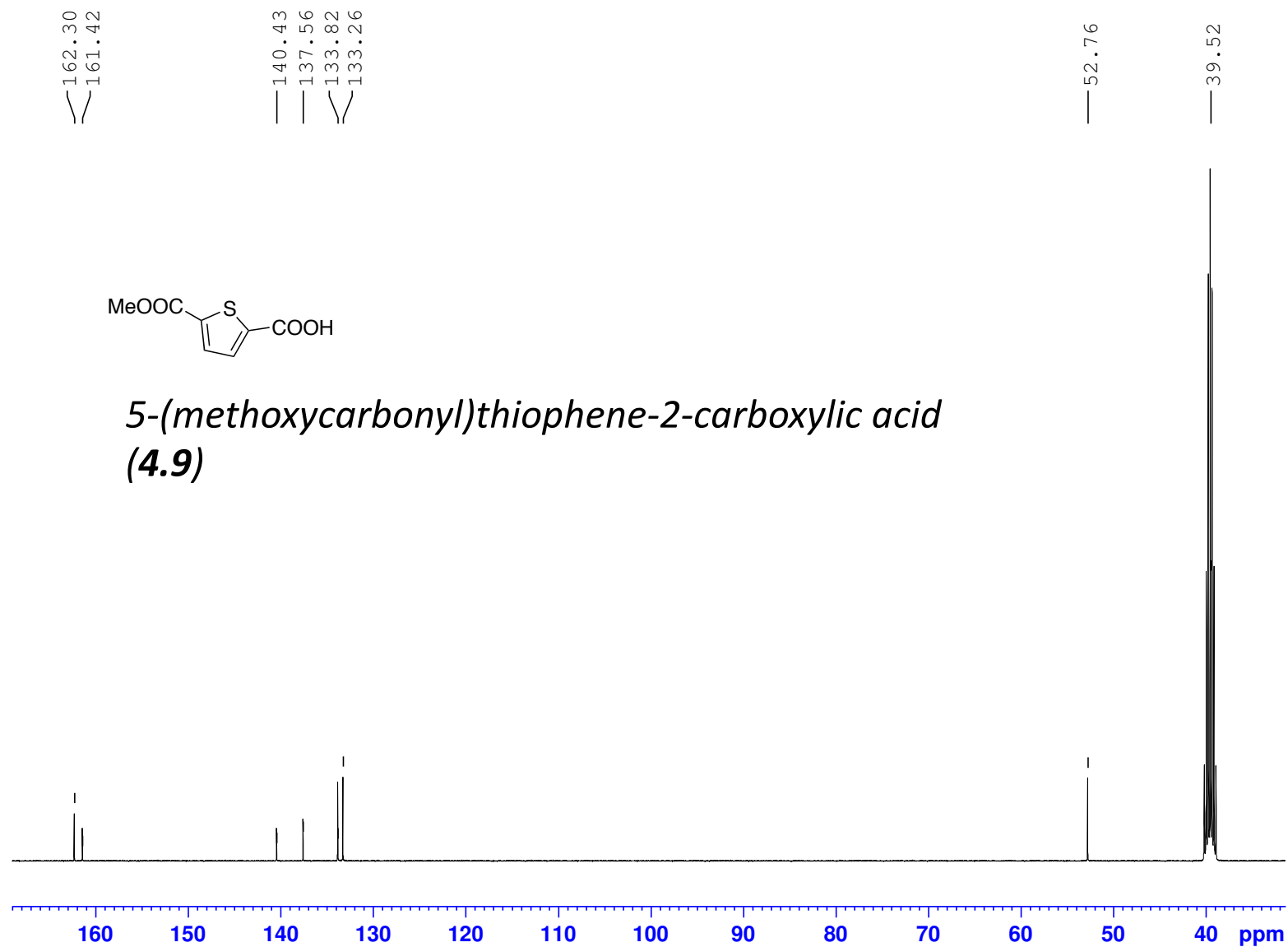
MZP647-10mg-1H-NMR-June-01-2017

(400 MHz, 297.2 K, DMSO-d6)

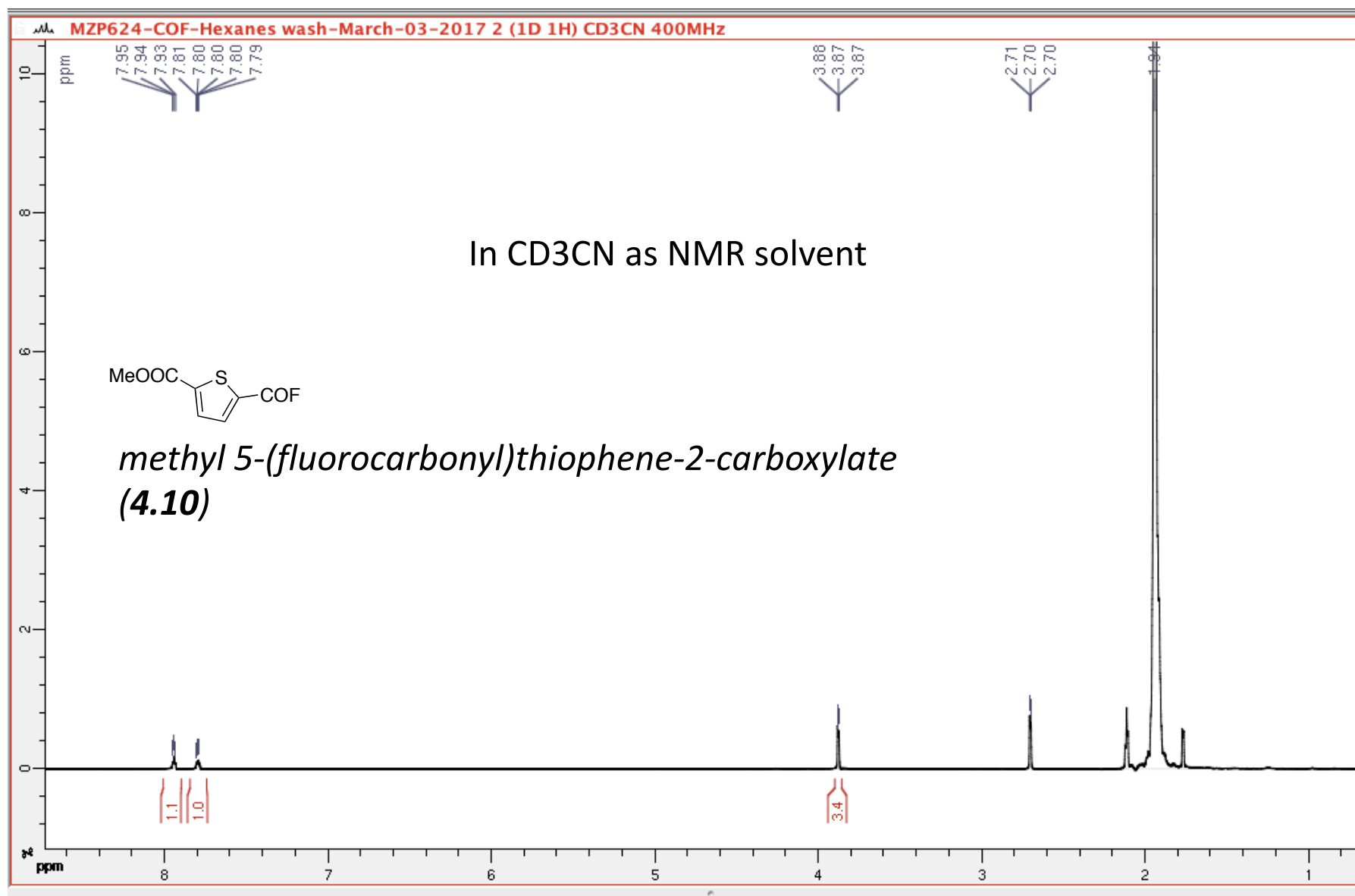


MZP647-10mg-13C-NMR-June-01-2017

(100 MHz, 297.2 K, DMSO-d6)

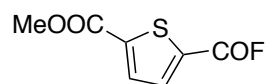


(400 MHz, 297.2 K, CD<sub>3</sub>CN)

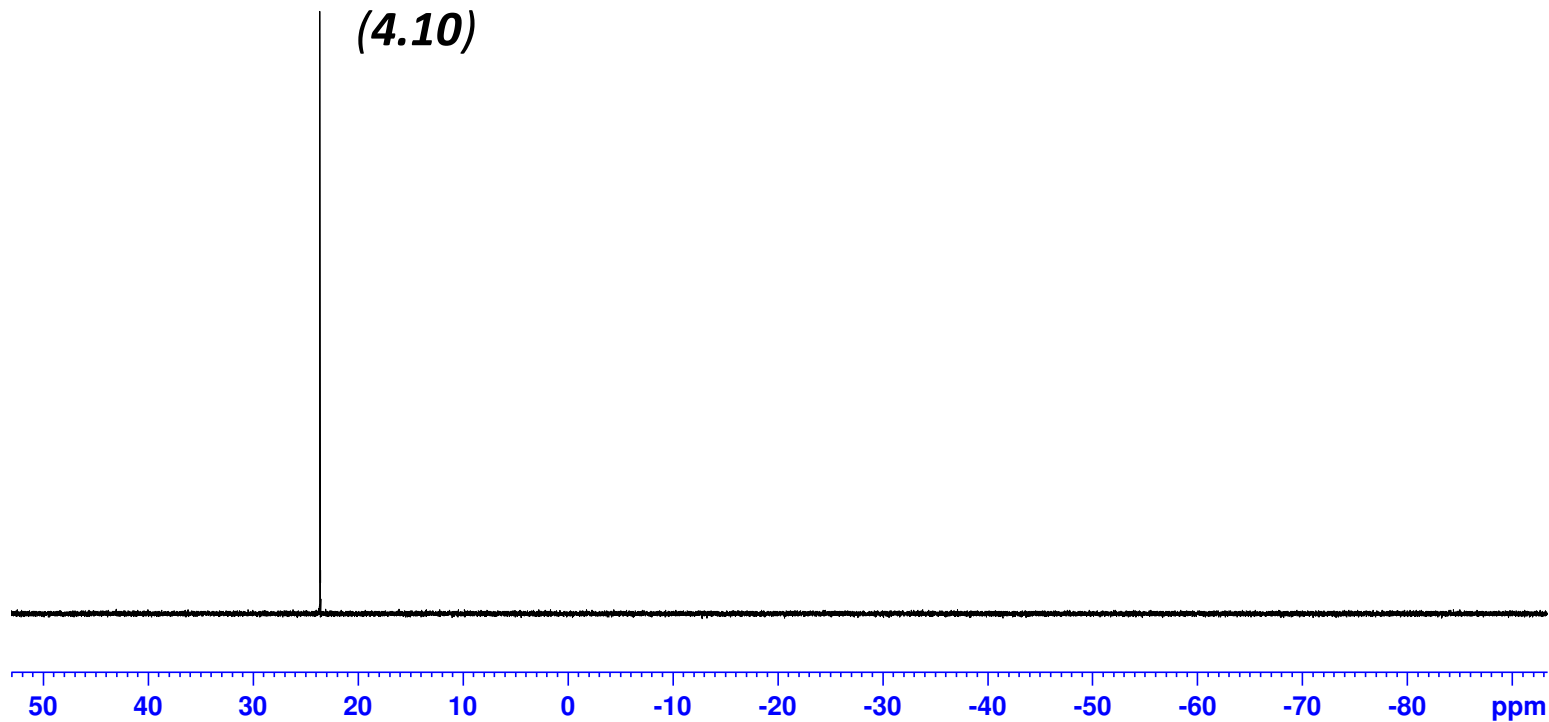


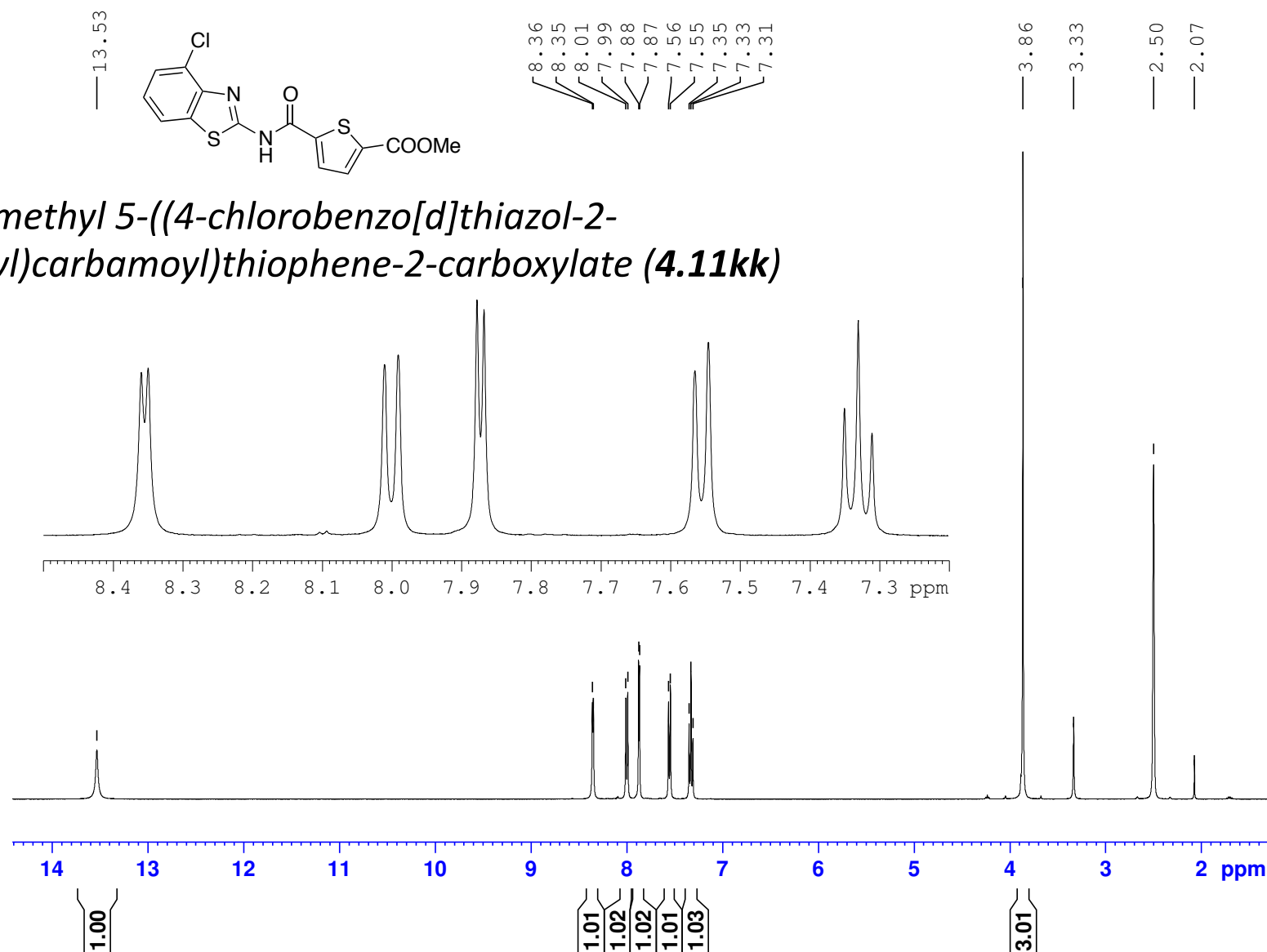
In CD<sub>3</sub>CN as NMR solvent

— 23.62

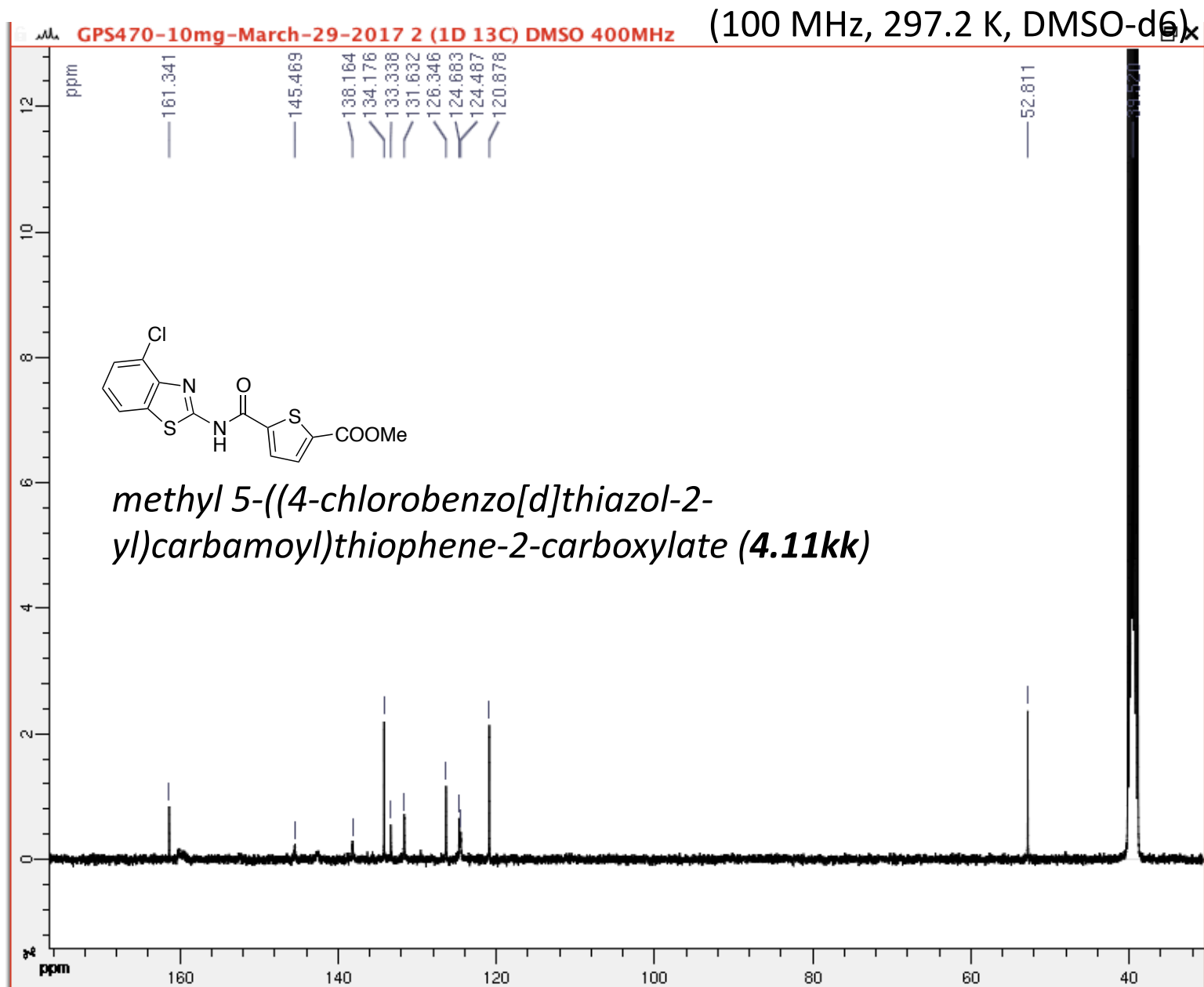


*methyl 5-(fluorocarbonyl)thiophene-2-carboxylate*  
**(4.10)**



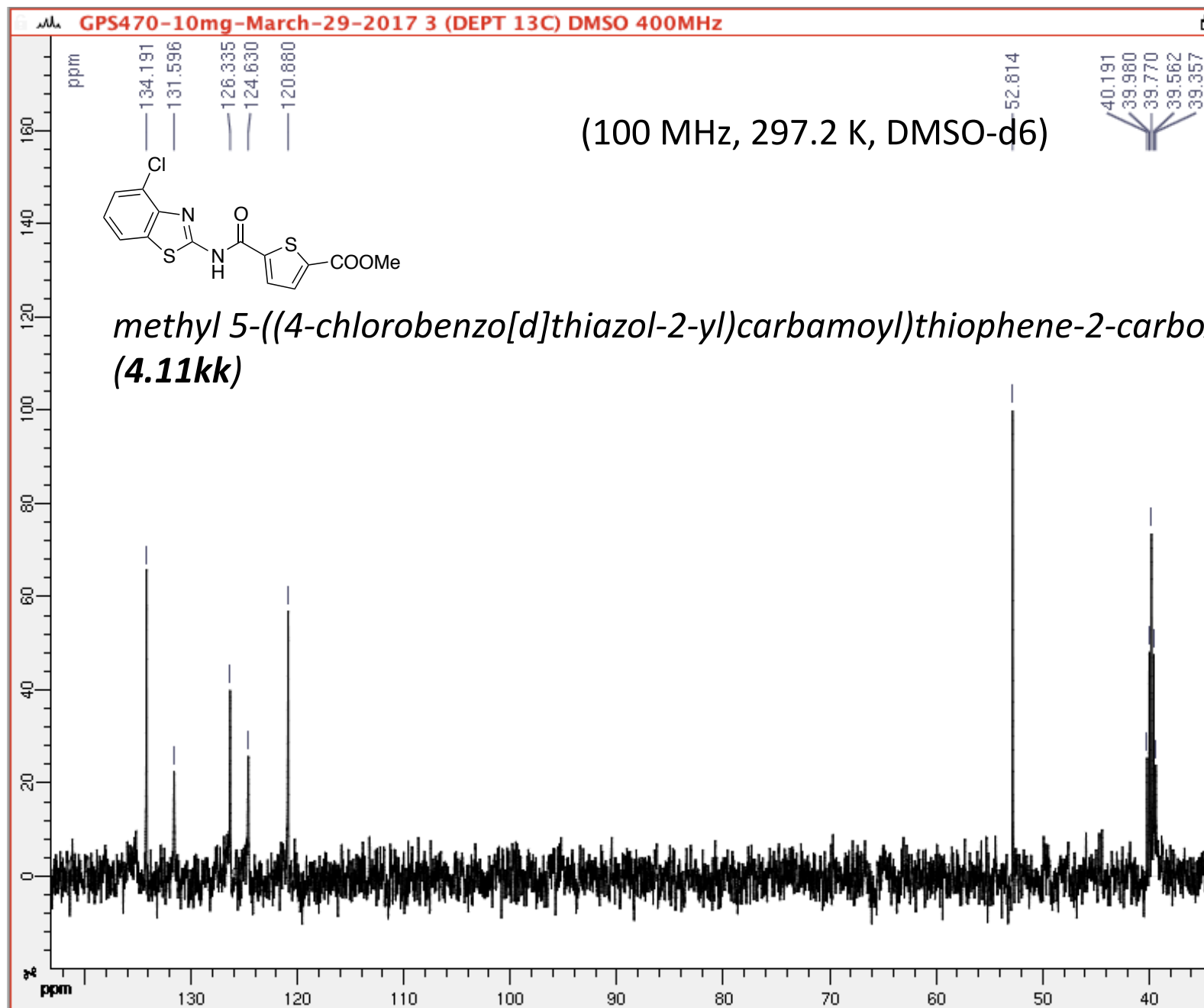


GPS470





GPS470



GPS472-MZP624-B77-10mg-1H-NMR-March-2017

(400 MHz, 297.2 K, DMSO-d6)

GPS472

— 13.68

— 9.09

8.33

8.30

8.28

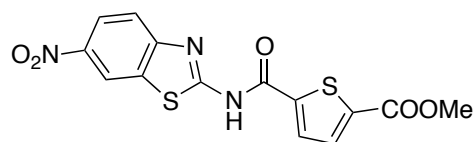
7.93

7.91

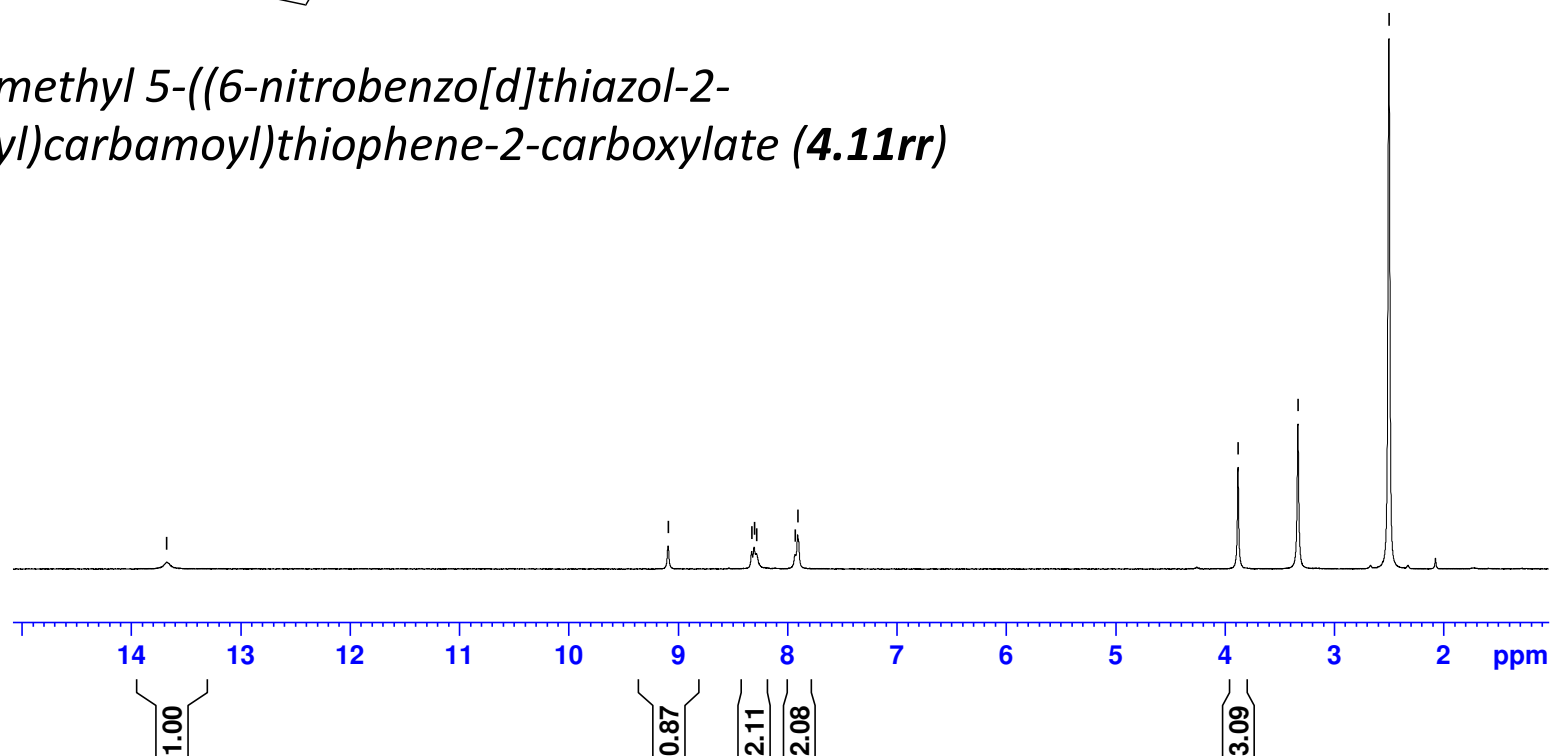
— 3.88

— 3.33

— 2.50

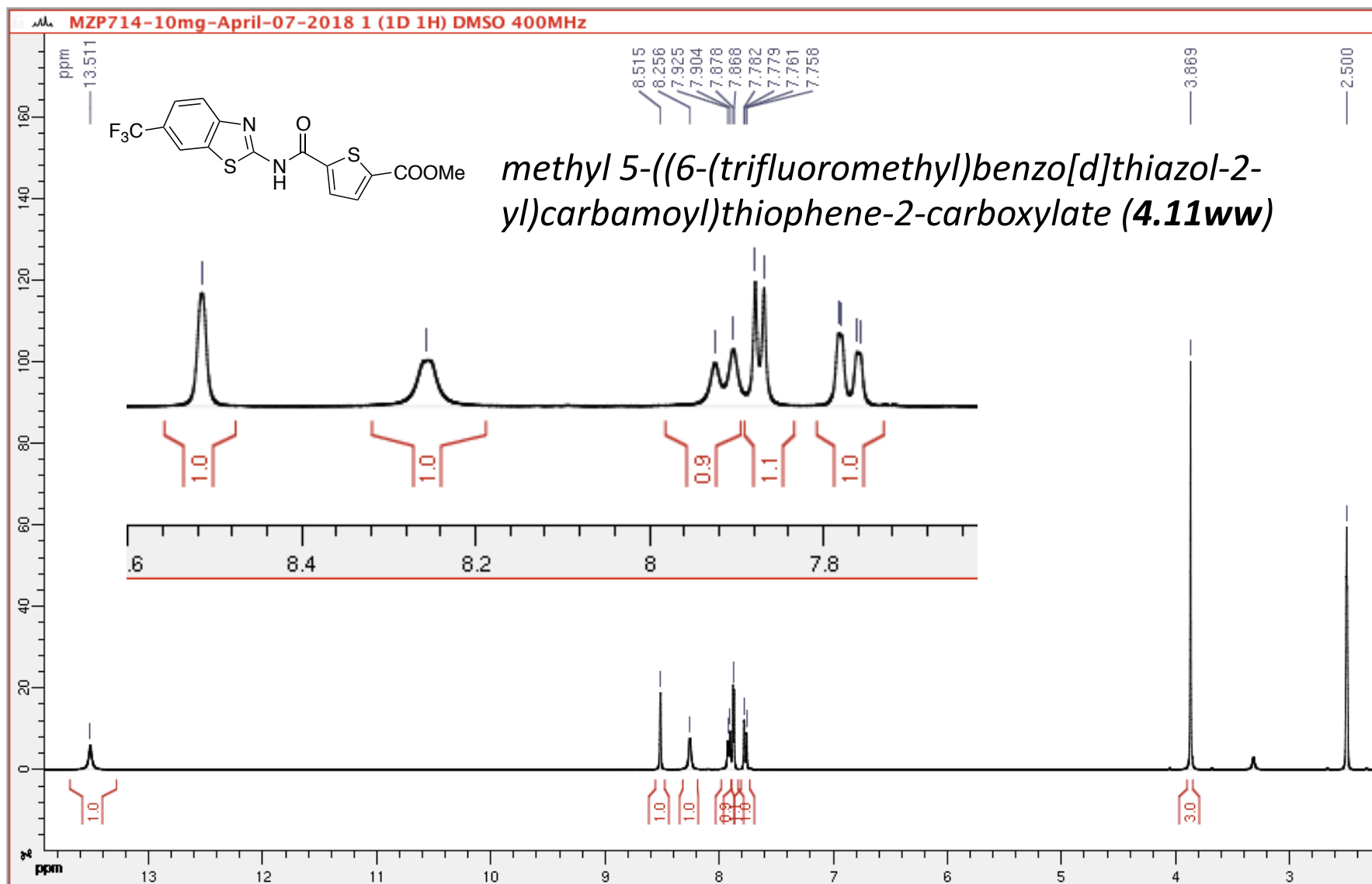


*methyl 5-((6-nitrobenzo[d]thiazol-2-yl)carbamoyl)thiophene-2-carboxylate (4.11rr)*

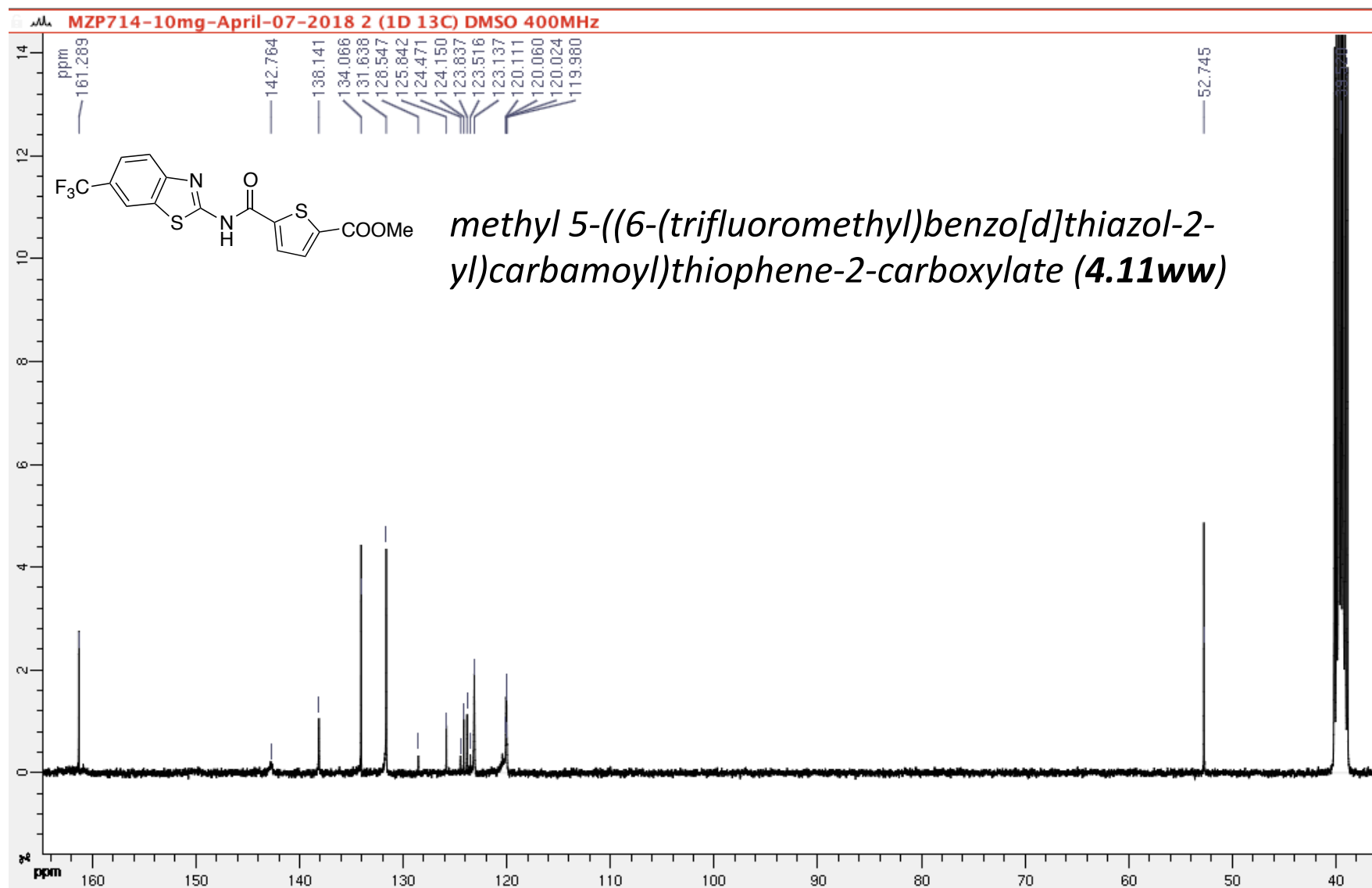


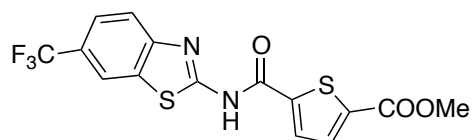
(400 MHz, 297.2 K, DMSO-d6)

GPS496



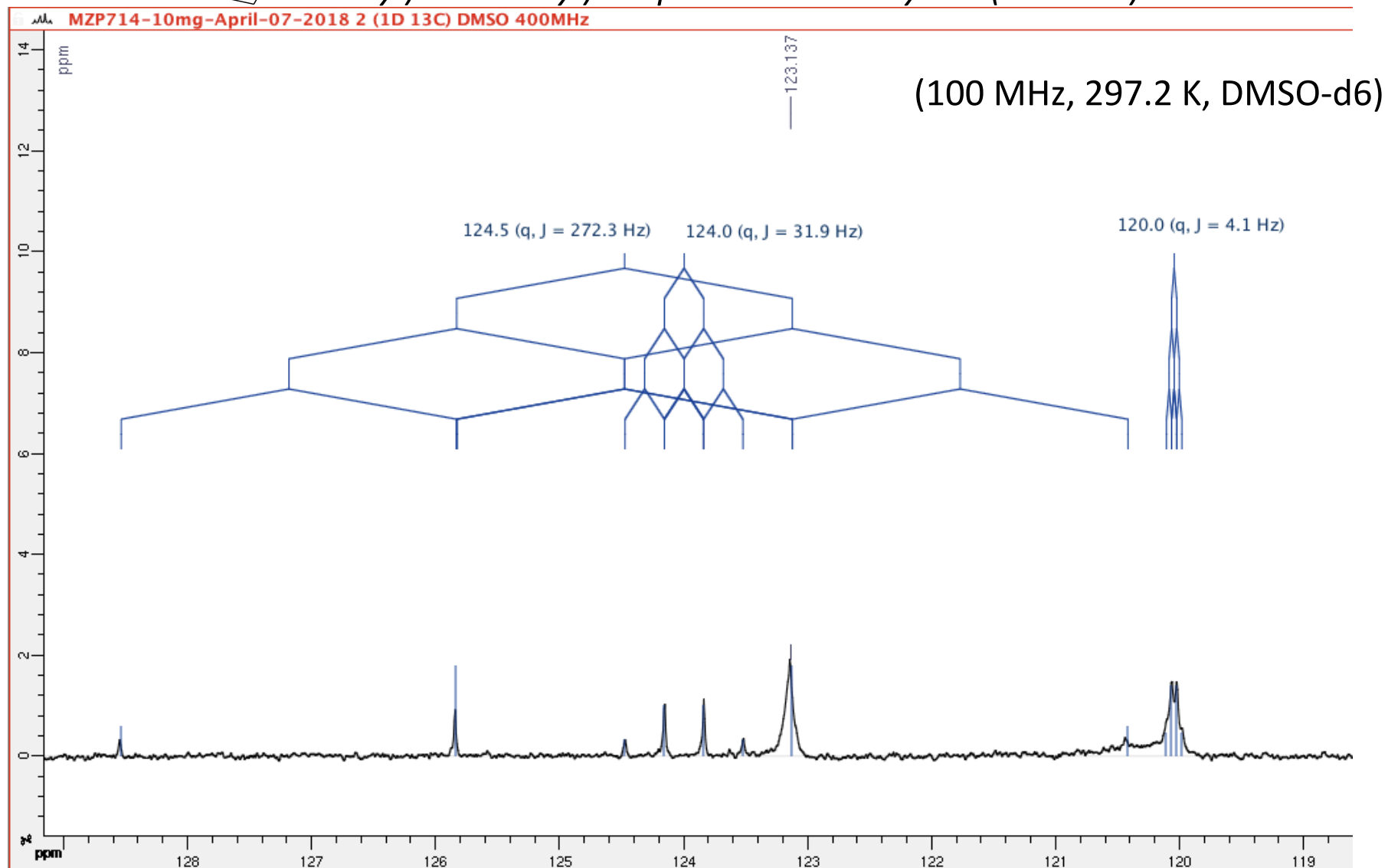
(100 MHz, 297.2 K, DMSO-d6) GPS496





*methyl 5-((6-(trifluoromethyl)benzo[d]thiazol-2-yl)carbamoyl)thiophene-2-carboxylate (4.11ww)*

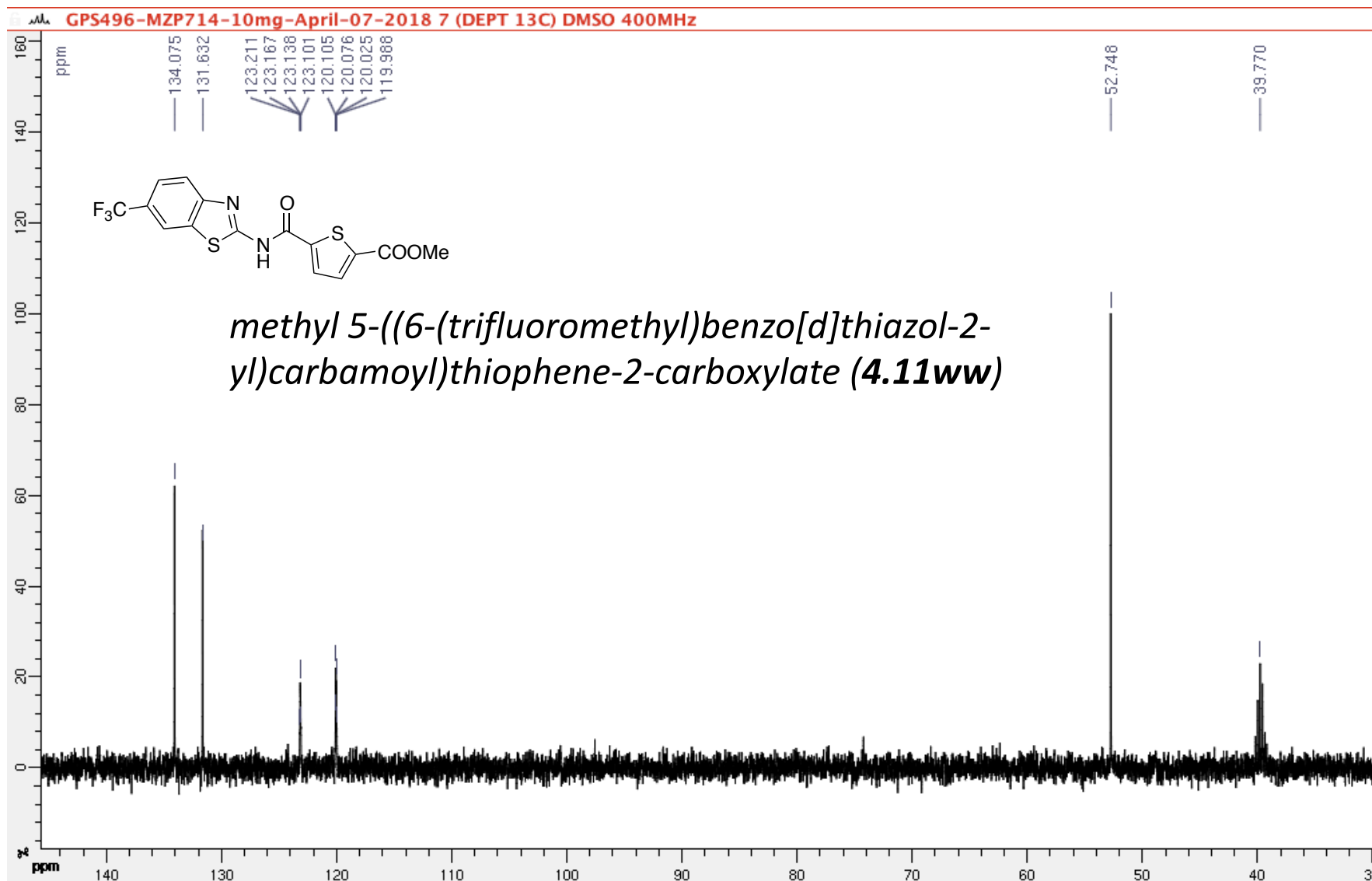
GPS496



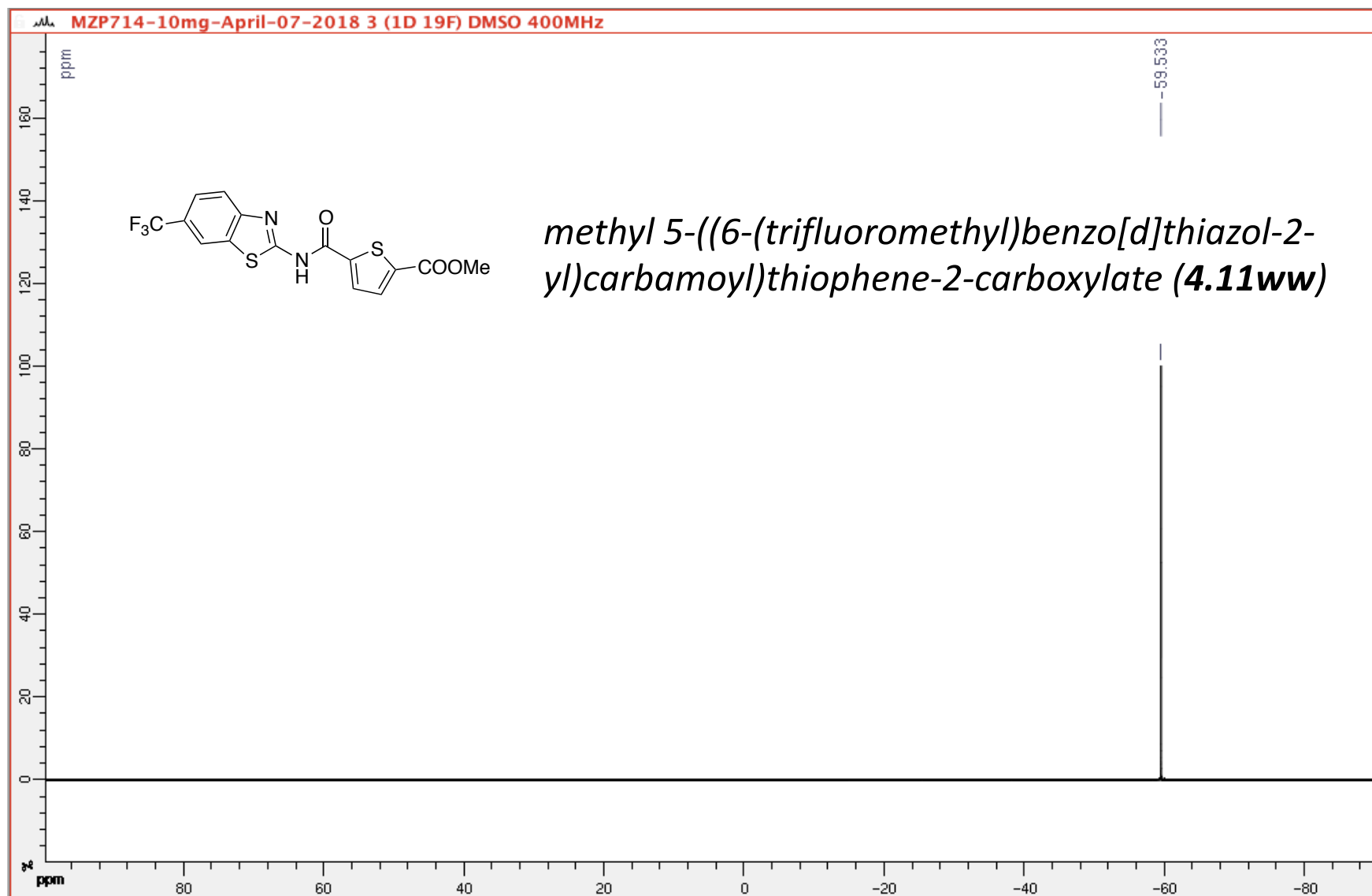
DEPT135

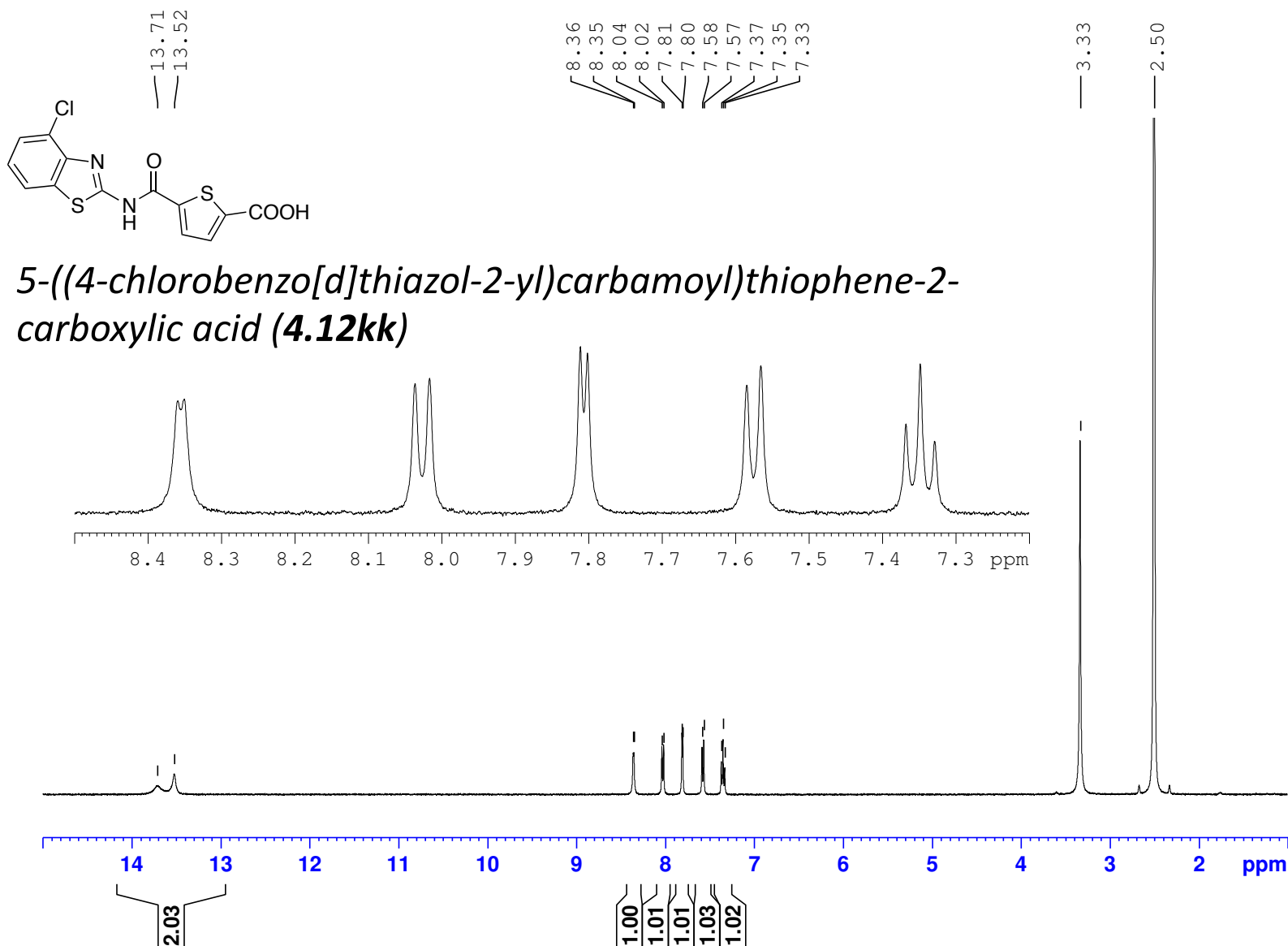
(100 MHz, 297.2 K, DMSO-d6)

GPS496



(400 MHz, 297.2 K, DMSO-d6) GPS496

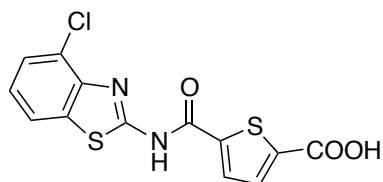




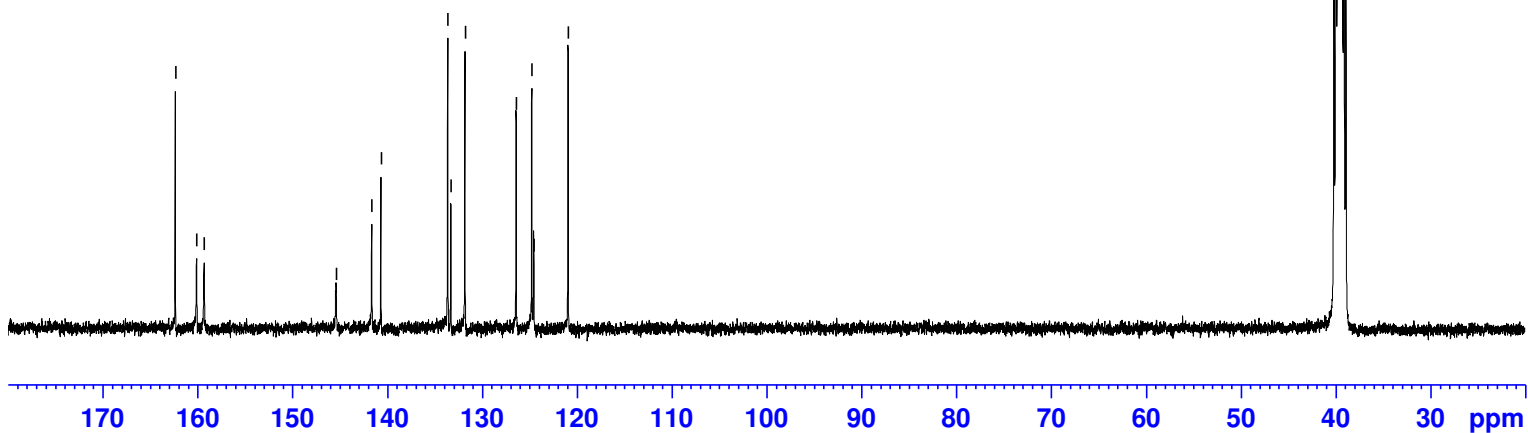


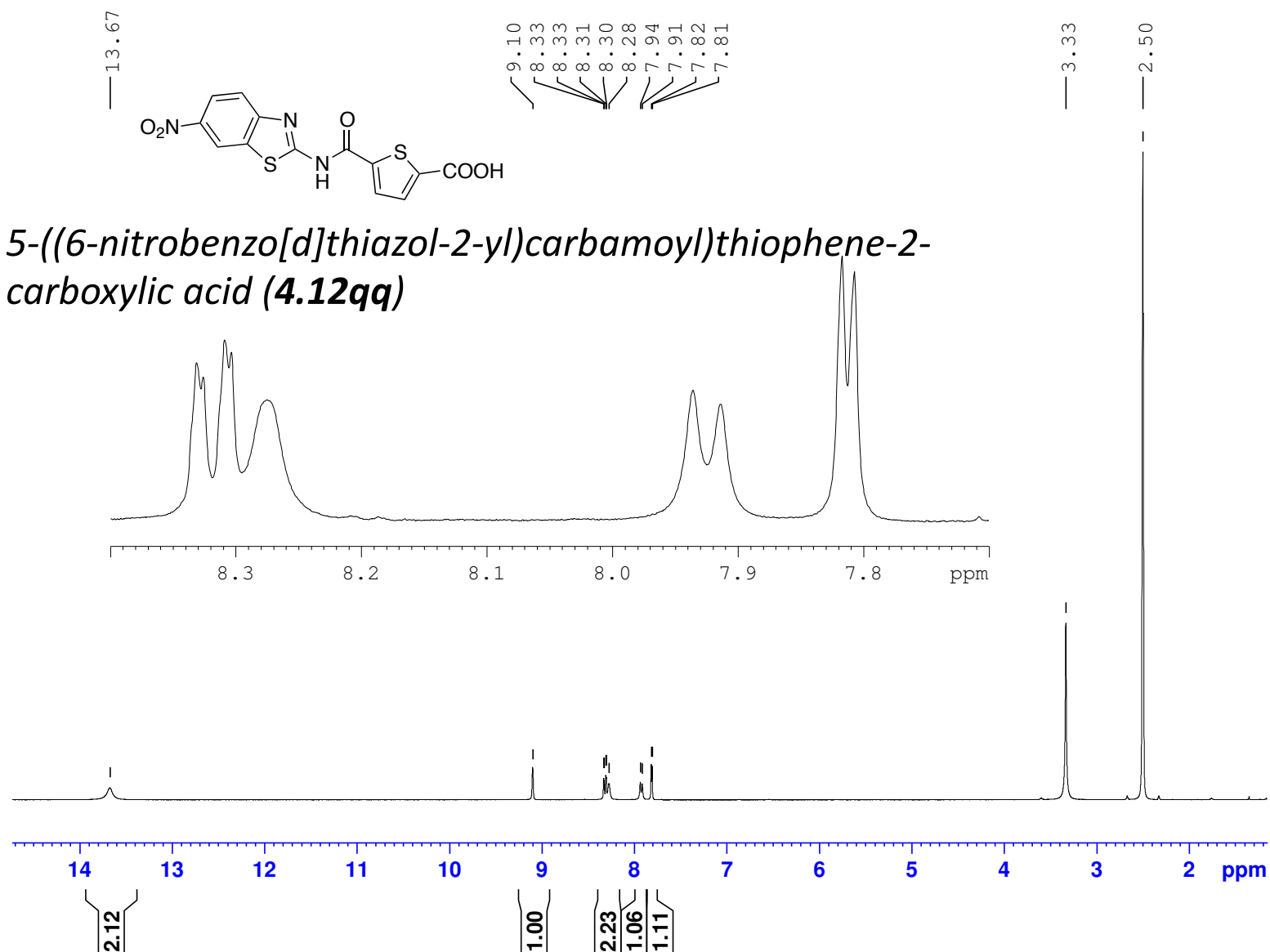
162.35  
160.12  
159.32  
  
145.41  
141.64  
140.68  
133.63  
133.30  
131.81  
126.41  
124.77  
124.56  
120.93

40.14  
39.93  
39.73  
39.52  
39.31  
39.10



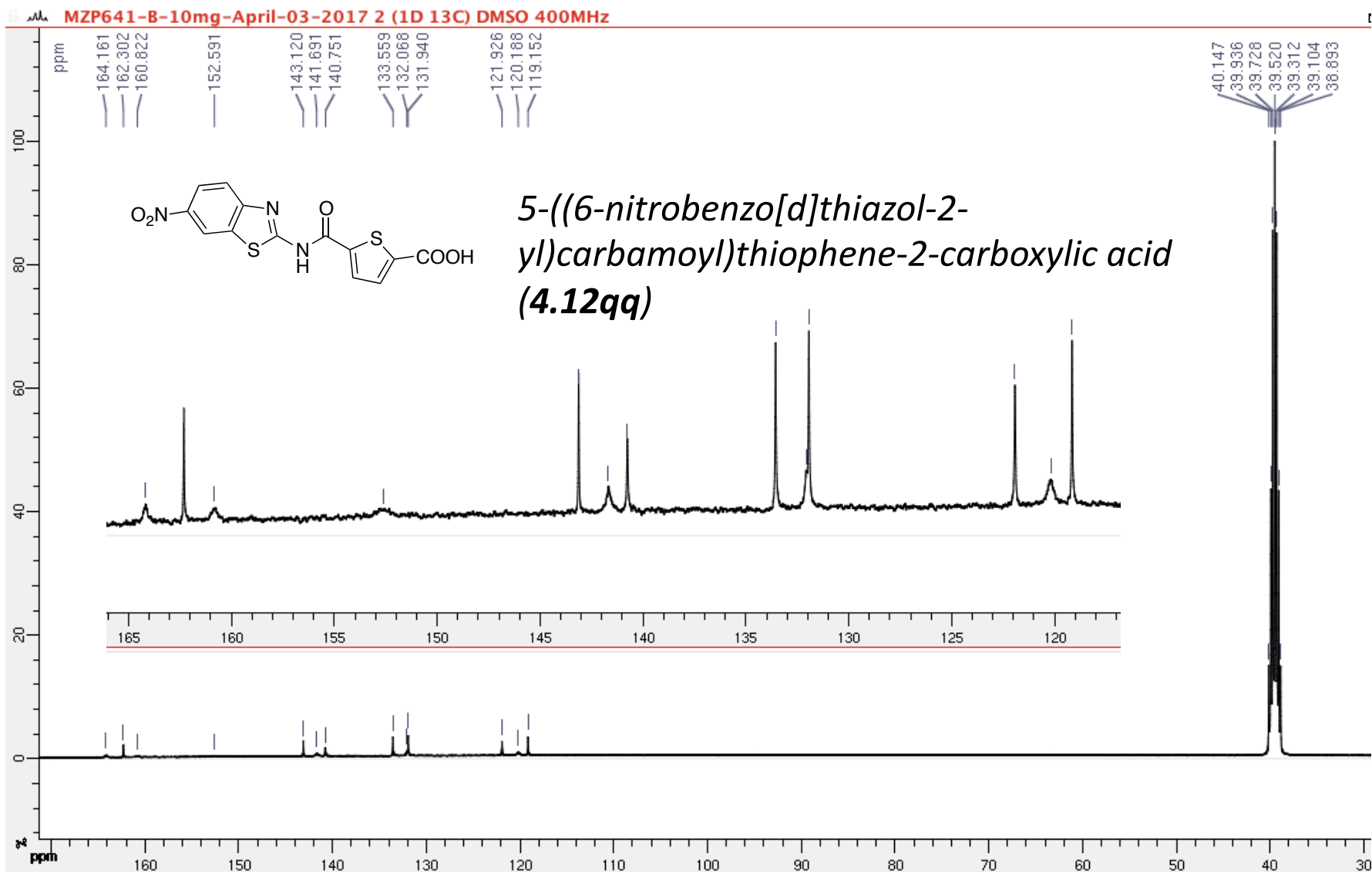
*5-((4-chlorobenzo[d]thiazol-2-yl)carbamoyl)thiophene-2-carboxylic acid (4.12kk)*





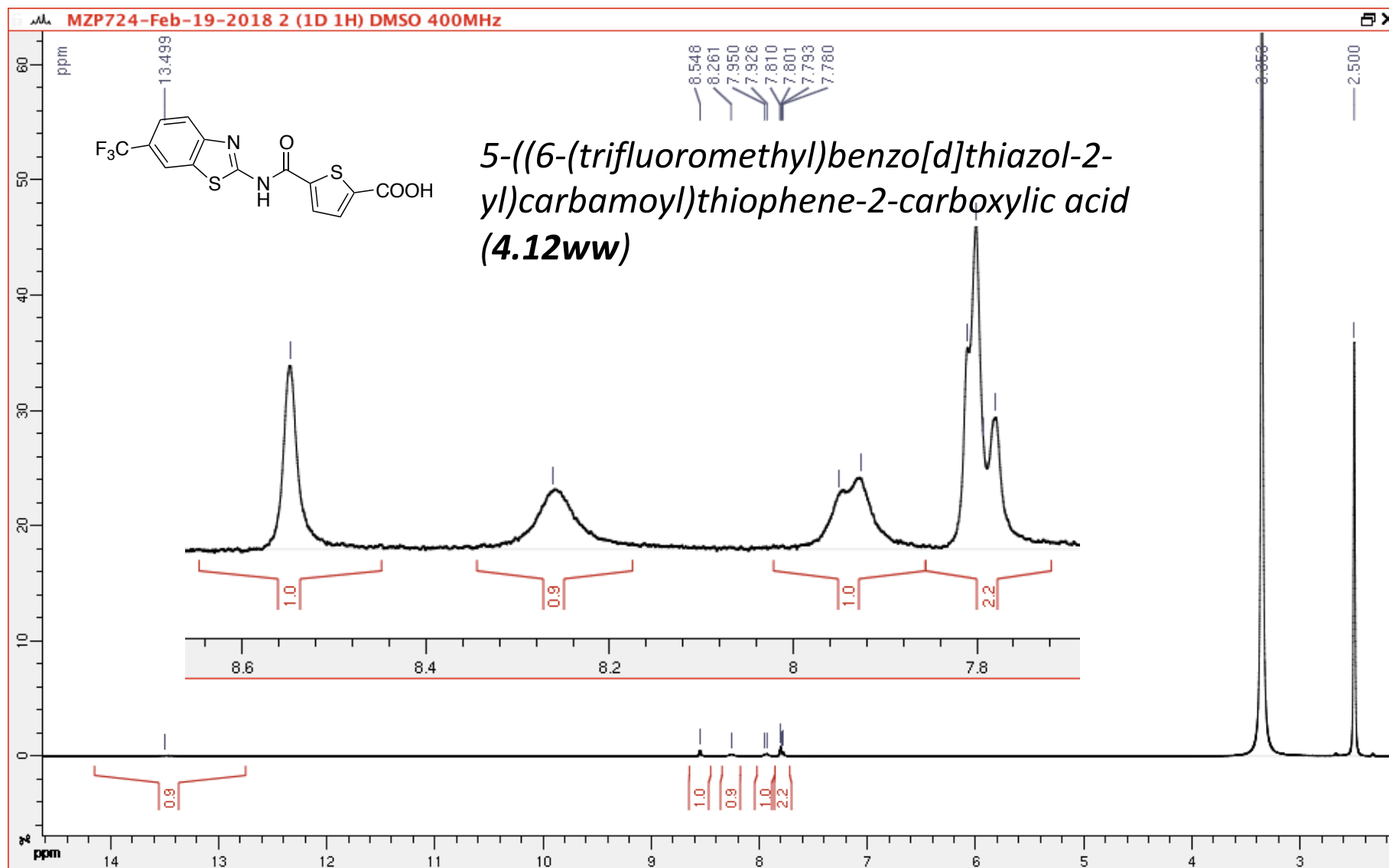
(100 MHz, 297.2 K, DMSO-d6)

GPS471



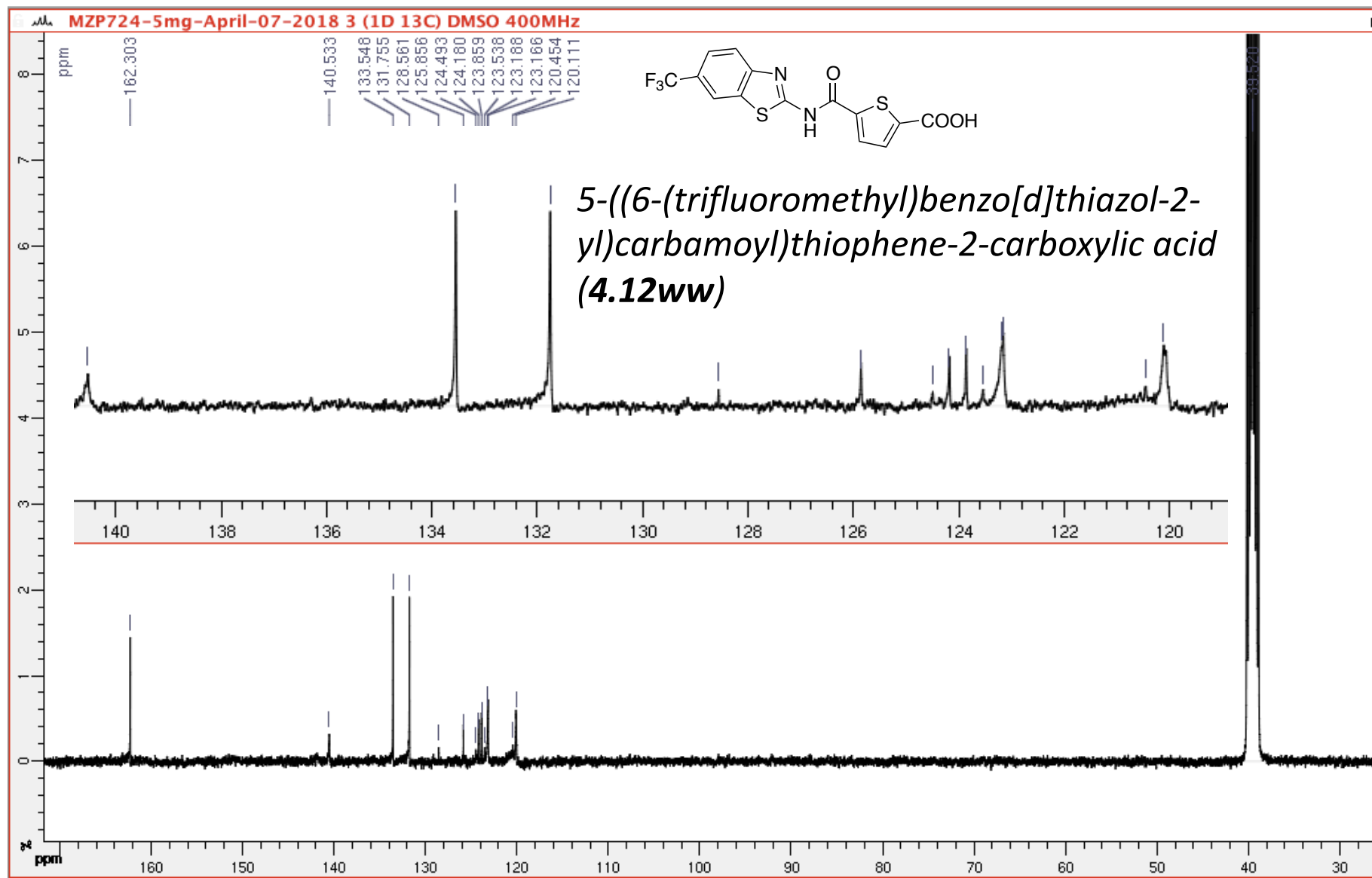
(400 MHz, 297.2 K, DMSO-d6)

GPS497

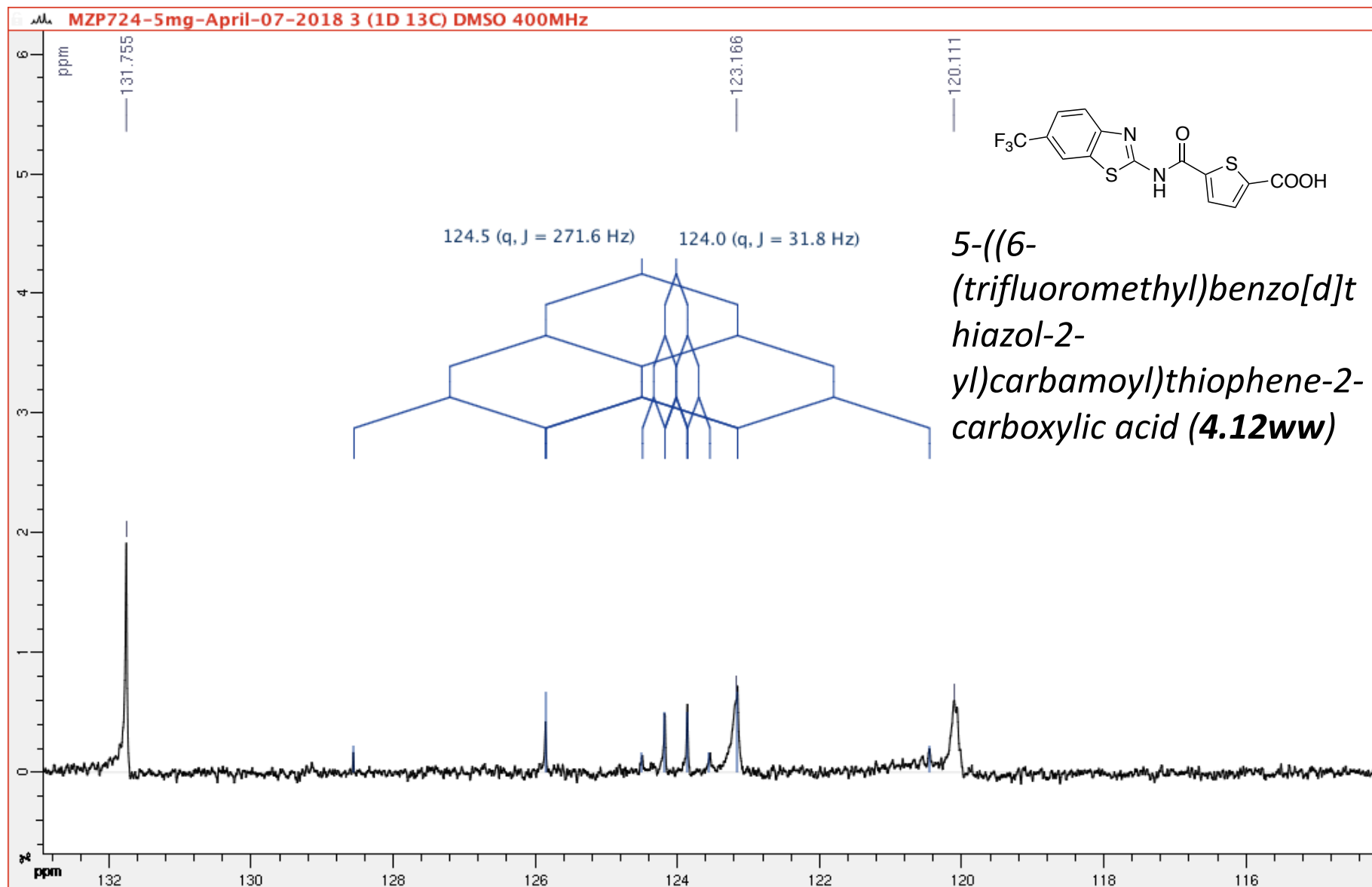


(100 MHz, 297.2 K, DMSO-d6)

GPS497



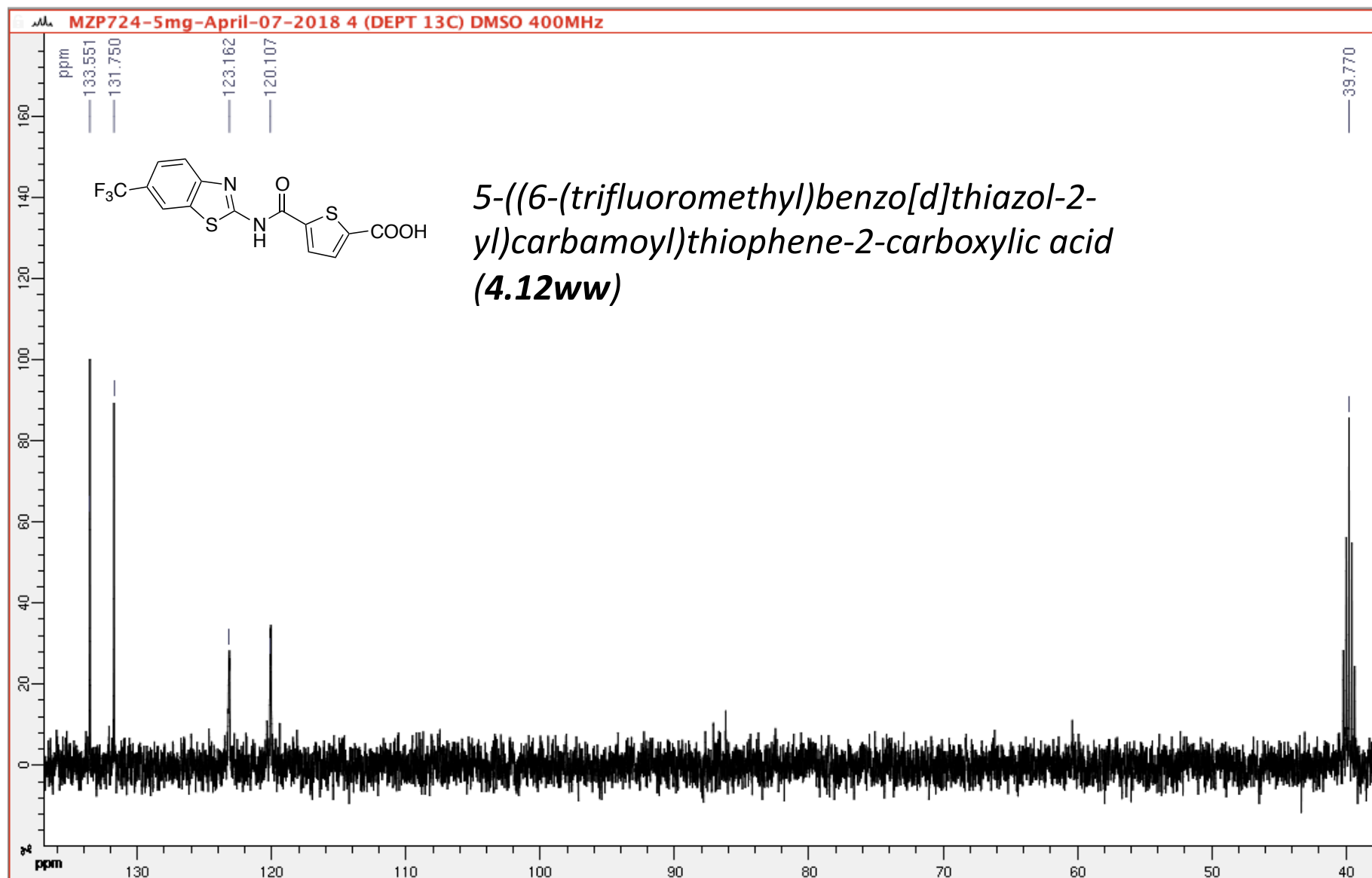
(100 MHz, 297.2 K, DMSO-d6) GPS497



DEPT 90

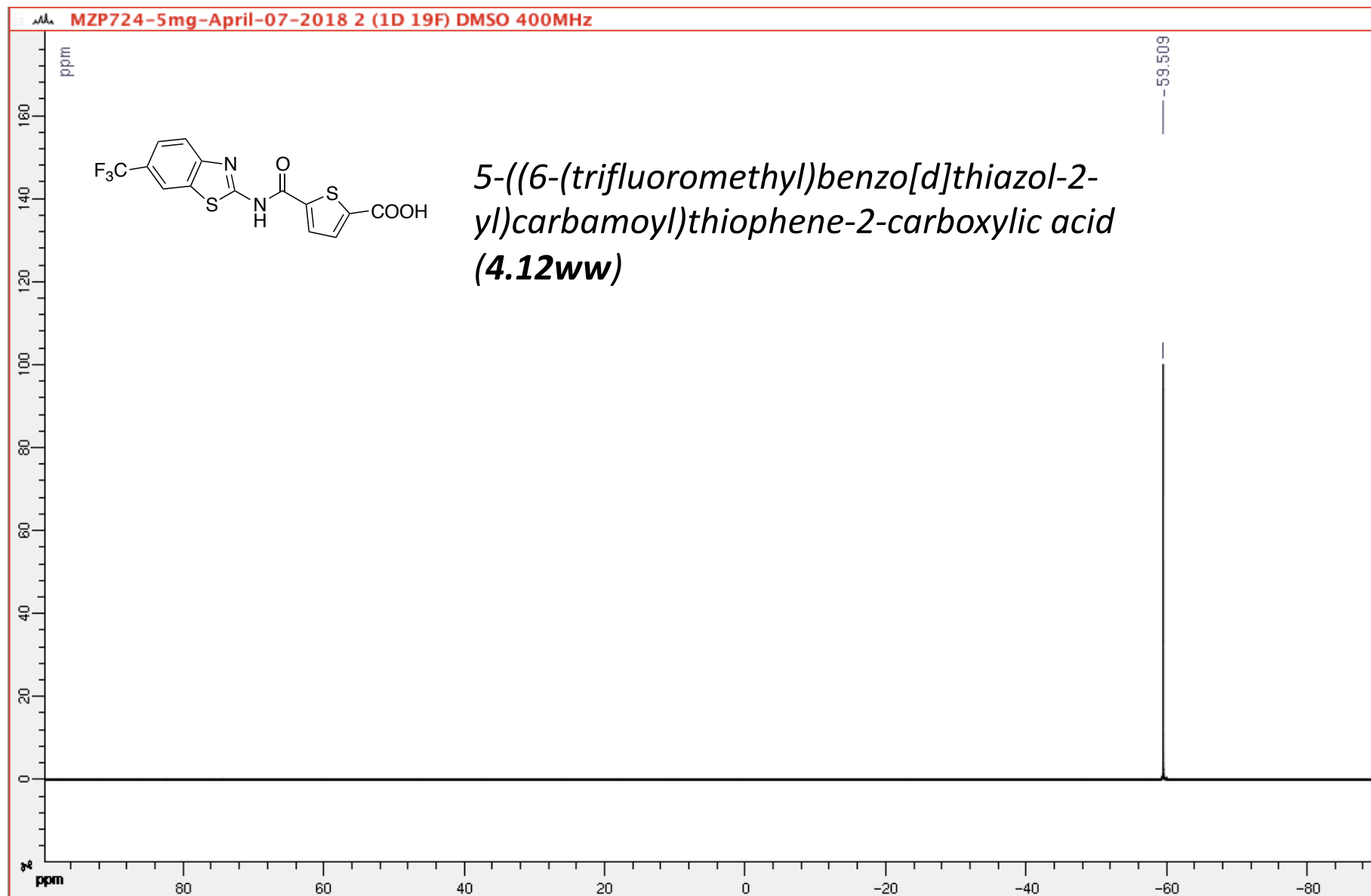
(100 MHz, 297.2 K, DMSO-d6)

GPS497

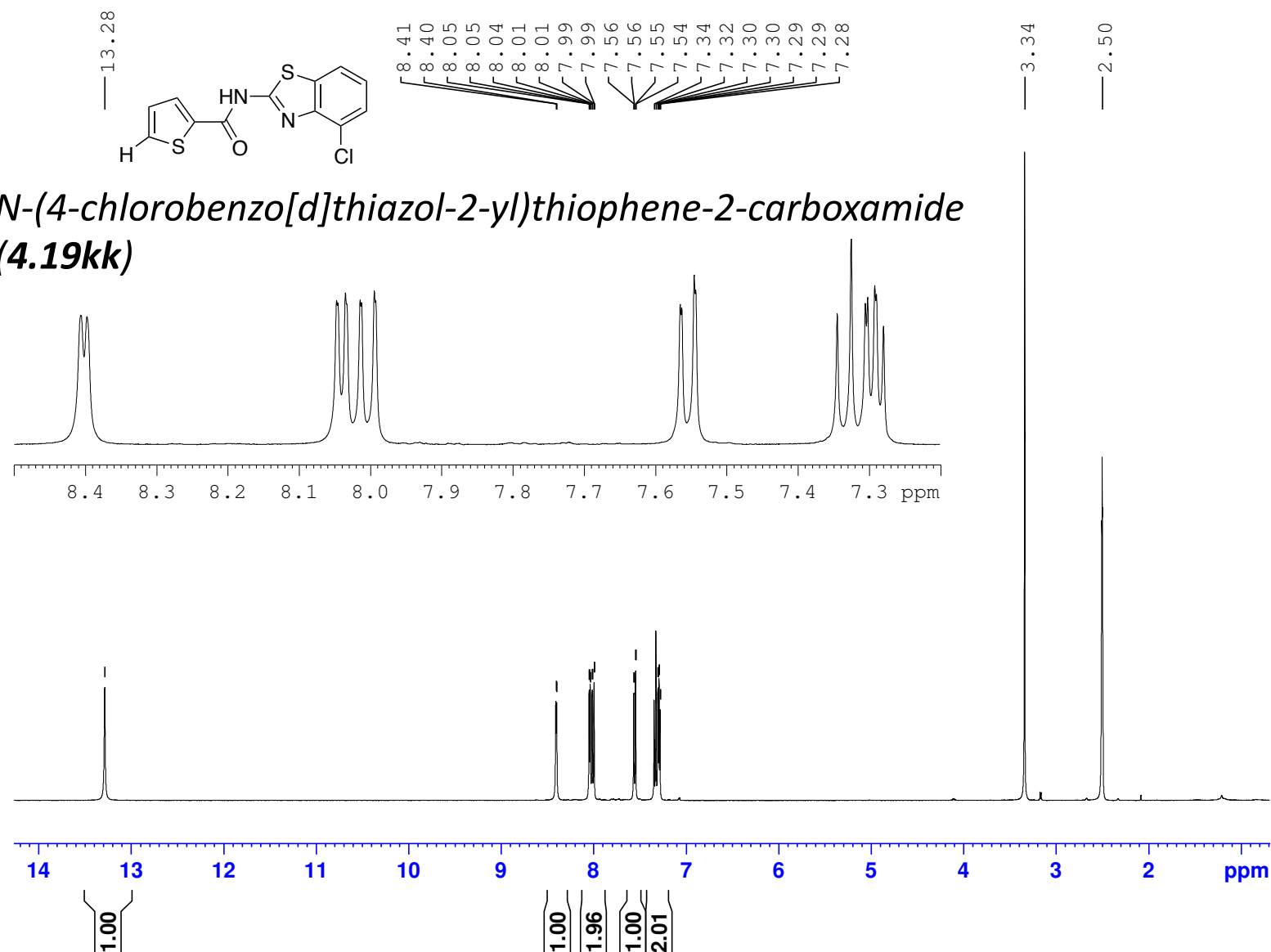


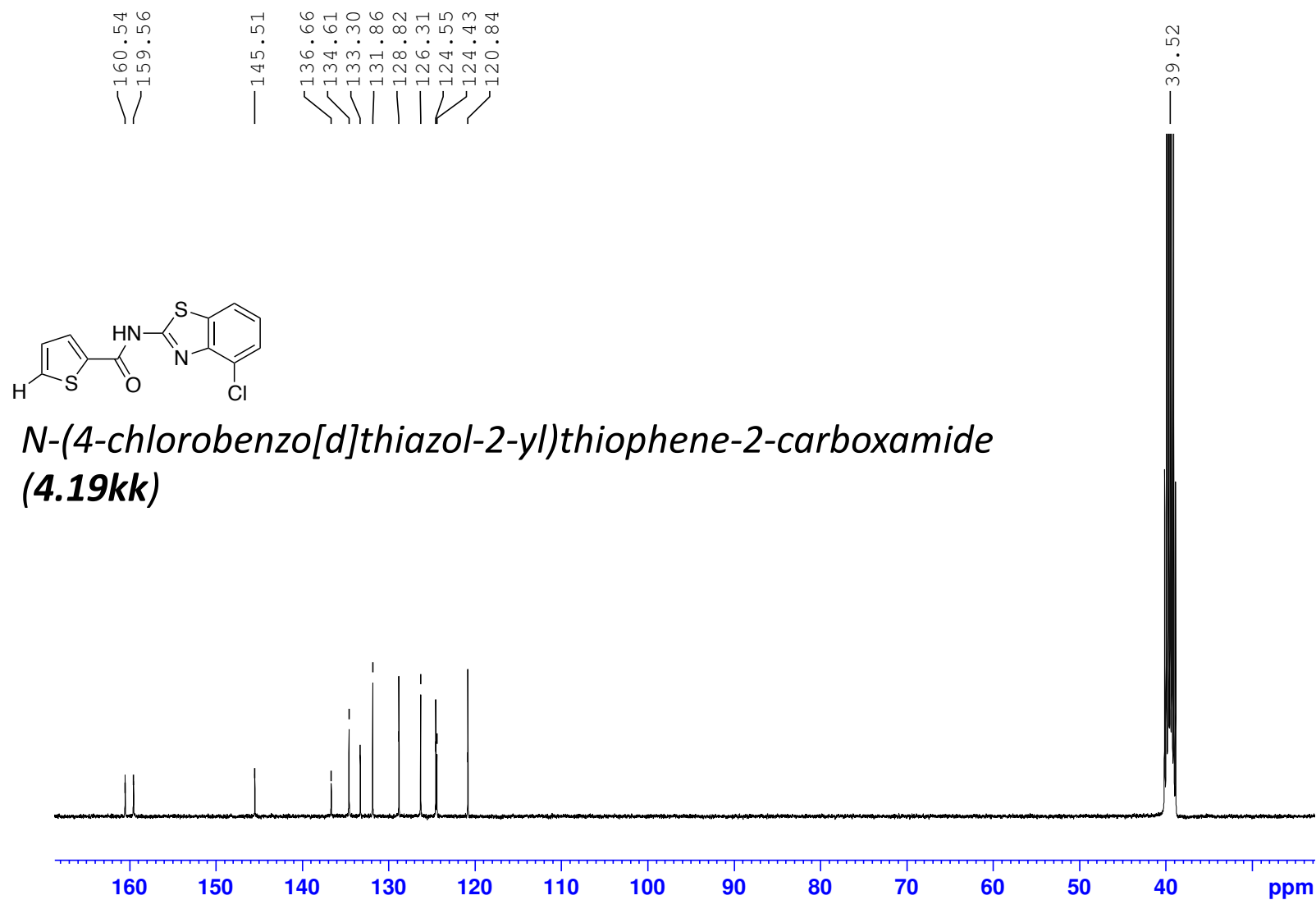
(400 MHz, 297.2 K, DMSO-d6)

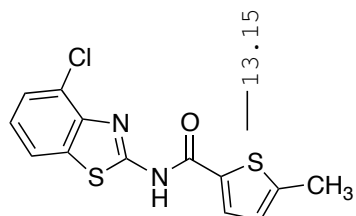
GPS497



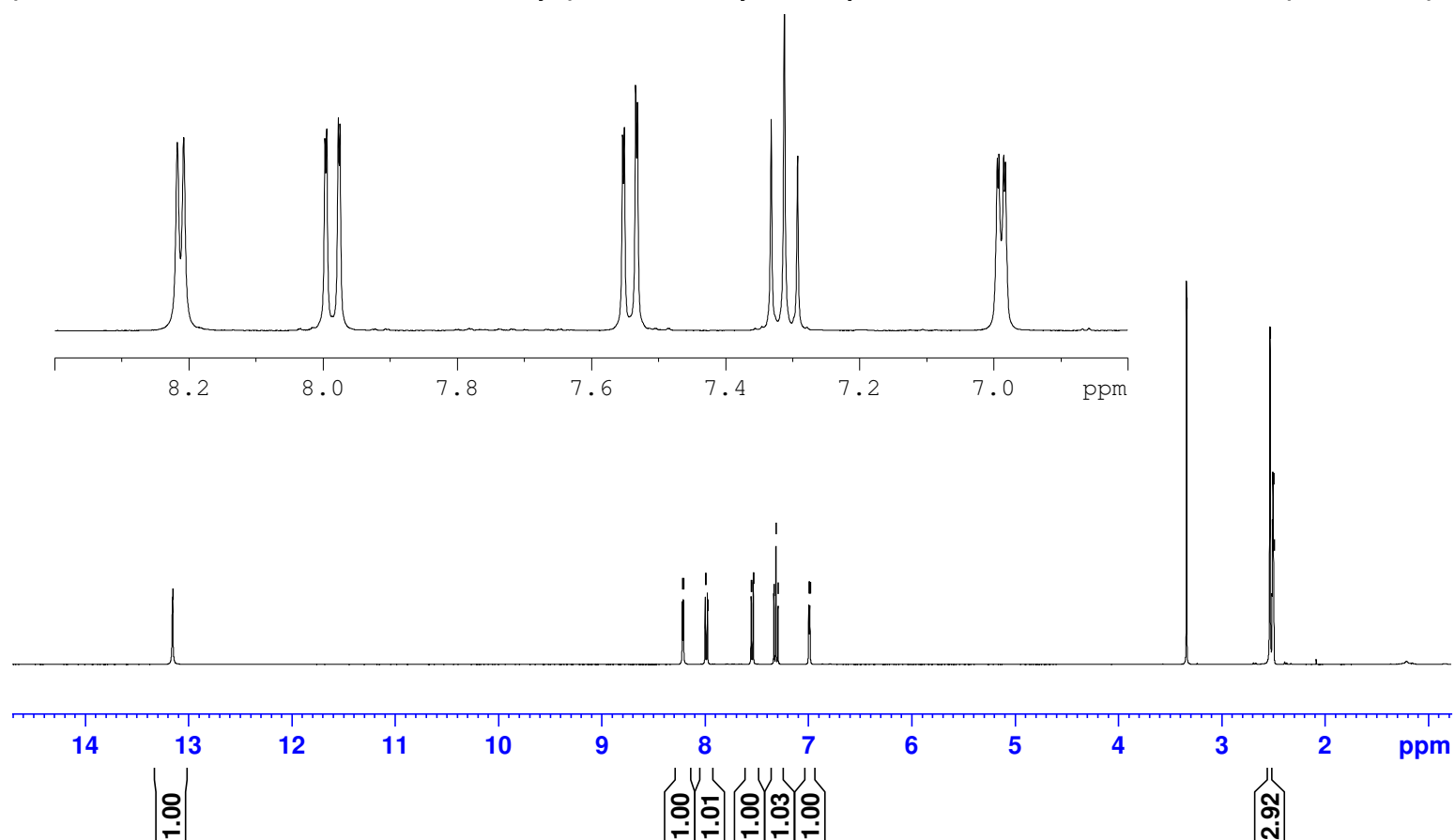








*N*-(4-chlorobenzo[d]thiazol-2-yl)-5-methylthiophene-2-carboxamide (**4.20kk**)

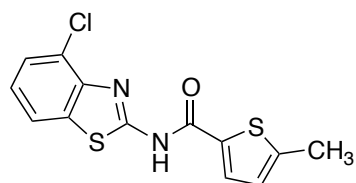


GPS482-MZP596C1-A42-13C-NMR-May-03-2017

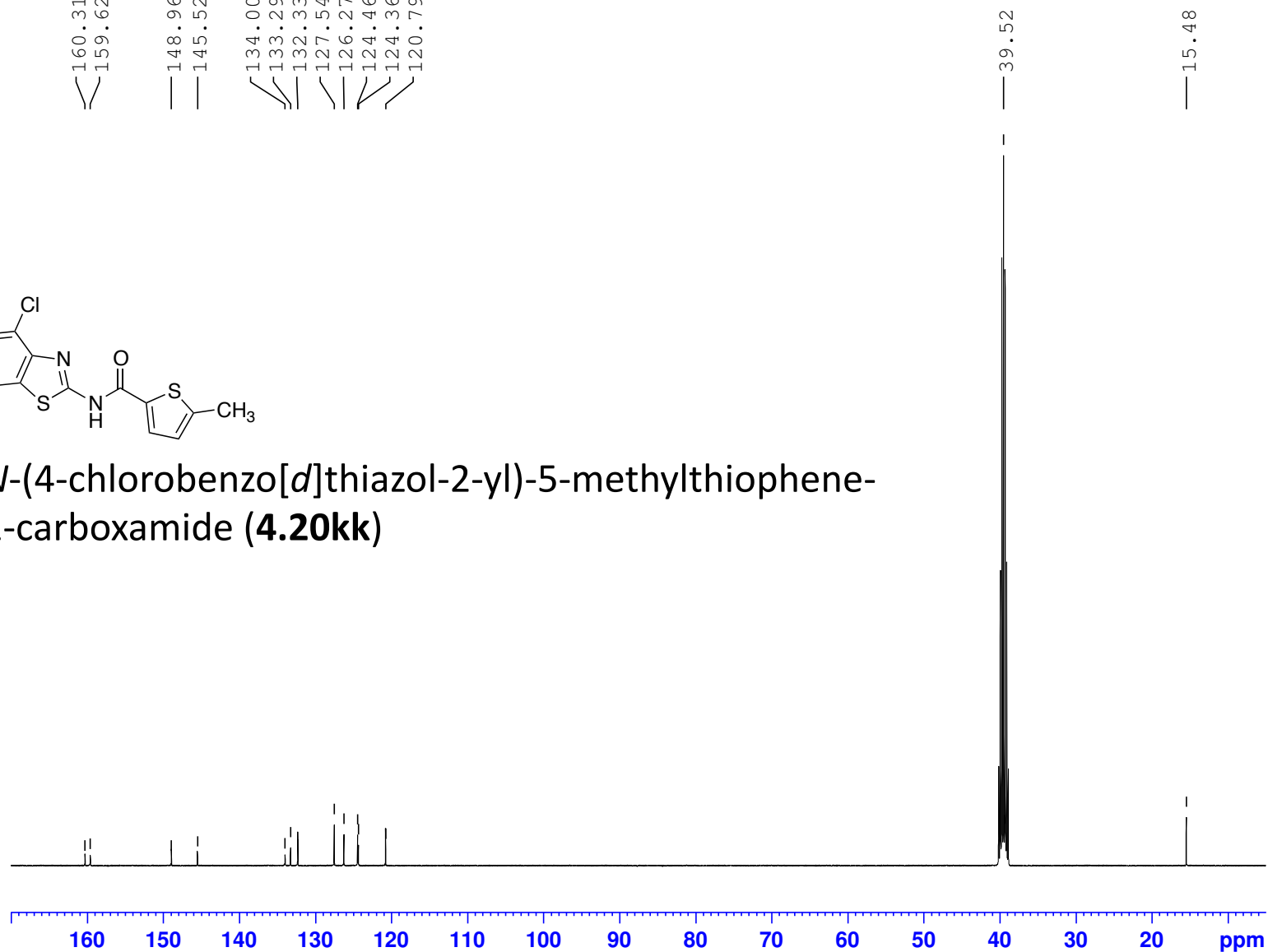
(100 MHz, 297.2 K, DMSO-d6)

GPS482

160.31  
159.62  
148.96  
145.52  
134.00  
133.29  
132.33  
127.54  
126.27  
124.46  
124.36  
120.79

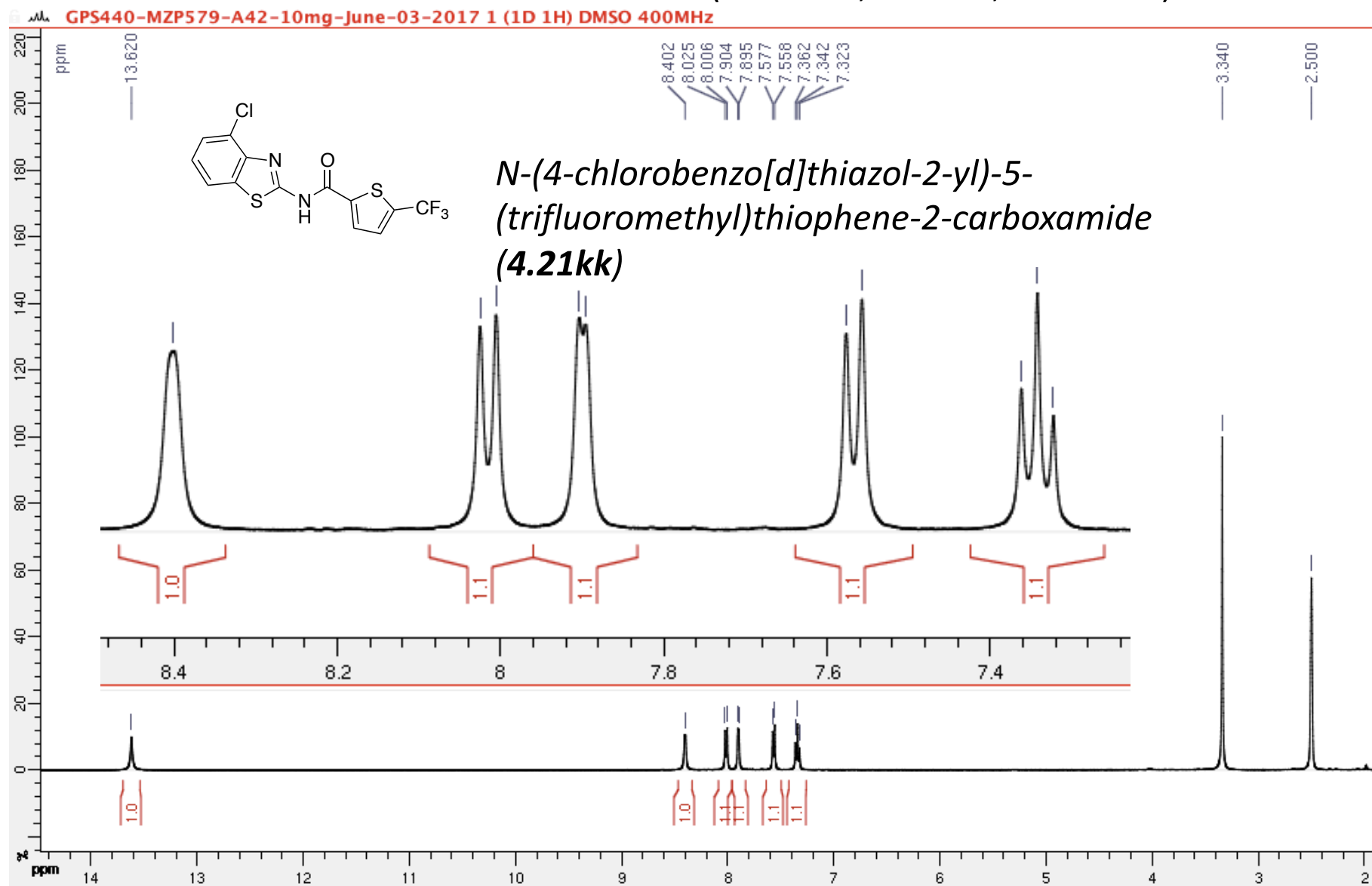


*N*-(4-chlorobenzo[d]thiazol-2-yl)-5-methylthiophene-2-carboxamide (**4.20kk**)



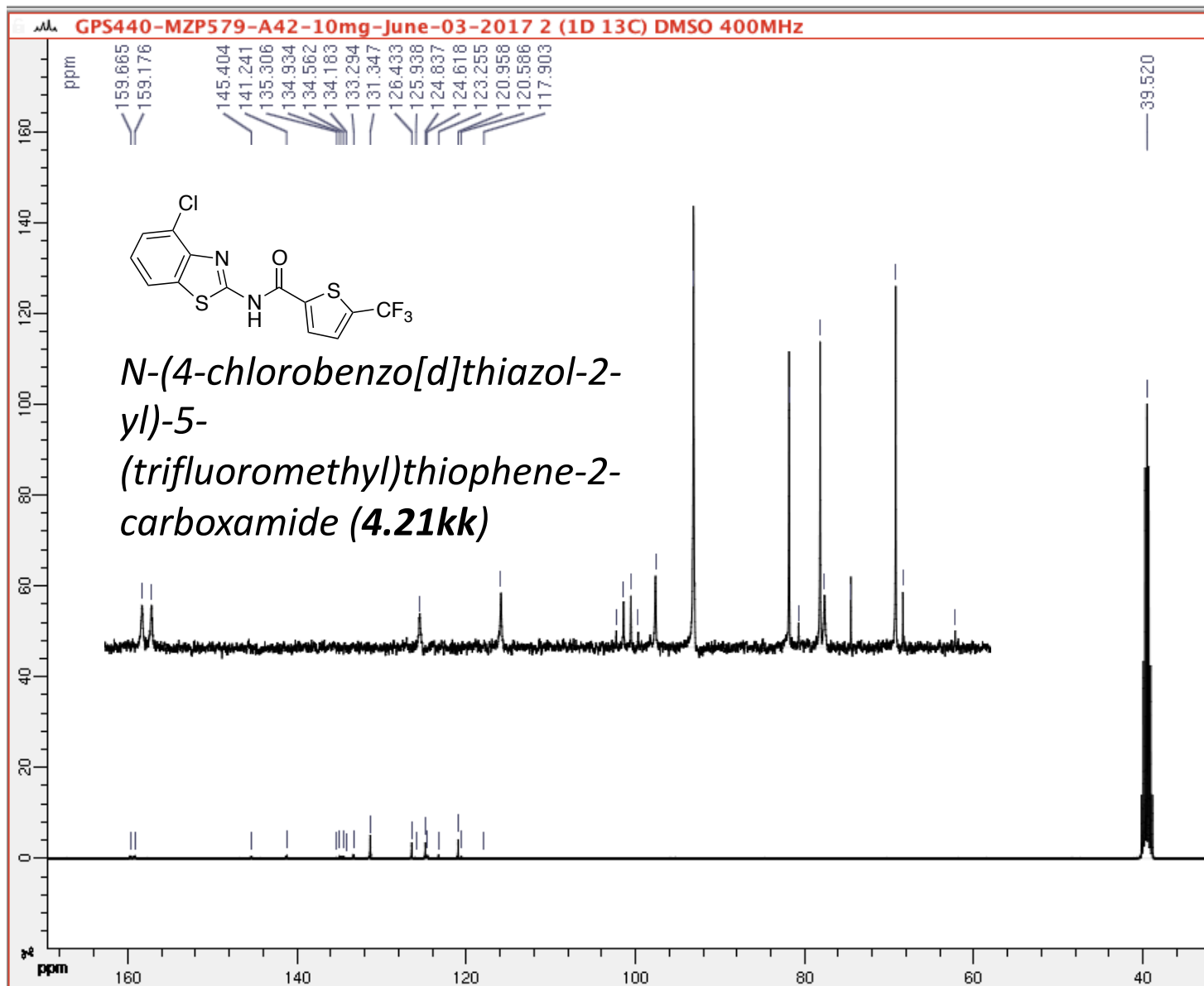
(400 MHz, 297.2 K, DMSO-d6)

GPS440



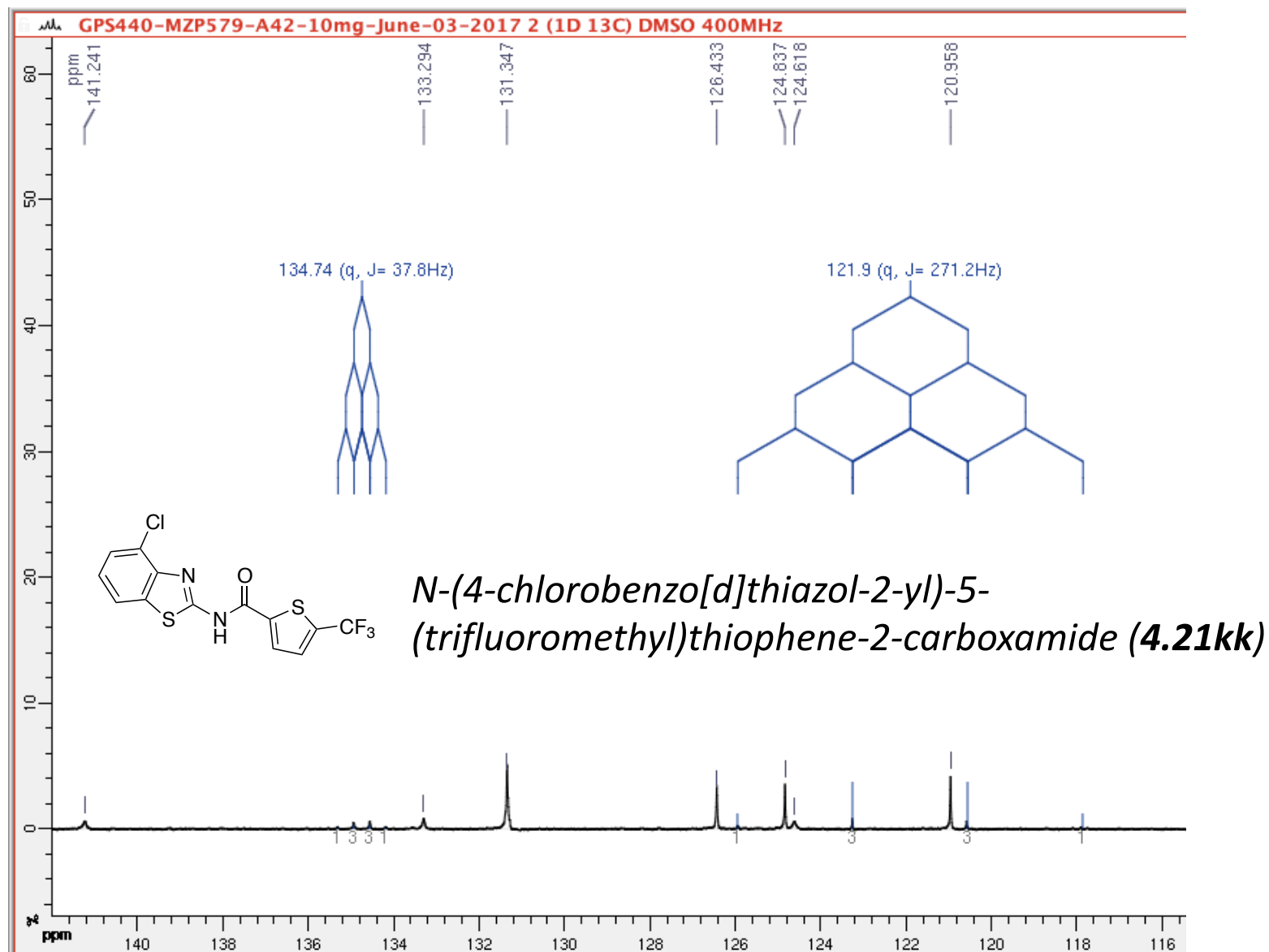
(100 MHz, 297.2 K, DMSO-d6)

GPS440



(100 MHz, 297.2 K, DMSO-d<sub>6</sub>)

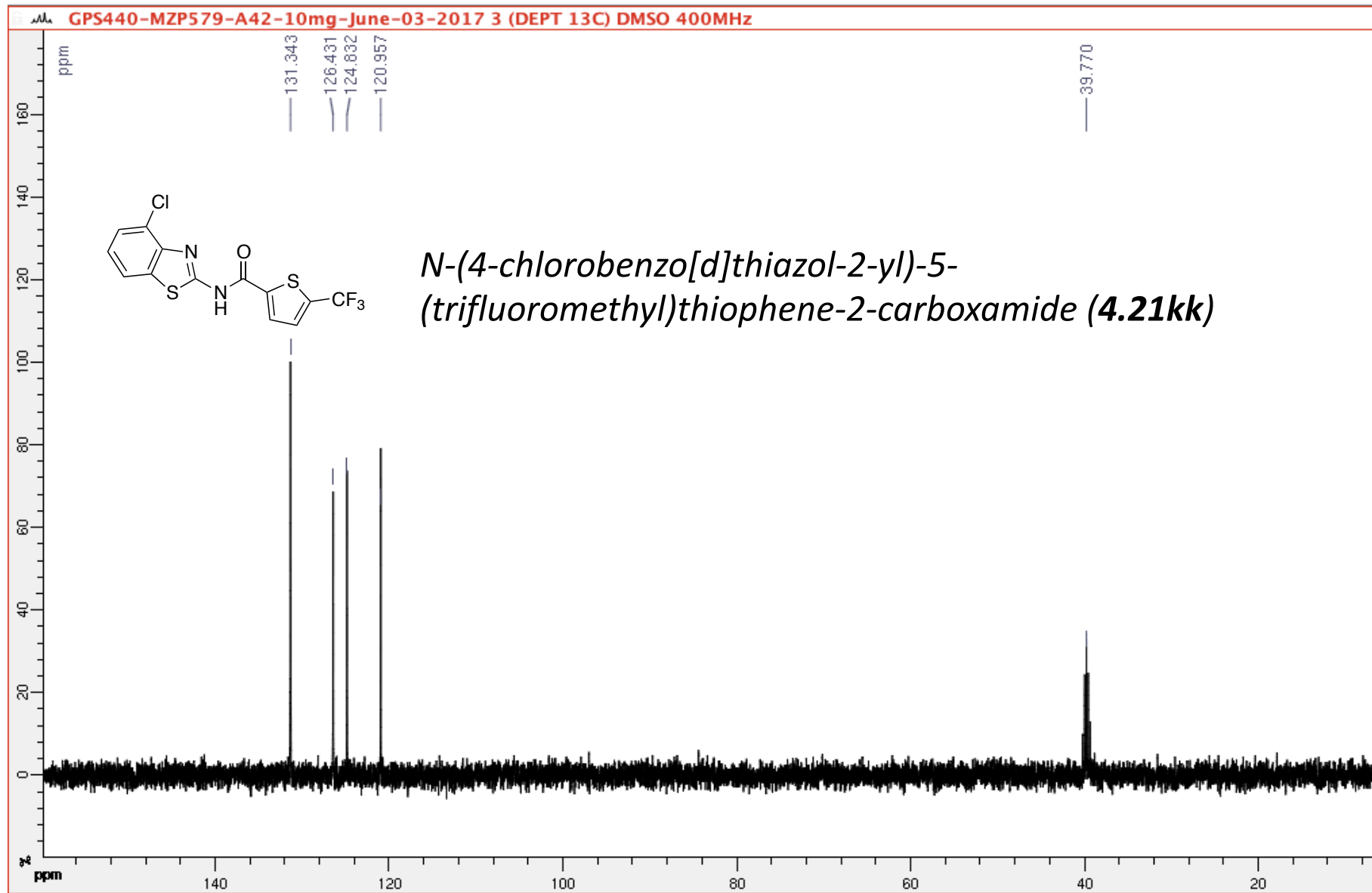
GPS440



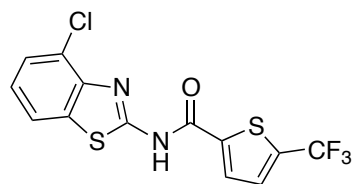
DEPT 135

(100 MHz, 297.2 K, DMSO-d6)

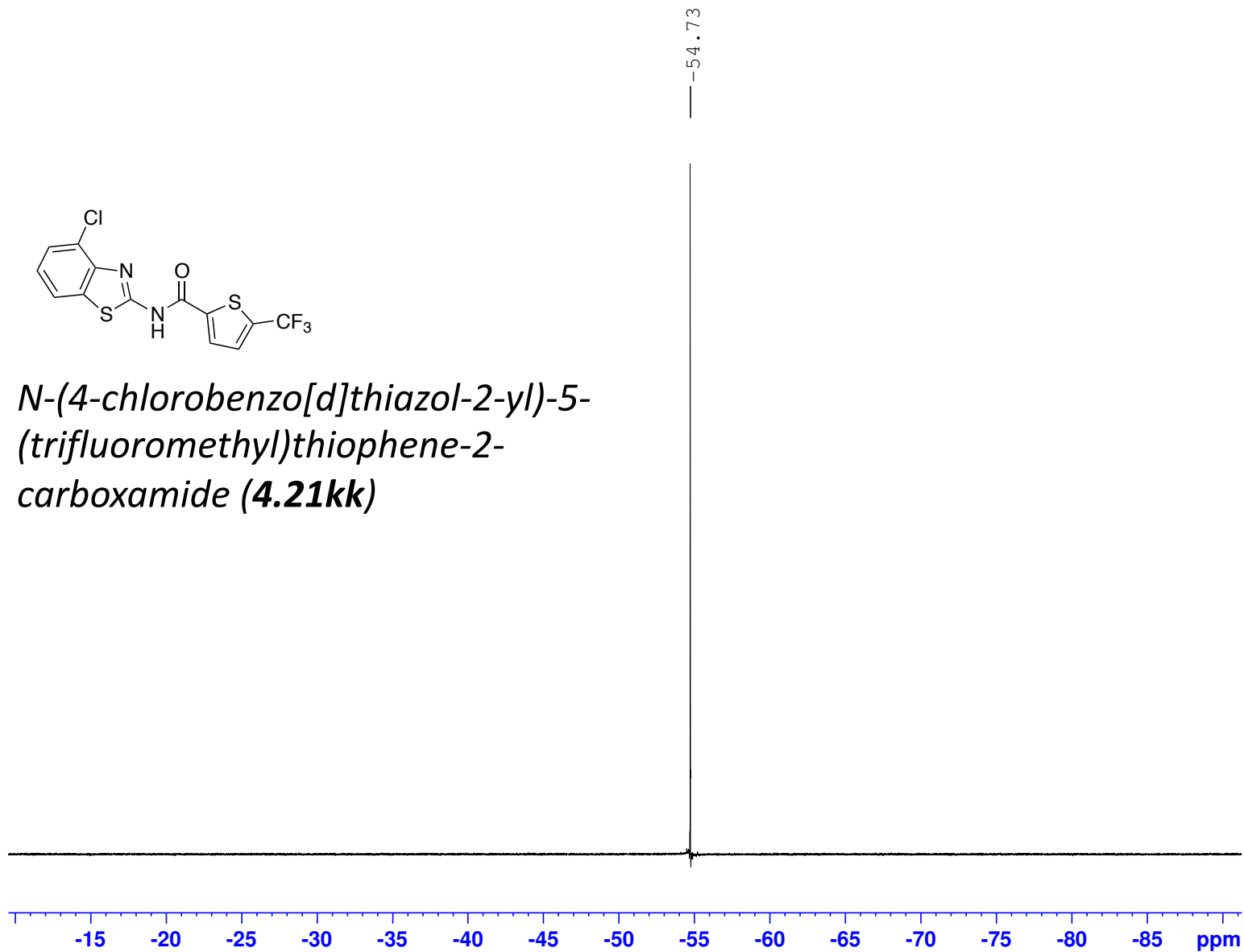
GPS440





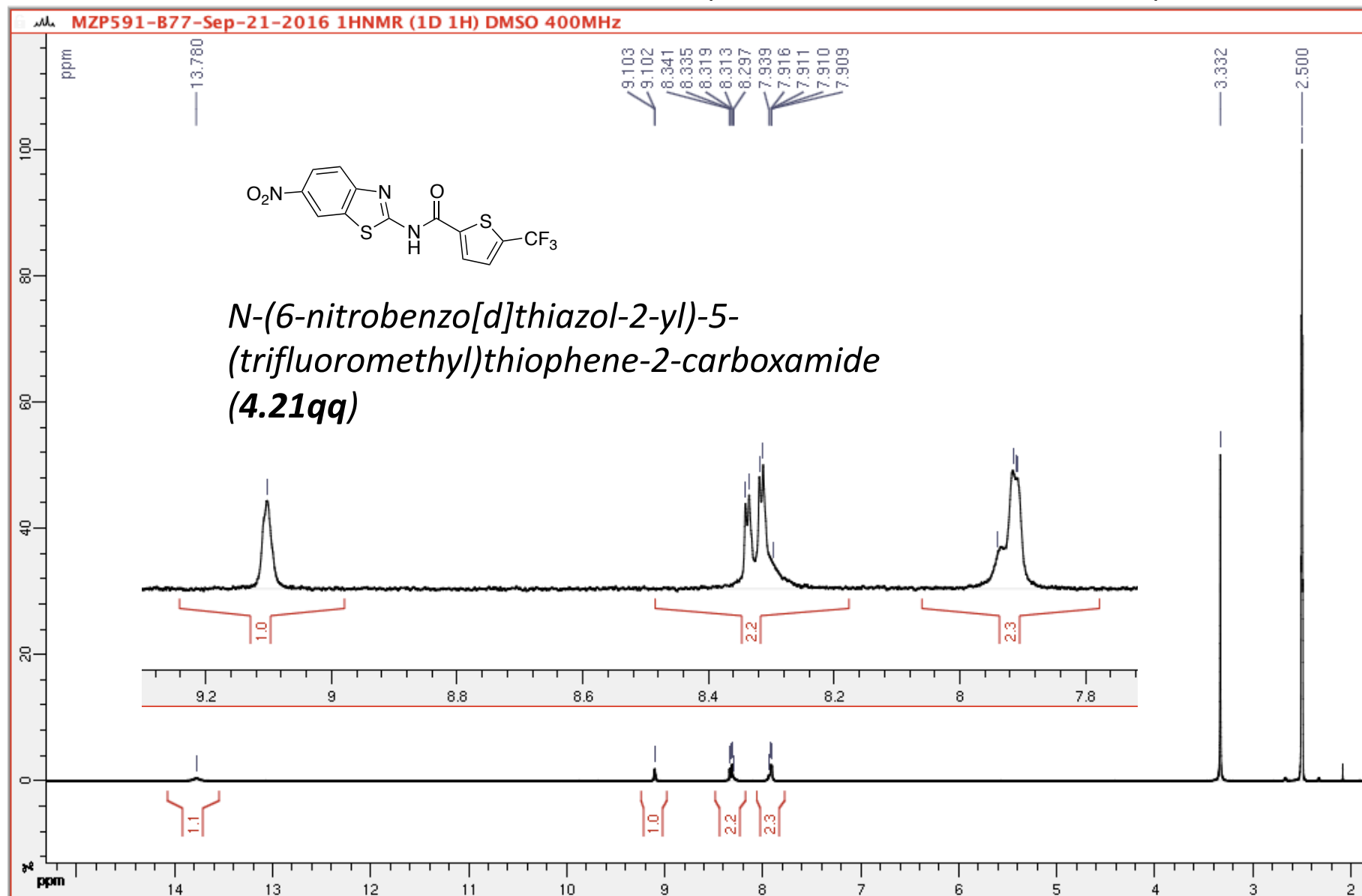


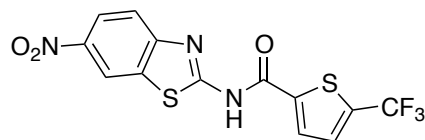
*N*-(4-chlorobenzo[d]thiazol-2-yl)-5-(trifluoromethyl)thiophene-2-carboxamide (**4.21kk**)



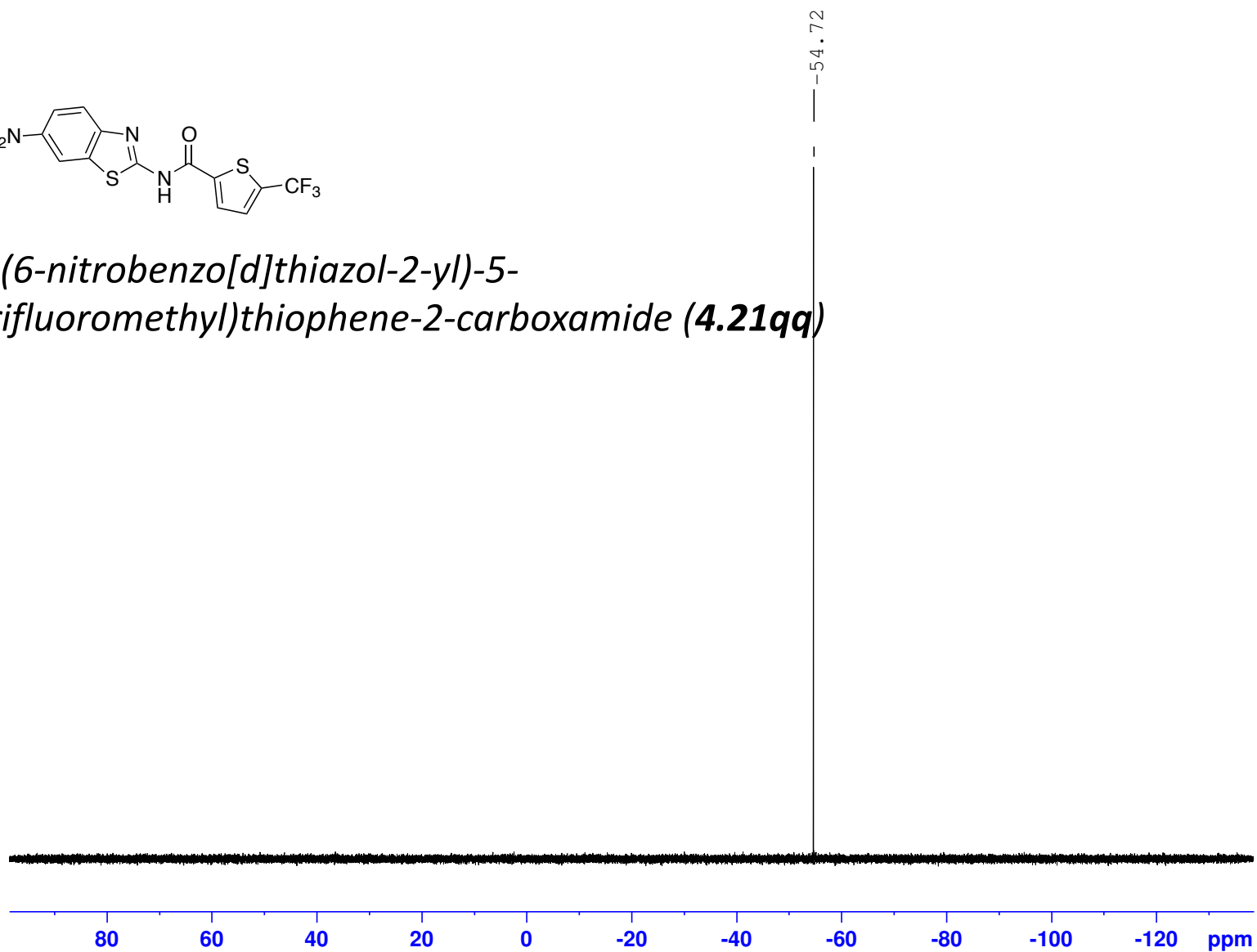
(400 MHz, 297.2 K, DMSO-d6)

GPS483



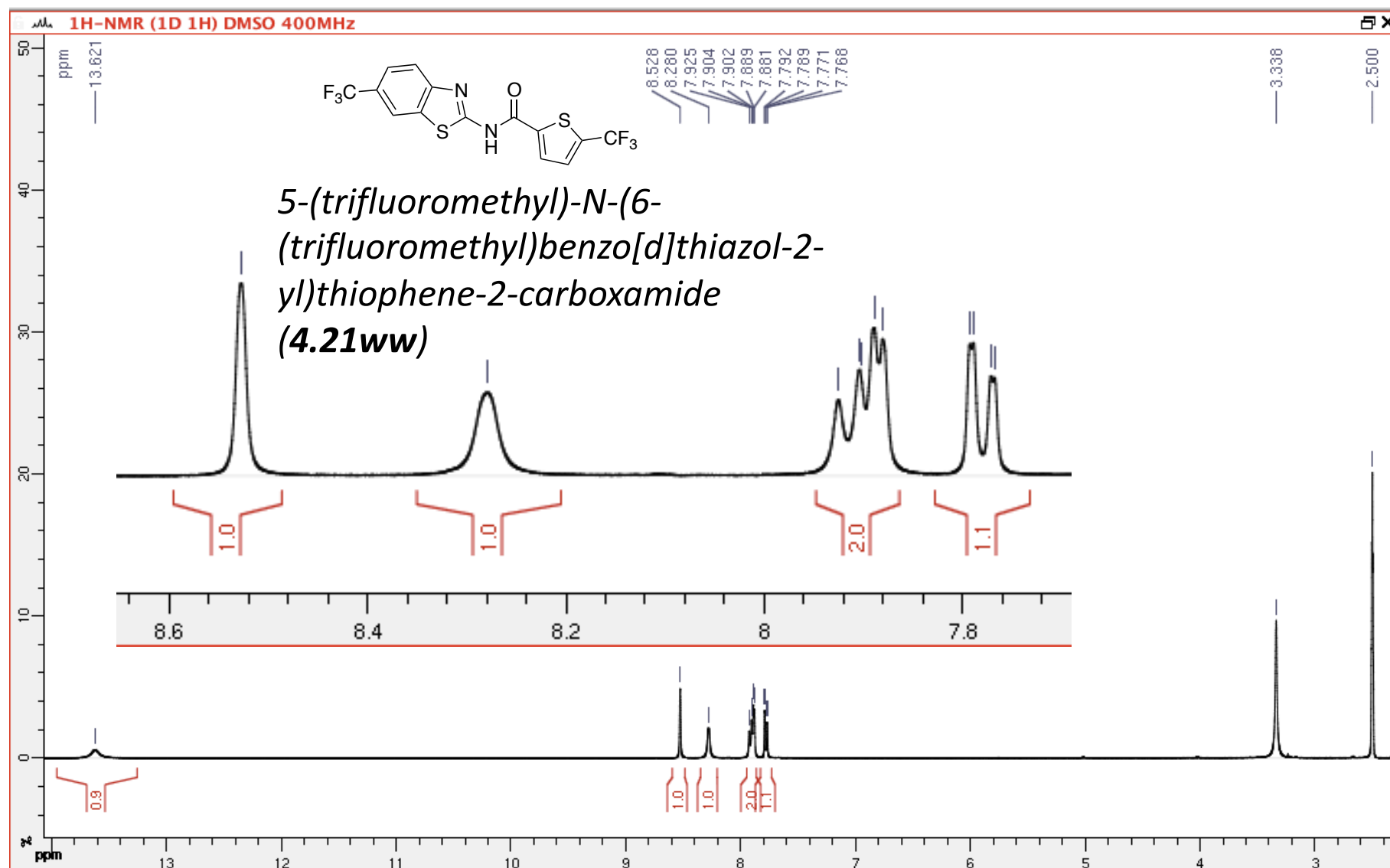


*N*-(6-nitrobenzo[d]thiazol-2-yl)-5-(trifluoromethyl)thiophene-2-carboxamide (**4.21qq**)



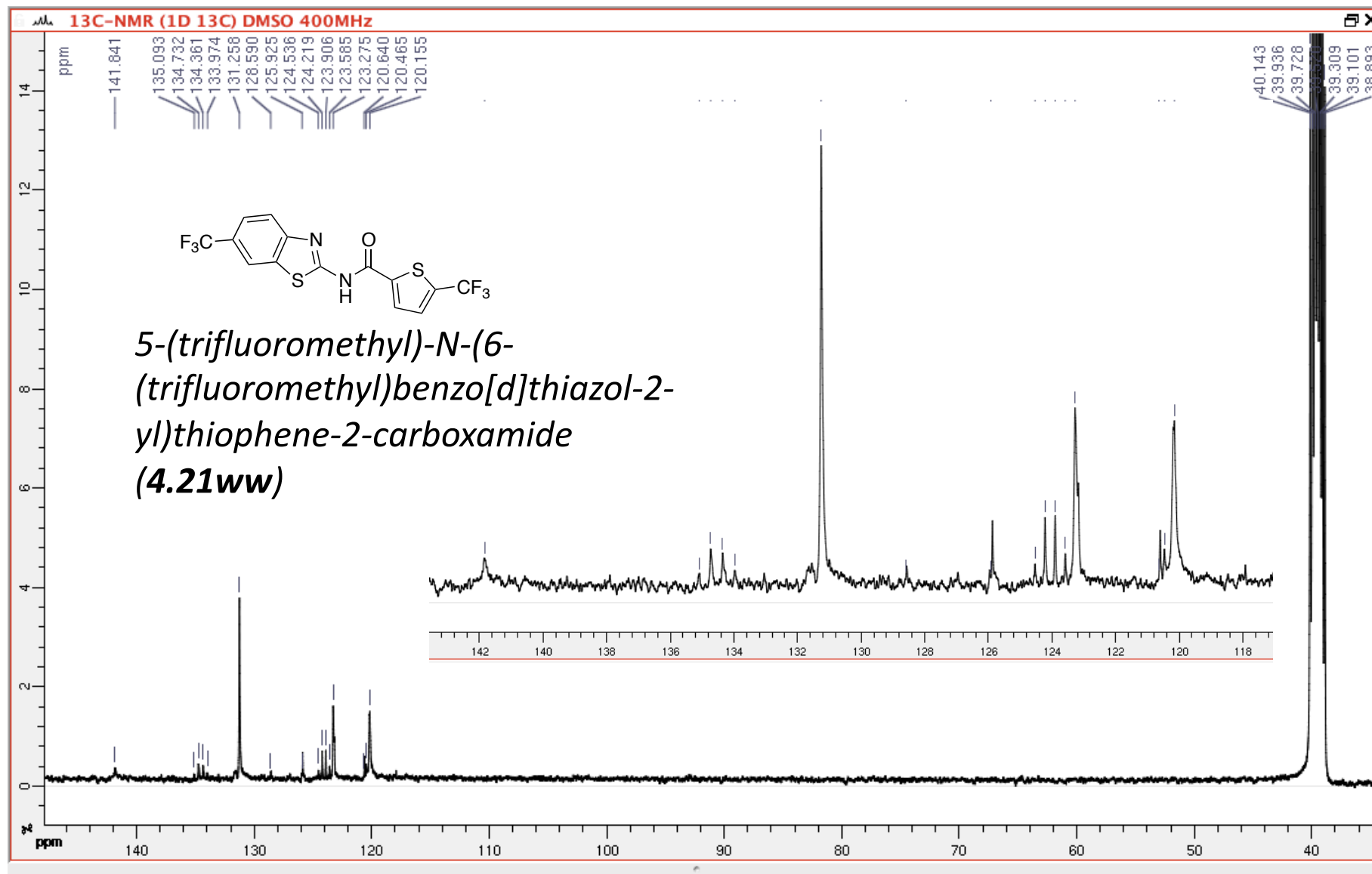
(400 MHz, 297.2 K, DMSO-d6)

GPS485



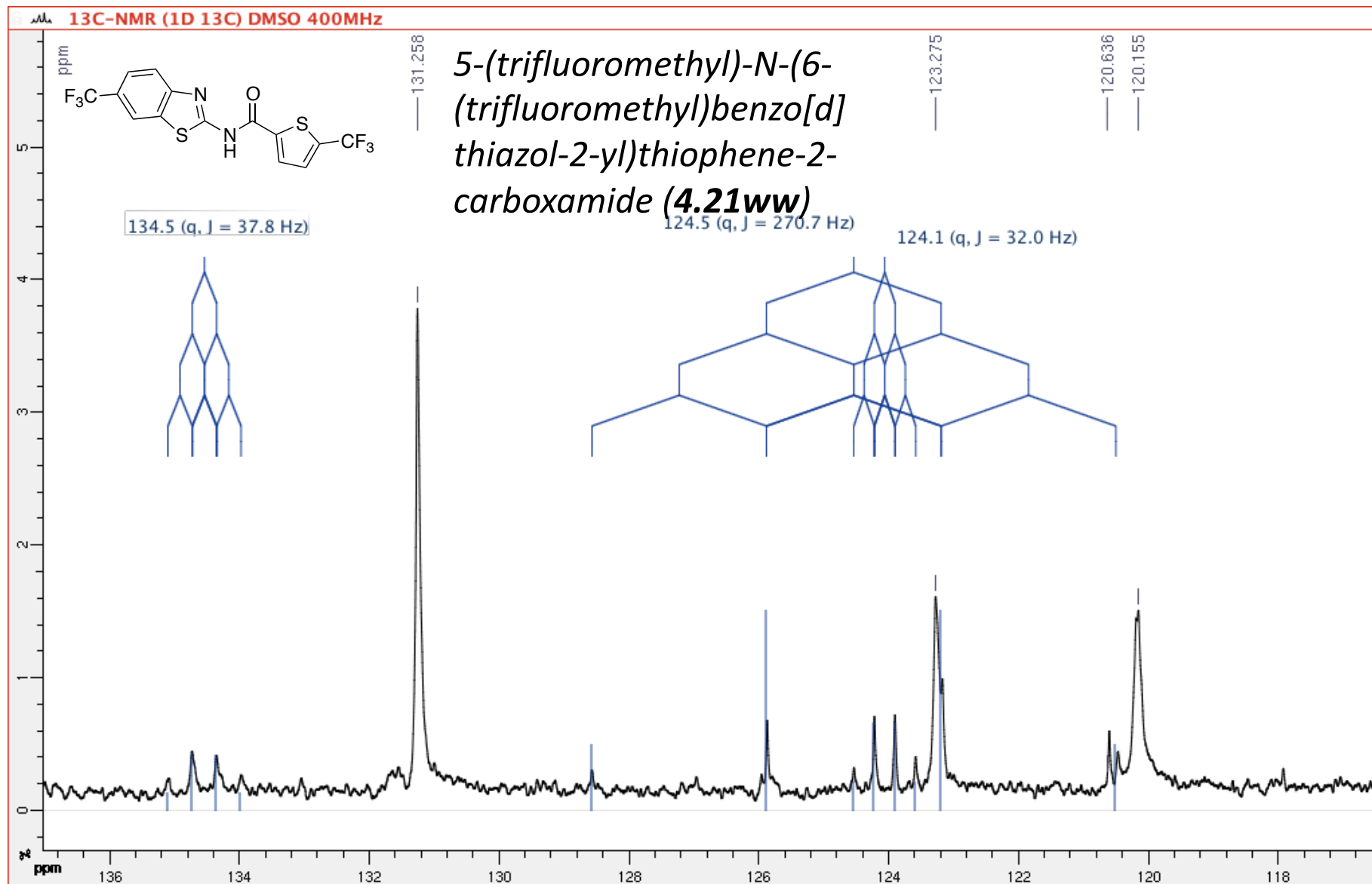
(100 MHz, 297.2 K, DMSO-d6)

GPS485



(100 MHz, 297.2 K, DMSO-d6)

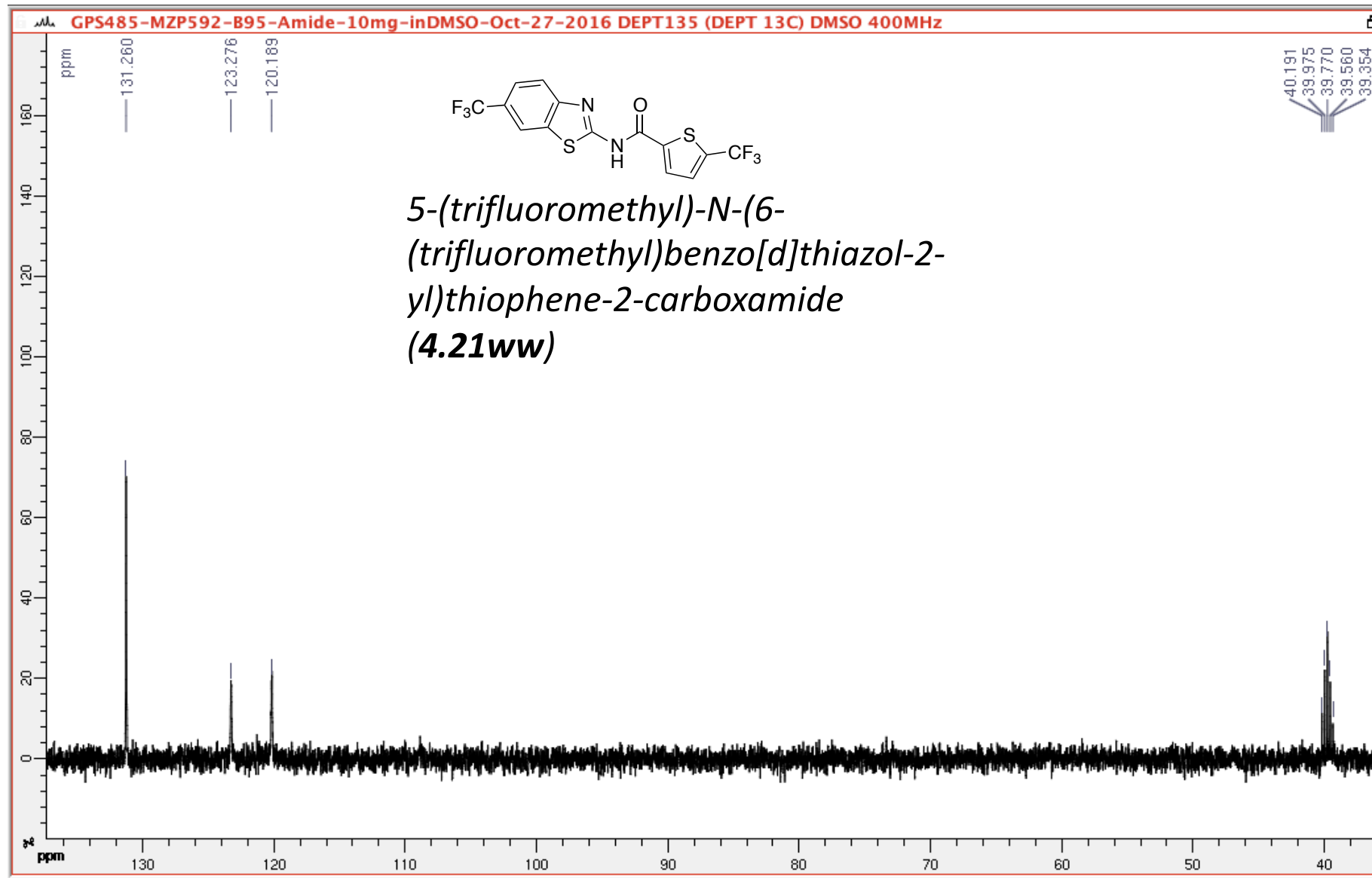
GPS485

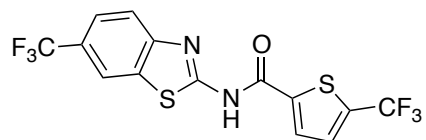


DEPT 135

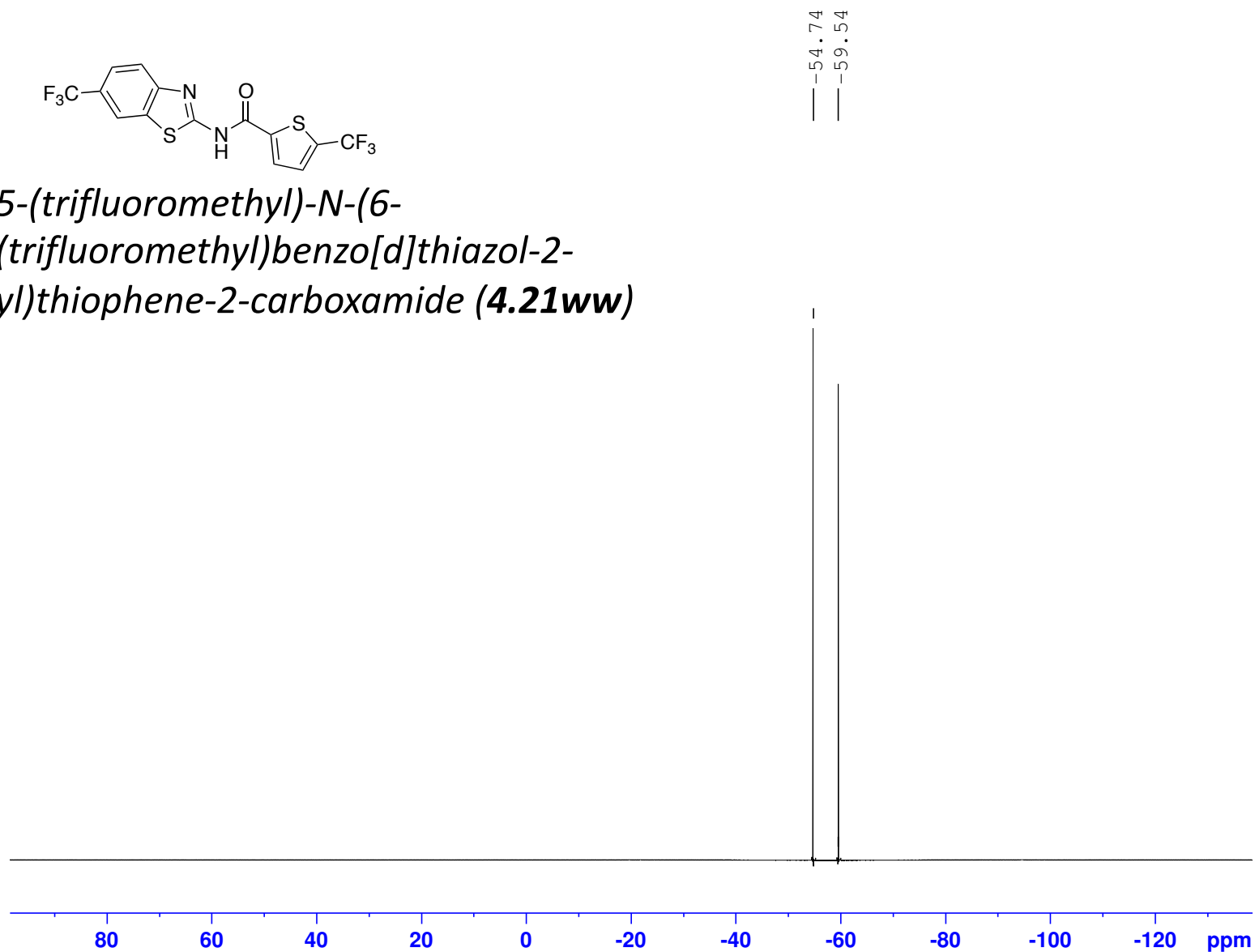
(100 MHz, 297.2 K, DMSO-d6)

GPS485





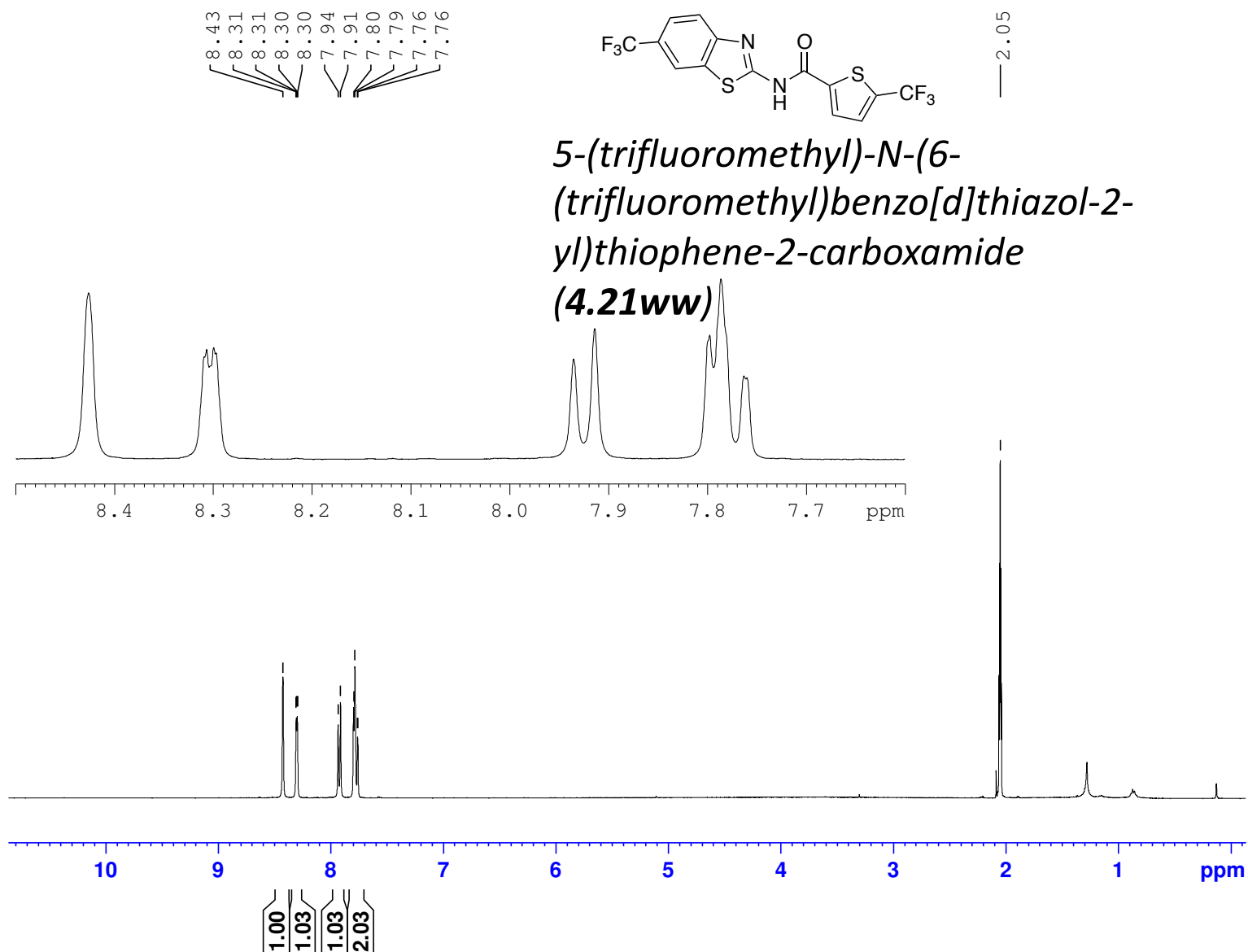
*5-(trifluoromethyl)-N-(6-(trifluoromethyl)benzo[d]thiazol-2-yl)thiophene-2-carboxamide (4.21ww)*





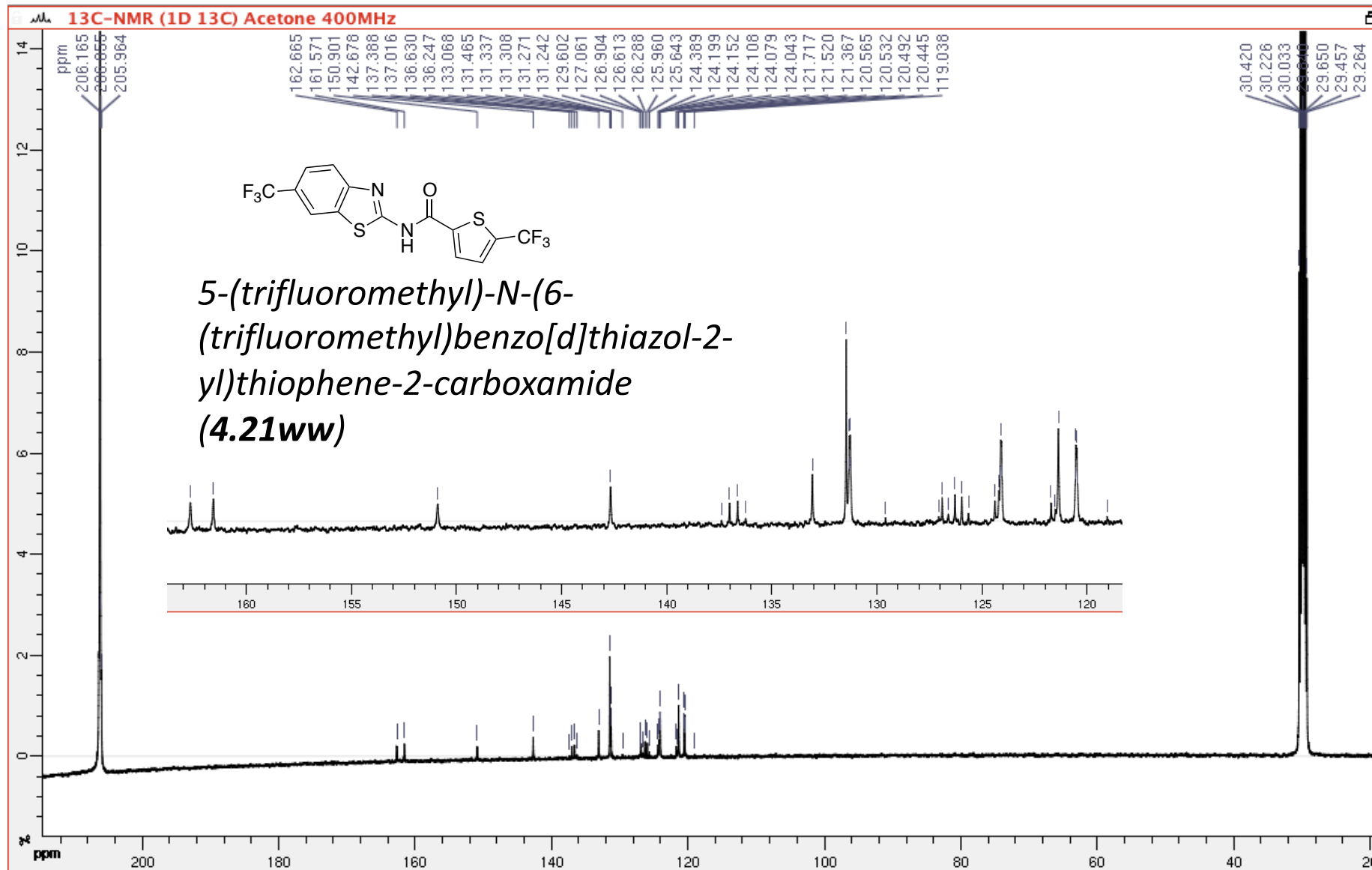
GPS485-MZP592=B95-in acetone-1H-NMR-Oct-26-2016

(400 MHz, 297.2 K, Acetone-d6) GPS485



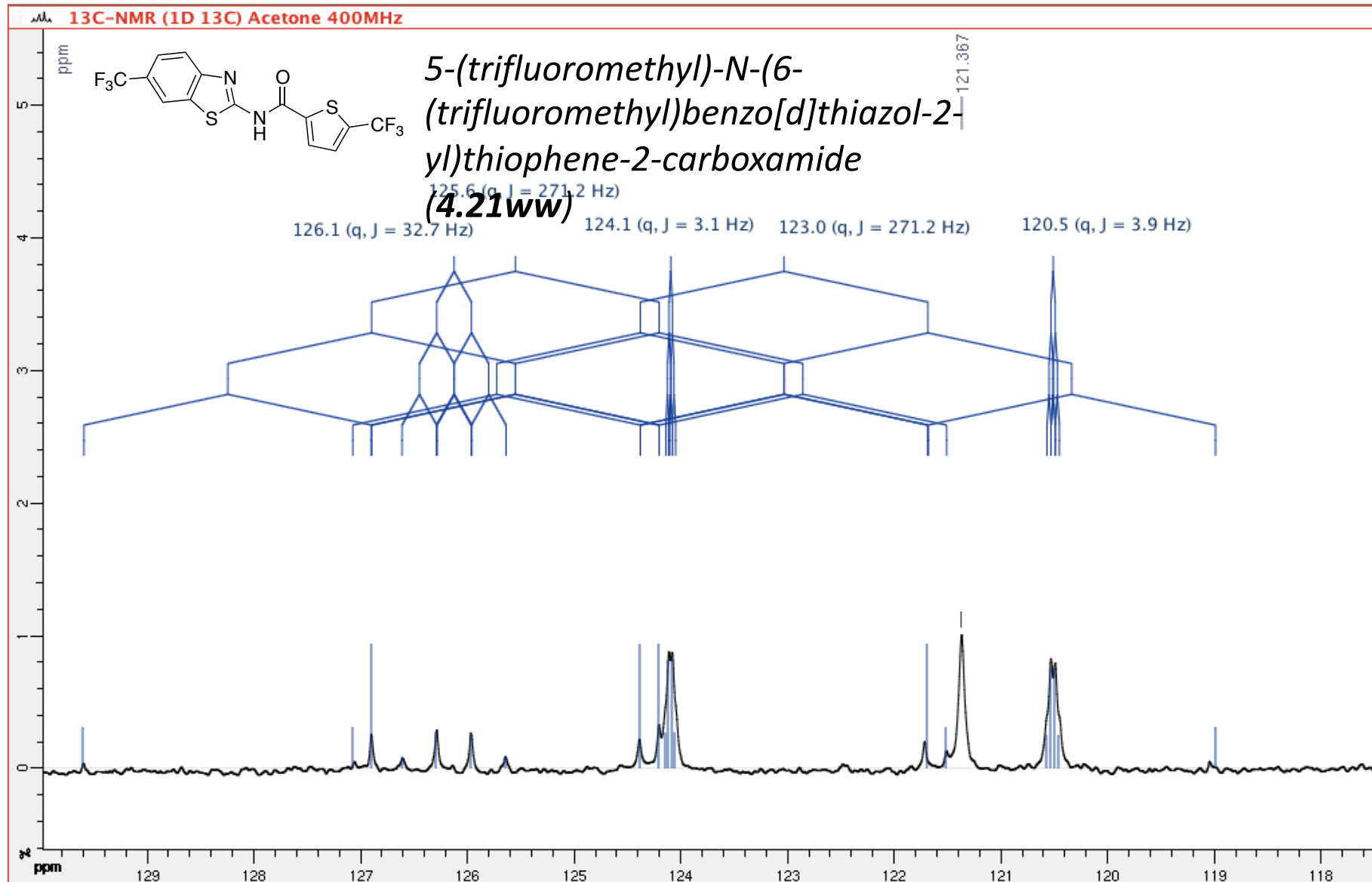
In acetone

(100 MHz, 297.2 K, Acetone-d<sub>6</sub>) GPS485



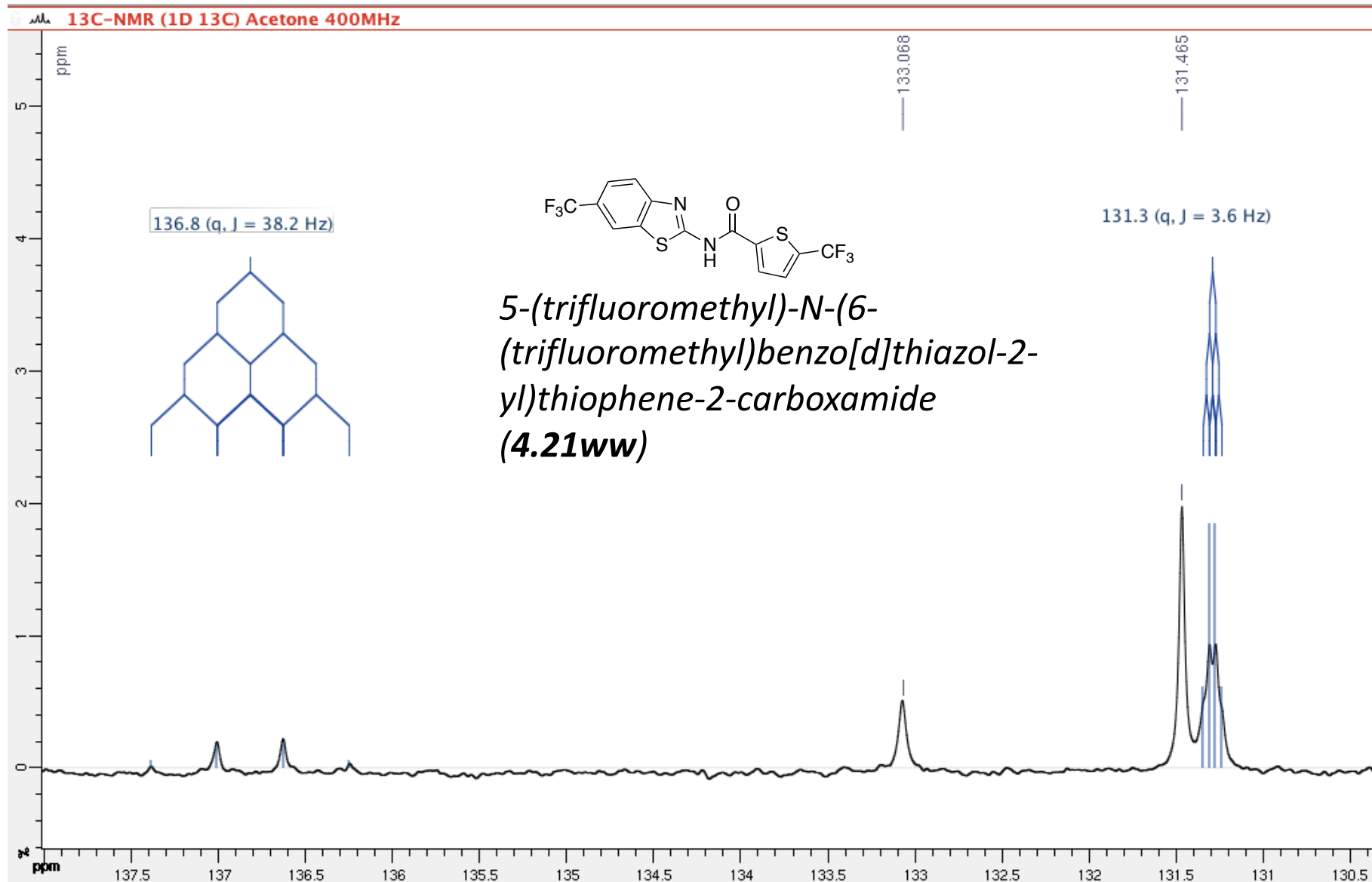
In acetone

(100 MHz, 297.2 K, Acetone-d6) GPS485



In acetone

(100 MHz, 297.2 K, Acetone-d<sub>6</sub>) GPS485

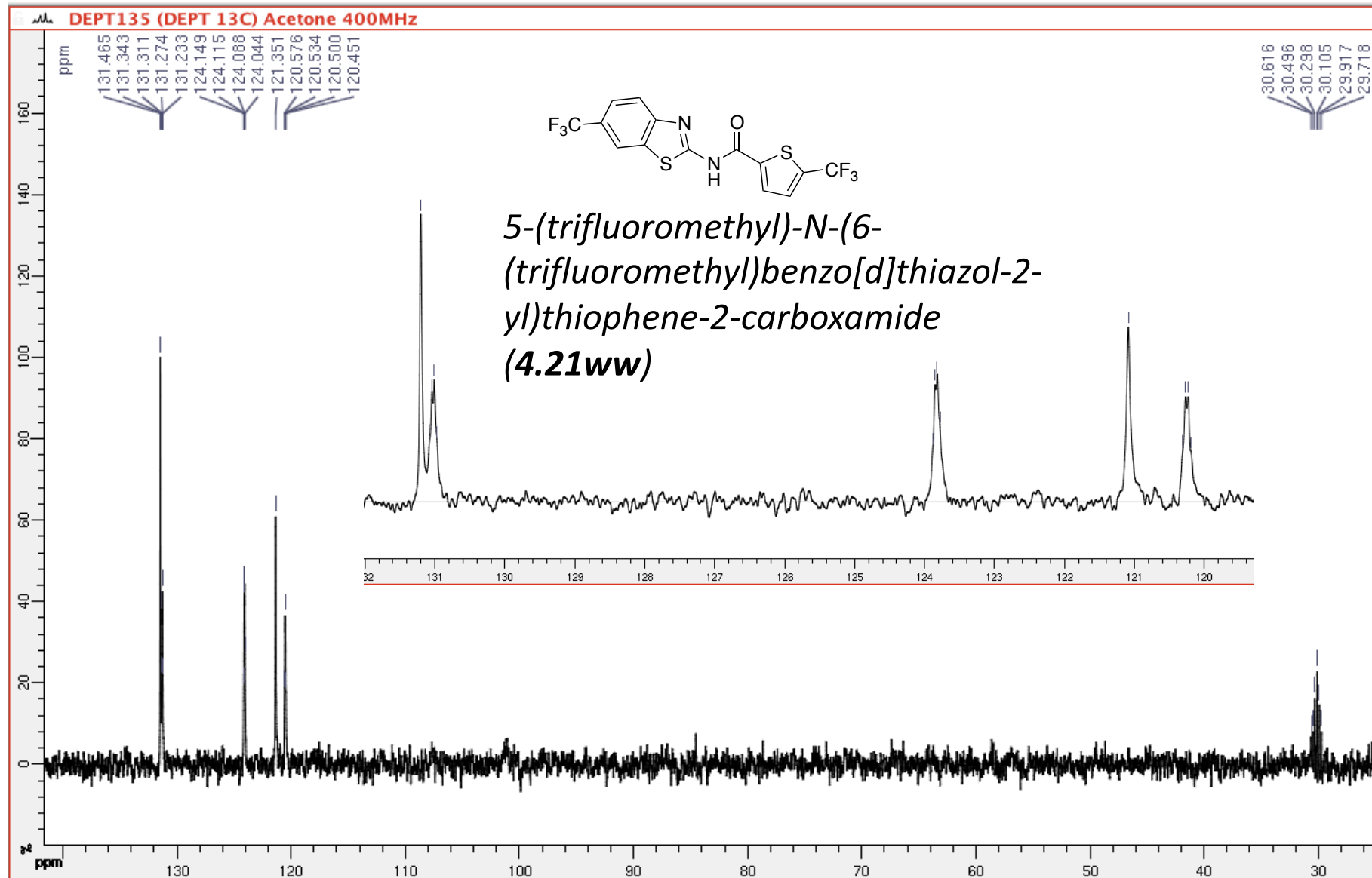


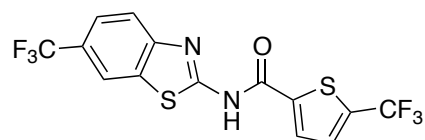
In acetone

DEPT 135

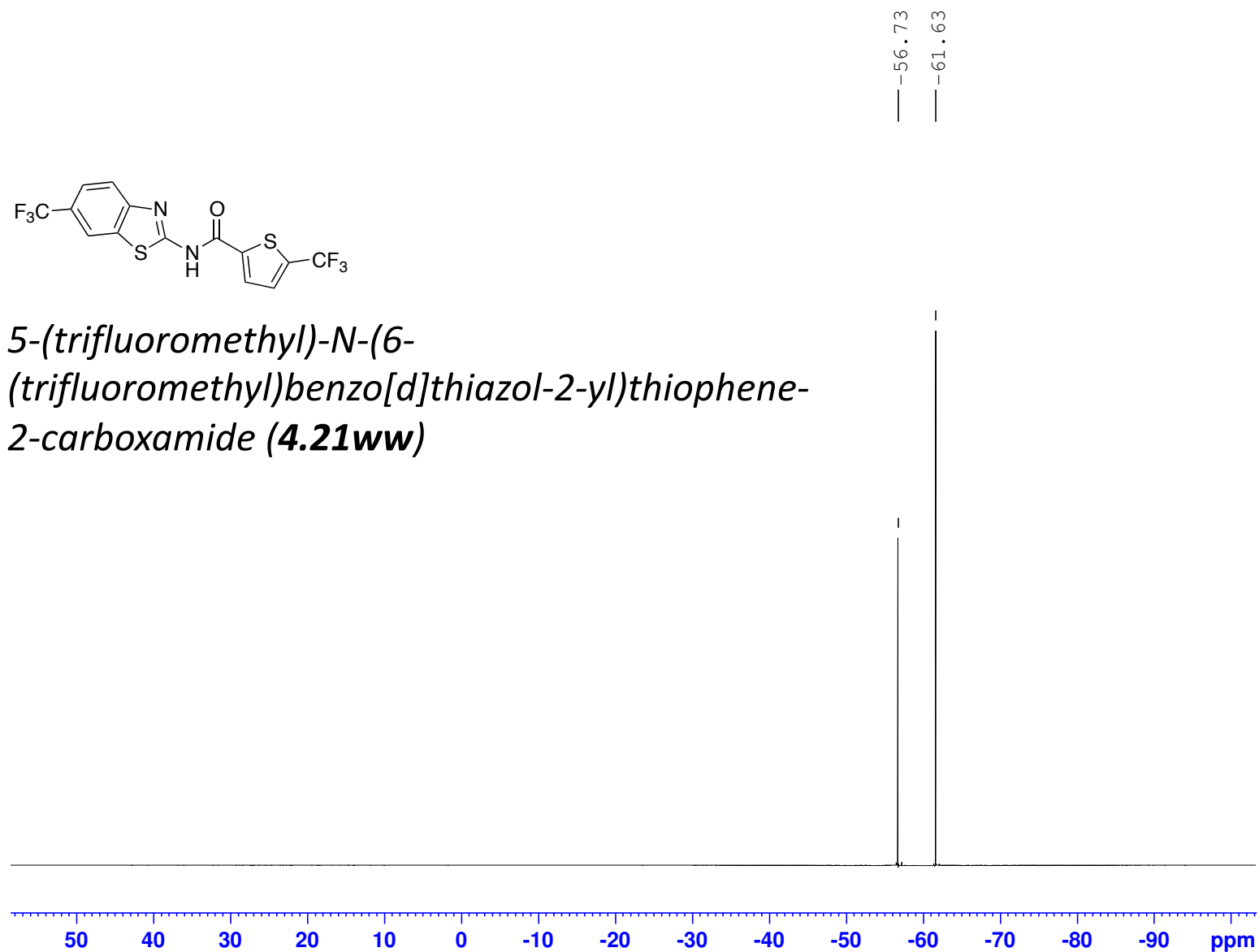
(100 MHz, 297.2 K, Acetone-d<sub>6</sub>)

GPS485

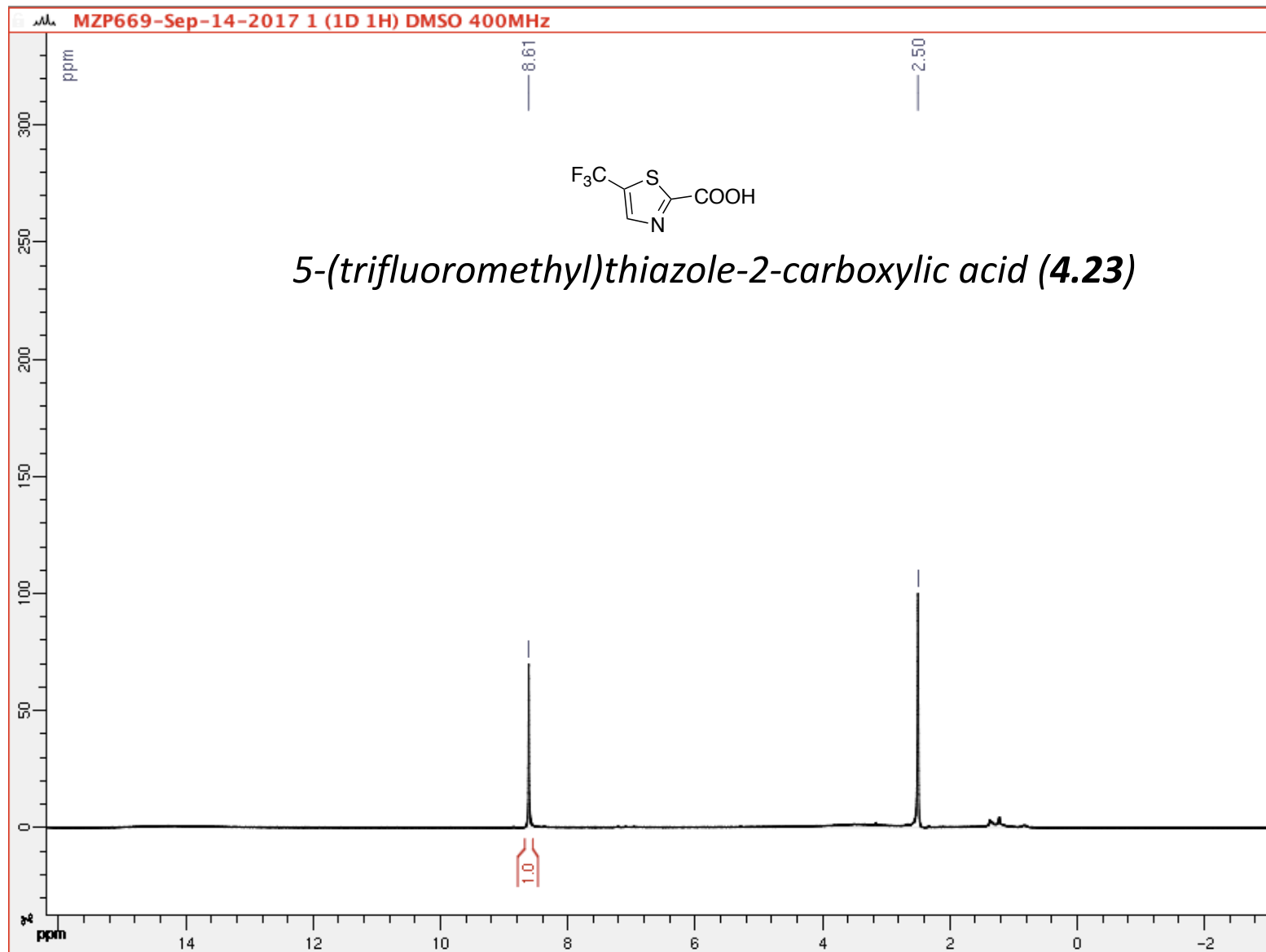




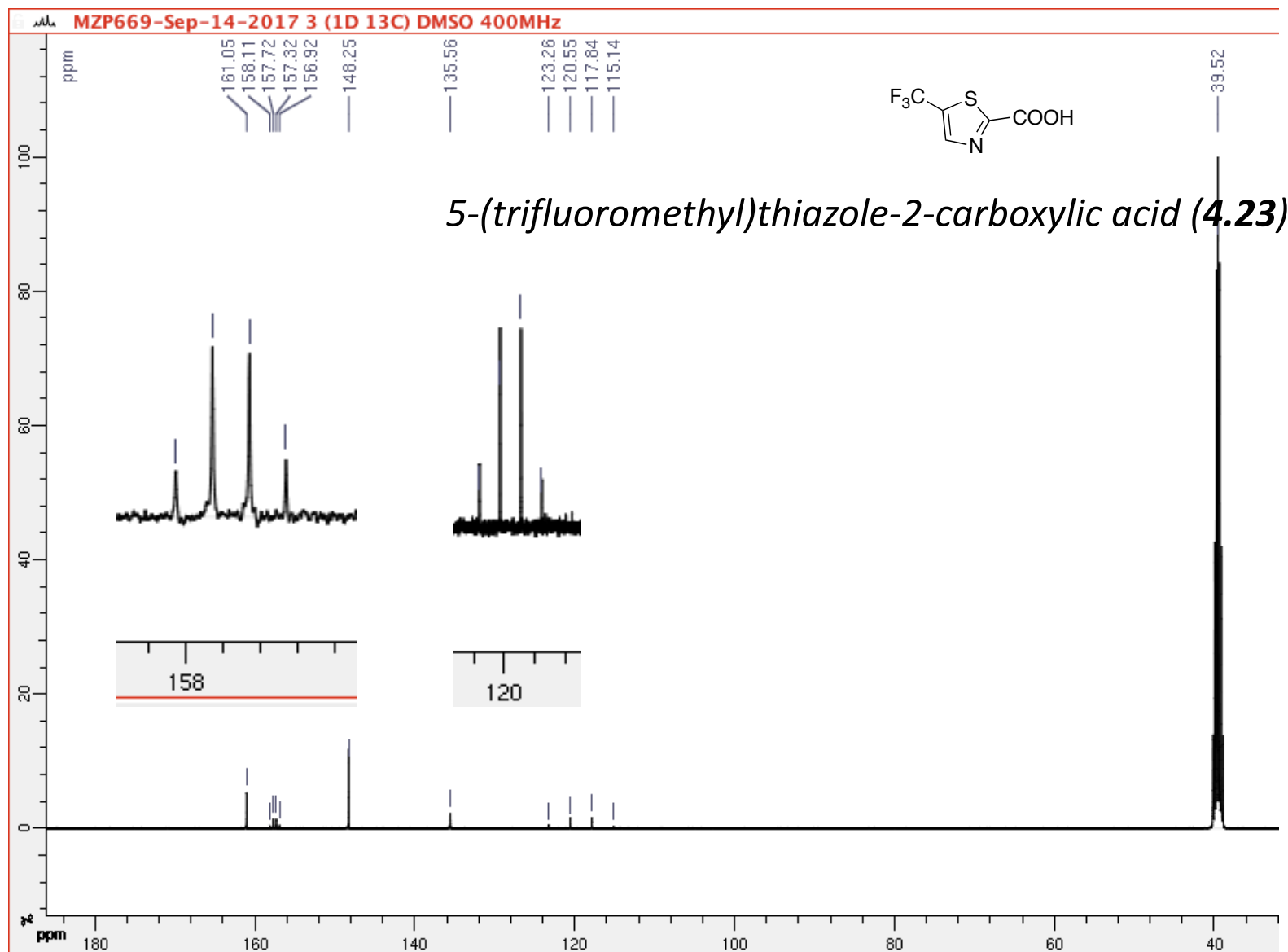
*5-(trifluoromethyl)-N-(6-(trifluoromethyl)benzo[d]thiazol-2-yl)thiophene-2-carboxamide (4.21ww)*



(400 MHz, 297.2 K, DMSO-d6)

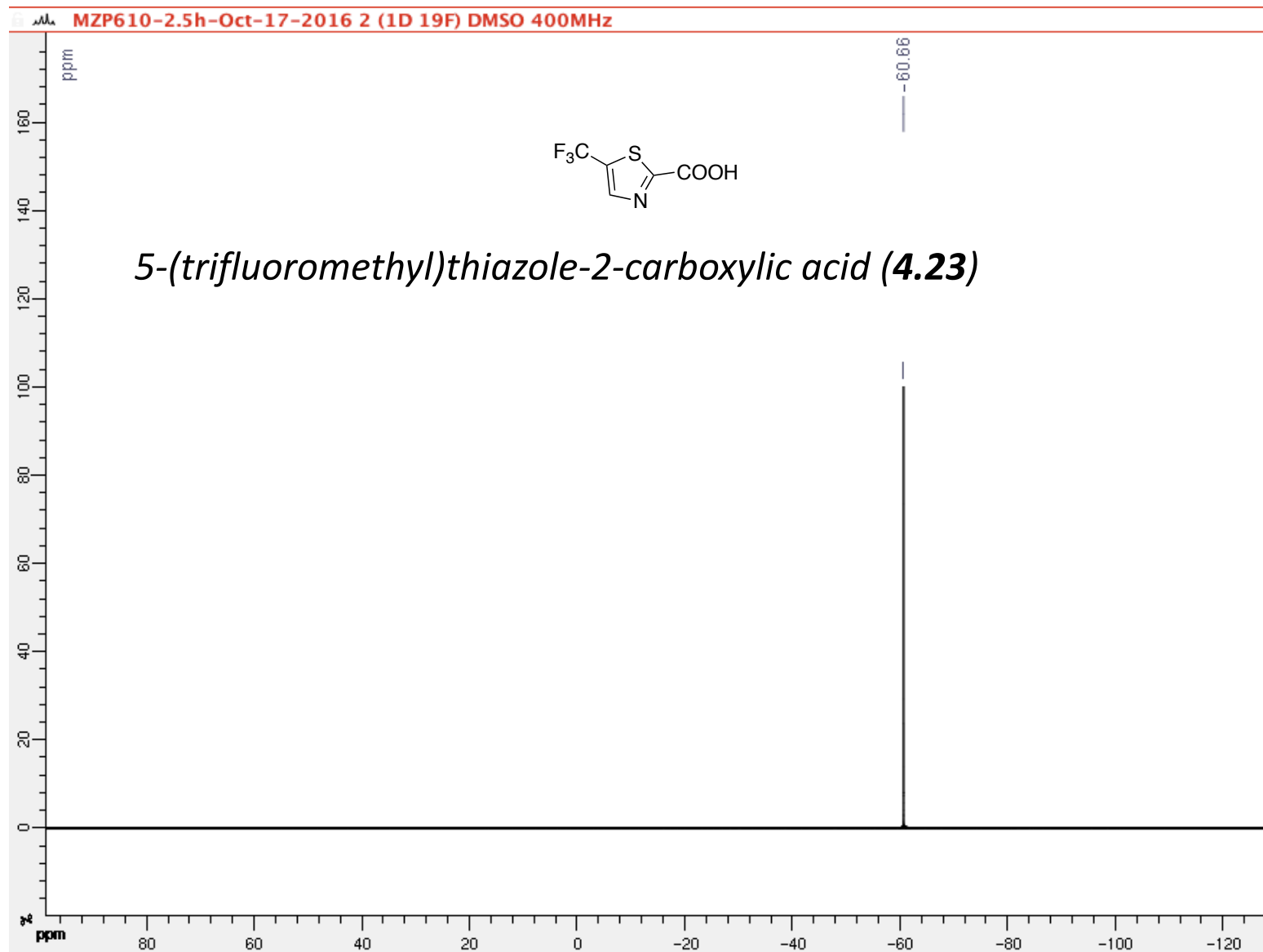


(100 MHz, 297.2 K, DMSO-d6)





(400 MHz, 297.2 K, DMSO-d6)

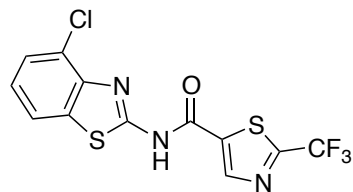


GPS488-MZP611-A42-10mg-1H-NMR-June-03-2017

(400 MHz, 297.2 K, DMSO-d6)

GPS488

13.84



9.10

8.04

8.02

7.59

7.57

7.38

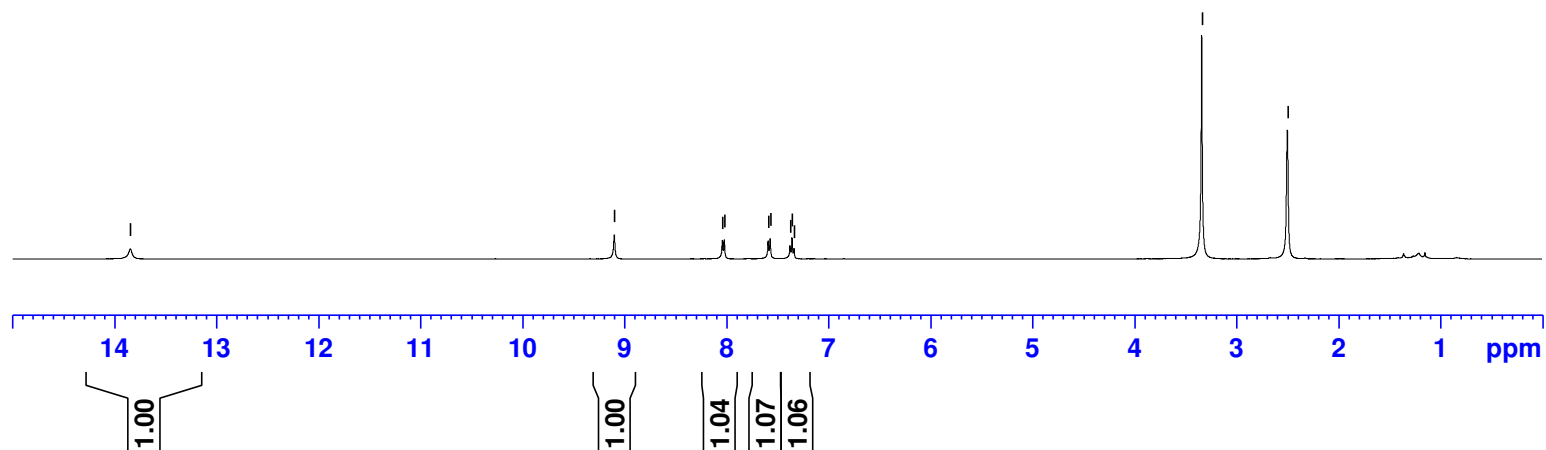
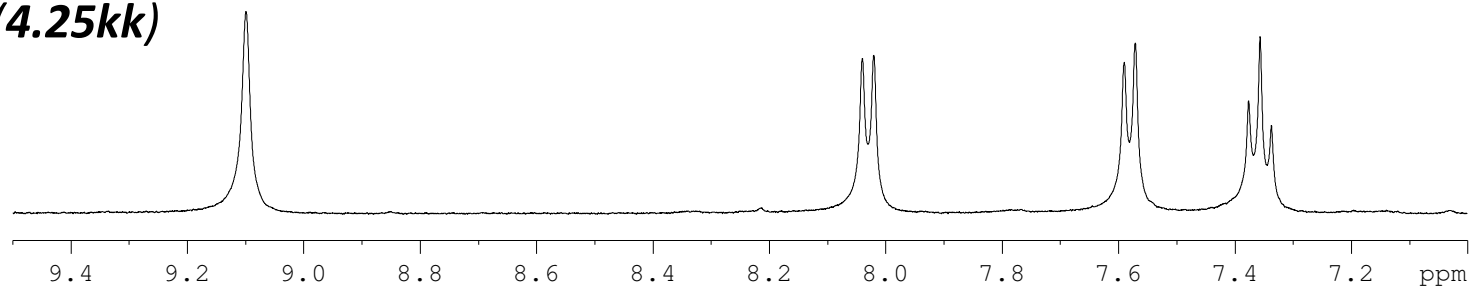
7.36

7.34

3.34

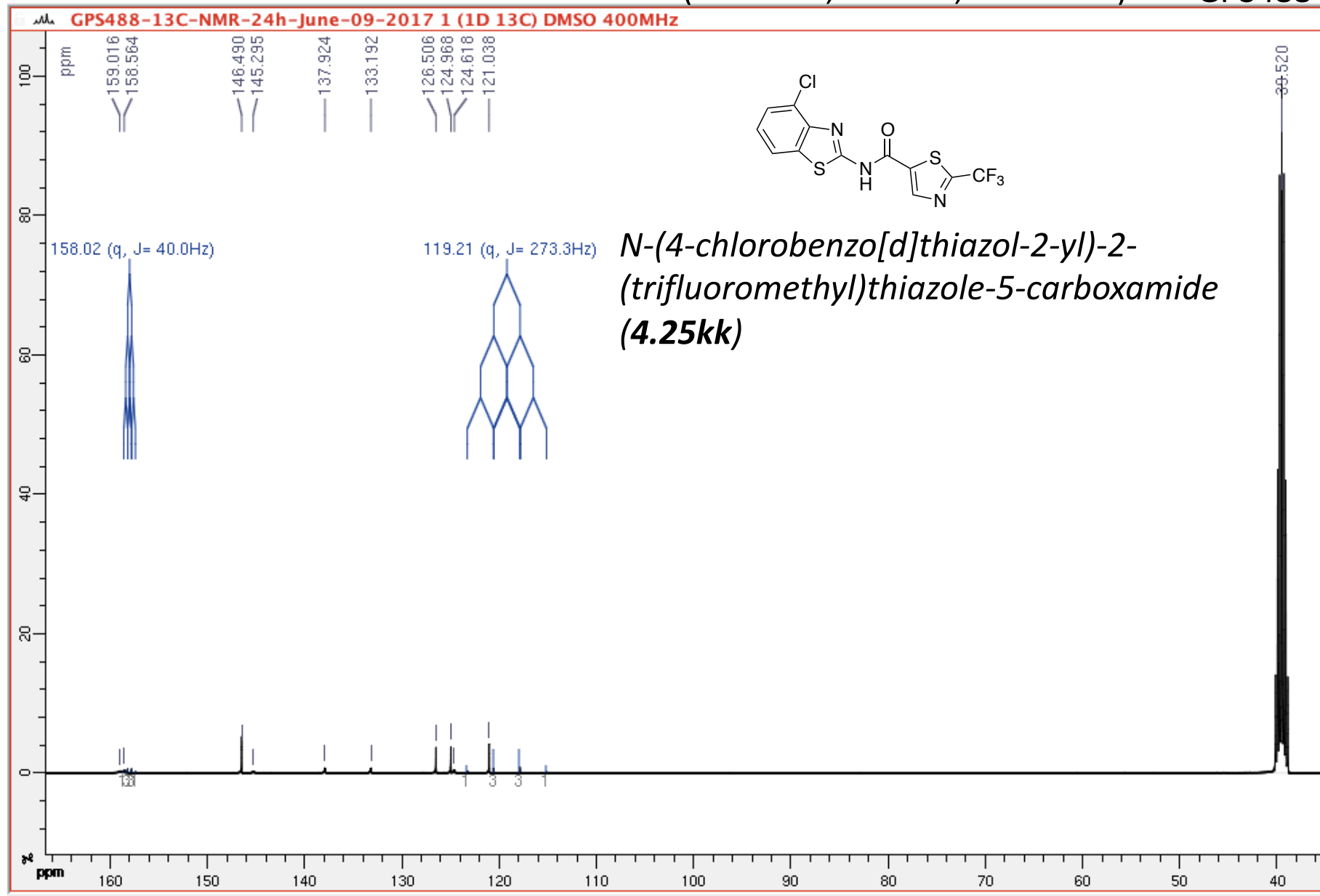
2.50

*N*-(4-chlorobenzo[d]thiazol-2-yl)-2-(trifluoromethyl)thiazole-5-carboxamide  
(4.25kk)



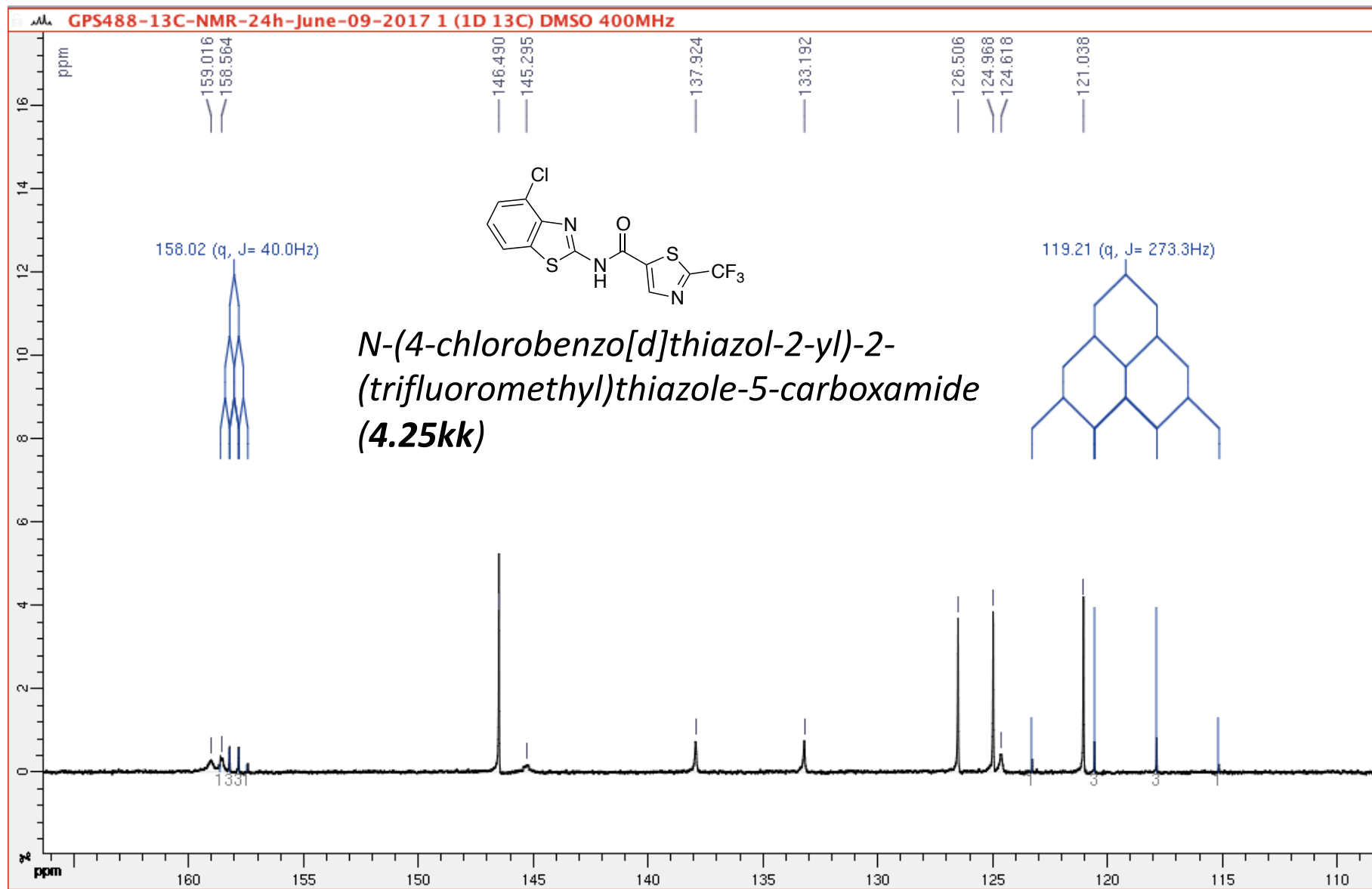
(100 MHz, 297.2 K, DMSO-d6)

GPS488



(100 MHz, 297.2 K, DMSO-d6)

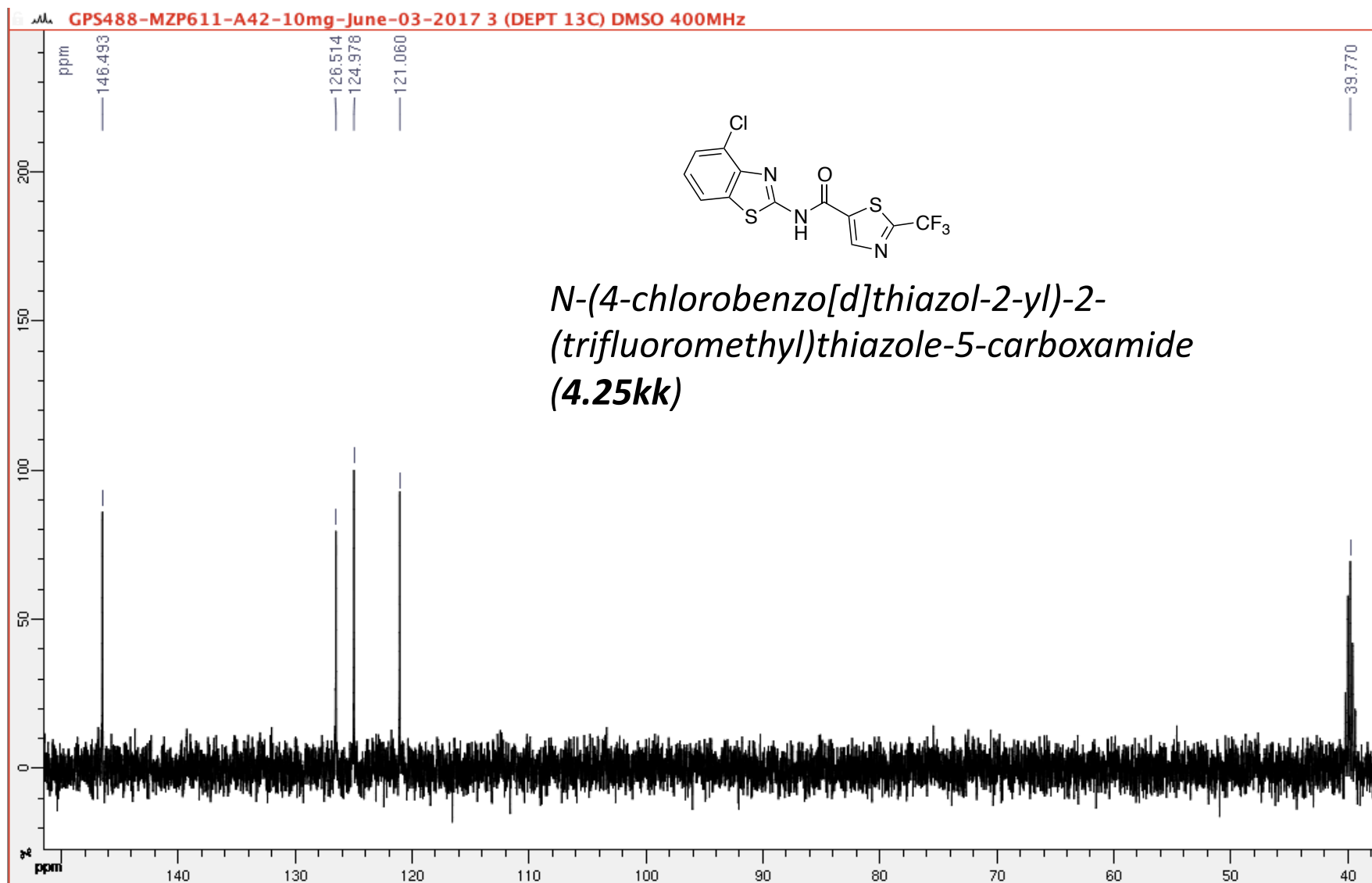
GPS488



DEPT 135

(100 MHz, 297.2 K, DMSO-d6)

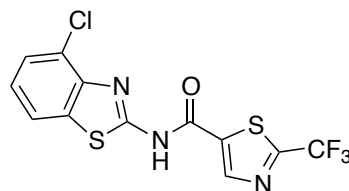
GPS488



GPS488-19F-NMR-June-07-2017

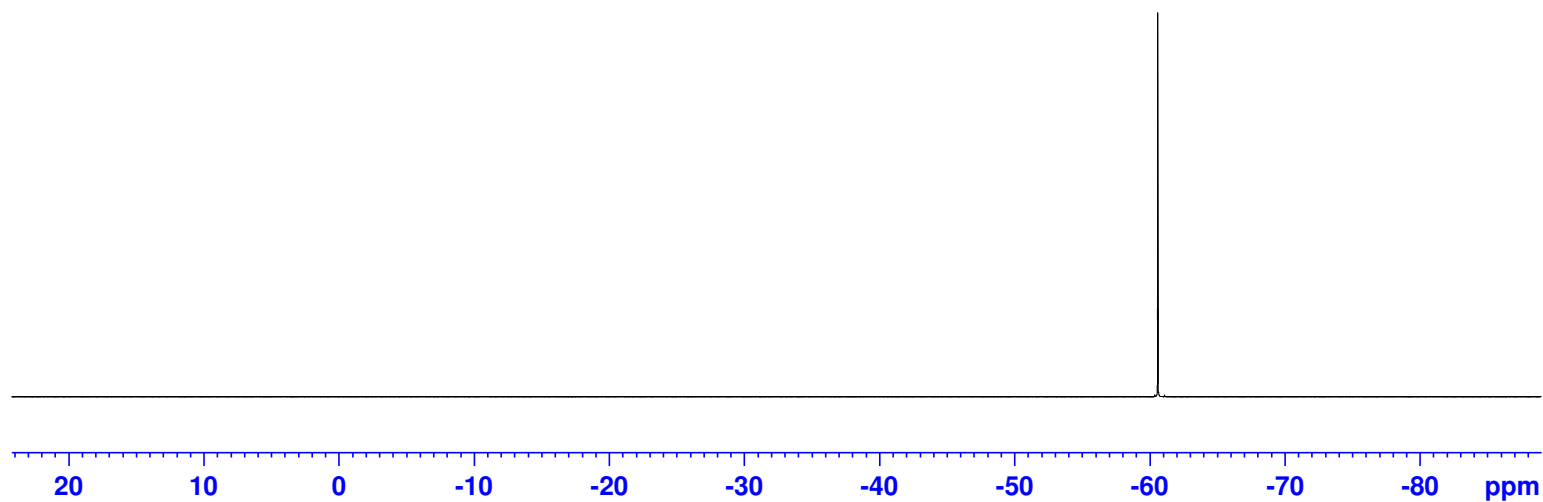
(400 MHz, 297.2 K, DMSO-d6)

GPS488



— -60.59

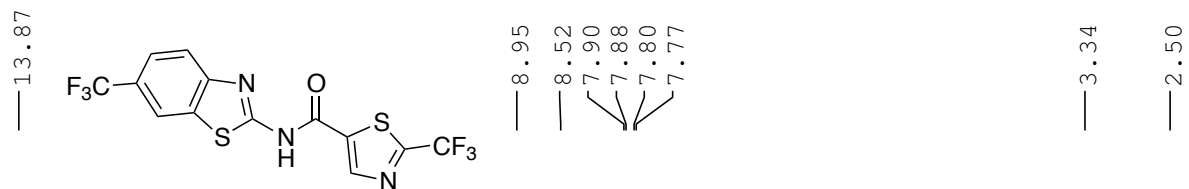
*N*-(4-chlorobenzo[d]thiazol-2-yl)-2-(trifluoromethyl)thiazole-5-carboxamide  
**(4.25kk)**



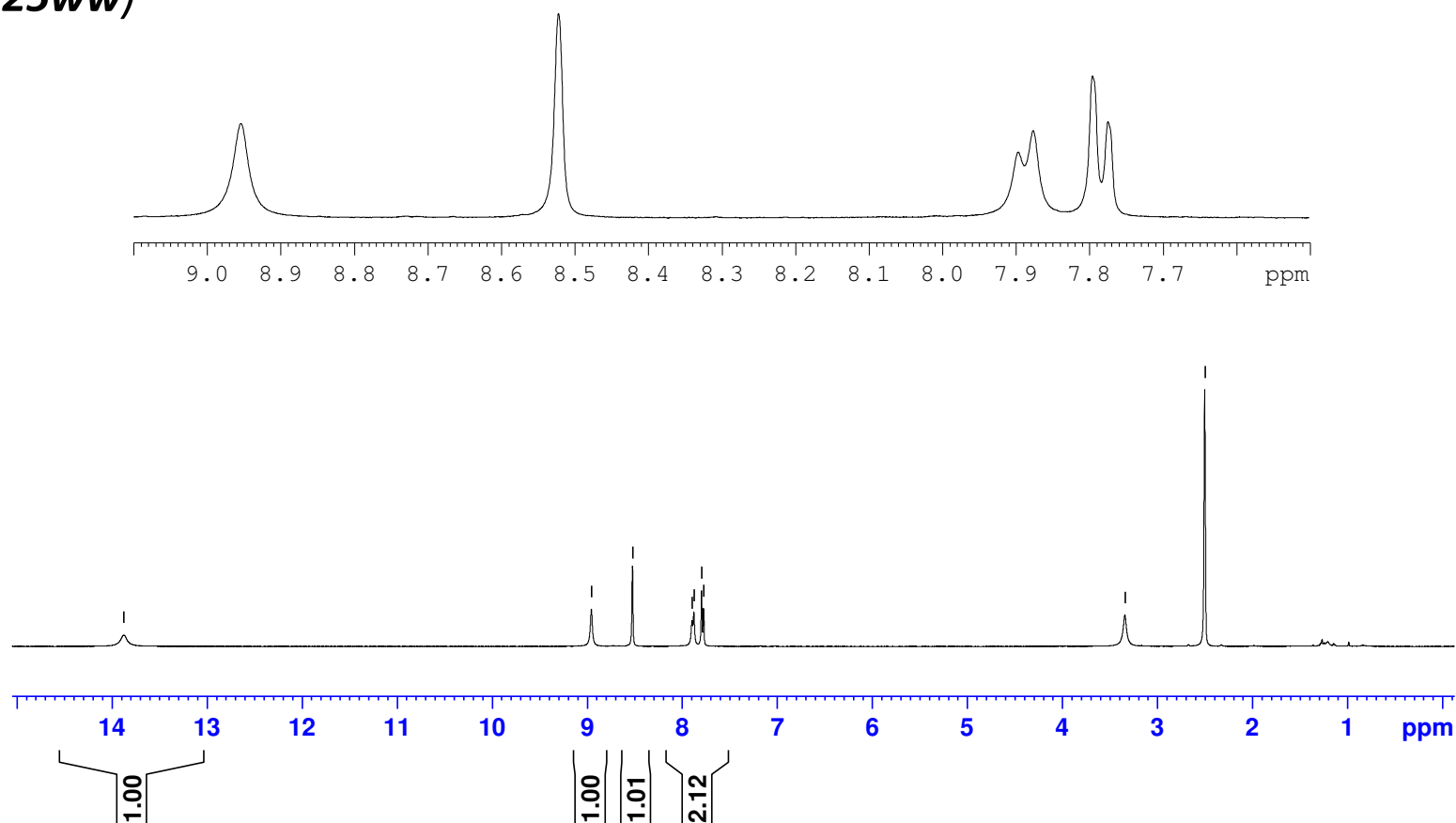
GPS491-10mg-1H-NMR-June-02-2017

(400 MHz, 297.2 K, DMSO-d6)

GPS491

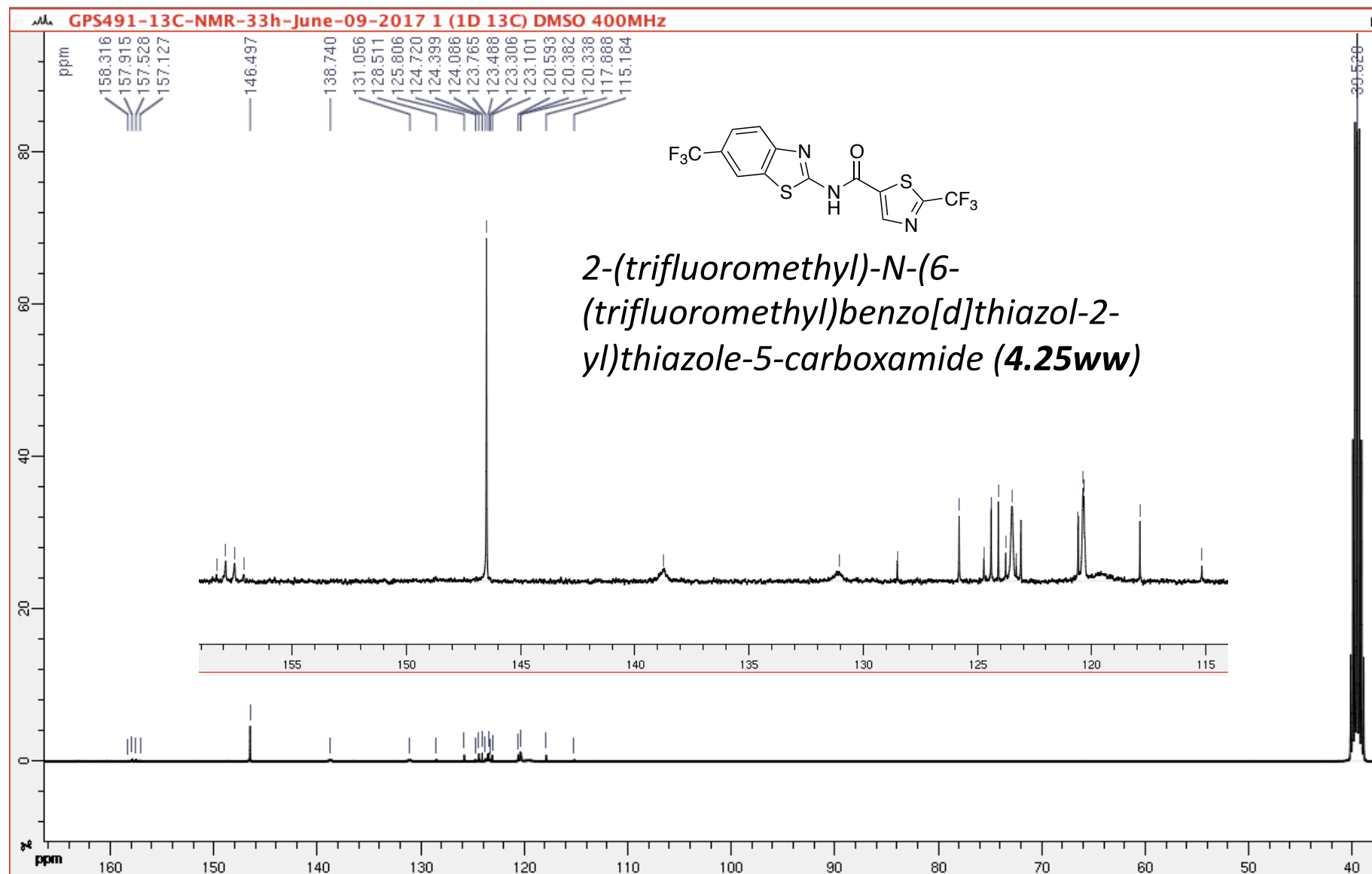


**2-(trifluoromethyl)-N-(6-(trifluoromethyl)benzo[d]thiazol-2-yl)thiazole-5-carboxamide (4.25ww)**



(100 MHz, 297.2 K, DMSO-d6)

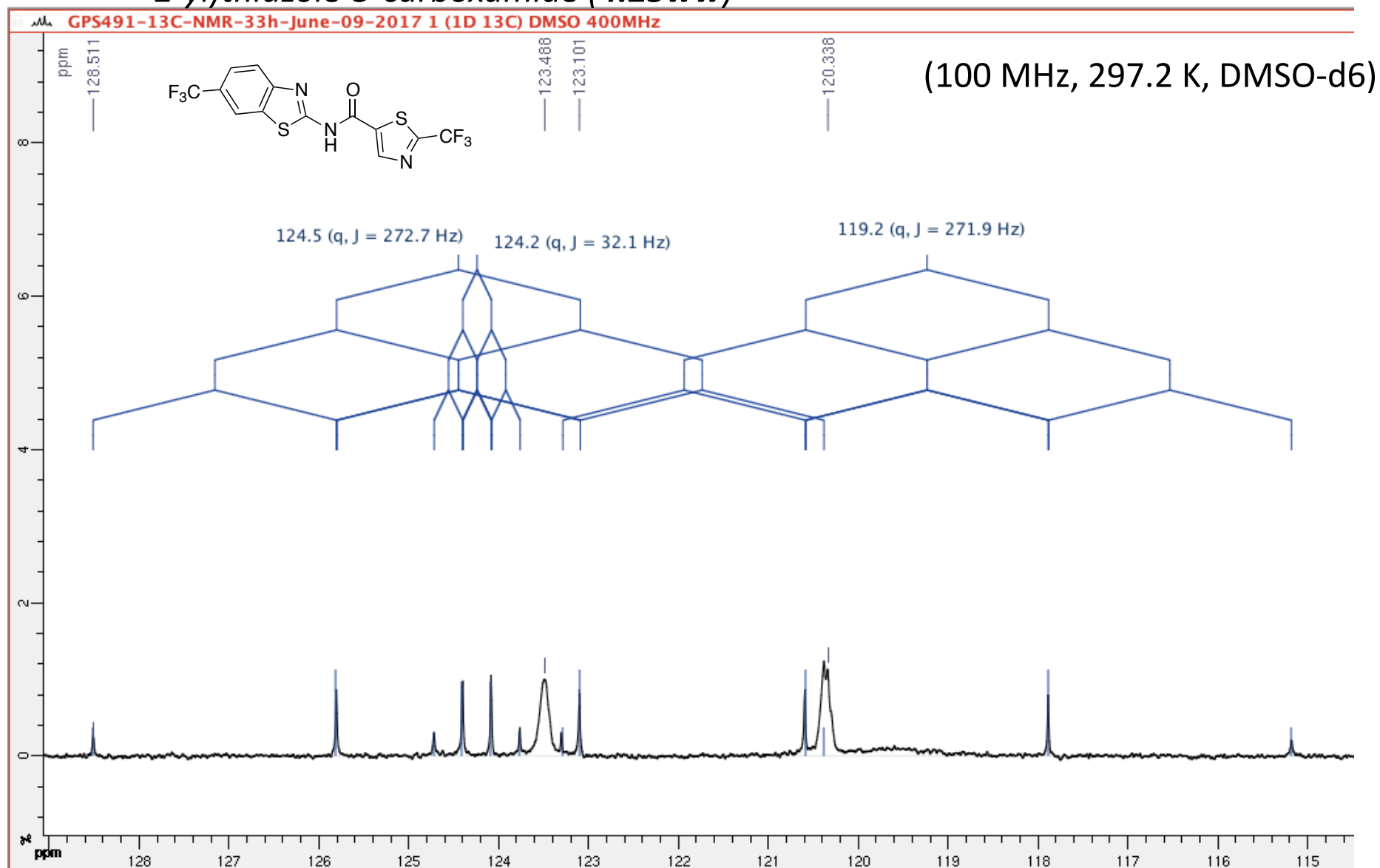
GPS491





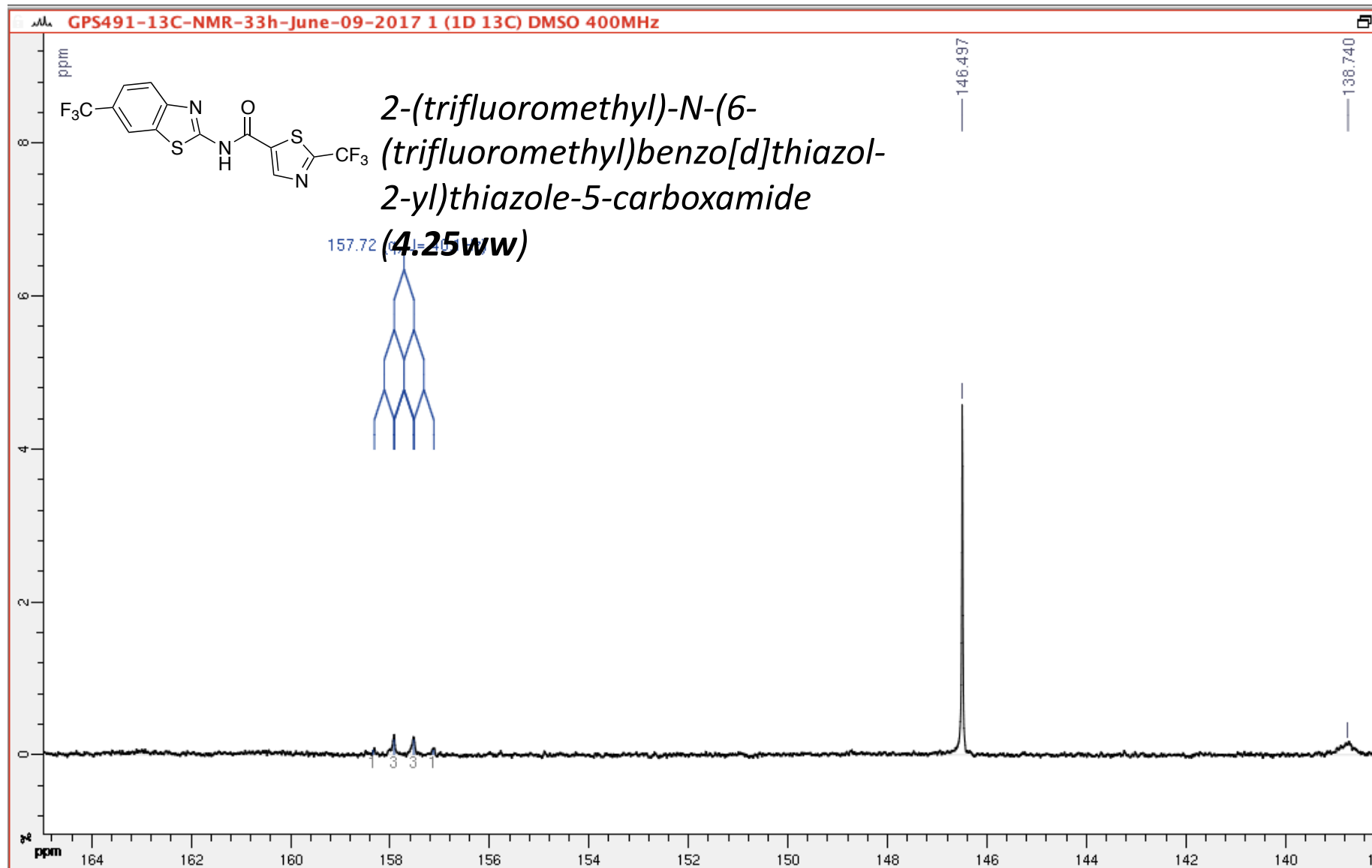
2-(trifluoromethyl)-N-(6-(trifluoromethyl)benzo[d]thiazol-2-yl)thiazole-5-carboxamide (**4.25ww**)

GPS491



(100 MHz, 297.2 K, DMSO-d6)

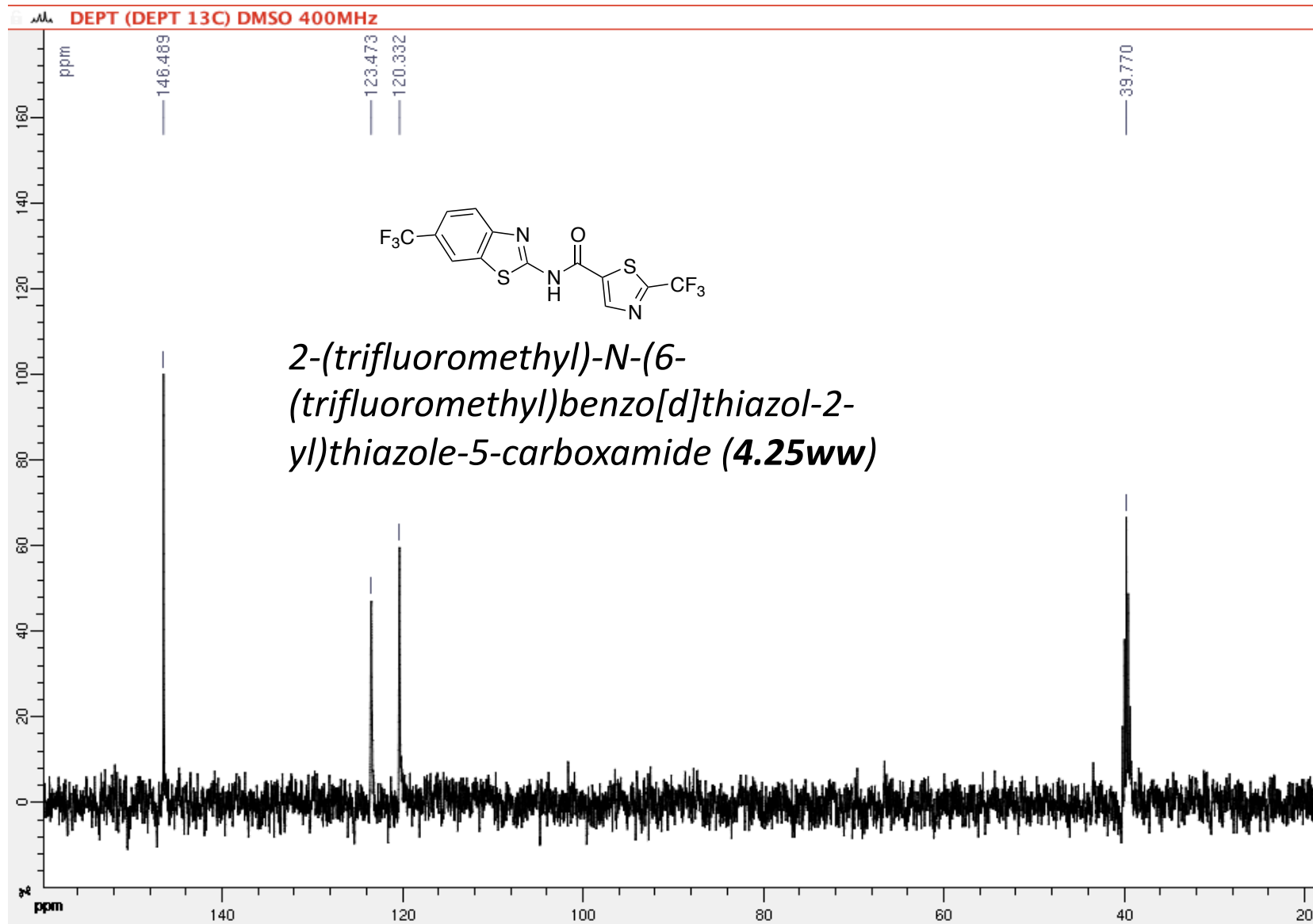
GPS491

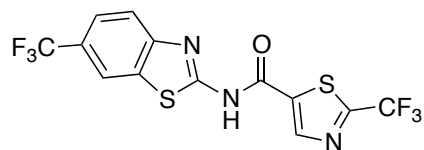


DEPT 135

(100 MHz, 297.2 K, DMSO-d6)

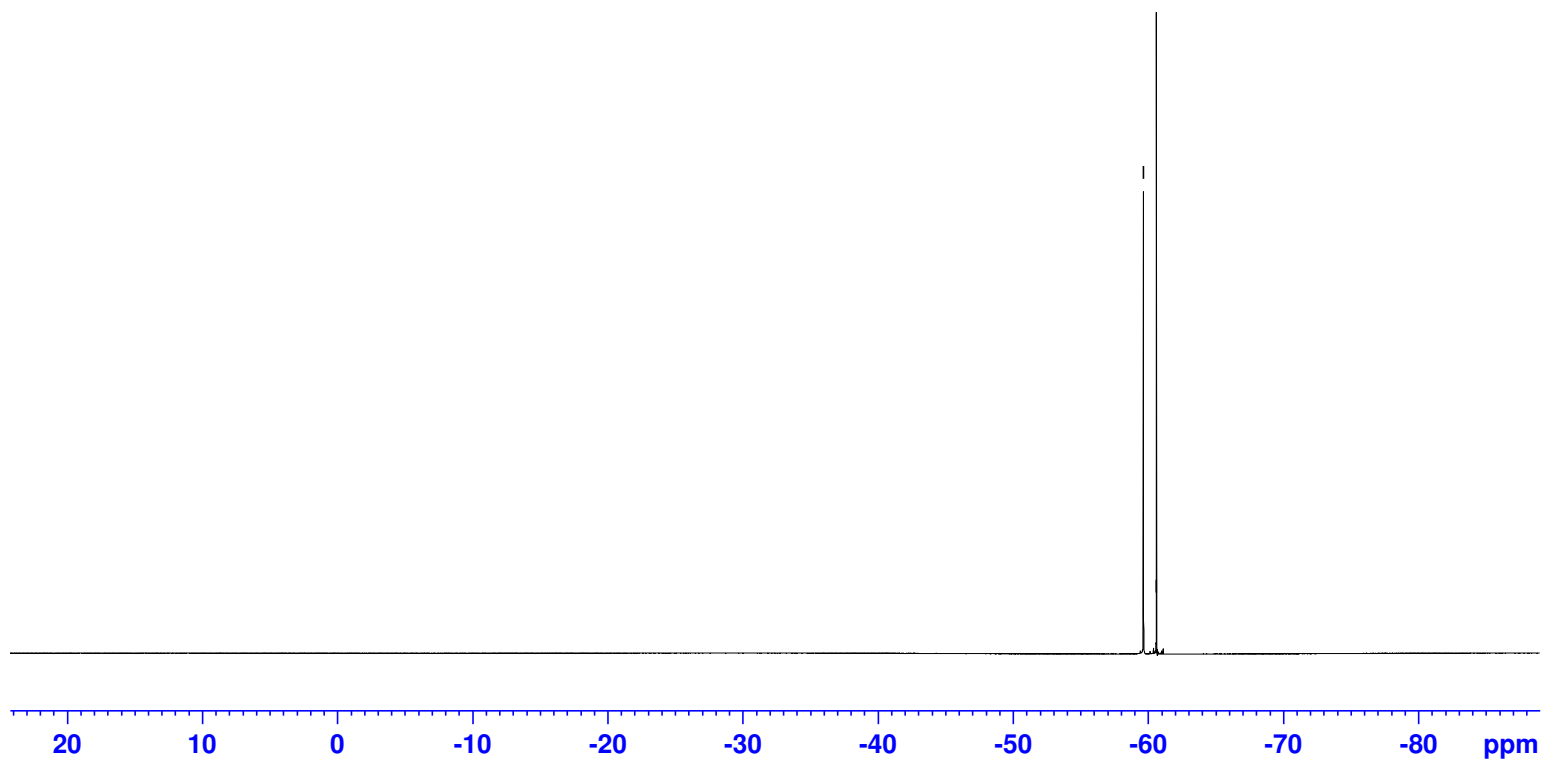
GPS491



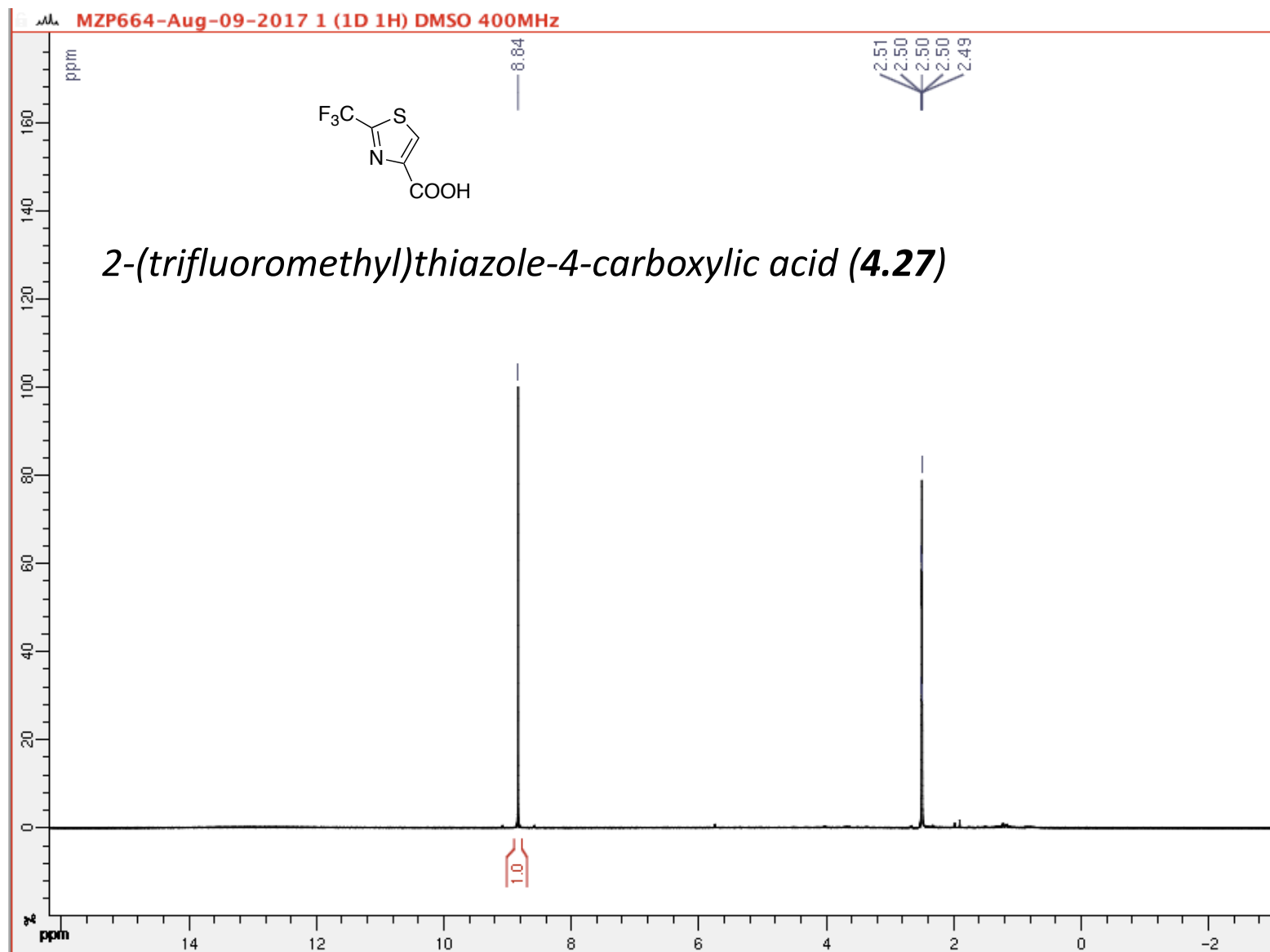


-59.63  
-60.59

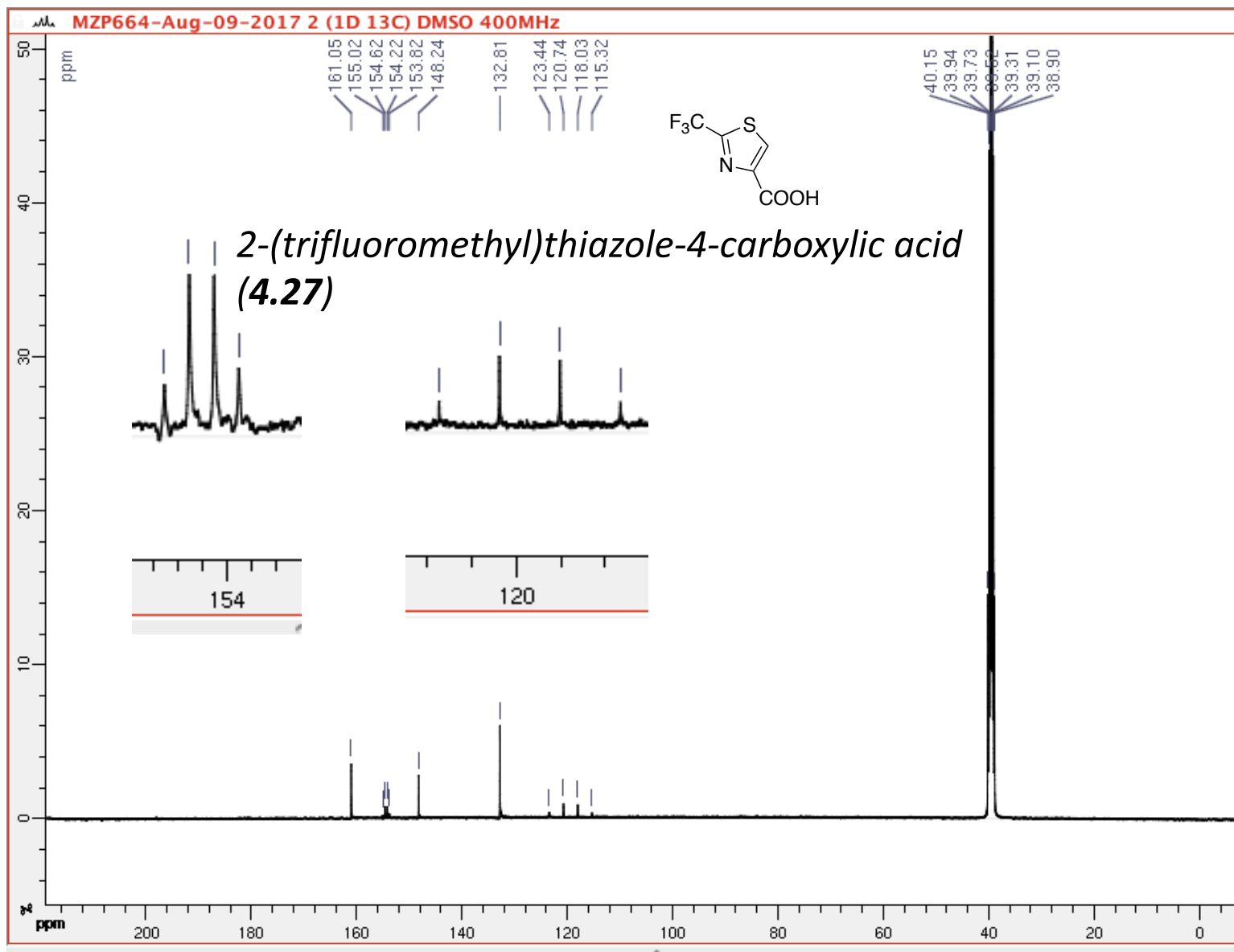
*2-(trifluoromethyl)-N-(6-(trifluoromethyl)benzo[d]thiazol-2-yl)thiazole-5-carboxamide*  
**(4.25ww)**



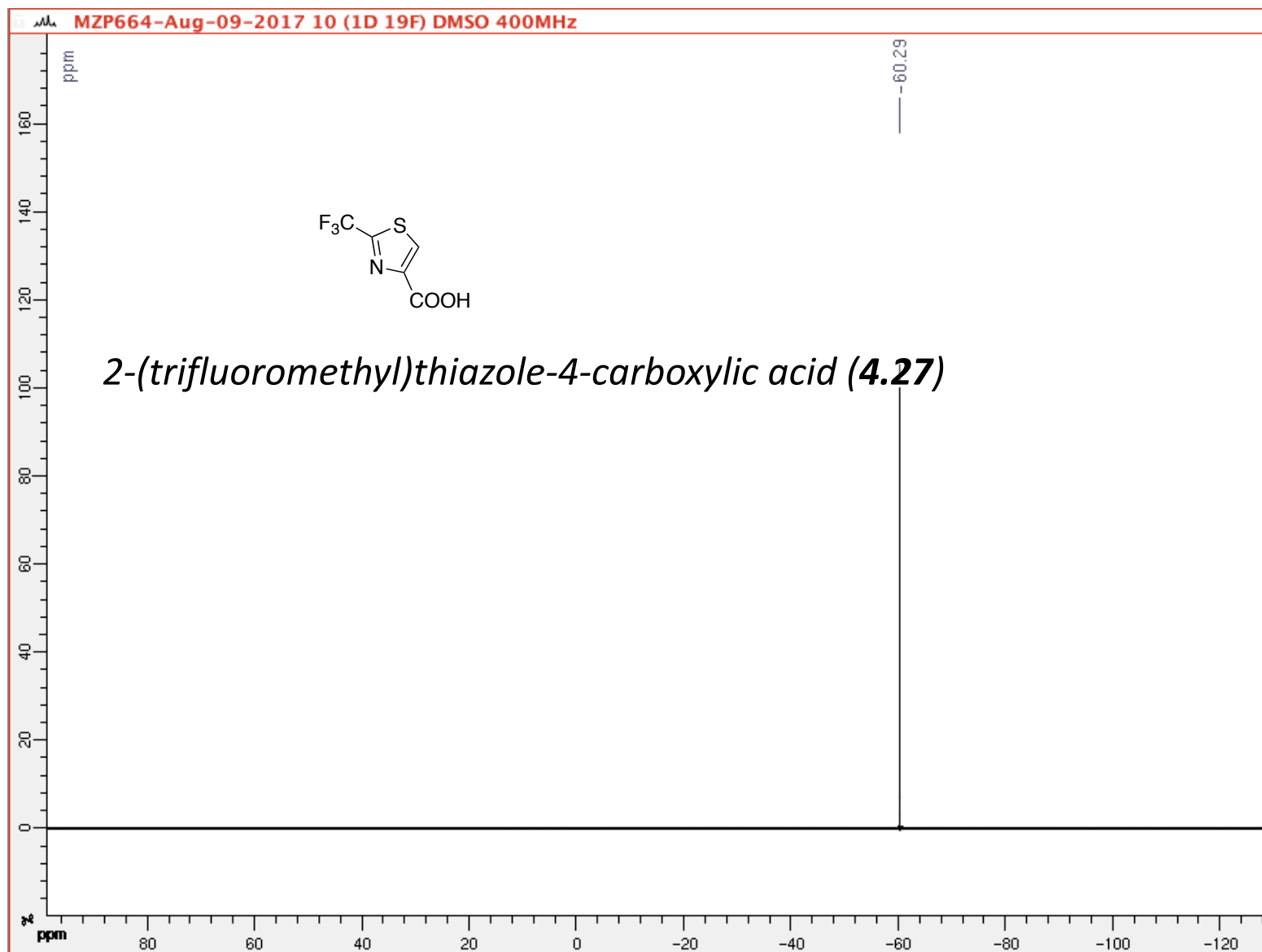
(400 MHz, 297.2 K, DMSO-d6)



(100 MHz, 297.2 K, DMSO-d6)

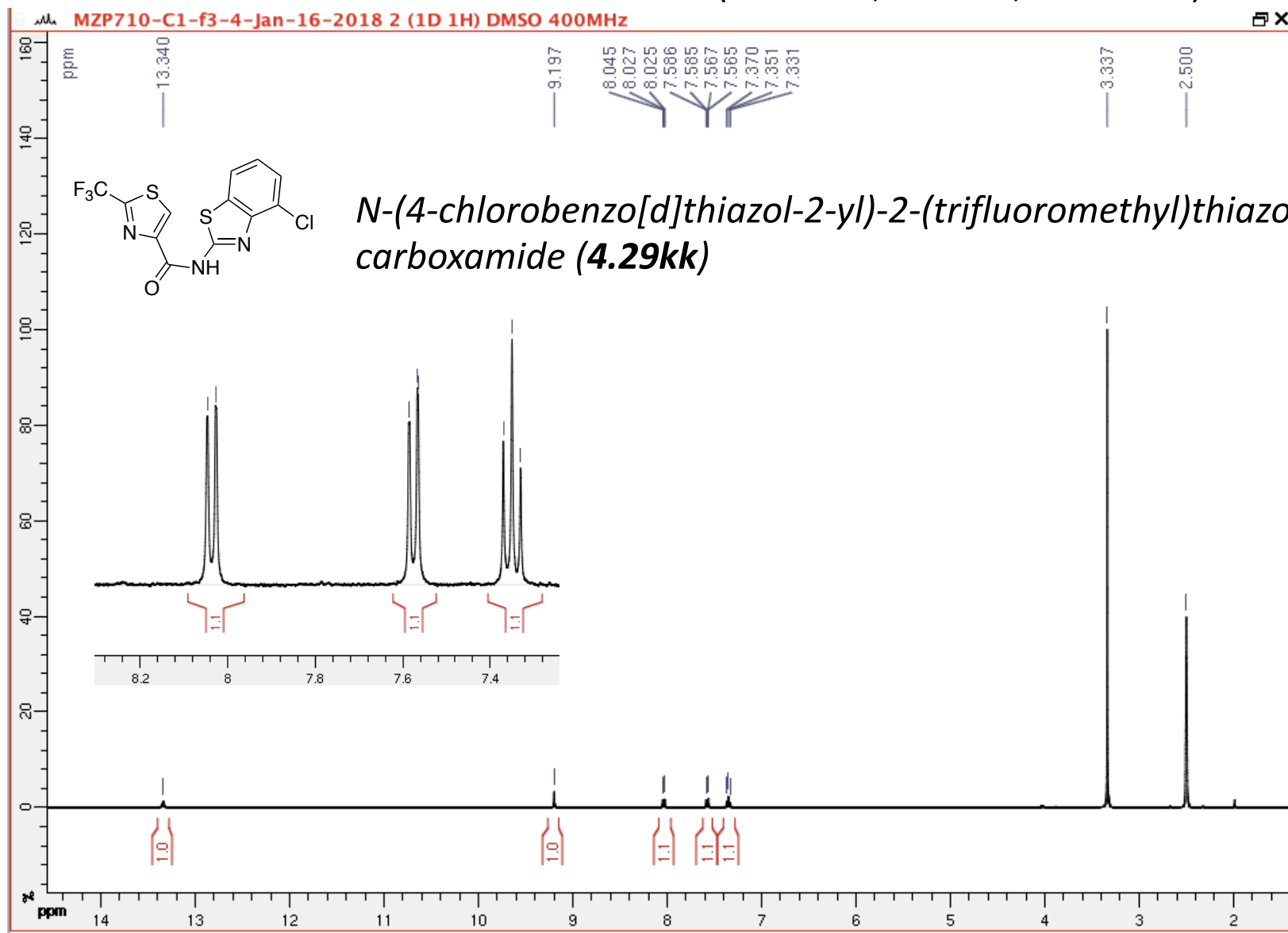


(400 MHz, 297.2 K, DMSO-d6)



(400 MHz, 297.2 K, DMSO-d6)

GPS500





(400 MHz, 297.2 K, DMSO-d6) GPS500

